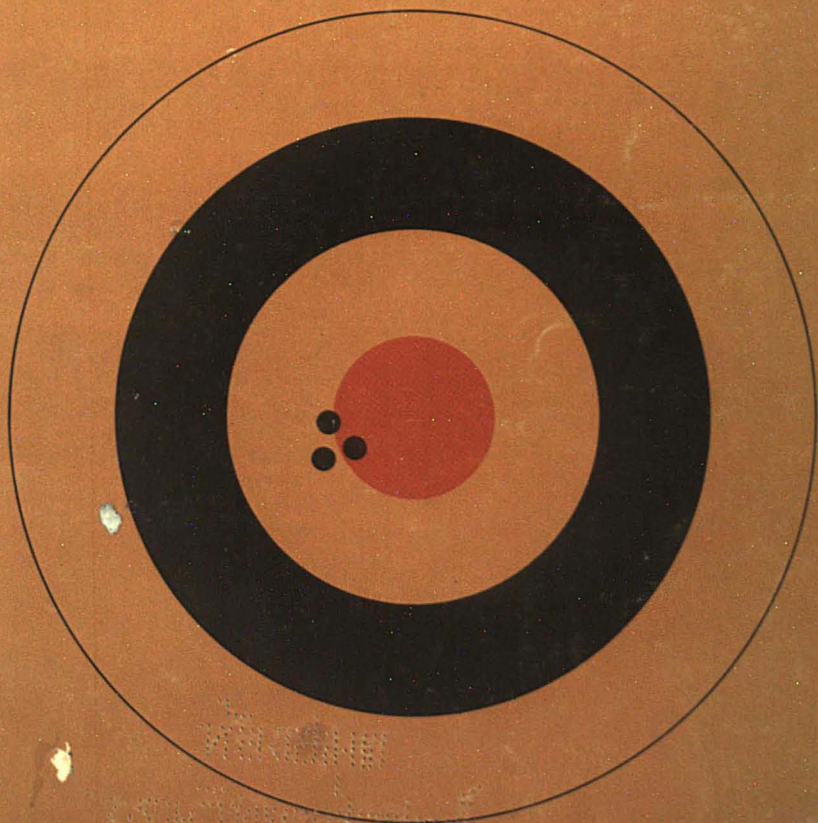


APRIL 1979

analytical chemistry

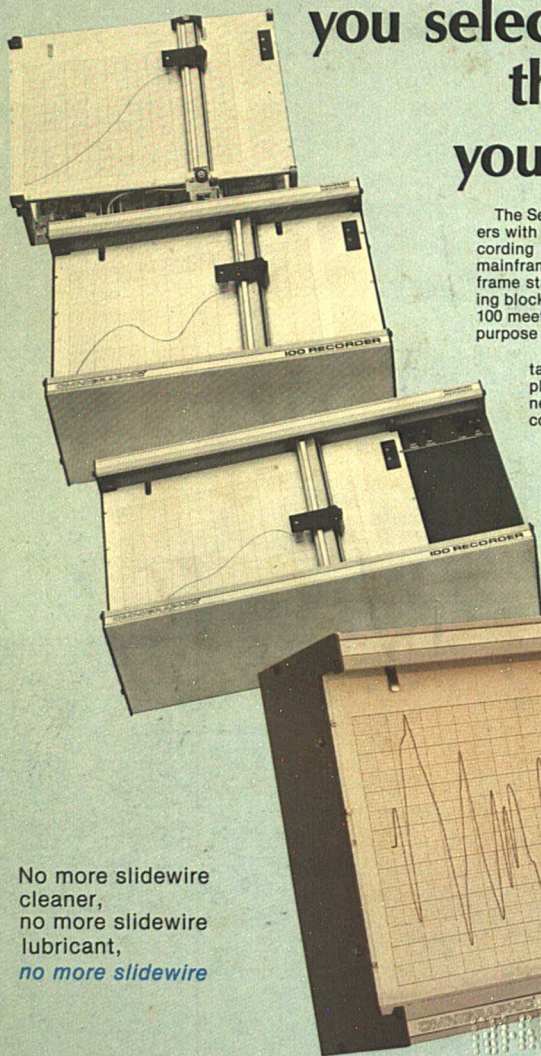
J F K A S S A S S I N A T I O N



B U L L E T A N A L Y S E S

Lab or field, production or process, OEM or general purpose...

The Omnigraphic® Series 100 lets you select the model that's right for your application



The Series 100 is a complete family of X-Y recorders with a model available to meet your specific recording need. Each model is built around a basic mainframe. The completely self-contained mainframe stands alone but can act as the basic building block for your particular application. The Series 100 meets both general purpose as well as special purpose system applications.

Houston Instrument's patented non-contacting capacitance feedback transducer replaces the slidewire and potentiometers, neatly eliminating the most troublesome components of X-Y servo systems.

For complete information contact Jim Bell, Houston Instrument, One Houston Square, Austin, Texas 78753 (512) 837-2820. Outside Texas call toll free 1-800-531-5202. In Europe contact Houston Instrument, Rochesterlaan 6 8240 Gistel Belgium. Phone 059/277445.

No more slidewire
cleaner,
no more slidewire
lubricant,
no more slidewire

Prices begin at \$970*
Quantity discounts available

* U.S. Domestic Price Only

* Registered Trademark of Houston Instrument

**houston
instrument**

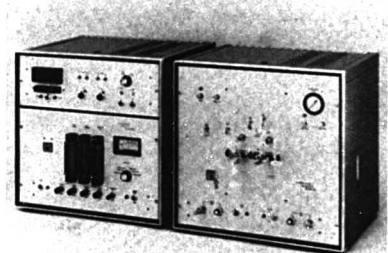
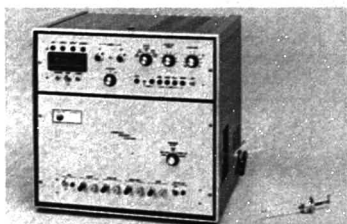
DIVISION OF BAUSCH & LOMB

"the graphics - recorder company"

Even Better Ways of Doing What Dohrmann Does Best

Measuring traces of nitrogen, sulfur, and halides

Dohrmann microcoulometric systems are leaders in the field for *fast, accurate* and *sensitive* determinations of traces of N, S, and Cl in solids, liquids and gases at the ppm level. Dohrmann's ongoing development of sampling accessories and methodology make this technique a powerful analytical tool in any laboratory. For details, call your local Dohrmann salesman or Doug Jones toll-free at (800) 538-7708.



Analyzing water for ppb organic carbon

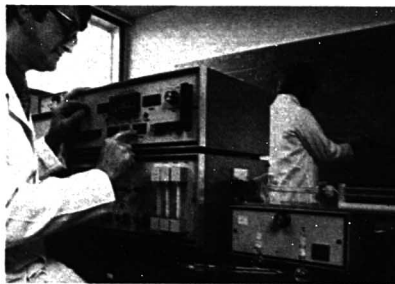
Dohrmann has added the DC-54 ultra-low-level organic carbon analyzer to its well established line of versatile TOC instruments. The DC-54 brings *speed, convenience* and *precision* to low-level TOC analysis: purgeables to ± 1 ppb, non-purgeables to ± 10 ppb.

If your TOC requirement runs from drinking to waste water, remember: **Dohrmann does it all.** For details on Dohrmann TOC analyzers, call your local Dohrmann salesman or Leon Hiam toll-free at (800) 538-7708.

The DN-10 Total Nitrogen Analyzer

Using oxidative pyrolysis and chemiluminescence detection, the DN-10 offers even greater *convenience* when measuring traces of nitrogen in organics. It's a proven, reliable performer for rapid, routine, low level analysis of nitrogen in feedstocks, light oils, and other petroleum products. For details, call your local Dohrmann salesman or Doug Jones toll-free at (800) 538-7708.

For literature on all products described above, write or circle the reader service number below.



ENVIROTECH



CIRCLE 60 ON READER SERVICE CARD

DOHRMANN

3240 Scott Boulevard
Santa Clara, California 95050

CALL TOLL FREE
(800) 538-7708

In Alaska, California,
Hawaii, Puerto Rico, call
collect (408) 249-6000

How to do High Performance TLC without mortgaging the ranch.

Introducing the Whatman LHP-K plate.

High Performance TLC (HPTLC) aims — in concept — to revolutionize TLC. It's fast, extremely sensitive (pg-ng), has excellent reproducibility, high separation capability; it can be correlated with HPLC and is in other ways virtuous for either qualitative or quantitative TLC.

Unfortunately it was also expensive and a little fussy.

Until now.

Now there's the Whatman LHP-K plate, high performance TLC with a preadsorbent area. ***You use it just as you use any preadsorbent TLC plate; no special spotting equipment or chambers; no special techniques.***

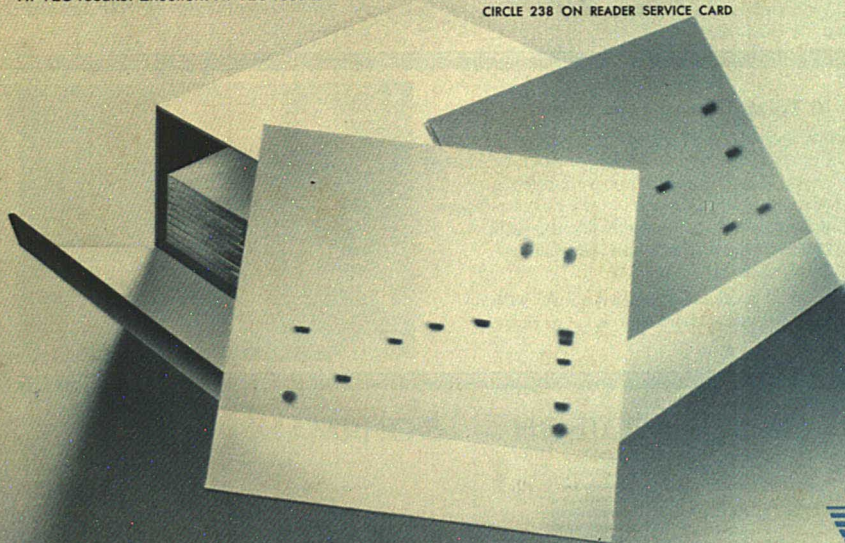
HPTLC results. Excellent HPTLC results.

You can spot relatively large volumes (up to 5 μ l) of low concentration samples with, for example, a Drummond 5 μ l Microcap. Develop in an ordinary chamber. Separate nanogram, even picogram, quantities in 1-4 minutes. Tight (1.5 - 2.5 mm) spots in a 3-7 cm run. The LHP-K plates incorporate a preadsorbent spotting area preceding the special, 5 μ m particle, silica gel. This virtually eliminates all spotting problems long associated with HPTLC. The layer is ultra smooth and highly reflective.

The LHP-K plate. Inexpensive HPTLC. Only from Whatman.

Details in our new literature. Yours for the asking. **Whatman Inc.** ■ 9 Bridewell Place, Clifton, N.J. 07014; tel: 201-777-4825.

CIRCLE 238 ON READER SERVICE CARD



Whatman 



analytical chemistry

CONTENTS

REPORT

F. W. Michelotti and J. T. Baker Chemical reviews the fundamentals of hazardous chemical safety with specific emphasis on flammable liquids, corrosive chemicals, insidious hazards, compressed gases, and cryogenic liquids **441 A**

INSTRUMENTATION

Gas chromatography-mass spectrometry applied to clinical chemistry is discussed by Nathan Gochman, Lermuel J. Bowie, and David N. Bailey. Three commercial systems are presented in detail **525 A**

THE ANALYTICAL APPROACH

Reexamination of the bullet-lead specimens from the JFK assassination by nondestructive neutron activation analysis is described by V. P. Guinn of U of California **484 A**

REGULATIONS

A Master Analytical Scheme for trace determinations in commercial products holds promise for simplifying and reducing the cost of compliance with regulations **458 A**

NEWS

The 32nd annual Summer Symposium on Analytical Chemistry will be held at Purdue University in June. The program on lasers and analytical chemistry is given **466 A**

BOOKS

Books on laser and coherence spectroscopy, computers in mass spectrometry, chemical microscopy, and pollution evaluation are reviewed by J. M. Harris, D. H. Smith, A. C. Reimschuessel, and R. K. Stevens **511 A**

EDITORS' COLUMN

A summary of a survey on problems of conversion to SI units and its effect on the teaching of chemistry is presented **521 A**

EDITORIAL

A newly formed subcommittee within the ACS Committee on Environmental Improvement plans to set forth the minimum criteria for the validation of an environmental analytical method. This is an important initial step toward improving data **465**

Permission of the American Chemical Society is granted for libraries and other users to make reprographic copies for use beyond that permitted by Sections 107 or 108 of the U.S. Copyright Law, provided that the copying organization pay the appropriate per-copy fee through the Copyright Clearance Center, Inc. Educational institutions are generally granted permission to copy upon application to the Office of the Director, Books and Journals Division, ACS, 1155 16th St., N.W., Washington, D.C. 20036.

Published monthly with review issue added in April and Laboratory Guide in August by the American Chemical Society, from 20th and Northampton Sts., Easton, Pa. 18042. Executive and Editorial headquarters, American Chemical Society, 1155 16th St., N.W., Washington, D.C. 20036 (202) 872-4600. Second class postage paid at Washington, D.C., and at additional mailing offices.

1979 Subscription prices—including surface postage

	1 yr	2 yr	3 yr
MEMBERS:			
Domestic	\$12	\$22	\$30
Canada, Foreign	21	40	57
NONMEMBERS:			
Domestic	16	29	42
Canada	25	47	69
Other Foreign	33	61	89

Airmail and air freight rates are available from Membership & Subscription Services, ACS, P.O. Box 3337, Columbus, Ohio 43210 (614) 421-7230.

New and renewal subscriptions should be sent with payment to the Office of the Controller at the ACS Washington address.

Subscription service inquiries and changes of address (include both old and new addresses with ZIP code and recent mailing label) should be directed to the ACS Columbus address noted above. Please allow six weeks for change of address to become effective.

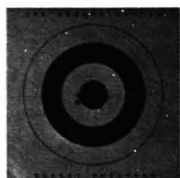
Claims for missing numbers will not be allowed if loss was due to failure of notice of change of address to be received in the time specified; if claim is dated (a) North America: more than 90 days beyond issue date, (b) all other foreign: more than one year beyond issue date; or if the reason given is "missing from files."

Microfilm and microfiche editions are available by single volume or back issue collection. Inquiries and payments to Microforms Program, ACS Washington address.

Single issues, current year, \$3.00 except review issue and Labguide, \$4.00; back issues and volumes: write or call Special Issues Sales, ACS Washington address (202) 872-4365.

Advertising Management: Centcom, Ltd., 25 Sylvan Road South, Westport, Conn. 06880 (203) 226-7131

Technical Contents/Briefs	430 A
Call for Papers	469 A
Meetings	470 A
Short Courses	476 A
New Products	500 A
Manufacturers' Literature	507 A
Advertising Index	544 A
Author Index	IBC
Future Articles	IBC



Our cover illustrates targets and bullets. Bullet analysis is the subject of this month's Analytical Approach

Briefs

Two-Dimensional Chemical State Plots: A Standardized Data Set for Use in Identifying Chemical States by X-Ray Photoelectron Spectroscopy 466

The two-dimensional graphs plot kinetic energy of the sharpest X-ray excited Auger line versus the binding energy of the most intense photoelectron line.

C. D. Wagner,* L. H. Gale, and R. H. Raymond, Shell Development Company, P.O. Box 1380, Houston, Tex. 77001
Anal. Chem., 51 (1979)

Surface Analyses by a Triboelectric Charging Technique 483

The technique's utility for detection of chemical transformations of surfaces and contamination by mass transfer is demonstrated.

Harry W. Gibson,* John M. Pochan, and F. C. Bailey, Webster Research Center, Xerox Corporation, Webster, N.Y. 14580
Anal. Chem., 51 (1979)

Auger Electron Spectra Intensity Variation with Potential-Modulation Differentiation 488

The intensity of Auger transitions for a number of KLL, MNN, and LMM series peaks are examined as a function of the modulation voltage.

G. E. McGuire* and B. R. Martin, Texas Instruments Incorporated, Dallas, Tex. 75265
Anal. Chem., 51 (1979)

Parameters for the Ratio Method by X-ray Microanalysis 491 ■

Atomic or weight ratios of elements can be calculated routinely from X-ray intensities of ultrathin samples using precalculated proportionality factors.

András G. A. Jánosy,* Kristóf Kovács, and Ida Tóth, Biological Research Center, Institute of Biophysics, POB 521, H-6701 Szeged, Hungary
Anal. Chem., 51 (1979)

Diagnosis and Correction of Wedging Errors in Absorbance Subtract Fourier Transform Infrared Spectrometry 495

The wedging effects in absorbance subtract spectrometry give the resulting concentration errors and residual spectra, and describe means for correcting for them.

Tomas Hirschfeld, Block Engineering, Inc., Cambridge, Mass. 02139
Anal. Chem., 51 (1979)

* Corresponding author.

■ Supplementary material available.

Determination of Oil Content in Oil Modified o-Phthalic Polyester Resins by Infrared Spectrometry 499

The calculated oil percentage is within the accuracy of a gravimetric procedure.

James A. Vance,* N. Bradford Brakke, and Paul R. Quinney, Analytical Laboratory, Lilly Industrial Coatings, Inc., 666 South California Street, Indianapolis, Ind. 46225
Anal. Chem., 51 (1979)

Nanosecond Time-Resolved Spectrometry with a Tunable Dye Laser and a Simple Pulse-Gated Photon Counter 502

Fluorometric system ($\Delta\lambda = 3.5$ nm, $\Delta t = 5$ ns) is constructed and used for the measurement of the time-resolved spectrum and of the lifetime. The sensitivity of $A\phi$ is 5×10^{-11} .

Totaro Imasaka, Teichiro Ogawa, and Nobuhiko Ishibashi,* Faculty of Engineering, Kyushu University, Fukuoka 812, Japan
Anal. Chem., 51 (1979)

Vapor Phase Determination of Blood Ammonia by an Optical Waveguide Technique 505

A linear relationship exists between absorbance and blood ammonia concentration in the clinically useful range of 0–400 $\mu\text{g/dL}$.

P. L. Smock, Department of Chemistry, University of Dayton, Dayton, Ohio 45469, T. A. Orofino and G. W. Wooten,* Monsanto Research Corporation, 1515 Nicholas Road, Dayton, Ohio 45407, and W. S. Spencer, St. Elizabeth Medical Center, Dayton, Ohio 45407
Anal. Chem., 51 (1979)

Effect of Sample Thickness on the Magnitude of Optoacoustic Signals 508

Published theoretical predictions of the effect of sample thickness on optoacoustic signal magnitude are substantiated experimentally using polymer films.

M. J. Adams,* G. F. Kirkbright, and K. R. Menon, Chemistry Department, Imperial College of Science and Technology, London SW7 2AZ, U.K.
Anal. Chem., 51 (1979)

Determination of Trace Elements in Light Element Matrices by X-ray Fluorescence Spectrometry with Incoherent Scattered Radiation as an Internal Standard 511

Analyses of approximately 0.5-g samples, prepared as thin uniform specimens, give results accurate to within $\pm 10\%$, when X-ray counting statistics are not the limiting factor.

Robert D. Giaque,* Roberta B. Garrett, and Lilly Y. Goda, Energy and Environment Division, Lawrence Berkeley Laboratory, University of California, Berkeley, Calif. 94720
Anal. Chem., 51 (1979)

ORION's "no lemon" meters will suit you to a T-shirt.

Model 501: New, low-cost digital pH meter readable to 0.01 pH. Features ATC and digital reading of temperature.

Model 407A: Versatile, top-of-the-line analog meter for pH and specific ion work. Also available in battery-powered field version, with carrying case.

Model 201: A low-cost, hand-held digital that reads to 0.05 pH. Comes with carrying case and line adaptor to permit laboratory use.

Model 701A: Research-grade digital pH/mV meter with 0.001 pH resolution. Features ATC and digital output for interfacing to ORION printer. Comes with swing arm electrode holder.

901 Microprocessor Analyzer: Unique "thinking" meter offers unmatched simplicity of operation, makes electrode analysis faster, easier. Pushbutton standardization and blank correction. No calibration curves to draw.

The famous ORION "no lemon" T-shirt, yours with a demo of any ORION "no lemon" meter.

Ask for a demonstration of any ORION "no lemon" meter and receive a "no lemon" T-shirt, free!

Take your pick of the "no lemon" crop! These are just a few of ORION's pH and specific ion meters, priced from as little as \$220. They're so reliable, each one comes with our famous "no lemon" guarantee: If your meter quits for any reason other than abuse within one year of purchase, we'll replace it with a brand new one. Immediately, and without charge. That's why we say, "ORION eats lemons!" Mail the coupon today for your demo and free T-shirt.



Please call me for a demo of (circle):

501 901 407A 201 701A

T-shirt size: ☐ medium ☐ large ☐ extra-large

Name _____

Title _____ Phone () _____

Organization _____

Street _____

City _____ State _____ Zip _____

ORION RESEARCH
380 Putnam Ave., Cambridge, MA 02139

A29D

Briefs

Comparison of Different Plasma Excitation and Calibration Methods in the Analysis of Geological Materials by Optical Emission Spectrometry 516

No buffers are needed for rock analyses by ICP in which the matrix effects are low. For MWP, large quantities of ionization buffers are needed.

Jan-Ola Burman and Kurt Bostrom,* Department of Economic Geology, University of Luleå, S-951 87 Luleå, Sweden
Anal. Chem., 51 (1979)

Determination of Microgram Quantities of Asbestos by X-ray Diffraction: Chrysotile in Thin Dust Layers of Matrix Material 520

Detection limits as low as $2 \mu\text{g}/\text{cm}^2$ (on a filter) are cited in the presence of mg quantities of matrix.

B. A. Lange* and J. C. Haartz, U.S. Department of Health, Education, and Welfare, Public Health Service, Center for Disease Control, National Institute for Occupational Safety and Health, 4676 Columbia Parkway, Cincinnati, Ohio 45226
Anal. Chem., 51 (1979)

Optimized Wide-Interval Rate Measurements of Substrate 526

Estimation of substrate amount from rate measurements over wide time intervals can exhibit an order of magnitude reduction in errors because of the rate constant variations.

J. E. Davis* and Brian Renoe, Division of Laboratory Medicine, Departments of Pathology and Medicine, Washington University and Barnes Hospital, St. Louis, Mo.
Anal. Chem., 51 (1979)

Optimization of the Coupled Enzymatic Measurement of Substrate 529

By proper selection of the time at which the reaction rate is measured, 20% variation in enzymatic activities will cause less than a 2% variation in the initial substrate concentration rate.

J. E. Davis* and Jeff Pevnick, Division of Laboratory Medicine, Department of Pathology and Medicine, Washington University and Barnes Hospital, St. Louis, Mo. 63110
Anal. Chem., 51 (1979)

Determination of Individual Ubiquinone Homologues by Mass Spectrometry and High Performance Liquid Chromatography 534

The detection limit for ubiquinone using the direct inlet selected ion monitoring method is 0.1 ng.

Sukehiro Imabayashi,* Tetsuya Nakamura, Yoshio Sawa, Jirō Hasegawa, Kenya Sakaguchi, Takeshi Fujita, Yutaka Mori, and Kiyoshi Kawabe, Eisai Research Laboratories, Eisai Co., Ltd., Koishikawa 4, Bunkyo-ku, Tokyo 112, Japan
Anal. Chem., 51 (1979)

Stoichiometry of the Reaction of Electrons with Bromotrichloromethane in an Electron Capture Detector 537

Results lend support to assumptions of chemical reactivity inherent in the use of the ECD as a gas-phase coulometer.

E. P. Grimsrud* and S. H. Kim, Department of Chemistry, Montana State University, Bozeman, Mont. 59717
Anal. Chem., 51 (1979)

Statistical Designs for the Optimization of the Nitrogen-Phosphorus Gas Chromatographic Detector Response 541

The average value of the ratio of nitrogen to hydrocarbon response with the nitrogen-sensitive detector is about 1000:1.

I. B. Rubin*, Bio/Organic Analysis Section, Analytical Chemistry Division, Oak Ridge National Laboratory, Oak Ridge, Tenn. 37830, and **C. K. Bayne,** Mathematics and Statistics Research Section, Computer Sciences Division, Oak Ridge National Laboratory, Oak Ridge, Tenn. 37830
Anal. Chem., 51 (1979)

Electron Impact Excitation of Ions from Organics: An Alternative to Collision Induced Dissociation 547

The spectra obtained using cyclotron resonance spectrometry are analogous to those obtained by collision induced dissociation and yield characteristic structural information.

R. B. Cody and B. S. Freiser,* Department of Chemistry, Purdue University, West Lafayette, Ind. 47907
Anal. Chem., 51 (1979)

Determination of Organosulfur Compounds Extracted from Marine Sediments 551

Method uses a dichloromethane extraction with a Cu column to eliminate elemental sulfur and a flame photometric detector. The detection limit for S is 1 ng with a precision of $\pm 10\%$.

Timothy S. Bates* and Roy Carpenter, Department of Oceanography, University of Washington, Seattle, Wash. 98195
Anal. Chem., 51 (1979)

Voltammetric Ion Selective Electrode for the Determination of Nitrate 554

Electrolysis cell with an anion-exchange membrane sheath responds to nitrate down to 6.7×10^{-6} M. Currents measured at 8 min yield working curves with a slope of $1.91 \pm 0.05 \times 10^6$ nA/M.

James A. Cox* and George R. Litwinski, Department of Chemistry and Biochemistry, Southern Illinois University of Carbondale, Carbondale, Ill. 62901
Anal. Chem., 51 (1979)

Spectroelectrochemical Determination of Heterogeneous Electron Transfer Rate Constants 556

Good agreement is obtained between values of k_{et} and α determined spectroelectrochemically ($k_{et} = 4.6 (\pm 0.2) \times 10^{-4}$ cm/s, $\alpha = 0.328 (\pm 0.006)$) and those determined by chronocoulometry ($k_{et} = 4.0 (\pm 0.2) \times 10^{-4}$ cm/s, $\alpha = 0.323 (\pm 0.008)$).

Douglas E. Albertson and Henry N. Blount,* Brown Chemical Laboratory, The University of Delaware, Newark, Del. 19711, and **Fred M. Hawkridge,*** Department of Chemistry, Virginia Commonwealth University, Richmond, Va. 23284
Anal. Chem., 51 (1979)

MEASURING MOLECULAR WEIGHT?

Chromatix does it better 5 ways!

1. All Polymers measured. We measure molecular weight of all types of polymers, including synthetic and biological, linear or branched, water or organic soluble, small or large, at low temperatures or high temperatures. In addition, we can supply everything you need for molecular weight data processing, detection, and separation—either as a system or as modular components.

2. Results in Minutes. We can provide answers in minutes to such complex data processing problems as the determination of molecular weight (MW) distributions or diffusion coefficients. For example, using Chromatix turnkey software, our powerful disk-based Laboratory Data System can calculate MW distributions from on-line gel permeation chromatographic data (GPC) and automatically plot the results. We also have turnkey software for automatic calculation of diffusion coefficients, particle sizes, absolute molecular weight and MW distributions. To build your own custom programs, we offer LDS system disks for FORTRAN and BASIC. Our system is also PDP-11 software compatible.



3. Unique MW Detector. To rapidly measure absolute molecular weight without external calibration, we offer the KMX-6 Low Angle Laser Light Scattering Photometer. This unique detector measures absolute molecular weight rather than relative weight or molecular size. It operates with very small sample volumes and minimal sample preparation. When used with a GPC, it provides on-line MW distributions independent of GPC column calibrations.

4. Aqueous Chromatography. For separation in liquid chromatography, our new line of Aquapore™ columns and our new constant flow HPLC pump are specifically designed for use with water soluble macromolecules. Yet,

they handle polar and non-polar organic solvents just as successfully. We also offer other types of columns, plus valves, injectors, and plumbing components.

5. Comprehensive Technical Backup. We offer a wide range of technical backup including detailed application literature, user training courses, and a fully staffed and equipped applications laboratory. For complete technical and application information, check #35 Laboratory Data System, #36 KMX-6 Detector, #37 Pump and Columns, #38 Applications in Synthetic Polymers, #39 Water Soluble Polymers, #40 Biopolymers, #41 Low Molecular Weight, #42 technical representative to call.

chromatix

Specialists in Molecular Weight

560 Oakmead Parkway
Sunnyvale, CA 94086 -
Phone: (408) 736-0300
TWX: 910-339-9291
D6903 Neckargemünd 2
Unterstrasse 45a
West Germany
Phone: (06223) 7061/62
Telex: 461-691

RUGGED 0.6 METER MONOCHROMATOR

The HRS is designed to offer ultra-high throughput with excellent resolution. Featuring holographic diffraction gratings up to 110 x 110 mm in a 600 mm system results in an incredible F4.9 aperture and very high stray light rejection.

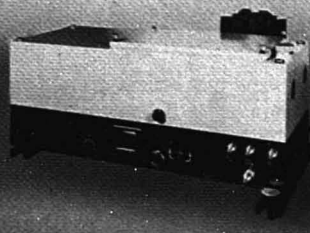
Ideal applications include fluorescence, absorption, plasma emission and laser spectroscopy. Send today for all the details.

Instruments SA, Inc., J-Y Optical Systems Division, 173 Essex Avenue, Metuchen, N.J. 08840. (201) 494-8660, Telex 844-516. In Europe, Jobin Yvon, Division d'Instruments SA, 16-18 Rue du Canal, 91160 Longjumeau, France, Tel. 909.34.93 Telex JOBYVON 842-62882.

**JOBIN
YVON**



Instruments SA, Inc.
J-Y Optical Systems Division



CIRCLE 91 ON READER SERVICE CARD

ULTRA-HIGH THROUGHPUT 1 M MONOCHROMATOR

The highest throughput monochromator available, the HR-1000 offers an aperture of F6.8 using a 120 x 140 mm holographic diffraction grating.

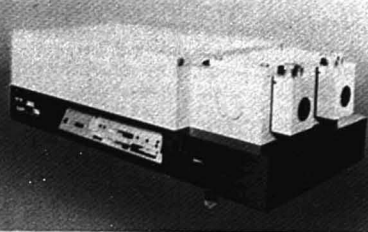
Featuring high resolution and full computer compatibility, the HR-1000 is ideal for plasma emission, fluorescence, absorption, kinetics using multichannel detection and, of course, laser spectroscopy. Send today for all the details.

Instruments SA, Inc., J-Y Optical Systems Division, 173 Essex Avenue, Metuchen, N.J. 08840. (201) 494-8660, Telex 844-516. In Europe, Jobin Yvon, Division d'Instruments SA, 16-18 Rue du Canal, 91160 Longjumeau, France, Tel. 909.34.93 Telex JOBYVON 842-62882.

**JOBIN
YVON**



Instruments SA, Inc.
J-Y Optical Systems Division



CIRCLE 92 ON READER SERVICE CARD

Briefs

Thin-Layer Spectroelectrochemistry for Monitoring Kinetics of Electrogenerated Species 561

Rate constants obtained for the acid-catalyzed benzidine rearrangement are $2.8 \times 10^{-3} \text{ s}^{-1}$ in 0.05 F HCl and $3.0 \times 10^{-2} \text{ s}^{-1}$ in 0.10 F HCl.

Elmo A. Blubaugh, Alexander M. Yacynych, and William R. Heineman,* Department of Chemistry, University of Cincinnati, Cincinnati, Ohio 45221 *Anal. Chem.*, 51 (1979)

Metallized-Plastic Optically Transparent Electrodes 565

Polyester sheets covered with thin films of gold or indium/tin oxide are used as optically transparent electrodes.

R. Cieslinski and N. R. Armstrong,* Department of Chemistry, University of Arizona, Tucson, Ariz. 85721 *Anal. Chem.*, 51 (1979)

Determination of Nitrogen and Oxygen Functional Groups in Coal-Derived Asphaltenes 569

Absorptivity values of OH (L/g-cm) and NH (L/g-cm) are $0.066 \pm 0.002 \text{ wt } \%$ OH and $0.052 \pm 0.006 \text{ wt } \%$ pyrrolic nitrogen.

Irving Schwager and Teh Fu Yen,* Chemical Engineering Department, University of Southern California, University Park, Los Angeles, Calif. 90007 *Anal. Chem.*, 51 (1979)

Determination of Nitrogen in Atmospheric Aerosols by Proton Activation Analysis 572

Sensitivity extends to $0.1 \mu\text{g}/\text{cm}^2$ corresponding to 200 ppm in a sample of thickness $500 \mu\text{g}/\text{cm}^2$. The accuracy, when compared with the destructive combustion method, is approximately 14%.

Mark Clemenson, Tihomir Novakov, and Samuel S. Markowitz,* Department of Chemistry and Lawrence Berkeley Laboratory, University of California, Berkeley, Calif. 94720 *Anal. Chem.*, 51 (1979)

Continuum Source Atomic Fluorescence Detector for Liquid Chromatography 575

Retention data reported for the acetylation reaction of ferrocene are in agreement with those obtained using the conventional UV molecular absorption detector.

Daryl D. Siemer,* Prabhakaran Koteel, Daniel T. Haworth,* William J. Taraszewski, and Stephen R. Lawson, Department of Chemistry, Marquette University, Milwaukee, Wis. 53233 *Anal. Chem.*, 51 (1979)

Aids for Analytical Chemists

Microprocessor-Controlled Digital Integrator for Nuclear Magnetic Resonance Measurements 579

F. Morley, I. K. O'Neill, M. A. Pringuer, and P. B. Stockwell,* Laboratory of the Government Chemist, Cornwall House, Stamford St., London SE 9NQ, United Kingdom *Anal. Chem.*, 51 (1979)

The Ohaus Brainweigh 1500D.

The electronic balance that thinks twice for you.

What makes our new Ohaus Dual-Range 1500D so smart? It gives you two ways to profit from one electronic balance.

- 1) 150g x 0.01g capacity and sensitivity or
- 2) 1500g x 0.1g capacity and sensitivity

By the touch of a bar you enjoy the advantages of two different balances. In one compact unit. With one low price tag—only \$1,595 (a lot less than some electronic balances with a lot less to offer).

The brain behind it all.

The tiny genius that controls the 1500D is our sophisticated microprocessor, which stores operator commands, then responds **only** after the reading is stable.

That means human interaction without human error, in more ways than one.

Consider all the intelligent features Ohaus squeezed into each compact 1500D...

- Die-Cast Construction. Stands up to abuse. Stain resistant. Wipes clean. Protects against dust and spills.
- Microprocessor "Brain". Fewer components for greater reliability.
- Compact Size. Ideal for lab table. Sturdy enough for production line.
- Clearly Labelled Controls. Right up front for quicker and easier operation.
- Large, Stable Platform. Takes variety of objects and unexpected overloads in stride.
- Big, Easy to Read Digits. Seen when seated or standing. If overloaded, "error" shows.
- Span Calibration Adjustment.

Recessed above tare bar.

- Rock-Steady Display. "g" lights up for stable reading.
- "Rapidtouch" Tare Bar. Recessed to avoid accidentally taring.

And you can learn to operate one in just a few minutes.

Give the new 1500D the twice over.

Send us this coupon—and we'll send you our full-color catalog about the 1500D and all the new Ohaus Brainweighs. The weigh of the future.

The Ohaus 1500D. Fully guaranteed. And backed by over 70 years of Ohaus quality engineering.

Once you have one, you won't have to think twice about it.

OHAUS

Ohaus Scale Corporation, Dept. 11-029
29 Hanover Road, Florham Park, N.J. 07932, (201) 377-9000

☐ Yes, show me the weigh of the future. Send me the full-color catalog on the Ohaus Brainweighs.

☐ I'm ready to see a demonstration. Please have a dealer sales rep call me.

NAME _____

TITLE _____

ORGANIZATION _____

CITY _____

STATE _____

ZIP _____

PHONE NUMBER _____

CIRCLE 157 ON READER SERVICE CARD



THE OHAUS BRAINWEIGHS™

The weigh of the future.

Briefs

Graphite Plate Sample Holders for X-ray Photoelectron Spectroscopy 581

David M. Aylmer, Hossein Razzavi, and James C. Carver,*
Department of Chemistry, Texas A&M University, College Station, Tex. 77843
Anal. Chem., 51 (1979)

Blank Limitations in Laser Excited Solution Luminescence 583

T. G. Matthews and F. E. Lytle,* Department of Chemistry, Purdue University, West Lafayette, Ind. 47907
Anal. Chem., 51 (1979)

Algorithm for the Determination of Decay Rate Constants by Reversal Current Chronopotentiometry 585

Donald A. Tryk and Su-Moon Park,* Department of Chemistry, The University of New Mexico, Albuquerque, N.M. 87131
Anal. Chem., 51 (1979)

Digestion Tube Diffusion and Collection of Ammonia for Nitrogen-15 and Total Nitrogen Determination 586

William A. O'Deen* and L. K. Porter, USDA, Science & Education Administration, Agricultural Research, P.O. Box E, Fort Collins, Colo. 80522
Anal. Chem., 51 (1979)

General Method for Overcoming Photoacoustic Saturation in Highly Colored Organic and Inorganic Solids 589

William H. Fuchsman,* Chemistry Department, Oberlin College, Oberlin, Ohio 44074, and Ann J. Silversmith, Gilford Instrument Laboratories, Inc., 132 Artino Street, Oberlin, Ohio 44074
Anal. Chem., 51 (1979)

Automatic Device to Monitor and Terminate a Distillation 591

Robert R. Lowry, Department of Agricultural Chemistry, Oregon State University, Corvallis, Ore. 97331
Anal. Chem., 51 (1979)

Correction. Anodic Stripping Peak Currents: Electrolysis Potential Relationships for Reversible Systems 592

Alberto Zirino and S. P. Kounaves

CALIBRATION GAS MIXTURES IN DISPOSABLE CYLINDERS

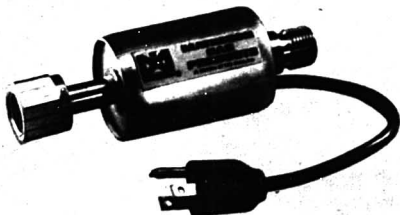
Matheson now offers a wide variety of gas mixtures and pure gases in convenient, disposable cylinders. Containing 14 liters of analyzed gas mixtures or pure gases, these cylinders are easy to handle, extremely portable, and weigh only 1½ pounds. A pressure regulator and unique syringe adapter are available. All products are shipped UPS for speed and economy. For a complete list of products and pricing contact Matheson, 1275 Valley Brook Avenue, P.O. Box E, Lyndhurst, NJ 07071.



CIRCLE 138 ON READER SERVICE CARD

N₂O ICING ELIMINATED

The new N₂O heater from Matheson prevents AA system icing caused by nitrous oxide at high flow rates. N₂O icing poses problems in automatic control since the system regulator cannot function properly when iced. Other controls and instruments such as valves and flowmeters can also become ineffective as ice layers build up. Installed between the N₂O cylinder and regulator, the N₂O heater eliminates regulator icing. It plugs into any 110V outlet and can heat N₂O at flowrates up to 751/m (160 cfh). The N₂O heater is thermostatically controlled so that the gas is not overheated and the heater can be left unattended without gas flow. Construction is of brass and the N₂O heater is rated at 3000 psi. Specifications and prices are available from Matheson, 1275 Valley Brook Ave., P.O. Box E, Lyndhurst, NJ 07071.



CIRCLE 139 ON READER SERVICE CARD

99.9999% MINIMUM PURITY HELIUM

Critical gas chromatography procedures to determine trace impurity levels can only be performed using very high purity carrier gas. Matheson now makes available the purest helium for this purpose. Most individual impurity levels are non-detectable at thresholds of 0.1 ppm. Complete information is available from Matheson, 1275 Valley Brook Ave., P.O. Box E, Lyndhurst, NJ 07071.

CIRCLE 140 ON READER SERVICE CARD

		<h1>Handle Gases the Right Way. Stay Out of the Equipment Maze.</h1> <p>When should you use a two stage regulator . . . or will a single stage suffice? When do you need a metering valve? Can I get a direct reading flowmeter? Matheson answers questions like this every day in every office.</p> <p>Different gases, different end uses require different answers.</p> <p>It's one of the reasons Matheson has over 2,000 specific pieces of equipment. You need that much to properly handle over 150 gases.</p> <p>At Matheson there is no Equipment Maze, just a well-organized product line with well-organized people to help you.</p> <p>We have prepared a guide for selecting the right regulator. Use the reader service number for your copy of our Regulator Selection Guide.</p>					



Lyndhurst, N.J. 07071

East Rutherford, N.J. 07073/Morrow, Georgia 30260/La Porte, Texas 77571
 Gloucester, Massachusetts 01930/Joliet, Illinois 60434/Gonzales, Louisiana 70737
 Cucamonga, California 91730/Newark, California 94560/Bridgeport, N.J. 08014
 Dorsey, Maryland 21227/Whitby, Ontario, Canada L1N 5R9
 Edmonton, Alberta, Canada T5B 4K6/B2431 Oveel, Belgium
 6056 Heusenstamm, West Germany
 CIRCLE 141 ON READER SERVICE CARD

The friendly desktop computer system...

They're solving big problems.

They've learned what computer power is all about. HP's System 45 desktop computer provides the simplest, most direct way to a solution—from the problem in your mind to a final report or plot, quickly and easily. That's why more and more problems thought to need a big computer are now being solved by System 45.

This powerful graphic, computational tool operates with a wide range of input, mass storage and output peripherals. As for software, we don't think you should have to write all the programs you need to solve your problems. That's why we have a wide array of practical, user-tested software to help you handle statistical analysis, engineering design, management science, business administration and much, much more.

In the graphics system shown, the input device is the HP digitizer (9874A), the mass storage is the internal dual tape drives, and the output is the HP 4-color plotter (9872A). You can interface System 45 with virtually any instrument found in the scientific



But not on a big computer.

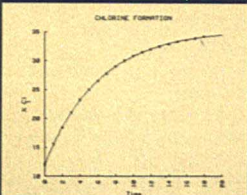
or engineering environment. All interface cards, cables and I/O slots are designed for quick "plug in and run" operation.

In addition, the System 45 Enhanced BASIC language allows you to upgrade any peripheral—internal printer to line printer, CRT graphics to 4-color plotter, tape drive to floppy disk—by simply changing one statement with no other software modification.

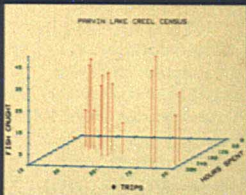
If you'd like to solve big problems on your own terms, at your own pace, and in your own work environment, you need the power and flexibility of the friendly HP System 45. Power in terms of fast, simple solutions, and the flexibility to solve more big problems than you probably thought possible.

For brochures describing System 45 and the HP programs of interest to you, call the HP Literature Center toll-free day or night.

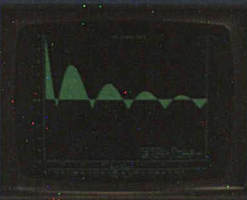
The number is 1-800-821-7700, Extension 400. (In Missouri, call 1-800-892-7655, Extension 400.) Or, call your nearest HP sales office for a demonstration.



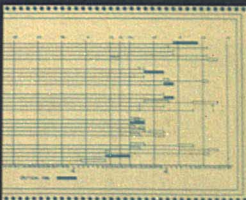
Hard copy record from CRT display of non-linear regression curve.



4-color plot of three-variable data in a scattergram.



CRT graphic display of input to Fast Fourier Transform.



Printer/Plotter output of project schedule (GANTT chart).

HEWLETT  PACKARD

3404 E. Harmony Road, Fort Collins, Colorado 80525

For assistance call: Washington (301) 948-6370, Chicago (312) 250-9800, Atlanta (404) 950-1500, Los Angeles (213) 877-1282.
Ask for an HP Desktop Computer representative.

CIRCLE 150 ON READER SERVICE CARD

INTRODUCING

The Model 384-1 Polarographic Analyzer System...



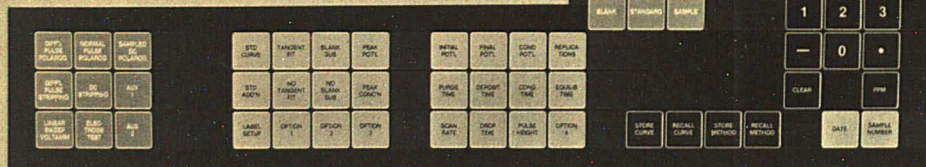
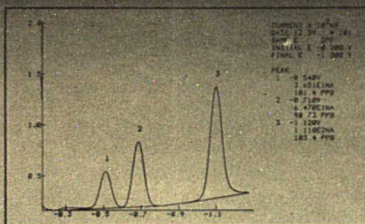
...because your analyses are not getting any easier.

The 384 has the MOST ADVANCED SOFTWARE for polarography

- Stores and recalls as many as 12 different analytical methods
- Stores and recalls as many as 9 complete analytical curves
- Accommodates up to 9 peaks in each scan
- Calculates concentration automatically by either standard addition or multi-point standard curve
- Labels header sheet with 24 experimental parameters
- Permits blank subtraction capability with unique blank for each curve
- Fits tangents for most accurate peak height measurements

The 384 has the
MOST ADVANCED HARDWARE
for polarography

- Micro-floppy disk



- 64 button control panel

- 40 character alphanumeric display



For more information on the Model 384-1 System, write or call today:

EG&G PRINCETON APPLIED RESEARCH
P. O. BOX 2565 • PRINCETON, NJ 08540 • 609/452-2111

493A

Circle 176 for Additional Information Only

Hazardous Chemical Safety in the Laboratory

F. W. Michelotti

J. T. Baker Chemical Co.
222 Red School Lane
Phillipsburg, N. J. 08865

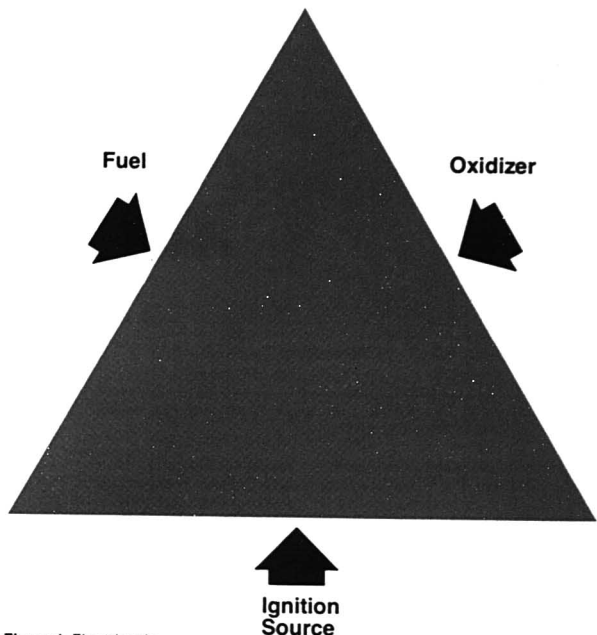


Figure 1. Fire triangle

Reprinted with permission from ref. 1.
Copyright 1976 Van Nostrand-Reinhold Co.

Since the birth of chemistry as a science over 200 years ago, there has been a veritable explosion of scientific knowledge that resulted in part from the rapid growth of instrumental methods of analysis. There are over 4 million chemical compounds that have been prepared and characterized in the laboratory. The NMR, IR, or UV spectra of many of these compounds are likely to be found in the literature. Unfortunately, there has been less progress in understanding their chemical hazards. In some aspects of these hazards, such as chronic toxicity, we are probably still a century behind.

Hazards in the laboratory may be divided into four major categories.

Mechanical: sharp objects, broken glass, unguarded machinery, compressed gases

Thermal: open flames, hot surfaces, cryogenic liquids

Electrical: faulty wiring, ungrounded equipment, lethal voltages.

Chemical: flammable liquids, corrosive chemicals, toxic substances, radioactive materials, and biohazards

This categorization is helpful in developing a checklist for use in carrying

out a periodic safety audit of a laboratory facility. Some hazards, of course, fall into more than one category. Excess pressure from a cylinder could rupture a glass vessel (mechanical) and release a toxic (chemical) gas. The discussion that follows will focus principally on chemical hazards.

FLAMMABLE LIQUIDS

Organic solvents present a very real hazard for fire or explosion. The combustion of 1 gal of toluene will destroy an ordinary two-man laboratory in 8 min. Persons present in the fire area will be killed within 1 min. It thus behooves us to be familiar with the physical chemistry of combustion and its application to the development of safe laboratory practices in the use of flammable liquids.

The Fire Triangle

The essential elements for combustion to be considered are shown in Figure 1 (fire triangle) (1).

Some authors refer to a fire tetrahedron (2) where a fourth leg represents uninhibited chain reactions. For

present considerations this fourth leg can be ignored, since it can be viewed as the mechanism by which the combustion proceeds.

The Fuel. The fuel (usually an organic compound) can be characterized by its vapor pressure, boiling point, liquid and vapor densities, heat of combustion, heat of vaporization, flashpoint, flammability range, and autoignition temperature.

The latter three parameters are most significant in assessing a fuel hazard.

Flashpoint. The flashpoint is defined as the lowest temperature at which a fuel-air mixture present above the surface of a liquid will ignite if an ignition source is introduced. This parameter is usually determined under open cup or closed cup conditions as prescribed by ASTM procedures (3). In general, open cup measurements result in flashpoints 5–10 °F higher than closed cup methods, the former representing combustion of liquids under fire conditions, and the latter, those more typical in a plant reactor or vessel. The flashpoint is generally considered the most significant

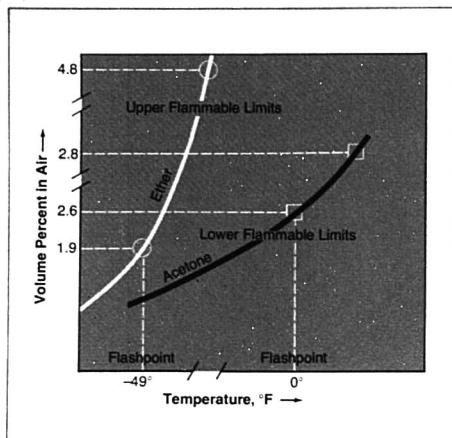


Figure 2. Relationship between flashpoint and flammability ranges for ether and acetone

parameter in assessing the flammable nature of liquids. The NIOSH system (4) (Table I) categorizes the relative hazards. The Department of Transportation (5) (DOT) considers a material neither flammable nor combustible if it has a flashpoint above 200 °F. The flashpoint of flammable liquids is provided by most laboratory suppliers on the label. It is important that the laboratory personnel familiarize themselves with the safety information supplied on the label.

Flammability Range. It is possible for a flammable liquid to be above its flashpoint, and yet not ignite in the presence of an adequate energy source. The explanation for this phenomenon lies in the composition of a fuel-air mixture that may be too lean or too rich for combustion. This is best seen from Figure 2 where the relationship between flashpoint and flammability ranges for ether and acetone, respectively, is shown. Table II lists flammability ranges and flashpoints for a number of common flammable liquids. LEL and UEL refer to lower and upper explosive limits, respectively. Because of its extreme hazard, ether is available only in metal con-

tainers for laboratory use. Carbon disulfide is almost as hazardous. The flammability range provides little margin of safety from the practical point of view since in a spilled solvent situation in the presence of an energy source, the flammability range is reached very quickly and a fire or explosion will ensue before a fuel-rich (nonflammable) range can be reached.

Autoignition Temperature. This is defined as the minimum temperature required to initiate and sustain combustion without an external energy source. Classical examples are white phosphorus and freshly prepared Raney nickel on filter paper (actually a test for its reactivity). A common hazard that can be considered falling in this category is carbon disulfide. This toxic, flammable liquid has been known to ignite spontaneously at steam bath temperature (autoignition temperature 212 °F). Interestingly, ether, which has a lower flashpoint than carbon disulfide, has a higher autoignition temperature (356 °F).

The Oxidizer. The most obvious and prevalent one is, of course, oxygen, which accounts for approximately 21% of the atmosphere. Enriched oxy-

gen atmospheres present a significantly increased hazard. Many materials normally considered noncombustible will burn in undiluted oxygen. However, there are a large number of less ubiquitous oxidizers that are at least as hazardous—chlorine, fluorine, ozone, perchloric acid, etc.

Ignition or Energy Source. This is the third leg of the fire triangle. An energy source can be a hot surface, a spark arising from faulty wiring or ungrounded equipment, friction from shoes, and so forth. Everyone is familiar with the increase in static electricity, particularly on cold dry wintery days. The minimum ignition energies of hydrocarbons and their derivatives are of the order of 0.2 J but may be as low as 0.02 J for hydrocarbons with double and triple bonds (6) and only 9 μ J for carbon disulfide. By comparison, electric discharges from a person to the ground have minimum energies of about 0.4 mJ (7).

Removal of at least one side of the fire triangle is the basis of fire prevention. It is usually impossible to remove all energy sources; few researchers work in truly explosion-proof laboratories. It is difficult to exclude oxygen routinely. Laboratory safety in handling flammable liquid hazards is therefore best achieved through careful control and protection of flammable liquids. The following guidelines are recommended.

Never have in the general work area more than one container of flammable solvent (i.e., only the one in use). In order of preference, have it in: a safety can with a spring-loaded closure, a metal can as provided by some suppliers (8), or a 1-pint bottle if it must be in glass.

Use flammable liquids (as all other categories of hazardous materials) only in a properly functioning, periodically checked fume hood. Guidelines for fume hoods are described elsewhere (9).

Store frequently used solvents only in an approved, solvent storage cabinet. According to the NFPA, these cabinets should be designed so that the internal temperature does not exceed 325 °F when subjected to a 10-min fire test using the standard time-

Table I. NIOSH System

Rating	Hazard	Flashpoint, °F
4	Extremely flammable	<73
3	Highly flammable	≥73–≤100
2	Moderately combustible	≥100–≤200
1	Slightly combustible	≥200–<1500
0	Noncombustible	>1500

Table II. Flammability Ranges and Flashpoints for a Number of Common Flammable Liquids

	LEL, %	UEL, %	Flashpoint, °F
Heptane	1.2	6.7	25
Carbon disulfide	1.3	44	-22
Ether	1.9	48	-49
Methyl alcohol	6.0	36.5	65

HPLC Solvents

by J.T. Baker



High performance liquid chromatography problems are frequently related to the *variability* of the reagents used. Specifically: spurious UV absorbance, particulate matter, residues, unknown or uncontrolled water, etc. 21 Baker HPLC solvents, however, now provide maximum reproducibility . . . new predictability . . . exceptional consistency.

How is such unusual consistency achieved? Extremely tight specifications coupled with superior product definition create consistency.

Examples? HPLC Acetonitrile is controlled for low UV absorbance at 220nm (0.01 max.), 254nm (0.01 max.), 280nm (0.01 max.) and at 350nm (0.01 max.); water 0.02% max.; residue 0.0005% max. Further characterization is provided by: GC assay (99.7% min.), consistent refractive index and fluorescence (at 450nm and emission maximum). Plus physical data. And as with all 'Baker Analyzed'® Reagents the *actual lot analysis* is always on the label as an assurance of quality and a time saving reference. You can always verify our claims for reproducibility beforehand.

Consistency? Here are ten consecutive lots of Baker HPLC acetonitrile.

Lot No.	626118	626119	626120	626121	626122	626123	626124	626125	626126	626127
Residue, %	0.00006	0.00007	0.00002	0.00003	0.00001	0.00008	0.00001	0.00008	0.00002	0.00004
Water, %	0.005	0.002	0.003	0.003	0.002	0.01	0.008	0.003	0.003	0.003
Absorbance at 220 nm	<0.005	<0.005	<0.005	<0.005	<0.005	0.007	0.007	0.005	0.008	0.008
Absorbance at 254 nm	<0.005	<0.005	<0.005	<0.005	<0.005	<0.005	<0.005	<0.005	<0.005	<0.005
UV Cut-off (nm)	188	188	189	189	189	189	189	188	188	188

Note, that residue after evaporation was controlled to an average value of 0.00012% (versus a specification of 0.0005% max.). The water content was controlled to an average of 0.004% for the ten lots (versus a specification of 0.02% max.). These consistent, low levels of residue and water prevent solvent interference in the separation of the sample. The extremely low absorbance values at 220nm and 254nm assure that the peaks detected can be attributed to the sample and not the solvent.

Baker's exceptional lot-to-lot and bottle-to-bottle consistency assure experienced experts and novice chromatographers of *reproducible separations*.

Baker HPLC solvents are stocked where you need them. Contact one of the more than 120 Baker distributor locations in the U.S. and Canada to implement a stocking program to suit your needs.

For emergency shipments on HPLC solvents, your distributor can provide special Baker Super Service by calling a Baker Super Service Center for immediate shipment to you.

For more information, write to J. T. Baker Chemical Co., Phillipsburg, N.J. 08865, or call 201/859-5411.



J. T. Baker Chemical Co.
Phillipsburg, NJ 08865

CIRCLE 20 ON READER SERVICE CARD

IR Accessories Supermarket

WILKS INFRARED
SPECTROSCOPY
ACCESSORIES

The new Wilks Infrared Spectroscopy Accessories Catalog contains over 30 pages of vital data on hundreds of the highest quality accessories for all commercially-available IR spectrophotometers. It includes transmission, microsampling, and reflectance accessories, pyrolysis equipment, crystals — everything from daily necessities such as NaCl cells and windows to research-grade long path gas cells.

**FOR YOUR FREE
COPY, CONTACT:**

Analabs, Inc.

A Unit of Foxboro Analytical
80 Republic Drive
North Haven, CT 06473
Tel. (203) 288-8463

FOXBORO

Wilks is a trademark of The Foxboro Company

CIRCLE 77 ON READER SERVICE CARD

temperature curve specified by NFPA. The NFPA code also allows the use of wooden cabinets. Tests made by the Los Angeles Fire Department (10) have shown properly constructed wooden cabinets (at least 1 in. thick) to be at least as effective, and in many cases better, than the steel cabinets.

When using a 1-gal solvent bottle, place it in a protective carrier.

When transferring a flammable liquid from one container to another in quantities of 1 gal or more, ground and/or bond the respective vessels.

Fire Fighting

Though the use of preventive measures cannot be overemphasized, one nevertheless must be prepared in the event of fire. Suitably placed fire extinguishers of appropriate size usually of the B or ABC type should be readily available. In special situations where reactive metals and/or their alloys or complexes are handled, D-type extinguishants are required. Periodic unannounced fire drills should be conducted; personnel should be drilled in actual fire fighting trials. Responsibility for fighting fires should be clearly assigned. Drills in the use of self-contained breathing apparatus are also important since an individual can asphyxiate himself because of unfamiliarity with the equipment.

Safety Showers

There have been reported cases in which otherwise knowledgeable chemists with their clothing on fire run past safety showers in search of help. It is critical that everyone in a laboratory know exactly where each and every safety shower is located and how it works. The shower itself should be a nonclogging deluge-type capable of delivering very large quantities of water (30–60 gal/min under a pressure of 20–50 psig), necessary to cover instantly the entire person with a virtual flood of water. It is best each shower not have a shutoff valve, but if such a valve is deemed necessary, it should be protected from tampering or unauthorized persons. Showers should be tested at least every 6 months, but preferably more often since plumbing fixtures corrode and some shower heads plug up. In areas where the water hardness is high, the showers should be checked every month.

Spill Control

Often, a spilled liquid (flammable solvent, corrosive, or the like) is the first of a series of accidents that can lead to bodily injury and even death. Today, effective spill control products that have been evaluated for effectiveness in a spectrum of spill situations are readily available (11). Since sever-

al types can be purchased for flammable liquid spill control, one should choose only those that effectively reduce the vapor pressure of the spilled solvent essentially to zero at ambient temperatures. It is important to note that two insidious properties are usually associated with volatile organic liquids: a density in the liquid state less than that of water that usually renders water ineffective in extinguishing a solvent fire; and a vapor density greater than that of air for all volatile organic liquids that could result in an unexpected fire flashback from a remote energy source in a spilled solvent situation.

CORROSIVE CHEMICALS

Corrosive chemicals are those substances that, by direct chemical action, are injurious to body tissue or destroy metal. The list of corrosive materials is vast. They exist in all three states of matter, and their ability to cause personal injury depends on the nature of the corrosive; the temperature and concentration of the corrosive at the time of contact; the site of contact or exposure—eyes, skin, lungs (inhalation), stomach (ingestion); and the duration of the contact or exposure.

For proper protection, the following guidelines should be observed.

Goggles or face shield should be worn at all times in all laboratory areas. Recommended eye and face protection for use in industry, schools, and colleges can be obtained from the American National Standards Institute (12). Contact lenses either of the soft or hard variety should not be permitted in research laboratories. Toxic, corrosive fumes are easily drawn by capillary action behind the contact lens and cause injury. Should injury result, trauma is increased by having to remove contact lens before flooding with large quantities of water.

Adequate respiratory protection (respirator, gas masks, self-contained breathing apparatus) should be available and used when required. Drills in the safe use of this equipment should be carried out periodically.

Adequate fume hoods that have a face velocity of at least 100 linear ft/min should be provided.

Intimate knowledge of the location and use of eye wash station is mandatory. Criteria for effective eye washes and safety showers have recently appeared (13). Portable eye wash stations are usually not recommended since they cannot supply copious quantities of water for at least 15 min. Additionally, stagnant water is an excellent environment for the growth of microorganisms.

Use of an acid safety carrier to

FX SERIES OF FT NMR SYSTEMS

FX-90Q

OMNI Probe™ System
10mm, 5mm, micro inserts

CIRCLE 131 ON READER SERVICE CARD



FX-60Q

Solids Probe (^{13}C) with
Magic Angle Spinning
High Resolution Probe ($^{13}\text{C}/^1\text{H}$)

CIRCLE 132 ON READER SERVICE CARD

FX-200

Dual Probe ($^{13}\text{C}/^1\text{H}$)
Broad Band (^{15}N to ^{31}P)
50 KHz Spectral Width

CIRCLE 133 ON READER SERVICE CARD

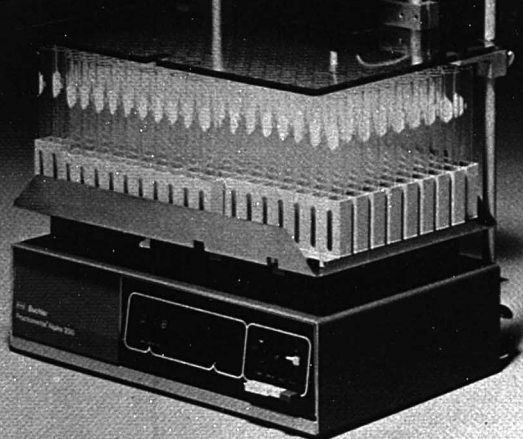
System Features

- Light Pen Control System
- Foreground/Background
- Digital Quadrature Detection
- Multi Frequency Observation
- Programmable Multi Pulser
- Module Performance Indicator Lights
- Comprehensive Auto Stacking
- T_1 -rho
- Double Precision (32 bit word length)
- Floppy; MH Disc Storage
- 50KHz Spectral Width
- CPU Expansion to 65K

JEOL

235 Birchwood Ave., Cranford, NJ 07016
201-272-8820

**RELIABLE
VERSATILE
COMPACT
COMPATIBLE**



Fractomettte® Alpha 200

Liquid Fraction Collector

RELIABLE: New single motor drive offers greater reliability than more complex mechanisms. Solid-state circuitry is designed for cold room use. Unit is overflow protected and includes a patented liquid detecting shutdown device.

VERSATILE: Push-button control of time, drop count or volume collection. An exclusive lift off collection platform provides unloading and cleaning convenience.

COMPACT: No other 200 tube collector is so compact. Occupies less than 1½ square feet of bench space; will fit in an ordinary household refrigerator.

COMPATIBLE: System compatible with metering pumps, column monitors, recorders and other accessories. Support rod lattice facilitates mounting. Yes, there are many reasons for you to select the Alpha 200 when your applications require a liquid fraction collector. In fact, no other fraction collector offers all the features available in the Buchler Fractomettte Alpha 200. Write for details.



Buchler Instruments, Inc.

1327 16th Street, Fort Lee, N.J. 07024
(201) 224-3333 (212) 563-7844

Made in U.S.A.
Sales and service worldwide.

CIRCLE 24 ON READER SERVICE CARD

transport acid bottles from one location to another should be mandatory. Concentrated sulfuric acid spills are particularly dangerous because of sulfuric acid's very slippery nature. Medical attention if required should be readily available. The medical staff should be made aware of the types of materials used in laboratories and recommended treatment measures. For all types of hazardous chemical injuries, knowing what was the offending agent can save valuable seconds in bringing rapid relief and attenuation of damage to the injured.

INSIDIOUS HAZARDS

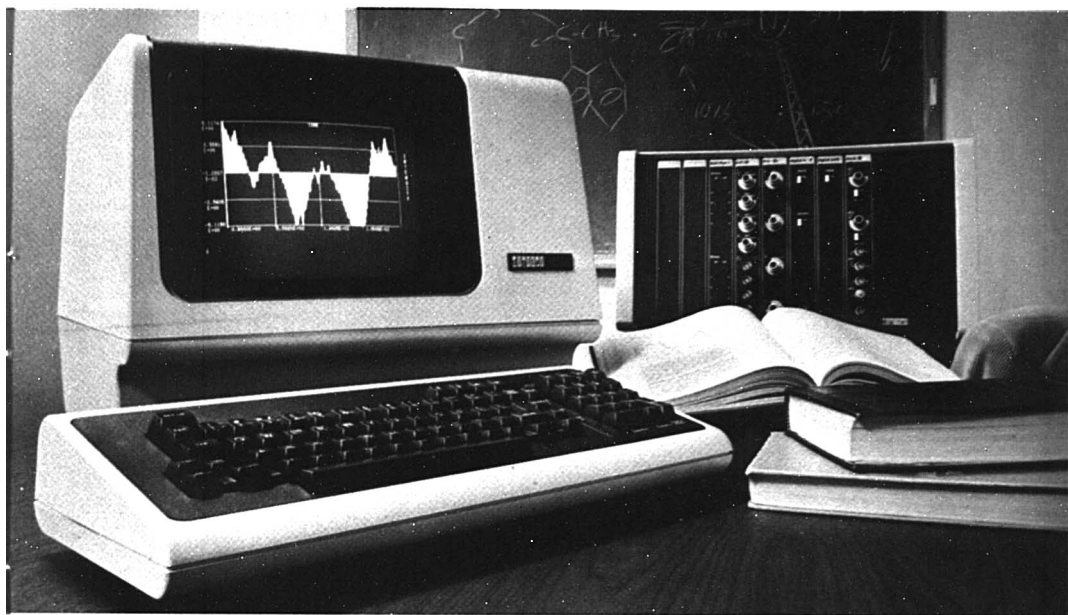
Insidious hazards are conditions within the laboratory that represent potential safety and health perils that are easily overlooked because they are not readily seen, smelled, tasted, or otherwise noted and therefore ignored. Several typical samples will be cited.

Mercury

One of the most common insidious hazards is mercury. Mercury poisoning affected Pascal and Faraday (14). In the laboratory, mercury is commonly found in thermometers, barometers, and in certain analytical instruments. Although there is general recognition of the physical properties of mercury (high density, surface tension, etc.), there does not seem to be a corresponding appreciation of its toxicity and need to retrieve quickly all mercury spills in the laboratory. At a room temperature of 25 °C, the equilibrium concentration of mercury vapor is about 20 mg/m³ or 200 times the threshold limit value (TLV) of 0.1 mg/m³ recommended as the maximum atmospheric concentration for the normal work schedule by the American Conference of Governmental Hygienists (15).

Control of Mercury Hazards. Mercury should be stored in unbreakable plastic bottles in a cool, well-ventilated area. Catch trays should be used beneath setups using significant amounts of mercury (greater than 1 g); such setups should preferably be made in a fume hood. Care should be exercised in handling mercury and mercury-containing instruments. Periodic monitoring of mercury vapor concentrations should be carried out in areas where mercury has been spilled or suspected of having been spilled. Instrumentation for such monitoring has been described by Biram (16) and others (17). Where mercury is routinely used, periodic medical checkups are recommended for those potentially exposed. Spill cleanup capability should be readily available (18). The traditional methods of mercury cleanup by

THINK MINC



**Digital made the computer
easy-to-use and easy-to-interface.
And you can buy it on a desk-top
calculator budget.**

Plug MINC in, turn it on, and you can plot charts, solve complex engineering and statistical problems, control instruments and acquire data. You have complete, ready-to-run BASIC software—true computer functionality. It's as easy as that. MINC's built around Digital's proven PDP-11 microcomputer. MINC has its own graphics terminal, one million character dual floppies and three serial line interfaces.

And MINC makes interfacing easy. Hooking up a lab instrument is as simple as plugging in a single connector to the IEEE Bus interface or one of the seven optional input/output modules. When you finish your experiment, you unplug the connector and wheel the MINC cart to the next job.

And, if you need more on-line data storage, there's the new DECLAB-11/MNC that combines the functionality and ease-of-use of MINC with 10 million character, random access disk drives, powerful FORTRAN software and Digital's versatile RT-11 operating system.

If you'd like the whole story on these easy-to-use systems, write Laboratory Data Products Group, Digital Equipment Corporation, Marlborough, Massachusetts 01752. Telephone (617) 481-9511, Ext. 6969. European headquarters: 12, av. des Morgines, 1213 Petit-Lancy/Geneva. In Canada: Digital Equipment of Canada, Ltd.



DECLAB-11/MNC



MINC

CIRCLE 49 ON READER SERVICE CARD

digital

AT LAST, A GC/MS DATA SYSTEM THAT PROVIDES HIGH RELIABILITY WITH BOTH QUADROPOLE AND MAGNETIC SECTOR SYSTEMS



Regardless of the type of GC/MS system you select, the RDS 150 is the only system that will insure complete versatility, reliability, adaptability and economy. That's because at RDS we continually work to upgrade the system to keep pace with your state-of-the-art analysis.

For example, the RDS Data System is the only GC/MS data system for magnetic sector mass spectrometers that will easily accommodate a wide range of selected ion monitoring. Selected ion monitoring analysis of m/z of 150 and m/z of 600 can be accomplished simultaneously.

This is because the RDS Data System is not a time based system. It's a true feedback system which uses either a Hall probe or the mass spectrometer's internal mass marker. This insures high reliability and improved accuracy during your mass assignments.

In addition, Simultaneous Acquisition and Data Reduction (SADR) is a revolutionary foreground/background software system that permits simultaneous real-time acquisition and reduction of your GC/MS data as well as fully unattended operation of such components as samplers and solvent divert valves. It also means unattended data reduction such as library search, spectral presentations and Bieman maximized mass reconstructed gas chromatograms.

And our RDS Distributive Processing System lets you acquire and analyze GC/MS data in half the time and do away with single component failure downtime.

At a cost comparable to other single CPU/GC/MS data systems, you get complete interaction of the computers without interdependence.

When you're ready to automate your GC/MS data acquisition and analysis, contact the people who offer you so much more. Call or write us today.



RIBER DATA SYSTEMS, INC.

1020 Corporation Way Palo Alto, CA 94303 (415) 961-2012 Telex 910-379-6474
CIRCLE 182 ON READER SERVICE CARD

use of polysulfides, flowers of sulfur, etc., have been shown to be ineffective (19).

Peroxides in Ether

Several ethers (diethyl ether, dioxane, tetrahydrofuran, and others) are used routinely in various analytical (GC, HPLC, etc.) and synthetic procedures. It is well established that these ethers, when uninhibited or when the inhibitor has been consumed, will form dangerous peroxides in the presence of oxygen by a free-radical chain mechanism (20). Diisopropyl ether in reaction with oxygen shows the characteristic autoacceleration and susceptibility to added radical sources or inhibitors of a radical chain autoxidation (21). This ether is particularly hazardous. These peroxides have caused many laboratory accidents and a number of hazardous disposal operations. Such incidences have been reported in the literature (22). Analytical tests have been described for the detection of peroxides in ethers and methods for their removal (23).

Though calcium hydride has been reported as useful in removing peroxides, great care should be exercised with tetrahydrofuran. A violent explosion was reported when THF (24) was heated under reflux with stirring in the presence of CaH_2 , a procedure previously carried out frequently without incident. It was suggested by the authors that the explosion might be attributable to cleavage of the THF molecule by CaH_2 in localized hot zones.

Perchloric Acid

Many analytical digestion procedures, nonaqueous titrations, etc., call for the use of perchloric acid. A review of the circumstances leading to a Los Angeles explosion that killed 15 people and injured 400 has been published (25). Harris concluded that the basic cause of accidents involving perchloric acid is due to contact with organic material, or to the formation of the anhydrous acid. This extreme reactivity is chemically related to a formal +7 oxidation state borne by chlorine rendering perchloric acid one of the strongest acids known (26) and an extremely powerful oxidizing agent. The anhydrous acid (greater than 85%) is extremely dangerous, and only experienced workers should handle it.

Handling Perchloric Acid in the Laboratory. The use of goggles is absolutely mandatory. All work should be carried out in a properly functioning fume hood. Aprons, gloves, and other protective clothing are strongly recommended. No organic material should be stored in a perchloric acid hood. Perchloric acid should

PREPARE SPECTROGRAPHIC SAMPLES RAPIDLY FROM...



DRILLINGS,
CHIPS,
CRUSHINGS,
METALLIC
POWDERS,
SCRAP PIECES,
ETC.

with the **LECOMELT™ 3.3**

INDUCTION / CENTRIFUGAL CASTING FURNACE.

- AVOID CONTAMINATION AND ELEMENT LOSS
- PREPARE HOMOGENEOUS SAMPLES IN ONE MINUTE

CONTACT LECO TODAY!



LECO CORPORATION 3000 Lakeview Ave. St. Joseph, MI 49085, U.S.A. Phone: (616) 983-5531
Offices: California (714) 957-8227 • Texas (713) 931-0000 • Pittsburgh (412) 776-4891 • Canada (416) 270-8010

CIRCLE 130 ON READER SERVICE CARD

free LC Assistance for Environmental Analysis

If you need assistance in understanding or performing environmental analysis, Waters Environmental Group would like to help.

If you are monitoring:



CIRCLE 210 ON READER SERVICE CARD



CIRCLE 211 ON READER SERVICE CARD



CIRCLE 212 ON READER SERVICE CARD

Waters can help solve your environmental application problem.

Circle Reader Service No. call or write:



Waters
Environmental Group
Waters Associates, Inc.
Maple Street, Milford, MA 01757
(617) 478-2000

never come into contact with strong dehydrating agents. In wet combustion and digestion procedures, the sample should be treated with nitric acid first to destroy easily oxidizable matter.

Fume Hood or Exhaust Systems.

The exhaust hood should have smooth surfaces for ease of cleaning. Nonabsorbent materials such as stainless steel should be utilized throughout the system. Omit the use of organic sealants or adhesives. Periodic washing of the entire structure is strongly recommended. Guidelines in the use of perchloric acid as well as cleaning procedures for perchloric acid-contaminated fume hoods are available from the National Safety Council.

Spill Control. Products now available will readily and efficaciously neutralize most acid spills including those of perchloric acid (27).

Azide Salts

Sodium azide has been used for many years as a bactericide in constant temperature water baths and in solutions used in hospital diagnostic laboratories. Over the years a number of explosions (usually in the plumbing systems) were traced to the use of soluble azide salts. The cause of these accidents was traced to an initial exchange reaction in metal plumbing forming heavy metal azides that are explosive when these diagnostic solutions are routinely disposed of by pouring down the drain. It is hoped that no one today makes use of soluble azide salts to inhibit microorganism growth. Alternate inhibitors such as 2-phenoxyethanol are preferred.

Reaction Preceded by Induction Period

These reactions usually proceed by a free radical mechanism (28). Typical examples are free radical-induced polymerizations, Grignard reactions, and decomposition of halocarbons, such as chloroform and carbon tetrachloride. The hazard common to these categories of reactions is the variable and unpredictable period of time (induction period) during which reactants are added to each other with no semblance of reactivity. Suddenly and sometimes violently, the reaction (exothermic) initiates spewing flammable, toxic liquids on heating mantles, electrical connections, hot surfaces, etc. The caution that must be exercised here is to forego adding more than 10-15% of a reactant prior to reaction initiation. The phenomenon is exacerbated as the volume of reactants increases:

$$V = 4/3\pi r^3$$

$$\frac{dV}{dr} = S = 4\pi r^2$$

where V , S , and r are the volume, surface, and radius, respectively, of a sphere. Thus, volume outstrips the surface available for cooling as one scales up.

Ozone

Organic chemists use ozone to rupture double bonds in structure determinations of organic molecules. It is an extremely powerful oxidizer and toxic (TLV, 0.1 ppm). Analytical chemists may at times be exposing themselves to dangerous levels of ozone in prolonged use of some UV and fluorescence spectrophotometers, particularly in poorly ventilated air. Whenever arcing or silent electric discharge conditions prevail, the generation of ozone must be suspected, and good ventilation conditions established.

COMPRESSED GASES

Liquids and solids as distinctive states of matter are nearly incompressible. By contrast, gases at ambient conditions rather easily compress. The reason for this marked difference is the very large free volume or intermolecular distances between molecules. If the air in a room $20 \times 20 \times 10$ ft were liquefied, the volume of the liquid would only be 0.1% of the original volume, and the molecules would still not be touching. This very large "free" space of gases also accounts for their much lower densities as compared to liquids and solids. Various laws (Boyle's, Charles') have been combined into what is called the ideal gas law, $PV = nRT$, which *real* gases obey at low pressures. However, at higher pressures, various divergences from ideality result (Figure 3).

Compressed gases represent a form of energy that can be devastating if not properly used and the phenomenon of pressure well understood. Compressed gases represent a unique hazard in that one is exposed simultaneously to major mechanical and chemical hazards dependent on the gas employed.

A compressed gas is defined by the Department of Transportation (DOT) as any material or mixture having in the container an absolute pressure exceeding 40 psi at 70 °F or, regardless of the pressure at 70 °F, having an absolute pressure exceeding 104 psi at 130 °F; or any liquid flammable material having a vapor pressure exceeding 40 psi absolute at 104 °F as determined by ASTM Test D-323 (29).

Compressed gases are divided into two categories: *pressurized*—those gases that do not liquefy easily because of very low boiling points [weak Van der Waals-type intermolecular attraction (30)] such as hydrogen and helium; and *liquefied*—gases that



ChromAR HPLC Solvents

The High Performance Winners.

High-performance racing cars are a different breed from standard automobiles. So are Mallinckrodt's ChromAR HPLC solvents in comparison to others. Mallinckrodt's Science Products Division was first to recognize that high-performance, high-pressure liquid chromatography requires specially processed solvents. Now, we offer an extensive array of ChromAR solvents to provide the wide selection of characteristics you need in your HPLC applications... with the uniform performance you have the right to expect.

• ChromAR solvents are rigidly controlled for low levels of water, free acid, evaporative residue, UV absorbance. Fluorescence levels are typical of those for quality reagent solvents.

ChromAR solvents are conveniently available from any of the more than 300 Mallinckrodt distributors. Contact Mallinckrodt Science Products Division today for more information and the name of the distributor nearest you.

Call the:

Mallinckrodt

(800) 325-7840

Hot Line

When you need something special
Mallinckrodt, Inc./Science Products Division
P.O. Box 5840/St. Louis, Missouri 63134

- They meet a 99% GLC assay or better (and we publish the limits for all impurities).
- Filtration through a 1-micron filter helps protect against damage to high-pressure pumps and columns.
- Each ChromAR solvent is specially processed. For example, our THF and ether are both packaged under nitrogen in specially-treated light-proof containers to eliminate peroxide formation without adding any optically-active stabilizers. ChromAR HPLC Chloroform contains no stabilizer affecting polarity or absorption.
- All ChromAR solvents are guaranteed for their intended use... and they're available at low prices you'll find pleasing to your budget.

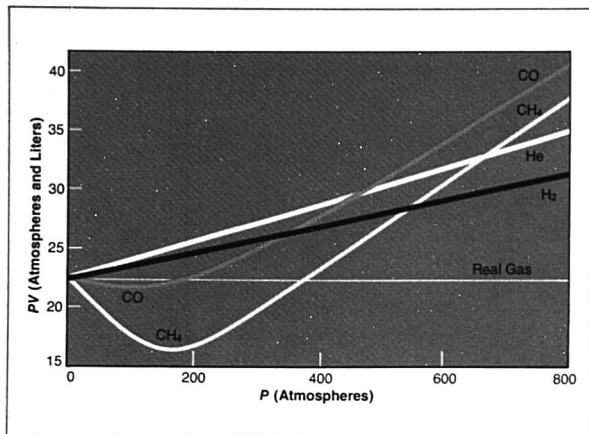


Figure 3. PV vs. P plot for several gases at 0°C

Reprinted with permission from ref. 31. Copyright 1951 Macmillan Co.

exist in a cylinder in liquid and gaseous states, such as propane, butane. The latter gases exhibit a constant gas pressure while the cylinder is discharging until all the liquid is volatilized. These gases (as all other gases at ambient temperatures except hydrogen and helium) have a positive Joule-Thompson coefficient, and the cylinder will cool on prolonged discharge. An exception to the two categories is acetylene, which is a gas dissolved in a liquid (acetone).

It is important to remember that pressure is force per unit area (usually expressed as pounds per square inch or kilograms per square centimeter). Thus, even relatively low pressures of 4–10 psig can be very dangerous in terms of total force exerted on a door or wall. It is also important to remember that the gauge reading represents pressure over atmospheric, i.e., $\text{psig} = \text{psia} - 14.7$, where psia represents absolute pressure.

Hazardous Properties of Compressed Gases

Compressed gases are characterized by very low boiling points and if gas is flammable, flashpoints below room temperature present an ever-present danger of fire or explosion.

Large amounts of potential energy as a result of compression.

Very high rates of diffusion. Hydrogen at 0°C has a diffusion rate of 184 000 cm/s or almost 2000 m/s (31). This effectively means almost instantaneous permeation throughout a laboratory if hydrogen is liberated. Higher molecular weight and flammable gases diffuse only slightly more slowly [Graham's inverse square-root law

(32)]. Leakage from cylinders can therefore cause an explosion or fire if the gas is flammable; injury or death if it is toxic; asphyxiate if it is "harmless" (e.g., nitrogen) (the ambient oxygen content of the air we breathe need drop to only 15% to asphyxiate); and exposure to radioactive danger if the gas is radioactive (e.g., tritium).

Gas Cylinders

Everyone using compressed cylinders should be familiar with the information provided on the cylinder itself.

DOT codes—specify materials of construction, capacities, test procedures, and the service pressure for which the cylinder is designed. A cylinder labeled DOT3A-2000 indicates that the cylinder has been manufactured in accordance with DOT specification 3A and a cylinder operating pressure of 2000 psi at 70°F .

Serial numbers—a number assigned to a cylinder as a means of identification.

Date of hydrostatic testing—usually carried out every 5 or 10 years. If metal stretches too much, cylinders will be replaced. Unless weakened by corrosion, cylinders last for many years.

A tag or proper label indicating the name of the contained gas.

A DOT diamond label, red for flammable gases, green for nonflammable. It is important to note that ammonia has a green label; yet, it is a flammable gas (flammability limits 16–25%) (33).

Safety Relief Devices

Provision is made for these devices on all DOT compressed gas cylinders

except those containing toxic gases where the potential exposure to the toxicant is considered to be a greater risk than cylinder failure. These devices are affixed to the cylinder valve, in the cylinder itself, or at both locations. Various devices are employed.

Safety Relief Valves. These valves are spring-loaded and are used mostly for low-pressure liquefied flammable gases. They will release gas until pressure is back to a safe range.

Frangible Discs. These are used mostly for high-pressure cylinders and will burst at a predetermined pressure considerably above the service pressure and release the entire contents of the cylinder. They are found on most cylinders alone or in combination with other safety relief devices.

Fusible Plug. This device is activated by temperature only. The frangible disk sometimes backed by a fusible plug will function only if the temperature is high enough to melt the metal, after which excessive pressure will burst the disk. Acetylene tanks are equipped with fusible plugs designed to function around 212°F releasing all of the gas to prevent an explosive polymerization or decomposition. Never tamper with any of these pressure relief devices.

Guidelines for Handling Compressed Gases

Always use a hand truck for transport even for short distances; chain cylinder to hand truck. Do not transport compressed gases in closed vehicles. Chain each cylinder in place at all times. Do not drop cylinders or expose them to any type of mechanical abuse. Leave valve cap on cylinder until ready for use. Use only in upright position. Shut off all valves when not in use. Use only recommended regulator for the particular gas; never use improvised adaptors. Always consider the cylinder to be full and handle accordingly. Discontinue using a high-pressure cylinder when the pressure approaches 30 psig, and clearly mark the cylinder as empty; this practice will prevent potential suck-back of reactive gases and moisture. Never pressurize glass equipment. Never lubricate or allow organic lubricants or oils to come into contact with oxygen cylinders. Never use copper or copper-containing alloys (brass) regulators. Never allow tubing to come in contact with acetylene. Place cylinders of flammable gases (hydrogen, acetylene, ethylene, etc.) outside in a protected area and pipe into the working area.

Storage of Compressed Gases

Store cylinders in a fireproof, well-ventilated area; storage temperature

RAPID SPECTRAL ANALYSIS

The TN-1710-I-DARSS* is a complete, computer-based system for rapid analysis of UV-Vis-NIR spectral data.

Complete spectra are acquired in milliseconds. Using the sequential scan module, up to 64 different spectra can be recorded at nearly 400 spectra/second for Time Resolved Spectroscopy and Chemical Kinetics measurements.

High spectral resolution measurements are accommodated with the TN-1149 spectrograph which can provide a dispersion as high as 0.036 nm per channel.

Highest S/N Ratio: The new TN-1223-4I large area intensified array has 2.5 mm x 0.025 mm channels for up to 15 times better S/N than other I-DARSS detectors.

Programmable operation: NBS traceable calibration sources are combined with advanced radiometric/photometric routines for correction of intensity data in Raman and general purpose QC measurements including CIE calculations. Programs and spectral data can be stored on an optional floppy disk device.

Highest Sensitivity: The I-DARSS is more sensitive than SIT and ISIT devices over most of its operational bandwidth. Further, the Gen II Intensifier gain can be varied from 200 to nearly 40,000 with a single control while maintaining a 4096:1 A-D conversion range.

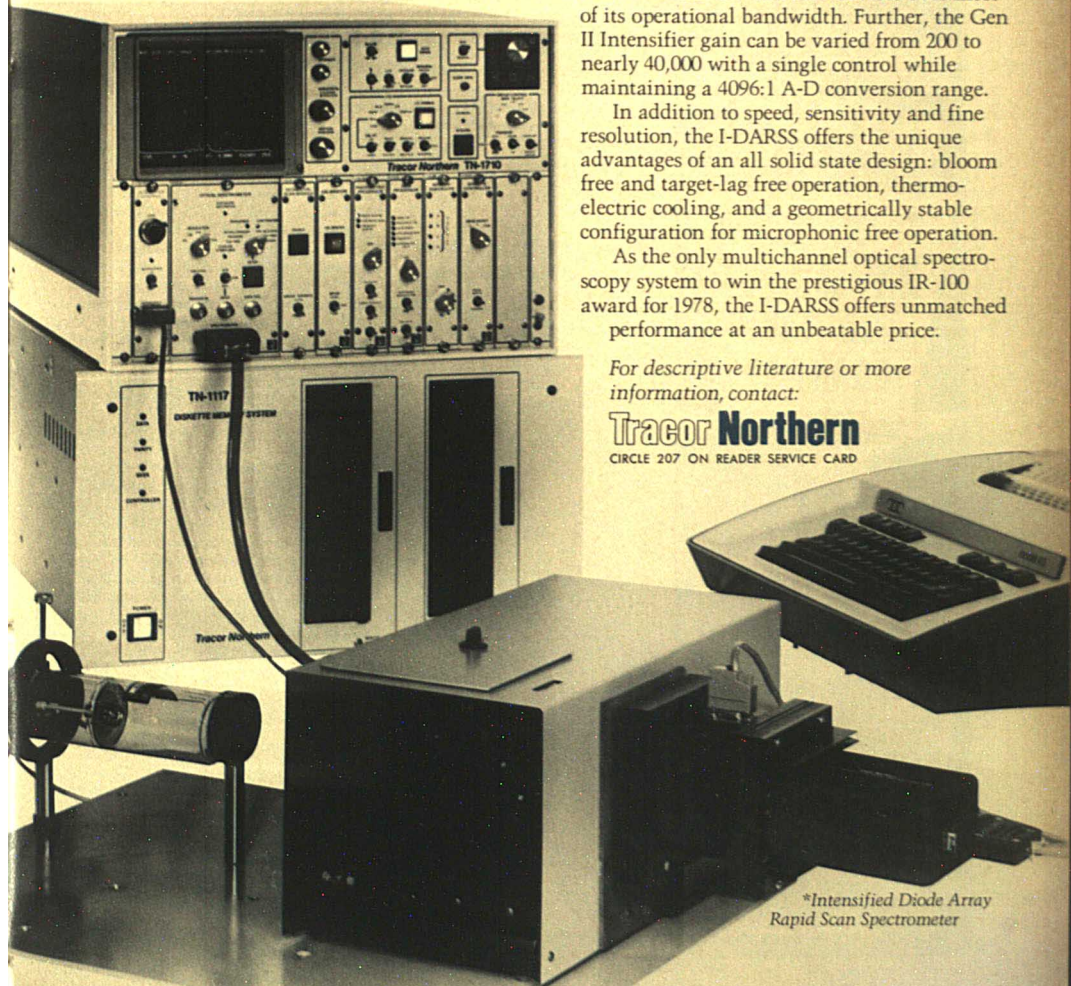
In addition to speed, sensitivity and fine resolution, the I-DARSS offers the unique advantages of an all solid state design: bloom free and target-lag free operation, thermoelectric cooling, and a geometrically stable configuration for microphonic free operation.

As the only multichannel optical spectroscopy system to win the prestigious IR-100 award for 1978, the I-DARSS offers unmatched performance at an unbeatable price.

For descriptive literature or more information, contact:

Tracor Northern

CIRCLE 207 ON READER SERVICE CARD



*Intensified Diode Array
Rapid Scan Spectrometer

GFS CHEMICALS

**YOUR MOST
DIRECT
SOURCE
FOR THE FINEST
COMMERCIALY
AVAILABLE**

**ANALYTICAL
CHEMICALS**

**IT'S WISE TO KNOW
YOU CAN
BUY DIRECT
in ANY
QUANTITY**

**FROM THE
MANUFACTURER**



ANALYTICAL CHEMICALS SINCE 1928

**G. FREDERICK SMITH
CHEMICAL COMPANY**

867 McKinley Ave.
Columbus, Ohio 43223

FOR PROMPT SHIPMENT
614 224-5343



Contact us on circle
Reader Service Card for
YOUR 50th ANNIVERSARY
GENERAL CATALOG
...it's FREE

GFS CHEMICALS

CIRCLE 192 ON READER SERVICE CARD

should not exceed 100 °F. Store only on level floors and protect from dampness, direct sunlight, and extreme weather conditions. Chain each cylinder in an upright position. Store oxidizing gases, oxygen, chlorine, etc., at least 25 ft from fuel gases or preferably in another storage area. Do not store oxygen cylinders on asphalt or near other combustible materials; enriched oxygen is extremely dangerous.

CRYOGENIC LIQUIDS

Cryogenics may be defined as low-temperature technology or the science of ultralow temperatures. To distinguish between cryogenics and refrigeration, a commonly used measure is to consider any temperature lower than -73.3 °C (-100 °F) as cryogenic.

There are currently more than 25 gases that are used cryogenically. Seven gases, however, account for the greatest volume of use and applications in research and industry. These are helium (bp, -269.9 °C), nitrogen (bp, -195.8 °C), fluorine (bp, -187 °C), argon (bp, -185.7 °C), oxygen (bp, -183 °C), and methane (bp, -161.4 °C).

Hazards of Cryogenic Liquids

The primary hazards of cryogenic liquids are fire or explosions, pressure buildup, embrittlement of structural materials, contact with, and destruction of, living tissue, and asphyxiation.

The fire or explosion hazard is obvious when gases such as hydrogen, methane, and acetylene are considered. The hazard may be greatly increased when gases thought to be non-flammable are used. Enriched oxygen will greatly increase the flammability of ordinary combustibles and may even cause some noncombustible materials like carbon steel to burn readily under the right conditions (34).

Wood or asphalt saturated with oxygen has been known to explode literally when subjected to shock. Since oxygen has a higher boiling point (-183 °C) than nitrogen (-195.8 °C), helium (-269.9 °C), or hydrogen (-252.7 °C), it is possible to condense oxygen out of the atmosphere and entrap it when using these lower boiling cryogenic liquids. Particularly with liquid hydrogen, conditions may exist for an explosion.

The danger of pressure buildup is ever-present. Since most cryogenic gases are above their critical temperature, volatilizing gases must always be vented, and expansion ratios in excess of 1000/1 are possible. Any attempt to contain these gases will result in an explosion, the violence of which will be proportional to the pressure exerted to contain the gas. Even in the case

of the most "harmless" gases such as nitrogen, helium, etc., one must be ever mindful of the potential hazard of asphyxiation.

Materials that normally are ductile at ambient temperatures may become extremely brittle when exposed to cryogenic temperatures. Some metals suitable for cryogenic temperatures are the 300 series of stainless steel and other austenitic series, copper, brass, and aluminum. A number of plastic materials such as Dacron, Teflon, Kel-F, mylar, and nylon also perform satisfactorily at low temperatures.

Even a very brief skin contact with cryogenic liquids is capable of causing tissue damage similar to that of thermal burns, and prolonged contact may result in blood clots with potentially very serious consequences.

The following guidelines should therefore be adopted in handling cryogenic fluids. Always wear eye protection, preferably a face shield. Wear gloves that are impervious to the fluid being handled, and loose enough that they can be tossed off. A potholder may be a desirable alternative. The area should be well ventilated. Do not allow the necks of the containers to become plugged with ice or other condensate. Use appropriate metal cryogenic containers. Avoid glass Dewars. If the latter must be used, tape them to prevent flying glass in case of implosion/explosion. Use a hand truck in transporting cryogenic liquids. Select working materials suitable for the temperatures involved. Cryogenic storage conditions should follow similar guidelines.

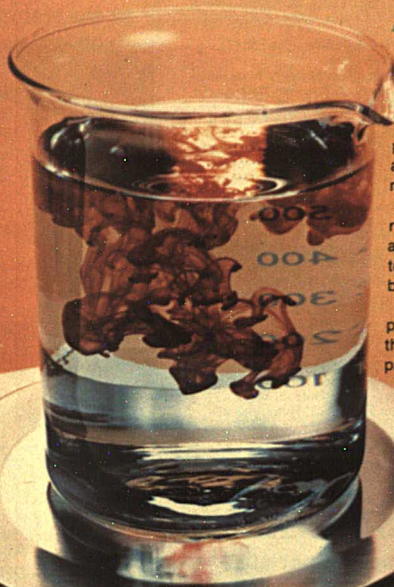
It is almost impossible to cover all aspects of hazardous chemical safety. Several topics such as waste disposal hazards have not been discussed because of space limitations. The important subject of acute and chronic toxicity has only indirectly been treated. The reader is strongly urged to consult the extensive literature and/or the corporate safety officer regarding any aspect of laboratory safety he/she may be concerned about. Safe laboratory conditions can be achieved only if they truly become *everyone's* objective.

References

- (1) Schieler-Pauze, "Hazardous Materials," p 11, Van Nostrand-Reinhold, New York, N.Y., 1976.
- (2) Walter M. Haessler, "The Extinguishment of Fire," 33 pp, Engineered Systems Division, Fyr-Fyter Co., Dayton, Ohio.
- (3) Eugene Meyer, "Chemistry of Hazardous Materials," p 47, Prentice-Hall, Englewood Cliffs, N.J.
- (4) An Identification System for Occupationally Hazardous Materials, HEW Publication No. (NIOSH) 75-126.
- (5) "Code of Federal Regulations," Vol 49, p 246.

DeltaRange DeltaRange DeltaRange DeltaRange

The movable fine range that simplifies precision weighing.



▲ This photo of the new PC4400 balance demonstrates one of the great benefits of DeltaRange. Here's a big-capacity balance—4000 g—weighing a drop of fluid with .01 g readability, although the balance already has nearly 1000 g tared into it.

It is weighing the drop on the 400 g DeltaRange. If you press the control bar, the full 400 g fine range will be available again. And again. And again. Items that weigh more than 400 g will get a result with .1 g readability.

You can really appreciate DeltaRange if you've ever run out of range when weighing formulas. And you'll appreciate it if you're tired of going from one balance to another to weigh heavy and light items. This one balance can do all your weighing.

Because PC Series balances are available with a plug-in microprocessor-based Application Input Device, they can save time when you need to count small parts, measure moisture loss in percent, do reference comparison weighing, or to highlight intermediate and final results during compounding or formula weighings. The device accepts keys that program the balance for each function.

Mettler PC balances are available in several capacities/readabilities. Contact your Mettler dealer—or write for a brochure to Mettler Instrument Corporation, Box 71, Hightstown, NJ 08520.

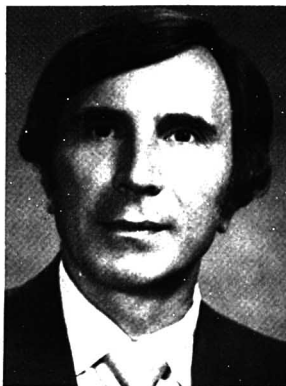
Mettler PC 4400

0.32 g

DeltaRange

Mettler

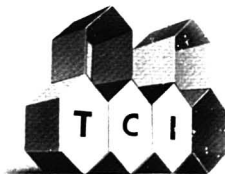
- (6) Haase Heinz, "Electrostatic Hazards, Their Evaluation and Control," p 32, Verlag Chemie, New York, N.Y., 1977.
- (7) Haase Heinz, *ibid.*, p 35.
- (8) Available from J. T. Baker and other major laboratory supply companies.
- (9) "Safety in the School Science Laboratory," M.S. Dept. of Health, Education and Welfare (NIOSH), Less No. 11, Cincinnati, Ohio 45226, Aug. 1977.
- (10) Los Angeles, Calif., Fire Department Standard No. 40, 1-1-60.
- (11) SAFE-T-DATA No. 2, J. T. Baker Chemical Co., Phillipsburg, N.J. 08865.
- (12) "American National Standard Practice for Occupational and Educational Eye and Face Protection," ANSI Std. Z 87.1-1968, American National Standard Institute, New York, N.Y.
- (13) Albert Weaver and Karen A. Britt, "Professional Safety," p 38, June 1977.
- (14) A. Giese, *Science*, 91, 476 (1940).
- (15) Norman V. Steere, "Handbook of Laboratory Safety," p 335, CRC Press, West Palm Beach, Fla.
- (16) J.G.S. Biram, *Vacuum*, 5, 77 (1957).
- (17) "Air Sampling Instruments for Evaluation of Atmospheric Contaminants," 2nd ed., Secretary of American Conference of Governmental Industrial Hygienists, Cincinnati, Ohio, 1962.
- (18) Mercury Spill Cleanup Kits (Mercury), J. T. Baker Chemical Co., Bulletin No. 4.
- (19) a. N. V. Steere, *Chem. Educ.*, 42 (7), 4529 (1965); b. F. W. Michelotti and J. W. Seidenberger, *Am. Lab.*, 77 (1978).
- (20) Cheves Walling, "Free Radicals in Solution," p 412, Wiley, New York, N.Y.
- (21) K. I. Ivanov, V. K. Savinova, and V. K. Mikhailova, *J. Gen. Chem. USSR*, 16, 65, 1003, 1015 (1946); A. Rieche and K. Koch, *Ber.*, 75, 1016 (1942).
- (22) a. I. B. Douglass, *J. Chem. Educ.*, 40, 469 (1963); b. N. V. Steere, *ibid.*, 41, A575 (1964).
- (23) A. G. Davies, *J. Roy. Inst. Chem.*, 386 (1956); A. G. Davies, "Organic Peroxides," Butterworths, London, England, 1961; R. N. Feinstein, *J. Org. Chem.*, 24, 1172 (1959); W. Dasler and C. D. Bauer, *Ind. Eng. Chem. Anal. Ed.*, 18, 52 (1946); "Manual of Techniques," Metal Hydrides, Inc., Beverly, Mass., 1958.
- (24) Rolf Halonfrenner, Wolfgang Klauel, and John S. Coates, *Chem. Eng. News*, 56 (6), 3 (1978).
- (25) E. M. Harris, *Chem. Eng.*, 56 (1), 116-7 (1949).
- (26) E. Meyers, "Chemistry of Hazardous Materials," p 133, Prentice-Hall, Englewood Cliffs, N.J., 1977.
- (27) J. T. Baker SAFE-T-DATA, No. 3, Phillipsburg, N.J., 08865.
- (28) Cheves Walling, "Free Radicals in Solution," p 169, Wiley, New York, N.Y.
- (29) Hazardous Materials Regulations of the Department of Transportation, R. M. Graziano, Tariff No. 31, issued by Graziano, Agent, 1920 L Street, N.W., Washington, D.C. 20036.
- (30) C. A. Coulson, "Valence," Oxford at the Clarendon Press, p 260, 1953.
- (31) Carl F. Prutton and Samuel H. Maron, "Fundamental Principles of Physical Chemistry," p 23, Macmillan, New York, N.Y., 1951.
- (32) Carl F. Prutton and Samuel H. Maron, *ibid.*, p 17.
- (33) National Fire Protection Assoc., "Fire Protection Guide on Hazardous Materials," 6th ed., 49-46, Boston, Mass.
- (34) Norman V. Steere, "Handbook of Laboratory Safety," p 575, CRC Press, West Palm Beach, Fla.



F. W. Michelotti is director of research for Laboratory Products at the J. T. Baker Chemical Co. He received degrees from Fordham University, AB, cum laude, and an MS degree in organic chemistry, before obtaining a PhD degree from Polytechnic Institute of New York (1957) in organic polymer chemistry. He is author of over 30 scientific papers and patents in organic, polymer, analytical, and diagnostic chemistry, and coauthor of the J. T. Baker Safety School Manuals on Hazardous Chemical Safety, and is director of research for the J. T. Baker Spill Control Products R&D effort. Most recently, he has written and presented several papers and lectured extensively on chemical hazards in the laboratory. He is a member of the American Chemical Society, the Division of Organic Chemistry, the Division of Health and Safety, Executive Committee of the Research Section of the National Safety Council, and the Association of Research Directors.

QUALITY! SELECTION! FAST DELIVERY!

All Yours From TCI—The Organic Reagent Specialist.



Organic Reagents
Fine Organic Chemicals
Rare Organic Chemicals
Custom Synthesis

Since 1922, TCI (Tokyo Kasei) has supplied leading chemical laboratories and industries worldwide with a broad selection of fine chemicals. Our current catalog includes over 10,000 different chemicals for every type of use. Virtually all orders are shipped within 12 hours of receipt. Five-gallon, 55-gallon and ton lots are available. Be sure of setting quality, selection and fast delivery. Buy TCI!

Write today for your free copy of the 750-page TCI Organic Chemicals Price List.



TOKYO KASEI KOGYO CO., LTD.

(Tokyo Chemical Industry Co., Ltd.)

9-4, Nihonbashi-Honcho 3-chome, Chuo-ku, Tokyo, 103 Japan

Telex: 222-4719 ASACMN J Cable: ASACHEMCO TOKYO Tel: 241-0861

CIRCLE 200 ON READER SERVICE CARD

BREAK THE GLASS HABIT

Nalgene® FEP Sep Funnels are as chemical resistant as glass.

Like glass, Nalgene® FEP Sep Funnel of Teflon® FEP resist any chemical used in an extraction. But unlike glass, they won't break or crack, even when dropped, so you can reduce replacement costs. And both the screw cap on top and the stopcock at the bottom make these Nalgene Sep Funnel leakproof when they're shaken.

Teflon® FEP construction lets you see clearly the interface of even colorless liquids all the way down to the stopcock housing.

Nalgene Sep Funnel are non-wetting, so they drain completely. They're non-stick, so they're easy to clean. The stopcock housing can be removed for easier cleaning, too.

Get extraordinary chemical resistance and convenience with these economical alternatives to fragile glass sep funnels.

Put Nalgene Labware to the test, and see why so many laboratories are breaking the glass habit. Send for our free Nalgene Labware catalog, featuring over 250 products for professional use. Write: Nalge Company, Division of Sybron Corporation, Nalgene Labware Department, Box 365, Rochester, New York 14602.

And unbreakable
Nalgene Labware
lasts longer.

Nalgene
Labware

Glass
Labware

SYBRON | Nalge

CIRCLE 155 ON READER SERVICE CARD

Reporting Impurities in Commercial Products

A Master Analytical Scheme to identify and measure trace organics in commercial products could solve the regulatory reporting dilemma faced by industry

An earlier article in this series (1) pointed to the necessity for an exhaustive analytical development program to meet proposed regulatory requirements by the U.S. Environmental Protection Agency for registration of pesticides. The *Federal Register* (2) calls for reporting all impurities in manufacturing use products and formulated use products at a concentration of 0.01% or higher. The applicant must also provide detailed analytical methods for all impurities reported. One manufacturer has estimated that the costs of complying with the analytical methods development requirements alone could be as high as \$4.5 million for the registration of a single household disinfectant. The bulk of these costs is in the development of analytical methods for complex matrices. It is reasonable to expect that similar premanufacturing information will be recommended for chemicals regulated by the Toxic Substances Control Act.

Because of these costs, industry and the ACS have both proposed that requirements for chemical analysis for trace impurities be limited to only those chemicals known to be toxic. Unfortunately, analytical experience to date has demonstrated that we cannot accurately predict what chemicals will be present at trace levels, and we cannot always predict toxic effects (PCB's were manufactured for about 40 years before research revealed their harmful impact on fish and wildlife). The need to know what is in commercial products and the astronomical costs of meeting this need under current proposals create a dilemma and a tremendous challenge to the analytical chemist—not a challenge to amass armies of analytical chemists applying traditional approaches to the problem but a challenge to develop innovative concepts that will provide adequate, if not entirely complete, information at a justifiable cost.

For example, a compromise might be reached between EPA and industry if a standard analytical protocol could be developed that would identify and measure all impurities at a concentration above a level low enough to be considered insignificant for the vast majority of chemicals. Separate, more sensitive procedures could be applied for the determination of the very few chemicals known to be of concern at lower concentrations (e.g., 2,3,7,8-tetrachlorodibenzo-*p*-dioxin). Application of such a protocol might appeal to both EPA and industry. The regulatory agency could be assured that a reliable and comprehensive analysis of the product had been made by a broadly tested protocol. The industry could be assured that it had fulfilled its regulatory obligations. The cost of applying such a protocol should be reasonable, particularly if commercial laboratories geared up to provide the analysis on a mass-production basis. Although a standard qualitative-quantitative scheme may not provide the best possible analysis for every impurity in every product, the uniform application of the protocol would likely provide, by far, the largest amount of valuable information at the lowest cost.

Development of a comprehensive analytical protocol for analysis for trace impurities is not a pipe dream. It can be done today by combining appropriate state-of-the-art techniques, and cost-effective and successful application can be predicted with considerable confidence. Experience with the EPA analytical screening protocol for consent decree priority pollutants provides encouragement. This protocol was hastily developed within a three-month period to identify and measure, by gas chromatography-mass spectrometry, 114 volatile organic compounds in industrial wastewaters at a detection level of about 10

ppb. Quantitation is precise only to an order of magnitude. Approximately 12 different commercial and government laboratories have applied the protocol to 5000 samples at an average cost of about \$700 per sample (less than \$7.00 per compound). The protocol is far from perfect, as pointed out in a previous article in this series (3), but its use is encouraging for several reasons: Even though the protocol is somewhat complex and requires sophisticated equipment, it has been broadly applied at reasonable cost; analysis of standard mixtures has demonstrated acceptably comparable results from different laboratories; and although only 114 compounds are identified and quantitated, GC retention times and detector responses and mass spectra are collected routinely on every sample for many additional compounds.

A logical next step is to put together a comprehensive method that provides for extraction of all compounds and identification and measurement of every compound for which a detector response and mass spectrum are obtained. Currently, EPA is developing just such a scheme through a contract to the Research Triangle Institute and Gulf South Research Institute (4). This scheme will be based on the use of a computerized GC-MS system. Sampling procedures, extractions, internal reference compounds, GC columns, and MS operating conditions will be specified so that all volatile organics (those that are amenable to gas chromatography) will be identified and measured from data collected on a single GC-MS run for each extract. Compounds are identified from automatic computer spectra matching. GC retention times and relative peak heights are computed by use of internal reference compounds; recovery factors and detector response factors for identified compounds are retrieved

**Jarrell-Ash on
Plasma Spectrometry:
the 1979
Seminar Series**

Please reserve a place for me at the
session to be held

Date

City

and rush me the details as to location, hours,
speakers, etc.

Name

Title

Organization

Address

City

State

Zip

**Important: please fill out this line so that we
can reach you with any final details.**

(Area Code/Phone No.)

**Jarrell-Ash on
Plasma Spectrometry:
the 1979
Seminar Series**

Please reserve a place for me at the
session to be held

Date

City

and rush me the details as to location, hours,
speakers, etc.

Name

Title

Organization

Address

City

State

Zip

**Important: please fill out this line so that we
can reach you with any final details.**

(Area Code/Phone No.)



NO POSTAGE
NECESSARY
IF MAILED
IN THE
UNITED STATES

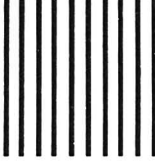
BUSINESS REPLY MAIL

FIRST CLASS PERMIT NO. 3902 PITTSBURGH, PA.

POSTAGE WILL BE PAID BY ADDRESSEE

Fisher Scientific Company
Jarrell-Ash Division
711 Forbes Avenue
Pittsburgh, PA 15219

ATTN: Plasma Seminars Coordinator



NO POSTAGE
NECESSARY
IF MAILED
IN THE
UNITED STATES

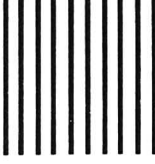
BUSINESS REPLY MAIL

FIRST CLASS PERMIT NO. 3902 PITTSBURGH, PA.

POSTAGE WILL BE PAID BY ADDRESSEE

Fisher Scientific Company
Jarrell-Ash Division
711 Forbes Avenue
Pittsburgh, PA 15219

ATTN: Plasma Seminars Coordinator



Get a plasma update from the experts.

New Jarrell-Ash seminar series starts May 7.

WEST

May 7 Minneapolis
May 8 Vancouver
May 10 San Francisco
May 11 Los Angeles

CENTRAL

May 14 Kansas City
May 15 Indianapolis
May 17 Houston
May 18 New Orleans

EAST

May 21 Pittsburgh
May 22 Raleigh/Durham
May 24 Greater New York
May 25 Toronto

Treat yourself to the latest information on plasma spectrometry. In a seminar right in your own area. From the plasma experts at Jarrell-Ash.

Last year, in 12 cities coast to coast, they discussed the history, theory and basic performance features of ICAP—inductively coupled argon plasma. How it brings you AA's sensitivity plus remarkable multi-element capability to expedite today's heavy analytical workloads.

Now there's an all-new Jarrell-Ash plasma series in the U.S. and Canada [see schedule, left]. It talks hardware and software, answers your most-asked questions.

□ **What system to buy.** Seminar details 5 different plasma choices. From surprisingly low cost workhorses to advanced research units. Plus the most effective software for each.

□ **You and the computer.** Because ICAP produces enormous amounts of data for over 48 elements in 60 minutes, you'll need help in data management. Seminar guides you through storage and retrieval, statistics, graphics capabilities — the works.

□ **Hardware specifics.** You'll learn about the versatile "N+1" channel: how it can add dual-an-element capability. Automatic background correction: what it is, when to use it. And much more.

□ **Plus** — the new Jarrell-Ash plasma movie. For anyone who missed last year's session — and an excellent review of theory, applications and techniques for **everyone**.

Plan now to attend. There's no charge — but enrollment is limited. Use special Jarrell-Ash postcard bound into this journal to get details on the session in your area, today.



Leaders in
Plasma Spectrometry

Jarrell-Ash Division
Fisher Scientific Company

590 Lincoln Street
Waltham, Massachusetts 02154
Phone (617) 890-4300

from a computer library of data previously established for each chemical class. Taken together, this information allows computerized quantitation without reanalyzing the sample and avoids the necessity to maintain thousands of reference compounds. Generally, concentrations should be accurate to within a factor of two.

The Master Analytical Scheme described above is designed for use with aqueous samples. Estimated detection limits will be 10 ppb for effluents, 1 ppb for ambient waters, and 0.1 ppb for finished drinking water. Cost of application is estimated at \$3 000 per sample. This cost is quite a bargain when compared to a cost of \$10 000 for providing quantitative information for just the 114 consent decree pollutants using the EPA protocol with sufficient spike and blank runs to compute recoveries and detector responses.

To analyze commercial products, the Master Analytical Scheme would have to be "front ended" to provide for dissolution of the product and its impurities. It would also have to be extended to nonvolatile compounds, probably by use of high-pressure liquid chromatography coupled with mass spectrometry. Insurmountable obstacles, then, no longer exist.

Assuming that these obstacles will

be overcome shortly, the analytical chemists can offer regulatory agencies and industry the solution to the dilemma of chemical analysis for trace impurities in commercial products. Application of the entire protocol could be made for \$20 000, satisfying the requirement to identify and report impurities. No additional methods development would be necessary; procedures for extracting only the compounds for which monitoring would be required would be already developed as a part of the protocol. The mass spectrometer could be replaced with less expensive detectors for monitoring previously identified compounds. (It is important to assert here that nonchemists should overcome their paranoia about GC-mass spectrometers. They are no longer "rare and exotic instruments.") They are used by more pollution control laboratories today than the number of pollution control laboratories using gas chromatographs 15 years ago. They are, for many purposes, more economical to use than gas chromatographs with other detectors.)

We hereby challenge the analytical chemist to complete the development of the proposed system that will solve the problem of identifying and measuring trace organic impurities in commercial products. Its development

and adoption can reduce the analytical measurements cost of developing new products while providing the best attainable information.

The successful application of the qualitative-quantitative approach requires that analytical chemists try the protocol that is to be standardized and collaborate in its improvement. If you want to join in this accomplishment, contact Dr. Wayne Garrison, who is in charge of EPA's program to develop the Master Analytical Scheme. His address is

U.S. Environmental Protection
Agency
Environmental Research Laboratory
College Station Road
Athens, Ga. 30605

References

- (1) R. A. Libby, *Anal. Chem.*, **50**, 1229A (1978).
- (2) *Fed. Regist.*, **43** (132), 29707-10 (10 July 1978).
- (3) R. O. Kagel, R. H. Stehl, and W. B. Crummett, *Anal. Chem.*, **51**, 223A (1979).
- (4) A. W. Garrison et al., "An Automatic Sampler, A Master Scheme, and A Registry System for Organics in Water," *Proc. 9th Annual Materials Research Symp.*, NBS, in press.

The award winning electronic balance

You can count on it...

and automatically perform a wide range of complex weighing and data conversions too.

That's why Wescon gave the Scientech 3300 Series top-loading electronic balance its Award of Merit for the best commercial application of a microprocessor for process and quality control.

It's the new generation of balances from Scientech, a pioneer in the development of intelligent weighing systems for laboratory and industry. The 3300 Series offers analytical laboratory precision, easy to use data input keyboard, bright digital readout, ruggedized construction and electronic digital tare...all at a "Made in USA" price.

Find out more about the capabilities of Scientech's new generation of electronic balances. Call or write for descriptive literature on the award winners from Scientech.

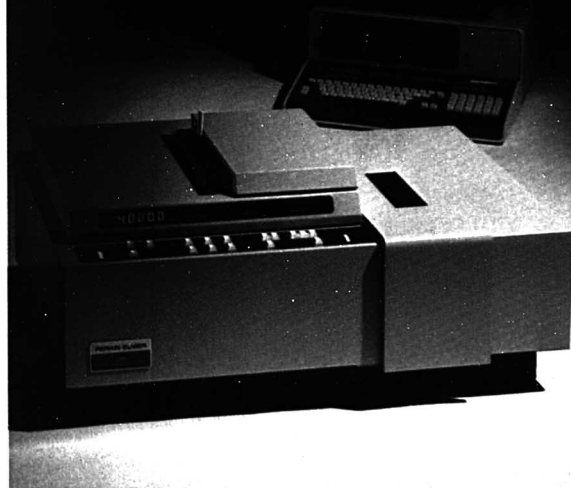
SCIENTECH, INC.
5649 Arapahoe Avenue • Boulder, Colorado 80303 • (303) 444-1361



CIRCLE 195 ON READER SERVICE CARD

PLAN AHEAD WITH PERKIN-ELMER

NEW 98 INFRAREDS



"The x98 series are instruments that let you plan ahead. They are ideal workhorse spectrometers, but with high performance that justifies coupling them to the revolutionary Perkin-Elmer Infrared Data Station. At any time you can upgrade from a basic instrument to a powerful system still costing no more than other spectrometers which offer far less."

The 98 Series

There are three instruments in the series, giving scan range options down to 200cm^{-1} . All employ the same high energy optical system to ensure good performance even with difficult samples and with a wide range of accessories.

Microprocessor control provides simple yet flexible operation, with pushbutton selection of all parameters to guarantee that conditions are set reproducibly even by inexperienced operators. The advanced electronic Flowchart recorder maintains chart calibration even when different scale expansions are used, and the digital wavenumber display keeps the operator in the picture.

Quantitative Accuracy

The increasing demand for quantitative measurements is met by the x98 series. Outstanding accuracy follows from the excellent ordinate reproducibility. For high sample throughput there's a multisampling accessory and selectable wavelength limits.

New Data System

A standard interface allows the x98 series to be used with almost all computers, but it's unlikely that any can match the Perkin-Elmer IR Data Station. This sophisticated micro-computer system is as easy to use as the instruments themselves. Current facilities include signal averaging, digital smoothing, and spectral subtraction. For the future, the possibilities are endless.

For further information Contact:

Perkin-Elmer Corporation, Main Avenue,
Norwalk, Connecticut 06856 U.S.A.

Perkin-Elmer Limited, Maxwell Road,
Beaconsfield, Buckinghamshire, HP9 1QA

Bodenseewerk Perkin-Elmer & Co. GmbH,
Postfach 1120, D-7770 Ueberlingen, West
Germany

PERKIN-ELMER

Expanding the world of analytical chemistry.

CIRCLE 177 ON READER SERVICE CARD

ANALYTICAL CHEMISTRY, VOL. 51, NO. 4, APRIL 1979 • 463 A

LIQUID CHROMATOGRAPHY



OUR NEW LC METHODS PROCESSOR—FOR AUTOMATED, UNATTENDED ANALYSES FROM INJECTION TO PRINTOUT.

The Perkin-Elmer Methods Processor for liquid chromatography gets the chemist out of instrument operation and back into chemistry. Out of routine, repetitive monotony and into useful work.

A revolutionary combination of data processing and control technology, it performs reliably, all by itself—all day, all night, all week-end. You can even run studies previously judged too difficult and tedious.

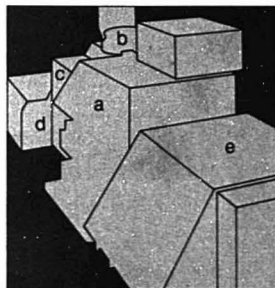
You tell it what you want through one of our cassette-tape programs that's been tested and proved. Or you can generate your own programs on the keyboard. And you don't have to be a computer expert, either.

FIVE MODULAR UNITS

To do so much, so precisely and efficiently, the Methods Processor is assembled from five separate Perkin-Elmer modular units—each a significant advance in its own field:

- the Series 3B pump module, which performs difficult qualitative and quantitative analyses with the convenience of micro-processor control,
- the Model 420 Automatic Sampler/Injector, which permits unattended injection of up to 42 different samples,
- the Model LC-100 column air-bath oven, offering precise temperature control from 10°C above ambient to 99°C,

- the Model LC-75 Detector and Autocontrol, which adds spectroscopy to separation,
- the SIGMA 10 Chromatography Data Station that processes data and delivers a printout.



With this combination, you get complete keyboard control of the analysis. You can install the pump method. Set in the data processor method. Designate a vial number in the Autosampler. Indicate sample name and date, time, and run number. Change solvents and wavelengths.

EFFICIENT PERFORMANCE

Your software control is crashproof and foolproof. You get error messages. You're reprogrammed for non-valid entries. You can modify the method without complete re-setup. The system won't "lock up."

Meanwhile, the Methods Processor is shrinking your costs. Solvent usage is reduced and operating time shortened. Repeatability and

timing of conditions, as well as overall initial results, are better than with manual operations.

The system handles multiple mixed samples, each in a different solvent program and data reduction method, if required. It lets you program and start complex analytical sequences by one-shot keyboard operation. It easily gets out of the software routine for simple manual operation. And it takes clear and complete prompting—in English.

INFINITE OPTIONS

All these capabilities in a single system bring you infinite options for finding exactly the kind of analysis you want. No other liquid chromatography system is so variable, versatile, or technologically advanced as this newest Perkin-Elmer development. It brings this analytical technique to its fullest potential.

MORE REMARKABLE FEATURES

There's a long list of other advantages you'll find in the Perkin-Elmer LC Methods Processor. All functions are performed without any system modification whatever, the result of Perkin-Elmer design and testing throughout.

Get the full story on this revolutionary development in LC analysis. Talk to your Perkin-Elmer representative. Or write Perkin-Elmer Corp., MS 12, Main Avenue, Norwalk, CT 06856.

PERKIN-ELMER

Expanding the world of analytical chemistry.

32nd Annual Summer Symposium

Lasers and Analytical Chemistry

"Lasers and Analytical Chemistry" is the subject of the 1979 Summer Symposium of the ACS Division of Analytical Chemistry. The symposium will be held June 27-29, 1979, on the campus of Purdue University in West Lafayette, Ind. The symposium program has been arranged by John C. Travis of the Center for Analytical Chemistry, NBS, and Gary M. Hieftje, Dept. of Chemistry, Indiana University. The local arrangements chairman is Fred E. Lytle of Purdue University. The symposium is sponsored by the ACS Division of Analytical Chemistry and ANALYTICAL CHEMISTRY.

About Purdue University

Purdue's main campus is located in West Lafayette, Ind., across the historic Wabash River from Lafayette. The university has a total student population of 31 000. The Dept. of Chemistry has 46 faculty members and 280 graduate students. The analytical group consists of R. Graham Cooks, Ben S. Freiser, Peter T. Kissinger, Fred E. Lytle, Dale W. Margerum, Harry L. Pardue, Sam P. Perone, and Nicholas Winograd. Any of the Chemistry Department faculty will be glad to discuss the research or teaching program of Purdue with interested attendees.

Travel

For participants traveling by air, the Purdue Airport is currently served by 11 flights a day from Chicago, 8 from Indianapolis, and 3 from Detroit. The Memorial Union is a short cab ride away from the airport. Also, from 6:00 a.m. until 6:15 p.m. the airport is served by buses every half-hour.

Housing and Symposium Arrangements

Housing for the symposium will be in the Purdue Memorial Union and local motels. Rooms in the Union are limited in number; therefore, it is suggested that delegates return the completed reservation form and registration fee as soon as possible. Daily rates at the Union are \$16.50 for single occupancy and \$21 for double. For those participants wishing to make their own housing reservations, a list of local motels with rates is available



Chemistry East at Purdue University

upon request. Payment for housing should be made in person and not sent with the registration fee. Meals are available at several locations in the Memorial Union or at local restaurants. No meal packages are offered.

If special facilities are required for handicapped participants, please contact Professor Lytle so that arrangements can be made.

Registration

The symposium will be held in the Stewart Center adjacent to the Union. The registration fee of \$40 includes admission to all sessions, symposium materials, refreshment breaks, university services, and a Thursday night cookout. All participants should send the registration form together with a check for \$40 made payable to Purdue University, before May 31, 1979. Advance registration is imperative to ensure that space will be available. After

arrival, badges and conference materials should be picked up in the lobby of Stewart Center on Tuesday evening between 7:00 and 9:00 p.m. or on Wednesday morning between 7:30 and 9:00 a.m.

Student registration for the technical session costs \$5.00. Extra tickets are available for the cookout at \$10 each.

Family Activities

Although no organized tours are planned, a variety of activities are available for family members during the symposium. The Tippecanoe Battlefield, Fort Ouiatenon, the Moses Fowler House, and Columbian Park with amusement rides and zoo are all in or close to town. Points of interest in the Indianapolis area include the Conner Prairie Pioneer Settlement, the Indianapolis Motor Speedway, the Indianapolis Museum of Art, and a su-

on Analytical Chemistry

Purdue University, West Lafayette, Ind., June 27-29, 1979

perb Children's Museum. In addition, there are several beautiful state parks within an hour's drive from Lafayette.

Symposium Format

The symposium is divided into five sessions. In the first session, Wednesday morning, the chairmen of each of the subsequent four sessions, Wednesday afternoon through Friday morning, will provide an overview of lasers in analytical chemistry and of the content of their respective sessions. This overview will assess the impact of lasers on specific areas in analytical chemistry. The other sessions will present a tutorially oriented discussion on the nature of lasers and radiation, and the operation, construction, and use of lasers.

In addition to these five sessions, a poster session, containing only contributed papers, will be held on Wednesday June 27, from 8:00 to 10:00 p.m. Abstracts and titles for poster papers must be submitted by

May 15, 1979, to either of the symposium program chairmen: Gary M. Hieftje, Dept. of Chemistry, Indiana University, Chemistry Bldg., Bloomington, Ind. 47401; or John C. Travis, Analytical Chemistry Division, NBS, Washington, D.C. 20234.

Wednesday Morning, June 27

Impact of Lasers on Analytical Chemistry—An Overview

G. M. Hieftje, J. C. Travis, *Presiding*

8:30 **Opening Remarks.** F. E. Lytle, Purdue U

8:45 **Fundamentals of Lasers.** F. E. Lytle, Purdue U

9:30 **Analysis by Laser-Induced Fluorescence.** J. C. Wright, U of Wisconsin

10:30 **Analysis by Absorption of Laser Radiation.** R. A. Keller, Los Alamos Scientific Lab

11:15 **Methods the Laser Made**

Possible. T. Hirschfeld, Block Engineering

Wednesday Afternoon

Fundamentals of Lasers

F. E. Lytle, *Presiding*

2:00 **General Laser Principles.** F. E. Lytle, Purdue U

2:40 **Tunable Laser Systems.** M. J. Wirth, U of Wisconsin

3:40 **Nonlinear Optics.** J. C. Wright, U of Wisconsin

4:20 **Pulsed Laser Systems.** J. M. Harris, U of Utah

Wednesday Evening

Poster Session—Contributed Papers

G. M. Hieftje, J. C. Travis, *Presiding*

8:00-10:00 **Contributed Papers**

Registration Form

32nd Annual Analytical Summer Symposium on Lasers and Analytical Chemistry

June 27-29, 1979, Sponsored by the

ACS Division of Analytical Chemistry and ANALYTICAL CHEMISTRY

Purdue University, West Lafayette, Ind. 47907

Name (please print) _____	Telephone _____	Registration Fee	\$40 _____
Mailing Address _____		Student Registration Fee	\$5 _____
_____		Extra Cookout Tickets _____ @ \$10	_____
Professional Affiliation _____		Total amount due and enclosed	\$ _____

Please check appropriate items:

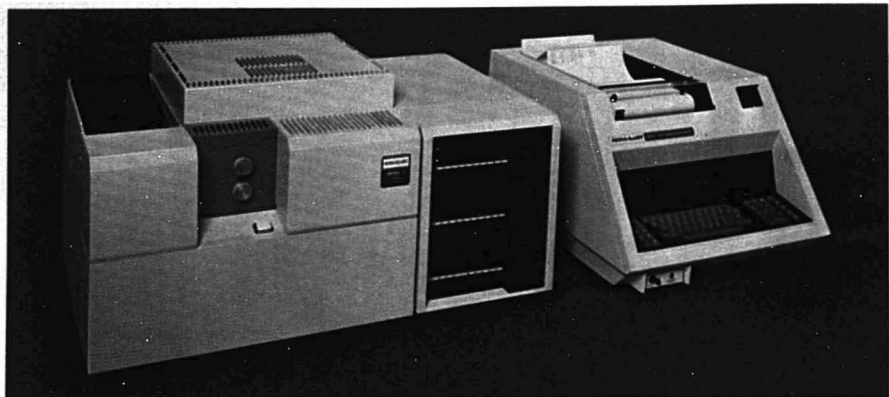
- ☐ I would like to share a room with _____
- ☐ I will share a double room with someone you assign.
- ☐ I prefer a single room.
- ☐ I will arrange for my own housing. Please send list.

DO NOT SEND MONEY IN ADVANCE FOR HOUSING.

Please return this form by May 31, 1979, with a check made payable to Purdue University to: Continuing Education Business Office, Room 110, Stewart Center, Purdue University, West Lafayette, Ind. 47907

For general information, contact: Fred E. Lytle, Dept. of Chemistry, Purdue University, West Lafayette, Ind. 47907 (317-494-8271)

PERKIN-ELMER'S SIGMA GC SERIES— MORE THAN EVER, YOUR SOUNDEST CHOICE.



Two years ago, we introduced our SIGMA gas chromatography concept. Today it has proved itself as the most advanced, common-sense move of its kind.

Because the SIGMA series gives you a unified set of instruments to match your applications and budget. Plus options. Plus accessories. Plus a microprocessor-controlled data handling unit that serves them all. And they've all demonstrated their capabilities fully, from the most sophisticated at the top of the line to the routine-use instrument that still shares the basic advantages of the whole series.

THE FULL LINE

The SIGMA 1 leads off. It combines one or more gas chromatographs with integral microprocessor control and multi-channel data handling. The internal printer/plotter gives the chromatogram, analytical conditions, and quantitative results.

The SIGMA 2 is a multi-detector, microprocessor-controlled instrument that combines versatility with operating ease. You set the analytical parameters on a keyboard that instructs you in the setup routine.

SIGMA 3 gas chromatographs are modestly priced but exceptionally versatile single or dual channel temperature programmed instruments. They may be equipped with an extremely wide choice of detectors. A simple numerical keyboard sets parameters and the microprocessor checks that no "impossible" values are entered.

SIGMA 4 instruments are excellent for routine applications. They are dedicated isothermal units offering the same detectors, injectors, and ovens as their more expensive counterparts.

MORE ACCESSORIES

Even the list of SIGMA accessories is longer now, widening the SIGMA capabilities for handling your applications. There's the new

HS-6 headspace sampler, especially useful for environmental analysis, simple in operation and low in cost. Others include an automatic gas analyzer for refinery gases and the AS-100 automatic sampler which injects up to 100 samples automatically. These new accessories join a long list of standard accessories including gas sampling valves, a pyrolysis injector, the MS-41 solid injector, spectroscopic detectors and a complete line of packed and capillary, glass and metal columns.

JOIN THE PARADE

Don't let more time pass before you start to enjoy the benefits of the most significant advance in GC today. Get the details now. Talk to your Perkin-Elmer representative. Or write Perkin-Elmer Corporation, MS-12, Main Avenue, Norwalk, CT 06856.

PERKIN-ELMER

Expanding the world of analytical chemistry.

CIRCLE 178 ON READER SERVICE CARD

Thursday Morning, June 28

Analysis by Laser-Induced Fluorescence

J. C. Wright, *Presiding*

9:00 Laser-Induced Matrix Isolation Fluorimetry. E. L. Wehry, R. R. Gore, R. B. Dickinson, Jr., U of Tennessee

9:30 New Laser-Based Methodologies for Determination of Organic Pollutants via Fluorescence. J. C. Brown, J. M. Hayes, G. J. Small, Ames Laboratory, USDOE

10:00 Use of Time Resolution in Analytical Spectroscopy. F. E. Lytle, Purdue U

10:40 Laser-Induced Fluorescence for Trace Element Analysis. P. J. Hargis, J. P. Hohimer, Sandia Labs

11:10 Laser-Excited Atomic Fluorescence Spectrometry. S. J. Weeks, NBS

11:40 Panel Discussion

Thursday Afternoon

Analysis by Absorption of Laser Radiation

R. A. Keller, *Presiding*

1:30 Potential Analytical Aspects of Laser Multiphoton Ionization Mass Spectrometry. L. Zandee, D. A. Lichtin, R. B. Bernstein, Columbia U

2:00 Review of Recent Visible and Infrared LIDAR Investigations. R. A. Baumgartner, SRI International

2:30 Detection of Free Radicals by Laser Magnetic Resonance. C. J. Howard, NOAA

3:15 Intracavity Absorption and Optoacoustical Spectroscopy. K. V. Reddy, Allied Chemical Corp.

3:45 Analytical Aspects of Thermal Blooming. R. L. Swofford, Standard Oil Co.

4:15 Optogalvanic Spectroscopy. J. C. Travis, NBS

4:45 Panel Discussion

Friday Morning, June 29

Methods the Laser Made Possible

T. Hirschfeld, *Presiding*

9:00 Analytical Applications of Nonlinear Raman Spectroscopy. A. L. Harvey, Naval Research Laboratory, Washington, D.C.

9:40 Spectroscopy in Supersonic Molecular Beams. D. Levy, U of Chicago

10:30 Heterodyne Astronomical Spectroscopy. A. L. Betz, U of California, Berkeley

11:10 Picosecond Studies of Chemical Phenomena. A. J. Campillo, Los Alamos Scientific Lab

11:50 Panel Discussion

12:15 End of Symposium

Program and Local Arrangements Chairmen



John C. Travis



Gary M. Hieftje



Fred E. Lytle

Evaluating an NMR Facility

A new high-resolution, 600-MHz nuclear magnetic resonance facility at Carnegie-Mellon University in Pittsburgh needs evaluating. Scientists are invited to submit one-page proposals for short-term (one week or less) projects that will put the instrument through its paces. A variety of projects then will be scheduled for this spring, and participating scientists also will take part in a symposium once projects are completed. Proposals may be submitted to Dr. K. D. Kopple, Chairman, NMR Facility Advisory Committee, Dept. of Chemistry, Illinois Institute of Technology, Chicago, Ill. 60616. 312-567-3433.

Lab Safety Guide

A supplementary reference issue of the *Chemical Bulletin* called "The Laboratory Safety Deskbook I: A Guide to OSHA Standards" is available. Those OSHA standards that

have a direct impact on chemical laboratories are compiled into this reference issue. The contents include the William Steiger Occupational Safety and Health Act, Code of the Federal Register, Title 29, Part 1910, and National Fire Protection Association Standard for Laboratories Using Chemicals. The guide can be purchased for \$10 per single copy or \$8.00 each for 10 or more copies. Send requests to Business Manager, Chemical Bulletin, 86 East Randolph St., Chicago, Ill. 60601. For further information, call Dolores Kenney at 312-236-3026.

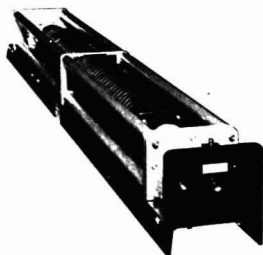
Call for Papers

93rd Annual Meeting of the Association of Official Analytical Chemists
Marriott Hotel, Twin Bridges, Washington, D.C. Oct. 15-18, 1979. Current

developments in analytical methodology pertaining to agricultural, environmental, and public health areas will be presented. Abstracts for papers to be presented must be received by July 6, 1979. All manuscripts must be postmarked by Aug. 31, 1979. For further details, contact: Kathleen Fominaya, AOAC, Box 540, Benjamin Franklin Station, Washington, D.C. 20044.

4th National School/Conference
Australian National University, Canberra, Australia, Feb. 4-8, 1980. Organized by the Australian X-ray Analytical Association. Contributions for the conference are now invited. Title and brief statement (200-300 words) outlining the proposed content to be submitted to the Conference Secretary by 1 August 1979. Further details from: Conference Secretary, AXAA Headquarters, c/o NSW Institute of Technology, P.O. Box 123, Broadway 2007, New South Wales, Australia.

ION? YAG?



We've got 'em all!

Whether you need an argon-krypton ion laser or a solid-state laser, Control Laser Corporation probably has a system to match your scientific/laboratory requirements. For work in the areas of photo-coagulation, blood plasma diagnostics, cauterization, particle analysis, primary pattern generation and the like, our ion laser line offers up to 20 W of output power with primary lines in the blue (488 nm) and the green (514 nm). On the other hand, our cw, pulsed and Q-switched lasers are ideal for tasks such as aligning laser fusion reactors, coherent anti-Stoke Raman spectroscopy, pollution monitoring and bloodless surgery. To make your job even easier, we will incorporate any of the lasers in to a laboratory work station containing (optionally) positioning stages, microscopes, cameras and the like.



For details, contact our Sales Department.



CONTROL LASER CORPORATION
HOLOBEAM LASER, INC. - A Subsidiary

11222 Astronaut Blvd. ■ Orlando, Florida 32809
305/851-2636

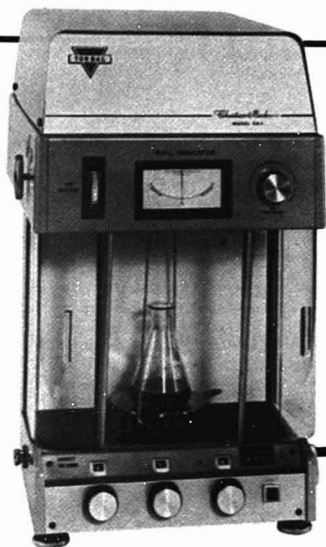
CIRCLE 33 ON READER SERVICE CARD

News

Meetings

- **Scanning Electron Microscopy/** 1979, Apr. 16-20, Sheraton Park Hotel, Washington, D.C. Contact: Om Johari, P.O. Box 66507, AMF O'Hare, Ill. 60666. 312-843-0862
- **International Conference on Electroanalysis in Hygiene, Environmental, Clinical, and Pharmaceutical Chemistry.** Apr. 17-20, Chelsea College, London. Sponsored by Electroanalytical Group, Analytical Div., the Chemical Society. Contact: W. F. Smyth, Dept. of Chemistry, Chelsea College, Manresa Rd., London, England
- **Progress in Chromatography (2nd Danube Symposium).** Apr. 18-20, Carlsbad, Czechoslovakia. Organized by Czechoslovak Chemical Society Chromatography Group. Contact: K. Macek, Institute of Physiology, CSAV, Prague 4, Budejovicka 1083, Czechoslovakia
- **2nd Canadian Chromatography Conference.** Apr. 19-20, Hampton Court Hotel, Toronto, Canada. Contact: Vijay Mohan Bhatnagar, Alena Enterprises of Canada, P.O. Box 1779, Cornwall, Ont. K6H 5V7, Canada
- **Chromatography Workshop.** April 23-24, George Washington Motor Lodge, Fort Washington, Pa. Contact: Frank van Lenten, E. I. du Pont de Nemours & Co., Jackson Labs, CD&P, Wilmington, Del. 19898
- **Symposium on Electron Microscopy and X-Ray Applications to Environmental and Occupational Health Analyses.** Apr. 23-25, Aspen, Colo. Contact: Philip A. Russell, Denver Research Institute, University of Denver, Denver, Colo. 80208
- **3rd International Symposium on Control of Sulfur and Other Gaseous Emissions.** Apr. 24-26, Salford, UK. Contact: R. Hughes, Dept. of Chemical Engineering, University of Salford, Salford, M5 4WT, UK
- **Symposium on Advanced Analytical Concepts for the Clinical Laboratory.** Apr. 26-27, Oak Ridge, Tenn. Contact: Charles D. Scott, Oak Ridge National Laboratory, P.O. Box X, Oak Ridge, Tenn. 37830. Page 1322 A, Dec.
- **70th Annual Meeting of the American Oil Chemists' Society.** Apr. 29-May 3, Fairmont Hotel, San Francisco. Contact: American Oil Chemists' Society, 508 S. Sixth

10 years ago it was the best analytical lab balance around. 2500 units later, the Torbal EA-1 still is.



The "All-American" Balance

Torbal EA-1 has been in continuous production since 1968. Almost every one made in those ten years is still in service, and most with never a service call.

What makes the Torbal so durable—so special—for laboratory use is its friction-free torsion design. There's no damage-prone knife edge to wear, or need replacement. Which is why **the Swiss and German makers are now switching to torsion suspension in their balances.** At Torbal we've been building torsion suspensions for over 80 years.

Unmatched reliability and quality.

Every Torbal balance is "new generation", combining the quality and the reliability of a non-fatiguing torsion band.

Now save as much as \$1000 over copy-cat imports.

The EA-1's combination of uncompromising quality and repair-free operation has always provided for inexpensive, long-run operation. **And right now, thanks to dollar fluctuations, it will cost you a lot less than a copy-cat import.**

We'd like you to see the EA-1. Unfortunately, size, weight and set-up time present some difficulties for your distributor salesman. So drop us a line and tell us where you are. We'll introduce you to a Torbal user in your area for a hands-on demo.

What makes Torbal the best?

- Friction-free torsion design.
- Electronic null indicator for fool-proof readouts.
- Large, easy-to-read digital readouts to 159.9999 grams.
- Accuracy to 0.1 mg without vernier or micrometer readings.
- 8 to 10 grams of infinitely variable dial-in-tare (with extended tare options to 208 grams).
- No knife-edges—no "beam arrest" required.

Write for illustrated brochure or a demonstration.



TORBAL

THE TORSION BALANCE COMPANY

Main Office and Factory: Clifton, N.J. 07012
Sales Offices: Chicago, IL; Temple City, CA

CIRCLE 199 ON READER SERVICE CARD

St., Champaign, Ill. 61820. 217-359-2344

- **3rd International Symposium on Capillary Chromatography.** Apr. 30-May 4. Hindelang, FRG. Contact: R. E. Kaiser, Inst. for Chromatography, P.O. Box 1308, D-6702 Bad Dürkheim-1, Federal Republic of Germany
- **American Society for Microbiology.** May 4-8. Los Angeles. Contact: Richard Bray, 1913 I St., N.W., Washington D.C. 20006
- **AOAC 4th Annual Regional Spring Training Workshop and Exposition.** May 6-9. Sheraton-Palace Hotel, San Francisco. Contact: Paul C. Bolin, Laboratory Director, Food and Drug Administration, 50 U.N. Plaza, San Francisco, Calif. 94102. 415-445-4763
- **9th Annual Symposium on the Analytical Chemistry of Pollutants.** May 7-9. Jekyll Island, Ga. Sponsored by Environmental Protection Agency, University of Georgia, and Environmental and Analytical Chemistry Division of the American Chemical Society. Contact: Elaine P. McGarity, Environ-

mental Research Laboratory, EPA, Athens, Ga. 30605; or Roland Frei, Dept. of Analytical Chemistry, Free University of Amsterdam, De Boelelaan 108, Amsterdam-Buitenveldert, The Netherlands

- **ACS 11th Central Regional Meeting.** May 7-9. Holiday Inn, 328 W. Lane Ave., Columbus, Ohio. Contact: A. Wojcicki, Dept. of Chemistry, Ohio State University, 140 West 18th Ave., Columbus, Ohio 43210. 614-422-4750
- **4th International Symposium on Column Liquid Chromatography.** May 7-10. Boston Park Plaza, Boston. Contact: Barry L. Karger, Chairman, Organizing Committee, 4th International Meeting on Column Chromatography, Northeastern University, Institute of Chemical Analysis, Boston, Mass. 02115
- **25th International Instrumentation Symposium.** May 7-10. Anaheim, Calif. Contact: Instrument Society of America, Test Measurement Div., 11009 Prospect N.E., Albuquerque, N.M. 87112
- **32nd Chemists' Conference.** May 16-17. Royal Hotel, Scarborough.

Contact: K. Speight, Conference Secretary, British Steel Corp., Sheffield Laboratories, Hoyle St., Sheffield, S3 7EY, England

- **Symposium on Progress in Electrochemical Corrosion Testing.** May 20-25. San Francisco, Calif. Contact: Jane B. Wheeler, ASTM, 1916 Race St., Philadelphia, Pa. 19103. 215-299-5413
- **Fifth Biennial Symposium in Clinical Chemistry.** May 21-22. Valley Forge Sheraton, Route 363, King of Prussia, Pa. Contact: Barry N. Elkins, Cochairman, 1979 Symposium Committee, 215-842-6612
- **Workshop on Thermal Analysis.** May 21-22. Gaithersburg, Md. Contact: Oscar Menis, B326 Chemistry Bldg., NBS, Washington, D.C. 20234. 301-921-2175
- **8th IMEKO Congress.** May 21-27. Moscow, USSR. Contact: IMEKO Secretariat, 1371 Budapest, P.O. Box 457, Hungary
- **5th Annual National Meeting of the Clinical Radioassay Society.** May 22-25. Washington, D.C. Contact: 5th CRS Meeting, Box 119, Fairfax, Va. 22030
- **New York Microscopical Society Sessions.** May 30-June 1. Statler Hilton Hotel, New York City. Contact: Ted Rochow, 3008 Charwood Pl., Raleigh, N.C. 27612
- **Chemical Conference of the Chemical Institute of Canada.** June 3-6. University of British Columbia, Vancouver, B.C., Canada. Contact: The Chemical Institute of Canada, 151 Slater St., Suite 906, Ottawa, Ont., K1P 5H3, Canada. 613-233-5623
- **27th Annual Conference on Mass Spectrometry and Allied Topics.** June 3-8. Seattle, Wash. Contact: H. M. Fales, Bldg. 10, Rm. 7N322, National Institutes of Health, Bethesda, Md. 20014
- **National Conference on Synchrotron Radiation Instrumentation.** June 4-6. Gaithersburg, Md. Contact: David Ederer, A251 Physics Bldg., NBS, Washington, D.C. 20234. 301-921-2301
- **ACS 13th Great Lakes Regional Meeting.** June 4-6. Rockford College, Rockford, Ill. Contact: A. A. Schilt, Dept. of Chemistry, Northern Illinois University, DeKalb, Ill. 60115
- **13th Annual Conference on Trace Substances in Environmental Health.** June 4-7. University of Missouri, Columbia. Contact: D. D. Hemphill, Environmental Trace Substances Research Center, Rte. 3, University of Missouri, Columbia, Mo. 65211

**SUB MICRON
PARTICLE SIZE ANALYSIS
DOWN TO 0.01 MICRON
IT'S SIMPLE WITH A JOYCE-LOEBL
DISC CENTRIFUGE 3**

Benefit from the wealth of experience established in our application's laboratory in analysing a wide spectrum of particulate materials. The results are summarised in a free booklet 'APPLICATION REPORTS' covering the following major end-user groups:

• Polymer Emulsions	• Magnetic Iron Oxide
• Inks and Pigments	• Carbon Black
• Titanium Dioxide	• And many others

For your copy circle the reader enquiry card or write to:



JOYCE-LOEBL
Marpleway, Team Valley
Gateshead NW11 0QW
England



**JOYCE
LOEBL**

Vickers Instruments Inc.
100A Commerce Way
Woburn
Massachusetts 01801
U.S.A.

CIRCLE 129 ON READER SERVICE CARD

Great Britain has added a new dimension to our analytical capabilities.

Johnson Matthey Chemicals Limited may not be a "household" laboratory name among American analysts, but it certainly is in the laboratories throughout Europe. That's because this 157-year-old English company has been providing European laboratories with their elements, compounds and capabilities for more than 67 years.

To name a few: SPECPURE

Materials of Defined Analyses:

A range of over 300 high purity substances covering 73 elements suitable for preparation of both solid and solution reference materials for use in instrumental and wet chemical analyses.

SPECPURE Fabricated Metals.

From aluminum to zirconium. Available in rods, wire and sheets.

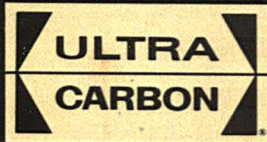
SPECTROFLUX

Analytical Fluxes: 18 standard compositions comprising mainly of alkali boraxes for use in flux fusion dissolution of refractory materials.

SPECTROMEL

Standard Powder Mixtures:

3 compositions which together contain a total of 73 elements which include rare earth and precious metal mixtures for preparation of reference materials in semi-quantitative emission spectrography.



the graphite specialists

CIRCLE 215 ON READER SERVICE CARD

R.U. Powder Mixture:

Containing 49 elements in a base of zinc, magnesium and calcium oxides for use in qualitative emission spectrography.

These are but a few of the capabilities that are now available to you from the company you depend on for ultra-high purity graphite products: Ultra Carbon Corporation, P.O. Box 747, Bay City, Michigan 48707.

SPECURE, SPECTROFLUX and SPECTROMEL are registered trademarks of Johnson Matthey Chemicals Limited.



- **Industrial Trace Analysis.** June 7-8. Vancouver, B.C. Contact: Ian Webber, B.C. Hydro R&D Lab, 8809 Heather St., Vancouver, B.C. V6P 3T1, Canada. 604-327-0211
- **Symposium on Accuracy in Powder Diffraction.** June 11-15. Gaithersburg, Md. Sponsored by NBS, National Research Council of Canada, and International Union of Crystallography. Contact: Stanley Block, A221 Materials Bldg., National Bureau of Standards, Washington, D.C. 20234. 301-921-2837
- **ACS 34th Northwest Regional Meeting.** June 13-15. Holiday Inn, Richland, Wash. Contact: M. H. Campbell, Exxon Nuclear Co., Research & Technology Center, 2955 George Washington Way, Richland, Wash. 99352. 509-943-7309
- **Microprocessors and Industry: Techniques and Applications.** June 18-20. London Press Centre, London. Contact: Carole Meads, Sira Institute Ltd., South Hill, Chislehurst, Kent BR7 5EH, England. 01-467-2636
- **International Symposium on Occupational Radiation Exposure** in Nuclear Fuel Cycle Facilities. June 18-22. Los Angeles, Calif. Contact: John H. Kane, Special Assistant for Conferences, Office for Technical Information, Dept. of Energy, Washington, D.C. 20545
- **10th International Symposium on Chromatography and Electrophoresis.** June 19-20. Venice, Italy. To be held in conjunction with the 6th International Symposium on Mass Spectrometry in Biochemistry and Medicine. Contact: Alberto Frigerio, Istituto di Ricerche Farmacologiche "Mario Negri," Via Eritrea, 62, 20157 Milan, Italy. Page 1322 A, Dec.
- **6th International Symposium on Mass Spectrometry in Biochemistry and Medicine.** June 21-22. Venice, Italy. To be held in conjunction with the 10th International Symposium on Chromatography and Electrophoresis. Contact: Alberto Frigerio, Istituto di Ricerche Farmacologiche "Mario Negri," Via Eritrea, 62, 20157 Milan, Italy. Page 1323 A, Dec.
- **72nd Annual Meeting of the Air Pollution Control Association.** June 24-28. Cincinnati Convention Center, Cincinnati. Contact: Air Pollution Control Assoc., P.O. Box 2661, Pittsburgh, Pa. 15230. 412-621-1090
- **Joint Congress on Clinical Chemistry.** June 25-29. Montreal, Que., Canada. Contact: Claire DuPont, Dept. of Biochemistry, Montreal Children's Hospital, 2300 Tupper St., Montreal, Que., Canada H3H 1P3
- **32nd Annual Summer Symposium on Analytical Chemistry.** June 27-29. Purdue University, West Lafayette, Ind. Contact: Fred E. Lytle, Chemistry Bldg., Purdue University, West Lafayette, Ind. 47907
- **XXI Colloquium Spectroscopicum Internationale—8th International Conference on Atomic Spectroscopy.** Jul. 1-6. Cambridge, England. Sponsored by the Royal Society, the Chemical Society, and the Institute of Physics. Contact: Association of British Spectroscopists, XXI CSI/8th ICAS, P.O. Box 109, Cambridge CB1 2HY, UK. Page 866 A, August
- **World Spectroscopy Conference.** Jul. 2-3. Sheraton Hotel, Lisbon,

INTRODUCING OmniSolvTM The new high purity, glass

OmniSolvTM Now there's only one name you need to remember for virtually all your solvent needs — OmniSolv. It's MCB's new line of multi-purpose, glass-distilled solvents. Forget about being understocked or overstocked with a different solvent for each application. There's always a fresh supply of OmniSolv as handy as your local MCB distributor. And you'll be pleased to find it's competitively priced.

MCB guarantees OmniSolv to be of the highest purity and to fulfill all the requirements for:

Portugal. Contact: Vijay Mohan Bhatnagar, Alena Enterprises of Canada, P.O. Box 1779, Cornwall, Ont. K6H 5V7, Canada

- **Third European Congress of Clinical Chemistry.** Jul. 3-8. Brighton, UK. Contact: P. J. N. Houarth, Dept. of Chemical Pathology, Guys Hospital Medical School, London SE1 9RT, UK
- **2nd World Chromatography Conference.** Jul. 5-6. Sheraton Hotel, Lisbon, Portugal. Contact: Vijay Mohan Bhatnagar, Alena Enterprises of Canada, P.O. Box 1779, Cornwall, Ont. K6H 5V7, Canada
- **AACC 31st National Meeting.** Jul. 15-20. New Orleans, Louisiana. Contact: AACC National Office, 1725 K St., N.W., Washington, D.C. 20006. 202-857-0717
- **National Conference on Weights and Measures.** Jul. 22-27. Portland, Ore. Contact: Harold Wollin, A211 Metrology Bldg., NBS, Washington, D.C. 20234. 301-921-3677
- **21st Rocky Mountain Conference on Analytical Chemistry.** Jul. 30-Aug. 1. Sponsored jointly

by Rocky Mountain Society of Applied Spectroscopy and Rocky Mountain Chromatography Discussion Group. Contact: H. E. Taylor, U.S. Geological Survey, 5293 Ward Rd., Arvada, Colo. 80002. Page 1323 A, Dec.

- **28th Denver Conference on Applications of X-Ray Analysis.** Jul. 30-Aug. 3. University of Denver. Contact: Mildred Cain, Denver Research Institute, University of Denver, Denver, Colo. 80208. 303-753-2141
- **Photo/Optoacoustic Spectroscopy and Detection.** Aug. 1-3. Iowa State University. Sponsored by the Optical Society of America and the Ames Laboratory-USDOE. Contact: The Optical Society of America, Suite 620, 2000 L St., N.W., Washington, D.C. 20036. 202-293-1420
- **Combined 37th Annual Meeting of the Electron Microscopy Society of America and 13th Annual Meeting of the Microbeam Analysis Society.** Aug. 13-17. San Antonio, Tex. Contact: Dale Newbury, Chairman, MAS Program Committee, NBS, Bldg. 222, Room

A121, Washington, D.C. 20234. 301-921-2875

- **1979 Symposium on Instrumentation and Control for Fossil Energy Processes.** Aug. 20-22. Denver Marriott, Denver. Topics include two-phase interface level measurement, on-line analysis and sampling, flow control systems, and reactor temperature measurement. Contact: M. L. Holden, Director, Conference Planning and Management, Argonne National Laboratory, Bldg. 223, 9700 S. Cass Ave., Argonne, Ill. 60439. 312-972-5585
- **5th Australian Symposium on Analytical Chemistry.** Aug. 20-24. Perth, Western Australia. Contact: Barry Codling, Analytical Division, Royal Australian Chemical Institute, 30 Plain St., Perth, Western Australia 6000
- **International Conference on Liquid Scintillation Counting: Recent Applications and Development.** Aug. 21-24. University of California at San Francisco. Contact: C. T. Peng, School of Pharmacy, University of California, San Francisco, Calif. 94143
- **27th IUPAC Congress.** Aug. 27-

OmniSolv

distilled solvent from MCB.

- Spectrophotometry • Chromatography • HPLC • Residue Analysis
- Pesticide Analysis • Gas Chromatography

For more information on the full OmniSolv line, consult your copy of the 1979 MCB Buying Guide. Then place your order with your local MCB distributor. For the name and address of the distributor nearest you,

write: MCB Reagents,
2909 Highland Avenue,
Cincinnati, Ohio 45212

MCB Reagents

Associate of E. Merck, Darmstadt, Germany



31. Helsinki, Finland. Contact: J. Larinkari, P.O. Box 244, SF-00131 Helsinki 13, Finland
- **XIV European Congress on Molecular Spectroscopy**, Sept. 3-7. Frankfurt/Main, Federal Republic of Germany. Contact: Sec'y Gen., EUC/MOS 1979, Gesellschaft Deutscher Chemiker, J. Wendenburg, P.O.B. 90 04 40, D-6000 Frankfurt (Main) 90, West Germany
- **3rd International Bioanalytical Forum**, Sept. 4-7. Guildford, UK. Contact: E. Reid, Wolfson Bioanalytical Centre, University of Surrey, Guildford GU2 5XH, UK
- **17th ACS National Meeting**, Sept. 9-14. Washington, D.C. Contact: A. T. Winstead, ACS, 1155 Sixteenth St., N.W., Washington, D.C. 20036. 202-872-4397
- **Symposium on Atomic Spectroscopy**, Sept. 10-14. Tucson, Ariz. Contact: J. O. Stoner, Dept. of Physics, University of Arizona, Tucson, Ariz. 85721
- **International Conference on Flow Analysis**, Sept. 11-13. Amsterdam, The Netherlands. Contact: Secretary FA-Amsterdam, Laboratory for Analytical Chemistry, University of Amsterdam, Nieuwe Achtergracht 166, 1018 WV Amsterdam, The Netherlands
- **6th Annual Meeting of the Federation of Analytical Chemistry and Spectroscopy Societies (FACSS)**, Sept. 16-20. Philadelphia, Pa. Contact: P. D. LaFleur, Director, Center for Analytical Chemistry, NBS, Washington, D.C. 20234. 301-921-2851
- **9th North American Thermal Analysis Society Meeting**, Sept. 23-26. Holiday Inn City-Centre, Chicago. Contact: Barbara L. Fabricant, Glass Thermochemistry R&D, Owens-Corning Fiberglass Technical Center, P.O. Box 415, Granville, Ohio 43023. 614-587-0610
- **2nd European Symposium on Particle Characterization**, Sept. 24-26. Nuremberg, West Germany. Contact: Secretariat, NMA Nurnberger Messe-und Ausstellungs-gesellschaft mbH, Messezentrum, D 8500 Nuremberg, West Germany
- **14th International Symposium on Advances in Chromatography**, Sept. 24-28. Lausanne, Switzerland. Contact: A. Zlatkis, Chemistry Dept., University of Houston, Houston, Tex. 77004. 713-749-2623
- **3rd Annual Arnold O. Beckman Conference**, Oct. 2-5. Colorado Springs, Colo. Contact: Michele Tuttle, Meeting Coordinator, AACC, 1725 K St., N.W., Washington, D.C. 20006
- **ACS 9th Northeast Regional Meeting**, Oct. 2-5. Hotel Syracuse, N.Y. Contact: R. J. Conan, Jr., Dept. of Chemistry, LeMoyne College, Syracuse, N.Y. 13214. 315-446-2882
- **23rd ORNL Conference on Analytical Chemistry in Energy Technology**, Oct. 9-11. Gatlinburg, Tenn. Contact: W. S. Lyon, Oak Ridge National Laboratory, P.O. Box X, Oak Ridge, Tenn. 37830
- **3rd Symposium on Biological/Biomedical Applications of Liquid Chromatography**, Oct. 11-12. Boston. Contact: Gerald L. Hawk, Waters Associates, Milford, Mass. 01757
- **1979 Midwestern Universities Analytical Chemistry Conference**, Oct. 11-13. University of Illinois at Urbana-Champaign. Contact: Kelsey D. Cook, School of Chemical Sciences, Dept. of Chemistry, Roger Adams Laboratory, Urbana, Ill. 61801
- **ACS 15th Western Regional Meeting**, Oct. 17-19. North Hollywood, Calif. Contact: J. Quaglino, 5943 Lubao Ave., Woodland Hills, Calif. 91364
- **International Exhibition on Laboratory Technology, Analyses, Procedures, and Automation in Chemistry**, Oct. 17-20. Graz, Austria. Contact: Media Consult GmbH, Kongresse und Ausstellungen, Conventions and Exhibitions, Klopstockgasse 34, Postfach 404, A-1171 Vienna, Austria
- **18th Annual Meeting of ASTM Committee E-19 on the Practice of Chromatography**, Oct. 21-24. Philadelphia. Contact: Tim Bradley, Spectra-Physics, 2905 Stender Way, Santa Clara, Calif. 95051
- **Instrument Society of America Conference & Exhibit**, Oct. 22-25. O'Hare Exposition Center, Chicago. Contact: ISA, 400 Stanwix St., Pittsburgh, Pa. 15222
- **Expochem 79**, Oct. 22-25. Houston, Tex. Contact: A. Zlatkis, Chemistry Dept., University of Houston, Houston, Tex. 77004. 713-749-2623
- **International Liquid Chromatography Symposium III—LC Analysis of Polymers and Related Materials**, Oct. 24-25. Strasbourg, France. Contact: Jack Cases, Waters Associates, Inc., 34 Maple St., Milford, Mass. 01757
- **ACS 31st Southeastern Regional Meeting**, Oct. 24-26. Roanoke, Va. Contact: J. Wolfe, Virginia Polytechnic Institute and State University, Blacksburg, Va. 24060
- **Separation Science and Technology for Energy Applications**, Oct. 30-Nov. 2. Gatlinburg, Tenn. Contact: A. P. Malinauskas, General Chairman, Oak Ridge National Laboratory, P.O. Box X, Oak Ridge, Tenn. 37830
- **Society of Forensic Toxicologists Annual Meeting**, Oct. 31-Nov. 2. Williamsburg, Va. Contact: R. V. Blanke, Medical College of Virginia, MCV Station, Box 696, Richmond, Va. 23298
- **Eastern Analytical Symposium**, Oct. 31-Nov. 2. Hotel Americana, New York City. Contact: Ivor L. Simmons, c/o M&T Chemicals, Inc., P.O. Box 1104, Research Laboratory, Rahway, N.J. 07065. 201-499-2464
- **ACS 15th Midwest Regional Meeting**, Nov. 7-10. Chase-Park Plaza Hotel, St. Louis. Contact: T. P. Layloff, National Center for Drug Analysis, FDS, 1114 Market St., Room 1002, St. Louis, Mo. 63101. 314-425-4135
- **American Nuclear Society Conference on "Measurement Technology for Safeguards and Materials Control"**, Nov. 26-29. Kiawah Island, Charleston, S.C. Contact: Tom Canada, Los Alamos Scientific Lab, MS-540, Los Alamos, N.M. 87544
- **ACS 35th Southwest Regional Meeting**, Dec. 5-7. Villa Capri Motor Hotel and Joe C. Thompson Conference Center, University of Texas, Austin. Contact: R. M. Gipson, Jefferson Chemical Co., P.O. Box 4128, Austin, Tex. 78765. 512-459-6543

Short Courses

ACS Courses. For more information, contact: Department of Educational Activities, American Chemical Society, 1155 Sixteenth St., N.W., Washington, D.C. 20036. 202-872-4508

Maintaining and Troubleshooting Chromatography Systems Workshop

Boston, May 5-6; Philadelphia (ASTM E-19 Meeting), Oct. 20-21. Q. Walker, M. T. Jackson, and M.P.T. Bradley. \$250, ACS members; \$300, nonmembers.

**now...
the complete spectrum
of GC capability**



**NEW HP 5880A
GAS CHROMATOGRAPH**

HEWLETT  PACKARD

NEW HP 5880A GAS

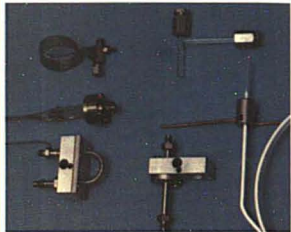
...tomorrow's gas ch

the most versatile and expandable gas ch



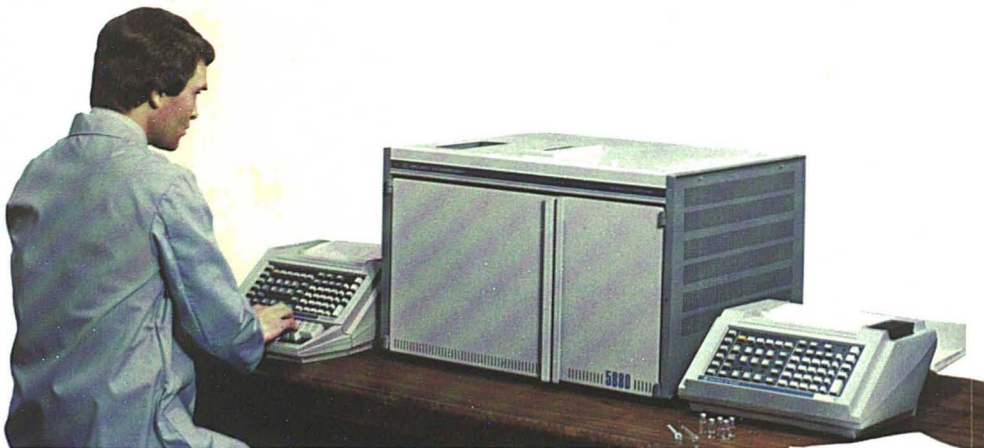
Unequalled **EXPANDABILITY** through four levels of friendly, functional keyboards for your needs . . . today and tomorrow

You can start with LEVEL 1, a simple, single-detector isothermal instrument with high-speed printer/plotter (35 characters per second) and retention time labeling. From there, you can upgrade through each level to a multi-detector, temperature programmed instrument with data handling and programming capabilities. Each level has numerous hardware and software options and can be upgraded to the next level without redundancy. An optional alpha/numeric keyboard provides report annotation, plus BASIC programming. A powerful HP cartridge tape unit allows off-line storage of information.



Accepts a wide range of optional accessories for extraordinary **VERSATILITY**

A wide range of all-glass accessories, cold trap and auxiliary oven, open up new application possibilities. In addition, six heated zones provide ample reserves for heated accessories such as transfer lines for sample collection, and catalyst tube for methanation of CO and CO₂ to improve minimum detectable limits.



S CHROMATOGRAPH

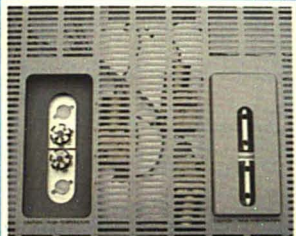
chromatograph today

chromatography system in the world today



Advanced AUTOMATION for easy operation

- The HP automatic sampler with cleverly designed injection-port-to-injection-port transport mechanism is keyboard controlled for automatic selection of all operating parameters.
- All GC functions are controllable through BASIC. New concepts in automation become feasible, including self-optimization of operating conditions.



Unmatched FLEXIBILITY with universal hardware mounting

This system permits simultaneous installation of glass capillary and conventional injection ports. Up to four single or two dual detectors can be accommodated. Choose from a wide range of detectors including new single-filament, inert TC Detector and FI Detector with auto-ignition. Up to four valves may be used in heated auxiliary zones between injection ports and detectors.



Brand new INTERFACING capabilities

- External connectors provide direct interfacing with HP 3350 Lab Automation Systems.
- The instrument's advanced design allows an additional conventional GC to use simultaneously all the data processing power of the HP 5880A, including BASIC.

the first and only microprocessor, keyboard-operated GC system with all these features . . .

- Multiple-channel capability with two printer/plotters
- Total instrument and sampler control through BASIC
- Two-channel, post run integrator and previously unavailable calibration procedures
- Large four column oven



Chemical Abstracts Workshops
Philadelphia, May 10-11; Los Angeles, June 7-8. CA staff. \$75, ACS members; \$135, nonmembers

Creative Problem Solving
Philadelphia, May 10-11. Moshe Rubinstein. \$225, ACS members; \$265, nonmembers

Interpretation of NMR Spectra
Philadelphia, May 10-12. LeRoy Johnson and Roy Bible. \$295, ACS members; \$340, nonmembers

Capillary Gas Chromatography
Philadelphia, May 11-12. S. P. Cram and Milos Novotny. \$250, ACS members; \$300, nonmembers

Gas Chromatography
Chicago, May 18-19; Atlanta, June 14-15. R. A. Keller and M. F. Burke. \$225, ACS members; \$265, nonmembers

Federal Regulations in the Chemical Industry
Chicago, May 18-19; Washington, D.C. (178th ACS National Meeting), Sept. 8-9. G. S. Dominguez. \$225, ACS members; \$265, nonmembers

Toxicology for Chemists
Chicago, May 22-24. Morris Joselow. \$485, ACS members; \$555, nonmembers

Planning for Safe Laboratory Handling of Highly Toxic Chemicals
Chicago, May 30-June 1. N. V. Steere and Maurice Golden. \$295, ACS members; \$340, nonmembers

Safety and Health for Academic Chemistry Laboratories
Chicago, June 2-3. N. V. Steere. \$130, ACS members and nonmembers

Liquid Chromatography, Theory and Practice
Blacksburg, Va. June 4-7, Dec. 10-13. H. M. McNair. \$450, ACS members; \$510, nonmembers

High-Pressure Liquid Chromatography Apparatus Workshop
Los Angeles, June 7-8; Philadelphia (FACSS Meeting), Sept. 15-16. D. H. Freeman. \$250, ACS members; \$300, nonmembers

Multinuclear NMR Spectroscopy
Los Angeles, June 7-9; Tallahassee, Fla., June 14-16. G. C. Levy. \$295, ACS members; \$340, nonmembers

Microprocessors and Minicomput-

ers—Interfacing and Applications
Blacksburg, Va. June 10-15, Sept. 23-28, Dec. 9-14. R. E. Dessy and the Chemistry Dept. Instrument and Design Group of VPI&SU. \$455, ACS members; \$515, nonmembers

Atomic Absorption Spectroscopy
Atlanta, June 14-15. Samuel Koirtyo-hann, Michael Epstein, and Theodore Rains. \$245, ACS members; \$290, nonmembers

Design and Analysis of Industrial Experiments
Atlanta, June 14-16; Philadelphia (FACSS Meeting), Sept. 14-16. John Hromi. \$295, ACS members; \$340, nonmembers

Carbon-13 NMR Spectroscopy
Washington, D.C. (178th ACS National Meeting), Sept. 7-9. G. C. Levy and Paul Ellis. \$295, ACS members; \$340, nonmembers

Effective Writing for Scientists and Engineers
Washington, D.C. (178th ACS National Meeting), Sept. 7-9. Henrietta Tichy and Sylvia Fourdrinier. \$295, ACS members; \$340, nonmembers

High-Performance Management
Washington, D.C. (178th ACS National Meeting), Sept. 8-9. J. H. Morrison. \$225, ACS members; \$265, nonmembers

Electroanalytical Chemistry
Philadelphia (FACSS Meeting), Sept. 14-16. Dennis Evans and P. E. Whitson. \$295, ACS members; \$340, nonmembers

Laboratory Automation: Micro-, Mini-, or Midcomputers?
Philadelphia (FACSS Meeting), Sept. 15-16. R. E. Dessy and the Chemistry Dept. Instrument and Design Group of VPI&SU. \$225, ACS members; \$265, nonmembers

Thermal Methods of Analysis
Philadelphia (FACSS Meeting), Sept. 15-16. W. W. Wendlandt and I. M. Sarason. \$225, ACS members; \$265, nonmembers

Gas Chromatography, Theory and Practice
Blacksburg, Va. Sept. 24-27. H. M. McNair. \$425, ACS members; \$485, nonmembers

Introduction to Gas Chromatography

Blacksburg, Va. May 9-11. *Contact:* David Stafford, Chemical Services Group, Box 63626, 800 Madison Ave., Memphis, Tenn. 38163

9th Gas Chromatography, Lecture and Laboratory
Villanova University, Villanova, Pa. May 16-18, \$100, \$125 (after April 15); May 18-19, \$60, \$80 (after April 15). *Contact:* R. L. Grob, Chemistry Dept., Villanova University, Villanova, Pa. 19085. 1-215-527-2100, exts. 496, 480, 481

Microprocessors for Scientists
University of British Columbia, Vancouver, B.C., Canada (62nd Annual Conference of the Chemical Institute of Canada), June 2-3. \$100, CIC members; \$125, nonmembers. *Contact:* Gary Horlick, Dept. of Chemistry, University of Alberta, Edmonton, Alt., T6G 2G2, Canada

X-ray Spectrometry and X-ray Powder Diffraction
University of Denver, Jul. 23-27. C. S. Barrett, D. E. Leyden, C. O. Ruud, J. J. Fitzpatrick, and specialists from industry. *Contact:* Mildred Cain, Denver Research Institute, University of Denver, Denver, Colo. 80208. 303-753-2141

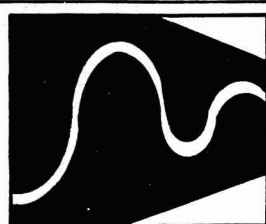
Interpretation of Infrared and Raman Spectra
Fisk University, Nashville, Tenn. Jul. 23-27. \$275. *Contact:* Nelson Fuson, Director, Fisk Institute, Box 8, Fisk University, Nashville, Tenn. 37203

Gas-Liquid Chromatography
Fisk University, Nashville, Tenn. Jul. 23-27. \$275. *Contact:* Nelson Fuson, Director, Fisk Institute, Box 8, Fisk University, Nashville, Tenn. 37203

Pollution Evaluation
Fisk University, Nashville, Tenn. Jul. 23-27. \$275. *Contact:* Nelson Fuson, Director, Fisk Institute, Box 8, Fisk University, Nashville, Tenn. 37203

For Your Information

Chromatography Newsletters, Vol. 6, No. 3, is available from the Perkin-Elmer Corp. The titles of the four articles in this Oct. 1978 issue are: Determination of volatile halogenated hydrocarbons in environmental water by glass capillary column gas chromatography and electron capture detection; a variable all-glass effluent splitter for



New Applications of Lasers to Chemistry

ACS Symposium Series No. 85

Gary M. Hietje, Editor
Indiana University

Based on a symposium sponsored by the Division of Analytical Chemistry of the American Chemical Society.

This collection of 12 papers represents an excellent cross section of topics depicting the scope of current applications of lasers to chemistry and the potential importance of lasers in the future of chemistry and chemical analysis.

Chemists, physicists, and engineers from academia, industry, and government give a precise account of the latest developments in laser technology and measurement systems as well as the use of lasers in detecting single atoms and molecules.

The book's main subject material reflects areas of chemistry in which the laser has had the greatest impact — namely, high-resolution spectroscopy, high sensitivity analysis, time-resolved or kinetic spectroscopy, and new techniques in laser Raman spectrometry.

CONTENTS

Selective Excitation of Probe Ion Luminescence (SEPI) • Applications of Tunable-Diode-Laser IR Spectroscopy to Chemical Analysis • Two-Photon-Excited Molecular Fluorescence • Laser-Excited Luminescence Spectrometry • Laser Fluorimetry: Detection of Aflatoxin B₁ in Contaminated Corn • Laser-Enhanced Ionization for Trace Metal Analysis in Flames • The Study of Biological Surfaces by Laser Electrophoretic Light Scattering • New Laser-Based Methods for the Measurement of Transient Chemical Events • Laser Applications in Photoelectrochemistry • Coherent Anti-Stokes Raman Scattering Spectroscopy • Spectroscopy by Inverse Raman Scattering • Vibrational Spectra in Nanosecond

244 pages (1978) Clothbound \$23.50
LC 78-22032 ISBN 0-8412-0459-4

SIS/American Chemical Society
1155 16th St., N.W./Wash., D.C. 20036

Please send _____ copies of SS 85 *New Applications of Lasers to Chemistry* (ACI 0459-4) at \$23.50 per copy.

☐ Check enclosed for \$_____. ☐ Bill me.
Postpaid in U.S. and Canada plus 75¢ elsewhere.
California residents please add 6% state use tax.

Name _____
Address _____
City _____ State _____ Zip _____

News

dual-detector operation and collection of GC fractions; the determination of traces of oxygen in vinyl chloride; and drug analysis by chromatography, a review. For a free copy, ask for order no. CHN-12 from Perkin-Elmer Corp., Instrument Division, Main Avenue, Mail Station 12, Norwalk, Conn. 06856. 203-762-6853

An analytical service that quickly determines if processed sugar derivatives have been added to natural fruit sugar products is available from **Geochron Laboratories** of Cambridge, Mass. Utilizing modified mass spectrometry equipment, Geochron Laboratories SIRA (stable isotope ratio analysis) has been approved on a first action basis by Federal agencies including FDA and the U.S. Customs Dept. The price is \$45/sample. For more information, contact: Geochron Laboratories, Division of Krueger Enterprises, Inc., H. W. Kreuger, 24 Blackstone St., Cambridge, Mass. 02139. 617-876-3691

A tentative standard that presents guidelines for the maintenance and service of clinical laboratory instruments is now available to the clinical laboratory community. Entitled "Guidelines for Service of Clinical Laboratory Instruments" (TSI-6), it provides the user of clinical laboratory instruments with a point-by-point outline of the specific types of training, maintenance, repairs, and service that a manufacturer may be expected to supply. Copies of TSI-6 are available at \$11 from NCCLS, 771 East Lancaster Avenue, Villanova, Pa. 19085.

Two courses, **Strategy of Experimentation and Strategy of Formulations Development**, will be held by the Du Pont Co. during 1979. The former course consists of 2½ days of seminars and workshops on the use of statistical methods for effective, well-designed experimentation. The latter course, 2½ days, teaches students to use statistics to develop formulations or mixtures that provide the best balance between product properties and manufacturing cost. Course schedules and other information may be obtained by writing to: Seminars, Du Pont Co., Rm B-1370, Applied Technology Division, Wilmington, Del. 19898. 302-774-6406

Pye Unicam Ltd., of Cambridge, England, is holding a series of analytical symposia during April and May 1979 in London, Manchester, and Glasgow. Lectures will be given in the fields of

GC, LC, AA, IR, and UV/VIS. For further information, call: T. Proctor or S.C.L. Webb at 0223 58866, ext. 25/26.

Analytical Express Service provides direct contact with Rice Division's laboratories for the analysis of regulated parameters of water and wastewater. The division laboratories offer GC/MS/data system, GC, and AA with flameless atomizers. For more information, call Analytical Express Service at 800-245-2730.

The guide, **Chemical Industries Information Sources** (595 pp, \$22), provides an indication of the broad range of data and information available from a variety of disciplines. In addition to published materials, this work furnishes details on numerous organizations and other sources of information on chemical and related industries. For further information, contact: Gale Research Co., Promotion Dept., Book Tower, Detroit, Mich. 48226.

A report from the IUPAC journal *Pure and Applied Chemistry*, Vol. 50, Nos. 11/12 (1978), entitled **Standard Potential of the Silver-Silver Chloride Electrode** is available. The report was prepared by the IUPAC Commission on Electroanalytical Chemistry. Copies of reprints may be obtained from: Chairman of the Commission, R. G. Bates, University of Florida, Gainesville, Fla. 32611.

Definitions of chemical terms are recommended in three reports published by IUPAC. Comments and suggestions are solicited from all chemists so that a final definitive report can be published. The three provisional reports soon to be published are in electroanalytical chemistry, polymer chemistry, and in thermodynamics. For further information, contact: Martin Gellender, Information Officer/Editor, Bank Court Chambers, 2-3 Pound Way, Cowley Centre, Oxford OX4 3YF, UK.

Growth in the sales of sophisticated instruments, especially overseas, has prompted EG&G, Inc., producer of research and health industry instruments, to form **EG&G Instruments, Inc.** The new worldwide marketing organization will handle the products of EG&G Princeton Applied Research Corp. and Brookdeal Electronics, an EG&G subsidiary in England. The new combined sales organization became effective Jan. 1, 1979.

THE ONLY WAY TO GET A TRACE THIS ACCURATE AND CRISP FROM A GOULD RECORDER IS TO USE ACCUCHART PAPER.

Gould Inc., Instruments Division

THE ONLY WAY.

That's because Accuchart paper is specially designed and produced by Gould for use in Gould recorders.

Only with Accuchart can you be certain of getting the precise and permanent traces Gould recorders are capable of producing. Unlike other papers, Accuchart will not compromise the accuracy or reliability of Gould recorders.

Just check some of these outstanding features Accuchart—and only Accuchart—can offer. Writing surfaces are exceptionally smooth and specially processed to instantly accept the trace with minimal pen friction. Exclusive formulas insure high tensile strength and dimensional stability. Overall accuracy of printed grid lines is better than 0.15% of any dimension.

Accuchart papers are available in many configurations, including semi-perforated chart rolls for use with either automatic Z-Folder or manually. And you can count on Gould's on-time delivery.

So remember. To get the finest quality traces from Gould recorders, use Accuchart paper. Easily identified by the Accuchart name on every roll. For more information, send for our free handy pocket guide by calling Gould toll free at (800) 325-6400, ext. 77. (In Missouri: (800) 342-6600). Or write Gould Inc., Instruments Division, 3631 Perkins Ave., Cleveland, Ohio 44114.



GOULD

An Electrical/Electronics Company

CIRCLE 85 ON READER SERVICE CARD

JFK Assassination: Bullet Analyses

Vincent P. Guinn

Department of Chemistry
University of California
Irvine, Calif. 92717



The world was shocked on November 22, 1963, when President John F. Kennedy was assassinated by rifle fire in Dallas, Tex. It rapidly became clear that either some or all of the bullets were fired at the President's motorcade limousine from a corner room on the sixth floor of the Texas School Book Depository, just after the motorcade turned onto Elm Street in Dealey Plaza. Within about 2 h after the shooting, Lee Harvey Oswald was captured a few miles away, but only after he had fired four revolver shots into Officer J. D. Tippit, killing him instantly. Initially arrested for the killing of Officer Tippit, it soon became evident that Oswald was probably also the assassin of President Kennedy. A search of the Book Depository sixth floor room resulted in the finding of three spent Western Cartridge Co. (WCC) 6.5-mm Mannlicher-Carcano (MC) cartridge cases on the floor of the room, and an Italian-made Mannlicher-Carcano military rifle with one unfired cartridge of the same type still in the gun. Oswald, an em-

ployee of the Book Depository, had been seen there that morning and also a few minutes after the assassination—disappearing soon thereafter.

During the next 48 h, Oswald was interrogated repeatedly, but consistently denied having killed either the President or Officer Tippit. While the investigation was still in progress, Oswald was shot and killed by Jack Ruby while Oswald was being transferred to other quarters.

Warren Commission Investigation

Within days, numerous rumors were afoot that Oswald was part of a conspiracy to assassinate the President, and that he had one or more confederates, firing from the same location or from another location. The facts, soon unearthed, that Oswald was an avowed Marxist, had recently lived for about three years in the Soviet Union where he married a Russian (Marina), and was an outspoken supporter of Fidel Castro's Cuba, led many people to suspect an international conspiracy. To investigate all of these possibilities in depth, and to provide the American public with a factual analysis of the assassination, the new President, Lyndon B. Johnson, appointed a Presidential Commission to conduct a thorough investigation of all aspects of the assassination. Headed by then Chief Justice Earl Warren, the 7-member Commission became known as the Warren Commission. Constituted only one week after the assassination, it conducted a 10-month investigation assisted mainly by the FBI, and published its findings in September of 1964 in the famous Warren Commission Report.

In this investigation, the Mannlicher-Carcano rifle was definitely proved to belong to Oswald (his palm print was found on it), the three recovered cartridge cases were proved to

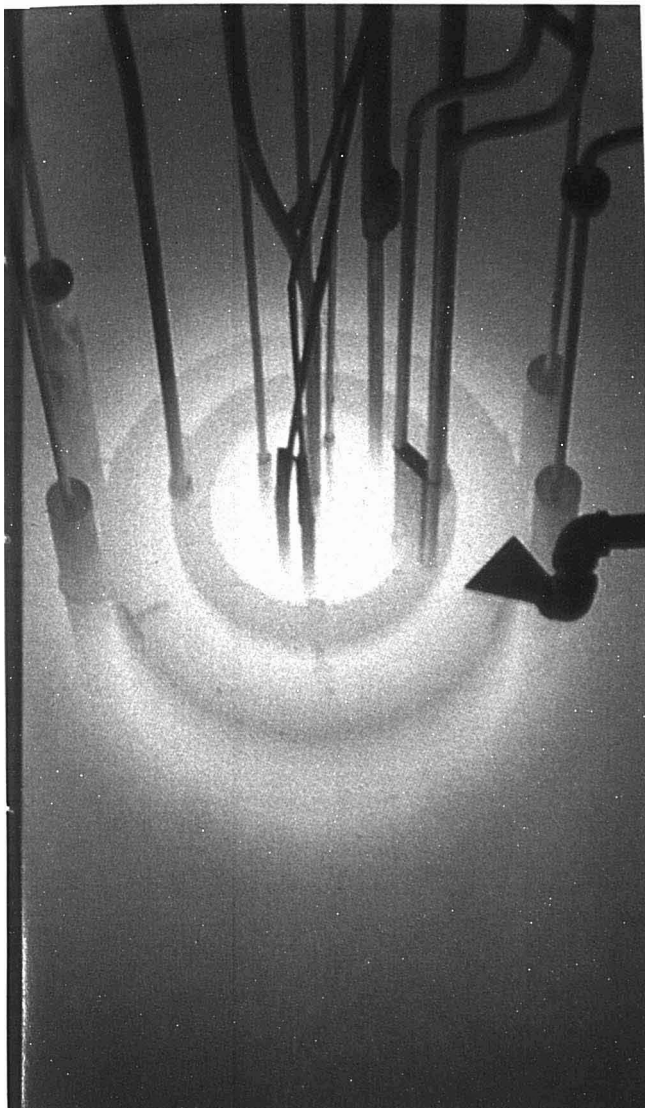
have been fired from it, and the almost undamaged copper-jacketed bullet found on Governor Connally's stretcher at the Parkland Memorial Hospital in Dallas and two large pieces (a nose portion and a base portion) of copper-jacketed bullet(s) found in the President's limousine were all shown to have been fired from that particular rifle. Clearly, Oswald appeared to be either the lone assassin or at least one of the assassins.

1963-1964 Analyses

All of the analytical measurements conducted by the Dallas police (inconclusive dermal nitrate tests run on paraffin casts taken of Oswald's hands and his right cheek soon after he was apprehended) and by the FBI Laboratory shed very little light on the subject. The FBI took the Oswald paraffin casts to the Oak Ridge National Laboratory and analyzed them by neutron activation analysis (NAA) for the possible presence of primer residue (barium and antimony) (1) still there even after the Dallas dermal nitrate tests. This effort was thwarted by the fact that the casts were badly contaminated, essentially as much Ba and Sb being found on the outside surfaces of the casts as on the inside surfaces—which had been in contact with Oswald's skin. The right cheek cast, if it had not been contaminated by improper previous handling, might have established that Oswald had very recently fired a rifle. The FBI Laboratory also analyzed the various bullet fragments recovered from the Dallas limousine, President Kennedy's brain, and Governor Connally's wrist plus the bullet recovered from his stretcher. These specimens were analyzed by emission spectrography. The results showed that all of the bullet-lead specimens were qualitatively generally "similar" in elemental composition,

The Analytical Approach

Edited by Claude A. Lucchesi



The core of the U.C. Irvine TRIGA Mark I nuclear reactor

and "could be" all of the same brand of ammunition. That was all of the chemical analysis work cited in the Warren Commission Report.

Surprise Letter Found in the National Archives

For a number of years after publication of the Warren Commission Report, the author, several other forensic scientists, and various critics of the Commission urged that the Dallas bullet-lead evidence specimens should be examined in more quantitative detail by some more powerful method, such as NAA, to test the Commission's conclusion that all of the specimens recovered were fired only by Oswald. The FBI, under J. Edgar Hoover, declined or ignored all such suggestions. And then a great surprise occurred late in 1973, almost 10 years after the assassination—a letter from J. Edgar Hoover to the Warren Commission, dated July 8, 1964, turned up in the National Archives. This hitherto unknown letter disclosed the fact that, after the generally not very informative emission spectrographic analyses, the bullet-lead specimens had been analyzed by the FBI, using the NAA method. The letter contained no numerical results at all, but merely stated that the NAA results were also inconclusive, and did not allow one to discern how many bullets were represented by the various recovered fragments, although it did state that some compositional differences were found. Why Mr. Hoover chose not to reveal that these NAA measurements had been made, and why there is no mention of them in the Warren Commission Report, is still a mystery.

1964 FBI NAA Data

Working with John Nichols, a forensic pathologist at the University of



Little things mean a lot in HPLC

Inlet filters. Rheodyne inlet filters can be connected between the sample injection valve and the column to protect the column from plugging. The 2 micron filter element prevents plugging caused by particles in the samples or by injection valve wear particles. Pressure rating of the filter assembly is 7000 psi (500 bar). Only type 316 stainless steel and PTFE contact the stream.

U.S. prices are \$45 for the Model 7302 Column Inlet Filter and \$20 for a package of 5 2 µm filter elements and gaskets.


Pressure Relief Valve. Rheodyne's Model 7037 Pressure Relief Valve protects your equipment against damage from over-pressure. You can set it anywhere in the range of 2000 to 7000 psi (140 to 500 bar). U.S. price is only \$270. So, when you consider the fact that you can blow a pressure gauge in less than 1 second, it's a real bargain.

Teflon Rotary Valves. Type 50 Rheodyne Valves are real workhorse accessories for your LC equipment.

Use them for sample injection, column switching, recycling, reagent switching, fraction collection, stream sampling and quantitative reagent injection. Available in four different versions, these valves are chemically inert with zero dead volume, operate at 300 psi. They are offered in 0.8 or 1.5 mm bore and in either manual or automatic versions.

U.S. price of 0.8 mm bore 3 and 4-way valves is \$80. The 6-position and sample injection valves are priced at \$95. Cost of 1.5 mm bore valves is \$2 more.

Write for more data. For full information, please address Rheodyne, Inc., 2809 Tenth Street, Berkeley, CA 94710. Phone (415) 548-5374.


RHEODYNE
THE LC CONNECTION COMPANY
CIRCLE 183 ON READER SERVICE CARD

Kansas Medical School, I joined in efforts to obtain a copy of the 1964 NAA data obtained by the FBI on the bullet-lead specimens. This also proved to be a slow uphill battle. Finally, and only by taking legal action under the amended Freedom of Information Act, Dr. Nichols succeeded in obtaining a copy of the FBI data—in April of 1975. Dr. Nichols immediately flew out to California with the data, and I began a detailed examination of the 70 pages of the raw NAA data and calculated results that had been obtained at the Oak Ridge National Laboratory in May 1964 by John F. Gallagher of the FBI Laboratory (now retired). The author's initial examination of these data tended to agree with Mr. Hoover's statement that the results were inconclusive. But I will discuss more about these data later.

WCC Mannlicher-Carcano Bullet Lead

At this point, Dr. Nichols and I urged a reexamination of the bullet-lead evidence specimens—this time using nondestructive instrumental neutron activation analysis (INAA) with a high-resolution Ge(Li) semiconductor gamma-ray detector instead of the low-resolution thallium-activated sodium iodide [NaI(Tl)] scintillation detector that had been used in 1964. During the period

1972–1976, I had analyzed a number of samples of WCC/MC 6.5-mm bullet lead, from all four of the production lots made by WCC, using instrumental NAA with Ge(Li) gamma-ray spectrometry. These known samples were supplied by Dr. Nichols and gave surprising results. The results showed that this type of ammunition was quite different from virtually all other brands of bullet lead I had ever analyzed before (2, 3). Although individual bullets were fairly homogeneous in their antimony and silver contents, they exhibited a great heterogeneity from bullet to bullet—even within the same production lot and even within an individual box of 20 cartridges. The range of Sb values was especially large, all the way from around 20 ppm up to 1200 ppm Sb. Although still in the range of unhardened lead, they clearly were not made from virgin lead but instead obviously contained appreciable and variable amounts of recycled lead—some of which was antimony-hardened lead. The silver levels ranged from about 5 ppm to around 15 ppm Ag. These background results showed that a more detailed analysis of the Dallas bullet-lead specimens, by INAA with Ge(Li) gamma-ray spectrometry, might be able to establish whether all of the specimens were or were not in the range of WCC/MC

bullet lead, and whether they corresponded to two, or more than two, bullets.

The Warren Commission, it should be noted, had concluded that Oswald fired three WCC/MC bullets; that one of them had missed completely; that one of them had struck the President in the back, exited from his throat, gone on to strike Governor Connally in the back (he was sitting in a jump seat right in front of the President), exited from the Governor's chest after fracturing one of his ribs, striking the Governor's right wrist—shattering it, exited from the under side of his wrist, and then came to rest in his left thigh after penetrating the flesh only slightly—finally to fall out on the Governor's stretcher at the hospital; and that a later (or last) one had struck the back of the President's head, exiting near the right front of his head, causing a massive and fatal wound. After issuance of the Commission's Report in 1964, numerous critics scoffed at their conclusion that a single bullet could cause the President's back wound and the Governor's back, wrist, and leg wounds—and still end up with only a slight dent in it and with only about a 1% weight loss. They dubbed it the "Magic Bullet." In addition, partly based on the Zapruder film and on eyewitness accounts of gunfire from a region in front of the limousine (the so-called "grassy knoll"), rather than from the rear, some critics claimed that the fatal head shot did not come from Oswald's location.

A Phone Call from the House Select Committee

In the early summer of 1977, the author received a phone call from a staff member of the U.S. House of Representatives Select Committee on Assassinations—inquiring (1) whether the author thought it might yield new information if the Dallas bullet-lead evidence specimens were reanalyzed, using improved INAA techniques; (2) what kind of information might be generated by such measurements; and (3) whether the author would be willing to conduct such analyses for the Select Committee. To (1) and (3) the answer was "yes," and the answer to (2) was a summary of the information possibly obtainable from such measurements, based upon the author's earlier studies of WCC/MC bullet lead. It was then agreed that the author would reanalyze the Dallas specimens, using the sensitive and nondestructive INAA method, with Ge(Li) gamma-ray spectrometry.

New INAA Measurements

In mid-September of 1977, James L. Gear of the National Archives flew

Flight cancelled.



When the stars come out in Mexico, and other parts of Latin America, hordes of vampire bats do also. These bats (*Desmodus rotundus*) have been attacking cattle, bleeding them and acting as dangerous vectors of paralytic rabies.

The cattle ranchers, suffering losses of \$350 million a year in meat and milk production, saw their livelihoods at stake. And while Count Dracula may have been kept in his place by a wooden stake, the ranchers needed a better solution.

The U.S. Agency for International Development (AID) funded U.S. Fish and Wildlife Service scientists who devised a control method. An anticoagulant solution, diphenadione, based on a Kodak intermediate, was developed by a chemical firm. It is smeared on vampire bats after they are trapped in nets. The bats, grooming each other, ingest it and die as they live—by bleeding. The purpose is not to eradicate the species, but to control them. Since other bat species do not associate with vampire bats, this method selectively controls only *Desmodus rotundus*, and only in those areas where they pose a threat to domestic livestock and human needs.

It's just one of the many creative uses of chemistry we've seen since 1918, when Kodak founded America's first industrial research laboratory to supply laboratories with organic chemicals.

Through a nationwide network of dealers, you can meet an enormous range of challenges with a choice of thousands of Kodak lab chemicals—available whenever and wherever needed. Just call your dealer for a fast response.

To learn more about the cancelled flight of vampires, write: Dept. 412L, Eastman Organic Chemicals, Eastman Kodak Company, Rochester, NY 14650.

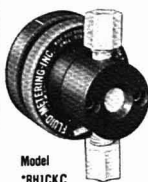
For the creative chemist.



Dealers handling EASTMAN Organic Chemicals: American Scientific & Chemical; Bioclinical Laboratories; Brand-Nu Laboratories, Inc.; Bryant Laboratory, Inc.; CAMX Scientific; Custom Chemical Laboratories, Inc.; Fisher Scientific; GAC Laboratories, Inc.; Labproducts, Inc.; Midland Scientific, Inc.; North-Strong, Inc.; Preiser Scientific; Sargent-Welch; Scientific Products; Scientific & Industrial Sales & Service, Inc.; VWR Scientific Inc.; Ward's Natural Science Establishment, Inc.

FMI METERING PUMPS

The FMI LAB PUMP line of valveless, variable metering pumps is available from stock at catalog prices. Models are available with maximum flow rates as low as microliters per minute or as high as one liter per minute at pressures to 200 PSIG. A wide variety of pump head materials offer superb chemical resistance. New items include: RYTON® liners, miniature panel mount pumps, and water flush gland option for use with problem fluids.



*This model has a variable displacement of 0.01 to 0.1 ml/revolution.
Price \$250.00

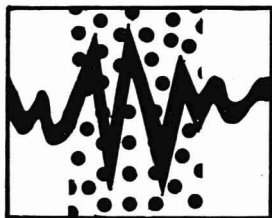


FLUID METERING, INC.

P.O. BOX 507, OYSTER BAY, N.Y. 11771 • (516) 922-6050

SINCE 1959

CIRCLE 78 ON READER SERVICE CARD



Nuclear Safeguards Analysis

Nondestructive and Analytical Chemical Techniques

ACS Symposium Series No. 79

E. Arnold Hakikila, *Editor*
Los Alamos Scientific Laboratory

Based on a symposium sponsored by the Division of Nuclear Chemistry and Technology of the American Chemical Society.

This comprehensive new volume reviews nondestructive and analytical chemical techniques in nuclear safeguards measurement methodology — a very topical subject in the forefront of nuclear research. Requirements in the area of standards and analysis of data are also discussed.

In view of a recent spurt of activity in the field, this book will be a valuable addition to the science libraries of chemists, nuclear materials management specialists, and NDA experts.

CONTENTS

Realm of Measurements • Standards for Chemical or NDA Measurements for Nuclear Safeguards • Standard Reference Materials Program • Decision Analysis • Calibration Curves • Verification of Reprocessing Input Analysis • Isotopic Safeguards Techniques • Energy-Dispersive Absorption Edge Densitometry • On-Line Alpha Monitors and Process Streams in a Nuclear Fuel Reprocessing Plant • Uranium and Plutonium Analyses • Portable Calorimeter System for Nondestructive Assay of Mixed-Oxide Fuels • Accountability Measurement System

214 pages (1978) clothbound \$22.00
LC 78-12706 ISBN 0-8412-0449-7

SIS/American Chemical Society
1155 16th St., N.W./Wash., D.C. 20036

Please send _____ copies of *SS 79 Nuclear Safeguards Analysis* (ACI 0449-7) at \$22.00 per copy.

☐ Check enclosed for \$ _____ ☐ Bill me.
Postpaid in U.S. and Canada, plus 75 cents elsewhere.

Name _____

Address _____

City _____ State _____ Zip _____

out to California with the Dallas bullet-lead specimens. During a three-day period, the author examined the specimens, prepared them for analysis, analyzed the samples in two reactor runs under different conditions, and returned the samples to him. An amusing aspect was that the measurements had to be conducted under tight security and secrecy—during every working hour of those three days Mr. Gear and the author were accompanied by two armed, uniformed federal guards. Needless to say, speculation amongst the U.C. Irvine students ran high! Later, reading the Ge(Li) pulse-height data from the samples and the Sb, Ag, and Cu standards back from the magnetic tape, I proceeded to calculate the ppm levels of these three elements in each sample.

Preparation of the samples for analysis was itself somewhat of a problem. The various samples ranged in size from about 1 mg on up to one large portion of a jacketed bullet (Q2) on up to an almost whole bullet (the Connally stretcher bullet, Q1). The smaller pieces were taken each in its entirety. From the large Q2 specimen, a piece of the bullet lead free of copper jacket was cut off with a stainless steel scalpel, for analysis. A sample of bullet lead was drilled out from the base of the stretcher bullet (Q1), using a 0.5-mm diameter carbon-steel drill.

Each sample was examined under magnification to be sure no specks of imbedded jacket material could be detected. To remove as much as possible of any external contamination from the samples, each was washed three times, alternately, with distilled/deionized water and reagent grade acetone. Each sample was weighed into a specially cleaned small polyethylene vial on an analytical balance. Several small standard samples each of Ag, Sb, and Cu were prepared in the same size vials, the solutions evaporated to dryness, and the materials cemented to the inside of the bottom of the vial by paraffin (using a few drops of 10% paraffin/CS₂ solution, followed by air drying). The conduct of the analyses was somewhat restricted by the security/secrecy requirements, and by the short time available to carry them out (precluding the possibility of doing replicate determinations of each sample, except for the silver determinations, which could be repeated, due to the short half life of ¹¹⁰Ag). Each night, all of the evidence specimens and the analytical samples had to be taken away for overnight security storage at the Laguna Niguel branch of the National Archives.

In the first run, the 1–50-mg samples and the standards were activated and counted one at a time, using the pneumatic-tube facility of the U.C. Ir-

INTRODUCING the Varian 5000 family of liquid chromatographs



**It makes
LC responsive
and simple**

The Varian 5000 Series is a family of powerful microcomputer-CRT-based liquid chromatographs that make LC easy for anyone.

It makes tough separations seem simple. The helpful CRT continuously displays all instrument conditions. Tells you everything you need to know, right now. Responds to you. Helps you build programs. Prompts and leads you. Makes LC easier than ever before.

It comes with full support. With your Model 5000 you receive a commitment from Varian to provide strong, continuing support—training, service and applications assistance—that will assure successful solution of your liquid chromatography problems.

Price/performance. There are six basic models in the 5000 Series: from simple isocratic to completely automatic gradient systems. Each is designed to offer unbeatable price/performance; to provide a new level of LC capability at system prices lower than most LC components.

Upward expandability. 5000 Series chromatographs are upward expandable and offer many options. You can configure a 5000 that is exactly right for your laboratory. Later, as your needs change, you can add whatever new capability you require.

For full details on a 5000 that may be exactly right for you, circle Reader Service Number 222.

To have a Varian representative contact you, circle Reader Service Number 223.



For gas chromatography you



For price/performance, versatility and reliability you can't beat the Varian 3700 series. In addition, every 3700 comes with full service and applications support to assure your success.

Can't beat the Varian 3700 series

The Varian 3700 series is a family of powerful gas chromatographs that puts the emphasis on performance. On giving you the greatest capability to handle your specific application plus unmatched flexibility to meet changing needs.

You can choose the right gas chromatograph.

The 3700 is modular so you can easily choose a chromatograph that is exactly right for your laboratory. All components—injectors, detectors, temperature programmers, flow controllers and automation systems—are upgradeable and interchangeable. You can begin with a basic dual column unit and add capability as you need it. Or, you can start right now with the world's most powerful, versatile and fully automatic GC system. And the 3700 continues to grow so you can always have the newest and best gas chromatograph.

You have better control of the analysis.

The 3700 controls, with ESP monitor and self-diagnostic display, give you more clear information about operating parameters and better control of injectors, column oven, detectors and flows. You don't have to interrogate the system and wait for a printout. You always know what is going on so you can take timely action.

Large dual-column oven makes it easier to do more.

It gives you more room to install columns side by side. Greater freedom to use any columns your application demands: packed or capillary, single or multiple, with column switching and valving inside the oven.

You can use the best detector for your application.

TCD, FID, ECD, FPD, TSD and multi-detector models are offered. Each of these new detectors is designed to provide excellent performance for its range of applications. See Figures 1, 2, and 3. Universal ionization detector bases let you interchange FID, ECD, FPD, and TSD detectors yourself in minutes.

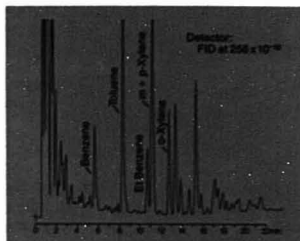


Figure 1. Benzene in Working Environment. The 3700 is widely used in industrial hygiene for detection and quantitation of solvents in the working environment.

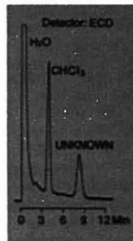


Figure 2. Halocarbons in Drinking Water. Analysis of drinking water injected directly onto a porous polymer column. Trihalocarbons at ppb levels can be detected with this technique.

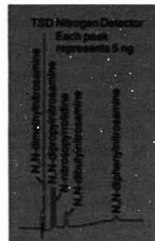


Figure 3. Volatile Nitrosamines. The 3700 equipped with a TSD, which is very selective for nitrogen, is excellent for screening food and cosmetics products for nitrosamines.

You can choose the best injection technique for your sample.

The versatile 3700 injector system permits you to choose: (1) heated or unheated true on-column injection right into the column packing, (2) heated, flash-vaporization with replaceable glass inserts, (3) two all glass capillary injectors with a choice of modes, or (4) valve injection using gas and liquid sampling valves.

You can use all the speed and power of capillary GC.

There are two high resolution, easy-to-use capillary systems to choose from. The new low cost system makes the power of capillary available to everyone. In both systems columns can be installed in minutes without tedious end straightening. A new capillary effluent splitter lets you detect your capillary separation with any two different ionization detectors. See Figure 4.

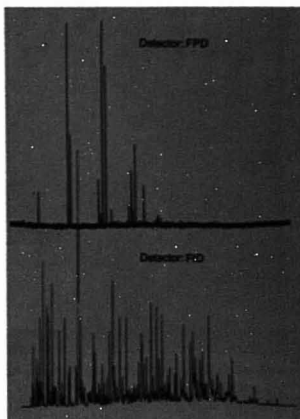


Figure 4. Coal Hydrogenation Product. In the analysis of very complex samples such as this coal hydrogenation product the 3700's capillary system gives high resolution of sample components. The capillary effluent splitter permits detection of the sulfur compounds with the FPD and the organics with FID.

Proven, powerful automation.

For total automation Model 3700 Gas Chromatograph combines with the proven Model 8000 AutoSampler™ and the powerful CDS-111 Chromatography Data System. These components can be purchased and used separately, or they can be combined in many different configurations to meet individual requirements. Result, you can choose the automation you want and you don't have to buy anything that you don't need.

Let us give you detailed information about an unbeatable 3700 system that will do great gas chromatography for you. **Circle Reader Service Numbers:** 244 3700 Series Gas Chromatographs, 245 CDS-111 Chromatography Data System, 246 Model 8000 AutoSampler, 247 Model 3711 Automatic Gas Chromatographs, 248 Have a representative call.



611 Hansen Way, Palo Alto, CA 94303 • Florham Park NJ (201) 822-3700 • Park Ridge, IL (312) 825-7772 • Houston, TX (713) 783-1800 • Los Altos, CA (415) 968-8141

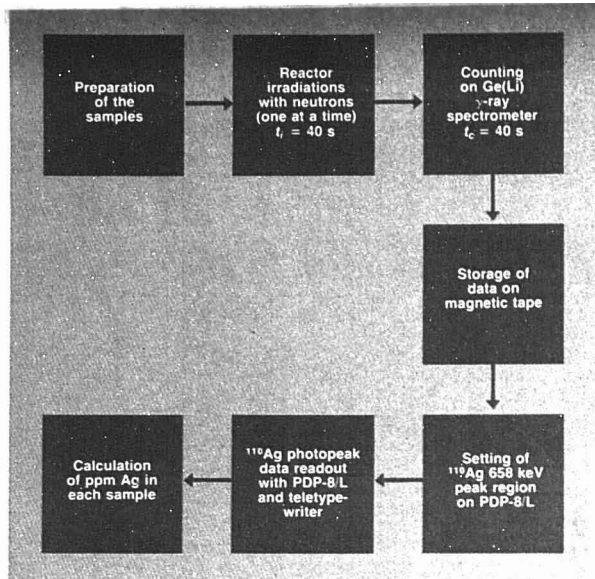


Figure 1. Schematic of INAA determination of silver in bullet-lead specimens via 24.4-s ^{110}Ag

vine TRIGA Mark I nuclear reactor. The conditions used were those of our rapid screening method (4), giving precision measurements for silver and less precise values for antimony and copper: irradiation, decay, and counting times of 40 s each. The samples were activated in a thermal-neutron flux of $2.5 \times 10^{12} \text{ n cm}^{-2} \text{ s}^{-1}$, and each was transferred to a fresh polyaluminum during the 40-s decay period. Each activated sample was counted with a 38 cm^3 Ge(Li) detector/4096-channel gamma-ray spectrometer, and the pulse-height data were promptly stored on magnetic tape. The most prominent induced activities detected were 24.4-s ^{110}Ag , 93-s $^{124\text{m}}\text{Sb}$, and 5.10-min ^{64}Cu . Quantitative results were based upon the largest photopeak of each (658, 498, and 1039 keV, respectively). The analytical sequence is shown schematically in Figure 1.

In the second run, the same samples (and standards) were activated and counted again, but this time all together in the 40-tube rotary specimen rack of the reactor—for 1 h at a thermal-neutron flux of $1.0 \times 10^{12} \text{ n cm}^{-2} \text{ s}^{-1}$. After about a 1-h decay, the samples and standards were counted as before, but this time for 5 min each. The most prominent induced activities were 2.80-day $^{122\text{Sb}}$ and 12.8-h ^{64}Cu , providing more precise values of the antimony and copper levels. Quantitative results were based upon the largest photopeak of each (564 and 511 keV, respectively).

Results of New INAA Measurements

As can be seen in Table I, samples Q1 and Q9 (the Connally stretcher bullet and fragments from Connally's wrist, respectively) are indistinguishable from one another in their Sb and Ag concentrations, but are clearly distinguishable from the Q2, Q4, 5, and Q14 samples (Q4, 5 being fragments recovered from two different areas in the Dallas limousine)—these latter three samples, in turn, being indistinguishable from one another. The results for copper follow the same pattern except that no reliable value for Cu could be obtained for sample Q9, because it was greatly contaminated with Cu from imbedded jacket material. From the induced 66.9-min $^{204\text{m}}\text{Pb}$ activities [an (n, n') fast-neutron product of lead] (5), it was also established that all of the samples were at least

90% lead. The sample Q designations, by the way, are those originally assigned to the evidence specimens by the FBI. The CE designations, which are also shown in Table I, are the Warren Commission Exhibit numbers assigned to them.

The conclusions derived from these results—interpreted in the context of my earlier measurements on background WCC/MC bullet-lead samples—are definite and straightforward: all of the Dallas samples are in the unusual (though not necessarily unique) concentration ranges of WCC/MC bullet lead; and the specimens show clearcut evidence for the presence of two, and only two, WCC/MC bullets—one of a composition of 815 ppm Sb and 9.3 ppm Ag, the other of a composition of 622 ppm Sb and 8.1 ppm Ag.

A Second Look at Earlier FBI Data

After I had obtained these new results, it seemed to me that the presence of two different compositions should have been discernible from the FBI's 1964 NAA data, in spite of the complication of the 20-fold poorer energy resolution of the NaI(Tl) scintillation detector that Mr. Gallagher used [the high-resolution Ge(Li) detector was not generally available in 1964]. My previous examination of the FBI data had revealed that the results had been obtained for silver (via the 24.4-s ^{110}Ag induced activity, as in the newer measurements) under one set of irradiation/decay/counting time conditions. His values for silver agreed closely with the new values. The complication, however, was that Mr. Gallagher measured antimony (via the 2.80-day $^{122\text{Sb}}$ and 60.4-day $^{124\text{Sb}}$ induced activities) under four different sets of irradiation/decay/counting time conditions—unfortunately obtaining four rather widely different Sb values for each sample. The wide spread of Sb values for each sample obscured any distinction between the Q1 and Q9 samples, on the one hand, and the Q2, Q4, 5, and Q14 samples, on the other—if all the results were viewed simultaneously. This confusion

Table I. Author's 1977 INAA Silver and Antimony Results ^a

Sample no.	ppm Ag	ppm Sb	Sample description
Q1 CE-399	8.8 ± 0.5	833 ± 9	Connally stretcher bullet
Q9 CE-842	9.8 ± 0.5	797 ± 7	Fragments from Connally's wrist
Q2 CE-567	8.1 ± 0.6	602 ± 4	Large fragment found in car
Q4, 5 CE-843	7.9 ± 0.3	621 ± 4	Fragments from President Kennedy's brain
Q14 CE-840	8.2 ± 0.4	642 ± 6	Small fragments found in car

^a The measurement precisions shown in Tables I and II as \pm values represent 1 standard deviation. Studies by the author on background samples of WCC/MC bullet lead show that the Sb variability within an individual bullet, particularly, is usually several times larger than the measurement precision on an individual sample.

Table II. 1964 FBI Antimony NAA Results from Four Sets of Measurements (and the One Set of Silver Results)

Sample no.	ppm Ag	ppm Sb			
		Set 1	Set 2	Set 3	Set 4
Q1	9.4 ± 0.3	945 ± 16	1002 ± 13	813 ± 43	705 ± 54
Q8	9.2 ± 0.1	977 ± 24	1090 ± 37	773 ± 22	676 ± 14
Q2	7.9 ± 0.9	745 ± 16	747 ± 20	626 ± 57	534 ± 30
Q4, 5	8.5 ± 0.4	783 ± 5	856 ± 46	614 ± 37	561 ± 32
Q14	8.5 ± 0.2	793 ± 10	879 ± 33	629 ± 18	562 ± 21

no doubt led Mr. Hoover to state that the results were inconclusive.

However, my second review of the FBI data (6) [benefiting, of course, from the hindsight gained from the newer Ge(Li) results] resolved this anomaly. Although not heretofore realized, the old FBI data also showed that samples Q1 and Q9 were similar to one another in their Sb and Ag contents (Cu was detected, but not measured), and distinct from samples Q2, Q4, 5, and Q14—which, in turn, were similar to one another. This conclusion was reached by examining the Sb results obtained by the FBI for all the samples under all four conditions—but with the data for each condition compared only with one another, rather than intercomparing the results obtained for each sample under all four conditions. Examined in this fashion, it was revealed that, for each of the four FBI measurement conditions, samples Q1 and Q9 matched closely, and were quite different from samples Q2, Q4, 5, and Q14, which in turn matched one another closely. The FBI results are displayed in this fashion in Table II. Apparently, some errors in some of the standards used, and/or in the counting conditions used in the four different measurements led to some consistent (determinate) errors that resulted in four different Sb values being obtained on the same sample. The FBI values for one of their conditions (set 3) agree closely with the newer Ge(Li) values, but their results for the other three conditions are numerically considerably different from the Ge(Li) results.

Presentation of Results Before the Select Committee

After I had submitted a detailed report to the Select Committee on my INAA results and conclusions concerning the Dallas bullet-lead evidence specimens, the Committee requested that I present these at their public hearings in Washington, D.C. On September 8, 1978, I presented a 90-min summary of my findings and conclusions (nationally televised on public service TV), the 90 min including questioning by various of the 12 Congressmen who constitute the Select Committee.

Thus, analytical chemistry—which in 1963-64 had not shed much light on the assassination—finally succeeded in producing significant useful information. The nondestructive instrumental neutron activation analysis results have demonstrated that, to a high degree of probability, all of the bullet-lead evidence specimens are of WCC/MC 6.5-mm brand, that there is evidence for the presence of portions of two—and only two—such bullets, and that the Connally stretcher virtually intact bullet indeed caused the fracture wound of Governor Connally's wrist—a previously hotly disputed part of the Warren Commission's theory. The back wounds of President Kennedy and Governor Connally involved essentially no damage to the bullet (or bullets) causing them, and thus produced no fragments for possible analysis. The new results cannot prove the Warren Commission's theory that the stretcher bullet is the one that caused the President's back wound and all of the Governor's wounds, but the results are indeed consistent with this theory.

And What Now?

In due time, my report to the Select Committee will be made public and available, and I will be submitting a series of several papers to the *Journal of Forensic Sciences* (of the American Academy of Forensic Sciences) that will cover this investigation in greater detail. These papers will also include additional studies in my laboratory, some of them still in progress at this writing, on background WCC/MC bullet-lead samples (further homogeneity studies) that will enable one to calculate actual numerical probabilities.

References

- (1) R. R. Ruch, V. P. Guinn, and R. H. Pinker, *Trans. Am. Nucl. Soc.*, **5**, 282, subsequent papers, AEC report (1962).
- (2) H. R. Lukens and V. P. Guinn, *J. Forensic Sci.*, **16**, 301 (1971).
- (3) H. R. Lukens, H. L. Schlesinger, V. P. Guinn, and R. P. Hackleman, "Forensic Neutron Activation Analysis of Bullet-Lead Specimens," U.S. AEC Report GA-10141, 48 pages, 1970.
- (4) V. P. Guinn and M. A. Purcell, *J. Radioanal. Chem.*, **39**, 85 (1977).
- (5) T. Izak-Biran and V. P. Guinn, *Trans. Am. Nucl. Soc.*, **28**, 94 (1978).
- (6) V. P. Guinn and J. Nichols, *ibid.*, p. 92.

Varian announces training courses in gas chromatography

Schedule for April, May and September 1979:

Basic Gas Chromatography

April 10-12, Park Ridge, IL
May 9-11, Florham Park, NJ
September 12-14, Walnut Creek, CA
Lecture & Lab, 3 days, \$225
Lecture only, 2 days, \$155

Glass Capillary Gas Chromatography

May 14-15, Florham Park, NJ
Lecture & Lab, 2 days, \$225

Maintenance of the Gas Chromatograph

April 16-17, Park Ridge, IL
September 17-18, Walnut Creek, CA
Lecture & Lab, 2 days, \$225

Automatic Gas Chromatography*

April 18-20, Park Ridge, IL
May 16-18, Florham Park, NJ
September 19-21, Walnut Creek, CA
Lecture & Lab, 3 days, \$200

To enroll in Park Ridge and Palo Alto courses, please contact the Varian Instrument Division Training Department, 2700 Mitchell Drive, Walnut Creek, CA 94598. Telephone (415) 939-2400 ext. 225. Enroll in Florham Park courses at Varian Instrument Division Training Department.

25 Hanover Road,
Florham Park, NJ 07932.
Telephone (201) 822-3700.

*One tuition-free course per Model 3711 purchase

CIRCLE 232 ON READER SERVICE CARD





Behind every EM-Series NMR Spectrometer stands **A team of experts to support you**

It's the team that has helped make the EM's what they are today: the fastest-selling permanent-magnet NMR spectrometers in the world.

The first member of the team you'll meet is the Varian Sales Representative, uniquely qualified to help you choose the EM instrument that best suits your needs. Perhaps the easy-to-use, low-cost EM-360A for routine 60-MHz analysis of proton-containing samples is best for you. Or perhaps you need the more flexible performance of the EM-360L to handle ^{19}F and ^{31}P observation as well as ^1H at 14 kG. For the ultimate in high-resolution performance, you may want to consider the 90-MHz EM-390, with the high sensitivity and chemical shift dispersion of a 21-kG magnet. Your Sales Representative also will be the one to tell you about the great features all EM's share: the low power consumption, the fact that they need no cooling water, their full compatibility with variable-temperature operation. And he'll even arrange for financing if you need it.

Now you are ready to meet the rest of the team.

Your order will be processed by an individual with a knack for handling the minute details of your requirements and the Product Specialist, who sees to it that these details, your applications needs, and your special wishes all come together to a happy union.

When your Varian EM-Series spectrometer is installed, a

trained Service Engineer will check its operation to make sure it performs to specifications and that you know how to operate it. But help with really getting to know your instrument comes from the Technical Writer who has put together a set of instruction manuals that in depth and competence counts among the finest in the industry. And you get powerful support from perhaps the least conspicuous member of the team: the Quality Assurance Administrator. He not only establishes and enforces Varian quality standards, he also stands in the wings to monitor the installation of your instrument and its performance.

Should you ever get stumped by a tricky application or a methods problem, you'll have an "inside" friend—the Varian Applications Scientist. Here's a storehouse of NMR expertise to draw from, and the answer to your problem may be as close as your telephone.

The team behind the EM-Series NMR Spectrometers is a bonus feature that makes a big difference. Ask any of the 1000-plus EM-owners!

For a package of information about the EM-Series NMR Spectrometers, circle Reader Service Number 218. To have the first member of the team call you, circle No. 219. Or write Varian Associates, Inc., Box D-070, 611 Hansen Way, Palo Alto, California 94303.



Varian SF-330 Spectrofluorometer

Stable, simple, economical...

It's designed to work for you.



Now the inherent sensitivity of fluorescence spectroscopy can be applied to a broad spectrum of quantitative determinations: in environmental studies, industrial hygiene, pharmaceutical assays, food/nutrition, and biological assays for enzyme activity, sialic acid, porphyrins, etc.

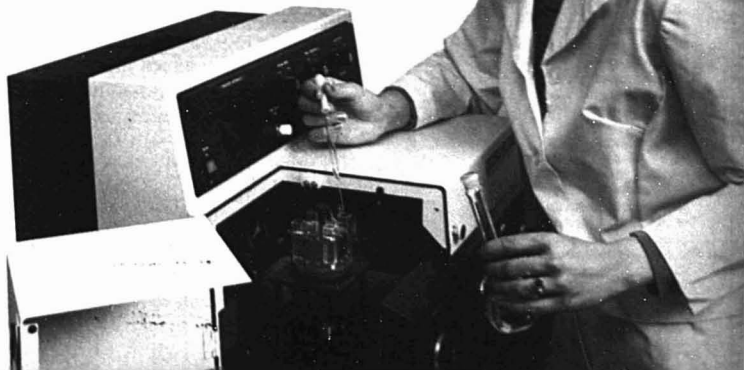
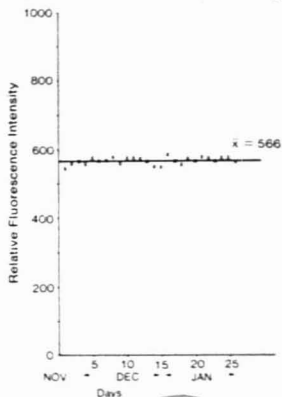
SF-330 gives you accurate, reproducible data, effortlessly. The ratio photometric system provides a new level of stability. Frequent calibrations are not necessary. Efficient optical system with concave grating assures high energy throughput over the entire operating range.

It's easy to vary operating parameters to suit your particular application. The convenient front panel provides simple, precise controls and clear, legible readouts that minimize guesswork. A large, four-turret sample compartment facilitates sample handling and interchange of accessories such as HPLC flow cells.

And the price is right. No other spectrofluorometer in this medium price range comes close in performance or convenience.

Circle 228 for more information. Circle 229 if you want our representative to call. Or write: Varian Associates, Inc., D-070, 611 Hansen Way, Palo Alto, CA 94303.

26 readings on a solid solution of Rhodamine B in a polymer block were taken over a two-month period. The same control settings were used throughout. An intentional source change was made between readings 9 and 10. Average intensity was 566 units $\pm 1.8\%$ RSD



The smartest label around.

High-Performance Liquid Chromatography Grade CH₃CN F.W. 41.05 Certificate of Actual Lot Analysis Full spectral curve for this lot available on request.		A-998 3.8 L (1 Gal)
Color (APHA) 5 Optical Absorbance at 254nm 0.01 220nm 0.05 200nm 0.20 Fluorescence Background (less than 1 µg/liter Quinine Sulfate) P.T. Refractive Index @ 25°C (traceable to NBS) 1.3410 Acidity (as CH ₃ COOH) 0.01% Alkalinity (as NH ₃) 0.002% Residue after Evaporation 0.001% % Water (H ₂ O) 0.1% Assay (as CH ₃ CN) 99.9%	LOT 790167	CERTIFIED HPLC-GRADE Acetonitrile UV cutoff — 190nm
Contains no preservatives. FILTERED THROUGH 0.5 MICRON FILTER WARNING! FLASH POINT 55°F HARMFUL IF INHALED OR ABSORBED THROUGH SKIN		CLASS 1B FLAMMABLE Made in U.S.A.

For laboratory and manufacturing use only, not drug, food or household use.

FISHER SCIENTIFIC COMPANY
 Chemical Manufacturing Division
 Fair Lawn, New Jersey 07410

Avoid breathing vapor.
 Keep away from heat, sparks, or open flame.
 Use with adequate ventilation.
 Keep container closed.
 Avoid contact with eyes, skin or clothing.
 First Aid: In case of contact immediately flush eyes or skin with plenty of water for at least 15 minutes while removing contaminated clothing, and obtain medical attention as soon as practicable.
 Contaminated shoes: Get a physician.

Fisher Certified HPLC Solvents. The label that tells you everything you want to know.

Optical absorbance at a variety of wavelengths (full spectral curves on request). Refractive index directly traceable to NBS. Background fluorescence. UV cutoff. Assay as mol % via GC. Water and preservative /inhibitor content. And much more.

Fisher HPLC solvents — so pure you can use them for **gradient elutions**. They're distilled in glass. And submicron-filtered to eliminate particulates.

After all, today's high-performance liquid chromatography columns, detectors and samples are valuable things. They deserve the **best**. That's why Fisher defines and certifies every parameter vital to their protection.

In stock at your nearest Fisher branch. Or have your branch set up a Customer Reserve Quantity arrangement, reserving your HPLC solvents needs for you alone, shipping automatically to your timetable. You can even reserve an **entire lot**, guaranteeing total uniformity month in, month out.

And remember: Fisher also stocks an impressive selection of auxiliary HPLC materials. Apparatus, appliances, supplies. This simplifies your ordering — and your laboratory life.

Write for HPLC catalog today!



Fisher Scientific Company
 711 Forbes Avenue Pittsburgh PA 15219

CIRCLE 76 ON READER SERVICE CARD



Our new 800 Series syringes are now available in six capacities—from 5 ul to 250 ul. All with the accuracy and reliability you've come to expect from Hamilton's syringe with a handle.

Bent plungers are eliminated by the 800's handle.

Larger, more substantial handle makes the 800 easier than ever to hold and use.

New blow-out stop prevents plunger blow-out under high pressures.

Removeable needles let you replace bent or plugged needles in seconds.

Interchangeable barrels make replacements fast and inexpensive.

Better than 1% accuracy and repeatability.

For more information, write Hamilton Company, P.O. Box 10030, Reno, Nevada 89510

HAMILTON

CIRCLE 96 ON READER SERVICE CARD



May we test grind 100 ml of cement, fertilizer, glass, mineral or such for you? In your choice of ceramic, steel or tungsten carbide container.

SHATTERBOX® 8510

The Polite Pulverizer
MEETS OSHA NOISE STANDARDS

WITHIN IS HOUSED A SHATTERBOX GRINDER—
the unexcelled workhorse which efficiently reduces up to 500 g of material to -325 mesh in 3 minutes.

CPX INDUSTRIES, INC.
P.O. BOX 788 METUCHEN, N.J. 08840
(201) 549-7144

CIRCLE 187 ON READER SERVICE CARD



NO POSTAGE
NECESSARY
IF MAILED
IN THE
UNITED STATES

BUSINESS REPLY CARD

FIRST CLASS Permit #27346 Philadelphia, Pa

POSTAGE WILL BE PAID BY ADDRESSEE

analytical
chemistry

P.O. BOX #7826
PHILADELPHIA, PA 19101



PROTECTION SIX WAYS

Our new 800 Series syringes are now available in six capacities—from 5 ul to 250 ul. All with the accuracy and reliability you've come to expect from Hamilton's syringe with a handle.

- ☐ Bent plungers are eliminated by the 800's handle.
- ☐ Larger, more substantial handle makes the 800 easier than ever to hold and use.
- ☐ New blow-out stop prevents plunger blow-out under high pressures.
- ☐ Removeable needles let you replace bent or plugged needles in seconds.
- ☐ Interchangeable barrels make replacements fast and inexpensive.
- ☐ Better than 1% accuracy and repeatability.

For more information, write Hamilton Company, P.O. Box 10030, Reno, Nevada 89510

HAMILTON

CIRCLE 96 ON READER SERVICE CARD

YOUR "READER SURVEY" VIEWS ARE VITAL

Analytical Chemistry occasionally presents a Reader Survey section that provides you with an opportunity to indicate your interests and activities. Your answers help us in planning editorial material that will be useful to you in your work.

To express your Reader Survey views, simply circle your answers on one of these adjacent reply cards and drop it in the mail. No postage is required.

APRIL 1979

VALID THROUGH
AUGUST 1979

TO VALIDATE THIS CARD, PLEASE CHECK
ONE ENTRY FOR EACH CATEGORY BELOW:

ADVERTISED PRODUCTS: 1 2 3 4 5 6

7	8	9	10	11	12	13	14	15	16	17
18	19	20	21	22	23	24	25	26	27	28
29	30	31	32	33	34	35	36	37	38	39
40	41	42	43	44	45	46	47	48	49	50
51	52	53	54	55	56	57	58	59	60	61
62	63	64	65	66	67	68	69	70	71	72
73	74	75	76	77	78	79	80	81	82	83
84	85	86	87	88	89	90	91	92	93	94
95	96	97	98	99	100	101	102	103	104	105
106	107	108	109	110	111	112	113	114	115	116
117	118	119	120	121	122	123	124	125	126	127
128	129	130	131	132	133	134	135	136	137	138
139	140	141	142	143	144	145	146	147	148	149
150	151	152	153	154	155	156	157	158	159	160
161	162	163	164	165	166	167	168	169	170	171
172	173	174	175	176	177	178	179	180	181	182
183	184	185	186	187	188	189	190	191	192	193
194	195	196	197	198	199	200	201	202	203	204
205	206	207	208	209	210	211	212	213	214	215
216	217	218	219	220	221	222	223	224	225	226
227	228	229	230	231	232	233	234	235	236	237
238	239	240	241	242	243	244	245	246	247	248
249	250	251	252	253	254	255	256	257	258	260

NEW PRODUCTS: 401 402 403 404 405 406 407

408	409	410	411	412	413	414	415	416	417	418
419	420	421	422	423	424	425	426	427	428	429
430	431	432	433	434	435	436	437	438	439	440
441	442	443	444	445	446	447	448	449	450	451
452	453	454	455	456	457	458	459	460	461	462
463	464	465	466	467	468	469	470	471	472	473
474	475	476	477	478	479	480	481	482	483	484
485	486	487	488	489	490	491	492	493	494	495

READER SURVEY: 301 302 303 304 305 306 307

308	309	310	311	312	313	314	315	316	317	318
319	320	321	322	323	324	325	326	327	328	329
330	331	332	333	334	335	336	337	338	339	340
341	342	343	344	345	346	347	348	349	350	351

Intensity of product need:

- ☐ 1. Have salesman call
- ☐ 2. Need within 6 mos.
- ☐ 3. Future project

Primary field of work:

- ☐ A. Energy
- ☐ B. Environmental
- ☐ C. Medical/Biological
- ☐ D. Drug/Cosmetic
- ☐ E. Forensic/Narcotic
- ☐ F. Textile/Fiber
- ☐ G. Metals
- ☐ H. Pulp/Paper/Wood
- ☐ I. Soaps/Cleaners
- ☐ J. Paint/Coating/Ink
- ☐ K. Electrical/Electronic
- ☐ L. Instrument Dev./Des
- ☐ M. Plastic/Polymer/Rub
- ☐ N. Agricultural/Food
- ☐ O. Inorganic Chemicals
- ☐ P. Organic Chemicals

Primary area of employment:

- ☐ INDUSTRIAL
- ☐ A. Research/Development
- ☐ B. Quality/Process Control
- ☐ MEDICAL/HOSPITAL
- ☐ C. Research/Development
- ☐ D. Clinical/Diagnostic
- ☐ GOVERNMENT
- ☐ E. Research/Development
- ☐ F. Regulate/Investigate
- ☐ COLLEGE/UNIVERSITY
- ☐ G. Research/Development
- ☐ H. Teaching
- ☐ INDEPENDENT/CONSULTING
- ☐ I. Research/Development
- ☐ J. Analysis/Testing

This copy of Analytical is:

- ☐ 1. Personally addressed to me in my name.
- ☐ 2. Addressed to other person or to my firm.

NAME: _____

TITLE: _____

FIRM: _____

STREET: _____

CITY: _____

STATE: _____ ZIP: _____

PHONE: (_____) _____

ION CHROMATOGRAPHY BREAKTHROUGH!

A simple and rapid means of analyzing complex mixtures containing both organic acids and inorganic ions at trace levels.

The dual system Ion Chromatograph 16 utilizes newly developed ion exchange columns which allow separation and detection of all ions in complex mixtures with pK_a less than (approximately) 7. This includes inorganic ions such as chloride, nitrate and sulfate as well as organic acids such as C_1 - C_{10} carboxylic acids, organic phosphonic and sulfonic acids, and carbonic acid.

The Dionex IC 16 is extremely versatile. Just dilute the sample and in the most complex matrix you can determine • a host of strong acids or their salts such as inorganic ions • Weak acids or their salts such as organic carboxylic acids in a single sample analysis • anions and cations simultaneously with a single sample injection (because the ion Chromatograph 16 is actually two systems in one).

There's more. The IC 16 includes auxiliary valves which allow the use of additional chromatographic detectors such as UV. Pre- or post columns can be used individually or coupled with this dual system and you can even use column gradients. Let your imagination run wild!

For information on this Dionex innovation, call or circle the appropriate reader service number.

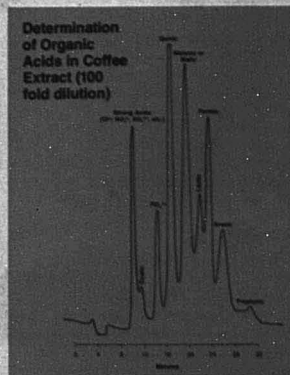
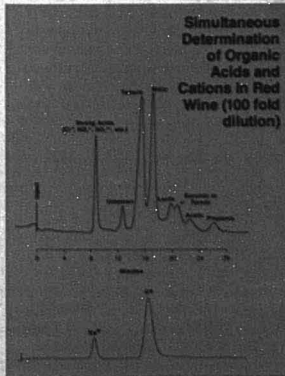
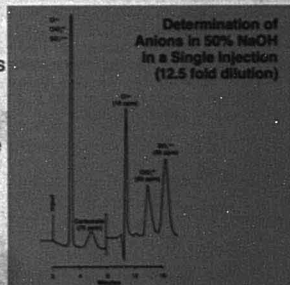
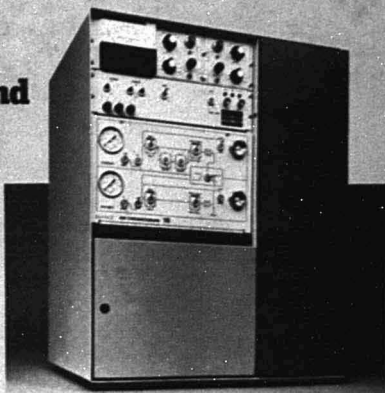
For information regarding applications of IC, circle the appropriate number:

Air Pollution 50	Brine Analysis 54
Water Pollution 51	Power Production 55
Elemental Analysis 52	Quality Control 56
Soil Analysis 53	IC 16 57

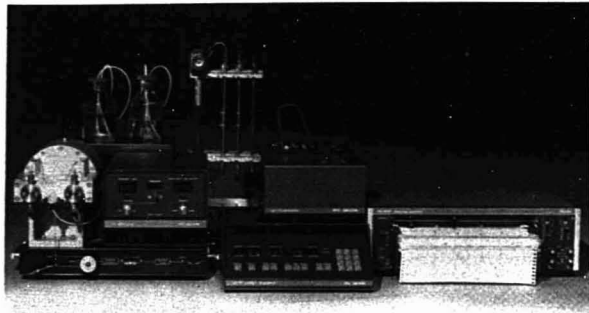
DIONEX

Ion Chromatography Systems

In the U.S.: 1228 Titan Way
Sunnyvale, CA 94086
Phone (408) 737-0700
In Europe: c/o A. The Buchan, Camberley, Surrey, GU15 3XB England



New Products



LC-XP series high-performance liquid chromatography instruments are modular in design with a basic configuration that consists of a single piston pump, UV detector, the desired column and injection system. Additions to the basic instrument include: LC-XP Dialamix unit which provides rapid selection of any mixture of two solvents; LC-FL fluorimetric detector; a series of isocratic and gradient elution liquid chromatographs based on the LC-XPD dual-piston reciprocating pump; and the LC-XP gradient programmer which is able to store up to 10 programs. Pye Unicam Ltd., Cambridge, England

401

Digital Image Analysis System

MOP, a digital image analysis system which consists of a microcomputer and a multipurpose measuring tablet, can measure up to eight parameters simultaneously and summarize and store data in up to 20 separate channels. The images can be analyzed from photographs—X-rays, projections, drawings—or a microscope. The system can determine percentages, averages, standard deviations, area differentials, and distribution analysis. Carl Zeiss, Inc.

410

Dye Laser

LFDL-1 longitudinal flow dye laser is a tunable high average power instrument that provides 1-2 W of power at a rep rate of 10-20 Hz. A regulated 1-kW high-voltage switching supply makes energy input/pulse independent of rep rate. A three-prism tuner is standard. Price is \$18 000. Candela Corp.

414

Liquid Chromatograph

Series 750 modular HPLC features a dual piston, pump, gradient programmer, column oven, and a UV detector with 200-280-nm range. Constant volume mobile phase delivery is provided from 0.1 to 9.9 mL/min with less than 1% pulsations peak-to-peak. A variety of accessories are available. Schoeffel Instrument Division of Kratos, Inc.

411

UV-VIS Spectrometers

The SP8-150 has reduced stray light at 220 nm of 0.01% and is fitted with a red-sensitive photomultiplier for a wavelength range extending to 900 nm. Accessories include modular units for first to fourth derivative and log A spectra. The SP8-250 is microprocessor controlled and has a double monochromator with stray light below 0.0002%. Both instruments feature master holographic gratings. Pye Unicam Ltd.

415

UV-VIS Spectrometer

A UV-VIS spectrometer, for continuous flow analysis and HPLC applications, features flow cell path lengths to 100 mm, a 50-fold amplifier, spectral range of 190-900 nm, and bandpass of 2 nm. Accessories include automatic sampler, temperature-controlled flow cell, and digital printer. Lachat Chemicals, Inc.

412

Centrifuge

Spinette Senior can centrifuge samples with volumes up to 90 mL at 3200 rpm (1286 xg), and accepts six 10-15-mL centrifuge tubes. It features covered rotating parts and a power interrupt interlock. International Equipment Co.

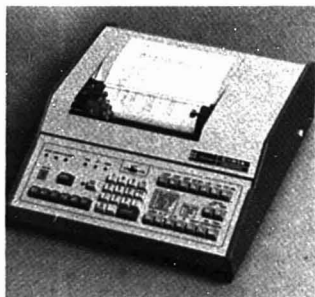
413

Particle Size Analysis

Autosieve automatically provides size distribution of particles in the 500-38- μ m range. Sieving, collection, weighing, washing, and data reduction are all microcomputer controlled. Micromeritics Instrument Corp.

416

For more information on listed items, circle the appropriate numbers on one of our Readers' Service Cards



Chromatopac C-R1A recording data processor features a thermal printer plotter, recording of names of components, processing of up to 339 peaks, processed exponential signals from FPD (sulfur compounds), measurement of peak heights, determining a calibration curve by the two-point method, and multiple-calculation function. Shimadzu Scientific Instruments, Inc.

402

End cap for
tight seal
during storage.

1/16" reverse
nut inlet/outlet,
adaptable to
virtually any
chromatograph.

4 mm ID 316
stainless steel
tubing with
Lichrospher
interior finish.

Choice of
packings for
adsorption,
reverse phase,
ion exchange
and exclusion
chromatography.

Zero dead volume
end fitting for
minimum band
spreading.

THE ANATOMY OF A QUALITY HPLC COLUMN

FROM BIO-RAD, OF COURSE!

You can have complete confidence in the performance of Bio-Rad's HPLC columns for the best of all possible reasons: we guarantee it. Specifically, we guarantee column efficiency, peak symmetry, and flow resistance. Furthermore, every Bio-Sil® column comes with a test chromatogram and a test solution sample so that you can verify performance yourself.

Bio-Rad offers a wide selection of columns—all competitively priced—and a wide choice of top quality packings including: • Bio-Sil HP-10 for adsorption • Bio-Sil ODS-10 for reverse phase • Bio-Sil GFC 100 for exclusion • Aminex® HP-C and Aminex A-9 for cation exchange • Aminex A-27

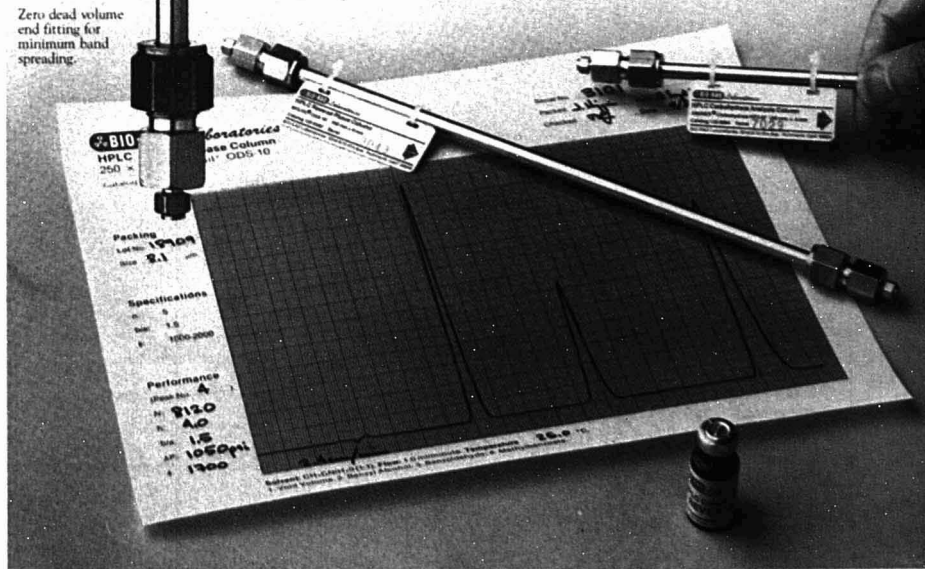
for anion exchange • A variety of custom packings for specific applications (HPX-87 and HPX-42 for carbohydrate analysis are two examples).

Request Bio-Rad Bulletin 1056 for details and our guide to HPLC column evaluation. Contact:

BIO-RAD Laboratories

2200 Wright Avenue
Richmond, CA 94804
Phone (415) 234-4130

Also in: Rockville Centre, N.Y.; Mississauga, Ontario; London; Milan; Munich; Vienna.



Where Small Differences Make a Big Difference

0.007A difference
on 2.6A background



New MIDAN™ Microprocessor Data Analyzer Enhances the Value of Data Generated by the DW-2a™ Spectrophotometer

Now you can expedite analyses of compounds in mixtures, correct baselines automatically, and perform other complex calculations using the new MIDAN Microprocessor Data Analyzer Accessory for our DW-2a Spectrophotometer.

With AMINCO's DW-2a Spectrophotometer, small sample differences can lead to new research territories in UV-VIS spectrophotometry. Our painstaking improvements in such parameters as photometric accuracy, stability, and system versatility extend your range of sample investigations and lead to substantial increases in overall system performance. And, the DW-2a Spectrophotometer's built-in flexibility and wide variety of capability-expanding accessories — like the MIDAN Analyzer — ensure continuing adaptability to your special applications needs.

AMINCO®

DIVISION OF TRAVENOL LABORATORIES, INC., Silver Spring, MD 20910-Phone 301-569-1727
European Headquarters: Rue Dautzenberg 36-38, 1190 Brussels, Belgium Phone 02-448 5412

© 1978 Travental Laboratories, Inc.



Cancer—The Outlaw Cell

Richard E. LaFond, Editor

An estimated 390,000 Americans will die of cancer this year alone and one out of every four will develop some form of this dread disease within their lifetime.

Statistics such as these show the need for a book that will explain our current state of the art in cancer research using simple, straightforward, non-medical language. *Cancer — The Outlaw Cell* successfully fulfills this need by making the latest advances in cancer research available to the general public in a clear, non-technical style that can be read and understood by both the professional scientist and non-scientist.

Written by leading experts at the forefront of their specialties and profusely illustrated in color, this collection of articles covers the great strides that have been made in understanding the causes of cancer, how this disease is spread, cancer as a biochemical problem, and non-surgical modes of therapy.

CONTENTS

Cancer — An Overview, Henry C. Pitot • *Tumor Growth and Spread*, Isaac J. Fidler and Margaret L. Kripke • *Control of Cell Growth in Cancer*, Arthur B. Pardee and David S. Schneider • *Cancer as a Problem in Development*, Armin C. Braun • *Puzzling Role of Cell Surfaces*, David J. Meyer and Max M. Burger • *Cancer-Causing Chemicals*, Elizabeth K. Weiszburger • *Cancer-Causing Radiation*, Robert L. Ulrich • *Michael Holland and John B. Storer* • *Cancer and Viruses*, Arnold J. Levine • *RNA Tumor Viruses*, Robert D. Cardiff • *Herpesviruses — A Link in the Cancer Chain*, Ariel C. Hollingshead and William A. Knuts • *Cancer and the Immune Response*, John L. Fahey • *Immunotherapy of Human Cancer*, Larry A. Schaller and Evan M. Herish • *Radiation Therapy*, Dana F. Nelson and Philip Rubin • *Chemotherapy of Cancer*, Joseph H. Burchenal and Joan R. Burchenal

192 pages (1978) clothbound \$15.00
LC 78-2100 ISBN 0-8412-0405-5
192 pages (1978) paperback \$8.50
LC 78-2100 ISBN 0-8412-0431-4

SIS/American Chemical Society

1155 16th St., N.W./Wash., D.C. 20036

Please send _____ copies of *Cancer — The Outlaw Cell*

_____ cloth \$15.00 _____ paper \$8.50
(ACK 0405-5) (ACK 0431-4)

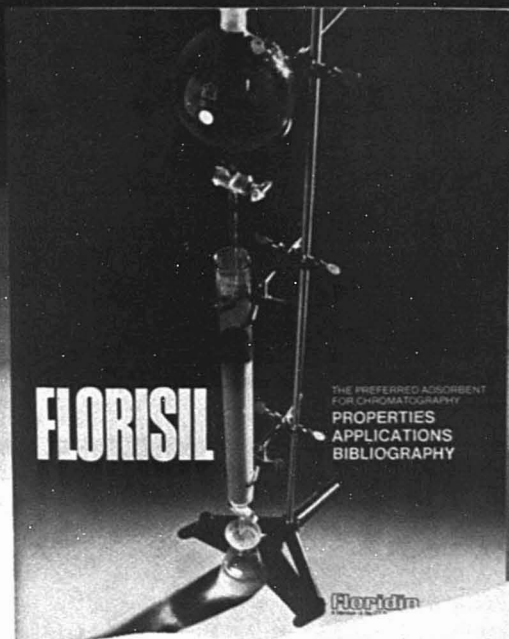
_____ Check enclosed for \$ _____ Bill me
Postpaid in U.S. and Canada, plus 75 cents elsewhere

Name _____

Address _____

City _____ State _____ Zip _____

WHO DID WHAT WITH FLORISIL IN CHROMATOGRAPHY. FREE.



You can get this 60-page chromatography bibliography free for the asking from Floridin. It'll tell you exactly why Florisil[®] is widely used to solve tough separation problems in column and thin layer chromatography. The bibliography includes

Florisil's chemical composition, physical properties and adsorptivity data. And a listing of who did what in chromatography with Florisil. Everything from Alkaloids to Thioesters.

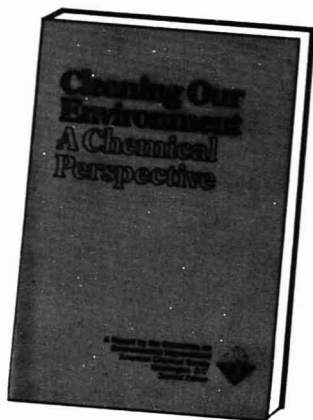
Free for all. Floridin's Chromatography Bibliogra-

phy. Contact Floridin Company, Dept. A-4, Three Penn Center, Pittsburgh, PA 15235. Phone: (412) 243-7500.

Floridin
A Member of the ITT System

CIRCLE 179 ON READER SERVICE CARD

PG-700



NEW! UPDATED! EXPANDED!

A totally revised edition of the
best selling single publication
ever produced by ACS

Cleaning Our Environment A Chemical Perspective

NEW!

- Analysis & Monitoring
- Toxicology
- Radiation

UPDATED!

- Air
- Water
- Solid Wastes
- Pesticides

The first edition of *CLEANING OUR ENVIRONMENT*, published in 1969, quickly became the ACS all-time best-selling book. But, because this is a changing world—*especially* in the environmental field—ACS has completely revised and expanded this important work. The four original topics (air, water, solid wastes, and pesticides) have been updated, and coverage has been added in three new areas—analysis and monitoring, toxicology, and radiation!

If you are interested as a professional or as a layman, *CLEANING OUR ENVIRONMENT* will bring you up to date on what is being done, what can be done, and what will be done!

Even if you already have the earlier edition—you will want this important and expanded revision! 457 pages. \$9.50 paperbound.

Essential reading for:

- educators
- researchers
- legislators
- administrators
- and a great refresher for environmentalists

Special Issues Sales

American Chemical Society
1155 Sixteenth Street, N.W.
Washington, D.C. 20036

PRICES

1-9 copies\$9.50 each
10-49 copies\$8.50 each
50 or more\$7.50 each

Enclose \$1.50 per order
for handling and postage.

California residents add
6% state use tax.

Please send me _____ copies of *CLEANING OUR ENVIRONMENT—A
CHEMICAL PERSPECTIVE*

☐ My payment is enclosed

☐ Bill me

Name _____

Address _____

City _____

State _____

Zip code _____

SPECTRACOMP 601[®]

PROGRAMMABLE UV-VISIBLE
SCANNING SPECTROPHOTOMETER

For Analytical, Research and Clinical Applications

First to provide these user-oriented benefits:

- Keyboard & Alphanumeric display for user interaction
- Total automation—no buttons, no complicated instructions
- A programmable computer & custom, user-designer programs
- Clear printouts of all instrument parameters
- Statistical analysis of spectral data
- A real time clock printout of time, date, & temperature
- Spectral data accumulation & printouts for up to 500 wave lengths
- Graphic displays of absorbance & transmittance values versus wave lengths on an incremental plotter
- Automatic selection of optimum scale expansion on recorder for both absorbance & wave lengths
- Magnetic stirring of sample & reference cuvettes, thermostatic control of samples, digital readout of temperature and standard TTY output.



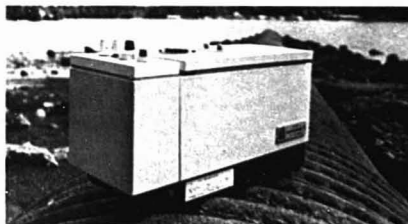
FOR FURTHER
INFORMATION CALL
OR WRITE:



**LACHAT
CHEMICALS, INC.**
INSTRUMENT DIVISION
10,500 N. Port Washington Road
Mequon, Wisconsin 53092 USA
Tel: (414)241-3872 Telex: 26-9681

CIRCLE 125 ON READER SERVICE CARD

The *Auto Analyzer*^{*} is the standard



and **ALPKEM**
rebuilds the standard.

- * Rebuilt AutoAnalyzer instruments
- * Full line of accessories & supplies
- * Applications Engineering

ALPKEM Corporation

14625 S.E. 82nd St., Clackamas, OR 97015
503-657-3010 or 800-547-6275

*Trademark Technicon Corp.

CIRCLE 2 ON READER SERVICE CARD

Gilson Spectra/Glo Fluorometer

—for liquid chromatography
column monitoring of
Fluorescence-labeled compounds

- MUCH GREATER SENSITIVITY
- SPECIFICITY OF MEASUREMENT
- NEWEST L.C. TECHNIQUE

More sensitive measurement
than UV or visible absorption
monitoring



More specific method of measurement because fewer compounds exhibit fluorescing property • Fluorophores are stable for L.C. uses • As little as 10 to 40 nanograms of protein can be detected.

Call or write
Gilson Medical Electronics, Inc.
Box 27, Middleton, WI 53562
Phone 608/836-1551 • Telex: 26-5478

CIRCLE 84 ON READER SERVICE CARD

The smallest balances with the largest selection.

Sartorius 1200 MP. Protected from obsolescence with micro processors.

The only line of electronic top-loaders offering...

...all in one housing: an analytical balance with 0.1 mg readability as well as a precision balance with 3.7 kg weighing range -

...micro processors as standard equipment -

...integration into commercial data processing systems plus connections to a wide variety of

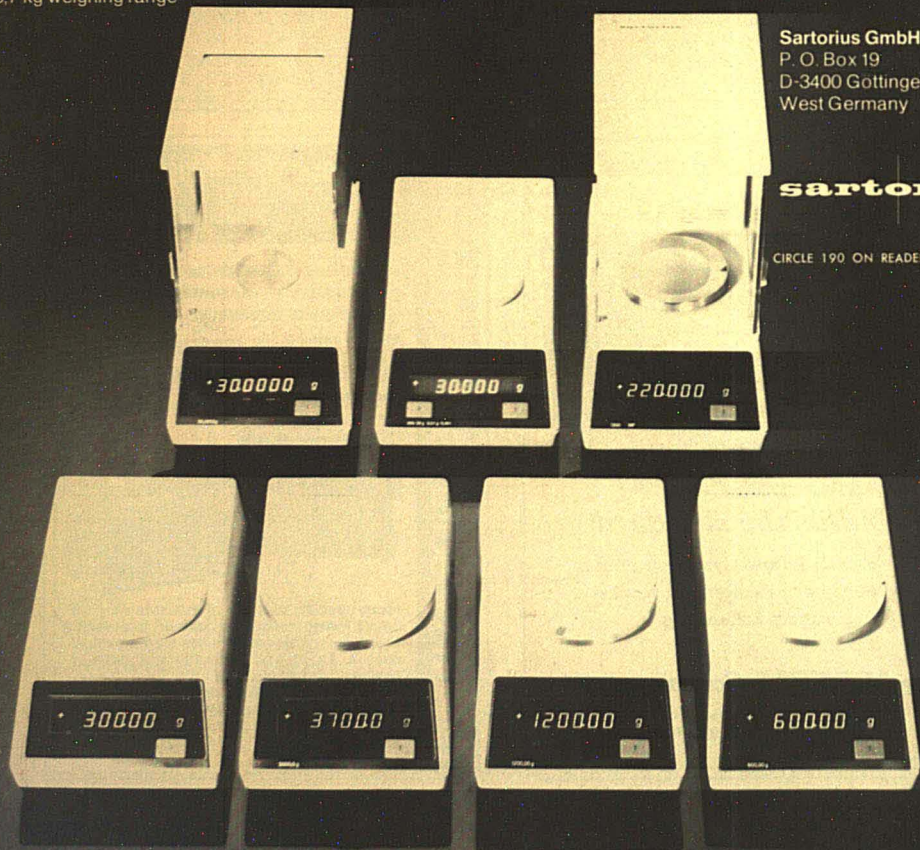
economical accessories for the solution of weighing problems.

Find out more about this line of future orientated miniature balances by requesting our 1978 catalog.

Sartorius GmbH
P. O. Box 19
D-3400 Göttingen
West Germany

sartorius

CIRCLE 190 ON READER SERVICE CARD



Manufacturers' Literature

Deuterium Gas. Specifications and principal uses of D₂ gas are defined in a specification sheet. 2 pp. Liquid Carbonic Corp. **435**

Isotopes Newsletter. Features the automation of mass spectrometric isotope ratio measurements. 4 pp. Micromass **436**

X-ray Absorption Analyzer. Operation and specifications of the Model 720 are outlined. 2 pp. Columbia Scientific Industries Corp. **437**

Chlorine Measurement System. Bulletin F-1000 gives information on the use of polarographic sensing technology for measuring various species of Cl. 6 pp. Delta Scientific Products, Envirotech Corp. **438**

Vacuum Filtration Manifold. Simultaneous filtration of multiple samples for individual analysis of filtrates, as well as retained or membrane-bound species, is described. 3 pp. Amicon Corp. **439**

Moisture Analyzer. Aquatest IV, a microprocessor-controlled titrator, is described. 4 pp. Photovolt Corp. **440**

Catalogs

TLC Products. A line of precoated TLC plates and accessory items is available. 36 pp. Analtech, Inc. **445**

Organic Chemicals. No. 50 data service catalog includes price list on more than 4000 chemicals. 224 pp. Eastman Kodak **446**

General Catalog. Over 9000 items for industrial research, health sciences, chemistry, agriculture, environmental and air pollution control are described in the 1979-80 edition. 468 pp. Cole-Parmer Instrument Co. **447**

Science Supplies. The 1979-80 edition includes items on pH, pumps, and spectrometry accessories. 240 pp. Markson Science Inc. **448**

Flow Meters. Sets of data for a wide variety of flow meters, basic specifications, applications, and theory of flow meters are given. 24 pp. Matheson Instruments **449**

Spectrometry Accessories. Smart printer and digital interface port are the accessories described for the Cary 219 spectrophotometer. 4 pp. Varian **430**

Semi-Q Accessory. The semiquantitative analysis accessory for the EEDS-II X-ray energy dispersive spectroscopy system is described. 2 pp. EG&G Ortec **431**

Liquid Chromatography Methods Development. The methods development processes involved in attacking a liquid chromatography separation problem—column and detector selection, sample pretreatment, chromatographic optimization—are detailed. Solvent property charts are included. 18 pp. Perkin-Elmer **429**

GC Detectors. Application bulletin (GCD-45) describes the GC-33 IR and GC-55 UV detector. 6 pp. Perkin-Elmer **425**

Septum. Low-bleed high-temperature silicone rubber septum called Thermo-green LB-1 is described in bulletin 780 entitled "GC Septa." 7 pp. Supelco, Inc. **428**

X-ray fluorescence. Tefal III, a tube-excited energy-dispersive fluorescence analyzer, is described in a brochure along with the advantages of the method in elemental assays. 16 pp. EG&G Ortec **427**

Valproic Acid. Bulletin 778 discusses the use of SP-1000, a terephthalic acid modified Carbowax, in analyzing valproic acid and other antiepileptic drugs. 2 pp. Supelco, Inc. **432**

Water Scale Analysis. Application note on the analysis of water-formed scale for major, minor, and trace elements by energy dispersive X-ray fluorescence is available. 7 pp. EG&G Ortec **434**



The proof is in the chromatogram.



When the quality is in the product, you can read it in the chromatogram. Glenco supplies a complete line of high-quality liquid chromatography products:

- HPLC System I
- A complete line of prepacked HPLC columns
- An exclusive line of classical LC columns
- High-quality packings, syringes and dispensers

Write for our new catalog.



Glenco Scientific Inc.

The total LC supplier since 1962

2802 White Oak Drive

Houston, Texas 77007

713/861-9123

CIRCLE 87 ON READER SERVICE CARD

THINKING SERIOUSLY ABOUT LIGHT SCATTERING?

THEN THINK
SERIOUSLY
ABOUT THE
C.N. WOOD

- MONOPHOTOMETER
(Single Detector)
- DUOPHOTOMETER
(Two Detectors)
- DIFFERENTIAL
REFRACTOMETERS
- ABSOLUTE
CALIBRATION

AVAILABLE WITH
MULTIPLE LIGHT SOURCES,
CONSTANT TEMPERATURE SYSTEM,
AUTOMATIC SCANNING, MANY ACCESSORIES.

Call (215) 968-4268 or send for literature and prices



CIRCLE 241 ON READER SERVICE CARD

New! 214nm Line Source

Now available for instrumentation applications requiring high intensity short wave UV. The Z-800 PEN-RAY® Zinc Lamp was designed for OEM application and is sized for retrofit in existing instrumentation. It's the first light source of its kind with a predominant spectral output at 214 and 308nm.

- Stable, reproducible transmission
- Low noise in the output
- Highest available brightness of the source
- Applicable for liquid chromatography systems and air pollution monitoring equipment.

Call or write today for more information.

ULTRA-VIOLET PRODUCTS, INC.
5100 Walnut Grove Avenue, San Gabriel, CA 91778 U.S.A.



New... from the research labs at UVP.

CIRCLE 216 ON READER SERVICE CARD



Edited by G.D. Meier 2nd Edition

In the five years since the first edition was published, *Hazards in the Chemical Laboratory* has become established as a vital handbook in all types of laboratory environment. However, over this period many developments have taken place which justify changes in scope and emphasis.

This second edition contains completely new chapters on Reactive Chemical Hazards, and Chemical Hazards and Toxicology. The authors of the chapters in the original volume have also brought their contributions up-to-date in the light of changing attitudes and legislative changes that are in progress. The section dealing with hazardous chemicals has been greatly expanded so as to provide detailed information on the properties, warning phrases, injunctions, toxic effects, hazardous reactions, first aid treatments, fire hazards and spillage disposal procedures for all common laboratory chemicals, together with short notes on the hazardous properties and reactions of several hundred other less common chemicals.

Brief contents

Introduction, Health and Safety at Work etc. Act 1974, Planning for Safety, Fire Protection, Reactive Chemical Hazards, Chemical Hazards and Toxicology, Medical Services and First Aid, Hazardous Chemicals, Safety in Hospital Biochemistry Laboratories, Precautions Against Radiations

**480 pages (1977) ISBN 0-85186-699-9
hardback \$15.75**

Distributed by The American Chemical Society
Published by The Chemical Society

SIS/American Chemical Society
1155 16th St., N.W./Wash., D.C. 20036

Please send _____ copies of *Hazards in the Chemical Laboratory* 2nd Edition at \$15.75 per copy.

☐ Check enclosed for \$_____ ☐ Bill me
Postpaid in U.S. and Canada, plus 40 cents
elsewhere

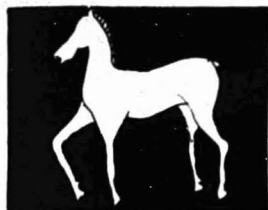
Name _____

Address _____

City _____

State _____

Zip _____



Archaeological Chemistry II

Advances in Chemistry Series No. 171

Giles F. Carter, Editor
Eastern Michigan University

A symposium sponsored by the Division of the History of Chemistry of the American Chemical Society.

Beautifully illustrated with 15 color plates and printed on high-quality enameled stock, this book highlights the great strides that have been made in understanding the origin and distribution of archaeological specimens composed of pottery, glass, metal, bone, and pitch, through the unfolding of new and improved analytical techniques.

Emphasis is on the historical knowledge derived from the chemical analysis and investigation of various artifacts including South American dyes, Egyptian glass, ancient Near Eastern ivory, Spanish ceramics, Chinese bronzes, prehistoric American copper, and copper-based Roman coins.

CONTENTS

Perspectives and General Techniques: Chemistry and Archaeology • Conservation of Archaeological Materials • Radiocarbon Dating • Spark Source Mass Spectrometry • Applications of X-Ray Radiography • **Organic Materials:** Trace Element Analysis in Bone • Amino Acid Analysis in Radiocarbon Dating of Bone Collagen • Amino Acid Racemization Dating of Bone and Shell • Ancient Near Eastern Archaeological Ivory Artifacts • Aliphatics from Middle Eastern Sites • The Identification of Dyes in Textiles • **Ceramics:** Analysis of Early Egyptian Glass • Spanish and Spanish-Colonial Mayolica Ceramics • Soapstone Artifact Characterization • Atomic Absorption Spectroscopy of Archaeological Ceramic Materials • **Metals:** Lead Isotope Ratios in the Manufacture of Pigments • Lead Isotope Analyses and Sources of Nigerian Bronzes • Ancient Chinese Bronze Compositions • Prehistoric Copper Artifacts • Chemical Compositions of Copper-Based Roman Coins

389 pages (1978) Clothbound \$46.00
LC 78-26128 ISBN 0-8412-0397-0

No. 138 *Archaeological Chemistry I*
254 pages (1974) Clothbound \$29.00

SIS/American Chemical Society
1155 16th St., N.W./Wash., D.C. 20036

Please send the following:

☐ Archaeological Chem. I • Archaeological Chem. II
(ACh 0211-7) \$29.00 ea (ACh 0397-0) \$46.00 ea

☐ Check enclosed for \$____ Bill me
Postpaid in U.S. and Canada plus 75¢ elsewhere
California residents please add 6% state use tax.

Name _____

Address _____

City _____

State _____

Zip _____

Solve your materials problems by Surface Area Pore Volume, Size or Chemisorption

More R & D and QC labs worldwide use industry proven Micromeritics instruments to measure physical properties of materials than those of any other manufacturer.

Micromeritics instruments reliably measure specific surface areas from 0.001 m²/g up, determine pore volume and pore size from 600 to 20 Å diameter, and do chemisorption studies to determine catalyst activity. Both manual and automatic instruments are available.

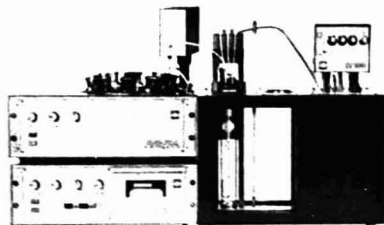
Micromeritics instruments use the classic, volumetric, gas adsorption (B.E.T.) technique employing a wide variety of adsorbates including argon, krypton, water vapor, nitrogen, or any non-corrosive gas.

For more information, contact Micromeritics Instrument Corp.
5680 Goshen Springs Road, Norcross, Georgia 30093 U.S.A.
(404) 448-8282 TELEX: 70-7450.

 **micromeritics**

CIRCLE 135 ON READER SERVICE CARD

VISCOSITY



Automated Measuring Saves Lab Time.

If you measure viscosity with the capillary method, there's a SCHOTT AVS System for you. If you don't, maybe you should. The fully automated AVS/PA will test up to 30 different samples without operator supervision. Select the program and let it go! Variable program capabilities include: number of rinses, number of repeat measurements, test temperature, sample temperature conditioning period, suction rates and more. Standard temperatures up to 150°C; High Temperature up to 220°C. Measuring accuracy 0.1% with a range up to 30,000 cSt. Semi-Automated models also available. Building block concept allows expansion from basic unit to fully automated unit.



SCHOTT
JENA GLAS JENA GLASWERK SCHOTT & GEN. INC.

**SEND FOR DESCRIPTIVE
COLOR BROCHURE NOW!**

11 EAST 26TH STREET, NEW YORK, N.Y. 10010/(212) 679-8535

CIRCLE 189 ON READER SERVICE CARD

Chemical and Biochemical Applications of Lasers, Vol. 4

Edited by C. BRADLEY MOORE

CONTENTS: A. Andreoni et al., Structural Studies of Biological Molecules Via Laser-induced Fluorescence: Acridine-DNA Complexes. B. E. Kohler, Site Selection Spectroscopy. R. Mathies, Biological Applications of Resonance Raman Spectroscopy in the Visible and Ultraviolet: Visual Pigments, Purple Membrane, and Nucleic Acids. R. P. Van Duyne, Laser Excitation of Raman Scattering From Adsorbed Molecules on Electrode Surfaces. S.

Druet and J.-P. Taran, Coherent Anti-Stokes Raman Spectroscopy. T. F. George et al., Theory of Molecular Rate Processes in the Presence of Intense Laser Radiation. R. L. Woodin et al., Multiphoton Dissociation of Gas Phase Ions Using Low Intensity cw Laser Radiation. J. E. Hearst, Photochemical Fixation of the Nucleic Acid Double Helix Utilizing Psoralens.

1979, about 403 pp., in preparation ISBN: 0-12-505404-1

Simplified Digital Automation with Microprocessors

By JAMES T. ARNOLD

CONTENTS: Automation, an Introduction. The Digital Approach To Information and Processes. Elementary Digital Logic. Introduction To More Complex Circuits. The Arithmetic Logic Unit. The Microprocessor. Microprocessor Operating Systems. Completing the Automated

System. Interface Devices and Auxiliary Circuits. An Exercise Design For A Microprocessor Automated Instrument System.

1979, \$22.50 ISBN: 0-12-063750-6

Additives for Plastics

Edited by RAYMOND B. SEYMOUR

FROM THE PREFACE: This two volume treatise was prepared by experts in the field to supply basic information of two sorts. The first volume consists of chapters to provide the fundamentals behind the subject. Each chapter in Volume 2 represents an expanded report of one of the presentations at the first Additives for Plastics Symposium sponsored by the Organic Coatings and Plastics Division of the American Chemical Society which was held at its National Meeting at Anaheim, California in April 1977. Chapters on specific additives were written by authors selected for their expertise in each phase of additive technology. The use of different types of coupling agents for fillers and plasticizers are discussed by researchers in these phases of plastic technology. Stabilizers for weather, fungal, heat resistance and resistance to ultraviolet radiation are also elucidated. Colorants which are most important esthetically are described. The state of the art reports published in Volume 1 and the research oriented reports published in Volume 2 are of vital interest to those who are closely associated with the plastics industry. Since additives are essential ingredients of almost all plastics, the information presented in these reports should be of interest to all who are concerned with the design, fabrication, and use of plastics.

VOLUME 1/STATE OF THE ART

CONTENTS: R. B. Seymour, Nonreinforcing Fillers for Plastics. M. P. Wagner, Natural and Synthetic Silicas in

Plastics. P. Hamed and A. Y. Coran, Reinforcement of Polymers through Short Cellulose Fibers. J. H. Kietzman, Asbestiform Fillers. J. V. Milewski, Whiskers and Microfibers. E. P. Pinedemann, Silane Coupling Agents. S. J. Monte and G. Sugerman, Nonsilane Coupling Agents. R. B. Seymour, Nonfiller Additives for Plastics. R. D. Deanin, Plasticizers. E. L. Cadmus, Biocides. W. S. Castor, Jr. and J. A. Manasso, Optical and Other Effects of White Pigments in Plastics. E. L. Weinberg, Heat Stabilizers. R. P. Levek, Flame Retardant Additives for Plastics.

1978, 288 pp., \$17.50 ISBN: 0-12-637501-1

VOLUME 2/NEW DEVELOPMENTS

CONTENTS: R. B. Seymour, Advances in Fillers for Plastics. J. V. Milewski, The Science and Potentials of Micropacking. H. S. Katz and L. Ehrenreich, Glass Fillers. M. P. Wagner and M. O. Fetterman, Silica-Filled Ethylene-Vinyl Acetate Resins. R. D. Deanin, Recent Advances in Plasticizers. E. P. Pinedemann and G. L. Stark, Effect of Additives on Viscosity of Filled Resins. S. J. Monte and G. Sugerman, Nonsilane Coupling Agents in Thermoplastics. C. E. Carraher, Jr. et al., Electrical, Solvent, Thermal, and Fungal Properties of Organotin-Containing Poly (Ethyleneimine). J. A. Manasso and W. S. Castor, Jr., Stabilization of Polyolefins for Weather Resistance. R. J. Pierotti, Jr. and R. D. Deanin, Ultraviolet Stabilization of High-Impact Polystyrene. V. J. Mumeau, Colorants for Plastics.

1978, 137 pp., \$9.50 ISBN: 0-12-637502-X

Liquid Chromatographic Analysis of Foods and Beverages, Vol. 1

Edited by GEORGE CHARALAMBOUS

Proceedings of a symposium organized by the Agricultural and Food Chemistry Division's Flavor Subdivision (American Chemical Society) on the occasion of the Joint ACS/Chemical Society of Japan Chemical Congress, Honolulu, Hawaii, April 1-6, 1979.

Modern liquid chromatography (HPLC) has progressed over the past decade from a quasi-probationary status to a fullfledged analytical method with particular relevance to the food and beverage field. It is a method that often complements and sometimes supersedes gas chromatography.

This book presents an update of practical and theoretical aspects of high performance liquid chromatography (HPLC) providing contributions from industrial and academic experts from the United States and abroad. It

shows how and why HPLC is now the method of choice for the separation, quantitative determination, and identification (often coupled with mass spectrometry) of both naturally-occurring and synthetic compounds of low volatility. *Liquid Chromatographic Analysis of Foods and Beverages* will benefit agricultural and food chemists, food scientists and technologists, packing and quality control specialists, flavorists and fragrance manufacturers and advanced students in these and related fields.

1979, 420 pp., in preparation ISBN: 0-12-169001-6

Send payment with order and save postage and handling charge. Prices are subject to change without notice.

ACADEMIC PRESS, INC.

A Subsidiary of Harcourt Brace Jovanovich, Publishers

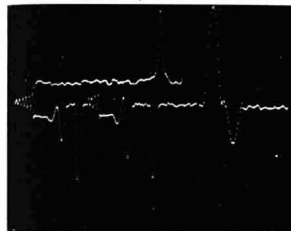
111 FIFTH AVENUE, NEW YORK, N.Y. 10003

24-28 OVAL ROAD, LONDON NW1 7DX

CIRCLE 3 ON READER SERVICE CARD

Laser and Coherence Spectroscopy

Edited by Jeffrey I. Steinfeld



Laser and Coherence Spectroscopy. J. I. Steinfeld, Ed. xv + 530 pages. Plenum Publishing Corp., 227 West 17th St., New York, N.Y. 10011. 1978. \$45
Reviewed by J. M. Harris, Dept. of Chemistry, University of Utah, Salt Lake City, Utah 84112

The introduction of the laser to the field of infrared and optical spectroscopy has had a significant influence on new directions in chemical analysis. Most analytical applications of the laser have, however, exploited only the high power per unit bandwidth and spatial coherence of the source to achieve lower detection limits and higher spectral resolution. This book considers an area of laser spectroscopy, which has generally been overlooked by analytical chemists, where the combined spatial and temporal coherence of laser radiation makes possible the coherent excitation of atomic and molecular energy states. Such excitation gives rise to optical analogues of familiar phenomena in magnetic resonance spectroscopy, such as double resonance, nutation, free induction decays, and echoes. Although the observation of these events is usually confined to low-pressure gases or low-temperature solids where the time scale for dephasing collisions or thermalization can be long compared to the period of the Rabi frequency, the additional information obtained on the dynamics of spectroscopic transitions, excited state relaxation, and spectral assignments will undoubtedly generate considerable interest among analytical spectroscopists.

In the first chapter, J. I. Steinfeld and P. L. Houston discuss double-resonance spectroscopy, where one radiation field probes the internal state distribution of an absorbing system

which has been perturbed by a second intense radiation field. A broad review covering microwave, infrared, and optical pumping with detection by microwave, infrared, or optical probing is presented. Optically detected microwave and infrared double resonance, in particular, are methods which have unique promise since they combine the selectivity and high resolution of rotational and vibrational spectroscopy with the sensitivity of laser-induced fluorescence. A well-written section on instrumentation in this chapter covering radiation sources, signal detection, and enhancement serves as background for the entire volume. T. G. Schmalz and W. H. Flygare, in the second chapter, consider coherent transients in the microwave region which have led to the recent development of a Fourier transform microwave spectrometer. This approach eliminates power broadening while providing higher sensitivity and higher Stark voltages for transitions with small dipole moments compared with continuous wave methods. Chapter 3, by R. L. Shoemaker, covers coherent transients in molecular vibrational transitions through a clear discussion of free induction decay and echoes. C. B. Harris and W. G. Breiland, in Chapter 4, discuss coherent phenomena in electronically excited states, with a particular emphasis on the study of zero-field spin sublevels of excited triplet states. The final chapter, by F. A. Novak, J. M. Friedman, and R. M. Hochstrasser, concerns coherent and time-dependent effects on resonant light scattering by molecules. The relationships between resonance Raman scattering and resonance fluorescence are considered in detail.

Overall, this volume is well written with a balanced presentation of theory, experimental detail, and results. Current literature is cited through 1976. Much of the theoretical material is repeated in Chapters 2-4, which would have been more effectively consolidated into an introductory chapter. The tabular presentation of double resonance results in Chapter 1 is a useful format which was disappointingly not used in other chapters. Generally, analytical spectroscopists should find this book a helpful review of coherent excitation phenomena

and, perhaps, a source of ideas for new approaches to spectroscopy.

Computers in Mass Spectrometry. J. R. Chapman. x + 265 pages. Academic Press, Inc., 111 Fifth Ave., New York, N.Y. 10003. 1978. \$9.80

Reviewed by D. H. Smith, Analytical Chemistry Division, Oak Ridge National Laboratory, Oak Ridge, Tenn. 37830

This is an excellent book. The layout is logically conceived, and each topic in turn is lucidly and concisely described by the author. The intent of the book is to cover all applications of computers to mass spectrometry from the software point of view. Computer programs are described in some depth, but no attempt is made to cover the details of electronic interfacing. The book is written with the specialist in mind, but can be read with advantage by any scientist concerned with data taking and processing.

The heart of the book concerns acquisition and processing of organic mass spectral data, for it is here that computers pay the biggest dividends to the analyst, both in terms of time saving and in terms of retrieval of information that would be impossible to obtain otherwise. Each major approach to data processing (library search, pattern recognition, and spectrum interpretation) is described in enough detail to give the reader a real feel for the problems involved and an appreciation of the ingenuity required to solve them.

The problems of spark source mass spectrometry are well covered in short sections in relevant chapters. An introduction to quantification of mass spectral data (organic and spark source) comprises the final chapter of the book.

Of particular value are the summaries at the end of each chapter, which are helpful to the nonexpert in placing its contents in context. Figures and tables are well chosen. References are thorough and are an excellent guide to further reading on any topic covered in the book.

There are, naturally, a few nits to pick. Use of acronyms, not infrequently before they are defined, is rampant and occasionally leads to such visually ambiguous combinations as MSS

Books

(mass spectrometers). Use of commas is erratic, causing this reader to re-read numerous sentences. Terms in equations could occasionally be better defined.

These are unimportant in light of the overall quality of the book. It fulfills a worthwhile function in bringing together descriptions of the principal applications of computers to mass spectrometry. As such, it belongs in the library of any scientist even peripherally involved in the area.

Handbook of Chemical Microscopy. 2nd ed., Vol. 2, *Chemical Methods and Inorganic Quantitative Analysis*. E. M. Chamot and C. W. Mason, xi + 438 pages. John Wiley & Sons, Inc., 605 Third Ave., New York, N.Y. 10016. 1940. \$27.50

Reviewed by A. C. Reimschuessel, *Applied Chemical Corp., Box 1021 R, Morristown, N.J. 07960*

The "Handbook of Chemical Microscopy," 2nd ed., Vol. 2 by the late

E. M. Chamot and C. W. Mason—professor emeritus, Cornell University, is a reprint of the revised 1940 edition. As a classic text it is a valuable source of information for any student of microscopy. Of particular interest, especially for the novice in microscopy, are chapters I, II, and XIII, that deal with general subjects such as "Manipulative Methods," "Methods of Applying Reagents," and "Sampling and Physical Examination." Both the study and practice of these techniques will without any doubt be beneficial to any microscopist.

Chapters III–XII deal with the actual chemical analyses—the detection of cations and anions—and represent a thorough treatise of classical microscopical chemical analyses and indeed provide a handy reference and guide for the interested user. The terminology used to describe the reaction products is lucid, and the respective micrographs are excellent illustrations of the morphology of corresponding compounds. In short the didactics of the book are outstanding.

The classical methods described are still of great value, especially when applied to the detection of light elements such as Li and Be. However, this reviewer is disappointed that the present edition has not been revised to include significant new developments and advances in chemical microscopy that have taken place during the past 20 years. Particularly missed is a discussion of techniques such as scanning electron microscopy in combination with both X-ray fluorescence analysis and secondary ion mass spectrometry, scanning transmission electron microscopy including electron energy spectroscopy, and scanning auger spectroscopy, because these techniques offer not only identification but also direct imaging of low and high atomic number elements. A text without adequate treatment of these methods can unfortunately not be considered up-to-date. This reviewer hopes that any following edition will be characterized by the inclusion of these new developments.

Pollution Evaluation: The Quantitative Aspects. W. F. Pickering, v + 199 pages. Marcel Dekker Inc., 270 Madison Ave., New York, N.Y. 10016. 1977. \$16.50

Reviewed by R. K. Stevens, *EPA, Environmental Sciences Research Laboratory, Research Triangle Park, N.C. 27711*

This book constitutes a brief introduction to pollution evaluation and an introduction to the principles of

NEW! from GOW-MAC

a teaching
LC good
enough
for QC



Model No. 80-500

a QC LC good
enough for
research



Model No. 80-600

and both priced good
enough for anybody

Both LC units employ rugged, modular GOW-MAC design for reliable operation. The basic Model 80-500 offers pulseless solvent delivery with a constant pressure pump (300 ml capacity to 1000 psi), a modular design for uniform manual injections, column holder, complete with 20 micron Silica Gel column, and reliable 254 nm, low volume (8 μ l) UV detector. Only \$1750.

The high-performance Model 80-600 offers a continuous solvent delivery system with constant volume, variable flow-rates from 0.5 $\text{cm}^3 \text{min}^{-1}$ – 5 $\text{cm}^3 \text{min}^{-1}$ with a low dead volume damping system. Pressures go to 3000 psi. For highly reproducible injections, a six-port rotary valve, modularly designed into column and detector system.

The 80-600 has a 10 micron Silica Gel column and a 254 nm, low volume (8 μ l) UV detector. \$3245.

Other detectors, columns and accessories are available. In addition, each unit shipped comes with a useful book, *Elementary Theory of Liquid Chromatography with Bibliography and Experiments*. For further information, inquire.



GOW-MAC INSTRUMENT CO.
P.O. Box 32, Bound Brook, NJ 08805
Telephone: 201/560-0600
Shannon Free Airport, Co. Clare, Ireland
Telephone: 61632 Telex: 6254

CIRCLE 86 ON READER SERVICE CARD

GREAT NEWS FOR ALL NMR USERS!

Just Published! **Handbook of NMR SPECTRAL PARAMETERS**

W. Brügel

AN EXHAUSTIVE COLLECTION OF PROTON NMR SPECTRAL DATA RELATED
TO CHEMICAL STRUCTURES, COVERING ALL THE MAJOR CHEMICAL CLASSES

- * Unique classification system lists 7,500 selected compounds and enables you to relate the data to hundreds of thousands more
- * Ideal for: Rapid elucidation of the structure of a compound from NMR data; Finding comparative values easily and quickly, in contrast to reference spectra; Simplifying the investigation and formulation of new compounds
- * Eliminates costly and time-consuming mathematical analysis; Cuts out tedious literature searches by giving over 1,800 references

ISBN 0 85501 170 X (3 volume set)

1016pp Casebound

Price: \$280.00

FULLY DESCRIPTIVE ILLUSTRATED BROCHURE AVAILABLE

TELEPHONE, TELEX OR WRITE NOW TO

HEYDEN

HEYDEN & SON INC., 247 South 41st Street, Philadelphia, PA 19104
Tel.: (215) 382 6673 Telex: 831-769

CIRCLE 93 ON READER SERVICE CARD

ANALYTICAL CHEMISTRY, VOL. 51, NO. 4, APRIL 1979 • 513 A

chemical analysis and statistics that are useful in activities of this kind. Included are chapters on the evaluation of land, water, and air pollution. The initial chapter treats the legal aspects to be considered in the course of planning a sampling program and the validity of data to be derived. The final chapter covers preconcentration (to improve sensitivity), masking (for interferences), and the selection of suitable methods. In all, a large subject is dealt with rather compactly in 188

pages plus an index of 10 pages. The exposition is therefore understandably brief but is supplemented by bibliographies with which to fulfill the reader's interests and needs.

The publisher claims that the book is unique in that it combines pollution evaluation methods and the basics of supporting analytical techniques in one volume. To accomplish this dual theme, the author presents alternate subject material in successive chapters. The odd-numbered chapters dis-

cuss pollution evaluation methods as well as the environmental factors to be considered. The even-numbered chapters discuss the fundamental principles of the analytical techniques referred to in the preceding chapter on evaluation.

The analytical topics are treated with differing degrees of emphasis and detail. The sections on the principles underlying gravimetry and titrimetry (redox and acid-base), although concise, are quite inclusive of fundamentals and are profitable reading. The descriptions of spectroscopy, gas chromatography, HPLC, and activation analysis, by comparison, are less extensive in scope. Those readers, who will want to explore these topics further, will not find a list of suggested reading material at the close of this chapter. The reviewer assumes that additional information (on these subjects) may be gleaned from the texts listed in the final chapter of the book.

Other serviceable techniques for pollution studies are introduced in the (odd numbered) chapters on air and water. The methods described are IR spectroscopy, atomic absorption (and flame emission), polarography, anodic stripping voltammetry, coulometric methods, potentiometric methods with ion-selective electrodes, and colorimetric methods. These chapters fulfill their prime purpose in discussing the methodology of pollution studies, planning and execution and are finished off with reading lists.

The book is largely free of typographical errors indicating that it has been proofread with some care. A few errors, which affect the sense of the text, are noted below: On page 138, in the paragraph describing self-absorption of emitted radiation, the following statement appears: "At any time the number of atoms in the ground state (N_0) greatly exceeds the number of excited states, and as the total concentration increases, the probability of emitted radiation meeting lower energy atoms before entering the dispersion system is markedly increased. The ground state atoms absorb characteristic emission . . ." The intended sense of this statement is somehow thwarted.

Additionally, in the listing of components of cigarette smoke on page 54, "benzopyrin" would read more familiarly as benzopyrene. The listing of another component as "butadiene" creates an ambiguity. Did the author intend butadiene or butanedione (diacetyl)?

In the course of discussions of spectroscopy, the author employs the

The symbol of excellence since 1959

Distilled in Glass™



Residue-Free Solvents from Burdick & Jackson

Purified to the exacting requirements of gas chromatography, liquid chromatography and spectrophotometric analysis.

Acetone
Acetonitrile
Benzene
Butanol-1
Butanol-2
n-Butyl Acetate
Butyl Chloride
Carbon Tetrachloride
Chlorobenzene
Chloroform
Cyclohexane
Cyclopentane
o-Dichlorobenzene
Dimethyl Acetamide
Dimethyl Formamide
Dimethyl Sulfoxide
Dioxane
2-Ethoxyethanol
Ethyl Acetate
Ethylene Dichloride
Ethyl Ether
Heptane, 98-99°
Hexadecane
Hexane, 68-69°
Isobutyl Alcohol

Iso-hexanes
Methanol
2-Methoxyethanol
Methylene Chloride
Methyl Ethyl Ketone
Methyl Isoamyl Ketone
Methyl Isobutyl Ketone
N-Methylpyrrolidone
Nonane
Pentane
Petroleum Ether, 30-60°
beta-Phenethylamine
Propanol-1
Propanol-2
Propylene Carbonate
Pyridine
Tetrahydrofuran
Tetramethyl Urea
Toluene
Trichloroethylene
1,1,2-Trichloro-
1,2,2-Trifluoroethane
2,2,4-Trimethylpentane, 99-100°
o-Xylene

Ask for Bulletin BJ-25 U.S. Agencies use F.S.S.

BURDICK & JACKSON LABORATORIES, INC.

1953 South Harvey Street, Muskegon, Michigan U.S.A. 49442 (616) 726-3171

CIRCLE 23 ON READER SERVICE CARD

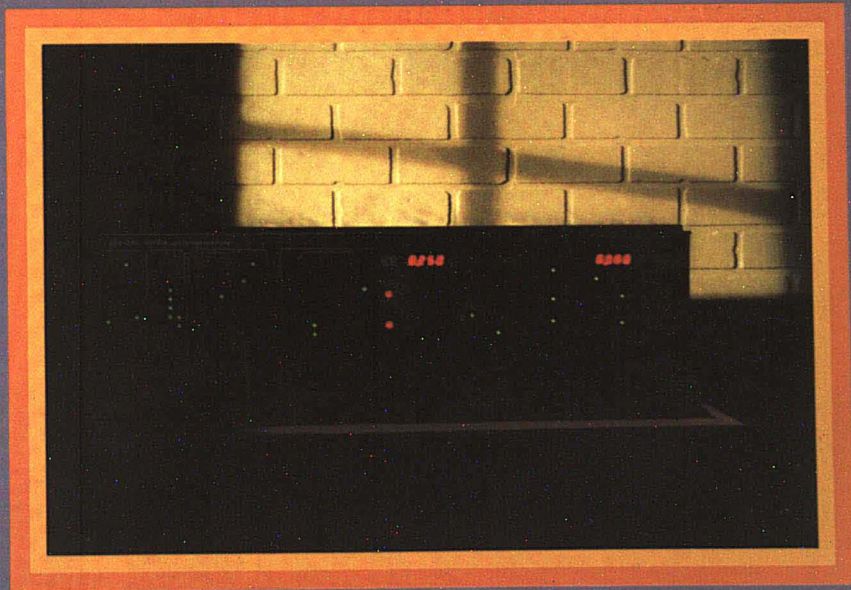


UV/VISIBLE SPECTROPHOTOMETERS

Master, blazed Holographic Gratings cut stray light.

To save costs, the gratings in commercial UV/visible spectrophotometers are usually produced by making replicas from a master, and in the process, fidelity and performance are lost.

Cutting no corners, Pye Unicam have fitted master holographic gratings throughout their new range of instruments, and a glance at the stray light specifications will prove our advantage.



Pye Unicam

A SCIENTIFIC INSTRUMENT COMPANY OF PHILIPS

A new range of UV/visible Spectrophotometers

Pye Unicam have many spectroscopic 'firsts' to their credit and now we introduce two more technological breakthroughs, pioneered in our own laboratories.

Our complete range now benefits from the increased performance of **master, blazed holographic gratings** and the durability conferred by **silica coated optics**.

SPECTROPHOTOMETRY MOVES INTO THE FUTURE

SP6 Series

- ☐ Improved performance
- ☐ Improved construction
- ☐ 195 or 325-1000nm
- ☐ Meter or digital display
- ☐ Colour-coded controls
- ☐ Automatic drift compensation

This highly popular range of single beam spectrophotometers is now relaunched with major improvements in performance, features and construction. The SP6 is available as four low-cost models with choice of visible or UV/visible ranges and meter or digital display. Simplicity of design and colour-coded controls allow the instruments to be used with speed and precision even by inexperienced operators. Their proven high reliability and rugged construction make the SP6 the perfect 'workhorse' instrument for any laboratory, as thousands of satisfied operators around the world can testify. Circle No. 110

**MASTER
HOLOGRAPHIC
GRATING**



SP8-100 and SP8-150

- ☐ Double beam scanning
- ☐ High performance
- ☐ Synchroscan recording principle
- ☐ Flexible, modular design
- ☐ Vast accessory range

The SP8-100 has rapidly established itself as a truly versatile UV/visible scanning spectrophotometer with very simple operation. As part of our policy of continuous product improvement, it is now offered with higher guaranteed performance and the SP8-150 is added to the range with an extended wavelength range and even better specification. Circle No. 111

SP8-200 and SP8-250

- ☐ Research performance
- ☐ Single or double monochromator
- ☐ Microprocessor control
- ☐ Keyboard operation
- ☐ Complete remote control facilities
- ☐ 185-950nm range

When the SP8-200 was announced, we challenged that its performance could only be significantly bettered by double monochromator instruments. That's still true, but with the introduction of the SP8-250 and its double, master holographic monochromator, there's no need to look beyond the Pye Unicam range for the ultimate in low stray light levels. Both instruments have the full range of slitwidths, scan speeds, chart expansions and other facilities expected of research performance spectrophotometers. Circle No. 112



Pye Unicam Ltd

York Street Cambridge England CB1 2PX
Telephone (0223) 58866 Telex 817331

Printed in England 7061.05.3011.11



GAS CHROMATOGRAPHY

Capillary chromatography: Pye Unicam know-how solves your separation problems.

Our full range of capillary columns and injection systems, including splitless, splitter and the superior Grob system, is backed as always, by the Pye Unicam reputation.

Write to us at the address below or use the reader service card to send for our brochure 'Capillary Columns and Injection Systems' detailing their use for the most demanding of separations and explaining the advantages over the use of conventional packed columns.



Manufacturers of the 204 chromatograph and the LC-XP liquid chromatograph



Pye Unicam

A SCIENTIFIC INSTRUMENT COMPANY OF PHILIPS

York Street, Cambridge, England CB1 2PX
Telephone (0223) 58866 Telex 817331

CIRCLE 97 ON READER SERVICE CARD



Pointers to better water analysis

The items below symbolise a major step forward in automatic water analysis.

They are part of Pye Unicam's AC6 Water Analysis System which is like no other because it works on a discrete rather than a continuous flow principle. Take a look at some of the points in its favour.

1 AC6 results emerge directly in concentration at the rate of 240/hr. – faster than continuous flow systems, even in three channel form.

2 Choice of Flowcells makes analytical ranges more flexible.

3 Numbered and coded racks guarantee positive sample identification. At any one time 100 samples can be loaded into the AC6 and the system genuinely left to get on with its job.

4 Exclusive 'VoluKey' syringe programming gives analysis changeover times of less than five minutes.

5 Pye Unicam method sheets demonstrate the unparalleled flexibility of the system – and its simplicity of operation.

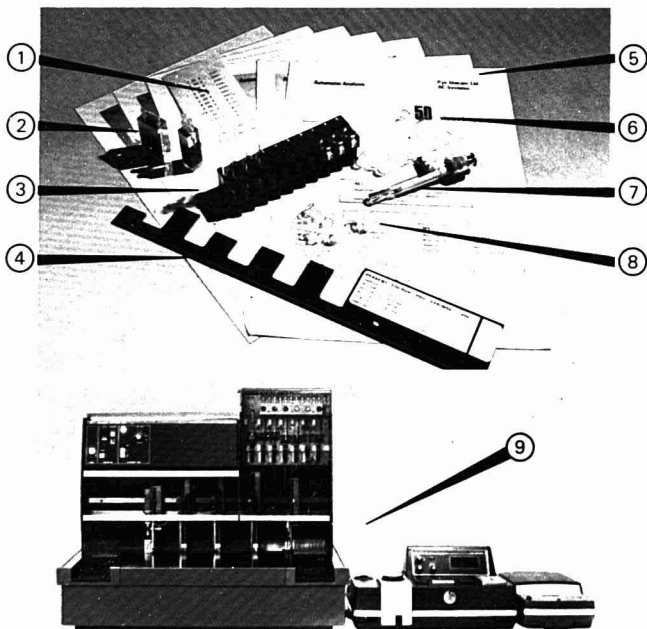
6/8 Separate test tube and disposable

sample cup for each sample solution keeps cross contamination to a minimum.

7 Various sizes of sample and disposable reagent syringes ensure a wider analytical range and improved precision compared with peristaltic systems.

9 The complete AC6 Water Analysis System – quite simply, it offers increased performance and versatility at lower cost.

For our brochure write, phone or use the reader reply service card today



Pye Unicam

A SCIENTIFIC INSTRUMENT COMPANY OF PHILIPS

York Street Cambridge CB1 2PX England
Telephone (0223) 58866 Telex 817331
CIRCLE 98 ON READER SERVICE CARD



Aren't you glad you waited before buying your new AA?



Because the new System SP9 now offers you so much more.

Flame or flameless, System SP9 has the microprocessor power and flexibility to solve your AA problems.

System SP9 has Computer Data Handling to give

- Calibration with up to 5 standards.
- Precision calculations and Running Mean.
- Peak height or peak area.

System SP9 has a unique Video Furnace Programmer providing

- Display of set parameters and status.
- EAROM storage of 10 furnace programs.
- Temperature or Voltage control.

And System SP9 has automation

via the world's most flexible flame and flameless autosamplers.

Now you've no need to wait any longer. Write, phone or use the reader reply service for further information on System SP9, the most cost effective AA system available.



Pye Unicam

A SCIENTIFIC INSTRUMENT COMPANY OF PHILIPS

York Street Cambridge CB1 2PX England
Telephone (0223) 58866 Telex 817331

CIRCLE 99 ON READER SERVICE CARD

A new level in HPLC sophistication and simplicity.



Micromeritics proudly introduces its new 7500 microcomputer-based Liquid Chromatograph—a beautiful blend of engineering sophistication and operating simplicity.

We've taken the most advanced features available in HPLC today and packaged them so you can have the exact system to fit your specific application. Both gradient and isocratic integrated systems are available to accommodate rigorous quality control and methods development needs or the complex analysis functions of research and development laboratories.

Simple keyboard entry

All operating commands can be made from a single microcomputer-based control module. An alphanumeric display readout continually informs the operator of entry status for such parameters as flow rate, pressure limits, solvent concentration and column temperature.

Total analysis reporting

Comprehensive analysis reporting is achieved through a printer/plotter which not only gives you the chromatograms, but also a printout of gradient/solvent conditions, flow rate, pressure, temperature and operational status. Sample retention times, peak area and height, percent of concentration, sample and injection numbers can also be printed out.

Total automation

The 7500 system can be totally automated to give you unattended analysis around the clock. It can initiate 192 analyses of up to 64 samples . . . automatically.

Other advanced design features

The new 7500 also has an all new Ternary Solvent Mixer for more accurate and reliable low pressure solvent blending; a precision heated column compartment for faster more stable analysis; a new



**Also available as components.
Buy what you need now, and
add more as you need it.**

pulseless solvent delivery system; and a choice of three detectors—variable wavelength, fixed wavelength or refractive index.

Available as components, too

And finally, you have the option of buying as much or as little of the system as you presently need. The 7500 system is also available as individual components. You can buy what you need now and add more later as you need it.

To learn more about the many features that separate the new 7500 from all the other HPLCs on the market, contact Micromeritics Instrument Corporation, 5680 Goshen Springs Road, Norcross, Georgia 30093 USA (404) 448-8282 TELEX: 70-7450.

micromeritics®

EUROPEAN SALES OFFICE

2 Orchard Way
Eaton Bray
Bedfordshire
England
Tel: 051-626249

AFRICA

NORTH
Coutronics France S.A.
Margency 95580 Andilly
France
Telephone: 989-9030

SOUTH
Coutler Electronics Pty. Ltd.
Transvaal
South Africa
Telephone: 805-2046/55/56

ARGENTINA
Instrumental S.R.L.
Buenos Aires
Telephone: 85-3121 86-1436

AUSTRALIA

Townson & Meier Ltd.
Lane Cove N.S.W.
Telephone: 426-1199

BELGIUM

Anals S.A.
Namur
Belgium
Telephone: 081-22 50 85

BRAZIL

Danon Sociedade Importadora
Equipamentos Científicos Ltda.
Rio de Janeiro
Telephone: 221-4480

DENMARK

Ble & Bernsen Ltd.
Rødovre
Telephone: 45-294-6822

EASTERN EUROPE

The GGI Forum
Thessaloniki
Greece
Telephone: 542-371

ENGLAND

Coutler Scientific Ltd.
Hertford
Telephone: Harp 63151

FINLAND

Oy Tainio AB
Helsinki
Telephone: 905-44011

FRANCE

Coutronics France S.A.
Margency 95580 Andilly
France
Telephone: 989-9030

GERMANY

Coutler Scientific GmbH
Gahringshof
West Germany
Telephone: 02156-755011

GREECE

The GGI Forum
Thessaloniki
Greece
Telephone: 542-371

GUADALUPE

Coutronics France S.A.
Margency 95580 Andilly
France
Telephone: 989-9030

INDIA

Blue Star Limited
Bombay
Telephone: 45-7867 or
45-6799

ITALY

Coutler Scientific S.p.A.
Milano
Telephone: 989-108

JAPAN

Shimadzu Sensakusho Ltd.
Kyoto
Telephone: (075) 8111111

KUWAIT

Bader Sultan & Bros. Co.
Kuwait
Telephone: 421-291 92 93

MAINTENANCE

Delta Electronics Sdn. Bhd.
Bangsar Baru
Kuala Lumpur
Telephone: 943629

MARTINIQUE

Coutronics France S.A.
Margency 95580 Andilly
France
Telephone: 989-9030

NETHERLANDS

Chemical Laboratory Instruments
Schynkel
Netherlands
Telephone: 04104-4035

NEW ZEALAND

Selby-Wilson Scientific Ltd.
Lower Hutt
Telephone: 697-099

RE UNION

Coutronics France S.A.
Margency 95580 Andilly
France
Telephone: 989-9030

SPAIN

Urra S.L.
Barcelona 15
Telephone: 2548100

SWITZERLAND

IG Instrumenten-Gesellschaft
Zürich
Telephone: 0166331

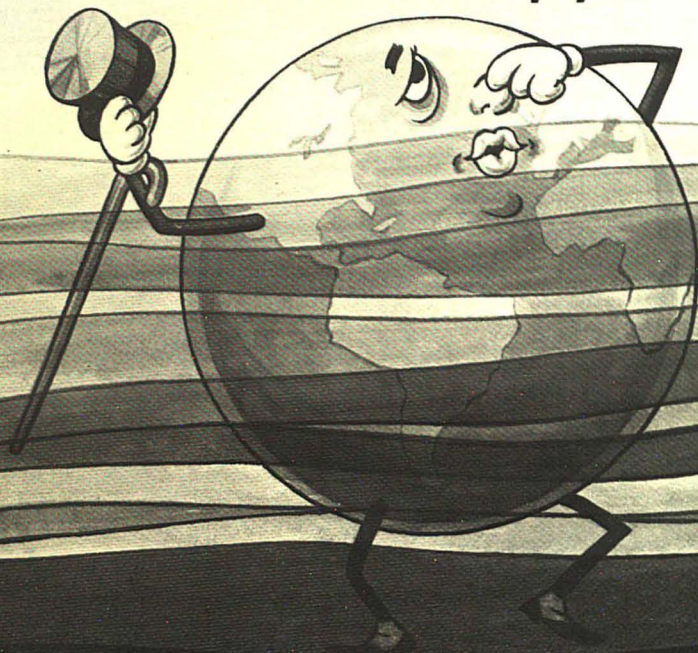
TAIWAN

Verter Corporation
Tapei, Taiwan
Telephone: 752-6452(3)

U.S.S.R.

Coutronics France S.A.
Margency 95580 Andilly
France
Telephone: 989-9030

**Listen world . . .
it's time to clean up your act**



Environmental Science & Technology

SHOWS WHAT CAN BE DONE, WHAT MUST BE DONE, AND HOW TO DO IT!

Environmental clean-up is not only a good idea — it is the law! And ENVIRONMENTAL SCIENCE & TECHNOLOGY gives you the practical, hard facts you need on pollution and control, covers techniques, feasibility, research, equipment (including products, services and supplies) as well as case histories.

Essential reading for businessmen, scientists, legislators, governmental executives, builders, manufacturers and the academic world, ENVIRONMENTAL SCIENCE & TECH-

NOLOGY covers a broad range of information from what is going on in research labs to how-to-put-it-to-work in the real world. Also included is up-to-date news of current and pending governmental regulations, industry trends, meeting guide, technology reports and much more!

Your Guarantee:

You may cancel your subscription any time you are not pleased and you will receive a refund, in full, for copies still due.

Environmental Science & Technology, American Chemical Society
1155 Sixteenth Street, N.W., Washington, D. C. 20036

1979

YES, I want to keep up-to-date on the hard facts of environmental clean-up. Please enter my subscription to ENVIRONMENTAL SCIENCE & TECHNOLOGY as follows:

ACS Member subscription, 1-year
Non-member subscription, 1-year
Institution, Company or Library subscription, 1-year

Please specify: ☐ Hard copy, or ☐ Microfiche
☐ Payment enclosed. ☐ Bill me. ☐ Bill company.

U.S.		Foreign	
<input type="checkbox"/> \$16.00	<input type="checkbox"/> \$22.00	<input type="checkbox"/> \$24.00	<input type="checkbox"/> \$30.00
<input type="checkbox"/> \$24.00	<input type="checkbox"/> \$30.00	<input type="checkbox"/> \$64.00	<input type="checkbox"/> \$70.00

Toll Free: New Orders: 800-638-2000
Md. only 301-949-1551

Name _____ Title _____

Organization _____
☐ Home
Address ☐ Business _____

City, State, Zip _____

Allow 60 days for your first copy to be put in the mail.

*ACS Member rates are for personal use only.

0034L

Solve Your Materials Problems 6 Ways

More R&D and QC labs use Micromeritics proven, precision instruments to measure physical properties of material than those of any other manufacturer in the world. These measurements include:

- 1 Automatic particle size distribution** gives rapid analysis from 100 to 0.1 μm diameter and 500 to 38 μm diameter.
- 2 Manual and automatic physical adsorption** for B.E.T. surface area from 0.001 m^2/g up; adsorption and desorption isotherms; pore structure (volume, size and shape) from 600 to 20 \AA diameter.
- 3 Manual and automatic chemisorption** measures active material availability; percent metal dispersion.

- 4 Mercury porosimetry** measures pore structure (volume, size and shape) from 354 to 0.0035 μm diameter; density, surface area and average particle size.

- 5 Manual and automatic density** determines absolute volume to $\pm 0.02\text{cc}$.

- 6 Electrophoretic mass-transport analysis** to study flocculation and dispersion; particle-liquid systems behavior; zeta potential.

We also invite you to use our complete Materials Analysis Laboratory Services. Let us show you how to solve your material problems. Call or write Micromeritics Instrument Corporation, 5680 Goshen Springs Road, Norcross, Georgia 30093. U.S.A. (404) 448-8282. Telex: 70-7450.

 **micromeritics**

CIRCLE 137 ON READER SERVICE CARD



EUROPEAN SALES OFFICE

2 Orchard Way
Easton Bray
Bedfordshire
England
Telex: 951426249

AFRICA

North
Coultronics France S.A.
Marsigny 95580 Andilly
France
Telephone: 989-9030

South

Coulter Electronics PTY. Ltd.
Transvaal
South Africa
Telephone: 805-2046 55 56

ARGENTINA

Instrumentaria S.R.L.
Buenos Aires
Telephone: 85-3121 86-1436

AUSTRALIA

Townsend & Mercer Ltd.
Lane Cove N.S.W.
Telephone: 428-1199

BELGIUM

Analis S.A.
Namur
Belgium
Telephone: 081-22 50 85

BRAZIL

Danon-Sociedade Importadora
Quemados Cientificos LTDA
Rio de Janeiro
Telephone: 221-4480

DENMARK

Be & Berntsen Ltd.
Rødovre
Denmark
Telephone: 45-294-8822

EASTERN EUROPE

Medata AB
Stockholm
Sweden
Telephone: 08-303370

ENGLAND

Coulter Scientific Ltd.
Hertford
Telephone: Harp 63151

FINLAND

O.Y. Tamm AB
Helsinki
Telephone: 90-544011

FRANCE

Coultronics France S.A.
Marsigny 95580 Andilly
France
Telephone: 989-9030

GERMANY

Coulter Scientific GmbH
Garching/Obad
West Germany
Telephone: 02156-755011

GREECE

The G.G. Orom
Thessalonica
Greece
Telephone: 542-371

GUADALOUPE

Coultronics France S.A.
Marsigny 95580 Andilly
France
Telephone: 989-9030

INDIA

Blue Star Limited
Bombay
Telephone: 45-7867 or
45-6799

ITALY

Coulter Scientific S.p.A.
Milano
Telephone: 98-80-108

JAPAN

Shimadzu Seisakusho Ltd.
Kyoto
Telephone: (075) 8111111

KUWAIT

Bader Sultan & Bros. Co.
Kuwait
Telephone: 421291 92 93

MALAYSIA

Datta Electronics SDN. BHD.
Kuala Lumpur
Telephone: 943629

MARTINIQUE

Coultronics France S.A.
Marsigny 95580 Andilly
France
Telephone: 989-9030

NETHERLANDS

Chemical Laboratory Instruments
Schjndel
Netherlands
Telephone: 04104-4035

NEW ZEALAND

Selby-Wilton Scientific Ltd.
Lower Hutt
Telephone: 697-099

REUNION

Coultronics France S.A.
Marsigny 95580 Andilly
France
Telephone: 989-9030

SPAIN

Izasa S.L.
Barcelona 15
Telephone: 2548100

SWITZERLAND

IG Instrumenten-Gesellschaft
Zürich
Telephone: 0166331

TAIWAN

Vertex Corporation
Taipei
Telephone: 752-4452(3)

U.S.S.R.

Coultronics France S.A.
Marsigny 95580 Andilly
France
Telephone: 989-9030

...for the
innovative
chemist

CHEMTECH

Created for the chemist who tackles life with a zest for solving problems and achieving results, CHEMTECH is a lively monthly publication with a brisk style and a down-to-earth approach.

You'll find it is written, not by staff writers, but by "shirt-sleeve" plant people, researchers, company heads, professors, economists, and scientists in many disciplines. CHEMTECH is edited from the perspective of the practitioner.

Consider some of the varied disciplines and topics it covers: agriculture, analysis, biology, business, catalysis, chemical science, energy, engineering, environment, government, management, marketing, plastics and polymers, and much, much more!

Most important, CHEMTECH helps you cope with live, real-world problems, from the preparation, characterization, and use of chemicals to engineering operation, distribution... even your problems as a practicing technologist.

Because you are a doer, an achiever, an innovator—join other active, interested chemists and subscribe to CHEMTECH NOW!

CALL TOLL FREE: New Orders (800) 638-2000/MD Only (301) 949-1551 or mail the coupon below.

CHEMTECH

American Chemical Society
1155 Sixteenth Street, N.W.
Washington, D. C. 20036

YES, please enter my one-year subscription to CHEMTECH as indicated:

	U.S.	Foreign**	
ACS Member*	<input type="checkbox"/> \$17.00	<input type="checkbox"/> \$21.00	1979
Nonmember, personal	<input type="checkbox"/> \$25.00	<input type="checkbox"/> \$29.00	
Institution	<input type="checkbox"/> \$85.00	<input type="checkbox"/> \$89.00	
Students	<input type="checkbox"/> \$ 8.50	<input type="checkbox"/> \$12.50	

☐ Payment enclosed. (Payable to American Chemical Society)

☐ Bill me. ☐ Bill company.

Name _____

Title _____

Organization _____

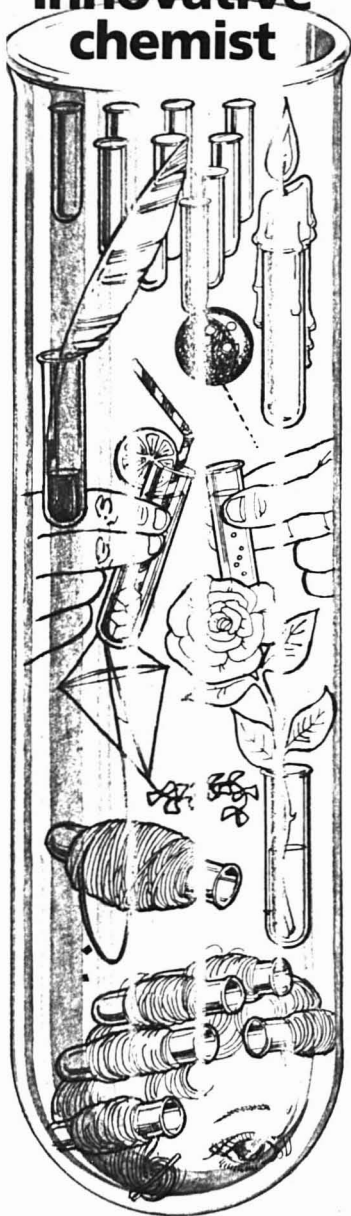
Address _____

City, State, Zip _____

*Member rates are for personal use only.

**Payment must be made in U.S. currency by international money order, UNESCO coupons, U.S. bank draft or order through your book dealer.

0034L



For Creative Chromatography Specify Spectra-Physics.



SP 4100: the first intelligent integrator

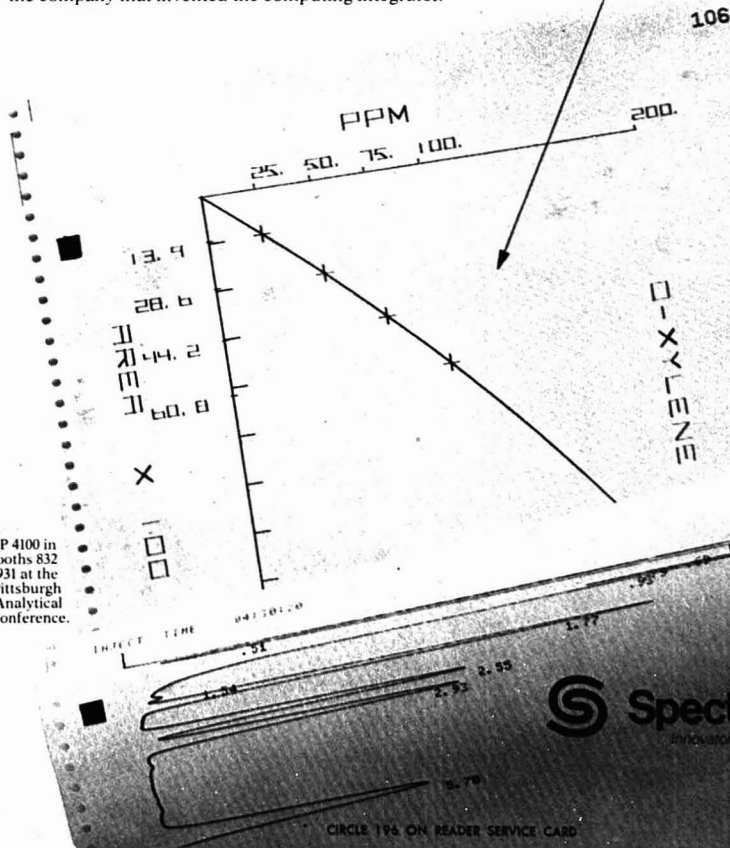
Our new single-channel SP 4100 Computing Integrator is really sophisticated, and yet costs far less than other units with fewer features. **SP 4100 is easy to use**—plug it in, touch a button, and you get Area and Area % report. If you want more, **it has truly intelligent dialog**—it asks only relevant questions for the data manipulation you want. **Dynamic integration is standard**—automatic integration with dynamic evaluation of parameters will integrate each peak optimally.

Let us show you how SP 4100 can help you do more creative chromatography. It's what you'd expect from Spectra-Physics, the company that invented the computing integrator.

BASIC programmability is standard—You can use SP 4100's extensive capability and flexibility to fit your individual needs.

Programmable X-Y plotting—You can enhance your data presentation with graphs such as this multilevel calibration.

USA headquarters:
Spectra-Physics
2905 Stender Way,
Santa Clara, CA
95051
Or call one of our
regional US sales
offices:
Midwest (Ill.):
(312) 958-0882
Mid-Atlantic (Md.):
(301) 345-7333
East (N.J.):
(201) 981-0390
South (Tex.):
(713) 688-9886
West (Calif.):
(408) 249-0105
European
headquarters:
Spectra-Physics
GmbH
Alsfelder Strasse 12,
6100 Darmstadt
West Germany.



See SP 4100 in
Booths 832
and 931 at the
Pittsburgh
Analytical
Conference.

Spectra-Physics
Innovators in Chromatography



LIF-O-GEN® SPECIALTY GASES

Lif-O-Gen® is a leading specialty gas manufacturing company with total capabilities in processing a broad range of high purity research gases, primary gas calibration standards, and gas mixtures as well as a complete line of gas handling equipment, instrumentation and analytical devices.

For particular gases or equipment to meet your own special requirements, please write or phone Lif-O-Gen®, Specialty Gas Department, P.O. Box 149 Woods Rd., Cambridge, Maryland 21613 (301) 228-6400 TWX: 710-865-9652

LIF-O-GEN® OFFERS

- Pure Gases • Gas Mixtures • Gas Handling Equipment
- Gas Chromatographs • Electronic Gases • Pollution Monitoring Gases • Calibration Gases • Complete range of refillable and disposable aluminum and steel cylinders • Lif-O-Gen® Gas Encyclopedia, the most complete and advanced encyclopedia of its kind in the world



LIF-O-GEN®

American Life Support Corp.

P.O. Box 149, Woods Rd.
Cambridge, Maryland 21613

A Subsidiary of Liquid Air Corp. of North America

Copyright 1979, Lif-O-Gen®

CIRCLE 217 ON READER SERVICE CARD

prevent vacuum leaks... stop laboratory glassware breakage use **APIEZON**
GREASES • OILS • WAXES

Apiezon lubricants are especially formulated for use with high vacuum laboratory equipment. These easily applied, high purity, low vapor pressure, stable products are resistant to organic solvents, most chemical vapors.

GREASES—anti-seize greases which eliminate costly breakage; for high vacuum use down to 5×10^{-11} torr at 15°C and moderate vacuum use to 10^{-4} torr. They won't leach out of ground glass joints or stop cocks.

OILS—ideal as vapor diffusion pump fluids. They greatly minimize the need for a cold trap, permit maximum pumping speeds, reduce operating and maintenance costs.

COMPOUND Q: a low cost, putty-like, versatile sealant.

WAXES—for sealing vacuum joints more permanently.

Write or call for your free copy of Bulletin 43a

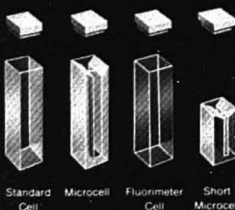
BIDDLE JAMES G. BIDDLE CO.
Plymouth Meeting, Pennsylvania 19462
Phone: (215) 646-9200 413

CIRCLE 26 ON READER SERVICE CARD

THE WIDEST SELECTION OF HIGH-PRECISION SPECTROPHOTOMETER CELLS

Available in glass, special glass, quartz, matched sets, and specials!

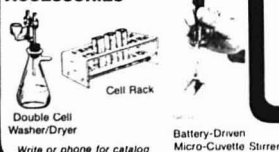
ALL FUSED CONSTRUCTION



HPLC FLOW CELLS



ACCESSORIES



Write or phone for catalog

PRECISION CELLS, INC.

560 SO. BROADWAY, HICKSVILLE, N.Y. 11801 • (516) 938-7772

CIRCLE 174 ON READER SERVICE CARD

usage, "infrared radiation which is sorbed" or "molecular sorption" of radiation. This is uncommon usage at best.

This reviewer prefers that techniques be identified by their distinctive names. In this volume some (important) techniques are unlabeled. It is the author's option to determine how limited or rudimentary the description should be, but naming the technique will help the interested reader to find information from other sources. In the section on statistics the author apparently introduces Student's *t* test but without a label. In another chapter the application of permeation devices to the calibration of monitors is nicely described, but there is no indication that these devices are called permeation tubes. The operation of the carbon monoxide monitor described in the section on air pollution is apparently based on the gas filter correlation cell. This is not indicated, however.

Nevertheless, the book is neatly arranged and reads smoothly. The volume would serve for an orientation in pollution evaluation for the practicing chemist.

New Books

Trace Element Analysis of Geological Materials. R. D. Reeves and R. R. Brooks. x + 421 pages. John Wiley & Sons, Inc., 605 Third Ave., New York, N.Y. 10016. 1978. \$27.50

This book is volume 51 in the series of chemical analysis that covers the sequence of processes necessary in the analysis of geological materials. Sampling techniques and the physical and chemical methods of sample pretreatment are discussed. The analytical methods used include gravimetry and titrimetry colorimetry and fluorimetry atomic emission, atomic absorption and fluorescence, X-ray emission, radiometry and radioactivation, electroanalytical, and mass spectrometry.

Physical Methods in Modern Chemical Analysis. Vol. 1. Theodore Kuwana, Ed. x + 320 pages. Academic Press, Inc., 111 Fifth Ave., New York, N.Y. 10003. 1978. \$33

This series contains chapters written by specialists on selected analytical methodologies at a depth level

greater than that of instrumentation-oriented textbooks. Volume one contains chapters on gas chromatography; principles, instrumentation, applications, scope, and structural problems of mass spectrometry; fluorescence and atomic absorption spectrometry; and flame and plasma emission analysis methods.

Patent Policy: Government, Academic, and Industry Concepts. Willard Marcy, Ed. x + 173 pages. American Chemical Society, 1155 16th St., N.W., Washington, D.C. 20036. 1978. \$19

This is number 81 in the ACS Symposium Series based on a symposium at the 175th Meeting of the ACS in Anaheim, Calif., March 13-14, 1978. The 13 chapters present historical insights along with an overview of the success of existing patent policies in providing a way to reward all of the parties at interest while safeguarding the public. Specific questions and answers concerning government, academic, and industry concepts are presented along with approaches that may enhance the usefulness of the patent system in the future.

THINK BAUSCH & LOMB PRODUCTIVITY

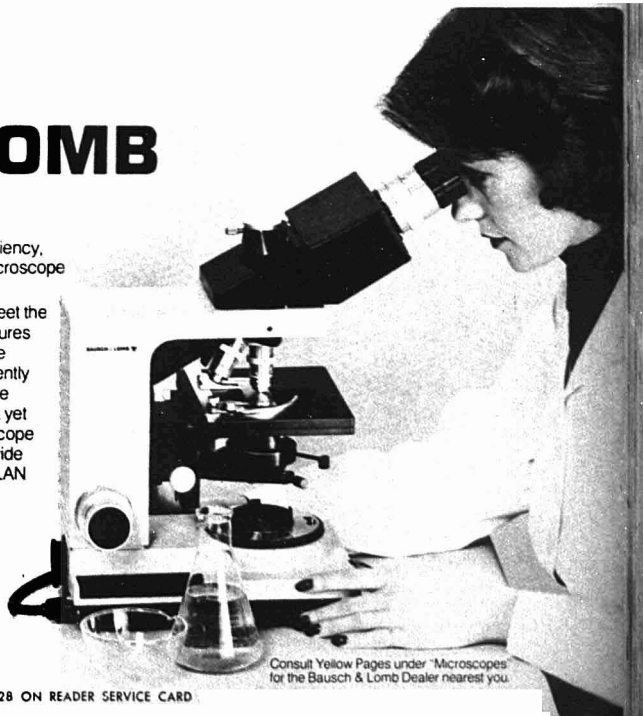
When your laboratory work requires maximum cost efficiency, testing accuracy and total output—think BALPLAN® Microscope productivity.

BALPLAN® Microscopes are specifically designed to meet the demands of a busy lab schedule. Each microscope features distortion-free, wide, flat fields that reduce viewing fatigue and the errors that might follow. All controls are conveniently positioned for comfortable operation, and the bright, white light of tungsten-halogen illumination offers the best look yet at any specimen. It all adds up to a hard working microscope that will increase the productivity in your lab. And worldwide Bausch & Lomb servicing is your assurance that BALPLAN Microscopes will stay on the job each and every day for many years to come. Write today for a detailed catalog or a BALPLAN demonstration. THINK BAUSCH & LOMB... Productivity since 1874.

BAUSCH & LOMB 
Scientific Optical Products Division

Rochester, New York 14602 USA
716-338-6000, TWX 510-253-6189
TELEX 97-8231, CABLE: Bausch & Lomb

In CANADA: Bausch & Lomb Canada Ltd., 2001 Leslie Street,
Don Mills, M3B2M3, Ontario, Canada, (416) 447-9101



Consult Yellow Pages under "Microscopes" for the Bausch & Lomb Dealer nearest you.

CIRCLE 28 ON READER SERVICE CARD

Lange's Handbook of Chemistry. 12th ed. J. A. Dean, Ed. xv + 1470 pages. McGraw-Hill Book Co., 1221 Avenue of the Americas, New York, N.Y. 10020. 1979. \$28.50

This edition features in-depth material on thermodynamic properties, the elements and selected organic compounds, recommended symbols, formation constants, acid dissociation constants for organic compounds, conversion factors including SI units, and mathematical and statistical relations.

Analysis of Airborne Particles by Physical Methods. Hanns Malissa and J. W. Robinson, Eds. 301 pages. CRC Press, Inc., 2255 Palm Beach Lakes Blvd., West Palm Beach, Fla. 33409. 1978. \$64.95; \$74.95, outside USA

The analytical procedures include X-ray fluorescence, emission, atomic adsorption, radioactivity measurements, spark source mass spectrometry, neutron activation, electron and ion probe microanalysis, X-ray diffraction, IR, and thermoanalysis.

Continuing Series

Progress in Nuclear Magnetic Resonance Spectroscopy. Vols. 10 and 11. J. W. Emsley, J. Feeney, and L. H. Sutcliffe, Eds. vii + 766 and vii + 298 pages. Pergamon Press Inc., Maxwell House, Fairview Park, Elmsford, N.Y. 10523. 1978. \$80 and \$40

Volume 10 contains articles on the through-space mechanism in spin-spin coupling; application of density matrix theory to NMR lineshape calculations; spin-spin coupling and the conformational states of peptide systems; and fluorine coupling constants. Volume 11 contains review articles on calculations of nuclear spin-spin coupling constants; quantitative applications of ^{13}C NMR; dynamic ^{13}C NMR spectra and structures of organotin compounds; semiempirical calculations of the chemical shifts of nuclei other than protons; dynamic ^{13}C NMR spectroscopy of metal carbonyls; and deuterium magnetic resonance, applications in chemistry, physics and biology.

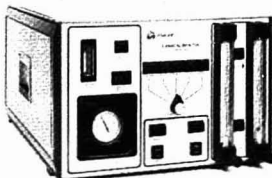
Analytical Methods for Coal and Coal Products. Vol. 2. Clarence Karr, Jr., Ed. xvi + 669 pages. Academic Press Inc., 111 Fifth Ave., New York, N.Y. 10003. 1979. \$55

Volume two is divided into four parts: structure, minerals in coal, coal carbonization products—coke, pitch, and coal combustion products. Theory and the practical laboratory detail of the various analytical methods are presented along with background references.

GLC and HPLC Determination of Therapeutic Agents. Vol. 9, Part 2. Kiyoshi Tsuji, Ed. xiv + 936 pages. Marcel Dekker Inc., 270 Madison Ave., New York, N.Y. 10016. 1978. \$45

Part two of a three-part series is divided into four sections: therapeutic drug monitoring, drugs affecting the nervous system, antimicrobial agents, and metabolic disease and endocrine function agents. Detailed descriptions for chromatographing drugs representative of each class are provided.

Now. Make gas phase calibrations with NBS-traceable certainty



To get accurate, useful outputs from your gas analyzer or chromatograph, precise calibration is critical. So when you do calibrate, use the most accurate instrument available—the Metronics Dynacalibrator. It delivers accurate and precise gas concentrations ranging from 0.0001 ppm to over 1000 ppm. As a result, you can use it to get NBS-traceable calibrations of almost any instrument—in the lab or in the field.

Further, since calibration is our only business, you get an instrument that is coldly objective and easy to use. It's also competitively priced. Yet, it has features no other calibrator can match:

- Self contained design, no need for gas cylinders and related apparatus
- Oven control within $\pm .05^\circ\text{C}$, NBS traceable
- Oven temperatures variable to 50°C , 110°C optional
- Flow calibrated and stable to within $\pm 1\%$ (full scale) or $\pm 3\%$ (low scale) for each reading.
- Our own disposable, calibrated permeation devices, certifications traceable to NBS standards. Available for hundreds of gases.
- All controls and indicators logically grouped on front panel for fast, error free operation
- Fast, easy device change or replacement via front panel
- Continuous, unattended automatic or remotely controlled operation
- Dynamic gas concentration ranges of 60:1

CIRCLE 148 ON READER SERVICE CARD

- Optional, "in-transit" maintenance of purge and temperature

It all adds up to calibrations that are above suspicion—your best protection against costly measurement errors. Three models meet every requirement. For detailed literature and a demonstration, call or write today. Metronics, 2991 Corvin Drive, Santa Clara, CA 95051. Phone: (408) 737-0550 Telex: 35-2129

Metronics
Calibration you can count on.





WE HAVE THE SOLUTIONS BEFORE YOU HAVE THE PROBLEMS.

Making specialty and rare gases is a lot tougher than using them. That may be tough for us, but it's good for you.

It's tough because our experts, like Frank Kramer, have to make sure every cylinder or other container of our pure gases and gas mixtures are exactly what we certify them to be. And we have to make sure they'll perform exactly as you expect them to perform.

We have to make sure there are no trace heavy-metals in your electronics gases. We have to know your NO calibration gases are not polluted with excess NO₂. And we want you to know that you will not get 0.12-ppm hydrocarbons in your 0.10 certified zero air.

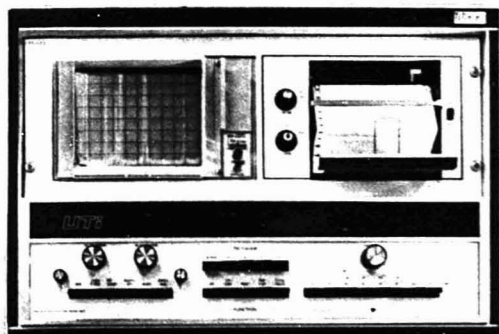
To do that, we use the same kind of instrumentation in our specialty gas production plants that you do in your facilities. Mass, emission, x-ray, infra-red and atomic absorption spectroscopy, flame ionization detectors, scanning and transmission electron microscopes, scanning electron microprobes,

x-ray fluorescence and, of course, gas chromatographs. (We regard the gas chromatograph as a piece of production equipment, and we probably have more GC experience than most of our customers combined.)

In addition, we often set up the same equipment in the same application environment that you do just to make sure everything you're doing will work without a hitch.

All of which is good for you because—whatever you're doing with your specialty gases and equipment—Airco people like Frank Kramer have probably done it before. Hundreds of times over.

We're happy to share our knowledge, experience and facilities—and even Frank—with you any time you like. Simply call or write our Specialty Gases and Equipment Dept., Airco Industrial Gases, 575 Mountain Ave., Murray Hill, NJ 07974. (201) 464-8100.



Albion, MI (517) 629-9161
Baton Rouge, LA (504) 383-1436
Chicago, IL (312) 468-4200
City of Industry, CA (213) 963-2871
Houston, TX (713) 225-6227
Phoenix, AZ (602) 273-1255
Pittsburgh, PA (412) 562-3723
Raleigh-Durham, NC (919) 549-0633
Riverton, NJ (609) 829-7878
Santa Clara, CA (408) 247-5470
South Acton, MA (617) 263-7767
Vancouver, WA (206) 695-1255

AIRCO
Industrial Gases

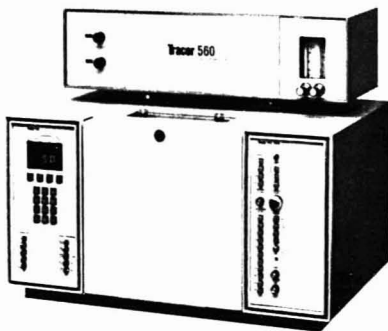
CIRCLE 6 ON READER SERVICE CARD

Tracor offers the widest selection of proprietary GC Detectors—including Flame Photometric, Linear Electron Capture (Ni63), Hall Electrolytic Conductivity*, Nitrogen/Phosphorous, Thermal Conductivity, Flame Ionization, **Gas Chromatography** Photo Ionization and exclusive Ultrasonic Detector for low level determination of fixed gases.

Water Analysis? Sulfur Analysis? Capillary GC? Tracor has an instrument for your application including new split/splitless glass capillary capability.

*New 700A

CIRCLE 202 ON READER SERVICE CARD



Tracor Chromatography



Data Processing Tracor's Analytical Processor (TAP) provides the most sophisticated software resulting in highest precision—and it's easy to use, too.

CIRCLE 203 ON READER SERVICE CARD



Liquid Chromatography Tracor's modular 900 Series Liquid Chromatograph featuring the 950 High Pressure Pump, 980A Solvent Programmer and the state-of-the-art 970A Variable Wavelength Detector. Also included is Tracor's new 965 Photo Conductivity Detector for Liquid Chromatography.

CIRCLE 205 ON READER SERVICE CARD

GC/LC News

Send for Tracor's FREE periodical RETENTION TIMES. This will keep you informed of recent developments in both gas and liquid chromatography.

Free subscription to Retention Times

CIRCLE 204 ON READER SERVICE CARD

Tracor Instruments

Tracor, Inc. 6500 Tracor Lane Austin, Texas 78721 Telephone 512:926 2800

Editors' Column

SI in Education

Communication among university, college, and school teachers is the aim of the Committee on Teaching of Chemistry (CTC) of the International Union of Pure and Applied Chemistry (IUPAC). The information gathered through the committee is disseminated in the "International Newsletter on Chemical Education". This publication is available free-of-charge from the Secretariat of IUPAC (Bank Court Chambers, 2-3 Pound Way, Cowley Centre, Oxford OX4 3YF, UK). However, there is no mechanism for automatic mailing of the newsletter except to subscribers of the IUPAC "Information Bulletin" (\$25 U.S., Pergamon Press, Headington Hill Hall, Oxford OX3 0BW, UK).

A recent issue of the newsletter (No. 10) presented a report on a survey on problems of conversion to SI units and its effect on the teaching of chemistry in schools. The survey, invited by the CTC, was conducted, and the report prepared, by Brian T. Newbold of the Université de Moncton, New Brunswick, Canada.

The questionnaire used in the survey included the following questions:

- Has your country introduced SI units into the school system?
- If yes, in what year and to what level (school years)?
- What year for chemistry and what levels of chemistry?
- Have booklets, etc., been prepared for teachers and pupils to help them to teach and learn how to use SI units in science and particularly chemistry? If yes, please give some idea of the scope of such booklets and their sources.
- What problems are encountered in using SI units to teach chemistry in schools? Please indicate specific areas in the curriculum that are affected, pedagogical difficulties, and any other problems involved.

• If SI units have yet to be adopted by the school system in your country, please indicate if introduction of said units is presently contemplated, and what year SI units are likely to be introduced.

CTC has National Representatives from 41 countries including the United States. All 41 were sent the questionnaire; 19 replies were received. The respondents represented Australia, Brazil, Canada, Denmark, Federal Republic of Germany, Finland, France, German Democratic Republic, Greece, Hungary, India, Japan, Netherlands, New Zealand, Republic of South Africa, Spain, Sweden, United Kingdom, and Yugoslavia.

SI units have been introduced into school systems in 17 countries. Except for Brazil (1962), France (1955), and Sweden (1966), the introduction has taken place in the 1970's. Greece is expected to convert within the next two years. It is expected that it will be quite some time before SI units are introduced into schools in Japan. The use of SI units is compulsory by law in Finland and the Federal Republic of Germany. The level at which the units are introduced in schools varies greatly, although in chemistry they appear to have been universally adopted.

In the majority of countries responding, instruction in teachers' colleges and publications for teachers and pupils are available on the use of SI. In France, there is no apparent need for special publications because of the long period of exposure to SI units. Except for Greece and Japan, textbooks using SI units are available.

What problems are encountered in using SI units to teach chemistry in schools? Denmark, Finland, France, Netherlands, Republic of South Africa, and Spain reported no problems. According to Newbold, the problems raised by the other countries can be briefly summarized as follows: values of equilibrium constants (Australia); pressure and concentration (Canada); joules (Federal Republic of Germany and Canada); computational difficulties (German Democratic Republic); textbooks using non-SI data (New Zealand and Canada); equipment calibrated in non-SI units (New Zealand); recalculation of constants based on the new definition of the standard state (Sweden); problems of technicians trained in the use of SI units having to use mixed units in industry (United Kingdom); and the resistance of teachers to the changeover to SI units (Canada, Federal Republic of Germany, German Democratic Republic, and Hungary). Overall, the problem with acceptance of SI units seems to be one of the teacher rather than of the pupil.

Obvious in this survey's results is the absence of any response from the United States. Perhaps, as in the case of Canada where data from only the provinces of New Brunswick, Quebec, Newfoundland, and Prince Edward Island, and the Northwest Territories were available, the coordination of data from 50 states was too complex. Or is the problem the same as Japan's where there is no strong push for SI units?

A. A. Husovsky

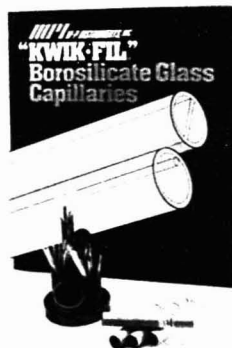
GET IT ALL TOGETHER! MICRO-ION SELECTIVE SYSTEM

PRECISION MEASUREMENTS FROM MACRO AND MICRO ION SELECTIVE AND pH ELECTRODES

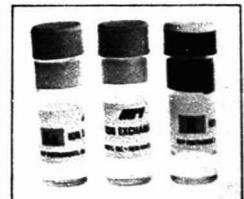


MODEL F-223A DUAL/DIFFERENTIAL ELECTROMETER

- 10 OHMS INPUT RESISTANCE • LOW INPUT CAPACITANCE
- 10 SUPPRESSES LEAKAGE CURRENT • ON BOARD PROBE TEST
- ACTIVE MINIMISE MODE • DIGITAL READOUT
- ELECTRODE RESISTANCE TEST



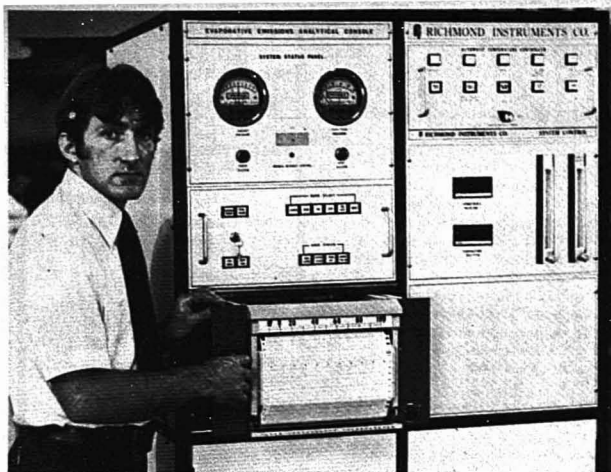
- FOR MICROPIPETTE ELECTRODES
- SINGLE AND MULTI-BARREL TYPES
- THETA AND QUAD TYPES
- THIN WALL TUBING



K⁺ & Na⁺ ION EXCHANGE RESINS LOW COST 1.0 ml. AMOUNT

M-P INSTRUMENTS, INC.
80 FITCH ST. • P.O. BOX 3110
NEW HAVEN, CT 06511
TEL. (203) 388-2163
TWX 710-460-2636 WPHNSTR HVN

CIRCLE 237 ON READER SERVICE CARD



"TI recorders help our systems operate 24 hours a day."

... says Dennis Mach, General Manager of Richmond Instruments Company, manufacturers of exhaust test systems.

"We have no problems with TI recorders. They are reliable, easy to mount, clean, and easy to service. That's why we use them in the vast majority of our emission systems. We like the resolution of the wide chart and the good inking system. In addition, the removable back panel makes special modifications easy."

"We especially like the reliable heavy-duty construction because our systems must operate with little or no down-time to keep our customers satisfied."

Richmond Instruments is only one of many satisfied users of TI strip chart recorders. The chances are good that you, too, can profit from the high quality, accuracy and heavy-duty construction of the TI recorders. There's a broad selection of designs to choose from.

Drives include unidirectional

and bidirectional synchro systems. Wide and dual-grid *servo/riter**II models give a choice of one to five full overlapping channels on a 8.75" grid. And if space saving is a requirement, the Lab/Test recorders use only 7 inches of panel height.

Options include full scale adjustable zero, variable spans and inputs, electric pen lifters, felt tip or capillary inking, bidirectional take-up system, synchro or digital drives, and stepper.

TI recorders are backed by more than twenty years of proven quality, reliability, accuracy and performance plus a nationwide network of sales and service offices to serve you.

For further information, please contact Texas Instruments Incorporated, P.O. Box 1443, M/S 619, Houston, Texas 77001. Or phone (713) 491-5115, ext. 3333, TWX 910-867-4702, Telex 775938.

*Trademark of Texas Instruments Incorporated



TEXAS INSTRUMENTS

INCORPORATED
CIRCLE 201 ON READER SERVICE CARD

PUBLICATIONS

Investigate the structure of ACS

EDUCATION

MEETINGS

DIVISIONS

EMPLOYMENT

Your benefits are compound.

Membership is simple.

American Chemical Society members receive *Chemical and Engineering News* each week. *C&E News* brings you the up-to-date happenings in the chemical world plus official ACS news.

AND THERE ARE MANY OTHER BENEFITS:

Publications—Members enjoy substantial savings on world renowned ACS publications.

Meetings—Two national meetings each year plus a host of regional and local meetings are held for your benefit.

Local Sections—provide you with activities of local interest and an opportunity to participate in Society affairs.

Divisions—28 subject divisions help you keep up with your special chemical interest.

Educational Activities—short courses, audio courses and interaction courses help you expand as a professional.

Employment Aids—give you a helping hand in today's tight job market.

But most important, your membership helps support the scientific and educational society that represents you as a professional.

110,000 Chemists and Chemical Engineers know the value of ACS membership.

Send coupon below today for an application.

American Chemical Society
Office of Member Services
1155 Sixteenth Street, N.W.
Washington, D. C. 20036

Yes, I am interested in membership in the American Chemical Society. Please send information and application.

Name

Address

City

State Zip

HOW many times

have you wished that you could scan ALL of the American Chemical Society's article titles in a matter of minutes?

The ACS Single Article Announcement (SAA) lets you do just that, twice a month, and for only 50¢ an issue (member rate).

Are you a chemist or engineer who likes to keep up... but can't afford to subscribe to all 18 of the ACS journals?

Then Single Article Announcement is the alerting service designed with just your needs in mind.

SAA offers a convenient, one-stop method for scanning the tables of contents of all our publications PLUS an ordering feature so you can easily and inexpensively obtain only those articles of interest to you.

For just \$12.00 a year (that's 50¢ an issue), members can receive this up-to-date alerting service. Nonmembers can subscribe for \$24.00 a year (only \$1.00 an issue).

Sound interesting???

If you'd like to examine a free sample issue, just fill out the coupon below and return it to:

Ms. Barbara E. Meyers
Research & Development Dept.
American Chemical Society
1155 Sixteenth Street, N.W.
Washington, D.C. 20036

YES! I'd like to receive a free sample issue of Single Article Announcement. Please send it to:

Name _____
Company _____
Address _____
ZIP _____

MCI Automatic Moisture Meter. Reliable, Fast and Easy.

Incorporates coulometry principle applied to Karl Fischer titration. Operation is full-automatic. Measuring time is shortened. Accuracy is within 5µg for 10µg-1mg H₂O and within 0.5% for 1-30mg H₂O. Wide-range applications include measurement of ultra-trace water content in liquids, solids and gases. Range: 10µg-30mg H₂O. An optional water vaporizer for speedy and accurate measurement of water content in plastics, grain, etc.

Printer (optional)



CA-02 Moisture Meter with Printer



MITSUBISHI CHEMICAL INDUSTRIES LIMITED
Instruments Dept., Mitsubishi Bldg., 5-2, Marunouchi 2-chome, Chiyoda-ku,
Tokyo, 100 Japan Telex: J24901 Cable Address: KASEICO TOKYO

CIRCLE 147 ON READER SERVICE CARD

The LC Detection System with a mind... ...not a mind of its own.



Now—using a Schoeffel variable wavelength absorption detector, you can stop the flow in your LC system and scan the spectrum for positive identification of an eluted fraction. Without having to worry about baseline variations. Without spending valuable time correcting for solvent and background absorbance. Because of the mind: Schoeffel's MM 700 Memory Module makes absorbance profiling ('fingerprinting') a snap. Solvent and background absorbance

are automatically removed from sample analysis. For fast, simple, more accurate qualitative determinations. Also useful in gradient elutions.

Best of all, the MM 700 is used with Schoeffel's UV-VIS absorption detector—the SF 770 Spectroflow Monitor—with motorized wavelength drive. An industry standard since its introduction in 1973. Write for our brand new literature—or phone us for a demonstration.

U.S.A.: 24 Booker Street, Westwood, New Jersey 07675
(201) 664-7263, Telex 134356
EUROPE: 2351 Trappenkamp, Celsiustrasse 5, W. Germany
(04323) 2021, Telex 299660

KRATOS Inc.
SCHOEFFEL
INSTRUMENT DIVISION

CIRCLE 191 ON READER SERVICE CARD

Finnigan simplifies Organics-in-Water analysis.

Routine analysis of organics in water a problem? Finnigan's OWA™ Organics-in-Water Analyzer is the problem-solving system designed to meet your analysis needs.

Simplified pre-programmed procedures make the Finnigan OWA system simple to operate. Yet it provides complete measurement of both gross and trace compounds in water. And it delivers the analytical capabilities of systems which cost many thousands of dollars more.

Finnigan further simplifies the solution to your organics-in-water analysis problem by offering training in system

operation, application techniques and laboratory management.

For nearly a decade, Finnigan systems have pioneered organics-in-water analysis. Let us show you how the Finnigan package — hardware, software and training — can solve your analysis problem. Call or write us today.



finnigan
Instruments

A TRIVISIO GROUP COMPANY
845 WEST MAUDE AVENUE
SUNNYVALE, CALIFORNIA 94086
(408) 732-0940

Finnigan will soon be demonstrating an OWA system in a city near you. Ask us for details.

CIRCLE 75 ON READER SERVICE CARD

Specialized Gas Chromatography—Mass Spectrometry Systems for Clinical Chemistry

Nathan Gochman and Lemuel J. Bowie

Veterans Administration Hospital, San Diego, Calif. 92161, and Departments of Chemistry and Pathology, University of California at San Diego, La Jolla, Calif. 92093

David N. Bailey

Division of Clinical Pathology, University of California Medical Center, San Diego, Calif. 92103

Mass spectrometry can be used to identify and quantitate almost any chemical compound of molecular weight less than 1500. This includes essentially all therapeutic agents and their metabolites. The main advantages of mass spectrometry as an analytical technique are its increased sensitivity (for some substances, in the picogram range) over other analytical techniques, and its specificity in identifying unknowns or for confirming the presence of suspected compounds. The enhanced sensitivity results primarily from the action of the analyzer as a mass filter to reduce background interference and from the sensitive electron multipliers used for detection. The excellent specificity results from characteristic fragmentation patterns, which can give information about molecular weight and molecular structure. Mass spectrometry has now permitted the development of definitive methodology against which suitable reference methods can be evaluated. An important example is the analysis of inorganic ions (sodium, potassium, chloride, calcium, magnesium, lithium, lead, and phosphate) by isotope-dilution mass spectrometry (1).

Since biological samples (e.g., human serum, urine) are complex mixtures, the combined gas chromatograph-mass spectrometer (GC-MS) has evolved as an ideal instrument for rapid separation and analysis with

minimal prior purification. Specific clinical applications of GC-MS have included the analysis of biogenic amines, amino acids, peptides, lipids, carbohydrates, prostaglandins, steroids, and bile acids (1, 2). Especially promising is the metabolic profiling of organic acids and volatiles, which permits a complete class of compounds to be monitored leading to enhanced diagnosis of a variety of metabolic disorders (1-3). Another new application is that of rapid identification of bacteria from their characteristic molecular fragments so that a definitive identification of the microorganism may often be made on the same day as sample collection (1).

Probably the most significant contribution of GC-MS to the clinical laboratory thus far has been made in clinical toxicology and therapeutic drug monitoring. Because of the structural similarity of many drugs, analysis by more conventional techniques (e.g., ultraviolet-visible spectrophotometry, gas-liquid chromatography) has often suffered from lack of specificity. In addition, the analysis is frequently complicated by the presence of several drugs ingested concurrently in overdose. Mass fragmentography (multiple ion detection and selected ion monitoring) is particularly well suited for drug analysis in these cases, since by its nature it permits simultaneous separation and analysis of multiple known compounds and quantita-

tion with far greater specificity than heretofore possible.

A comprehensive review of mass spectrometry, prepared by Roboz (4), covers instrumentation, techniques, and applications in clinical chemistry.

Basic Design

The basic components of most systems are shown in Figure 1 and are described below.

Gas Chromatograph. As previously indicated, the major function of the gas chromatograph is to resolve components of complex mixtures. A second function, which may not be as obvious, however, is to present the compounds to the mass spectrometer in a form (i.e., gas phase) readily acceptable for mass spectrometric analysis. The difficulty of accomplishing this second function has limited the adaptation and integration of other chromatographic techniques (e.g., high-performance liquid chromatography) to mass spectrometry. Since the mass spectrometer must operate under high vacuum, the GC carrier gas (e.g., helium or nitrogen) must be removed prior to introduction into the spectrometer. Even high capacity pumps cannot maintain high vacuums with carrier gas flow rates of greater than 10 mL/min (4). This problem is alleviated by placing a separator between the GC and mass spectrometer.

Molecular Separators. The two most popular types of devices used to

We can't really show off Inficon's versatile surface analysis system.



Until you show up with a sample for comparative analysis.

The best way to demonstrate Inficon's LHS-10 surface analysis system is by direct application. So bring in any vacuum compatible sample—give us two weeks' notice, please—and we'll analyze it.

And we'll prove ours is the simplest, most cost-effective system for your surface analyses.

Whatever your analytical problem, the LHS-10 will help you obtain more complete surface characterizations, correlate data faster, and reach firmer experimental conclusions.

LHS-10's universal analysis chamber allows customizing to your exact needs—whether it's catalyst efficiency testing, elemental or quantitative analysis, trace detection, depth profiling, or chemical fingerprinting.

You can have ESCA (XPS), UPS, AES, SAM, SIMS, ISS modules now, or add any later at minimal cost. Even add a computer system for simultaneous instrument operation and data manipulation.

No matter what techniques you select for present or future use, all can be employed on the same sample area—without specimen manipulation—for rapid sample analysis.

For now, let the other surface analysis companies first demonstrate their capabilities—then let Inficon give you proof positive of the LHS-10's superior performance, versatility and simplicity.

Write or call today. We'd like to see you and your sample soon.

We also offer contract surface analysis and assistance with special problems.



The plexiglas model of our universal chamber clearly shows our versatile analysis techniques.

INFICON
LEYBOLD-HERAEUS

6500 Fly Road, East Syracuse, New York 13057
315/437-0377 ■ TWX 710 541-0594

CIRCLE 121 ON READER SERVICE CARD

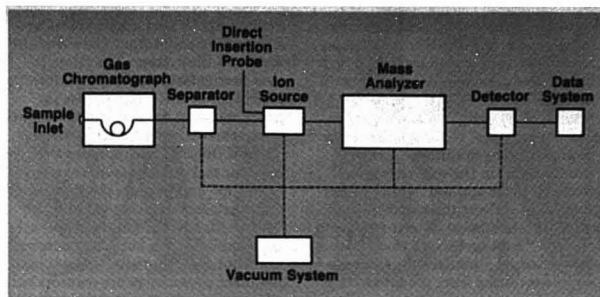


Figure 1. Major components of typical GC-MS system

remove carrier gas from sample molecules are gas-jet separators and membrane separators. The jet separator forces the entire GC effluent through a narrow orifice under a vacuum. Another orifice is placed in close proximity to retrieve sample molecules. Since the lighter carrier gas molecules preferentially diffuse away from the center of the stream under vacuum, as much as 99% of the carrier gas can be removed. The function of membrane separators is based upon the higher relative solubility (and therefore permeability) of organic compounds than of carrier gases in silicone polymers. Membrane separators have higher sample yields compared to jet separators, but the permeability of molecules is highly temperature dependent. A comprehensive discussion of both types of devices can be found in ref. 5.

Direct Insertion Probe. Solid samples may be introduced into the mass spectrometer by heating and

volatilizing in a vacuum. Direct insertion probes are designed to hold a small amount of sample, introduce it into the system via a vacuum seal, and heat the probe tip to temperatures sufficient to volatilize the molecules present. This technique is very useful for identifying pure substances and simple mixtures that do not require prior GC separation and can be volatilized without decomposition.

Ion Sources. In order for the mass analyzer to separate molecules or fragments, they must be ionized. This can be accomplished by various methods, but the two most widely used approaches are electron impact ionization (EI) and chemical ionization (CI). A detailed discussion of the principles and relative advantages of the two techniques is beyond the scope of this article. In general, CI is a gentler means of ionizing, gives simpler fragmentation patterns, and is especially useful for compounds where higher

molecular weight fragments (e.g., molecular ion) are sought. Electron impact ionization, on the other hand, is somewhat simpler to accomplish since it does not require a reagent gas, and by giving more fragments, may give more structural information. With both techniques, ions are formed from the neutral gas molecules, focused into a beam, and accelerated before entering the mass analyzer.

Mass Analyzers. Although there are a number of designs for mass analyzers, the most popular in recent years has been the quadrupole analyzer. In this approach, rf and dc voltages are applied to parallel rods in such a manner to permit only a specific mass to traverse without annihilation at any one combination of voltages. In contrast to most magnetic analyzers that use a magnetic field for resolving various masses, the resulting mass spectrum is linear. Magnetic analyzers are theoretically more sensitive at higher masses and with advanced designs may become more popular.

Detectors. Currently, most mass spectrometers use electron multipliers to detect the ions emerging from the analyzer. These devices are capable of amplifying the ion current as much as 10^7 by use of a series of dynodes in a manner similar to that used in absorption and fluorescence spectroscopy.

Data System. Because of the wealth of information and the speed at which data are generated, most conventional systems accumulate data with the aid of dedicated micro- or minicomputers. A combination of direct computer storage and storage on magnetic tapes and/or discs is used to compile all of the data and to reconstruct mass spectra or chromatograms on request. Cathode-ray tubes are frequently used to provide real time display of data acquisition.

Vacuum System. The separator, ion source, mass analyzer, and detector must be maintained at high vacuum (commonly 10^{-7} torr). Both the speed at which the instrument can be operational after cleaning or opening to atmospheric pressure and the efficiency of maintaining high vacuum are related to the capacity and speed of the vacuum system. Most systems use combinations of oil diffusion pumps to maintain high vacuum (10^{-7} torr) with conventional forepumps to reduce the initial pressure to approximately 10^{-3} torr.

Selected Systems

Despite the potential for application of GC-MS in the clinical laboratory, historically, it has been almost exclusively limited to the research laboratory because of its technical complexity and high cost of instrumentation and operation. With the recent interest in biomedical applications of

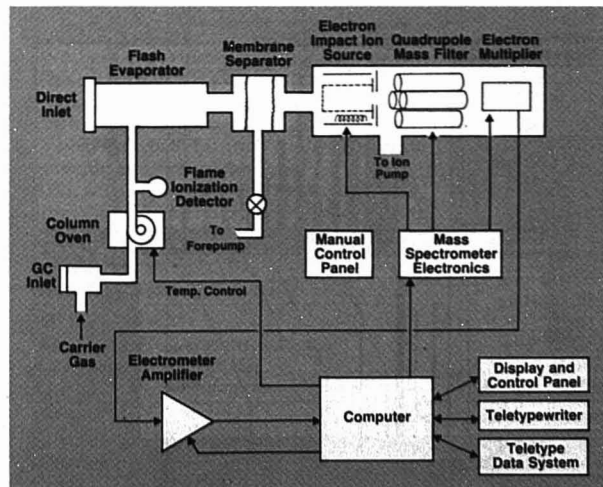


Figure 2. Block diagram of Olfax IIA

GC-MS, however, several systems have been streamlined in design or simplified in operation, and therefore may be more suitable for routine application in the clinical laboratory. Three such systems that will be discussed in greater detail are: Olfax IIA (Vitek Systems, Inc., Division of McDonnell Douglas Corp., Hazelwood, Mo.); HP 5992 (Hewlett-Packard, Palo Alto, Calif.); and DP-102 (E. I. du Pont de Nemours & Co., Inc., Wilmington, Del.).

Vitek Olfax IIA

Historically, the Olfax was the first system specifically designed for use in the clinical laboratory. The basic instrumentation (Figure 2) consists of a 400 atomic mass unit (amu) electron-impact quadrupole mass spectrometer with a two-stage membrane separator. This is interfaced with a single-column gas-liquid chromatograph (Perkin-Elmer Model 3920) and a microprocessor (Intel 8008) with 27K in read only memory (ROM) and 4K in random access memory (RAM). An additional 60K is available for on-line tape storage. The microprocessor controls all mass scanning, chromatograph temperatures, and temperature programs. It also continuously monitors such system parameters as pressure and mass spectrometer temperatures. A printer-cassette reader (Texas Instrument Silent 700) is integrated into the system to print analytical data, to load identification programs, and to enable the user to interact with the system.

The Olfax system utilizes the principle of selected ion monitoring (SIM) in which several characteristic mass fragments (usually 5–10) are chosen for monitoring in lieu of the complete mass spectrum. Figure 3 demonstrates a typical contracted spectrum using phenobarbital analysis as the example.

The uniqueness of the Olfax derives from its ability to analyze mixtures of compounds even when they elute from the chromatograph with the same or similar retention times. This ability is built upon the concept of probability-based matching (PBM) of selected mass fragments (6) and eliminates the need for a search library. The probability that a given compound is present is indicated by a "confidence index" (K). Thus, 2^K represents the average number of compounds selected at random whose mass spectra must be examined to find characteristic mass fragments that match the target spectrum to the same degree as the unknown. The probability (P) that the mass spectral data could arise from a compound selected purely at random is then $1/2^K$.

The specific K for the compound sought is the summation of individual

values (K_j) found for each mass fragment used in the identification whose abundance falls within user-specified limits. The overall K is a linear combination of four parameters: $K = \Sigma K_j = \Sigma(U_j + A_j + W_j - D)$, where U is the "uniqueness" of the particular fragment being examined, A is its "abundance" in the reference spectrum, W is the applied "window tolerance" that reflects the narrowness of the peak-abundance criteria used, and D is the "dilution factor" that reflects the decreased abundance in the target sample resulting from the presence of contaminants contributing the same or similar fragments.

The "uniqueness" (U) of a given mass fragment in a specific spectrum is derived from a previous study of fragments from more than 17 000 compounds based on the probability that the abundance of the particular fragment in question would be more than 50% of that of the base peak of a spectrum taken at random (6). The parameter " V " (the sum of U and A) reflects how "characteristic" a given mass peak is; this number is generated by the Olfax after the reference compound is introduced. The " V " value aids the user in selecting the most characteristic mass peaks for his identification program (fragments with the highest V values are usually the most characteristic). By use of the concept of PBM, a compound is identified as "positive" if its overall K exceeds the threshold set by the user. The more contaminants present in the sample, the greater the chance for the same or similar mass peaks to be contributed and the lower the resultant K . Quantitative analysis of mixtures of com-

pounds can be performed following appropriate calibration and standardization of the system. The Olfax is thus particularly useful for performing toxicology profiles in overdose in which multiple drugs are often ingested concurrently. In addition, the use of PBM frequently eliminates the need for meticulous sample extract "cleanup" and permits the analysis of crude extracts of biological samples.

The Olfax IIA is simple to operate, and sophistication in mass spectrometry is not a prerequisite. Critical instrument parameters are continuously self-monitored and conveyed to the user by a series of diagnostic messages. The user can easily generate his own compound identification programs after selecting up to 17 characteristic mass peaks (based on the computer-generated " V " values). Up to 16 different compounds can be included and sought simultaneously in one identification panel. For the user who is not inclined to develop his own programs, commercially developed identification programs are available for a variety of compounds, mostly drugs. Whether user developed or commercially supplied, the programs are stored on magnetic tape cassettes, which are loaded into memory through the printer-reader. These programs also contain all chromatographic information including temperature programs necessary for operation. While most analytical work is performed in the "Auto ID" mode using PBM identification, an "Interactive Data System" mode is also available to permit generation of traditional mass spectra and to allow the user to interact with the system.

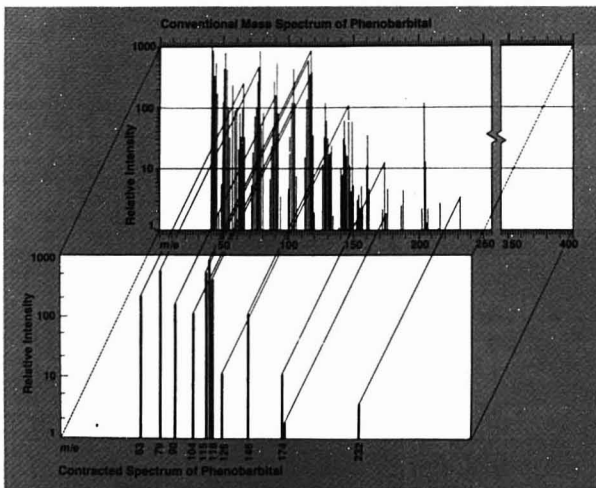
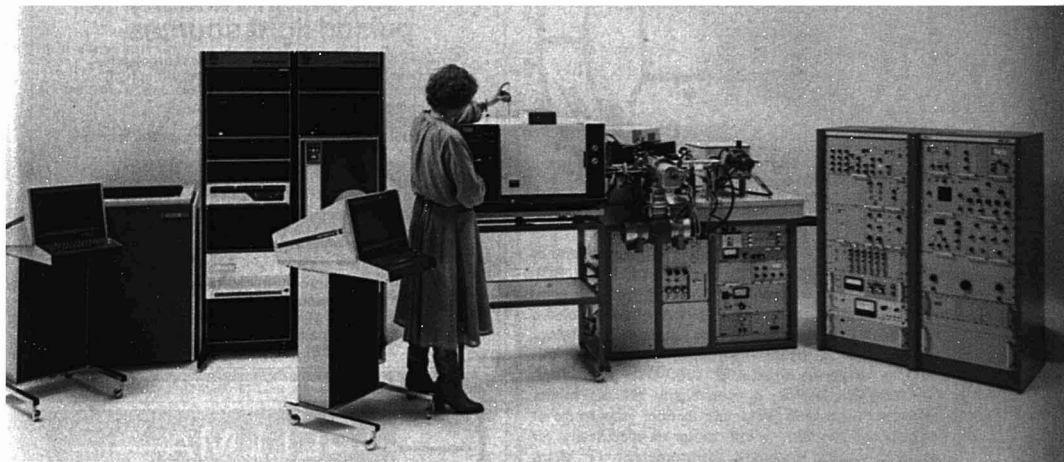


Figure 3. Schematic representation of SIM

ON SALE NOW!



The new Varian MAT 212 and 312 mass spectrometers are so attractively priced you'll think they're on sale.

If you've always been a Varian admirer, now's an excellent opportunity to be a Varian owner.

Reason: Varian has put together some great "packages" combining our new MAT 212 and 312 mass spectrometers with our popular SS200P* data systems which feature simultaneous data acquisition and evaluation.

And, whether a 212 or 312 package catches your eye, you'll like our irresistibly low prices.

The MAT 312 is an advanced version of our popular MAT 311A. It has an improved source

with more accessories and greater versatility for applications including field desorption studies.

The versatile MAT 212 brings a proven track record to CI/EI studies, not to mention such great options as GC/MS analysis with packed columns (jet separator); multi-ion selection analysis, DCI (direct chemical ionization or desorption CI) collisional activation analysis, negative ion detection and much more.

Now, to the bottom line . . . price. We suggest you call us. You'll be pleasantly surprised and may want to arrange a demonstration. For information or literature contact:

Performance at a glance!

MAT 312

Resolving power: up to 35,000 (10% valley)
Mass Range: 1 to 3600 amu
Accuracy: better than 2 ppm

MAT 212

Resolving power: up to 20,000 (10% valley)
Mass Range: 1 to 1200, switchable to 3600 amu
Accuracy: better than 3 ppm

Varian MAT Mass Spectrometry, 25 Hanover Road, Florham Park, NJ 07932. Phone (201) 822-3700

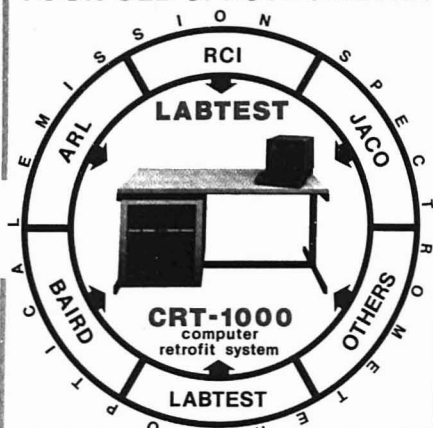
Varian MAT GmbH, Postfach 14 4062
Barkhausenstr 2, 2800 Bremen 10
West Germany. Phone (0421) 5493-1

Varian Associates, Ltd., 28 Manor Road
Walton-on-Thames/Surrey
United Kingdom. KT12 2QF
Phone (43741)



*Outside U.S. — SS 188.

MODERNIZE YOUR OLD SPECTROMETER



We like the optical end of OLD spectrometers made by ARL, Baird, JACO, RCI, and others. By-and-large they are still doing a good optical job. But technological advances have obsoleted their readout equipment. And modern laboratory demands have outpaced their capability. To solve this problem we designed the CRT-1000 Data Acquisition and Readout System. It is a highly reliable micro-processor controlled data acquisition, spectrometer control, and readout system designed specifically for use with optical emission spectrometers. IT WILL BRING YOUR SPECTROMETER UP TO CURRENT TECHNICAL STANDARDS FOR ABOUT 1/3 THE COST OF A COMPLETE NEW SYSTEM. The CRT-1000 will satisfy your existing readout requirements and provide additional features such as video display and/or hard copy printout of percent concentration, interelement corrections, averaging, automatic standardization, daily logging, and many other features. And you don't need a computer programmer to run it.

Over 100 major corporations have selected Labtest computer products and Labtest software. And Labtest computer installations have already logged hundreds of thousands of hours of field operation.

If reliability, low maintenance, flexibility, speed, and freedom from operator error are important in YOUR laboratory—modernization of your existing spectrometer system with the CRT-1000 may be the answer to your needs. Call us collect today to discuss your application. Ask for the Retrofit Project Manager.

LABTEST

EQUIPMENT

COMPANY

11828 La Grange Avenue, Los Angeles, CA 90025
Telephone (213) 478-2518 478-1610

subsidiary **SYSTRON DONNER** corporation

CIRCLE 127 ON READER SERVICE CARD



PRA's high intensity pulsed light sources.

The PRA 610 microsecond pulsed light sources offer maximum versatility for applications requiring high ultraviolet intensities.

- Discharge energy per pulse to 100 joules
- Repetition rate 1 to 100 pps
- Spectral range 200 nm to 1200 nm with peak intensities in UV
- Various pulse widths 1.5-50 μ sec.
- Non magnetic lens aperture for ESR/NMR applications
- Carefully designed for minimized RFI

PRA manufactures pulsed light sources with a variety of pulse widths and discharge energies and has people with broad experience in optical systems design to advise you.

PRA

Photochemical Research
Associates Inc.

45 Meg Drive, London, Ontario
Canada N6E 2V2
(519) 686-2950 Telex 064-7597

CIRCLE 175 ON READER SERVICE CARD

OS* QH* QS* OF* QU* QI*

Hellma—the largest assortment of highest precision glass and quartz cells.
Standard • Flow-through • Constant-temperature
Anaerobic • Special Designs
Also available—ULTRAVIOLET-LIGHT SOURCES
Deuterium Lamps • Mercury Vapor Lamps
Hollow Cathode Lamps • Power Supplies

HELLMA
CELLS, INC.

Write for literature
Box 544
Borough Hall Station
Jamaica, New York 11424
Phone (212) 544-9534

CIRCLE 94 ON READER SERVICE CARD

WHY WAIT



A MONTH... OR MORE... FOR THAT ROUTED COPY OF ANALYTICAL CHEMISTRY TO REACH YOUR DESK?

For only \$16.00 a year... (\$12.00 if you're a member of A.C.S.)... you can own your very own subscription.

Why use a worn-out copy or wait until it comes to rest in the library? You can have your own copy to clip, to read at leisure, and to add to your personal file of vital information.

You'll receive FOURTEEN information-packed issues including THE ANNUAL LABORATORY GUIDE TO INSTRUMENTS, EQUIPMENT, AND CHEMICALS and the special APRIL ANNUAL REVIEWS.

All you have to do is fill in the order form below. We'll do the rest!

Please send me ANALYTICAL CHEMISTRY at the following subscription rate:

	U.S.	Canada	All Other Countries
ACS Members*			
1-Year	<input type="checkbox"/> \$12.00	<input type="checkbox"/> \$21.00	<input type="checkbox"/> \$21.00
3-Years	<input type="checkbox"/> \$30.00	<input type="checkbox"/> \$57.00	<input type="checkbox"/> \$57.00
Nonmembers			
1-Year	<input type="checkbox"/> \$16.00	<input type="checkbox"/> \$25.00	<input type="checkbox"/> \$33.00
3-Years	<input type="checkbox"/> \$42.00	<input type="checkbox"/> \$69.00	<input type="checkbox"/> \$89.00

Name _____

Address _____

City _____

State/Country _____

Zip _____

Your _____

Nature of Company's
Business _____

☐ Bill company

☐ Bill me for \$ _____

☐ Payment enclosed in the amount of \$ _____

Note: Subscriptions at ACS Member Rates are for personal use only.
Please allow 60 days for your first copy to be mailed.

2

0586C

Please send me ANALYTICAL CHEMISTRY at the following subscription rate:

	U.S.	Canada	All Other Countries
ACS Members*			
1-Year	<input type="checkbox"/> \$12.00	<input type="checkbox"/> \$21.00	<input type="checkbox"/> \$21.00
3-Years	<input type="checkbox"/> \$30.00	<input type="checkbox"/> \$57.00	<input type="checkbox"/> \$57.00
Nonmembers			
1-Year	<input type="checkbox"/> \$16.00	<input type="checkbox"/> \$25.00	<input type="checkbox"/> \$33.00
3-Years	<input type="checkbox"/> \$42.00	<input type="checkbox"/> \$69.00	<input type="checkbox"/> \$89.00

Name _____

Address _____

City _____

State/Country _____

Zip _____

Your _____

Nature of Company's
Business _____

☐ Bill company

☐ Bill me for \$ _____

☐ Payment enclosed in the amount of \$ _____

Note: Subscriptions at ACS Member Rates are for personal use only.
Please allow 60 days for your first copy to be mailed.

2

0586C

**BUSINESS REPLY CARD**

FIRST CLASS PERMIT NO 10094 WASHINGTON, D. C.

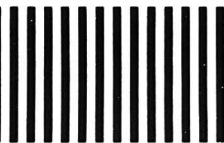
POSTAGE WILL BE PAID BY ADDRESSEE

AMERICAN CHEMICAL SOCIETY

Attn: Gayle Hebron

1155 Sixteenth Street, N.W.

Washington, D. C. 20036

NO POSTAGE
NECESSARY
IF MAILED
IN THE
UNITED STATES**BUSINESS REPLY CARD**

FIRST CLASS PERMIT NO 10094 WASHINGTON, D. C.

POSTAGE WILL BE PAID BY ADDRESSEE

AMERICAN CHEMICAL SOCIETY

Attn: Gayle Hebron

1155 Sixteenth Street, N.W.

Washington, D. C. 20036

NO POSTAGE
NECESSARY
IF MAILED
IN THE
UNITED STATES

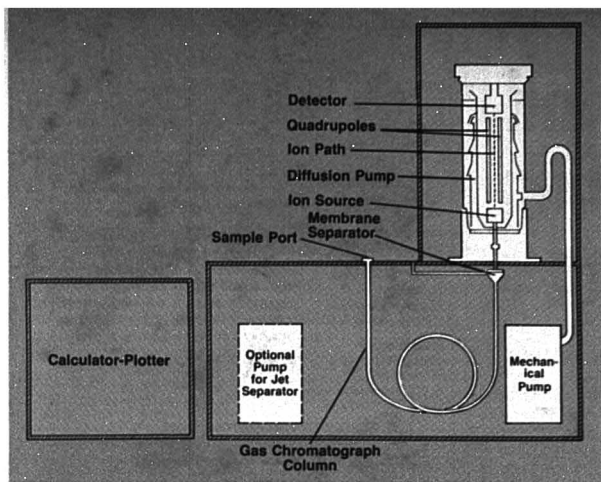


Figure 4. Schematic representation of HP 5992

Although it has high potential for clinical use, particularly when analysis of mixtures is desired, the Olfax system also has several limitations. Its scan range encompasses only 400 amu, and its analytical sensitivity is somewhat limited. These two limitations have rendered the instrument most applicable to the analytical workup of drug overdose (in which the analyte is usually a drug of molecular weight less than 400, and concentrations are relatively high) and to therapeutic monitoring of drugs such as the anti-convulsants and theophylline, which attain relatively high concentrations in plasma.

Hewlett-Packard HP 5992

The Hewlett-Packard 5992 is the first truly bench-top gas chromatograph-mass spectrometer system. The unit is similar in overall size and configuration to Hewlett-Packard's microprocessor-controlled gas chromatograph (Model 5830) with the substitution of a mass spectrometer as the detector instead of the more conventional flame-ionization or thermal-conductivity detectors. This was made possible by a unique and innovative design for the mass spectrometer unit. The ion source, quadrupole mass analyzer, and detector units are all located within a concentric diffusion pump. The relative orientation of the mass analyzer, the gas chromatograph, and the associated microprocessor/plotter are shown in Figure 4. The gas chromatograph and mass analyzer are housed in a single module, whereas the desk-top computer and plotter are separate. The computer is Hewlett-Packard's standard Model 9825A cal-

culator/plotter, which has been modified slightly for control and monitoring functions of the GC-MS unit. The gas chromatograph uses the standard Hewlett-Packard 5700A series oven and has similar features with regard to column size, oven temperature control, and injection port temperature control. The overall system is compact and can fit easily onto a laboratory bench (requires approximately 5 ft in length, 2.5 ft in width, and 5.5 ft in overhead clearance).

A key feature of the HP 5992 is the insertion of the major components of the mass spectrometer into a convoluted diffusion pump. This design contributes to the compactness of the system and probably to the lower cost. A detailed representation of the vacuum system and analyzer assembly is seen in Figure 5. In this concentric arrangement, the ion source, mass analyzer, and detector are all surrounded by a spun-steel cylinder. This is surrounded by a cavity containing vapors from the boiling pump fluid. At the various pump stages, the wall has openings that direct the vapors downward and sweep along the gases that are to be pumped off by the forepump. This entire assembly is then enclosed in another water-cooled steel cylinder that facilitates both condensation of the pump vapors and their return to the boiler.

This design results in a number of convenience and performance features. The combination of the small area to be evacuated and the large opening for pump-down results in fast evacuation. The overall design also permits easy access to the mass spectrometer assembly and makes it possi-

**All the information
that appeared
in C&EN
last year
is at your
fingertips
with the**

C&EN INDEX Annual 1977

Whether you are interested in wide coverage of a general topic or just a brief letter to the editor—if C&EN published it last year, you will find it listed in this comprehensive index. Consider a broad field such as fibers, for example: under that listing you will find research (acrylonitrile outlook promising); development (rayon fibers gather new interest with technological improvements); business (DuPont sales in Europe top \$1 billion); international news (Yugoslavia's polyester fiber plant operational) and twenty more listings! Most of them cross-indexed to be found easily under other headings, too.

In addition, you'll find information on many other broad fields—grants, health, OSHA, and so on—many with 50 or more listings! Individual topics, too—ovonic modification, kerogen, bathing caps.

Legislation, research, economics, processing... whatever aspect of the subject you want to know about... you will find it quickly and easily.

Just published, this comprehensive, useful index is available paperback or in microfiche... \$25.00.

Save time and effort... use the coupon below to order your C&EN INDEX, Annual 1977 edition now!

Special Issues Sales
American Chemical Society
1155 Sixteenth Street, N.W.
Washington, D.C. 20036

YES, please rush _____ copies of the
new C&EN INDEX Annual 1977 @ \$25.00
each.

- ☐ Paper ☐ Microfiche
☐ Payment enclosed. ☐ Bill me.
☐ Bill company.

Name _____

Organization _____ Title _____

Address _____

☐ Home ☐ Business

City, State, Zip _____

Take the grind out of grinding and mixing

with the complete grinding and mixing system from the Tygon® tubing people

We make it easy. The complete Norton grinding & mixing system — including jar mills, mill jars and grinding media — is designed to minimize effort, minimize time, and maximize results.



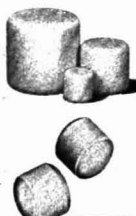
JAR MILLS

A size and style for nearly every application. Norton jar mills are built tough to give long service life, and their exclusive "no-creep" design means jars stay in place. Jar mills are available in single-tier, single jar; single-tier, three jar; two-tier and three-tier models.



MILL JARS

Norton Roalox mill jars offer four times the wear-life yet only half the contamination of conventional porcelain jars. Jars feature a simple all-in-one lid and handle system that makes opening, closing and locking a snap. Capacities range from 1/2 pint to 3.4 gallons.



GRINDING MEDIA

Both Burundum™ and Zirconia grinding media provide excellent grinding characteristics with a minimum of contamination. Burundum has a specific gravity of 3.42, and is designed for general grinding applications. For even faster milling times and less contamination, Zirconia is suggested (specific gravity 5.5). Both types are available in several sizes.



GET THE FACTS WITH THIS COMPREHENSIVE BROCHURE

Just call your local lab supply house, or call us toll-free at 800-321-9634 (Ohio call collect 216-630-9230).

34 236

NORTON PLASTICS AND SYNTHETICS DIVISION

PO BOX 250 AKRON OHIO 44309 TEL (216) 830-8230

CIRCLE 153 ON READER SERVICE CARD

Flavor Chemistry of Animal Foods



ACS Symposium Series No. 67

Roger W. Bullard, Editor
U.S. Fish and Wildlife Service

A symposium sponsored by the Division of Agricultural and Food Chemistry of the American Chemical Society.

The recent revolution in animal foods has produced high quality, more palatable foods for domestic pets and food-producing animals. Now research is also being directed toward meeting the needs of threatened wildlife species as well as toward controlling their destruction of human food supplies.

Since animals cannot directly appraise food or food additives, there are many unique problems in animal flavor research that require the cooperation from specialists in many different fields. This volume covers the problems and recent advances in this field. Many domestic and non-domestic animals are discussed by specialists in organic and analytical chemistry, biochemistry, behavior, biology, nutrition, and physiology.

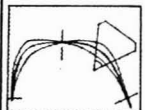
CONTENTS

Animal Flavor Research • Food Preference Behavior • Methodology of Behavioral Testing • Chemical Fractions from Estrus Urine • Bacterial Action and Chemical Signaling • Taste and Smell • Carnivore Taste Systems • Diets for Food-Producing Animals • Palatable Foods for Domestic Pets • Repellents to Protect Crops

175 pages (1978) clothbound \$19.00
LC 77-27295 ISBN 0-8412-0404-7

Order from:
SIS/American Chemical Society
1155 16th St., N.W./Wash., D.C. 20036

High Performance Mass Spectrometry: Chemical Applications



New methods and techniques in mass spectral fragmentation have boosted the field of mass spectrometry into a major scientific discipline. Ongoing research in chemical analysis problems through identification and quantification of trace amounts of material with high performance mass spectrometry methods is reviewed in these 18 chapters.

ACS Symposium Series No. 70

Michael L. Gross, Editor
University of Nebraska

A symposium co-sponsored by the University of Nebraska — Lincoln, the National Science Foundation, Kratos Ltd., and INCOS/Finnegan

Special emphasis is placed on structure, property, and energy surface determinations of gas-phase ions. These mass spectrometry methods include chemical and field ionization, ultra-high resolution, new methods of defocused metastable scans, collisional activation spectrometry, field ionization, kinetics, spark source ionization and new techniques in gas chromatography/mass spectrometry.

CONTENTS

Metastable Transitions • Unimolecular Reactions of Organic Ions • Ions from Collisional Activation Spectra • Kinetic Energy Spectrometry • Field Ionization Kinetic Studies of Gas Phase Ion Chemistry • Organic Trace Analysis • Gas Chromatography/High Resolution Mass Spectrometry • Positive and Negative Ion Chemical Ionization Mass Spectrometry • Selective Reagent Ions • Selectivity in Biomedical Applications • Field Desorption Mass Spectrometry • Applications in a Pharmaceutical Laboratory • Minor Nucleotides in Intact DNA • Ultra High Resolution Mass Spectrometry Analysis of Petroleum and Coal Products • Using a Double Focusing Mass Spectrometer • Multielement Isotope Dilution Techniques • Computer Applications • Computer Analysis of High and Low Resolution Mass Spectral Data

Order from:
SIS/American Chemical Society
1155 16th St., N.W.
Wash., D.C. 20036

358 pages (1978) \$28.00 clothbound
LC 78-789 ISBN 0-8412-0422-5

ble for all pump-down and venting operations to be performed automatically. The existence of only one high-vacuum flange minimizes the chance for leaks. Another major benefit of the location of the mass spectrometer assembly is the controlled-temperature environment that is provided. The sample transfer line is heated by the boiler to about 250 °C to prevent condensation of sample in transit from the gas chromatograph. The ion source and quadrupole are heated by the interior wall of the pump, which is maintained at uniform temperature by the pump vapor. The resultant temperature of 180–190 °C is sufficient to prevent condensation without destroying molecular ions. The quadrupole mass analyzer uses hyperbolic rods instead of the conventional round rods to preserve peak shapes and resolution at high mass (7). The detector

is maintained near room temperature since it is located slightly above the highest pump stage and is suspended from the vacuum flange.

The GC-MS system is controlled by a 9825 desk-top computer with 32K words (16 bits each) of semiconductor memory. Programs and data are stored on a cartridge tape unit (250K bytes capacity with a transfer rate of 2750 bytes/s). All information can be plotted on Hewlett-Packard Model 9866 B printer/plotter mounted directly on top of the computer, although a 32-character display and 16-character wide printer can be used for certain limited functions. The speed and computational power of the computer are sufficient to handle control, monitoring, and output functions without processing delays.

A number of convenient and useful software programs, including pro-

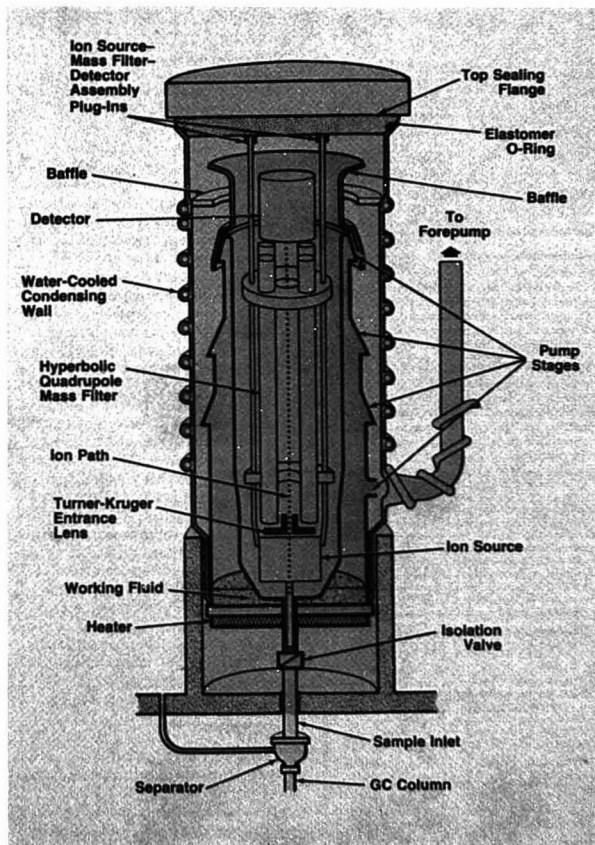


Figure 5. Detailed representation of vacuum system and analyzer assembly for HP 5992

WESCAN's Model 212 Conductivity Meter



- Direct Reading
- Digital Display
- Wide Range
- Zero Suppression
- Analog Recorder Output

The WESCAN Model 212 Conductivity Meter is a convenient, general purpose instrument designed to perform most laboratory conductivity measurements. Applications vary from single determinations using a temperature compensated dip-cell, to continuous monitoring of liquid chromatography effluents using a micro-volume flow cell. A variety of cells are available to satisfy various application methods.

For more information, contact:
WESCAN INSTRUMENTS, INC.
3018 Scott Blvd.
Santa Clara, CA 95050

WESCAN
INSTRUMENTS, INC.

CIRCLE 240 ON READER SERVICE CARD

NOW!

A DRY BLOCK HEATER THAT STIRS!



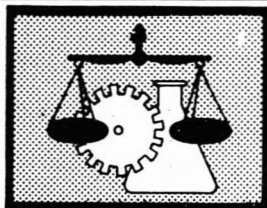
18900 Reacti-Therm[®]
Heating/Stirring Module, 110 volts \$162

FOR
ACCELERATING
AND PRECISELY
CONTROLLING
MINI AND MICRO
REACTIONS

For more information on
Pierce's new Reacti-Therm[®]
Heating/Stirring Module
please circle number below
on response card.

PIERCE
CHEMICAL COMPANY
Box 117 Rockford, Illinois 61101

CIRCLE 172 ON READER SERVICE CARD



Legal Rights of Chemists and Engineers

Advances in Chemistry Series No. 161

Warren D. Niederhauser, Editor
Rohm and Haas Company
E. Gerald Meyer, Editor
University of Wyoming

A symposium cosponsored by the
Division of Professional Relations and
the Council Committee on
Professional Relations of the American
Chemical Society.

Here is the first volume of its kind to cover
an entire spectrum of legal rights of chemists
and engineers and the problems they
encounter as professionals.

Included in twelve highly instructive papers
are well-established legal precedents,
legislation currently before Congress,
suggested new legislation, and extensive
bibliographies which permit the reader to
pursue particular areas of interest.

The collection contains a great deal of new
information and data useful to university
chemistry and engineering departments,
law schools, patent attorneys, medical
scientists, architects and technicians,
chemical process companies, and
professional associations.

CONTENTS

Careers Combining Chemistry and The Law •
Patent Law Revision • Special Compensation for
Salaried Chemists and Rewards for Invention •
Confidentiality, Secrecy Agreements, and Trade
Secrets • Employment Contracts • Legalization of
Employment Guidelines • Layoffs and Serious
Grievances • Union's Effect on Legal Obligations •
Social Responsibilities of Chemists • Equal
Opportunity Employment • Tax Effects of
Retirement Plans • Federal Tax Law

109 pages (1977) cloth-bound \$16 (H)
LC 77-9364 ISBN 0-8412-0357-1

SIS/American Chemical Society
1155 16th St., N.W./Wash., D.C. 20036

Please send _____ copies of *Advances 161*
Legal Rights of Chemists and Engineers at \$16 (H)
per copy.

☐ Check enclosed for \$ _____ Bill me.
Postpaid in U.S. and Canada, plus 40 cents
elsewhere.

Name _____

Address _____

City _____

State _____

Zip _____

grams to automatically monitor peaks
and store the associated mass spectra
on tape for search against several
identification libraries, are available.
Perhaps the two most useful programs
are the selected ion monitoring pro-
gram and on-line search program. The
SIM program monitors 1-6 ions simul-
taneously during the course of the
chromatography, after which it can
plot chromatograms of all of the ions
monitored, integrate the areas of
peaks, normalize the areas to any one
peak or to the sum of all areas, and
print a quantitative report. This pro-
gram is most useful for quantitative
analysis of samples from drug users.
The on-line search program operates
in real time. Whenever a GC peak is
detected, its mass is immediately cor-
rected for background, recorded on
tape, and searched against a library
stored in core. This is accomplished
rapidly enough that, in the event of
a match, the retention time, the name
of the compound, and the peak height
are recorded directly on the chromato-
gram as the peak is being eluted. The
system also has a diagnostic program
to aid the user in performing in-house
maintenance.

Another convenient program is the
Autotune program, which automati-
cally calibrates the mass spectrometer
and optimizes sensitivity and resolu-
tion. This is accomplished by intro-
ducing (automatically on the B series,
manually on the A series) a calibration
gas, perfluorotributylamine (PFTBA).
Subsequently, the software automati-
cally establishes correct voltages for
ion source, mass analyzer, and detec-
tor components and then optimizes
for resolution and sensitivity at select-
ed high and low masses.

Hewlett-Packard's innovative de-
sign, which has substantially reduced
the complexity of mass spectrometry,
places the entire mass spectrometer
on top of a standard GC and makes
it essentially a highly sophisticated
GC detector. This has made this sys-
tem the least expensive of all GC-MS
instruments. Nevertheless, this design
has a major drawback in that it makes
it impossible to utilize chemical ion-
ization. Although this may present
difficulties in the analysis of certain
compounds that do not render molec-
ular ions with electron impact ioniza-
tion, the simplicity, compactness, and
low cost of the system make it very
useful for selected applications.

Du Pont DP-102

The Du Pont DP-102 has the capa-
bilities of an advanced analytical mass
spectrometer but, due to its simplicity
and ease of operation, should prove
to be useful in the clinical laboratory
environment. As shown in Figure 6,
the system is housed in two separate
modules, one for the gas chromato-



Talk to Joyce Loebel...

who has three languages in Image Analysis

Joyce-Loebel has many software languages for their wide range of computer aided image analysis systems. From simple routine tasks through to the most complex scientific programming there's the right instrument and software package to suit your application and your budget. Check the package that best suits your requirements.

Magiscan

The Magiscan is a television based, wholly software controlled, quantitative image analysis system. The instrument has a high speed image processor to do the difficult feature extraction tasks, and a powerful mini computer to do the arithmetic orientated quantitative analysis task. The image processor operates on the fully digitised image and can therefore perform complex algorithms analysing not only density levels, but also operating on gradients, textures etc. The Magiscan software



approach enables it to handle feature extraction tasks other systems are incapable of, such as defining cell boundaries in a non-uniformly stained sample, separating overlapping spheres, and rejecting out-of-focus particles. The Magiscan has an evergrowing library of software for today's problem and an open-ended potential for further software development.

Microdensitometer 6

The competitively priced, all new Microdensitometer 6 combines the best features of the now world famous Microdensitometer 3CS with the latest advances in electro-optical techniques and computer data processing. It's a classical flat-bed microdensitometer, operating in transmission and reflectance mode. Optical density measurements are made using double-beam optics to assure high linearity, and precision over a wide range of optical density. Optical density or transmission data are recorded in digital form at a data rate of up to 1000 points per second. The 360° rotatable table can accommodate samples up to 250mm x 250mm. A projection screen provides excellent sample acquisition. The Microdensitometer 6 is interfaced to a mini computer, and Joyce-Loebel "Wizard" software language allows the user to programme the system to do any task from a straight forward raster scan to complex real-time data reduction analyses.



Scandig 3/Filmwrite 2

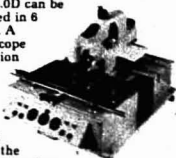
This system combines a high speed rotating drum microdensitometer and a photographic recorder respectively. Interfaced to a digital computer they form an Image Analysis system that can digitise, enhance, and record photographic images in either transmission or reflectance up to



an area 250mm x 250mm. Scandig 3 incorporates the very latest developments in solid state photometrics ensuring a repeatability not previously possible. Scanning apertures cover the range 12.5 to 200 microns through an optical density range of 0 to 3D (1 to 4D option). Filmwrite 2 generates instant hard copy on a 250mm x 250mm photographic paper. The integral photographic processor gives you instant prints without the need for a darkroom. Joyce-Loebel's famous FSPP software provides simple control of both Scandig and Filmwrite as well as a range of picture processing algorithms.

Microdensitometer 3CS

This instrument is a versatile double beam, high resolution flatbed recording microdensitometer providing an output in the form of an analogue graph on an integral X-Y recorder. Sample to graph X axis variable from 1 to 1 up to 1000 to 1. Density measurements from 0.2D up to 6.0D can be achieved in 8 ranges. A microscope projection



system allows the operator to view the sample through the variable calibrated measuring slit. Colour filters can be fitted as can a wide range of accessories for special application. Microdensitometer 3CS may be interfaced to a mini computer.



Joyce-Loebel

A Division of Vickers Limited

Great Britain Team Valley, Gateshead, NE11 0QW ENGLAND. Telephone (0632) 822111, Telex 53257
North America 100A Commerce Way, Woburn, MA 01801 USA. Telephone (617) 935-3113, Telex 94-0413
West Germany 7417 Pullingen, Röhrenstrasse 90, WEST GERMANY. Telefon (07121) 73021, Telex 0729 651

CIRCLE 122 ON READER SERVICE CARD

Come to Barnes for analytical accessories. You'll be in good company.

Analytical accessories are a Barnes specialty, the only spectroscopy products we make. We deliver promptly, off the shelf, analytical accessories compatible with Beckman, Perkin-Elmer, and other IR spectrophotometers. Windows, liquid and solid sampling items, gas cells, reflectance units, and much more.

Barnes quality, too, is compatible with the best. But the prices are a little lower. Because we have a special department that makes a big deal out of accessories, while for others it's only a sideline.

Solve your accessory problem toll free
(800) 243-3498. Or in Conn. (203) 348-5381
Barnes Engineering Company
30 Commerce Road, Stamford, Conn. 06904



CIBA GEIGY / DUPONT / EASTMAN KODAK / DOW
CHEMICAL / PERKIN-ELMER / GULF OIL CHEM. /
IBM / MONSANTO / MOBIL CHEM. / AMERICAN
CYANAMID / FORD MOTOR / ICI AMERICA /
HUGHES AIRCRAFT / GTE SYLVANIA /
AMOCO / EXXON RESEARCH /
MIT / GENERAL ELECTRIC /
STAUER ELECTRIC /
WESTERN ELECTRIC /
PFIZER CORP. /
3M CO.

CIRCLE 25 ON READER SERVICE CARD

graph and mass spectrometer and the other for the data system and computer/plotter. The GC-MS incorporates a number of features that warrant further discussion. The gas chromatograph accommodates both packed and capillary columns and offers a separate flame ionization detector and an automatic sampler as accessories. For high-resolution capability, a special capillary column accessory (not shown) admits gas coaxially at the end of the column to minimize loss of capillary column liquid phase and to maintain maximum sample transmission and GC resolution through the jet separator. Conventional capillary inlets that allow entry of sample directly into the ion source can lead to decreases in operating efficiency and to increased maintenance. As previously indicated, the DP-102 utilizes a jet separator to remove carrier gas. This system offers chemical ionization as well as electron impact ionization, and reagent gas for CI can be introduced automatically under computer control. The tip of the direct insertion probe forms an integral part of a novel rejuvenating ion source that will be discussed in more detail later. The probe, which can be automatically inserted into the ion source under computer control, ensures that all vacuum valves are operated in proper sequence and thereby prevents accidental loss of vacuum. The probe can also be temperature programmed to permit microdistillation and MS analysis of relatively unstable solid substances. The mass analyzer uses a 58° magnetic sector and scans with rapid accelerating voltage changes to achieve linear separation of masses. The magnetic analyzer is used because of its theoretically increased sensitivity and resolution at high mass. This system is capable of scan speeds approaching 1000 amu/s. A unique electron multiplier/computer interface provides a dynamic range of 10^9 (significantly larger than even most research mass spectrometers). This makes it possible to detect small peaks accurately in the presence of major components without saturating the data system on the large peaks or sacrificing sensitivity on small peaks. Consequently, it is possible to use a single internal standard concentration for a very broad range of sample concentrations, thereby eliminating the need for sample dilution or repeat analyses at different instrumental settings. The data system consists of an interactive keyboard control center and cathode-ray tube (CRT) for display. The dedicated minicomputer has 64K words of direct memory and a high-capacity disc storage capability of 20 megabytes. A Tektronix hard-copy unit can reproduce images displayed on the CRT.

Perhaps one of the most unique fea-

A FAST, EFFICIENT ALTERNATIVE TO KJELDAHL...

The Microprocessor Controlled MODEL 707 Provides Nitrogen/ Protein Analysis . . . In as Little as 30 Seconds!



MODEL 707

- Uses proven chemiluminescent detection principle
- Microprocessor controlled for greater stability and repeatability
- Programmed temperature parameters
- Handles from 5 to 120 samples per hour
- Accommodates up to 1g sample size
- 1 nanogram sensitivity with dynamic range of 10^6
- Extended range accessory (Model 732) allows combined nitrogen in percentage range



ANTEK[®] INSTRUMENTS, INC.

6005 North Freeway
Houston, Texas 77076
TELEPHONE (713) 691-2265 TWX: 910-881-1792

CIRCLE 5 ON READER SERVICE CARD

SIEMENS

In X-ray spectrometers, cost-effectiveness is far more important than cost.

There's no arguing. The SRS 200 is the most cost-effective sequential spectrometer on the market today.

Depending on model, it can accommodate up to 80 specimens. And it's specially designed for full automation.

It analyzes solids in any configuration, powders and liquids. For all elements from fluorine to uranium ... in standard concentrations from 0.0001% to 100%. And, with special sample preparation, trace analyses in the ppm or sub-ppm ranges.

Control it with your own computer ... or with our floppy-disk-oriented

system. Either way, you can feed it our software packages for sophisticated data manipulation and the latest correction methods.

The computer also controls the filter aperture changer, and X-ray tube power setting. A 10-position sample changer is standard.

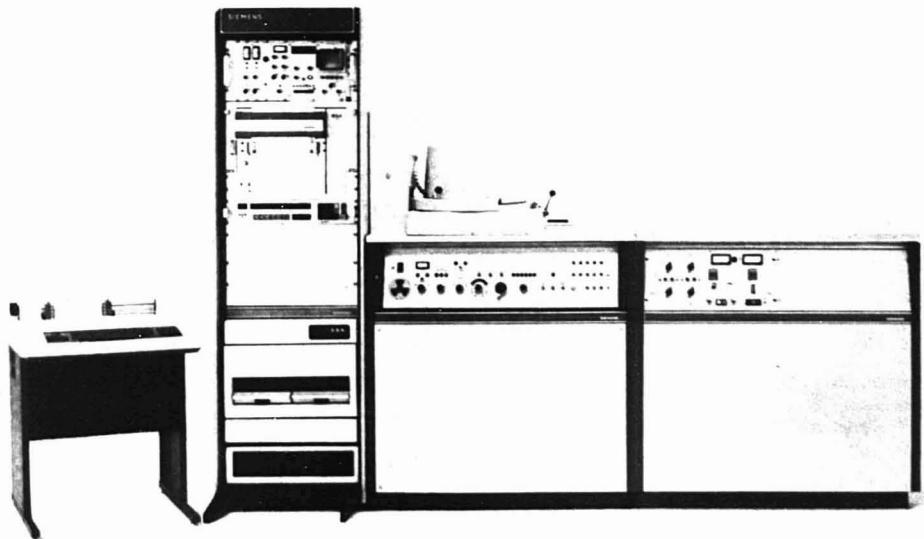
The SRS 200 has a 4-KW output generator powerful enough to operate two tubes simultaneously. So when you're ready to expand, you've got built-in economy.

It also features a detector pulse spectroscopy for initial setup and observation of the pulse-height

selector. And an X-ray tube that can be changed in five minutes.

So next time someone talks about cost, ask him to talk about effectiveness.

For complete information on the SRS 200, use the reader-response card. For more information on our full range of X-ray analyzers plus a free 30 x 43-inch, four-color wall chart of the X-ray periodic table of the chemical elements, call or write Mr. Pedro Arredondo, **Siemens Corporation**, 2 Pin Oak Lane, Cherry Hill, New Jersey 08034. (609) 424-9210.



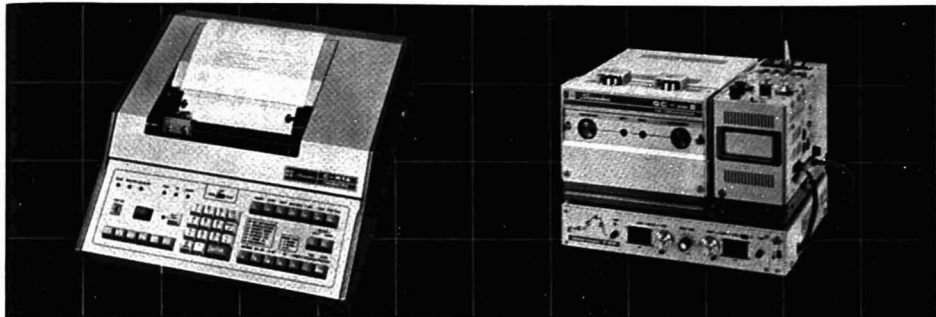
Siemens SRS 200. A little more the day you buy it, but more for your money for years.

CIRCLE 193 ON READER SERVICE CARD

ANALYTICAL CHEMISTRY, VOL. 51, NO. 4, APRIL 1979 • 537 A

FROM SHIMADZU

Shimadzu, one of the largest and oldest manufacturers of gas chromatographs in the world, offers a new line of unique gas chromatograph systems featuring the utmost in accuracy, versatility, speed, performance, and efficiency at a price anyone can afford. All Shimadzu GC use the latest technologies to ensure simple maintenance and maximum reliability. When you think of GC, think of Shimadzu.



Chromatopac C-R1A Recording Data Processor

Other chromatograph data processors can calculate common standard calculation routines such as area normalization, normalization with response factors, external standardization and internal standardization, but only the C-R1A goes a step further and calculates calorific value, steam pressure, liquid specific gravity, deviation from a standard value, mole density (%)—weight density (%), and other factors from the results of these calculations.

Other outstanding features of the C-R1A include a thermal printer/plotter for chromatograms and data recording, recording of the names of components, recording of up to 339 peaks, measurement of peak-top height or average height, all-new grouping function, and self-diagnostic function. These features not only ensure fast, precise analysis, but also free the chromatographer from troublesome, time-consuming manual calculations for more important work.

GC-MINI2 Gas Chromatograph

This surprisingly light weight, compact GC system has the performances of much larger more expensive systems. Dual column flow and on-column/on-detector system ensure excellent stability, high sensitivity, and perfect accuracy. Flow rates and pressures of the gases can be easily measured using one-touch connectors and flow monitors in the gas flow lines.

Unique oven temperature control system maintains the oven at room temperature, even when the injection port temperature is high. Contamination-free flame ionization detector exhausts the vapor from the flame directly from the jet to a cylindrical ion collector and vent at the top.

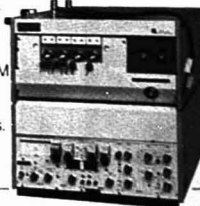
GC-MINI2 easily disassembles into four main modules—column oven, injection port/detector, flow control unit, and electric control unit—for quick, easy maintenance. The electric control unit further disassembles into six sub-units, thus simplifying maintenance still further.

GC-7AG Series Ghost-Cut Gas Chromatograph



Add the GC-7AG and GC-6AM and you have a complete system capable of meeting your ever changing GC needs.

GC-6AM Series Cartridge Gas Chromatograph



• Write today for more information on these and other Shimadzu labor and cost saving instruments.



SHIMADZU
SCIENTIFIC INSTRUMENTS, INC.

SHIMADZU SCIENTIFIC INSTRUMENTS, INC.
9147 Red Branch Road, Columbia, Md. 21045, U.S.A. Phone (301)997-1227 Telex 67959
SHIMADZU (EUROPA) GmbH
4300 Düsseldorf 1, Jülicherstr. 155, Germany Phone (0211)314061 Telex 0859639
SHIMADZU SEISAKUSHO LTD.
1, Nishinokyo-Ku, Nakagyo-Ku, Kyoto 604, Japan Telex 05422-166

CIRCLE 194 ON READER SERVICE CARD

MOST USED

...because
it's most
useful.

The annual ACS **LabGuide** is the definitive directory to scientific instruments, equipment, chemicals, services, books, trade names, manufacturers and their sales offices.

It leads all others in editorial pages, in advertising pages, and in reader usage: **more than 70,000 inquiries every year.**

Table I. Comparison of GC-MS Features*

	Hewlett-Packard HP 5992A	Vitek Olfax IIA	Du Pont DP-102
Mass analyzer	Hyperbolic quadrupole	Quadrupole	Magnetic sector
Ionization mode	Electron impact	Electron impact	Electron impact and chemical ionization
Source renewal	In situ alternate filament	Open system and replace source	Automatic source rejuvenation
Separator	Membrane	Dual membrane	Jet separator
Mass range (amu)	10-800	400	1000
Max scan rate (amu/s)	1100	150	1000
Pump-down time (min)	60	60	45 (10 min with turbomolecular pump)
Computer storage	32K (core) 250K (tape)	31K (core) 60K (tape)	64K (core) 20 000K (disc)
Cost (\$)	49 500	60 000	135 000

*Standard configurations are described; other options are available on request.

ization modes, switching from EI to CI can be accomplished almost instantly (6 s) either under computer control or by direct instruction from the keyboard. The system can thus produce EI and CI spectra on the same GC peak, thereby giving both structural and molecular weight information.

Due to the speed and capacity of the data system, the DP-102 provides a variety of useful software routines. Like the Hewlett-Packard 5992, the DP-102 offers a computer-directed tune-up procedure. Unlike the 5992, however, this tune-up procedure is not fully automatic, and the operator retains control. Nevertheless, the procedure is as rapid as the fully automatic methods and takes only a few minutes to complete. The procedure simultaneously optimizes resolution and sensitivity for EI as well as CI. The system can acquire and store mass spectra conventionally, perform SIM for up to 9 ions, and can do a combination of continuous scanning and SIM. The latter approach makes possible presumptive searches at high sensitivity in selected areas of the chromatogram by SIM while allowing for full searches in other areas of the chromatogram where unknowns may elute. The system provides real time displays and on-line searches against a library of more than 31 000 spectra so that peaks can be identified as they elute. Various display formats are available and can include as many as four separate chromatograms or operations (e.g., total ion chromatogram plus one or two selected mass chromatograms plus a selected mass spectrum) and a library search. All of these can be listed on the same printout.

As a result of its high capacity data system and overall system flexibility,

the DP-102 competes effectively with the most advanced research mass spectrometers. It is more costly than the other systems discussed here, but for the user who requires the additional flexibility, it provides many convenient and useful features.

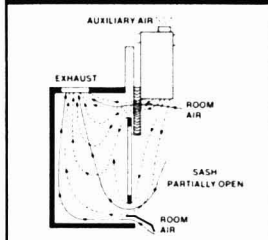
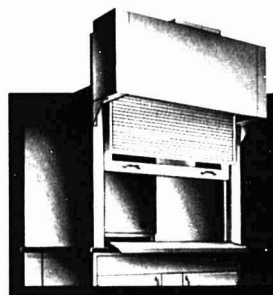
Summary

Key characteristics of the three GC-MS systems are detailed in a comparative format in Table I. As with all instrumentation, the potential laboratory user must consider his present and future analytical needs as well as the performance capabilities, design compromises, and price of the equipment.

Clearly, the two lower-cost systems (HP and Vitek) fall into a separate category from the Du Pont, based solely on the size of the laboratory's budget. The Du Pont instrument illustrates the additional flexibility that can be obtained in GC-MS and the price increment required. In particular, the availability of chemical ionization in an automatic mode with this system provides for ease of operation and increases the analytical sensitivity to larger molecular weight ions. Data storage and reporting modes are greatly enlarged and provide more extensive search capabilities for identification of unknowns. Automatic source rejuvenation and numerous other convenience features are included in the package.

The only system designed specifically for clinical laboratory analytical applications is the Vitek Olfax; yet, it retains most of the classical capabilities of GC-MS systems. The mass range limit is lowest (400 amu) and the maximum scan rate is least (150 amu/s). Nevertheless, the Olfax's efficient use of the probability-based

Kewaunee **HOODAIRE** Auxiliary Air System



- Upgrades the Performance of Existing Fume Hoods
- Reduces Energy Consumption
- Improves Laboratory Safety

Most manufacturers now offer—and strongly recommend—fume hoods with integral auxiliary air systems to reduce the loss of conditioned air exhausted through laboratory fume hoods. But what about laboratories with several existing non-auxiliary air type fume hoods? Are these facilities to be forced to "scrap" their present equipment in order to meet higher velocity requirements and avoid the increased energy costs?

To solve this problem, Kewaunee now offers a practical and highly ef-

fective way to upgrade the performance of existing fume hoods—the HOODAIRE Auxiliary Air System. Utilizing a unique patented design, the HOODAIRE System reduces the loss of expensive conditioned air by as much as 70% while, at the same time, it substantially improves fume hood safety. It readily adapts to most existing laboratory fume hoods, and it can provide a complete range of important safety features.

For complete information, call or write

kewaunee
Kewaunee Scientific Equipment Corp.
Metal Furniture Division
Adrian, Michigan 49221
Phone: 517-263-5731

CIRCLE 128 ON READER SERVICE CARD



Sampling 2 or 3 μ l. is no laughing matter.

Are you injecting 2 or 3 μ l samples, or even less, using a 10 μ l syringe and experiencing traditional difficulties of bending plungers and fixed needles? Not to mention loss of accuracy due to doubtful short-scale readings.

The SGE 5 μ l syringe with removable needle (RN) and guided plunger (GP) takes care of that.

The illustrated 5A-RN-GP syringe has an extended barrel and reinforced plunger plus a leak-free removable needle which combine to give the syringe strength and durability for a long service life. Injection is smooth and accurate. Also available in 10, 15 and 25 μ l versions.

And that is really something to smile about.

Please write for our "Precision Microlitre Syringe" catalogue.

LAUGHING
KOOKABURRA
Dacelo Gigas.

Scientific Glass Engineering Pty. Ltd.

Head Office
Scientific Glass Engineering Pty. Ltd.
111 Arden St., North Melbourne, 3091
Australia
Tel: (03) 329 6633

European Office
Scientific Glass Engineering (U.K.) Ltd.
637 North Circular Road, London NW2 7AY
Great Britain
Tel: 01 492 6244

U.S.A. Office
Scientific Glass Engineering Inc.
2800 Longhorn Blvd., Suite 104
Austin, Texas 78759 U.S.A.
Tel: (512) 837 7190



CIRCLE 188 ON READER SERVICE CARD

ANALYTICAL CHEMISTRY, VOL. 51, NO. 4, APRIL 1979 • 541 A

matching technique permits its successful application to the analysis of a wide variety of drugs and other biological compounds in complex matrices and under conditions in which they may not be totally resolved by the gas chromatograph.

The Hewlett-Packard product is a highly efficient, compact GC-MS that offers considerable performance at the lowest system price. The system includes HP components that have been previously utilized in other applications (e.g., the gas chromatograph and calculator/plotter). The unique construction of the diffusion pump and mass spectrometer components produces a compact and convenient overall instrument design, and the only major disadvantage is the inability to use chemical ionization.

We expect that other manufacturers will note the opportunities for specialized GC-MS systems and that new instruments will be introduced with competitive features. More widespread application of GC-MS techniques in the fields of clinical toxicology, therapeutic drug monitoring, forensic analysis, and analysis of environmental toxic substances should be expected.

Acknowledgment

The authors appreciate the helpful discussion with Cecil Hornbeck, Laboratory Service, Veterans Administration Hospital, San Diego. We also thank Harmon Brown, Hewlett-Packard, E. M. Chait and Paul Strauss, Du Pont, and W. E. Potter and J. Heslop, Vitek, for the information provided

about their companies' instruments and for technical discussions.

References

- (1) A. L. Burlingame, C.H.L. Shackleton, I. Howe, and O. S. Chizhov, *Anal. Chem.*, **50**, 346R (1978).
- (2) A. M. Lawson, *Clin. Chem.*, **21**, 803 (1975).
- (3) E. C. Horning and M. G. Horning, *J. Chromatogr. Sci.*, **9**, 129 (1971).
- (4) J. Roboz, *Adv. Clin. Chem.*, **17**, 109 (1972).
- (5) W. McFadden, "Techniques of Combined Gas Chromatography/Mass Spectrometry," Wiley-Interscience, New York, N.Y., 1973.
- (6) F. W. McLafferty, R. H. Hertel, and R. D. Villwock, *Org. Mass. Spectrom.*, **9**, 690 (1974).
- (7) W. M. Brubaker and W. S. Chamberlain, in "Recent Developments in Mass Spectrometry," K. Ogata and T. Hayakawa, Eds., University of Tokyo Press, Tokyo, Japan, 1970.

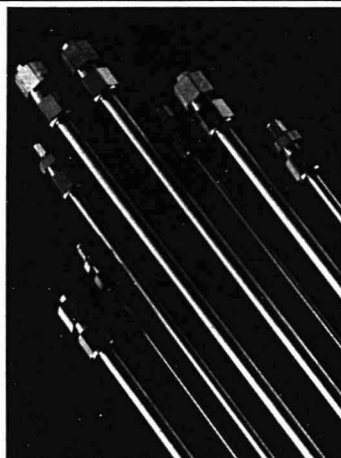


Nathan Gochman (left), chief, Clinical Chemistry Section (VA Medical Center) and associate adjunct professor of chemistry and pathology (Univ. of Calif. at San Diego); Lemuel J. Bouie (center), assistant chief, Clinical Chemistry Section (VA Medical Center) and assistant adjunct professor of chemistry and pathology (Univ. of Calif. at San Diego); and David N. Bailey, director, Toxicology Laboratory (UCSD Medical Center) and assistant professor of pathology (Univ. of Calif. at San Diego).

BETTER THREE FROM TSK

TSK-GEL PACKINGS & PACKED COLUMNS

Various types and grade covering total field of HPLC
Fully porous microspheres with narrow size distribution
High theoretical plate number
Stable physical and chemical properties
Little swelling and shrinkage



TSK STANDARD POLYMER Available in two models:
TSK STANDARD POLYSTYRENE for organic solvents
20 types, covering mol wt range from 300 to 20,000,000
TSK STANDARD POLY(ETHYLENE OXIDE) for aqueous solvents
7 types, covering mol wt range from 20,000 to 1,500,000



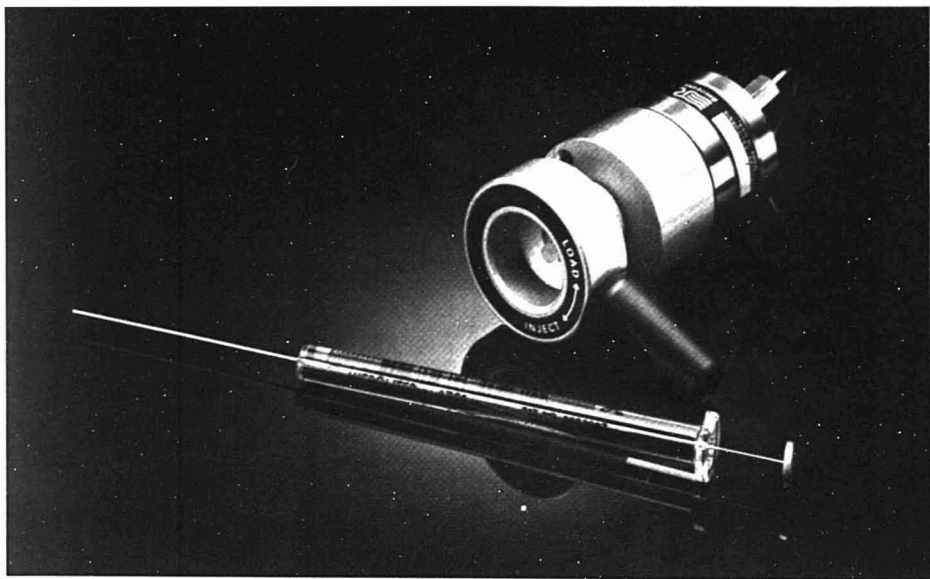
TSK-GEL TOYOPEARL

TOYOPEARL is hydrophilic polymer made, semirigid and spherical gel, particularly design for preparative GFC. Supplied as bulk packings suspended in water. Use of TOYOPEARL in place of the conventional soft gels will give you many advantages.

TSK TOYO SODA MANUFACTURING CO., LTD.

Head Office: Toso Building, 1-7-7 Akasaka, Minato-ku, Tokyo 107, Japan Tel. (03) 5585-3311 Cable Address: TOYOSODA TOKYO Telex J24475 TOYOSODA
New York Office: 200 Park Avenue, Suite 303E, New York, N.Y. 10017 U.S.A. Tel. New York 212-986-9447 Cable Address: SODATOKYO NEW YORK Telex 223355 TOYOSODA
London Office: Europe House, World Trade Centre, London, E19 6AA, England Tel. 01-488-2400 Telex: 884871 WORLDTRADELON TOYOSODA
Amto International b.v. Amsteldijk 166, Amsterdam, The Netherlands Tel. 020-461-858 Telex 18573 AMTO NL

CIRCLE 198 ON READER SERVICE CARD



Rheodyne simplifies LC sample injection again. We made the best injector even better.

Rheodyne's Model 7120 Syringe Loading Sample Injector has carved out an outstanding reputation in the LC field. Last year sales more than doubled. People seem to think it's the best around — and we modestly agree. Now we've made it even better — with new features that make sample injection simpler than ever before.

Flushing now unnecessary.

With the improved valve, Model 7125, the entire contents of the microsyringe is injected into the sample loop and flows to the column. No sample is left behind in the valve. Consequently, you don't have to flush the valve between injections unless you're doing trace analysis.

Further improvements.

The needle seal is now self adjusting. An optional switch signals time of injection. And mounting panels for LC systems are available.

Our new Model 7125 replaces the popular 7120 in all applications. Does all the 7120 does and more. Has the same mounting dimensions. Price is \$540.

New automatic model.

Our automatic Model 7126 combines the new 7125 with pneumatic actuators and time-of-injection switch so you can use it in automatic LC systems.

Compact. Sturdy. Reliable. May be used in the manual injection mode anytime you wish. Price is \$780.



Get the details now.

Contact Rheodyne Inc.,
2809 Tenth Street, Berkeley,
California 94710. Phone
(415) 548-5374.


RHEODYNE
THE LC CONNECTION COMPANY

CIRCLE 184 ON READER SERVICE CARD

ANALYTICAL CHEMISTRY, VOL. 51, NO. 4, APRIL 1979 • 543 A

LABORATORY SERVICE CENTER

β -Aminobutyric Acid • Ammonium Pyrrolidinedithiocarbamate • Anisoin
Cesium Chloride • 5-Chloroanthranilic Acid • 2,4-Diaminophenol DIHCl
Dichloroacetic Acid • 1,4-Dichlorobutane • N,N-Diethylformamide
2,3-Dimercaptosuccinic Acid • p-Dimethylaminobenzaldehyde • Esculin
Ethyl Pyruvate • Galloyanine • D(-)-Glutamic Acid • L(-)-Malic Acid
Malonic Acid • α -Naphtholbenzoin • o-, m- & p-Nitrobenzaldehydes
Potassium Acid Phthalate • 2-Pyridine Aldehyde • Sodium Pyruvate
Sodium- β -Hydroxybutyrate • Tetramethylammonium Chloride & Hydroxide

Write for our Products List of over 3000 chemicals

Tel: 516-273-0900

TWX: 510-227-6230

EASTERN CHEMICAL

BOX 2500 K

Division of GUARDIAN CHEMICAL CORP.

HAUPPAUGE, N. Y. 11787

Laboratory Service Center (Equipment, Materials, Services, Instruments for Leasing), Maximum space — 4 inches per advertisement. Column width, 2-3/16"; two-column width, 4-9/16". Artwork accepted. No combination of directory rates with ROP advertising. Rates based on number of inches used within 12 months from date of first insertion. Per inch: 1" — \$69; 12" — \$68; 24" — \$65; 36" — \$64; 48" — \$63.

CALL OR WRITE BARBARA AUFDERHEIDE

ANALYTICAL CHEMISTRY

25 Sylvan Road, So.

Westport, Ct. 06880

203-226-7131

LC Laboratories
1254 Chestnut Street
Newton, MA 02164
Problem-Solvers
in Organic and
Polymer Chemistry
(617) 244-9222
LIQUID CHROMATOGRAPHY SERVICES

SOLVENTS—Highest Purity

Call or write for prices.

Pollard & Co. Box 7131 Wilmington, DE
19803

Phone: 302-656-0060

LAB SAFETY

Send for 1979 Catalog

LAB SAFETY SUPPLY CO.

P.O. Box 1368, Janesville, WI 53455

USE LABORATORY SERVICE CENTER

INDEX TO ADVERTISERS IN THIS ISSUE

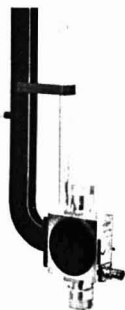
CIRCLE INQUIRY NO.	ADVERTISERS	PAGE NO.	CIRCLE INQUIRY NO.	ADVERTISERS	PAGE NO.
3	*Academic Press Flamm Advertising	510A	60	*Dohrmann Fred Schott & Associates	427A
6	*Airco Industrial Gases Hammond Farrell Inc.	519A	63	*Eastman Kodak Company Rumrill-Hoyt, Inc.	487A
2	*Alpkem Corporation Alpkem Advertising Company	505A	75	*Finnigan Instruments Robert Pease & Company Adv.	524A
xxx	*The American Instrument Company Industrial Advertising Associates	502A	76	*Fisher Scientific Company Tech-Ad Associates	496A
5	*Antek Cooley & Shillinglaw, Inc.	536A	78	*Fluid Metering, Inc. Arnold H. Nachman Associates	488A
10	*J. T. Baker Chemical Company Naimark & Barba, Inc.	443A	77	*Foxboro Analytical Shepherd, Tibball, & Galog	444A
25	*Barnes Engineering Company Jarman, Spitzer & Felix, Inc.	538A	84	*Gilson Medical Electronics, Inc. Towell, Inc.	505A
28	*Bausch & Lomb Scientific Optical Products Div. Wolff Associates, Inc.	517A	87	*Glenco Boone Advertising, Inc.	507A
26	*James G. Biddle Company Ferguson Advertising	516A	85	*Gould Inc. Carr Liggett Advertising, Inc.	483A
27	*Bio-Rad Laboratories Fred Schott & Associates	501A	86	*Gow-Mac Instrument Company Kenyon Hoag Associates	512A
21	*Brinkmann Instruments, Inc. Blatt Advertising, Inc.	0BC	96	*Hamilton Company Healer & Emerson Adv.	497A, 498A
22	*Bruker Instruments, Inc. Schwietzer Advertising	546A	94	*Helma International, Inc. Miller Advertising Agency, Inc.	530A
24	*Buchler Instruments Jud Jaffe Advertising	446A	1000	*Hewlett-Packard Benn Associates, Inc.	477A-480A
23	*Burdick & Jackson Laboratories, Inc. Studio 5 Advertising	514A	150	*Hewlett-Packard Tallant/Yates Advertising, Inc.	438A-439A
35-42	*Chromatix, Inc. David R. McClurg	433A	93	*Hayden & Son	513A
33	*Control Laser Corporation Sphere Advertising	470A	95	*Houston Instrument Cooley & Shillinglaw, Inc.	IFC
49	*Digital Equipment Corporation Creamer, Inc.	447A	121	*Inficon Paul, John & Lee, Inc. Adv.	526A
50-57	*Dionex Fred Schott & Associates	499A	91-92	*Instruments SA, Inc., J-Y Optical Systems Div. Kathy Wyatt & Associates	434A
			xxx	*Jarrell-Ash Div., Fisher Scientific Co. Tech-Ad Associates	459A-461A

INDEX TO ADVERTISERS IN THIS ISSUE

CIRCLE INQUIRY NO.	ADVERTISERS	PAGE NO.	CIRCLE INQUIRY NO.	ADVERTISERS	PAGE NO.
131-133	JEOL Analytical Instruments Weinrich Associates Inc.	445A	198	Toyo Soda Manufacturing Co., Ltd. Diamond Agency Co., Ltd.	542A
122, 129	Joyce-Loebel S. & M.E. Winship	472A, 535A	202-205	*Tracor Analytical Instruments Aim Advertising Agency	520A
128	*Kewaunee Scientific Equipment Corp. Guldberg Vandegrift Inc	541A	207	*Tracor Northern, Inc. Aitchnew Energetics	453A
127	Labtest Equipment Company Clarke Advertising	530A	215	Ultra Carbon Bradshaw Advertising	473A
125	Lachal Chemicals, Inc. Consulting Associates	505A	216	Ultra-Violet Products, Inc. Walnut Grove Industrial Advertising	508A
130	Leco Corporation LECOM	449A	217	U.S. Divers Co.-Lif-O-Gen Div. International Communications Inc.	516A
145	Mallinckrodt Goldberg & Brumbaugh, Inc.	451A	218-219, 222- 223, 228-229, 232, 244-248	*Varian 489A, 490A-491A, 493A, 494A, 495A Moran, Lanig & Duncan Adv.	495A
138-141	*Matheson Kenyon Hoag Associates	436A, 437A	235	*Varian M.A.T. Shepherd, Tibbalt & Galog	529A
143	*MC/B Manufacturing Chemists Northlich, Stolley, Inc.	474A-475A	237	W-P Instruments, Inc.	521A
148	*Metronics Murphy Advertising, Inc.	518A	210-212	*Waters Associates Marketing Dimensions, Inc.	450A
146	*Mettler McKinney, Inc.	455A	240	*Wescan Instruments, Inc. W.W. Love Advertising	533A
135	*Micromeritics Adgraphics	509A	238	*Whatman, Inc. J.S. Lanza & Associates	428A
136, 137	*Micromeritics Adgraphics	514G-514H, 514J	241	*C.N. Wood Manufacturing Co. Blavat Advertising, Inc.	508A
147	*Mitsubishi Chemical Industries Ltd. Global Advertising Co., Ltd.	523A			
155	*Nalge Labware Hutchins/Y & R	457A			
153	*Norton Plastics Northlich, Stolley of Akron, Inc.	532A			
157	*Ohaus Scale Corporation Michel-Cather, Inc.	435A			
xxx	*Orion Research OBC Advertising	431A			
179	*Pennsylvania Glass Sand Corporation	503A			
177, 178, 180	*Perkin-Elmer Corporation Marquardt & Roche, Inc. Adv.	463A, 464A-465A, 468A			
175	*Photochemical Research Associates Quantum Communications	530A			
172	*Pierce Chemical Pierce Ad-Graphics	534A			
174	*Precision Cells Inc. Arnold H. Nachman Associates	516A			
176	*Princeton Applied Research Corporation The Message Center	440A			
97, 98, 99, 110-112	*Pye Unicam Ltd.	514B-514C, 514D, 514E, 514F			
183, 184	*Rheodyne Bonfield Associates	486A, 543A			
182	*Riber Data Systems Marken Communications	448A			
190	*Sartorius GmbH Agentur Busche	506A			
191	*Schoeffel Instrument Mar-Bet Associates	523A			
189	*Schott & Gen, Inc. Bloom-Zagoren, Inc. Adv.	509A			
195	*Sciencetech, Inc. Prescott, Purcell, Karsh & Hagan	462A			
188	*Scientific Glass Engineering Arden Advertising Agency	541A			
194	*Shimadzu Seisakusho Ltd. General Advertising Agency, Inc.	539A			
193	*Siemens Hogan Gazzara Associates	537A			
192	*G. Frederick Smith Chemical Co. Andrew Shaw Advertising	454A			
196	*Spectra Physics Paul Pease Advertising, Inc.	515A			
187	*SPEX Industries Seymour Nussenbaum	497A			
201	*Texas Instruments, Inc. Morris & Adams	522A			
200	*Tokyo Kasei Kogyo Co., Ltd. Global Advertising Co., Ltd.	456A			
199	*The Torsion Balance Company Douglas Turner, Inc.	471A			

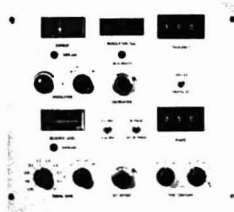


BRUKER EPR

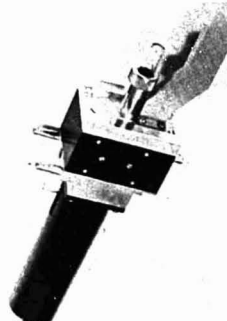


Introducing the NEW ER-200 SERIES D EPR SPECTROMETERS

TM High Sensitivity Resonator



Modulation Synthesizer - 1 kHz-999 kHz



High Temperature Resonator System

FEATURING:

- NEW high power microwave bridge: 200 mW leveled power, 600 mW max.
- NEW high dynamic range option with dual digitally-programmed rotary vane attenuators
- NEW directly measured digital microwave power readout
- NEW 100 kHz/12.5 kHz modulation channel with 2nd harmonic at both frequencies for ST-EPR
- Digitally controlled time base for slow sweep and built-in rapid scan unit
- TM mode cavity for high sensitivity
- Modulation synthesizer option tunable from 1 kHz to 999 kHz
- High temperature resonator system

... and many features available only from BRUKER including the best commercially available ENDOR accessory made.

For complete information, call or write:

BRUKER INSTRUMENTS, INC.

Manning Park, Billerica Mass. 01821
Phone (617) 667-9580

539 Beall Avenue
Rockville, Md. 20850
Phone (301) 762-4440

Old Mill Office Complex
201 San Antonio Circle, Suite 152
Mountain View, Calif. 94040
Phone (415) 941-3804

2410 Dunwin Drive, Unit 4
Mississauga, Ont., Canada L5L 1J9
Phone (416) 828-2830

CIRCLE 22 ON READER SERVICE CARD

Use this card to receive
your own monthly copy of

1979

ANALYTICAL CHEMISTRY

Toll Free: New Orders: 800-638-2000/Md. only 301-949-1551

	U.S.	Canada**	Foreign**
ACS Members*	<input type="checkbox"/> \$12.00	<input type="checkbox"/> \$21.00	<input type="checkbox"/> \$21.00
Nonmembers	<input type="checkbox"/> \$16.00	<input type="checkbox"/> \$25.00	<input type="checkbox"/> \$33.00

Bill me ☐ Bill Company ☐ Payment enclosed
(Make payable: American Chemical Society)

Name _____

Position _____

Your Employer _____

Address ☐ Home ☐ Business _____

City _____ State _____ ZIP _____

Employer's business ☐ Manufacturing ☐ Academic
☐ Government ☐ Other _____

If manufacturer, type of products produced _____

*Subscriptions at ACS member rates are for personal use only.
**Payment must be made in U.S. Currency, by international money order,
UNESCO coupons, U.S. bank draft, or through your book dealer.

Allow 60 days for your first copy to be put in the mail. 9998-G

Use this card to receive
your own monthly copy of

1979

ANALYTICAL CHEMISTRY

Toll Free: New Orders: 800-638-2000/Md. only 301-949-1551

	U.S.	Canada**	Foreign**
ACS Members*	<input type="checkbox"/> \$12.00	<input type="checkbox"/> \$21.00	<input type="checkbox"/> \$21.00
Nonmembers	<input type="checkbox"/> \$16.00	<input type="checkbox"/> \$25.00	<input type="checkbox"/> \$33.00

☐ Bill me ☐ Bill Company ☐ Payment enclosed
(Make payable: American Chemical Society)

Name _____

Position _____

Your Employer _____

Address ☐ Home ☐ Business _____

City _____ State _____ ZIP _____

Employer's business ☐ Manufacturing ☐ Academic
☐ Government ☐ Other _____

If manufacturer, type of products produced _____

*Subscriptions at ACS member rates are for personal use only.
**Payment must be made in U.S. Currency, by international money order,
UNESCO coupons, U.S. bank draft, or through your book dealer.

Allow 60 days for your first copy to be put in the mail. 9998-G

Mail this postage-free card today

Mail this postage-free card today



BUSINESS REPLY MAIL

FIRST CLASS PERMIT NO 10094 WASHINGTON D C

POSTAGE WILL BE PAID BY ADDRESSEE

AMERICAN CHEMICAL SOCIETY

Attn: Gayle Hebron
1155 Sixteenth Street, N.W.
Washington, D. C. 20036

NO POSTAGE
NECESSARY
IF MAILED
IN THE
UNITED STATES



BUSINESS REPLY MAIL

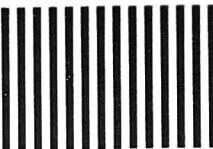
FIRST CLASS PERMIT NO 10094 WASHINGTON D C

POSTAGE WILL BE PAID BY ADDRESSEE

AMERICAN CHEMICAL SOCIETY

Attn: Gayle Hebron
1155 Sixteenth Street, N.W.
Washington, D. C. 20036

NO POSTAGE
NECESSARY
IF MAILED
IN THE
UNITED STATES



Editor: **Herbert A. Laitinen**

EDITORIAL HEADQUARTERS

1155 Sixteenth St., N.W.
Washington, D.C. 20036
Phone: 202-872-4570 Teletype: 710-8220151

Managing Editor: Josephine M. Petruzzi

Associate Editors: Andrew A. Husevsky, Barbara Cassatt

Associate Editor, Easton: Elizabeth R. Rule

Editorial Assistant: Andre D'Arcangelo

Associate Editor, editing: Nancy J. Oddenino

Production Manager: Leroy L. Corcoran

Art Director: John V. Sinnett

Designer: Alan Kahn

Advisory Board: L. S. Birks, Peter Carr, David Firestone, Kurt F. J. Heinrich, Philip F. Kane, Barry L. Karger, J. Jack Kirkland, Marvin Margoshes, Robert S. McDonald, James W. Mitchell, Royce W. Murray, Harry L. Pardue, Garry A. Rechnitz, Walter Slavin, John P. Walters

Instrumentation Advisory Panel: Gary D. Christian, Catherine Fenselau, Gary M. Hietje, Tomas Hirschfeld, Peter T. Kissinger, C. David Miller, Carter L. Olson, Sidney L. Phillips, Thomas H. Ridgway

Regulations, Analytical Division Ad Hoc Committee: Robert A. Libby (Chairman), Warren B. Crummett, William T. Donaldson, Donald T. Sawyer

Contributing Editor: Claude A. Lucchesi
Department of Chemistry, Northwestern University, Evanston, Ill. 60201

Published by the
AMERICAN CHEMICAL SOCIETY
1155 16th Street, N.W.
Washington, D.C. 20036

Books and Journals Division

Director: D. H. Michael Bowen

Journals: Charles R. Bertsch

Magazine and Production: Bacil Guiley

Research and Development: Seldon W. Terrant

Circulation Development: Marion Gurtein

Manuscript requirements are published in the January 1979 issue, page 171. Manuscripts for publication (4 copies) should be submitted to ANALYTICAL CHEMISTRY at the ACS Washington address.

The American Chemical Society and its editors assume no responsibility for the statements and opinions advanced by contributors. Views expressed in the editorials are those of the editors and do not necessarily represent the official position of the American Chemical Society.

Cleaning Our Environment—An Update

The ACS Committee on Environmental Improvement has issued a new edition of its report "Cleaning Our Environment" with the subtitle "A Chemical Perspective" as a follow-up to its 1969 report, subtitled "The Chemical Basis for Action". In an AC editorial in November 1969, the recommendations contained in the report were examined from the viewpoint of their analytical implications. Of the 33 recommendations, six were specifically directed to research in analytical chemistry and instrumentation, while many others had direct or indirect analytical components. It was clear in 1969 that to make significant progress in implementing the recommendations it would be necessary to include a great deal of highly competent analytical work, both as a service function and as research and development in its own right.

The new edition differs markedly from the old in devoting a separate chapter to Chemical Analysis and Monitoring, rather than scattering this material through the various sections on air, water, solid wastes, and pesticides. In this chapter, recognition is given to the accomplishments of analysts in refining existing techniques and to developing new methods for identifying and measuring previously unsuspected constituents of the environment. At the same time, it is acknowledged that "progress in environmental measurement has been slow, in part because of the persistent shortage of specialists in the field. Analysis too often is treated as a secondary activity and assigned to unqualified personnel. One result has been masses of environmental data that frequently are useless for the intended purposes."

Four recommendations in this chapter deal with the needs for additional funding for training in analytical chemistry and for research and development on new and improved analytical methods. Analytical scientists are urged to take the initiative in quality assurance of environmental analytical methods, and to give balanced attention to two types of techniques, namely those aimed at specific compounds and those aimed at classes of substances. Simple, low-cost methods suitable for mass application are to be preferred. Many of the recommendations in other chapters also involve analytical methods and instrumentation.

The ACS Committee on Environmental Improvement has appointed a Subcommittee on Environmental Analytical Chemistry with Dr. Warren B. Crummett of Dow Chemical Co. as Chairman. The goal of the Subcommittee is to set forth the minimum criteria for the validation of an environmental analytical method. Brief statements concerning sampling and sample handling, calibration and standardization, measurement validation, data handling, and establishing acceptability are to be formulated. This action should constitute an important initial step toward improving the usefulness, credibility, and reliability of environmental analytical data.



Two-Dimensional Chemical State Plots: A Standardized Data Set for Use in Identifying Chemical States by X-Ray Photoelectron Spectroscopy

C. D. Wagner,^{1*} L. H. Gale, and R. H. Raymond

Shell Development Company, P.O. Box 1380, Houston, Texas 77001

The combined use of both photoelectron and X-ray excited Auger lines increases the utility of ESCA for identifying chemical states. A useful format for displaying reference data is the two-dimensional plot where the kinetic energy of the sharpest Auger line is plotted vs. the binding energy of the most intense photoelectron line. A compilation of data for 24 elements is presented, including critically evaluated data from the literature which have been referenced to a uniform calibration line. The format of the plots is applicable to data obtained with ionizing photons of any energy. The data included for silicon, bromine, and tungsten were obtained with higher energy X-rays from a Au X-ray source.

The ESCA (Electron Spectroscopy for Chemical Analysis) or XPS (X-Ray Photoelectron Spectroscopy) technique has a special value among methods for analysis of surfaces because it furnishes information on the nature of chemical states. This is possible because the X-radiation used ordinarily does not produce chemical changes in the surface layers.

In the original concept (1), chemical shifts in photoelectron energies were stressed as the means by which chemical states can be identified. This feature is limited, however, since ranges in chemical shifts for some elements are small, and because there are difficulties in defining accurately the spectral line energies from insulating samples due to static charging.

There are other spectral features that can be useful in identifying chemical states. It has been found that chemical shifts in X-ray excited Auger lines are usually larger and very different from those in photoelectron lines (2). Those Auger lines that originate from Auger transitions resulting in vacancies in core levels have at least one sharp, intense component (3). Chemical shifts in this component can be measured as accurately as those in photoelectron lines, and this extra information is of significant value.

Since the chemical shifts of photoelectrons and Auger electrons are different, the differences between their kinetic energies constitute a special spectral property. This difference has been called the Auger parameter (4) and its numerical value is unique to each chemical state. It is more accurately determinable than either the photoelectron or Auger electron energy alone, because the static charge corrections in these lines then cancel. The chemical shift in the Auger parameter between two chemical states is related to the difference in extra-atomic relaxation energy between the two chemical states (5).

The Auger parameter is still a one-dimensional quantity, like the photoelectron energy or the Auger electron energy alone. A concept that makes independent use of the energies of the photoelectrons and the Auger electrons, as well as the Auger parameter, is the two-dimensional chemical state plot (6). In this, for each element, the kinetic energies of pho-

toelectrons for various chemical states are plotted on the abscissa, and those of corresponding Auger electrons on the ordinate. Each chemical state then occupies a unique position on the two-dimensional grid. An Auger parameter grid is also drawn as a family of parallel lines with slope +1. All points on any one of these lines have the same value of the Auger parameter. Points representing insulating chemical states, plotted to indicate error probability, take the form of rectangles about 0.7 eV long and 0.2 eV wide, parallel to the lines of the Auger parameter grid. The long dimension represents the error due to static charge correction. At right angles, this correction cancels and the error is minimized.

The form of the plot has evolved in several stages. At present we have arrived at a format we feel will be generally satisfactory for data presentation in the future. Accordingly, we present herewith, in this form, our present collection of data from this laboratory for a number of elements. We also include the available data from the literature for each element, corrected by static charge referencing to the same standard values. Data from other laboratories are not included when we do not have confidence in their method of static charge correction (7) (see below). Data for elements not included are scattered and few and do not warrant presentation in these plots; but many of them have been collected in tabular form (8).

Format of the Plots: The Modified Auger Parameter. Our previous format involved direct plotting of kinetic energies of Auger and photoelectrons. Values of the Auger parameter were shown on the diagonal grid. Disadvantages were: (1) kinetic energies of photoelectrons and hence values of the Auger parameter were dependent upon the photon energy used, and (2) values of the Auger parameter were often negative. We are indebted to Gaarenstroom and Winograd (9) for modifying the Auger parameter, by adding the Auger kinetic energy and the photoelectron binding energy. This has advantages in this presentation. In this approach, we plot Auger kinetic energy on the ordinate and photoelectron binding energy decreasing on the abscissa (essentially, still, a plot with kinetic energy increasing on the abscissa). The sum of the photoelectron binding energy and the Auger kinetic energy is then the Auger parameter plus the photon energy, according to:

$$\alpha = KE_A - KE_p$$

$$KE_p = h\nu - BE_p$$

$$\alpha + h\nu = KE_A + BE_p = \alpha'$$

where α is the Auger parameter, KE_A is the kinetic energy of the Auger electron, and KE_p and BE_p are the kinetic energy and binding energy of the photoelectron all referred to the Fermi level.

The quantity $\alpha + h\nu$ or α' , which we call the modified Auger parameter, is independent of the photon energy since both KE_A and BE_p are independent of photon energy. Thus, these

¹ Present address: 29 Starview Drive, Oakland, California 94618.

Table I. Suitable Lines for Chemical State Plots

radiation	element	photo-electron line	Auger line
Al K α (1486.6 eV)	F	1s	KVV
	Ne, Na	1s	KL _{2,3} L _{2,3} (D)
	Mg	1s, 2p	KL _{2,3} L _{2,3} (D)
	Ar, K, Ca, Sc	2p _{3/2}	L _{2,3} M _{2,3} M _{2,3} (P) + L _{2,3} M _{2,3} (D)
	Ti, Mn	2p _{3/2}	L _{2,3} M _{2,3} V
	Fe, Co, Ni	2p _{3/2}	L _{2,3} VV
	Cu, Zn, Ga	2p _{3/2}	L _{2,3} M _{2,3} M _{2,3} (G ₄ , ³ P, D ₂)
	Ge, As	2p _{3/2}	L _{2,3} M _{2,3} M _{2,3} (G ₄ , ³ P, D ₂)
	Se	3d	L _{2,3} M _{2,3} M _{2,3} (G ₄ , ³ P, D ₂)
	Ru, Rh, Pd	3d _{5/2}	M _{2,3} VV
Au M α (2122.9 eV)	Ag, Cd, In, Sn, Sb, Te, I, Xe, Cs, Ba	3d _{5/2}	M _{2,3} N _{2,3} N _{2,3} (G ₄ , D ₂)
	Hg, Tl, Pb, Bi	4f _{7/2}	N _{2,3} O _{4,5} O _{4,5}
	Al, Si	1s	KL _{2,3} L _{2,3}
	Se, Br, Kr, Rb, Sr, Y	2p _{3/2}	L _{2,3} M _{2,3} M _{2,3}
	Hf, Ta, W, Re, Os, Ir	3d _{5/2}	M _{2,3} N _{2,3} N _{2,3}
	P, S, Cl	1s	KL _{2,3} L _{2,3}
	Zr, Nb, Mo, Ru	2p _{3/2}	L _{2,3} M _{2,3} M _{2,3}
	Pt, Au, Hg, Tl, Pb, Bi	3d _{5/2}	M _{2,3} N _{2,3} N _{2,3}
	Ar, K, Ca	1s	KL _{2,3} L _{2,3}
	Rh, Pd, Ag, Cd, In, Sn, Sb, Te	2p _{3/2}	L _{2,3} M _{2,3} M _{2,3}
Ti K α (4510.9 eV)	Th, U	3d _{5/2}	M _{2,3} N _{2,3} N _{2,3}

plots can be constructed with no notation of the photon energy used, and can be applied to ESCA data obtained using any X-ray source.

Suitable Spectral Lines. Spectral lines suitable for this approach are shown in Table I. A new series of Auger lines not previously cited is included, the N_{2,3}O_{4,5}O_{4,5} lines, which should be useful for Hg, Tl, Pb, and Bi (10). Gold, silver, and titanium X-rays are shown as examples of X-rays of higher energy, by which suitable Auger lines can be recorded for elements that provide no useful Auger lines with Mg or Al X-radiation (11). Three of the chemical state plots included herewith were developed with AuM X-radiation (Si, Br, and W) (11).

Intensity of the Auger Lines. In most cases, the photoelectron used is from the process that results in the initial core shell vacancy involved in the subsequent Auger transition. The total number of Auger electrons resulting from vacancies in a given core shell should almost equal the number of photoelectrons, since the fluorescence yield in this energy range is extremely small. However, since there are a number of different energies of Auger electrons arising from the initial vacancy in one shell, the yield at any one energy is considerably less than the photoelectron yield. Nevertheless, normally the intensity (peak height) of the sharpest Auger line ranges from 15–40% of the parent photoelectron line when both are of similar kinetic energy. Instrument transmission and electron mean free path considerations change this ratio when the kinetic energies are disparate. The width of the Auger line used is similar to that of the photoelectron line.

When L X-rays (such as Ag) or M X-rays (such as Au) are used, the characteristic X-radiation contains a strong β component, and the individual X-ray lines themselves are

significantly wider (ca. 2 eV) than that from Mg or Al. Therefore, the photoelectron lines are wider and are split into two major components. Moreover, there is enhanced ionization from bremsstrahlung, so that the Auger line intensity is enhanced. Thus, with these sources of radiation, the Auger line is sharper and usually considerably more intense than the parent photoelectron line.

Valence-Type Auger Lines. Most of the plots shown here are for core-type Auger lines (final vacancies in core levels). Those transitions involving valence levels are usually more complex, leading to wide lines and sometimes Auger line groups of very different distributions. Included in the plots are valence-type Auger lines for F, Ti, Mn, Fe, Co, Ni, Cu, Ru, Rh, Pd, and Ag. Those from F, Ni, Cu, and Ag appear to be quasi-atomic transitions (12) and the lines are sharp resembling closely the core-type lines of higher Z elements. The valence Auger lines of Ti, Mn, Fe, Co, Ru, Rh, and Pd are nevertheless useful.

EXPERIMENTAL

Data in this laboratory were obtained with a Varian IEEE-15 spectrometer operated with Mg or Al X-rays at 10 kV, 100 mA, scanning in 0.1–0.2 eV steps by varying the retarding voltage applied to the sample. The analyzing energy was a constant 100 eV, giving a 1.0-eV instrumental line width. Samples were cylindrical in shape, ca. 1 cm o.d. by 1 cm long. Conducting samples were prepared by direct fabrication, cleaning, and then abrasion in nitrogen, or by vapor deposition in the instrument. They were mounted in electrical contact with the retarding voltage supply. Insulating samples were ground in an alumina mortar in a nitrogen glove box, dusted onto polymer film tape mounted on an aluminum cylinder, and transferred to the instrument without access to air.

Data were obtained in 10–20 volt scans, summing channel data until counts in the peak channel were at least several thousand above background.

Calibration and Charge-Referencing. Spectral energy data useful for identification of chemical states must be quoted with respect to an energy scale accurate in magnitude and with its absolute position established. The voltage scale used here was checked by measuring the difference in binding energy between initial and final states of known X-ray transitions, such as Mg K α , Zn L α , and Ge L α X-rays (7, 13). These intervals checked the known X-ray energies within 0.1 eV. A spectrometer work function was assumed so that the Au 4f_{7/2} line appeared at 83.8 eV. With this setting the Cu 2p_{3/2} line was at 932.4 eV. Residual hydrocarbon on standard abraded copper and gold appeared consistently at 284.6 eV. This value agrees with that expected from the C 1s – Au 4f_{7/2} value of 200.8 eV obtained by Jorgensen and Berthou (14) and Kinoshita et al. (15). The value of 284.6 eV for adventitious hydrocarbon was then used to correct energies of lines from insulators for static charging, which, in the Varian instrument, amounted to up to 5 eV.

Inclusion of data from the literature requires, in many cases, transposition to this voltage scale. Data for conducting samples were modified when the instrumental voltage scale was specified so that Au 4f_{7/2} is at other than 83.8 eV. Since data were almost never supplied in those papers to enable checking the magnitude of the voltage scale (e.g., the position of a natural line at high binding energy), the assumption had to be made that the voltage scale magnitude was accurate. Nevertheless, some literature values appeared out of line, and in exceptional cases these were rejected under the assumption of voltage scale inaccuracy.

Literature data on insulating samples were used if the charge referencing method was believed to be valid (7). Methods include:

- (1) Use of thin samples, if they are so thin that conductive backing lines are detected in good intensity.
- (2) Use of the gold decoration method, if it seems to be done properly (7).
- (3) Use of the adventitious hydrocarbon C 1s line.
- (4) Use of the C 1s line of internal hydrocarbon groups in the sample. Cyano ligands were also used.
- (5) Use of vapor deposition with co-condensation of a hydrocarbon. Values used throughout were 83.8 eV for Au 4f_{7/2} and

284.6 eV for C 1s. Validity of the latter value for internal referencing using cyano groups seems justified by the work of Vannerberg (16).

Data acquired by certain other methods were not included (7). These especially include charge referencing by physically mixing a calibrant powder. Use of a C 1s signal from polymer film sample mount was also rejected as inherently invalid, for the same reasons. Auger energies derived from electron beam ionization were not included, since the companion photoelectron energies must be obtained from separate experiments involving photon irradiation.

Construction of the Plots. The data for each element is shown as a rectangle containing the chemical structure. Those data points obtained from the literature contain superscripts indicating the literature reference. Tables within the plots include other data that are either off-scale or that cannot be included because of crowding. Off-scale points are shown at the border of the plots at the proper value of the Auger Parameter.

Limited label size makes it necessary to use some abbreviations. These are: R = alkyl; Me, Et, Pr, Bu, etc. = specific alkyl groups; Ph = phenyl; L = $P(C_6H_5)_3$; acac = acetylacetonate; N = NH_4 ; ox = surface oxidized in air; sulf = surface treated with H_2S ; NH_4^+ = $(NO_3)_3$; aq = hydrate; CN_n = $(CN)_n$; tu = thiourea; tm = tetramethylthiourea; Ac = CH_3CO ; and cp_n = (cyclo- C_6H_5) $_n$.

Data for many compounds from this laboratory have appeared in several articles (2-4, 6, 8, 11) but no effort is made here to indicate the data that have been previously published.

COMMENTS ON THE PLOTS

Fluorine. The fluorine KVV line has the distinctive $KL_{23}L_{23}$ character of core-type Auger lines, even though final vacancies in the transition are in valence levels. Covalent fluorine compounds (organic) are grouped in the lower left hand corner (low kinetic energies for the Auger and photoelectron lines). Compounds containing complex fluoroanions are grouped in the middle of the plot, while binary fluorides tend to be grouped in the upper right hand corner (high kinetic energies). A fluorinated graphite with the composition C_4F , which is conductive, has an expected high α' of 1343.9. In contrast, the bulk of the fluorine compounds are between 1339 and 1342.

Sodium. Sodium exhibits the typical core-type Auger line. The photoelectron chemical shift is small, less than 2 eV. In contrast, the Auger line exhibits a ca. 6.5-eV range. Compounds containing fluoride and complex fluoranions have low values for α' , ca. 2060, while all other compounds fall between 2060 and 2063.

Magnesium. Magnesium also exhibits a very small chemical shift for the photoelectron line; however, the shift in the Auger line is very large, almost 8 eV between Mg metal and MgF_2 . Two plots are shown, one for the low kinetic energy 1s photoelectron line and one for the higher kinetic energy 2p line.

Silicon. Data for solids were obtained with Au M_{23} X-rays (2122.9 eV). The value of α' for the insulating solids are similar, ca. 1712, 3 eV below that for Si, and 2 eV above those of the gaseous compounds (11).

Titanium. The $L_{23}M_{23}V$ group was selected as the representative Auger group because it is sharper than the somewhat more intense LVV line. The chemical shifts of both the $L_{23}M_{23}V$ and the $2p_{3/2}$ photoelectron line span more than 8 eV. The Auger parameter exhibits a large spread of 5 eV.

Manganese. With manganese, there are substantial chemical shifts in the most intense lines ($2p_{3/2}$, $L_{23}M_{23}V$) but the Auger group is often broad (5-8 eV fwhm) and somewhat variable in intensity.

Iron. With iron, the $L_{23}VV$ peak appears best for use. The dispersion on the plot is very great, providing a very meaningful and potentially useful chemical state plot in spite of the frequent great width of Auger peak. Some of the peaks, particularly those for the oxides, have ca. 8-10 eV fwhm. On the other hand, the conductive FeS_2 has a very sharp Auger

peak that can hardly be differentiated spectrally from Fe metal. The Auger peaks tend to be sharp in the diamagnetic compounds.

Cobalt. Cobalt compounds are dispersed on the plot as widely as iron compounds. Again, one sulfide is not significantly different from the pure metal in terms of line shape and position. Some of the paramagnetic compounds exhibit wide and blunt Auger peaks.

Nickel. The nickel $L_{23}VV$ Auger peak has developed a quasi-core character and is very sharp in many nickel compounds. However, NiO is a great exception. The intense Auger group is nearly square, extending over more than 10 eV. The points plotted on the chart are for the center of this extended group.

Copper. The Auger lines with copper assume a more consistent character, upon the transition to core-type (12). Note that there is no significant chemical shift in the $2p_{3/2}$ line for cuprous type copper, but the Auger line shift permits differentiation of these compounds. Cupric compounds are dispersed rather widely.

Zinc. The Auger group shows the typical distribution of the LMM core-type Auger lines. There is almost no chemical shift in the photoelectron line but a good shift in the Auger line of several electron volts.

Arsenic, Selenium. These plots, utilizing the many data of Bahl et al., exemplify the ideal—a slope of ca. 3 and very large dispersion. The theory (4) predicts a chemical shift in the Auger line three times that in the photoelectron line. There are two plots for arsenic, one for the high binding energy $2p_{3/2}$ line and another for the low binding energy 3d line.

Bromine. Au M_{23} (2122.9 eV) photons were used to record the higher BE $2p_{3/2}$ photoelectron and the high KE $L_{23}M_{23}M_{23}$ Auger electrons (11). Very little dispersion in Auger parameter was observed with the few solid compounds tested, but, as with silicon, values of α' for gaseous compounds were lower.

Rhodium. Significant dispersion is achieved here with a rather large number of compounds.

Palladium. At Pd, the final state in the Auger transition is not yet in a core level, but the $M_{45}VV$ group is broadening, prior to dividing into the M_4 and M_5 components. While the spectrometer does not resolve them, the peak corresponding to the M_5 component provides a clear and measurable peak.

Silver. Silver has essentially no chemical shift in the $3d_{5/2}$ line at all, but a good one in the $M_4N_{45}N_{45}$ line. The latter, now separated from the M_5 component, is quite sharply defined.

Cadmium. Again, there is almost no chemical shift in the photoelectron line but a good dispersion in the Auger line.

Indium. Here the dispersion is good, with a slight photoelectron chemical shift as well.

Tin, Antimony, Tellurium. With these, the plots have the ideal slope of ca. 3, and very large chemical shifts.

Iodine. Data are difficult to collect because of interference of the Auger peak with O(KVV), but data available indicate little chemical shift among simple iodides. There seems to be little variation in the Auger parameter, even between periodate and iodide.

Tungsten. Extensive data were recorded with Au, M radiation, to test the concept applied to the heavy transition metal series. The $M_{45}N_7N_7$ Auger groups are intense and sharp, 30% of the intensity of the W $3d_{5/2}$ line as recorded. Line position data for the compounds show excellent dispersion in chemical shift in two dimensions. This should be roughly representative of data for all the heavy metals.

Use of the Chemical State Plots. The positions of the photoelectron and Auger lines from an unknown sample should be located on the appropriate elemental plot. Chemical states which have lines located more than ca. 1 eV away from

the data point of the unknown can generally be excluded from consideration. Chemical compounds which coincide or are close to the data point for the unknown are potential candidates if they are consistent with other knowledge of the chemical composition. The possibility should, of course, be borne in mind that a chemical compound not recorded on the plot may have these coordinates.

One further caution needs to be exercised. A conductive state in a state of nearly atomic subdivision on an insulator may emit photoelectrons as much as 1 eV lower kinetic energy, and Auger electrons as much as 3 eV lower kinetic energy. This shift results from the loss of polarization energy in the conduction electrons. Conversely, lines of an extremely thin insulator on a conductor may be shifted to higher kinetic energies, because of a gain in polarization energy or extra-atomic relaxation energy.

CONCLUSION

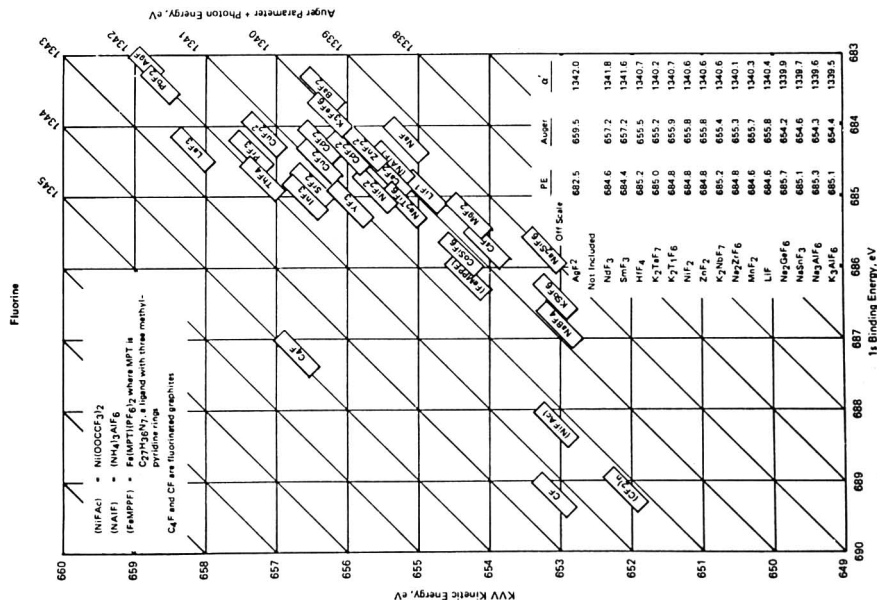
Twenty-six chemical state plots for twenty-four elements are presented. Data for three of them were obtained using radiation of higher photon energy than that of Al K α .

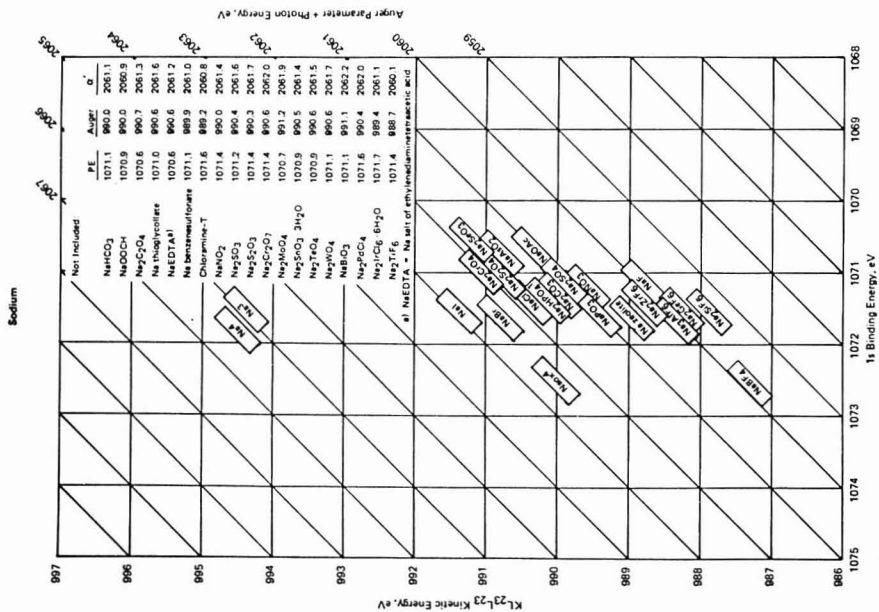
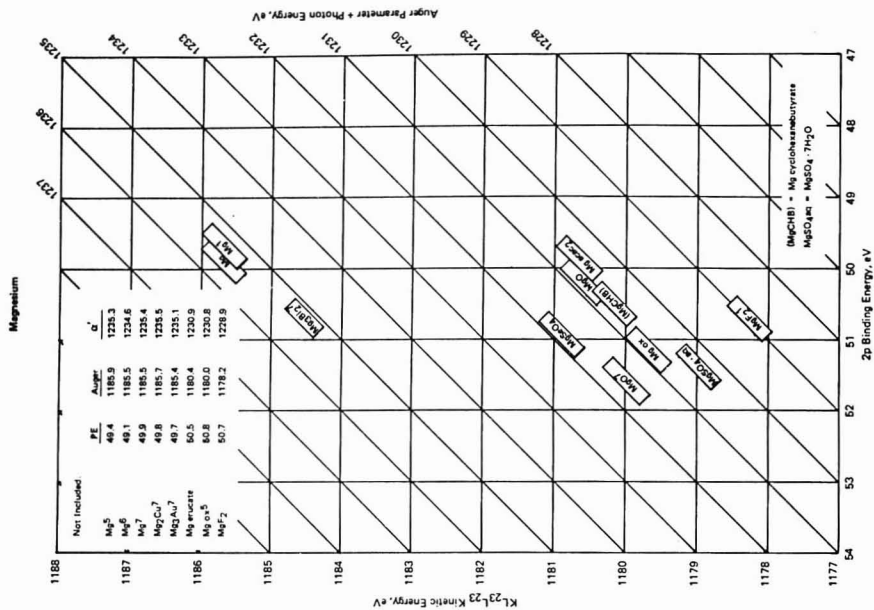
The data are presented not only as a convenient aid for spectroscopists using ESCA or XPS for analytical purposes,

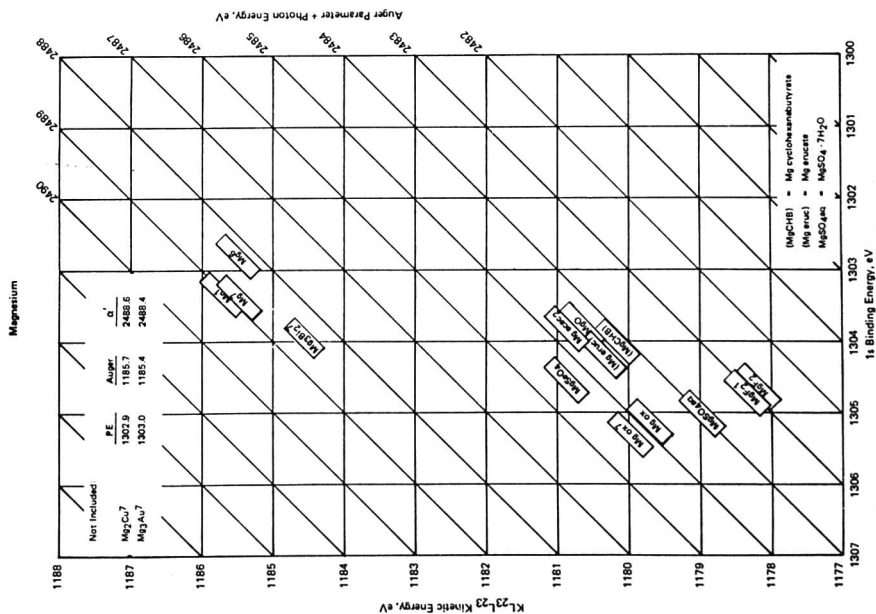
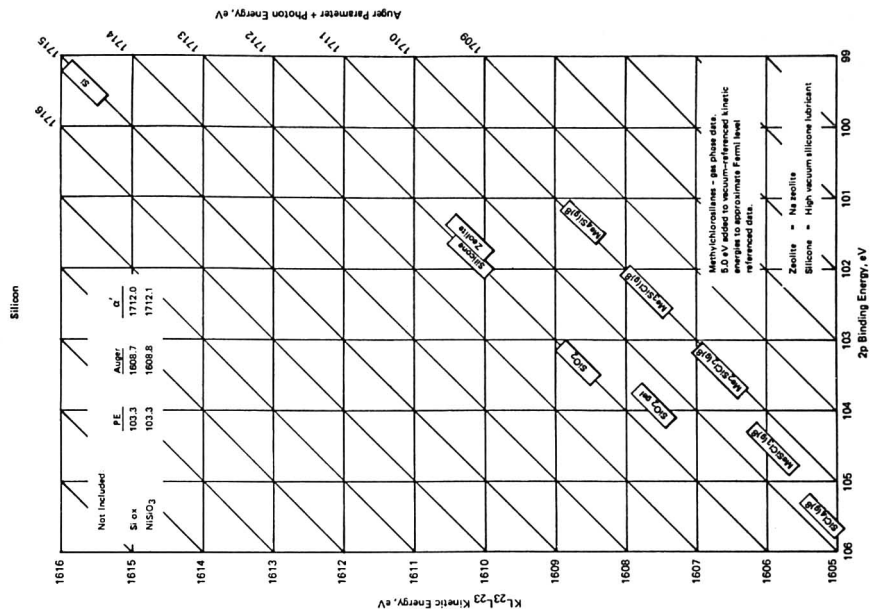
but also to establish a convenient standard format for presentation of such line position data in the future.

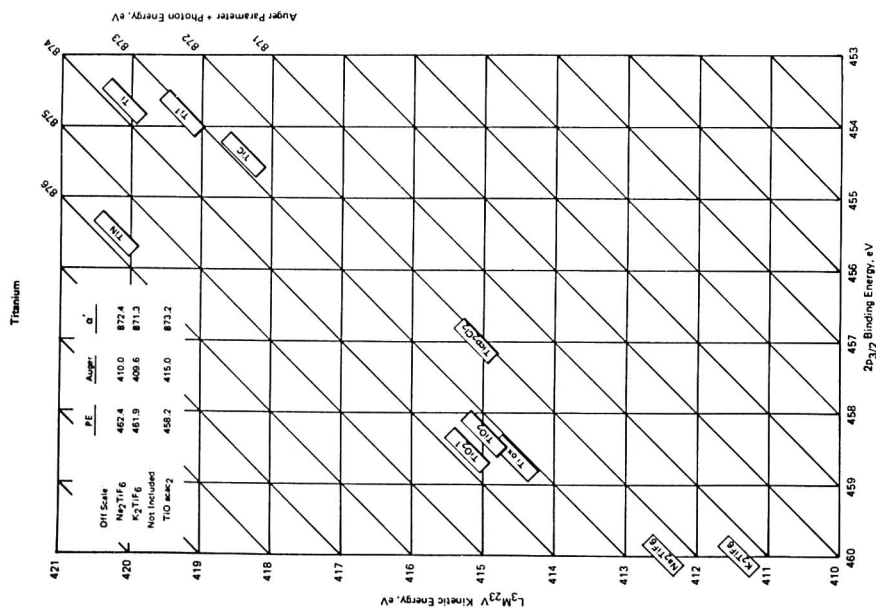
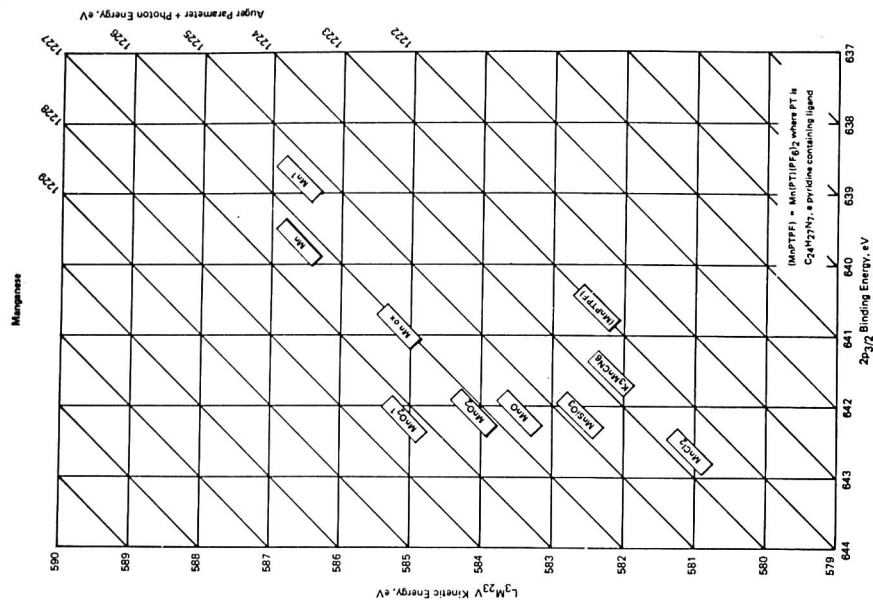
LITERATURE CITED (TEXT)

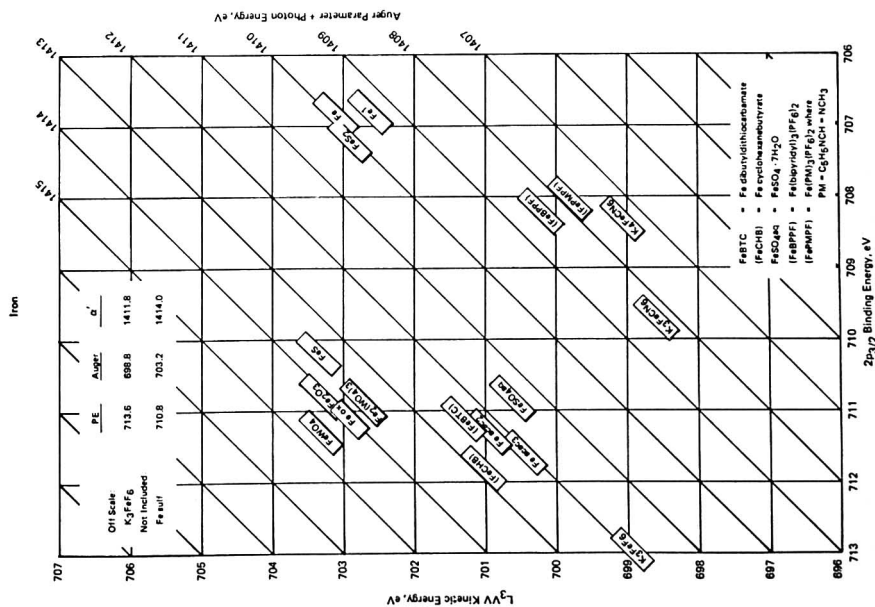
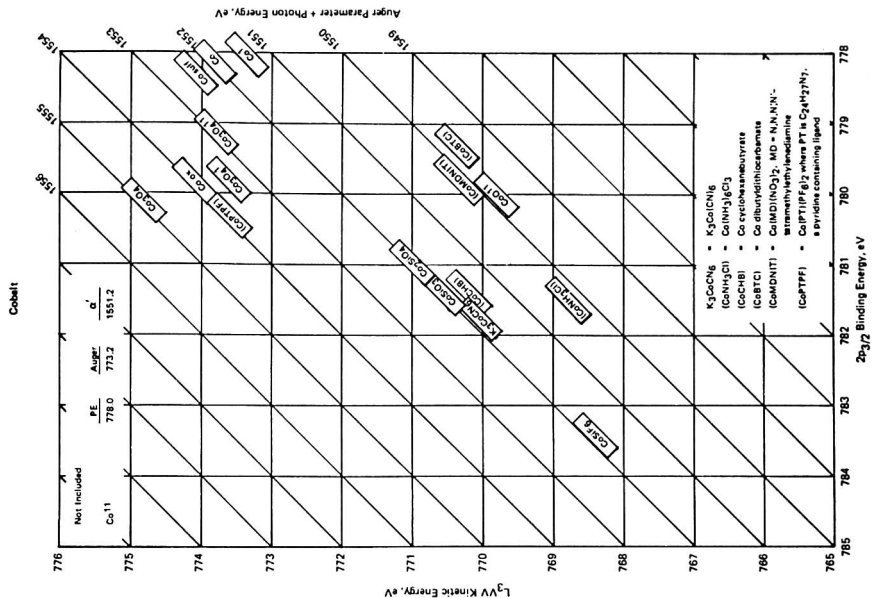
- (1) K. Siegbahn, C. Nordling, A. Fahlman, R. Nordberg, K. Hamrin, J. Hedman, G. Johansson, T. Bergmark, S. Karlsson, I. Lindgren, and B. Lindberg, "Atomic, Molecular, and Solid State Structure Studied by Means of Electron Spectroscopy, ESCA", Almqvist and Wiksells, Uppsala, 1967.
- (2) C. D. Wagner and P. Bileon, *Surf. Sci.*, **35**, 82 (1973).
- (3) C. D. Wagner, *Anal. Chem.*, **44**, 967 (1972).
- (4) C. D. Wagner, *Faraday Discuss. Chem. Soc.*, **60**, 291 (1975).
- (5) S. P. Kowalczyk, L. Ley, F. R. McFeely, R. A. Pollak, and D. A. Shirley, *Phys. Rev. B*, **9**, 381 (1974).
- (6) C. D. Wagner, *J. Electron Spectrosc. Relat. Phenom.*, **10**, 305 (1977).
- (7) "Energy Calibration in Electron Spectrometers", C. D. Wagner, *ASTM Spec. Publ.*, in press.
- (8) "The Role of Auger Lines in Photoelectron Spectroscopy", C. D. Wagner, in "Handbook of Ultra-violet and X-ray Photoelectron Spectroscopy", Heyden and Sons, Ltd., London, 1977, Chap. 7.
- (9) S. W. Gaarenstroom and N. Winograd, *J. Chem. Phys.*, **67**, 3500 (1977).
- (10) J. F. McGilp, P. Weightman, and E. J. McGuire, *J. Phys. C*, **10**, 3445 (1977).
- (11) C. D. Wagner, *J. Vac. Sci. Technol.*, **15**, 518 (1978).
- (12) L. Yin, I. Adler, T. Tsang, M. H. Chen, and B. Crasemann, *Phys. Lett. A*, **46**, 113 (1973).
- (13) J. A. Bearden, *Rev. Mod. Phys.*, **39**, 78 (1967).
- (14) C. K. Jorgensen and H. Barthou, *Chem. Phys. Lett.*, **31**, 416 (1975).
- (15) S. Kinoshita, T. Ohta, and N. Kuroda, *Bull. Chem. Soc. Jpn.*, **49**, 1149 (1976).
- (16) N.-G. Vannerberg, *Chem. Scr.*, **9**, 122 (1976).

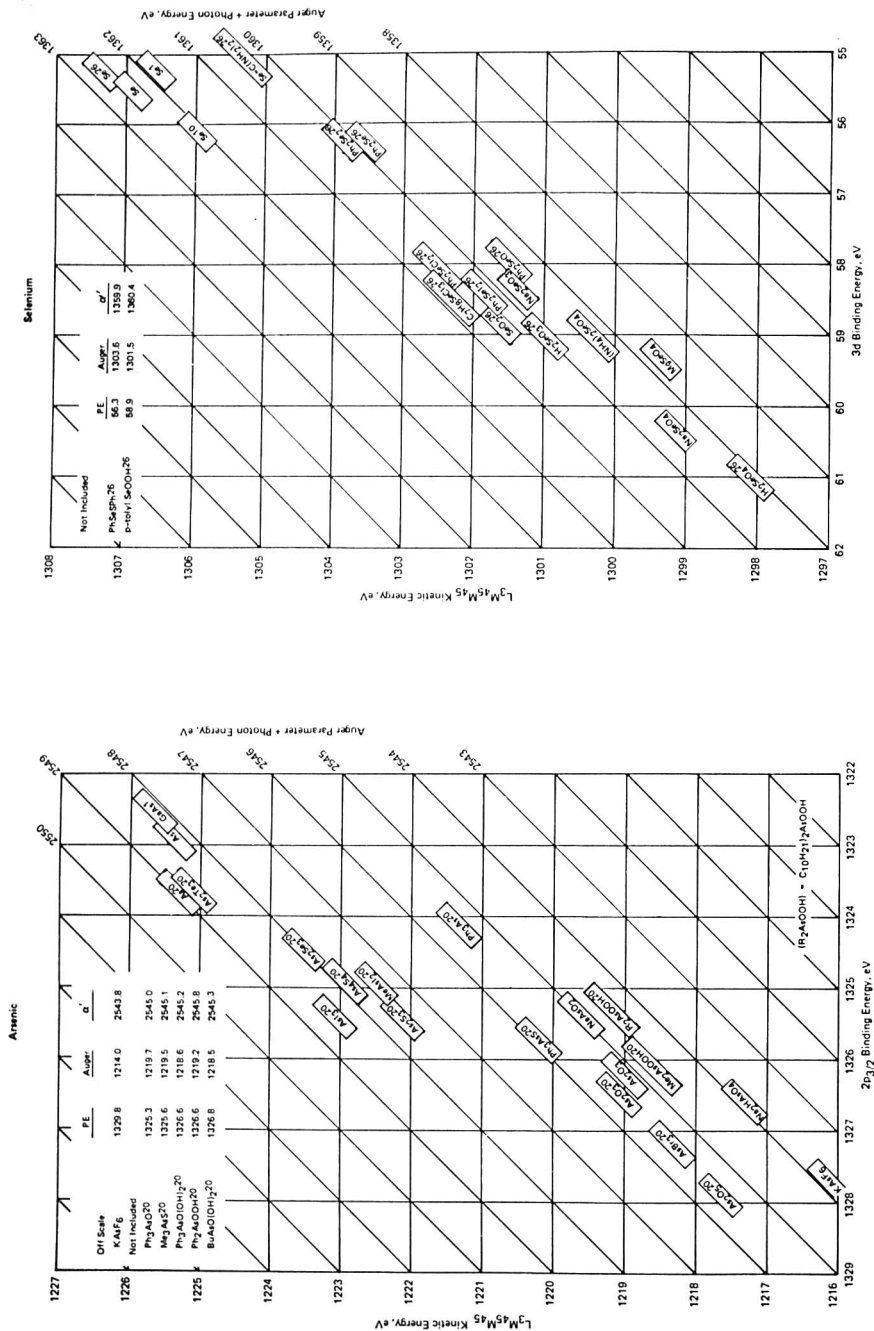


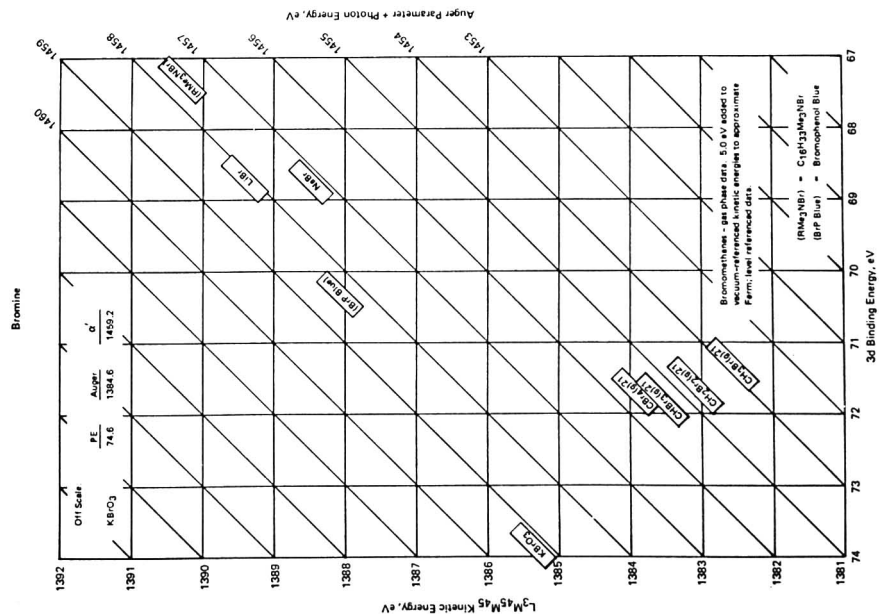
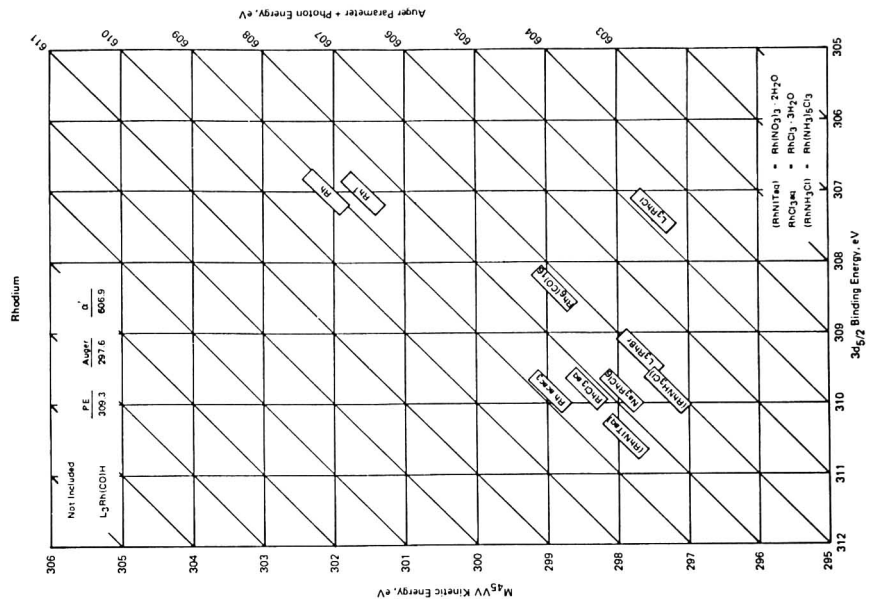


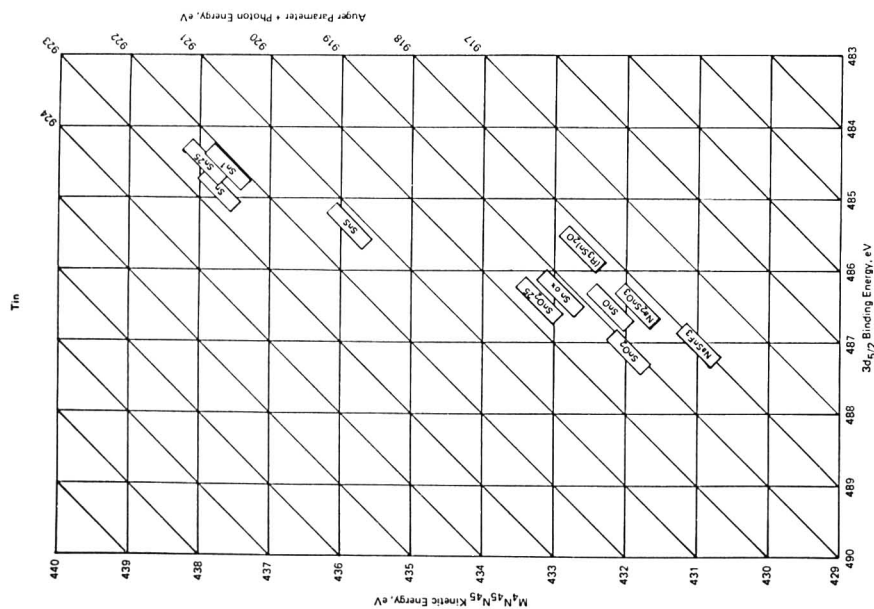
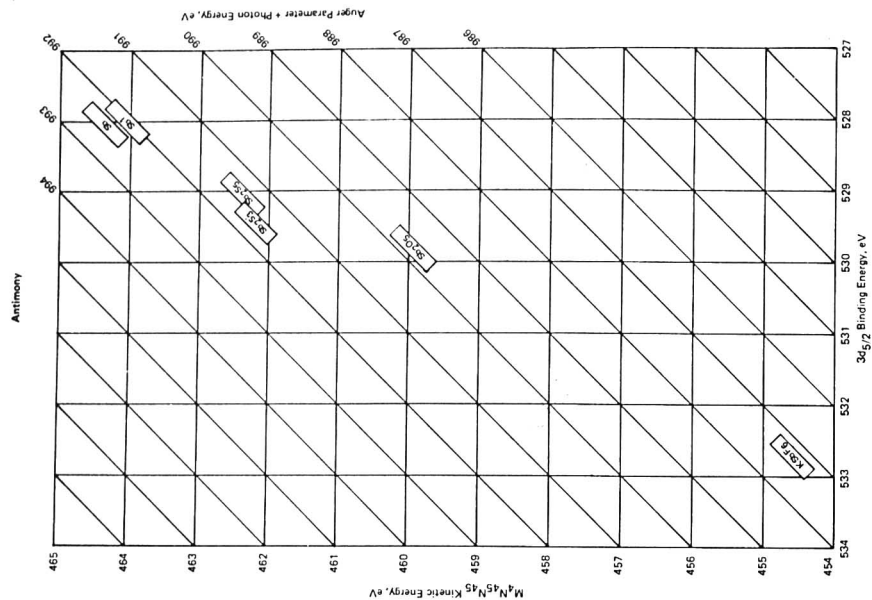


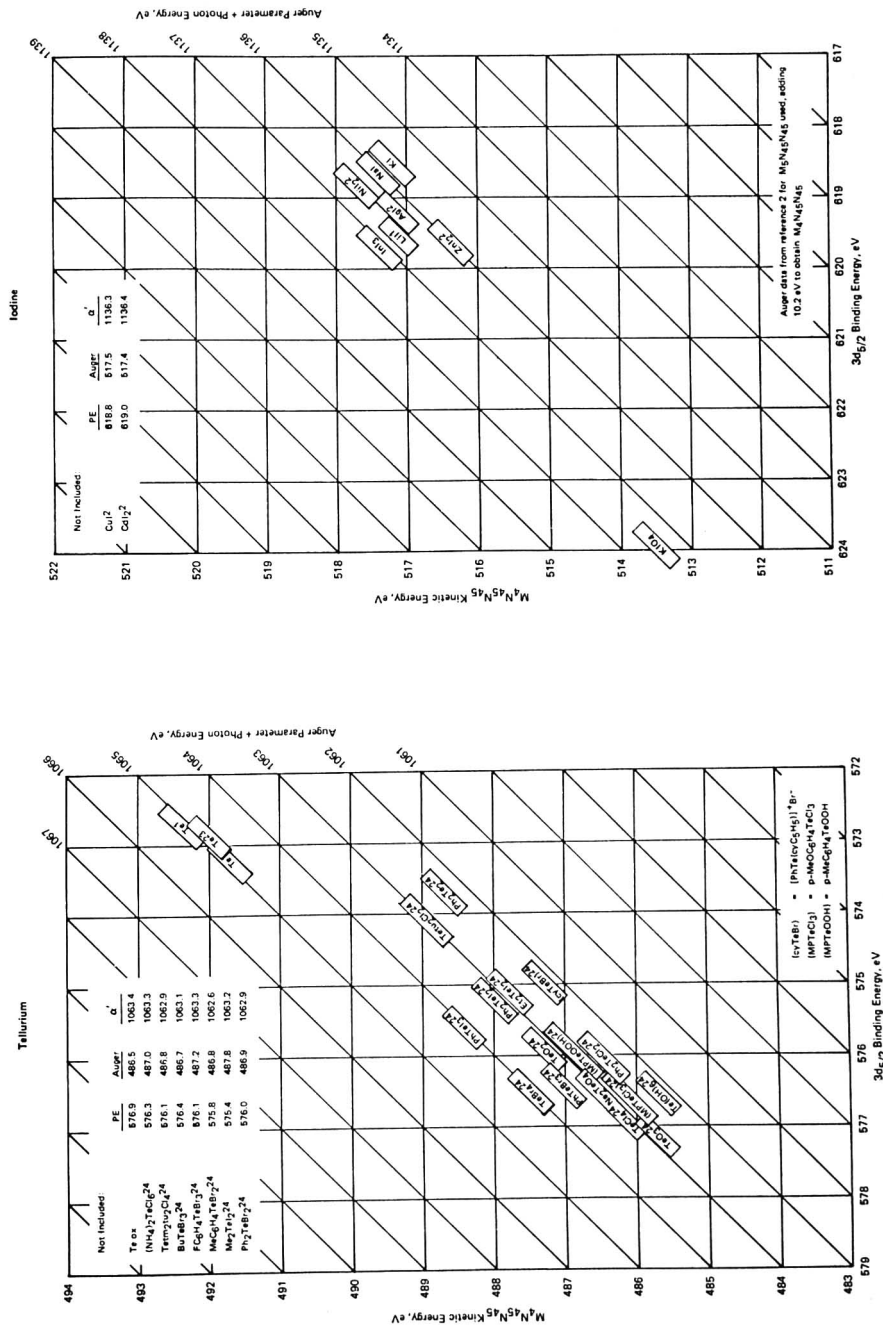


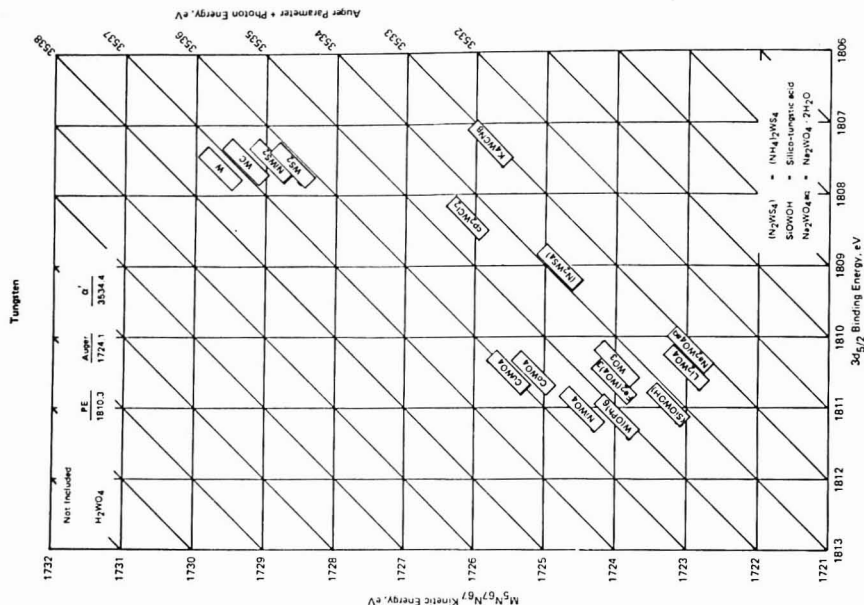












LITERATURE CITED (CHEMICAL STATE PLOTS)

- (1) L. E. Davis, Physical Electronics Industries, data to be published.
- (2) S. W. Gaarenstroom and N. Winograd, *J. Chem. Phys.*, **67**, 3500 (1977).
- (3) S. P. Kowalczyk, L. Ley, F. R. McFeely, R. A. Pollak, and D. A. Shirley, *Phys. Rev. B*, **8**, 3583 (1973).
- (4) A. Barrie and F. J. Street, *J. Electron Spectrosc.*, **7**, 1 (1975).
- (5) R. Hoogewijs, L. Fiermans, and J. Vennik, *J. Electron Spectrosc.*, **11**, 171 (1977).
- (6) L. Ley, F. R. McFeely, S. P. Kowalczyk, J. G. Jenkin, and D. A. Shirley, *Phys. Rev. B*, **11**, 600 (1975).
- (7) J. C. Fuggle, L. M. Watson, D. J. Fabian, and S. Alffrossman, *J. Phys. F*, **5**, 375 (1975).
- (8) K. Siegbahn, Uppsala University Report UIIP940, June 1976, Uppsala, Sweden.
- (9) R. Hoogewijs, L. Fiermans, and J. Vennik, *J. Microsc. Spectrosc. Electron.*, **1**, 109 (1977).
- (10) J. E. Castle and D. Epler, *Proc. R Soc. London, Ser. A*, **339**, 49 (1974).
- (11) J. Haber and L. Ungier, *J. Electron Spectrosc.*, **12**, 305 (1977).
- (12) N. S. McIntyre, T. E. Runnery, M. G. Cook, and D. Owen, *J. Electrochem. Soc.*, **123**, 1105 (1976).
- (13) G. Schön, *Surf. Sci.*, **35**, 96 (1973).
- (14) S. P. Kowalczyk, R. A. Pollack, F. R. McFeely, L. Ley, and D. A. Shirley, *Phys. Rev. B*, **8**, 2387 (1973).
- (15) J. C. Fuggle, E. Källne, L. M. Watson, and D. J. Fabian, *Phys. Rev. B*, **16**, 750 (1977).
- (16) G. Schön, *J. Electron Spectrosc.*, **2**, 75 (1973).
- (17) S. P. Kowalczyk, L. Ley, F. R. McFeely, R. A. Pollak, and D. A. Shirley, *Phys. Rev. B*, **9**, 381 (1974).
- (18) J.-M. Mariot and G. Dufour, *Chem. Phys. Lett.*, **50**, 219 (1977).
- (19) E. D. Roberts, P. Weightman, and C. E. Johnson, *J. Phys. C*, **8**, 1301 (1975).
- (20) M. K. Bahl, R. O. Woodall, R. L. Watson, and K. J. Irgolic, *J. Chem. Phys.*, **64**, 1210 (1976).
- (21) R. Spohr, T. Bergmark, N. Magnusson, L. O. Werme, C. Nording, and K. Siegbahn, *Phys. Scr.*, **2**, 31 (1970).
- (22) G. Schön, *Acta Chem. Scand.*, **27**, 2623 (1973).
- (23) M. K. Bahl and R. L. Watson, *J. Electron Spectrosc.*, **10**, 111 (1977).
- (24) M. K. Bahl, R. L. Watson, and K. J. Irgolic, *J. Chem. Phys.*, **66**, 5526 (1977); **68**, 3272 (1978).
- (25) A. W. C. Lin, N. R. Armstrong, and T. Kuwana, *Anal. Chem.*, **49**, 1288 (1977).
- (26) M. K. Bahl, R. L. Watson, and K. J. Irgolic, to be published.

RECEIVED for review November 20, 1978. Accepted December 19, 1978.

Surface Analyses by a Triboelectric Charging Technique

Harry W. Gibson,* John M. Pochan, and F. C. Bailey

Webster Research Center, Xerox Corporation, Webster, New York 14580

A device for measuring triboelectric charge exchange is described. Triboelectric charging is a surface phenomenon. It is sensitive to the chemical (molecular) structure of the surface. The utility of the technique for detection of surface contamination by mass transfer and of chemical transformations of surfaces is demonstrated by description of several examples. Not only can such changes be detected, but by a knowledge of the relationship between triboelectric charging and molecular structure, deductions as to the nature of the new surface species can be made.

Triboelectrification is a well known phenomenon (1, 2). It is essential in the processes of xerography (3, 4), electrostatic painting (5), and electrostatic separations (6), among others (6-8). While most of the work on triboelectric charging is directed toward these ends, the sensitivity of triboelectrification to the presence of foreign species on the surface also offers the opportunity for its utilization in analytical techniques for surfaces. The present communication describes the utility of triboelectrification to detect surface contamination in one system in some detail. Then several examples of the sensitivity of the technique to chemical alterations of surfaces are discussed.

EXPERIMENTAL

Triboelectric Charging Measurements. The device of Figure 1 was employed. The angle of the incline was 45°. The drop height from the hopper to the film was 1 cm. The path length was 7 inches. The hopper of 1-inch width was centered on the width (4 inches) of the film. The electrometer was a Keithley Model 610C (solid state) operated in the fast feedback mode on the 10⁶ coulomb scale. A Mettler P1200N balance was employed for mass measurements. The entire setup except for the electrometer was housed in a dry box maintained at zero humidity under a positive pressure of air passed through several drying columns. Films and beads were dried as indicated in the vacuum antechamber of the dry box prior to examination.

Film Preparation. Films were cast from solutions as indicated by use of a motorized Gardner Laboratory draw bar coater, typically with 10 wt % solutions and an 8-mil draw bar.

Metal Beads. The 100- μ m nickel berry beads were obtained from Sherritt-Gordon Co. The 100- μ m steel beads were acquired from Nuclear Metals Co. All beads were washed, dried and stored as per Table I.

Organic Materials. J. Yanus of Xerox Corporation supplied a sample of bis(4-diethylamino-2-methylphenyl)phenylmethane (1). General Electric Co. supplied Lexan 145 (2) in pellet form, which was precipitated once from chloroform into methanol prior to use. R. L. Schank of Xerox Corporation provided a sample of acetone oxime blocked toluene-2,4-diisocyanate (5). At temperatures above 110 °C, this blocked diisocyanate efficiently reverts to acetone oxime and toluene-2,4-diisocyanate (9). Dow 666U polystyrene that had been precipitated once from tetrahydrofuran into methanol was employed in the oxidation experiment. For the sulfonation experiment, a free-standing film of Dow Trycite, type 1000 was used.

Reaction of Blocked Diisocyanate 5 and Copolymer 7. A film was prepared as described above from the following solution: 0.4751 g of 7 (0.288 mequiv of hydroxyl) (10), 0.498 g of 5 (0.312 mequiv of isocyanate groups) and 10 mL of THF. The film was dried at room temperature in vacuo for several hours. Then it

Table I. Effect of Exposure^a to 1 on the Charging^b of Metal Beads^c vs Fresh Lexan Films^d

bead	bead charge (nC/g) ^e		
	clean bead (1st)	bead exposed to 1 (2nd)	clean bead (3rd)
100- μ m nickel berry	+1.24 \pm 0.09	-1.32 \pm 0.05	+0.595 \pm 0.055
100- μ m steel	-1.64 \pm 0.13	-2.86 \pm 0.15	-2.10 \pm 0.16

^a Exposed by cascading clean beads once over a pure film of 1 on cascade device (Figure 1). Film of 1 was cast from 10 wt % CH₂Cl₂ solution onto brush grained aluminum using an 0.008-inch draw bar; dried at 25 °C, 1 mm Hg for 48 h. Thickness ~ 20 μ m. ^b Charging measurements on cascade device of Figure 1 at zero humidity.

^c Washed successively with n-hexane, acetone, water, methanol, methylene chloride, carbon tetrachloride, chloroform, and diethyl ether; dried at 45 °C, 4 mm Hg for 64 h; 25 °C, 1 mm Hg for 6 h; stored in grounded capped aluminum bottles in dry box at 0% relative humidity. ^d Films cast onto brush-grained aluminum substrates using 10% by weight methylene chloride solutions and 0.008-inch draw bar; dried at 25 °C, 1 mm for 16-63 h; thickness ~ 20 μ m. Fresh in this context means that the film has not been contacted with anything prior to the experiment. ^e Average of 3 to 9 determinations (2-8 g each) \pm standard deviation.

was heated in an oven at 185 °C incrementally. After each heating period, the triboelectric charging capacity of the film was determined.

When this reaction was carried out on a NaCl disk, the infrared spectrum underwent a sharpening and increase in intensity of the 1715 cm⁻¹ (C=O) peak, loss of the 3360 cm⁻¹ (OH) peak, and slight enhancement of the weak 3420 cm⁻¹ (NH) peak.

DISCUSSION

Triboelectrification Measurements. The device used to measure the triboelectrification is shown in Figure 1. It consists of a grounded inclined plane. A film of the substance to be examined is mounted on this plane. Typically these films are cast from solution onto an aluminum sheet, but free-standing films can be used. At the top of the incline is a grounded metal hopper which contains metal beads. The metal beads are allowed to cascade down the film and are caught in a metal receptacle isolated from the surroundings by a metal Faraday cage. The receptacle is not grounded but rather is attached to an electrometer, which is used to measure the charge on the beads. By measuring the mass of the beads, the charge to mass ratio (Q/M) characteristic of the film and metal bead is obtained. Q/M is independent of mass over the range of masses employed. The device is an adaptation (11) of an apparatus previously reported (6). Good reproducibility is generally obtained with the device. For example, using six Lexan polycarbonate films on aluminum substrates and four to seven individual charging determinations on each film, the average charging value was +1.11 \pm 0.14 nanocoulombs (nC) per gram of 100- μ m diameter nickel berry.

Our experience of eight years of such measurements indicates that the precision of the technique as estimated by standard deviation is 10% or less of the average value from

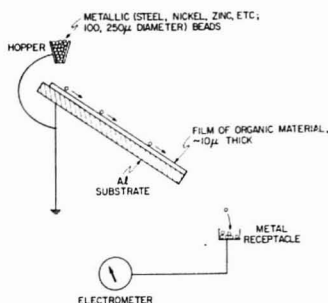


Figure 1. Device for measurement of triboelectric charging

film to film. For a given film the standard deviation is usually less, on the order of 5%, except for very high (>10 nC/g) or very low (<0.2 nC/g) charging levels, where standard deviations of 10% are more usual. Variations in the metal beads from batch to batch can be large, presumably due to varying surface oxidation, etc.

The depth sampled by the measurement will most likely vary with the magnitude of the charge. Moreover, the influence of a particular species is expected to vary exponentially with its distance from the surface contact. Nonetheless, some idea of the depth probed can be gleaned in specific instances. In the case of steady state charging, depths up to $4 \mu\text{m}$ in polystyrene are probed (12). In the apparatus under discussion here, however, very short contact times ($\sim 10^{-5}$ s) are involved (13) and the quantity of charge is viewed as a kinetic parameter. Therefore, the depths involved are probably much less. In the cases of polystyrene sulfonates and bare metals, the depth probed is about $1.5 \mu\text{m}$ (14). In systems such as those under discussion here, depths of less than $1 \mu\text{m}$ are most likely involved.

One of the problems encountered in the study of triboelectric charging of organic solids has been the lack of corroborative techniques. Few techniques have the requisite sensitivity. One which does, though it probes a shallower sample depth, is ESCA. In a study involving selective surface enrichment of a two-component system, ESCA and the triboelectric charging technique described herein were shown to be equally sensitive when conditions were such that probe depths of the two methods were similar (15).

The presence of water vapor can affect the charging results, presumably because it is adsorbed onto both surfaces involved, the metal bead and the organic film. For example, the charge acquired on $100\text{-}\mu\text{m}$ steel beads by cascading them over a film of poly(*p*-nitrosyrene) increases from $+1.8$ nC/g at zero humidity to $+3.1$ nC/g at 62% relative humidity and decreases to $+1.4$ nC/g at 100% relative humidity. In some cases, charging increases with increasing humidity, while in others it decreases. In some cases, effects are larger while in others they are smaller. For these reasons all of the experiments herein were performed under dry conditions.

Our interpretation of triboelectric charging is that it involves electron exchange between the two bodies (16). Therefore, it is dependent upon the relative solid-state energy levels of the two bodies. This is shown schematically in Figure 2. For a metal, the Fermi level defines both acceptor and donor levels. For an organic solid, acceptor states may be identified as being derived from lowest unoccupied molecular orbitals and donor states from highest occupied molecular orbitals. Inasmuch as solid-state energy levels of organics are generally related to gas phase or solution phase isolated molecular energy levels by the relatively constant polarization energy term (17),

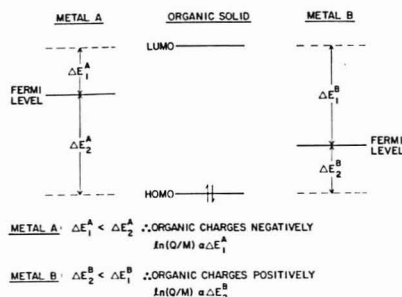


Figure 2. Relationship of molecular orbital energy levels, metal Fermi levels, and triboelectric charging

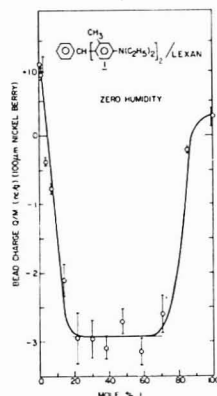
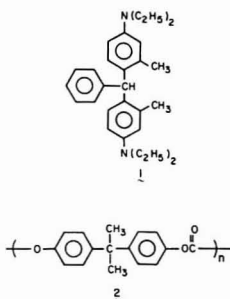


Figure 3. Triboelectric charging as a function of composition of films of bis(4-diethylamino-2-methylphenyl)phenylmethane (1) and Lexan polycarbonate (2). (Mole percentages determined on the basis of the repeat unit of 2)

relative charging tendencies of organic solids have been shown to be related to such gas or solution phase energy levels (18, 19). Since correlations of gas and solution phase isolated molecular orbital energy levels with structure are available (20-22), generalized predictions regarding charging tendencies can be made on the basis of chemical structure (23) and conversely deductions of chemical structure can be made on the basis of triboelectric charging. The following sections demonstrate this fact for two distinct situations: (i) the case of contamination of a surface by very small amounts of a second species, and (ii) the case of alteration of the chemical structure of a solid in situ or otherwise.

Example of Determination of Surface Contamination.

In connection with our work on triboelectricification (18, 19), the effect of composition of solid solutions was of interest. Therefore, solid solutions comprised of bis(4-diethylamino-2-methylphenyl)phenylmethane (1) and Lexan (2, bisphenol-A polycarbonate from General Electric) were examined. The fact that solid solutions formed was confirmed by optical microscopy and differential scanning calorimetry. The cascade triboelectric charge measured on the nickel beads as a function of film composition is shown in Figure 3. Note that the bead charge does not vary smoothly between the two pure components as might be expected, but rather exhibits a minimum of opposite sign.



Effect of Exposure of Metal Beads to Film of 1. In order to investigate the anomaly of Figure 3 the following experiment was done. First 100- μ m nickel berry beads were cascaded down a freshly prepared film of pure Lexan (2) to establish a reference point. Another batch of clean beads was then cascaded down a film of pure amorphous 1, which forms a stable glass ($T_g \sim 20^\circ\text{C}$) via solvent casting or thermal quenching from above the melting point. This latter batch of beads was collected and cascaded in smaller batches down the Lexan film to measure the bead charge. These results are given in Table I. These results were verified by a second set of experiments. As can be seen, the beads exposed to 1 acquired a negative charge vs. Lexan, whereas the clean beads became positively charged. The beads were obviously altered by exposure to 1. By inference, 1 or some product thereof was picked up by the beads. Moreover, by exposure to these "contaminated" beads, the Lexan film itself was contaminated (presumably via a second mass transfer of 1) as evidenced by the lower positive value with clean beads after use of the 1 exposed beads. After several exposures to these contaminated beads, the Lexan film even charged clean beads negatively.

Also shown in Table I are results for steel beads which reveal qualitatively similar results.

Effect of Intentional Coating of Nickel Beads. A second set of experiments was carried out to verify that beads coated with 1 charge negatively against Lexan. A batch of the washed 100- μ m nickel berry beads was coated with 0.5% by weight of 1. These were then measured against a fresh Lexan film, subsequent to clean beads on the same film. The results are given in Table II. These results were also verified by a separate set of experiments. The conclusion is that coating of the beads with 1 does indeed result in their acquiring a negative charge when exposed to Lexan, in agreement with the results given above.

To ensure that the results were not complicated by mass transfer from the coated beads to the hopper of the cascade device and then to the clean beads, a batch of coated beads was run through the hopper. Then clean beads were cascaded over a fresh Lexan film. The bead charge ($+1.37 \pm 0.13$ nC/g, seven determinations, 2 to 6 g each) was the normally observed value.

Lexan was expected to charge negatively against 1 on the basis of the relative energy levels of model monomers (8, 9). To test this, Lexan pellets were dried in vacuo and cascaded down a film of 1. The Lexan pellets acquired a net negative charge (-0.64 ± 0.19 nC/g, 4 determinations, 0.4 to 3 g each). Since Lexan is an insulator, grounding the cascade hopper would not remove residual charge on the Lexan and, therefore, this residual as measured via directly pouring Lexan pellets into a Faraday cage was subtracted from the measured cascade value.

The fact that the beads coated with 1 acquire negative charge while the film of 1 charges positively vs. Lexan pellets

Table II. Charging^a of 100- μ m Ni Berry Beads vs. a Lexan Film^b

Q/M on beads (nC/g)	clean beads ^c	1 coated ^d
	$+1.25 \pm 0.10^e$ (1st)	-1.03 ± 0.04^e (2nd)

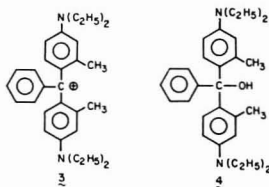
^a Charging measurements on device of Figure 1 at zero humidity in dry box. ^b Film as per footnote d, Table I. ^c As per footnote c, Table I. ^d By rolling clean 100- μ m Ni berry, 0.5% by weight 1 and methylene chloride in a rotary evaporator to remove solvent, drying while grounded at 25°C , 1 mm Hg for 18 h. ^e Average of 4 to 9 determinations (3 to 8 g each) \pm standard deviation.

is rationalized to be a result of positive space charge formation in the coating due to electron donation to the nickel bead. This effect and its ramifications are being reported separately (24).

Extraction of Nickel Beads Exposed to Film of 1. With this body of evidence for transfer of 1 to the nickel and steel beads and subsequently to the Lexan film, independent evidence of the mass transfer was sought. A large quantity of clean nickel beads was cascaded down a film of 1 in the usual manner. The beads were then removed from the dry box and extracted ten times with chloroform. The extract yielded about 0.1% (by weight of starting beads) of colorless solid. The infrared spectrum of this solid possesses several peaks characteristic of 1. In addition it possesses weak peaks at 1725 and 1750 cm^{-1} , presumably carbonyl absorption, but possibly aromatic C-H overtone bands. It also contains absorptions corresponding to tertiary OH (3630 cm^{-1}) (25).

A blank experiment was carried out as follows. A volume of chloroform equal to that used in the extraction of the nickel beads was taken to dryness, leaving a small amount of amorphous residue. The infrared spectrum contains weak points at 3680, 1730, and 1600 cm^{-1} . Thus, the bead extract absorptions at 3640 and 1750 cm^{-1} are real, but those at 3680, 1725, and 1600 cm^{-1} are, at least in part, artifacts.

We conclude that the beads had a coating probably consisting of 1, the product of reaction of the oxidized (dye) form (3) of 1 with water, the alcohol 4, and perhaps some other



products of oxidation.

The anomalous triboelectric charge vs. composition curve (Figure 3) for 1 in Lexan is therefore explicable in terms of mass transfer of 1 from the polymer film to the nickel berry bead during the initial contact event. The amount of 1 coating on the bead is presumably related to the amount of 1 available at the surface of the film. This coated bead subsequently contacts the 1/Lexan composite as it cascades down. The charging is controlled by both the composition of the film and the composition of the bead. As we have seen, nickel coated with 1 charges negatively against Lexan. The minimum results from the opposing effects of the amount of 1 transferred and the charge developed between the coated bead and the film; both variables depend upon film composition.

This study provides an excellent example of the sensitivity of triboelectric charging to the presence of very small amounts of contamination on surfaces of metals and polymers.

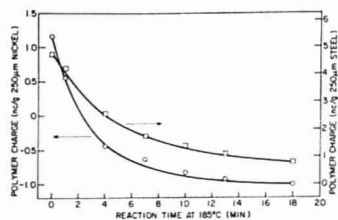
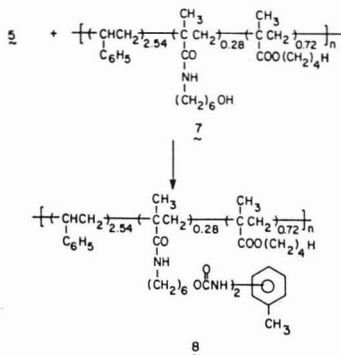
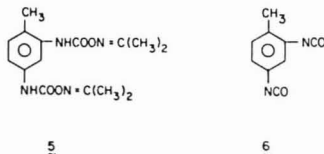


Figure 4. Triboelectric charging as a function of reaction time at 185°C for a film comprised of polymer 7 and blocked diisocyanate 5 (conversion of 7 to 8)

Examples of Detection of Chemical Reactions. Triboelectric charging is known to vary with the nature of the two contacting bodies (26-31). Recently we have found a dependence upon substituent constants in both aromatic (18) and aliphatic (19) systems that is taken to indicate a dependence upon molecular orbital energetics (20-22). Therefore, in principle, any chemical changes that take place at the surface are detectable by a change in the triboelectric properties. In this section several applications in fact will be described.

Chemical Modification by Thermal Treatment. This example demonstrates the utility of triboelectric charging to detect alteration of chemical structure, in this case throughout the bulk of film in situ. Isocyanates are very reactive toward hydroxyl and amino moieties. This reactivity is exploited for cross-linking by the use of diisocyanates (32). A common technique is to "block" the diisocyanate to yield a compound which thermally reverts to the diisocyanate. One such compound is the urethane 5; upon heating it reverts to acetone



oxime and toluene-2,4-diisocyanate (6) (9). The blocked diisocyanate was incorporated into films of polymer 7 (10) cast from solution onto aluminum. The cascade triboelectric charging of the polymer film was measured incrementally as

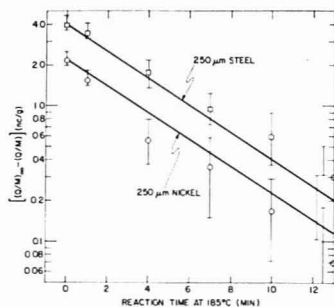


Figure 5. Logarithm of absolute difference between final triboelectric charge and triboelectric charge as a function of reaction time at 185°C for a film comprised of polymer 7 and blocked diisocyanate 5 (conversion of 7 to 8)

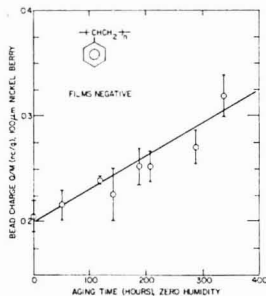


Figure 6. Triboelectric charging of a film of polystyrene (~20 μm thick) on brush grained aluminum as a function of aging time in dry air

a function of reaction time at 185°C. Heating causes release of diisocyanate 6, which in turn reacts with polymer 7, acylating it and yielding polymer 8. As can be seen from Figure 4, the charging approaches an asymptotic limit.

On the basis that the charging is directly related to the extent of reaction, the data may be replotted in the form $\log [(Q/M)_\infty - (Q/M)]$ vs. time. As can be seen in Figure 5, a straight line results for each of the two data sets. This is indicative of a first order reaction (33), as expected if conversion of 5 to 6 is the rate limiting step in conversion of 7 to 8. This is confirmed by the fact that a superimposable plot is obtained when the concentration is 5 is halved. Thus, triboelectric charging can in fact be used to follow the kinetics of the reaction.

Oxidation of Polystyrene. In a study involving the use of polystyrene films, it was noted that the triboelectric charging value varied as the film aged in dry air in a dry box; little, if any, ultraviolet light struck the film because of the safety glass window. A systematic kinetic study was carried out. The results are shown in Figure 6. Note that the amount of negative charge acquired by the film increases with aging time, a factor of 50% over 350 h. Others have reported similar effects (34).

A freshly prepared polystyrene film was examined by electron spectroscopy (ESCA, XPS). No oxygen could be detected on the surface (top ~50 Å). A film that was aged for 400 h was similarly examined. A strong oxygen is signal was observed (35).

Oxidation of polystyrene is well known (36). It is also known (36) that oxidation leads to ketone, aldehyde, quinone, car-

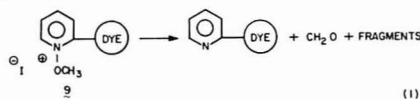
boxyl, etc. functionalities. These are known to be good electron-accepting moieties (37-39). Thus, in accord with expectation (18, 19, 23) the negative charging of the polystyrene film increases as the oxidation to these species occurs. Measurement of the triboelectric charging capacity thus affords a sensitive measure of surface oxidation.

Photooxidation of polystyrene is also well known (40). Brief ultraviolet irradiation in air causes a tenfold increase in negative charging of polystyrene films with mercury (41). In fact this process causes sufficient change in the charging capacity that it forms the basis of a patent for an imaging system (42).

Oxidation of Polyethylene. Ozonolysis of branched polyethylene, which contains olefinic bonds, was shown by infrared analysis to produce a carbonyl component with a concomitant reduction in the amount of unsaturation (34). Exposure of branched polyethylene either to air or ozone also caused a dramatic (tenfold) increase in the negative charging capacity of the film (34, 41). When one considers that the amount of unsaturation was only about 0.01% of the bulk sample, the sensitivity of the triboelectricification technique to surface chemical changes is obvious!

Oxidation of Coal. Moreover, in the only other analytical application of triboelectricification that we are aware of, the kinetics of the oxidation of surfaces of finely divided coal were followed by measuring the charging capacity under fixed conditions (43). It was found that the virgin coal charged positively and with increasing exposure time to air at 350 °C became less positive and then negative. The direction of change of charging is consistent with the data above and previously reported work (18, 19, 23).

Photochemical Transformations. The detection of surface chemical changes by the triboelectricification technique is not limited to oxidative processes, however. For example, a recent patent discloses the use of a photochemical surface reaction as an imaging system (44). It is based upon the change in triboelectric charging capacity between light struck and non-photolyzed areas of the surface. The reaction can be generalized as shown in Equation 1.



Surface coverage by the photoactive species (9) can be as low as 0.2 mg per square foot or about one monolayer!

Sulfonation of Polystyrene. Another example of the sensitivity of the triboelectric measurement to surface chemical transformations is provided by the following case. Very brief sulfonation of free-standing polystyrene film surfaces by a known method (45) results in a dramatic increase in the positive charging capacity of the film. With 100- μm nickel berry, a sign change occurs; the virgin polystyrene charges positively (0.2 nC/g), while a film sulfonated to the extent of about 1 monolayer charges negatively and an order of magnitude higher (15 nC/g). The direction of change upon sulfonation is consistent with results of our previous work (18, 19, 23).

Utility of the Method. While this triboelectric charging technique cannot be employed for molecular determination,

it provides a very sensitive probe for detection of mass transfer and changes in molecular structure. In fact, kinetic determinations are possible. The technique is very sensitive, especially to changes at or near the surface. It has the additional advantages of being simple, requiring relatively little sample, and being nondestructive.

ACKNOWLEDGMENT

We are grateful to John Yanus and Richard L. Schank of Xerox Corporation for samples of 1 and 5, respectively.

LITERATURE CITED

- (1) "Encyclopaedia Britannica", Vol. 8, Chicago, Ill., 1955, p. 169.
- (2) W. Gilbert, "De Magnete", London, 1600.
- (3) J. H. Dessauer and H. E. Clark, "Xerography and Related Processes", Focal Press, New York, 1965.
- (4) J. W. Weigl, *Angew. Chem., Int. Ed. Engl.*, **18**, 374 (1977).
- (5) S. Wu, *Polym. Plast. Tech. Eng.*, **7**, 119 (1976).
- (6) M. B. Donald, *Appl. Res. Ind.*, **11**, 19 (1958).
- (7) A. D. Moore, "Electrostatics and Its Applications", Wiley, New York, 1973.
- (8) I. I. Inoué, *J. Electrostatics*, **4**, 175 (1978).
- (9) R. L. Schank and T. C. Williams, U. S. Patent 3,449,289 (1969); *Chem. Abstr.*, **71**, P14000C (1969).
- (10) H. W. Gibson and F. C. Bailey, *J. Polym. Sci., Polym. Chem. Ed.*, **10**, 3017 (1972).
- (11) D. A. Hays, Xerox Corp., private communication, 1970.
- (12) T. J. Fabish, H. M. Saltsburg, and M. L. Hair, *J. Appl. Phys.*, **47**, 930 (1976).
- (13) R. W. Stover, presented at Ninth Ann. Meeting IEEE Ind. Appl. Soc., Pittsburgh, Pa., Oct. 1974.
- (14) H. W. Gibson and F. C. Bailey, unpublished results.
- (15) M. W. Williams, C. J. Au Clair, G. P. Ceasar, and J. M. Short, *Conf. Rec. Ind. Appl. Soc., IEEE Ann. Mtg.*, Sept. 1975, p. 436.
- (16) See also J. Fuhrmann, *J. Electrostatics*, **4**, 109 (1977/78).
- (17) L. E. Lyons, *J. Chem. Soc.*, 5001 (1957).
- (18) H. W. Gibson, *J. Am. Chem. Soc.*, **87**, 3832 (1975).
- (19) H. W. Gibson and F. C. Bailey, *Chem. Phys. Lett.*, **51**, 352 (1977).
- (20) H. W. Gibson, *Can. J. Chem.*, **51**, 3065 (1973).
- (21) J. E. Kuder, H. W. Gibson, and D. Wychick, *J. Org. Chem.*, **40**, 875 (1975).
- (22) H. W. Gibson, *Can. J. Chem.*, **55**, 2637 (1977).
- (23) H. W. Gibson, F. C. Bailey, J. L. Mincer, and W. H. H. Gunther, *J. Polymer Sci., Polym. Chem. Ed.*, in press.
- (24) J. M. Pochan, H. W. Gibson, F. C. Bailey, and D. F. Hinman, submitted to *J. Chem. Phys.*
- (25) K. Nakashishi, "Infrared Absorption Spectroscopy", Holden-Day, San Francisco, Calif., 1964, p. 30.
- (26) J. C. Wicke, "Disputatio Physica Experimentalis de Electricitatis Contris", Academy of Rostock, 1757.
- (27) H. W. Balton, *Text. Res. J.*, **24**, 146 (1954).
- (28) S. P. Hersh and D. J. Montgomerie, *Text. Res. J.*, **25**, 279 (1955).
- (29) J. Henniker, *Nature (London)*, **196**, 474 (1962).
- (30) E. Tsuchida, M. Kitajima, T. Yao, and I. Shinohara, *Kogyo Kagaku Zasshi*, **69**, 1978 (1966).
- (31) M. W. Williams, *J. Macromol. Sci., Rev. Macromol. Chem.*, **14**, 251 (1976).
- (32) D. H. Solomon, "The Chemistry of Organic Film Formers", Wiley, New York, 1967, Chap. 8.
- (33) A. A. Frost and R. G. Pearson, "Kinetics and Mechanism", Wiley, New York, 1962, pp. 27-40.
- (34) D. A. Hays, *J. Chem. Phys.*, **60**, 1455 (1974).
- (35) W. R. Salaneck, A. Paton and H. W. Gibson, *IEEE Trans. Ind. Appl.*, **1a-14**, 443 (1978).
- (36) "Encyclopedia of Polymer Science", Interscience, New York, 1966, Vol. 4, p. 707.
- (37) G. Brieble, *Angew. Chem., Int. Ed. Engl.*, **3**, 617 (1964).
- (38) M. Batley and L. E. Lyons, *Nature (London)*, **188**, 573 (1962).
- (39) W. E. Wentworth, L. W. Kao, and S. Becker, *J. Phys. Chem.*, **79**, 1161 (1975).
- (40) B. Rányi and J. F. Rabek, "Photodegradation, Photo-oxidation and Photostabilization of Polymers", Wiley, New York, 1975, pp. 165-184.
- (41) D. A. Hays and P. K. Watson, *Soc. Photo. Sci. Eng., Second Int. Conf. Electrophotog.*, 108 (1974).
- (42) J. T. Bickmore and W. L. Goffe, U.S. Patent 3,518,081 (1970).
- (43) D. G. A. Thomas, *Brit. J. Appl. Phys., Suppl. No. 2*, 555 (1953).
- (44) J. G. McNally, U.S. Patent 3,748,128 (1973).
- (45) T. Matsuda and M. H. Litt, *J. Polym. Sci., Polym. Chem. Ed.*, **12**, 489 (1974).

RECEIVED for review July 5, 1978. Accepted January 8, 1979.

Auger Electron Spectra Intensity Variation with Potential-Modulation Differentiation

G. E. McGuire* and B. R. Martin

Texas Instruments Incorporated, Dallas, Texas 75265

Auger electron spectra are normally taken as $dN(E)/dE$ vs. E with a potential-modulation differentiation scheme used to suppress the high background caused by inelastically scattered electrons. The observed Auger peak-to-peak intensity does not increase linearly over the range of modulation voltages currently available on commercial instruments. Auger spectra for a large number of elements were taken while varying the modulation potential to correlate signal amplitudes taken under varying modulation conditions. Detection limits have been estimated from the signal amplitudes based upon the reported detection limit of phosphorus in silicon.

The use of Auger electron spectroscopy (AES) as an analytical tool has seen explosive growth since the introduction by Harris (1) of a potential-modulation differentiation scheme to suppress the high background caused by inelastically scattered electrons. The derivative is obtained by superimposing a small sinusoidal potential-modulation on the analyzer pass energy and synchronously detecting the current passed through the analyzer. It is a common practice in electron-excited AES to use the peak-to-peak signal strength in the derivative spectrum as a relative quantitative measure of elemental surface concentration (2). In addition, the energy positions of the negative-going peaks in the derivative spectrum are used to identify the Auger transition energy values (3).

One judgment that must be made by the user of AES is the tradeoff which must be made between sensitivity and resolution in setting the amplitude of the potential-modulation employed in electronic differentiation (4). By electronically varying the modulation voltage, one has versatile control over signal to noise. The lowest order information concerning an Auger feature is available if one is interested only in detecting a signal. The signal strength is increased by the use of large oscillation amplitudes. The limiting amplitude would essentially be the separation between features.

The AES features actually contain more detail than is frequently utilized. The structures usually consist of a main peak followed by additional features on the low energy side because of various couplings of the Auger transition to the valence band electrons. The shape of the Auger feature depends on the chemical environment of the atoms being studied (5). The peak-to-peak amplitude in the derivative mode is dependent on the shape of the Auger peak as well as its size. As the modulation amplitude approaches the width of the Auger peak, the relationship becomes sensitive to the detailed shape of the feature (6).

However, the use of large modulation voltages would be beneficial when quantitative measurements are affected by the primary electron beam current, as the improved signal to noise could be traded off for either faster energy analysis or a reduction in primary electron beam current. Since the first harmonic signal strength is nonlinear (6, 7), it would be desirable to know the signal strength of the characteristic Auger transitions for various elements as a function of modulation voltage. Data taken with large modulation

voltages optimizing signal-to-noise can then be compared to data taken at low modulation voltages optimizing resolution. Since there is no accepted "standard" modulation voltage, these curves will also aid in comparing the Auger literature. Curves for the first-harmonic signal strength vs. modulation voltage have been compiled for some of the most commonly encountered elements and referenced to relative sensitivity factors compiled by Davis et al. (8).

EXPERIMENTAL

The Auger results reported here were obtained with a single-pass cylindrical mirror analyzer (CMA) manufactured by Physical Electronics Inc. (PHI Model 10-155). Samples were mounted at an angle of 30° with respect to the incident 5-keV, 5-μA electron beam. The electron gun is coincident with the CMA. Prior to analysis, the sample surface was cleaned by 2-keV argon ion bombardment for a minimum of 15 min at a pressure of 3.8×10^{-3} pascal. Ion sputtering at normal incidence was continued during data analysis to ensure a clean surface. Characteristic Auger spectra were recorded while varying the modulation potential from 1 to 10 eV peak-to-peak.

RESULTS AND DISCUSSION

In taking Auger electron spectra, one has two forms of instrumental broadening; from the analyzer itself and the dynamic broadening due to the potential-modulation scheme. The effects of potential-modulation distortion have been analyzed, assuming a Gaussian Auger peak shape for a deflection type analyzer (9). It was found that the first harmonic signal strength increased linearly with modulation amplitude up to an amplitude of about 0.3 p , where p is the Gaussian root mean square width. The signal then passed through a maximum and subsequently decreased at a rate near the inverse square root of the modulation amplitude for values in excess of about 3 p .

Figure 1 demonstrates how the modulation amplitude can affect the relative peak-to-peak (p-p) intensities of two characteristic Auger transitions from the same element. The low energy NOO transition of Ta shows a nearly linear response up to a modulation voltage of 3 eV where the high energy Ta MNN shows a nearly linear response up to 8 eV. Broadening of the high energy peak may be occurring due to potential-modulation or due to the analyzer since the energy resolution of 0.5% at 1680 eV is approximately 8 eV. At 4 eV p-p modulation, the Ta NOO transition intensity is at least 50% greater than the Ta MNN intensity but at 10 eV p-p modulation, their intensities are almost identical.

This would not normally be a problem since most data are taken at a set modulation voltage and referenced to standards examined using the same conditions. However, attempts to optimize the sensitivity vs. resolution trade-off over the entire energy range have resulted in selectable or ramped modulation schemes (4). The ramped modulation compensates for the direct dependence of the absolute resolution of the analyzer on pass energy. An alternate method is to retard the electron pass energy to a constant voltage as in the Physical Electronics double pass analyzer (PHI 15-255G). In addition the data generated by Davis et al., which is the most complete set of reference spectra available, was taken at 2 eV-6 eV p-p

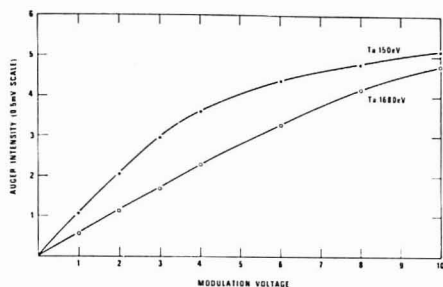


Figure 1. Relative peak-to-peak Auger intensity for the low energy Ta NOO transition and high energy Ta MNN transition as a function of modulation voltage demonstrates the nonlinearity of the response. A linear response occurs up to $0.3 p$ where p is the Gaussian root mean square width. Broadening may be due to the potential modulation or to the analyzer energy resolution

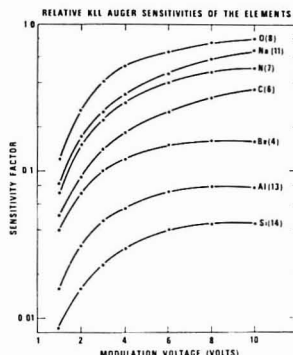


Figure 2. Relative sensitivity factors of the KLL Auger transition series plotted vs. the modulation amplitude for various elements

modulation. In general, the approach taken by Davis et al. was to use a modulation voltage of 3 eV p-p for Auger transition below 1000 eV and 6 eV p-p for those above 1000 eV and reference all of these to the Ag MNN transition taken at a modulation voltage of 3 eV p-p and an electron beam energy of 3 keV. Known exceptions to this are the LMM transitions of Ga, Ge, and As which were taken at 3 eV p-p modulation. In order to compare data in the "Handbook of Auger Electron Spectroscopy" (8), it is necessary to know the relative intensities taken at 3 eV and 6 eV p-p modulation. In the open literature, it is possible to find an even broader range of modulation voltages.

As an analytical aid to the Auger spectroscopist, the relative intensities of the KLL, LMM, and MNN Auger transitions taken at modulation voltages from 1–10 eV p-p for a large number of elements have been referenced to the data compiled by Davis et al. (8). The intensities are expressed as relative sensitivity factors and are plotted with respect to the modulation voltage in Figures 2, 3, and 4.

The family of curves that are generated varies smoothly over the range of modulation voltages typically increasing at the lower modulation voltages, then leveling off at the higher modulation voltages. Exceptions to this occur for the MNN transition series where the large modulation voltages result in convolution of the closely spaced doublet.

Detection limits may be estimated from these curves with proper calibration of one element. Morabito and Tsai (10)

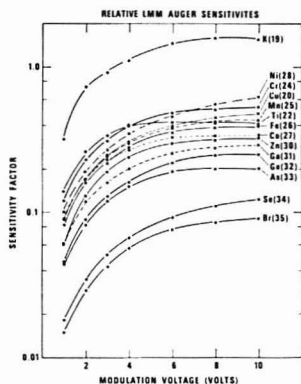


Figure 3. Relative sensitivity factors of the LMM Auger transition series plotted vs. the modulation amplitude for various elements

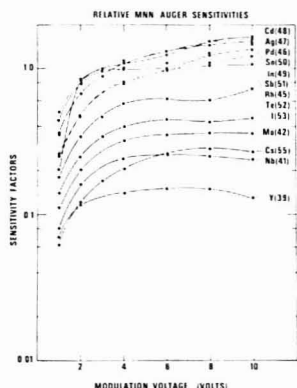


Figure 4. Relative sensitivity factors of the MNN Auger transition series plotted vs. the modulation amplitude for various elements

used ion implantation as a means of calibrating AES spectra for quantitative chemical analysis. A detectability limit in the range of $\sim 5 \times 10^{19}$ to 10^{20} atoms/cm³ for boron, phosphorus, and arsenic in silicon was established with in-depth profiling. Good depth resolution is necessary to establish the peak locations of the implant distribution. This limits the sensitivity because of the use of analysis times consistent with optimum depth resolution. Measurements on bulk doped phosphorus samples (11) and surface absorption of PH₃ gas (12) have been used to establish a detectability of $\sim 8 \times 10^{18}$ atoms/cm³ for phosphorus in silicon. Using this value, it is possible to estimate the bulk detectability of the elements in the periodic table using Figures 2, 3, and 4 and the data compiled in ref. 8. These values are presented in Figure 5.

CONCLUSION

Although it has been shown that the area under the $N(E)$ curve is linear as a function of modulation voltage (6), the most common format for data presentation for AES data has been in the derivative mode where the response is nonlinear. Data taken in the derivative mode are presented which show the nonlinear sensitivity factor as a function of modulation voltage. Using these values, it is possible to compare data taken under

AUGER SPECTROSCOPY ESTIMATED
LIMITS IN PPMA DETECTION

																																																																																																																																																																																																																																																																																																																																																																																																																																																																																																																																																																																																																																																																																																																																																																																																																																																																																																																																																																																																																																																																																																																																																																																																																																																																																																																																																																																																																					</
--	--	--	--	--	--	--	--	--	--	--	--	--	--	--	--	--	--	--	--	--	--	--	--	--	--	--	--	--	--	--	--	--	--	--	--	--	--	--	--	--	--	--	--	--	--	--	--	--	--	--	--	--	--	--	--	--	--	--	--	--	--	--	--	--	--	--	--	--	--	--	--	--	--	--	--	--	--	--	--	--	--	--	--	--	--	--	--	--	--	--	--	--	--	--	--	--	--	--	--	--	--	--	--	--	--	--	--	--	--	--	--	--	--	--	--	--	--	--	--	--	--	--	--	--	--	--	--	--	--	--	--	--	--	--	--	--	--	--	--	--	--	--	--	--	--	--	--	--	--	--	--	--	--	--	--	--	--	--	--	--	--	--	--	--	--	--	--	--	--	--	--	--	--	--	--	--	--	--	--	--	--	--	--	--	--	--	--	--	--	--	--	--	--	--	--	--	--	--	--	--	--	--	--	--	--	--	--	--	--	--	--	--	--	--	--	--	--	--	--	--	--	--	--	--	--	--	--	--	--	--	--	--	--	--	--	--	--	--	--	--	--	--	--	--	--	--	--	--	--	--	--	--	--	--	--	--	--	--	--	--	--	--	--	--	--	--	--	--	--	--	--	--	--	--	--	--	--	--	--	--	--	--	--	--	--	--	--	--	--	--	--	--	--	--	--	--	--	--	--	--	--	--	--	--	--	--	--	--	--	--	--	--	--	--	--	--	--	--	--	--	--	--	--	--	--	--	--	--	--	--	--	--	--	--	--	--	--	--	--	--	--	--	--	--	--	--	--	--	--	--	--	--	--	--	--	--	--	--	--	--	--	--	--	--	--	--	--	--	--	--	--	--	--	--	--	--	--	--	--	--	--	--	--	--	--	--	--	--	--	--	--	--	--	--	--	--	--	--	--	--	--	--	--	--	--	--	--	--	--	--	--	--	--	--	--	--	--	--	--	--	--	--	--	--	--	--	--	--	--	--	--	--	--	--	--	--	--	--	--	--	--	--	--	--	--	--	--	--	--	--	--	--	--	--	--	--	--	--	--	--	--	--	--	--	--	--	--	--	--	--	--	--	--	--	--	--	--	--	--	--	--	--	--	--	--	--	--	--	--	--	--	--	--	--	--	--	--	--	--	--	--	--	--	--	--	--	--	--	--	--	--	--	--	--	--	--	--	--	--	--	--	--	--	--	--	--	--	--	--	--	--	--	--	--	--	--	--	--	--	--	--	--	--	--	--	--	--	--	--	--	--	--	--	--	--	--	--	--	--	--	--	--	--	--	--	--	--	--	--	--	--	--	--	--	--	--	--	--	--	--	--	--	--	--	--	--	--	--	--	--	--	--	--	--	--	--	--	--	--	--	--	--	--	--	--	--	--	--	--	--	--	--	--	--	--	--	--	--	--	--	--	--	--	--	--	--	--	--	--	--	--	--	--	--	--	--	--	--	--	--	--	--	--	--	--	--	--	--	--	--	--	--	--	--	--	--	--	--	--	--	--	--	--	--	--	--	--	--	--	--	--	--	--	--	--	--	--	--	--	--	--	--	--	--	--	--	--	--	--	--	--	--	--	--	--	--	--	--	--	--	--	--	--	--	--	--	--	--	--	--	--	--	--	--	--	--	--	--	--	--	--	--	--	--	--	--	--	--	--	--	--	--	--	--	--	--	--	--	--	--	--	--	--	--	--	--	--	--	--	--	--	--	--	--	--	--	--	--	--	--	--	--	--	--	--	--	--	--	--	--	--	--	--	--	--	--	--	--	--	--	--	--	--	--	--	--	--	--	--	--	--	--	--	--	--	--	--	--	--	--	--	--	--	--	--	--	--	--	--	--	--	--	--	--	--	--	--	--	--	--	--	--	--	--	--	--	--	--	--	--	--	--	--	--	--	--	--	--	--	--	--	--	--	--	--	--	--	--	--	--	--	--	--	--	--	--	--	--	--	--	--	--	--	--	--	--	--	--	--	--	--	--	--	--	--	--	--	--	--	--	--	--	--	--	--	--	--	--	--	--	--	--	--	--	--	--	--	--	--	--	--	--	--	--	--	--	--	--	--	--	--	--	--	--	--	--	--	--	--	--	--	--	--	--	--	--	--	--	--	--	--	--	--	--	--	--	--	--	--	--	--	--	--	--	--	--	--	--	--	--	--	--	--	--	--	--	--	--	--	--	--	--	--	--	--	--	--	--	--	--	--	--	--	--	--	--	--	--	--	--	--	--	--	--	--	--	--	--	--	--	--	--	--	--	--	--	--	--	--	--	--	--	--	--	--	--	--	--	--	--	--	--	--	--	--	--	--	--	--	--	--	--	--	--	--	--	--	--	--	--	--	--	--	--	--	--	--	--	--	--	--	--	--	--	--	--	--	--	--	--	--	--	--	--	--	--	--	--	--	--	--	--	--	--	--	--	--	--	--	--	--	--	--	--	--	--	--	--	--	--	--	--	--	--	--	--	--	--	--	--	--	--	--	--	--	--	--	--	--	--	--	--	--	--	--	--	--	--	--	--	--	--	--	--	--	--	--	--	--	--	--	--	--	--	--	--	--	--	--	--	--	--	--	--	--	--	--	--	--	--	--	--	--	--	--	--	--	--	--	--	--	--	--	--	--	--	--	--	--	--	--	--	--	--	--	--	--	--	--	--	--	--	--	--	--	--	--	--	--	--	--	--	--	--	--	--	--	--	--	--	--	--	--	--	--	--	--	--	--	--	--	--	--	--	--	--	--	--	--	--	--	--	--	--	--	--	--	--	--	--	--	--	--	--	--	--	--	--	--	--	--	--	--	--	--	--	--	--	--	--	--	--	--	--	--	--	--	--	--	--	--	--	--	--	--	--	--	--	--	--	--	--	--	--	--	--	--	--	--	--	--	--	--	--	--	--	--	--	--	--	--	--	--	--	--	--	--	--	--	--	--	--	--	--	--	--	--	--	--	--	--	--	--	--	--	--	--	--	--	--	--	--	--	--	--	--	--	--	--	--	--	--	--	--	--	--	--	--	--	--	--	--	--	--	--	--	--	--	--	--	--	--	--	--	--	--	--	--	--	--	--	--	--	--	--	--	--	--	--	--	--	--	--	--	----

logms = 4.98×10^{-16} atoms/cc

Silicon

Figure 5. Auger spectroscopy detection limits in parts per million atomic in silicon are estimated based on the relative sensitivity factors of the KLL, LMM, and MNN Auger transitions and the bulk detectability of phosphorus in silicon.

varying modulation voltages and to estimate a detection limit.

LITERATURE CITED

- (1) L. A. Harris, *J. Appl. Phys.*, **39**, 1419 (1968).
- (2) R. E. Weber and A. L. Johnson, *J. Appl. Phys.*, **40**, 314 (1969).
- (3) H. E. Bishop and J. C. Riviere, *Surf. Sci.*, **17**, 462 (1969).
- (4) D. J. Pocker, *Rev. Sci. Instrum.*, **48**, 105 (1975).
- (5) T. W. Haas and J. T. Grant, *Appl. Phys. Lett.*, **16**, 172 (1970).
- (6) J. T. Grant, T. W. Haas, and J. E. Houston, *Surf. Sci.*, **42**, 1 (1974).
- (7) R. W. Springer, D. J. Pocker, and T. W. Haas, *Appl. Phys. Lett.*, **27**, 368 (1975).

- (8) L. E. Davis, N. C. MacDonald, P. W. Palmberg, G. E. Riach, and R. E. Weber, "Handbook of Auger Electron Spectroscopy", 2nd ed., Physical Electronics Inc., Inc., Eden Prairie, Minn., 1976.
- (9) N. J. Taylor, *Rev. Sci. Instrum.*, **40**, 792 (1969).
- (10) J. M. Morabito and J. C. C. Tsai, *Surf. Sci.*, **33**, 422 (1972).
- (11) J. H. Thomas III and J. M. Morabito, *Surf. Sci.*, **41**, 629 (1974).
- (12) A. J. Van Bommel and J. E. Crombeen, *Surf. Sci.*, **38**, 773 (1973).

RECEIVED for review August 18, 1978. Accepted December 14, 1978.

Parameters for the Ratio Method by X-Ray Microanalysis

András G. S. Jánosy,* Kristóf Kovács,¹ and Ida Tóth

Biological Research Center, Institute of Biophysics, POB 521, H-6701 Szeged, Hungary

Atomic or weight ratios of elements can be calculated routinely from X-ray intensities of ultrathin samples without recourse to standards by the "ratio method", using precalculated proportionality factors. The derivation of the ionization cross section (Q), fluorescence yield (ω), line intensity fraction (L) and spectrometer efficiency (T) parameters, needed for the calculation of the proportionality factors, is discussed and suggested "best values" are given. Failure of the ratio method as commonly used to give adequate results with L- or M-lines is attributable to breakdown of the ionization cross-section formula. A simple procedure is given for calculation of line intensity fractions, and the results are compared with previous methods.

Determination of the elemental composition of a very large variety of materials by sophisticated instrumental techniques is a field of surpassing importance (1-3). Atomic or weight ratios of elements above atomic number 10 can be calculated from simultaneously recorded X-ray intensities of ultrathin samples without the need for standards by the so-called "ratio" or "no-standards" method. The calculation is straightforward and can be performed by hand if a suitable table with the necessary proportionality factors is available. The method was originally proposed by Duncumb (4); it was further developed and adapted for biological applications by Russ (5-7) and for materials science by Cliff and Lorimer (8). The main advantages of the technique are that weight ratios can be calculated directly without tedious measurements on suitable standards (which are not always easy to obtain) and without instrumental adjustments; thus it seems to be especially useful for biological applications. However, it must be kept in mind that samples must be thin enough (0.1 to 0.5 μ m for biological samples and even less for inorganic materials) to avoid any interelement effects (atomic number, absorption, and fluorescence effects), and that the accuracy of the results depends on the reliability of the individual terms involved in the calculation of the proportionality factors. The method is not applicable to the problem of monitoring one element in an organic matrix for obvious reasons, but the relative values can be turned to absolute concentrations if (i) all the elements present in the probed mass have been monitored or (ii) the absolute concentration of one of the elements can be de-

termined by other means (9). The proportionality factors can be calculated from terms such as fluorescence yield, ionization cross section, spectrometer efficiency, etc., which are compiled in tables or calculable independently (6); or else they can be determined empirically for a given instrument by calibration standards once and for all (10). For many problems of X-ray microanalysis the knowledge of relative concentrations is quite sufficient. In the course of adapting the ratio method to our existing microanalyzer system, we met several discrepancies; therefore we reexamined the technique itself and the terms involved.

EXPERIMENTAL

Sample Preparation. A series of microcrystal standards were prepared by pipetting 0.01 to 0.1 M aqueous solutions of salts onto Formvar coated copper grids. Details of sample preparation were published recently (11).

Instrumentation. A JEOL 100B transmission electron microscope with attached Si(Li) detector and analyzer system (EDAX 707B) was used for measurements. The nominal accelerating voltage was (if not stated otherwise) $E_0 = 80.6$ kV, takeoff angle was 35°, electron probe diameter 0.1 μ m, measurement duration 100 s. Although the low electron dose and short observation time yielded relatively low total X-ray intensities (30 000 to 50 000 counts) adding to the statistical error of measurements, this was the safest way to ensure stability of the materials used under the electron beam. The detector efficiency was as stated below. The energy window settings on the analyzer were: 250 eV in range 0.8 to 3.4 keV, 350 eV in range 3.45 to 20.0 keV, and 450 eV above 20.0 keV. For analysis, crystals not larger than 0.3 μ m were selected.

X-RAY PRODUCTION IN THIN FILMS

The number of ionization events (dn_x) of a pure element (x) per incident electron is:

$$dn_x = Q_x N \rho \frac{ds}{A_x} \quad (1)$$

where Q_x is the ionization cross section of the particular shell, N is Avogadro's number, ρ is the density of the specimen, ds is the electron path length and A_x is the atomic weight of element x . For a composite sample, the number of atoms of element x per unit volume is $C_x N \rho ds / A_x$, where C_x is the weight fraction of element x , thus Equation 1 modifies to:

$$dn_x = C_x C_x N \rho \frac{ds}{A_x} \quad (2)$$

If the specimen thickness is much smaller than the electron mean free path, then the total number of ionizations (n_x) per

* Present address, Technical University for Chemistry, Department of Silicate Chemistry, POB 28, H-8200 Veszprém, Hungary

Table I. Bethe Parameters b_i and c_i as Used in Different Ionization Cross-Section Formulas

author	b_K	b_L	b_M	c_K	c_L	c_M	remarks
(a) Russ (6)	1	1	1	1	1	1	$Z_i = 1$
(b) Powell (16)	0.9	0.75	0.75	0.65	0.6	0.6	$4 < U < 30$
(c) Mott and Massey (17)	0.35	0.25	0.25	2.42	2.42	2.42	$4 < U < 30$
(d) Worthington and Tomlin (18)	0.35	0.25	0.25	$\frac{4}{1.65 + 2.35 \exp(1 - U)}$			$2 < U < 30$

Table II. Comparison of Calculated and Measured Ionization Cross-Section Ratios Q_K/Q_L and Q_L/Q_M at $E_0 = 80.6$ kV

formula and reference	$\left(\frac{Q_K}{Q_L}\right)_{Ag}$	$\left(\frac{Q_K}{Q_L}\right)_{Br}$	$\left(\frac{Q_K}{Q_L}\right)_I$	$\left(\frac{Q_L}{Q_M}\right)_{Os}$	$\left(\frac{Q_L}{Q_M}\right)_{Au}$	$\left(\frac{Q_L}{Q_M}\right)_{Pb}$
(a) (6)	0.0513	0.0540	0.0470	0.0939	0.0948	0.0961
(b) (16)	0.0118	0.0143	0.0094	0.0361	0.0360	0.0361
(c) (17)	0.0242	0.0229	0.0242	0.0486	0.0494	0.0506
(d) (18)	0.0228	0.0228	0.0209	0.0486	0.0494	0.0504
measured	0.0222	0.0225	0.0197	0.0532	0.0523	0.0471

incident electron along the electron trajectory (Δs), which is assumed to be the specimen thickness, will be:

$$n_x = Q_x C_x N \rho \frac{\Delta s}{A_x} \quad (3)$$

The generated X-ray intensity (I'_x) (photons per electron) is obtained by multiplying n_x by the fluorescence yield ω_i :

$$I'_x = Q_x \omega_i C_x N \rho \frac{\Delta s}{A_x} \quad (4)$$

If the analyzed film is thin enough so that interelement effects such as X-ray absorption, secondary fluorescence, and atomic number effect can be neglected (thin film criterion), the generated intensity is equal to the intensity leaving the specimen. We must also take into account that only a fraction of all generated X-ray photons actually reaches the detector, thus Equation 4 has to be multiplied by a detector efficiency factor (T_x):

$$I''_x = Q_x \omega_i T_x C_x N \rho \frac{\Delta s}{A_x} \quad (5)$$

Finally, it must be considered that only a fraction (L_x) of all X-ray lines of a series are counted in the selected energy window of the analyzer. Thus we get the total detected X-ray intensity I_x with electron beam current i_0 (= number of impinging electrons per unit time), measured in counts per second:

$$I_x = i_0 Q_x \omega_i L_x T_x C_x N \rho \frac{\Delta s}{A_x} \quad (6)$$

If two elements x and y are monitored simultaneously, their X-ray intensities I_x and I_y can be related to their concentrations C_x and C_y as:

$$\frac{I_x}{I_y} = \frac{C_x Q_x \omega_i L_x T_x A_y}{C_y Q_y \omega_i L_y T_y A_x} = \frac{C_x}{C_y} \frac{P_x}{P_y} \quad (7)$$

where the proportionality factors P_x and P_y can be calculated or determined empirically and tabulated for each element and accelerating voltage used. Naturally, Equation 7 can be extended to any desired number of elemental ratios. In the following we examine in detail the origin and use of the terms involved in Equation 7.

RESULTS AND DISCUSSION

Ionization Cross Section Q_i . Several ionization cross-section formulas have been proposed in the past, all derived from an equation introduced by Bethe (12). This can be written as:

$$Q_i = \frac{6.51 \times 10^{-14} Z_i b_i}{E_i^2 U_i} \ln(c_i U_i) \quad (8)$$

where Z_i is the number of electrons in the particular inner shell ($Z_K = 2$, $Z_L = 8$, $Z_M = 18$, etc.) involved in ionization, E_i is the critical excitation energy or absorption edge energy in eV (13, 14), $U_i = E_0/E_i$ is the overvoltage ratio of accelerating potential to absorption edge energy, while the parameters b_i and c_i are assumed to be constant for a particular shell. For the acceleration voltages used in the transmission electron microscope (usually 60 to 100 kV), a relativistic correction is suggested by Goldstein et al. (15), in order to get the actual electron wavelengths that interact with the specimen:

$$E_i^* = (1 + 9.875 \times 10^{-7} E_0) E_0 \quad (9)$$

(E_0 in eV). This correction has been used throughout our calculations.

We have tested some of the most commonly used formulas for Q_i which differ in the choice of the Bethe parameters b_i and c_i only. For convenience, these parameters are summarized in Table I. Since there is little information available on the Bethe parameters of M lines, we have tried different arbitrarily chosen values and found that $b_L = b_M$ and $c_L = c_M$ give the best results.

We have measured the intensity ratios of Ag $K\alpha/L\alpha$, I $K\alpha/L\alpha$, Sb $K\alpha/L\alpha$, Au $L\alpha/M\alpha$, Os $L\alpha/M\alpha$, Pb $L\alpha/M\alpha$, and U $L\alpha/M\alpha$ at 40.5, 60.4, and 80.6 kV nominal accelerating voltage and compared calculated ionization cross section ratios Q_K/Q_L and Q_L/Q_M with measured ratios via Equation 7. An excerpt from our results for $E_0 = 80.6$ kV is displayed in Table II. The simplified formula (a) (cf. Table I) which is used by Russ in his original "no-standards" model (6) gives the highest deviations (in some cases over 100%) which forbids its use whenever lines of different series are used. This is not surprising since the Bethe parameters are set equal to unity in this case. The formula (b) of Powell (16) gives deviations around 40% and the use of Bethe parameters as suggested by Mott and Massey (17) yields some 20% deviations on the average. The formula (d) of Worthington and Tomlin (18) seems to give the best results, as average deviations never exceeded 10%. This is the only formula which remains valid in the overvoltage range below 4, but it is suggested that it should not be used below $U = 2$.

The next question is, which absorption edge energy should be taken for L and M lines, where more than one edge will be excited. Figure 1 illustrates the problem, where some of the L-lines of silver are displayed with a typical fwhm (full width at half maximum) of 139 eV (corresponding to the measured resolution of 165 eV for the fwhm of Mn $K\alpha_1$ along with their energies in keV, relative line intensities, and line designation).

It is easy to see from Figure 1 that an energy window of 250 eV involves several other L-lines besides the principal line $L\alpha_1$,

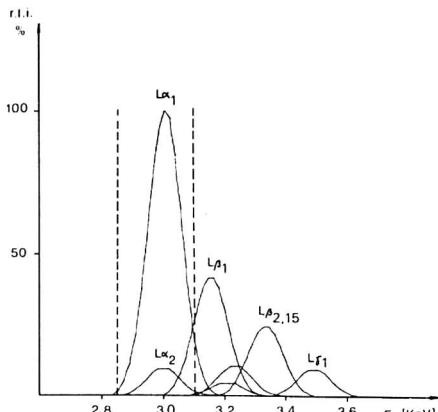


Figure 1. Some of the L-lines of Ag ($Z = 47$), fwhm = 139 eV for $L\alpha_1$ (ideal Gaussian shape). The broken lines at 2.850 and 3.100 keV represent the limits of an "energy window" of 250-eV width as usually set on multichannel analyzers.

such as $L\eta$, $L\alpha_2$ and $L\beta_5$ (all generated on the L_{III} edge), $L\beta_1$ (generated on the L_{II} edge), $L\beta_4$, $L\beta_3$ (generated on the L_I edge). (For clarity, minor L-lines have been omitted from the figure.) In this case a feasible compromise is to calculate an averaged "effective" absorption edge energy E_L from the individual energies, weighted by the relative line intensities (19). As an example, this calculation gives $E_L = 3.441$ keV for Ag from $E_I = 3.810$, $E_{II} = 3.528$, and $E_{III} = 3.352$ keV.

Fluorescence Yield ω . According to universal practice in microprobe analysis (3), average fluorescence yields are used instead of separate values for lines within a series. A good method to calculate such average values was proposed by Burhop (20):

$$\left(\frac{\omega}{1-\omega}\right)^{1/4} = A + BZ + CZ^3 \quad (10)$$

where Z denotes the atomic number and the values of the constants depend on the shell being excited as follows:

shell	K	L	M
A	-0.03795	-0.11107	-0.00036
B	0.03426	0.01368	0.00386
C	-1.163×10^{-6}	-2.177×10^{-7}	2.01×10^{-7}

This algorithm is considered superior (14, 21) to others like the Wentzel formula (22) which is also widely used in the microprobe literature.

Spectrometer Efficiency T . The spectrometer efficiency term allows for the fact that (i) part of the low energy (<2 keV) X-rays are absorbed in the Be window, Au contact layer, and Si dead layer of the detector, and that (ii) some of the very high energy X-ray photons (>20 keV) are not detected at all in the active Si layer. If detector specifications are known with sufficient accuracy, the spectrometer efficiency can be calculated by:

$$T_x = \frac{d\Omega}{4\pi} \exp \left[-\left(\frac{\mu}{\rho}\right)_{Be}^{E_x} t_{Be} \rho_{Be} - \left(\frac{\mu}{\rho}\right)_{Si}^{E_x} t_{Si}^d \rho_{Si} - \left(\frac{\mu}{\rho}\right)_{Au}^{E_x} t_{Au} \rho_{Au} \right] \left[1 - \exp \left(-\left(\frac{\mu}{\rho}\right)_{Si}^{E_x} t_{Si}^a \rho_{Si} \right) \right] \quad (11)$$

where $d\Omega/4\pi$ is the detector solid angle (which cancels in the ratio), $(\mu/\rho)^{E_x}$ is the mass absorption coefficient for the monitored X-ray energy E_x , t_{Be} , t_{Si}^d , and t_{Au} denote the

thickness of the absorbing Be, Si, and Au layers, t_{Si}^a is the detector active layer thickness and ρ is the density of the absorbing material. The spectrometer efficiency can also be described satisfactorily by the exponential function (7):

$$T_x = \frac{d\Omega}{4\pi} \exp \left[-\frac{k_1}{E_x^{2.8}} \right] \left[1 - \exp \left(-\frac{k_2}{E_x^{2.8}} \right) \right] \quad (12)$$

where the empirical constants k_1 and k_2 can be obtained from detector specifications. We calculated for our system with the manufacturer's stated specifications ($t_{Be} = 7.5 \mu\text{m}$, $t_{Si}^d = 0.15 \mu\text{m}$, $t_{Au} = 0.02 \mu\text{m}$, $t_{Si}^a = 4 \text{ mm}$):

$$k_1 = 1.12$$

$$k_2 = 20700$$

According to a suggestion of Russ (7), the spectrometer efficiency can be determined from the measured intensity ratio $I_{L\alpha}/I_{K\alpha}$ of Cu by combining Equation 7 with Equation 12 and solving for k_1 (the second exponential term in Equation 12 should be essentially zero at these X-ray energies). We obtained

$$k_1 = 1.03 \pm 0.05$$

Similarly, we calculated k_2 from measured intensity ratio $I_{K\alpha}/I_{L\alpha}$ of Ag (now the first exponential term of Equation 12 should be unity) to

$$k_2 = 20000 \pm 1500$$

With these values, the recalculated Be window thickness is $6.7 \pm 0.3 \mu\text{m}$ and the detector active layer thickness is $3.9 \pm 0.3 \text{ mm}$, in good agreement with the above stated specifications.

Line Intensity Fraction L . As already shown in Figure 1, an energy window of some particular width contains only a fraction of all excited lines of a series. This means that we have to consider further the ratio of observed line intensity to total line intensity, which we shall call the *line intensity fraction* to avoid confusion with the term "relative line intensity" as used above. This must be calculated for each principal X-ray line and it depends on both the width of the selected energy window and the fwhm of the lines concerned. The fwhm of any X-ray line can be calculated by:

$$\text{fwhm [eV]} = \sqrt{R^2 + 2.735 (E_x - 5898)} \quad (13)$$

where R is the spectrometer resolution (= fwhm of Mn $K\alpha_1$) and E_x is the energy of the line concerned, both in eV. As the resolution of the energy dispersive spectrometer is given in terms of the fwhm of the composite Mn $K\alpha_{1,2}$ line and not for a separate line Mn $K\alpha_1$, a distinction must be made between the two (23). We have measured 170 eV for the fwhm of Mn $K\alpha_{1,2}$ which is composed of $K\alpha_1$ at 5898 eV and $K\alpha_2$ at 5887 eV in the intensity ratio of 100:50. Gaussian analysis yielded 165 eV for Mn $K\alpha_1$, and this value has been used for the subsequent calculation of line intensity fractions. (An error of 5 eV for R would cause around 1% error for L , whereas the displacement of the energy window by one channel would result in 5 to 10% error for L .) We calculated the line intensity fractions L for our detector system for the $K\alpha$, $L\alpha$, and $M\alpha$ lines commonly used in X-ray analysis by numerical integration of the Gaussian normal distribution within the limits of the particular energy window, considering the actual line widths and the relative line intensities as given in the tabulation of Johnson and White (19). A computer program generally applicable for the calculation of the line intensity fraction L is provided in the Appendix.

Determination of Weight Ratios. We calculated the above discussed terms for our existing microanalyzer system and tabulated them together with the proportionality factors P_x of Equation 7 for the accelerating voltages commonly used

Table III. X-Ray Intensity Ratios Measured at $E_0 = 80.6$ kV on Microcrystal Standards and Comparison of Expected and Measured Weight Ratios Calculated after Russ (5) and the Present Model

specimen	measured intensity ratio $\left(\frac{I_x}{I_y}\right) \pm \text{s.e.m.}^a$	expected weight ratio $\left(\frac{c_x}{c_y}\right)_e$	measured weight ratio calculated after			
			Russ (5)		present model	
			$\left(\frac{c_x}{c_y}\right)_R$	Δ^b	$\left(\frac{c_x}{c_y}\right)_M$	Δ^b
NaCl	$\frac{I_{NaK\alpha}}{I_{ClK\alpha}} = 0.208 \pm 0.021$	0.649	0.500	-23.0%	0.563	-13.3%
KCl	$\frac{I_{KK\alpha}}{I_{ClK\alpha}} = 1.108 \pm 0.019$	1.103	1.123	+1.8%	1.127	+2.2%
KBr	$\frac{I_{KK\alpha}}{I_{BrK\alpha}} = 1.204 \pm 0.044$	0.489	0.452	-7.6%	0.514	+5.1%
CaHPO ₄	$\frac{I_{CaK\alpha}}{I_{PK\alpha}} = 1.519 \pm 0.008$	1.294	1.478	+14.2%	1.342	+3.7%
MnSO ₄	$\frac{I_{MnK\alpha}}{I_{SK\alpha}} = 1.495 \pm 0.010$	1.716	2.007	+17.0%	1.802	+5.0%
FeSO ₄	$\frac{I_{FeK\alpha}}{I_{SK\alpha}} = 1.489 \pm 0.009$	1.745	2.073	+18.8%	1.827	+4.7%
KMnO ₄	$\frac{I_{KK\alpha}}{I_{MnK\alpha}} = 0.804 \pm 0.011$	0.712	0.625	-12.2%	0.677	-4.9%
KAl(SO ₄) ₂	$\frac{I_{KK\alpha}}{I_{AlK\alpha}} = 2.128 \pm 0.022$	1.450	1.667	+15.0%	1.569	+8.2%
	$\frac{I_{KK\alpha}}{I_{SK\alpha}} = 0.610 \pm 0.008$					
KI	$\frac{I_{AlK\alpha}}{I_{SK\alpha}} = 0.287 \pm 0.013$	0.421	0.382	-9.2%	0.395	-6.2%
PbI ₂	$\frac{I_{KK\alpha}}{I_{IL\alpha}} = 1.045 \pm 0.033$	0.308	0.206	-33.2%	0.321	+4.1%
	$\frac{I_{PbL\alpha}}{I_{IL\alpha}} = 0.440 \pm 0.027$					
	$\frac{I_{PbM\alpha}}{I_{IL\alpha}} = 1.273 \pm 0.026$	0.816	3.264	+300%	0.887	+8.7%

^a s.e.m. = standard error of the mean. ^b Percent deviation of measured from expected weight ratio.

for analysis. (An excerpt from this tabulation is given in the Appendix for $E_0 = 80.6$ kV and some of the most commonly analyzed elements.) As a test of the model presented, microcrystal standards of known composition were analyzed and weight ratios calculated from measured intensity ratios after Russ (5) and our model. Results of these measurements are summarized in Table III. The measured intensity ratios represent the mean of 12 individual determinations per sample. As can be seen in column 2 of the table, the standard error of the mean could be kept within reasonable limits, despite the low total intensities. Deviations from expected ratios are somewhat larger with the method of Russ if only K-lines are considered, but errors grow prohibitively large if lines of different series are involved, whereas results are quite satisfactory with our model. This is due to deviations in calculated ionization cross-section values.

Undoubtedly, the largest remaining uncertainties stem from the choice of the numerical values for the ionization cross section Q_i . A relativistic correction for the acceleration voltage E_0 (which is normally not used in the conventional microprobe literature with typical excitation voltages around 20 kV, but should not be neglected with the much higher voltages of the transmission electron microscope) was used, together with average absorption edge energies for L- and M-shells. We found that the formula of Worthington and Tomlin (18) is superior to the others and useful in a wider overvoltage range. Another important point which we have taken into account

is the proper consideration of the line intensity fraction L_i which depends mainly on the energy window setting and the fwhm of the lines involved. This is easier, less time-consuming, and less prone to error than to consider all lines excited, which necessarily involves multiple peak deconvolution of the unknown spectrum. These improvements, while not all-inclusive, substantially increase the accuracy of rapid calculation of weight ratios by X-ray microanalysis.

ACKNOWLEDGMENT

The authors are indebted to C. P. Keszthelyi for many helpful suggestions during preparation of the manuscript. The thorough discussion of the section on line intensity fractions by L. Keszthelyi was highly appreciated.

Supplementary Material Available: Appendix A containing a BASIC program for Gaussian calculation of line intensity fraction and Appendix B containing the terms for calculation of proportionality factors P_i for selected X-ray lines at $E_0 = 80.6$ kV nominal accelerating voltage for the given analyzer system of the authors (3 pages) will appear following these pages in the microfilm edition of this volume of the journal. Photocopies of the supplementary material from this paper of microfiche (105 × 148 mm, 24X reduction, negatives) may be obtained from Business Operations, Books and Journals Division, American Chemical Society, 1155 16th St., N.W., Washington, D.C. 20036. Full bibliographic citation (journal, title of article, author) and prepayment, check or money order for \$5.50 for photocopy (\$7.00 foreign) or \$3.00 for microfiche (\$4.00 foreign) are required.

LITERATURE CITED

- (1) D. R. Beaman and D. M. File, *Anal. Chem.*, **48**, 101 (1976).
- (2) J. Papp, E. Czárán, and A. Jánosy, *Anal. Chem.*, **50**, 1265 (1978).
- (3) D. R. Beaman and J. A. Isasi, "Electron Beam Microanalysis", ASTM STP 506, American Society for Testing and Materials, Philadelphia, Pa., 1972.
- (4) P. Duncumb, *J. Microsc. (Paris)*, **7**, 581 (1968).
- (5) J. C. Russ, in Proceedings, Symposium on Thin-Section Microanalysis, St. Louis, Mo., EDAX Laboratories, 1972, p. 115.
- (6) J. C. Russ, *J. Submicrosc. Cytol.*, **6**, 55 (1974).
- (7) (a) J. C. Russ, *J. Microsc. Biol. Cell. (Paris)*, **22**, 283 (1975); (b) *Microsc. Acta, Suppl.*, **2**, 217 (1978).
- (8) G. Cliff and G. W. Lorimer, in Proceedings, Fifth European Congress on Electron Microscopy, Inst. Physics, London, 1972, p. 140.
- (9) D. Neumann and A. G. S. Jánosy, *Planta*, **134**, 151 (1977).
- (10) A. J. Morgan, T. W. Davies, and D. A. Erasmus, *J. Microsc. (Oxford)*, **104**, 271 (1975).
- (11) A. G. S. Jánosy and D. Neumann, *Microsc. J.*, **7**, 225 (1976).
- (12) H. Bethe, *Ann. Phys.*, **5**, 325 (1930).
- (13) E. W. White, G. V. Gibbs, G. G. Johnson, Jr., and G. R. Zechman, Jr., "X-Ray Emission and Absorption Wavelengths and Two-Theta Tables", ASTM DS 37A, American Society for Testing and Materials, Philadelphia, Pa., 1970.
- (14) E. P. Bertin, "Principles and Practice of X-Ray Spectrometric Analysis", Plenum Press, New York, London, 2nd ed., 1975, p. 968.
- (15) J. I. Goldstein, J. L. Costley, G. W. Lorimer, and S. J. B. Reed, "Scanning Electron Microscopy/1977", Vol. I, Proceedings, Workshop on Analytical Electron Microscopy, IITRI, Chicago, Ill., 1977, p. 315.
- (16) C. J. Powell, *Rev. Mod. Phys.*, **48**, 33 (1976).
- (17) N. F. Mott and H. S. W. Massey, "The Theory of Atomic Collisions", 2nd ed., Oxford University Press, London, 1949, p. 243.
- (18) C. R. Worthington and S. G. Tomlin, *Proc. Phys. Soc. (London), Sect. A*, **69**, 401 (1956).
- (19) G. G. Johnson, Jr., and E. W. White, "X-Ray Emission Wavelengths and keV Tables for Nondiffractive Analysis", ASTM DS 46, American Society for Testing and Materials, Philadelphia, Pa., 1970.
- (20) E. H. S. Burhop, *J. Phys. Radium*, **16**, 625 (1955).
- (21) J. W. Colby, *Adv. X-Ray Anal.*, **11**, 287 (1968).
- (22) G. Wentzel, *Z. Phys.*, **43**, 524 (1927).
- (23) R. H. Geiss and T. C. Huang, *X-Ray Spectrom.*, **4**, 196 (1975).

RECEIVED for review July 21, 1978. Accepted December 11, 1978. Presented at the Hungarian Symposium on X-Ray Microanalysis, July 11–13, 1978, Szeged, Hungary.

Diagnosis and Correction of Wedging Errors in Absorbance Subtract Fourier Transform Infrared Spectrometry

Tomas Hirschfeld

Block Engineering, Inc., Cambridge, Massachusetts 02139

The errors produced by wedging in IR spectra are calculated from theory and also shown experimentally. The effect of these errors is magnified in absorbance subtract spectrometry, and is particularly serious at the very high sensitivities FT-IR makes possible. The concentration errors and residual spectra produced by various types of absorbance subtract procedures are shown mathematically and graphically. For known wedging, a correction procedure is shown. If the wedging cannot be measured directly, it can be obtained spectrally from the appearance of known sample bands.

Sample spatial nonuniformity effects, such as wedging, have long been recognized as error sources in absorption spectrometry (1). Their numerical values have been described for the wedging case in a paper (2) which also described the resulting peak shape distortion in normal and difference spectrometry.

Difference spectrometry has recently grown into the FT-IR absorbance subtract spectrometry field (3). Here very small sample changes are detected by subtracting sample and appropriately weighed reference spectra in computer memory and scale-expanding the difference as much as a 1000-fold.

Under these conditions, even small sample nonuniformities give significant artifacts. And furthermore, almost any sample which is free from the even worse error source, interference fringes, must necessarily show a significant nonuniformity. The problem is thus not only severe, but far more common than usually realized.

A detailed mathematical analysis of the problem has only now become meaningful, since previous analyses (2) involved two unspoken and unfulfilled assumptions: Uniform beam irradiance (4), and negligible photometric effects due to beam deflection by the sample "prism" (5). These requirements have now been met by FT-IR, making the spatial nonuniformity errors predictable and eventually correctable.

Therefore, this paper will use the absorbance error due to wedging to calculate analytically the consequent concentration

errors and residual spectrum shape and amplitude to be expected for each of the weighing procedures used in absorbance subtract spectrometry.

Furthermore, a procedure for spectrometric wedging determination will be described, and its use to generate wedging-free results described.

ABSORBANCE ERRORS DUE TO SAMPLE WEDGING

If $f(x)$ is the probability distribution function of the sample thickness, its integral mean absorbance can be seen to be

$$\bar{A}(\nu) = -\log \frac{\int_0^\infty f(x) e^{-\ln 10k(\nu)c x} dx}{\int_0^\infty f(x) dx} = -\log \int_0^\infty f(x) e^{-\ln 10k(\nu)c x} dx \quad (1)$$

where $k(\nu)$ is the absorptivity as a function of the frequency ν and c is the sample concentration.

The simplest sample nonuniformity, sample wedging in an uniform beam makes all sample thicknesses in a range Δl around a mean l equally probable. Thus, $f(x)$ is a constant, and we can write

$$f(x) \int_{l-(\Delta l/2)}^{l+(\Delta l/2)} dx \approx 1; \therefore f(x) = \frac{1}{\Delta l} \quad (2)$$

Substituting this into Equation 1 now gives

$$\bar{A}(\nu) = -\log \frac{e^{-\ln 10k(\nu)c} [e^{\ln 10k(\nu)c(\Delta l/2)} - e^{-\ln 10k(\nu)c(\Delta l/2)}]}{\ln 10k(\nu)c} \quad (3)$$

and if we write $A(\nu)$ for the true absorbance

$$\bar{A}(\nu) - A(\nu) = \log \frac{\ln 10 \frac{A(\nu)}{2} \frac{\Delta l}{l}}{\sinh \left[\ln 10 \frac{A(\nu)}{2} \frac{\Delta l}{l} \right]} \quad (4)$$

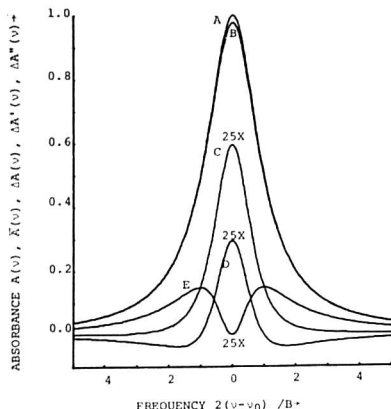


Figure 1. True absorbance, error spectrum, effect of wedging, and residual spectra for various absorbance subtract techniques as a function of frequency for peak absorbance 1.0, and a $\pm 25\%$ thickness range. A: true absorbance for a Lorentzian band; B: absorbance in the presence of wedging; C: error spectrum from "no negative value" subtract; D: residual spectrum from "peak integral nulling" subtract; and E: residual spectrum from "peak center nulling" subtract

This in turn can be expanded as a Taylor's series in $A(v)$ $(\Delta l/l)$ to give

$$\begin{aligned} \bar{A}(v) - A(v) &= \frac{\ln 10}{24} A^2(v) \left(\frac{\Delta l}{l} \right)^2 \left[1 - \frac{\ln^2 10}{120} A^2(v) \times \right. \\ &\quad \left. \left(\frac{\Delta l}{l} \right)^2 + \frac{\ln^4 10}{120720} A^4(v) \left(\frac{\Delta l}{l} \right)^4 - \dots \right] = \\ &0.09594 A^2(v) \left(\frac{\Delta l}{l} \right)^2 - 4.239 \times 10^{-3} \times A^4(v) \left(\frac{\Delta l}{l} \right)^4 + \\ &2.234 \times 10^{-5} A^6(v) \left(\frac{\Delta l}{l} \right)^6 - \dots \quad (5) \end{aligned}$$

Figure 1 shows this error for $A(v_0) = 1$ and a $\pm 25\%$ thickness range. It can be seen that the error is not severe until fairly significant $A(v)(\Delta l/l)$ values are reached.

WEDGING ERRORS IN ABSORBANCE SUBTRACT SPECTROMETRY

The preceding conclusion is drastically altered in absorbance subtract spectrometry, where the subtraction of similar spectra and large scale expansion of the remainder gives spectra which may easily be dominated by this error source.

Figure 1 shows the appearance of a Lorentzian spectral peak of true peak absorbance $A(v_0) = 1.0$, for both a flat sample and one having a thickness variation of $\pm 25\%$. The third curve shows a $25\times$ expansion of the difference, showing a nice "difference" spectral peak produced only by the wedging error.

Current practices in absorbance subtract spectrometry use both higher peak absorbance spectra and much higher scale expansions. The probability of the results containing spurious effects due to even slight wedging is therefore high.

While on the subject of current practices in absorbance subtract spectrometry, there is one that greatly disturbs me. Partially at least in response to earlier reports on studying intermolecular interaction effects by absorbance subtract spectrometry (6), a habit has grown up of automatically

blaming on them any anomalies encountered in this technique. "Intermolecular effects" sounds impressive enough, and since they are little understood and presumed to be unavoidable, nothing needs to be done.

This facile assignment of a scapegoat about which one is then fatalistic has been discouraging to a serious effort to understand and correct many real errors in absorbance subtract spectrometry. What is more, many of these other problems are potentially or actually curable, as shown in this paper, and account for a substantial part of the so-called "intermolecular effect" residuals.

Actually, spurious difference spectra due to wedging need not always have the appearance of Figure 1: Absorbance subtract spectrometry is usually done with an adjustable weighing factor on one of the spectra, which is adjusted to obtain the optimal end result.

Three end points can be distinguished in this process, all of which are commonly used. The first consists of carrying the subtraction to the point where negative values just appear on the peak shoulders. In a pure wedging situation, this gives a residual spectrum precisely as shown in Figure 1, whose intensity is given by

$$\Delta A(v) = \log \frac{\sinh \left[\frac{\ln 10}{2} A(v) \frac{\Delta l}{l} \right]}{\frac{\ln 10}{2} A(v) \frac{\Delta l}{l}} \approx \frac{\ln 10}{24} A^2(v) \left(\frac{\Delta l}{l} \right)^2 \quad (6)$$

Figure 2 gives $\Delta A(v) = A(v)(\Delta l/l)$. For a Lorentzian peak, Equation 6 becomes

$$\Delta A(v) = \log \frac{\sinh \left[\frac{\ln 10}{2} \frac{A(v_0)}{1 + 4(v - v_0)^2/B^2} \right]}{\frac{\ln 10}{2} \frac{A(v_0)}{1 + 4(v - v_0)^2/B^2}} \approx \frac{\ln 10}{24} \frac{A^2(v_0)}{[1 + 4(v - v_0)^2/B^2]^2} \left(\frac{\Delta l}{l} \right)^2 \quad (7)$$

where B is the bandwidth at half-height and v_0 the peak frequency.

More refined end-point criteria involve nulling the intensity at the initial peak location, or nulling the integral of the residual spectral peak either by estimation or by automatic computation.

WEDGING ERRORS IN PEAK CENTER NULLING ABSORBANCE SUBTRACT SPECTROMETRY

The weight assigned to the spectrum being subtracted can be modified for nulling purposes. Since this weight ultimately stems from the concentration of the molecule whose spectrum is subtracted, assigning it an incorrect value amounts to deriving an erroneous sample concentration.

Nulling the intensity at the peak location can be therefore expressed as

$$\bar{A}(v_0) - K(v_0)(c + \Delta c)l = \log \frac{\sinh \left[\frac{\ln 10}{2} k(v_0)c\Delta l \right]}{\frac{\ln 10}{2} k(v_0)c\Delta l} - k(v_0)\Delta c l \equiv 0 \quad (8)$$

which can be transposed to

$$\frac{\Delta c}{c} = \frac{1}{A(\nu_0)} \log \frac{\frac{\ln 10}{2} A(\nu_0) \frac{\Delta l}{l}}{\sinh \left[\frac{\ln 10}{2} A(\nu_0) \left(\frac{\Delta l}{l} \right) \right]} \approx \frac{\ln 10}{24} A(\nu_0) \times \left(\frac{\Delta l}{l} \right)^2 \left[1 - \frac{\ln^2 10}{120} A^2(\nu_0) \left(\frac{\Delta l}{l} \right)^2 + \dots \right] A(\nu_0) \frac{\Delta l}{l} \ll 1 \quad (9)$$

giving significant errors in the calculated concentration. Furthermore, there will be a residual spectrum, given by $\Delta A(\nu) = A(\nu) - k(\nu)(c + \Delta c)l =$

$$\log \frac{\frac{\ln 10}{2} A(\nu) \frac{\Delta l}{l}}{\sinh \left[\frac{\ln 10}{2} A(\nu) \left(\frac{\Delta l}{l} \right) \right]} - \frac{\log \frac{\frac{\ln 10}{2} A(\nu_0) \frac{\Delta l}{l}}{\sinh \left[\frac{\ln 10}{2} A(\nu_0) \left(\frac{\Delta l}{l} \right) \right]}}{\frac{A(\nu)}{A(\nu_0)}} \approx \frac{\ln 10}{24} [A^2(\nu) - A^2(\nu_0)] \left(\frac{\Delta l}{l} \right)^2 \times \left[1 - \frac{\ln^2 10}{120} A^2(\nu) \left(\frac{\Delta l}{l} \right)^2 + \dots \right] \quad (10)$$

which for a Lorentzian band becomes

$$\Delta A(\nu) = \frac{\frac{\ln 10}{2} \frac{A(\nu_0) \frac{\Delta l}{l}}{1 + 4(\nu - \nu_0)^2/B^2}}{\sinh \left[\frac{\ln 10}{2} \frac{A(\nu_0) \frac{\Delta l}{l}}{1 + 4(\nu - \nu_0)^2/B^2} \right]} - \frac{1}{1 + 4(\nu - \nu_0)^2/B^2} \times \log \frac{\frac{\ln 10}{2} A(\nu_0) \frac{\Delta l}{l}}{\sinh \left[\frac{\ln 10}{2} A(\nu_0) \left(\frac{\Delta l}{l} \right) \right]} \approx \frac{\ln 10}{24} \left(\frac{\Delta l}{l} \right)^2 \times \left[\frac{A^2(\nu_0)}{[1 + 4(\nu - \nu_0)^2/B^2]^2} - A^2(\nu_0) \right] \times \left[1 - \frac{\ln^2 10}{120} A^2(\nu_0) \left(\frac{\Delta l}{l} \right)^2 + \dots \right] \quad (11)$$

This residual spectrum peaks at $\nu = \nu_0 \pm B/2$, where its value is

$$\Delta A(\nu_0 \pm B/2) = \log \frac{\left\{ \frac{\ln 10}{4} A(\nu_0) \frac{\Delta l}{l} [e^{(\ln 10/2) A(\nu_0) (\Delta l/l)} - e^{-(\ln 10/2) A(\nu_0) (\Delta l/l)}] \right\}^{1/2}}{e^{(\ln 10/4) A(\nu_0) (\Delta l/l)} - e^{-(\ln 10/4) A(\nu_0) (\Delta l/l)}} \approx \frac{\ln 10}{96} A^2(\nu_0) \left(\frac{\Delta l}{l} \right)^2 \quad (12)$$

showing a 4-fold reduction in the residual spectrum peak intensity from that given by the no negative value technique. However, the shape of the spectrum now becomes quite different.

The shape and values of $\Delta A(\nu)$ for the above example can be seen in Figure 1, while Figure 2 shows $\Delta A(\nu_0 \pm B/2)$ as a function of $A(\nu_0)(\Delta l/l)$. Finally, $(\Delta c/c)/(\Delta l/l)$ as a function of $A(\nu_0)(\Delta l/l)$ can be seen in Figure 3.

WEDGING ERRORS IN PEAK INTEGRAL NULLING ABSORPTION SPECTROMETRY

Nulling the integral of the residual peak in absorbance

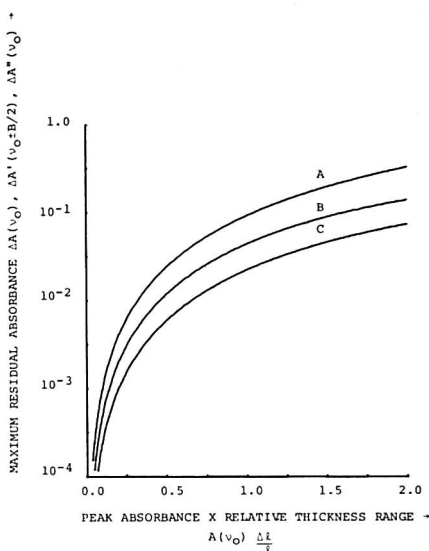


Figure 2. Maximum residual absorbances for the various absorbance subtract techniques as a function of the peak absorbance-relative thickness change product. A: "no negative value" subtract; B: "peak integral nulling" subtract; and C: "peak center nulling" subtract

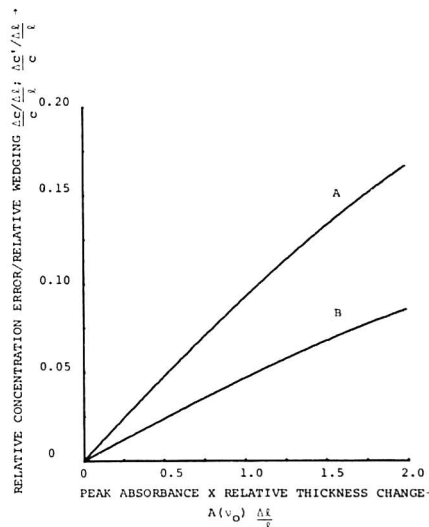


Figure 3. Concentration errors produced by wedging for the various absorbance subtract techniques as a function of the peak absorbance-relative thickness change product. A: "peak center nulling" subtract; and B: "peak integral nulling" subtract

subtract spectrometry can be approximated manually or done automatically. (The corresponding computer routine, Autosubtract, is available from Digilab for its FTS instrumentation.) The end result in either case can be expressed

$$\int_0^\infty [\bar{A}(\nu) - k(\nu)(c + \Delta c)l] d\nu = \int_0^\infty \log \frac{\sinh \left[\frac{\ln 10}{2} A(\nu) \frac{\Delta l}{l} \right]}{\frac{\ln 10}{2} A(\nu) \frac{\Delta l}{l}} d\nu - \Delta c l \int_0^\infty k(\nu) d\nu = 0 \quad (13)$$

which can be rearranged to

$$\frac{\Delta c'}{c} = \frac{\ln 10}{24} c l \frac{\Delta l}{l} \times \int_0^\infty k^2(\nu) \left[1 - \frac{\ln^2 10}{120} c^2 l^2 \left(\frac{\Delta l}{l} \right)^2 k^2(\nu) + \dots \right] d\nu \quad (14)$$

giving for a Lorentzian peak

$$\frac{\Delta c'}{c} = \frac{\ln 10}{24} A(\nu_0) \left(\frac{\Delta l}{l} \right)^2 \times \int_0^\infty \frac{1}{1 + 4(\nu - \nu_0)^2/B^2} \left[1 - \frac{\ln^2 10}{120} A^2(\nu_0) / [1 + (\nu - \nu_0)^2/B^2] + \dots \right] d\nu / \int_0^\infty \frac{d\nu}{1 + 4(\nu - \nu_0)^2/B^2} \quad (15)$$

which to first order reduces to

$$\frac{\Delta c'}{c} \approx \frac{\ln 10}{24} A(\nu_0) \left(\frac{\Delta l}{l} \right)^2 \frac{\int_0^\infty \frac{d\nu}{[1 + 4(\nu - \nu_0)^2/B^2]^2}}{\int_0^\infty \frac{d\nu}{1 + 4(\nu - \nu_0)^2/B^2}} = \frac{\ln 10}{48} A(\nu_0) \left(\frac{\Delta l}{l} \right)^2 \quad (16)$$

which is $1/2$ the error arising from the peak center nulling technique. This technique also gives a residual spectrum, described by

$$\Delta A''(\nu) = \bar{A}(\nu) - k(\nu)(c + \Delta c)l = \log \frac{\sinh \left[\frac{\ln 10}{2} A(\nu) \frac{\Delta l}{l} \right]}{\frac{\ln 10}{2} A(\nu) \frac{\Delta l}{l}} - k(\nu) \Delta c l \quad (17)$$

which, to first order and for a Lorentzian line, becomes

$$\Delta A''(\nu) = \frac{\ln 10}{48} A^2(\nu_0) \left(\frac{\Delta l}{l} \right)^2 \frac{1 - 4(\nu - \nu_0)^2/B^2}{[1 + 4(\nu - \nu_0)^2/B^2]^2} \quad (18)$$

which has a central peak at ν_0 for which

$$\Delta A''(\nu_0) = \frac{\ln 10}{48} A^2(\nu_0) \left(\frac{\Delta l}{l} \right)^2 \quad (19)$$

half the value given by the no negative value technique, and subsidiary minima given by

$$\Delta A''\left(\nu_0 \pm \frac{\sqrt{3}B}{2}\right) = \frac{\ln 10}{384} A^2(\nu_0) \left(\frac{\Delta l}{l} \right)^2 \quad (20)$$

one quarter the size of those given by the peak center nulling method. Figure 1 shows $\Delta A''(\nu)$ for the above example, while Figure 2 shows $\Delta A''(\nu_0)$ as a function of $A(\nu_0)(\Delta l/l)$ and Figure

3 gives $(\Delta c'/c)/(\Delta l/l)$ as a function of $A(\nu_0)(\Delta l/l)$.

MATHEMATICAL CORRECTION OF WEDGING ERRORS

If the value of $\Delta l/l$ can be determined independently, the wedging errors can be strongly reduced by performing the correction

$$A_c(\nu) = \bar{A}(\nu) + \frac{\ln 10}{24} \bar{A}^2(\nu) \left(\frac{\Delta l}{l} \right)^2 \quad (21)$$

where $A_c(\nu) \approx A(\nu)$ is the corrected spectrum and $\bar{A}(\nu)$ the measured one. All further calculations using $A_c(\nu)$ will then have error levels lower by

$$f \approx \frac{\ln^2 10}{120} A_c^2(\nu) \left(\frac{\Delta l}{l} \right)^2 \quad (22)$$

If $\Delta l/l$ cannot be directly measured, it can be found spectrometrically for bands of known shape by observing the band distortion. If the true band shape is known and l and c are known for scaling purposes, the calculation is fairly simple.

Thus we have to first order

$$\frac{\Delta l}{l} = \left[\frac{24}{\ln 10} \frac{k(\nu)cl - \bar{A}(\nu)}{k^2(\nu)c^2l^2} \right]^{1/2} \quad (23)$$

If, on the other hand, either l or c are unknown, the reference spectrum can be used to calculate $k(\nu)$, and a system of equations solved for two different frequencies to give

$$c\Delta l = \sqrt{\frac{24}{\ln 10}} \frac{1}{k(\nu)} \sqrt{\frac{\bar{A}(\nu') \frac{k(\nu)}{k(\nu')} - \bar{A}(\nu)}{1 - \frac{k(\nu')}{k(\nu)}}} \quad (24)$$

as well as

$$cl = \frac{\bar{A}(\nu') \frac{k^2(\nu)}{k^2(\nu')} - \bar{A}(\nu)}{k(\nu) \left[\frac{k(\nu)}{k(\nu')} - 1 \right]} \quad (25)$$

giving

$$\frac{\Delta l}{l} = \sqrt{\frac{24}{\ln 10}} \frac{k(\nu)}{k(\nu')} \sqrt{1 - \frac{k(\nu')}{k(\nu)}} \sqrt{\frac{A(\nu') \frac{k(\nu)}{k(\nu')} - A(\nu)}{\bar{A}(\nu') \frac{k^2(\nu)}{k^2(\nu')} - \bar{A}(\nu)}} \quad (26)$$

which for $\nu = \nu_0$ and ν' at the half-height location, reduces to

$$\frac{\Delta l}{l} = 4 \sqrt{\frac{3}{\ln 10}} \frac{\sqrt{2\bar{A}(\nu_0 \pm B/2) - A(\nu_0)}}{4\bar{A}(\nu_0 \pm B/2) - A(\nu_0)} \quad (27)$$

The accuracy of this measurement decreases very rapidly with decreasing $\Delta l/l$, but precisely so does the need for this accuracy. In practice, the reference spectrum of the same compound may be obtainable from the same sample if a much thinner sample of it is obtainable, as wedging errors can be neglected in the optically thin limit. An alternative procedure is to vignette the beam down to a much smaller sample area, over which Δl will be much smaller, again providing a "wedging free" reference. This lower thickness or lower beam size

reference can then be used to correct the full thickness, full beam size spectra which are most advantageous for absorbance subtract spectrometry.

CONCLUSIONS

Wedging in appreciably absorbing samples will produce absorbance errors which are greatly magnified in absorbance subtract spectrometry. The extent of this error can be calculated by the exact or simpler approximate formulas described here, and is shown graphically.

In absorbance subtract spectrometry, the significant resulting errors depend on the procedure used for setting the weighing coefficient for the subtracted spectrum. For the simplest procedure of using the highest weight that just fails to produce negative values in the peak's difference spectrum, the weighing coefficient will give the correct concentration, but produce a residual spectrum of peak intensity $(\ln 10/24) A^2(\nu_0)(\Delta l/l)^2$ and slightly distorted appearance.

If, instead, nulling the peak center intensity is used as a criterion, $(\Delta l/l)^2$ the concentration found will have a relative error $(\ln 10/24) A(\nu_0)(\Delta l/l)^2$. There also will be residual spectrum peaking at both half-height locations on the band with an intensity $(\ln 10/96) A^2(\nu_0)(\Delta l/l)^2$.

Lastly, if one nulls the peak integral, which can be done with an automatic program, one obtains a relative concentration error of $(\ln 10/48) A(\nu_0)(\Delta l/l)^2$, and a somewhat distorted residual spectrum of peak intensity $(\ln 10/48) A_2(\nu_0)(\Delta l/l)^2$. This increases the residual spectrum amplitude but reduces the concentration error.

The whole problem can be greatly reduced by using absorbance corrected for wedging if $\Delta l/l$ is known. This can also be measured spectrometrically if the true shape of at least one band is known, by using its distortion to calculate $\Delta l/l$ by equations given here. This true band shape can be obtained from reference samples or from reduced thickness or reduced beam size sample spectra.

LITERATURE CITED

- (1) R. N. Jones, *J. Am. Chem. Soc.*, **74**, 2681 (1952).
- (2) J. Koenig, *Anal. Chem.*, **38**, 1045 (1964).
- (3) T. Hirschfeld, *Appl. Spectrosc.*, **30**, 550 (1976).
- (4) A. L. Olsen, K. B. LaBaw, L. W. Nichols, *J. Opt. Soc. Am.*, **54**, 813 (1964).
- (5) A. P. Andreev, A. V. Malyi, N. S. Golyandin, and V. M. Zolotarev, *Sov. J. Opt. Technol.*, **43**, 641 (1977).
- (6) T. Hirschfeld and K. Kizer, *Appl. Spectrosc.*, **20**, 345 (1975).

RECEIVED for review April 11, 1977. Accepted December 5, 1978.

Determination of Oil Content in Oil Modified *o*-Phthalic Polyester Resins by Infrared Spectrometry

James A. Vance,* N. Bradford Brakke,¹ and Paul R. Quinney²

Analytical Laboratory, Lilly Industrial Coatings, Inc., 666 South California Street, Indianapolis, Indiana 46225

In the analysis of oil modified, *o*-phthalic polyester resins (alkyd resins), determination of phthalic anhydride and oil (triglyceride) are common. Lengthy, wet chemical methods exist for these determinations. The objective of this work is to develop an infrared technique to determine the percent oil in phthalate-glycerol alkyd resins, within the accuracy of the gravimetric procedure. Using integrated intensities for phthalates and triglycerides, it can be shown that the area under the carbonyl absorption band is the total of the component areas. By determining the concentration of phthalic anhydride gravimetrically, the area due to that concentration may be determined. The area due to the oil may then be obtained by subtracting the area due to the phthalate from the total area under the absorption band. The corresponding concentration may then be calculated. The results show that the calculated oil percentage is within the accuracy of the gravimetric procedure.

Phthalic anhydride content of alkyd resins is a determination outlined in ASTM designation D563-52 (1). This procedure has proven itself to be simple, yet accurate and reproducible. ASTM designation D-1398 (2) outlines a procedure for the isolation and quantitative determination

of fatty acids in alkyd resins. This method is considerably long and tedious.

We are searching for a method of alkyd resin analysis for the determination of oil that is rapid, yet quantitatively reliable and reproducible. For a quick, quantitative method for the determination of oil, when the concentration of phthalic anhydride is known, would save analysis time. Infrared spectrometry, being a powerful tool in this industry, seems a logical vehicle to obtain what we want.

In a typical phthalate alkyd resin the carbonyl absorption, occurring at 1735 cm^{-1} , is due to two components: oil and phthalate. If we could measure the area of the carbonyl absorption band, and having known the percentage of phthalic anhydride (thus its effect upon the carbonyl absorption of the resin), then it would be possible to deduce the concentration of the oil.

$$\text{area (total carbonyl)} = \text{area (oil-carbonyl)} + \text{area (phthalate-carbonyl)}$$

The integrated intensity, B , is defined as:

$$B = \frac{1}{bc} \text{area}$$

where b = the cell path length (in cm), c = the concentration (in mol/L), and the area is that under the absorption band (in cm^{-1}). Several methods for the determination of integrated intensities have been reported in the literature (3-5). We will use the Ramsey method (4) and the Cabana method (5), as well as direct integration, to obtain integrated intensity values for phthalates and triglycerides.

* Present address, Lilly Chemical Products, Inc., Athol Road, P.O. Box 188, Templeton, Mass. 01468.

² Permanent address, Butler University, 4600 Sunset Boulevard, Indianapolis, Ind. 46208.

Table I. Average *B* Values for Phthalates and Triglycerides

compound	<i>B</i> (direct integration)	<i>B</i> (Ramsey)	<i>B</i> (Cabana and Sandorfy)
dimethyl phthalate	1.16	1.45	1.24
dibutyl phthalate	1.22	1.64	1.32
dioctyl phthalate	1.17	1.45	1.25
dibutyl terephthalate	1.21	1.60	1.30
triacetin	1.07	1.30	1.16
tributyrin	1.00	1.13	1.08
trilaurin	1.00	1.31	1.13
tristearin	1.01	1.27	1.11

EXPERIMENTAL

Determination of *B* Values. The initial step is to prove that the hypothesis holds true for a selected number of known, pure reagents. The following compounds were run at conditions set below, and their respective integrated intensities calculated. These materials are dimethyl phthalate, dibutyl phthalate, dioctyl phthalate, dimethyl isophthalate, tributyrin, triacetin, trilaurin, and tristearin.

Each material was diluted in solution with spectral grade carbon tetrachloride to a concentration that would yield a carbonyl absorbance between 0.4 and 0.8 *A*. After a few trials, it was evident that 0.10 mole of carbonyl per liter was the appropriate concentration. Three solutions of each reagent were made: 0.08, 0.10, and 0.12 moles of carbonyl material per liter.

These solutions were run in a liquid cell whose pathlength had been previously determined. They were run on a Beckman IR-12 spectrophotometer, using the following conditions: glower current, 0.6 A; coarse gain, 10; fine gain, 2.0%; period, 2; slit width, 1.1 at 1000 cm⁻¹; abscissa expansion, 20 cm⁻¹/inch; mode, absorbance; chart speed, 20 cm⁻¹/min; and scanning range, 1650 cm⁻¹ to 1850 cm⁻¹.

The resulting spectra of the absorptions were then treated in the following fashion. Dibutyl phthalate is used as an example, Figure 1. Integrated intensities were calculated using the Ramsey, Cabana and Sandorfy, and direct integration methods.

(A) Ramsey Method.

$$\epsilon = A/bc$$

$$B = (K)(\epsilon)(\Delta\gamma^{a_{1/2}})$$

(B) Cabana and Sandorfy Method.

$$B = \frac{1}{cb} \int \frac{T_0}{T} [0.549(\Delta\nu_{1/8}K'_{1/8} + \Delta\nu'_{1/8}K'_{1/8}) + 0.156(\Delta\nu_{1/4}K'_{1/4} + \Delta\nu'_{1/4}K'_{1/4}) + 0.169(\Delta\nu_{1/2}K'_{1/2} + \Delta\nu'_{1/2}K'_{1/2}) + 0.124(\Delta\nu_{3/4}K'_{3/4} + \Delta\nu'_{3/4}K'_{3/4})]$$

(C) Direct Integration Method.

area by planimeter = 4.84 sq. in.

The chart paper we are using on the Beckman IR-12 is a 1-inch square grid. Since we are running at 20 cm⁻¹ per inch on the abscissa and 1 inch is equal to 0.1 *A*, we can convert square inch readings to wavenumber-absorbance units by multiplying by a factor of 2.

$$\text{area by planimeter} = 9.68\text{cm}^{-1} - A$$

$$B = \frac{1}{bc} \text{area}$$

Table I contains average *B* values obtained by the three methods for the known compounds studied.

Testing the Validity of *B* Values with Known Mixes. The known materials were paired into the following groups: dimethyl phthalate-triacetin, dibutyl phthalate-tributyrin, dioctyl

Table II. Areas of Known Binary Mixes

mix	area, cm ⁻¹ ·A	
	measured	calculated
dibutyl phthalate/tributyrin		
1:1 mix	19.01	19.08
2:1 mix	22.01	21.68
1:2 mix	21.56	21.46
dimethyl phthalate/triacetin		
1:1 mix	19.32	19.44
2:1 mix	18.52	18.79
1:2 mix	18.42	18.47
dioctyl phthalate/trilaurin		
1:1 mix	18.11	18.14
2:1 mix	18.51	18.44
1:2 mix	16.99	17.19
dimethyl isophthalate/tributyrin		
1:1 mix	20.54	21.27
2:1 mix	19.22	21.18
1:2 mix	20.64	20.27

Table III. Phthalic Anhydride Determinations

resin	% PA	
	theoretical	found
A	43.74	45.01
B	49.07	49.41
C	43.99	44.05
D	38.90	39.30
E	33.22	33.12
F	32.98	31.81

phthalate-trilaurin, and dimethyl isophthalate-tributyrin.

Three synthetic mixtures were made of each pair. These mixes were in the ratios of 1:1, 1:2, and 2:1. They were run under the same conditions cited above. The absorption bands were integrated by planimeter. Calculations were made and compared to the concentration data as follows: a dibutyl phthalate-tributyrin mix will be used as an example.

Remembering that we have calculated a *B* value for the dibutyl phthalate and the tributyrin separately, we can now compare a theoretical calculated area with an area that we measure. The measured area of the dibutyl phthalate-tributyrin mix is 21.55 wavenumber-absorbance units. Using the *B* values that we obtained from the Ramsey method, the theoretical area should be:

$$(B_{\text{dibp}})(c_{\text{dibp}})(b_{\text{cell}}) + (B_{\text{tby}})(c_{\text{tby}})(b_{\text{cell}}) = (1.64)(6.66 \times 10^{-2})(1.06 \times 10^{-2}) + (1.26)(12.26 \times 10^{-2})(1.06 \times 10^{-2}) = 27.82 \text{ cm}^{-1} \cdot A$$

Using the *B* values obtained from the Cabana and Sandorfy method, the theoretical area should be:

$$(1.33)(6.66 \times 10^{-2})(1.06 \times 10^{-2}) + (1.12)(12.26 \times 10^{-2})(1.06 \times 10^{-2}) = 23.83 \text{ cm}^{-1} \cdot A$$

Using the integrated intensity values which we obtained from direct integration, the calculated area should be:

$$(1.22)(6.66 \times 10^{-2})(1.06 \times 10^{-2}) + (1.00)(12.26 \times 10^{-2})(1.06 \times 10^{-2}) = 21.50 \text{ cm}^{-1} \cdot A$$

Table II contains data on the mixtures, their measured areas and the theoretical areas calculated. The seemingly large differences in areas from method to method will be discussed in the Results and Discussion section of this paper.

Testing Hypothesis in Production Resins. Oil modified, α -phthalic polyester resins that are made commercially were analyzed by the gravimetric method cited earlier for the determination of phthalic anhydride (1). These determinations were compared to the theoretical phthalic anhydride content of the polymer, and the results can be found in Table III.

Samples of these resins, 0.2 to 0.5 gram, were taken and placed into 25-mL volumetric flasks. To each flask, a few drops of benzene were added to reduce the sample and cover the bottom of the flask. The flask and its contents were then placed into a

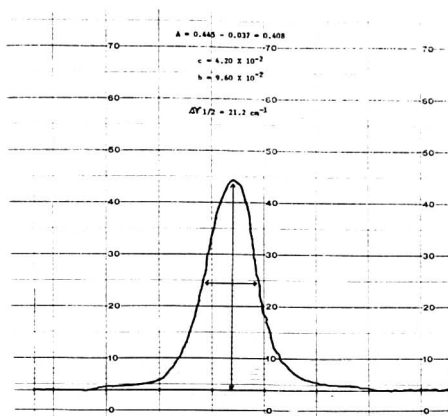


Figure 1. Dibutyl phthalate

vacuum oven and heated at 60 °C for a period of 0.5 to 1 h to drive off all volatile material. At this point, the flask was removed and allowed to cool. The contents were diluted with carbon tetrachloride to a volume of 25 mL. A sample of this solution was placed in a liquid cell and the region of 1650 cm^{-1} to 1850 cm^{-1} was scanned in the infrared. The area under the carbonyl absorption band was taken and the calculations made as follows: Resin C will be used as an example.

% phthalic anhydride (theoretical) = 43.99%

% phthalic anhydride (found) = 44.05%

total area integrated = 7.23 $\text{cm}^{-1} \cdot \text{A}$

To calculate the area due to the phthalic anhydride content:

$$\frac{(\text{g of polym})}{(\text{volume})} \times \frac{(\text{wt \% P.A.})}{(1)} \times \frac{(1 \text{ mol})}{(148.12 \text{ g})} \times \frac{(2 \text{ C=O units})}{(1 \text{ molecule})} \times \frac{(B)}{(1)} \times \frac{(b_{\text{cell}})}{(1)} = \frac{(0.1976 \text{ g})}{(0.025 \text{ L})} \times \frac{(44.05\%)}{(1)} \times \frac{(1)}{(1)} \times \frac{(1.22)}{(1)} \times \frac{(1.09 \times 10^{-2})}{(1)} = 6.21 \text{ cm}^{-1} \cdot \text{A}$$

To calculate the area due to the oil content:

$$\text{total area} - \text{area due to phthalate} = \text{area due to oil} = 7.23 - 6.21 = 1.03 \text{ cm}^{-1} \cdot \text{A}$$

To calculate the concentration of oil from this area the equation is:

$$\frac{(\text{g of polym})}{(\text{volume})} \times \frac{(\text{area})}{(878 \text{ g/mol})} \times \frac{(1 \text{ mol})}{(1 \text{ molecule})} \times \frac{(3 \text{ C=O units})}{(1)} \times \frac{(B)}{(1)} \times \frac{(b_{\text{cell}})}{(1)} = \% \text{ oil}$$

$$\frac{(1.976 \text{ g})}{(0.025 \text{ L})} \times \frac{(1.03 \text{ cm}^{-1} \cdot \text{A})}{(878 \text{ g})} \times \frac{(1)}{(1)} \times \frac{(1.00)}{(1)} \times \frac{(1.09 \times 10^{-2})}{(1)} = 35.15\%$$

Integrated intensities for dibutyl phthalate and tristearin were

Table IV. Weight Percent Oil in Production Resins

resin	% oil		
	theoretical	IR method	gravimetric
A	27.37	26.90	25.50
B	29.63	29.41	27.57
C	36.67	35.96	33.72
D	45.20	43.90	42.98
E	52.80	49.71	49.14
F	51.57	51.78	49.87
Average difference from theoretical		1.00	2.41

used here because they are the reagents we had that are closest in molecular weight to phthalic anhydride and a triglyceride in a resinous structure.

Resins with an oil content of 30% to 50% were analyzed by this method, and the results, along with a comparison to comparable methods, can be found in Table IV.

RESULTS AND DISCUSSION

We conclude that the hypothesis that $\text{area}_{\text{total}}$ is equal to the sum of the area from the phthalate and the oil is valid. For the quantitative aspect, the integrated intensity method appears to yield satisfactory results.

The B values shown in Table I indicate a disagreement between the various methods. We believe that the Ramsey method yields higher values because the absorptions we are working with are not ideal in shape, rather ones that are skewed to one side or the other. The Cabana and Sandorfy method yields better results, but for the quantitative work shown, the direct integration method seems to work best. B values obtained by this method agree to within $\pm 2\%$.

The synthetic mixtures also indicate that the direct integration method is the best. In most cases, the calculated area is within 2% of the measured area.

Finally, the results of the production polymers indicate that the method is valid. In comparison to the gravimetric method, the integrated intensity method is within the accuracy and precision of the gravimetric method.

The single, largest limiting factor for this method is the placement of the base line. A slight deviation in placement of the base line can yield a 10% difference in the B value.

All of the polymers studied were solubilized in xylene isomers. If resins reduced in higher boiling solvents were to be studied, then a more efficient vacuum would be needed to completely evacuate all volatile materials.

ACKNOWLEDGMENT

The technical assistance of the resin laboratory of Lilly Industrial Coatings, Inc., is gratefully acknowledged.

LITERATURE CITED

- (1) ASTM Designation D563-52, Part 20 (1973).
- (2) ASTM Designation D1398-69, Part 20 (1973).
- (3) E. B. Wilson, Jr., and A. J. Wells, *J. Chem. Phys.*, **14**, 578 (1946).
- (4) O. A. Ramsey, *J. Am. Chem. Soc.*, **74**, 72 (1952).
- (5) A. Cabana and C. Sandorfy, *Spectrochim. Acta*, **16**, 335 (1960).

RECEIVED for review August 24, 1978. Accepted January 5, 1979.

Nanosecond Time-Resolved Spectrometry with a Tunable Dye Laser and a Simple Pulse-Gated Photon Counter

Totaro Imasaka, Teichiro Ogawa, and Nobuhiko Ishibashi*

Faculty of Engineering, Kyushu University, Fukuoka 812, Japan

The design and construction of a fluorometric system with a nitrogen-laser-pumped dye laser ($\Delta t = 4$ ns, $\Delta\lambda = 3.5$ pm) excitation source and a gated ($\Delta t = 4$ ns) photon counter signal processor is described. The time resolution of the system is about 5 ns. The system can be applied to the lifetime measurement of nanosecond decays. The system was used for the measurement of time-resolved spectra and for the detection of molecular fluorescence at $A\phi = 5 \times 10^{-11}$, where A is the absorbance and ϕ the fluorescence quantum yield.

The development of high-power, high-resolution, and reliable lasers has accelerated the use of fluorescence spectrometry as an analytical tool. Above all, a nitrogen-laser-pumped dye laser has been a very useful excitation source for atomic (1) and molecular (2) fluorometry because of its wide tuning range.

Since this laser has a very short pulse, an excellent time-correlated detection system is essential. A boxcar integrator offers a range of variable sampling gate widths down to 10 ns and plug-in heads with the minimum width of 100 ps. However, the system of analog detection and boxcar averaging places a severe limitation on the sensitivity. A photon counting technique can increase the sensitivity, and techniques using a sampling oscilloscope (3, 4) or a time-to-amplitude converter (TAC) (5, 6) have been developed to take advantage of their high sensitivity and their high time resolution. However, the maximum counting rates of such a system are relatively low. A pulse-gated photon counting technique has been applied to detect very weak Raman scattering (7-9); however, the time resolution of the previous apparatus did not allow the nanosecond time-resolved spectrometry.

The design and the construction of an apparatus for nanosecond time-resolved spectrometry with a nitrogen-laser-pumped dye laser and with a simple pulse-gated photon counter will be described in this paper. The apparatus is very sensitive and is capable of observing multiple photons per laser pulse for long-lived photoemission.

INSTRUMENT DESIGN

The basic components of the experimental apparatus are a nitrogen-laser-pumped dye laser and fluorescence detection equipment, as shown in Figure 1. Each element will be described in detail in subsequent sections.

Nitrogen Laser. The nitrogen laser was constructed on the design of a LC inversion type. It consists of a 65-cm long discharge tube, 100-nF capacitors (Nichicon, 5 nF \times 20), and a pressurized spark gap switch. The nitrogen laser was operated at the repetition rate of 15-25 Hz. The output power and the pulse width were about 100 kW and 8 ns, respectively. Forced air cooling was requisite to its stable operation. Adequate shielding against the large quantity of radio frequency interference (RFI) was very important for photon counting.

Dye Laser. The dye laser cavity follows the design of Hensch (10), consisting of a grating, a beam expander (Oriel, \times 20), the dye cell, and an output mirror. A 600 grooves/mm

reflecting grating (30 \times 30 mm) blazed for 500 nm was used in 7th order of the back of the facets (11, 12).

Monitoring Circuit for Dye Laser Output. The intensity of the dye laser was monitored by an HTV R905 photomultiplier. The dynode voltage divider was tapered for a pulsed signal (13). The signal was amplified by an operational amplifier (Teledyne Philbrick 1029); the time constant was adjusted to 4.5 s for smoothing the pulsed signals. This circuit is also useful for the measurement of the time-integrated spectrum when the fluorescence intensity is considerably strong (12).

Wavelength Isolation. Photoemission was focused by a lens onto the entrance slit of either a 1-m single (JASCO CT-100) or a 0.4-m double (JASCO CT-40D) monochromator. The former was used for the high-resolution spectrometry of gaseous molecules and the latter for the measurement of very weak photoemission. The photons were detected with a fast response squirrel-cage photomultiplier (R928) having a red sensitive photocathode (185-930 nm). The base was wired for single photon counting according to the manufacturer's recommendations except charging capacitors which were wired to the tube socket (13).

Gated Electronics. An electronic system with fast time response and high sensitivity has been constructed for the time-resolved spectrometry. The advantages of the present technique are simplicity, low cost, and easy construction. A photodiode (LSD 39A, rise time 0.35 ns) received the dye laser and triggered the gate pulse generator shown in Figure 2. The circuit consists of two monostable multivibrators made of a digital IC (SN74S00, 3.5 ns). The time delay and the gate width can be changed by adjusting capacitors and resistors. The widths were monitored by a synchroscope.

The photoelectron signal was gated and amplified with a videoamplifier (MC 1445, 3.5 ns), as shown in Figure 3. A transistor was used for adjusting the characteristic impedance to 50 Ω . This circuit was connected just below the photomultiplier (R928) in order to minimize the RFI noise and to improve the time resolution by reducing stray capacitance.

The signal pulse was counted by an NF PC-545A photon counter (10 MHz). The output signal was recorded either on a digital printer or on a strip chart recorder.

EXPERIMENTAL

The 4-methylumbelliferone (4-MU), 2-phenyl-5-(4-biphenyl)-1,3,4-oxadiazole (PBD), and aluminum Calcein Blue (Al-CB) were the laser dyes used. The fluorescence cell for a liquid sample was cylindrical, 6 cm in height and 4 cm in diameter. That for atmospheric NO_2 had several iris diaphragms to reduce the scattered light (14). The fluorescein was obtained from Tokyo Kasei and it was purified from water. The NO_2 was continuously generated by use of a permeation tube (Kitazawa); the air was purified by a silica gel column and a carbon column. The time-resolved spectrum was measured several times and the data were accumulated and replotted manually. Typically it took about 8 h for recording a spectrum.

RESULTS AND DISCUSSION

Wavelength Resolution. The line width of the dye laser is of importance for the measurement of the high-resolution excitation spectrum especially for gaseous molecules. With

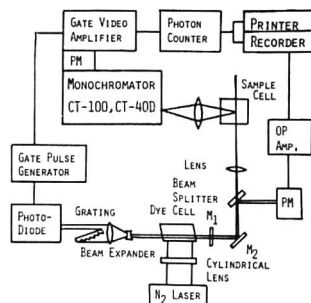


Figure 1. Block diagram of the experimental apparatus

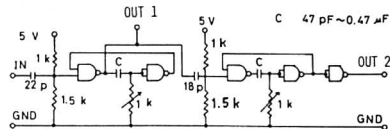


Figure 2. Circuit design of gate pulse generator. The time delay of the output signal (OUT 1) is 0 ns and the gatewidth can be adjusted to 0–1 ms. The time delay and the gatewidth of the output signal (OUT 2) can be adjusted to 40 ns–1 ms and 0–1 ms, respectively. All the measurements were carried out by using the gate pulse (OUT 1) except for the time-profile measurement

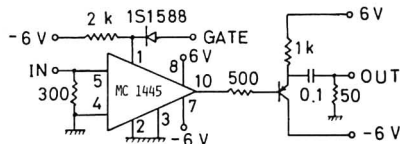


Figure 3. Circuit design of gated videoamplifier. Although the rise times of MC 1445 are 3.5 ns, the gate operation at the first stage in the MC 1445 and the discrimination of the low electron pulse in the photon counter seem to improve the resolution of this system

careful adjustment of the collimating telescope and the grating, a line width of 3.5 pm of full width at half-maximum (fwhm) was obtained for the 4-MU laser. The resolution of the dye laser system was limited by the area of the grating (450 nm/600 grooves \times 30 mm \times 7th order = 0.0036 nm). When the line width was of little importance, the first-order diffraction of the grating was used for obtaining higher output power. The reproducibility of the wavelength was confirmed by measuring the high-resolution excitation spectrum of NO₂ (15).

Time Resolution The time resolution of the photon counting system was evaluated by observing the response of the Raman scattering of water, since it appears instantaneously. The time profile is shown in Figure 4(A). The fwhm of the pulse, hence the time resolution of the total system, was about 5 ns. The pulse width of the dye laser was measured to be 4 ns by a photodiode (0.35 ns) connected to a SS-6200 synchroscopie (1.7 ns); then, the resolution of the detection system was estimated to be about 4 ns. Most of the published pulse-gated photon counting systems have not been so fast. The present apparatus allows nanosecond time-resolved spectrometry and nanosecond lifetime measurements.

Counting Rate. The maximum counting rate of the present system was limited by the counting rate of the photon counter and by the repetition rate of the dye laser. A distinct

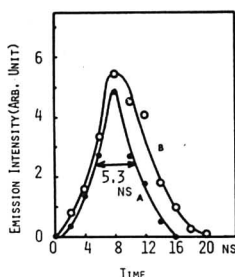


Figure 4. Raman and fluorescence intensity–time profiles. (A) ●—●—● Raman signal of water, (B) O—O—O fluorescence signal of fluorescein in water (10^{-9} M; pH 13, NaOH). The measurement was carried out under the conditions of 0.5 count/pulse in the duration of 0–100 ns. The maximum count rate was 0.02 count/pulse at 8 ns after excitation. Oxygen was not excluded from the sample. Excitation source, PBD laser: λ_{ex} = 377.1 nm, $\Delta\lambda_{ex}$ = 0.4 nm

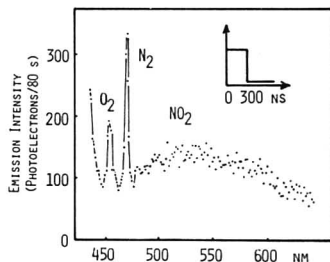


Figure 5. Fluorescence spectrum of atmospheric NO_2 (100 ppm). Fluorescence was monitored in the duration of 0–300 ns. Excitation source, Al-CB laser, $\lambda_{\text{ex}} = 424.3 \text{ nm}$, $\Delta\lambda_{\text{ex}} = 0.25 \text{ nm}$; $\Delta\lambda_{\text{em}} = 5 \text{ nm}$. The ordinate shows the number of photoelectrons per 80 s

advantage of this system is that for long-lived emitters it is possible to detect multiple-photons per laser pulse. When the present circuitry is combined with a low repetition rate N_2 laser, the counting rate is similar to that of a typical TAC system for fluorophors of very short lifetimes (<10 ns). However, when very high repetition rate sources are used, the present circuitry has a distinct advantage since it works at much higher repetition rates than a typical TAC system. Thus, the present circuitry is especially useful for long-lived emitters and for very high repetition rate sources.

Sensitivity. The sensitivity of a fluorometric system can be evaluated on the basis of $A\phi$ at its lower detection limit, where A is the absorbance (ccl) and ϕ the fluorescence quantum yield.

The fluorescence of atmospheric NO_2 is very weak, since the absorptivity and the fluorescence quantum yield are known to be very small; thus, it is difficult to measure the spectrum by a conventional spectrophotometer. The fluorescence spectrum of atmospheric NO_2 (100 ppm) is shown in Figure 5. The broad band in the spectrum is due to fluorescence from NO_2 and the sharp lines are assigned to Raman lines of N_2 and O_2 . A linear analytical curve was observed and the detection limit was determined to be 0.6 ppm, which corresponds to $A\phi = 5 \times 10^{-11}$ (14). The background signal interfered with the detection of yet lower levels of NO_2 ; this may be caused by fluorescence from the aerosol in the air. The detection of the molecular fluorescence at $A\phi = 5 \times 10^{-12}$ would be possible if such background signals could be removed as in the case of low-pressure gaseous

molecules. In such cases, the sensitivity would be limited by the noise from the nitrogen laser (about 1 pulse/100 s).

It would be possible to detect 2×10^{-11} M of fluorescein with a conventional spectrophotometer (Hitachi MPF-4); it corresponds to $A\phi = 2 \times 10^{-7}$. The results show that the present apparatus is more than four orders of magnitude more sensitive than the conventional spectrophotometer. The detection limit of fluorescein with the present system was $A\phi = 6 \times 10^{-10}$; the residual contamination of the solvent water did not allow the yet lower detectivity (16).

Linearity. An important consideration in the operation of the photon counting instrument is the range of linear response to varying intensities of photoemission. If the separation of two photoelectron pulses is very short, it is impossible to resolve individual photon counts. This multiple-photon event leads to saturation of the signal. The relation between the observed counting rate R_o and the actual counting rate R is given by (8),

$$R = -\ln(1 - R_o) \quad (1)$$

A study of the counting rate vs. photoemission intensity confirmed the validity of Equation 1. For qualitative measurements, it is possible to operate this system up to the observed counting rate of 0.5 count/pulse for short-lived emitters (<10 ns). The above correction is required for higher counting rate operation.

Application. The present apparatus has high time resolution, high sensitivity, and high wavelength resolution.

The time profile of photoemission of fluorescein is shown in Figure 4 (B). From the slope of the semilogarithmic plot, the radiative lifetime can tentatively be calculated to 2.4 ns.

The system was used for the ultra-trace analyses of atmospheric NO_2 (14) and of organic molecules in the condensed phase (16, 17).

The electronic excited state of NO_2 was investigated; the high wavelength resolution of the exciting source made it

possible to resolve the rotational levels of the excited state, and the high sensitivity allowed the measurement of the high resolution fluorescence spectrum (15). The time-resolved spectra provided information about the inter- and intramolecular relaxation processes of NO_2 (18).

ACKNOWLEDGMENT

The authors thank H. Kadone and M. Kunitake for their cooperation. The authors also thank R. N. Zare of Stanford University for his critical reading of the manuscript.

LITERATURE CITED

- (1) S. J. Weeks, H. Haraguchi, and J. D. Winefordner, *Anal. Chem.*, **50**, 360 (1978).
- (2) T. F. V. Geel and J. D. Winefordner, *Anal. Chem.*, **48**, 335 (1976).
- (3) J. M. Harris, R. W. Chrisman, F. E. Lytle, and R. S. Tobias, *Anal. Chem.*, **48**, 1937 (1976).
- (4) J. M. Harris and F. E. Lytle, *Rev. Sci. Instrum.*, **48**, 1469 (1977).
- (5) K. G. Spears, L. E. Cramer, and L. D. Hoffland, *Rev. Sci. Instrum.*, **49**, 255 (1978).
- (6) R. S. Meltzer and R. M. Wood, *Appl. Opt.*, **16**, 1432 (1977).
- (7) P. P. Yaney, *J. Opt. Soc. Am.*, **62**, 1297 (1972).
- (8) M. I. Bell and R. N. Tyte, *Appl. Opt.*, **13**, 1610 (1974).
- (9) J. I. Levatter, R. L. Sandstrom, and S. C. Lin, *J. Appl. Phys.*, **44**, 3273 (1973).
- (10) T. W. Hänsch, *Appl. Opt.*, **11**, 895 (1972).
- (11) J. E. Lawler, W. A. Fitzsimmons, and L. W. Anderson, *Appl. Opt.*, **15**, 1083 (1976).
- (12) T. Imasaka, T. Ogawa, and N. Ishibashi, *Bunseki Kagaku*, **26**, 96 (1977).
- (13) F. E. Lytle, *Anal. Chem.*, **46**, 545A (1974).
- (14) N. Ishibashi, T. Imasaka, and T. Ogawa, submitted to *Bunseki Kagaku*.
- (15) T. Imasaka, T. Ogawa, and N. Ishibashi, *J. Chem. Phys.*, in press.
- (16) N. Ishibashi, T. Ogawa, T. Imasaka, and M. Kunitake, unpublished data.
- (17) T. Imasaka, H. Kadone, T. Ogawa, and N. Ishibashi, *Anal. Chem.*, **49**, 667 (1977).
- (18) T. Imasaka, T. Ogawa, and N. Ishibashi, submitted to *Chem. Phys.*

RECEIVED for review July 7, 1978. Accepted December 4, 1978. This research was partially supported by a Grant-in-Aid for Scientific Research from the Ministry of Education (Grant No. 211204) and by a Fund Incorporated for Technological Development for Abandonment and Removal of NO_x from Steel Plants.

Vapor Phase Determination of Blood Ammonia by an Optical Waveguide Technique

P. L. Smock¹

Department of Chemistry, University of Dayton, Dayton, Ohio 45469

T. A. Orofino and G. W. Wooten*

Monsanto Research Corporation, 1515 Nicholas Road, Dayton, Ohio 45407

W. S. Spencer

St. Elizabeth Medical Center, Dayton, Ohio 45407

A technique utilizing light attenuation in optical waveguides is described for vapor-phase determination of ammonia in blood and serum. The general approach is applicable to clinical determinations normally carried out in the vapor phase and, with modifications, also to liquid-phase analyses. Results are examined for linearity and correlation with a reference method: (1) a linear relationship exists between absorbance and blood ammonia concentration in the clinically useful range of 0–400 $\mu\text{g/dL}$; (2) comparison with the reference method showed a correlation coefficient of 0.92. Preliminary results are also reported for application to determination of blood urea nitrogen, creatinine, and total amino acids.

The purpose of this communication is to report some results on development of a new technique for determination of ammonia levels in whole blood. The analytical procedure combines collection of ammonia from the vapor phase with colorimetric determination of its concentration, according to the response of a diffusion-controlled reaction involving ninhydrin at the surface region of an optical waveguide. The optical technique has been investigated for other applications (1, 2). In the context of the present investigations, results reported here indicate the technique may be useful for a number of whole blood and serum analyses.

Blood ammonia levels are of interest clinically because of the relationship between elevations in venous and arterial concentrations of this substance and diseases of the liver. The liver is the site for the most important detoxification process for ammonia, wherein it is transformed into a few usable synthetic products and the waste product urea (3). Hyperammonemia and the associated cerebral encephalopathy arise when abnormalities of the liver exist which prevent the transformation reactions from occurring. The problems associated with breakdowns in this detoxification process include the hepatic coma syndrome, cirrhosis of the liver, Reyes Syndrome, and the rare infant abnormality termed hereditary hepatic orinithine transcarbamalase (E.C. 2.1.3.3) deficiency (3–6).

Modern techniques for blood ammonia determination include use of ion-exchange resins to absorb ammonium ions from plasma (7–12) followed by one of the several common colorimetric methods for ammonia determination. Other recent approaches include use of ammonia-specific ion electrodes (13, 14) and the enzymatically regulated NAD-

NADH reaction followed by changes in sample absorbance at 340 nm (15) or NADH fluorescence (16). All the methods in this category offer great sensitivity, but their complexity can detract from utility in routine analyses.

Blood ammonia is often determined clinically by the Seligson technique (17, 18), which involves adding potassium carbonate to a blood sample to release the ammonia, collecting the gas on a rod dipped in sulfuric acid, and determining the product of a colored reaction using Nessler's reagent. This determination generally requires an hour to complete and involves a number of steps in collecting, extracting, and reacting the ammonia. The absorbance of the final colored reactant is a function of the blood ammonia concentration. The optical waveguide method presently described for determination of blood ammonia would simplify some of the steps involved in the Seligson procedure.

ANALYTICAL PRINCIPLE

The basis for the analytical technique investigated in this work is the partial attenuation of a light signal traversing a cylindrical optical waveguide by successive total internal reflections. The waveguide in this case is a quartz rod 2 cm in length and 0.1 cm in diameter with square, polished ends. The rod is uniformly coated, except at the ends, with a suitable polymer film which is transparent and contains a dispersion of a chemical reactive toward the component of interest (ammonia). The coatings are conveniently applied by casting from solution, followed by drying and trimming of the waveguide ends. In the present application, transport of the component into the coating is from the vapor phase surrounding the waveguide.

The reaction between the component and the coating chemical is selected to produce an optical change in the coating. In the ammonia application, the reactive chemical incorporated is ninhydrin and the optical change is generation of the wavelength specific, characteristic Ruhemann Purple color. However, in general, the principle of the method also is served by incurring changes in coating refractive index or turbidity.

The analytical detection method is shown in Figure 1, where the basic principle of total internal reflection responsible for propagation of light in optical fibers or other waveguides is illustrated. A longitudinal cross-section of a coated cylindrical waveguide is shown, in which the refractive index of the transparent coating n_2 slightly exceeds that of the glass or quartz cylinder n_1 . A light ray entering the flat, polished end of the cylinder from the air (n_0) is refracted somewhat upon penetrating the coating. At the coating-air interface, conditions are present to cause total internal reflection, according to the optical laws of refraction and reflection. Total reflection

¹ Present address, E. I. du Pont de Nemours & Co., Inc., Glasgow, Del.

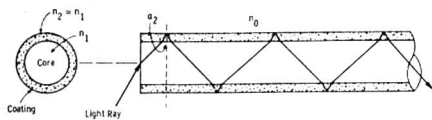


Figure 1. Light propagation in the optical waveguide

(less interface losses due to scattering) occurs for all angles greater than the critical angle α_2 given by the relationship

$$n_2 \sin \alpha_2 = n_0 \sin 90^\circ \approx 1 \quad (1)$$

If the critical condition is met, the ray continues to propagate along the length of the rod by successive internal reflections. In the process, the ray passes repeatedly through the coating and is attenuated according to the optical density of the coating. In practical application, light from a polychromatic source is passed through suitable lenses, masks, and filters to isolate the desired absorption wavelength and to launch a converging, hollow cone of illumination into one face of the waveguide. The intensity of the light signal traversing the length of the waveguide is measured photometrically.

If the concentration c of color bodies absorbing at some wavelength with extinction coefficient K is present in the coating, the intensity of light traversing the waveguide before (I_0) and after (I) color formation will be given to a first approximation by the relationship

$$A = -\log(I/I_0) = Kbc \quad (2)$$

where A is absorbance and b is total path length through the coating. If, further, the concentration accumulated is the result of a time exposure period of the coated waveguide, t , to a steady vapor concentration, C (of ammonia), c becomes a function of both t and C . In the simplest case, direct proportionality prevails and one finds a relationship of the form

$$A = K'Ct \quad (3)$$

Here, K' is a constant most conveniently assigned from experiments involving controlled vapor exposure. Its value is determined by the particular parameters of the diffusive and chemical reaction processes involved in the mass transport sequence. Equation 3 provides a means of determining C by optical measurements before and after exposure of the sensitized waveguide to an ammonia atmosphere, under controlled conditions.

From the general principles outlined, it is evident that a number of conditions are important in development and application of a useful system. These include: (1) ability to reproducibly release from the sample of interest and maintain in the vicinity of the waveguide the component to be measured; (2) selection of waveguide coatings which are transparent, compatible with the reactant and its products, and which provide a medium of low chemical potential to collect the component diffusing in from the surroundings; (3) specificity and stability of the light-attenuating reaction product; and (4) sufficient dynamic range, precision, and accuracy of the overall system for analytical use.

EXPERIMENTAL

Apparatus. A simple laboratory apparatus (Figure 2) was designed and fabricated to determine the feasibility of applying the optical waveguide approach to blood ammonia and ammonia-related determinations.

The reaction is carried out in a 50-mL Pyrex flask fitted with a side tube through which blood sample and reagents are admitted. A tapered Teflon plug with an integral clamping arrangement serves to seal the reaction vessel and hold the waveguide in place during exposure. The reaction flask is very similar to that used in the Seligson method.

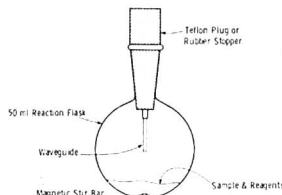


Figure 2. Apparatus for determination of blood ammonia by the optical waveguide technique



Figure 3. Rod holder for dip coating with beaker of polymer solution

Other equipment required for the measurements are the cylindrical quartz rods (Thermal American Fused Quartz, Montville, N.J.); a waveguide holder for the coating process with machined orifices and set screws as shown in Figure 3 (Monsanto Research Corporation); and a suitable dip-coating apparatus (Fisher-Payne). The optical-electronic device for measurement of waveguide transmission before and after exposure has been described elsewhere (1).

Materials and equipment used for preparation of coating solution include poly(vinyl alcohol) (Grade 92-125 [Elvanol] E. I. du Pont de Nemours & Co., Inc.), ammonia-free water, poly(vinyl pyrrolidone) (Monsanto Company), ninhydrin (Pierce Chemical Company, Rockford, Ill.), magnetic stirrer-heater, water bath, digital pH meter, and Gardner bubble viscometer.

Waveguide Preparation. In preparing the waveguides for use prior to the dipping procedure, they must first be cleaned in a chromic acid solution, thoroughly rinsed in water, and dried with a methanol rinse. The waveguides should then be microscopically inspected to ensure that no chipped ends or grooves are present.

Polymer solutions are prepared by pre-wetting 10 g of polymer in 100 mL of ammonia-free water, slowly heating to 80 °C while continuously stirring the solution, then cooling to 40 °C. Ninhydrin solutions in the proper weight percentage are added at this point, the solution is stirred to uniformity, and characterization of the solution in terms of pH, viscosity, and color is completed. Solutions are stored covered until use, to eliminate chance contamination by ammonia vapor.

Once the coating solution has been prepared, the waveguides are inserted into the holder, and, using the Fisher-Payne dip coater as a device to ensure an even pull from solution, they are coated twice—once from each end.

After coating, the polymer patches covering the ends of the rods are carefully removed and the waveguides are then ready for the reaction sequence.

Analytical Development. The basic analytical procedure involved in both development and application of the coated

Table I. Recommended Reaction Conditions for Blood Ammonia Determination

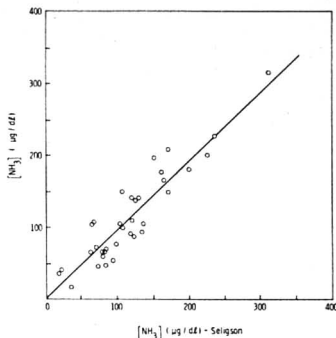
Waveguide Characteristics	
(a) waveguide dimensions:	2 cm length \times 0.01 cm diameter
(b) waveguide characteristic:	smooth surface, polished flat ends, no chips
(c) concentration:	30% ninhydrin in coating, by wt, based on polymer
(d) coating:	double-dipped coating process, coating solution viscosity = 12.9 Stokes (Gardner Bubble Viscometer), coating thickness: 0.004 cm
Reaction Solution	
(a) 1 mL sample	
(b) 1 mL borate/OH buffer	
(c) 1 mL ammonia-free water	
Reaction Variables	
(a) pre-humidification of coated waveguides:	2 h
(b) reaction time:	30 min
(c) reaction temperature:	$25 \pm 1^\circ \text{C}$
(d) post-reaction color development:	15 min

waveguide method for blood ammonia comprised three steps: initial measurement of waveguide optical transmission at selected wavelengths of incident light; exposure of the waveguide to a vapor-phase source of ammonia generated from the blood or serum sample under controlled conditions; final measurement of waveguide absorbance and interpretation of results. In the development stage, it also was necessary to investigate the role of various components of the system in determining quantitative analytical response.

Selection of a suitable coating material for the waveguides and incorporation of the active ninhydrin reagent were important considerations. Criteria for the coatings included optical clarity, physical integrity, compatibility with the reagents added, affinity for the moisture needed to sustain the reaction, and the consistency of analytical response. A number of candidates were investigated, including poly(vinyl acetate), poly(vinyl alcohol), and physical blends. A high molecular weight poly(vinyl alcohol), Elvanol 92-125, was finally selected, as it performed well under high humidity conditions. Coating integrity was maintained even after a 5-h exposure of 100% water vapor. Data on replicate analyses for ammonia standards in the 0 to 300 $\mu\text{g}/\text{dL}$ range showed good levels of precision.

The ionic nature of the ammonia-ninhydrin reaction indicated that the water content of the polymer coating could influence reaction sensitivity. This was found to be one of the most important effects to be considered, in that the amount of water incorporated into the polymer film at the time of reaction had a profound effect on reaction sensitivity and reproducibility. This was quantitatively demonstrated by exposing coated rods for varying time periods to 100% relative humidity environment, previous to reaction with 100, 200, and 300 $\mu\text{g}/\text{dL}$ aqueous ammonium sulfate standards. The exposure times indicated that an equilibrium state for coating water content, with respect to the water vapor content of the pre-treatment tank and reaction vessel, is reached in about 3 h pre-treatment time. Plotting these same data in standard curve form indicated that a reproducible absorbance value for a given standard appeared with 2 to 3 h prior exposure. Thus, prehumidification of the waveguide was adopted as part of the standard procedure.

The ammonia ninhydrin reaction also depends upon pH, with respect to the optimum value for the formation of the Ruhemann Purple chromophore. After much experimentation, it was determined that the addition to the polymer coating solution of potassium hydrogen phthalate, a water-soluble and polymer-compatible buffering agent, induced a pH of 5.0 in this solution, earlier determined as optimum for the reaction in the work of Stein and Moore (19). Rods coated with this solution and properly humidified always developed a purple color on reaction with ammonia, indicating the formation of the desired Ruhemann Purple.

**Figure 4. Correlation curve for blood ammonia: optical waveguide technique vs. modified Seligson**

Analytical Procedure. Recommended reaction conditions for the blood ammonia determination which we arrived at from our studies are summarized in Table I.

The procedure begins with measurement of optical transmission in the pre-humidified waveguide. To initiate the reaction in the vessel of Figure 2, 1 mL of sample (standard or unknown) containing the ammonia is pipetted into the flask. To this is added by pipette 1 mL each of the alkalinizing agent and ammonia-free water. The solution is stirred throughout the reaction by means of a small magnetic stirring bar in the reaction vessel. Temperature is maintained throughout the process by a suitable water or air thermostat. After reaction, the waveguide is removed from the vessel, allowed to complete post-reaction, and again optically characterized for transmission.

RESULTS

The optical waveguide technique was applied to the measurement of ammonia levels in a series of whole blood samples obtained from St. Elizabeth Medical Center, Dayton, Ohio. In these analyses, pooled samples obtained from routine daily clinical services were utilized. The specific technique outlined in Table I was employed for all experiments.

A batch of coated waveguides was prepared and first employed in construction of a standard curve based on replicate measurements on ammonium sulfate standards at the 0, 100, 200, 400, and 500 $\mu\text{g}/\text{dL}$ levels. Within-run precision was represented by a relative standard deviation of 10-12%.

Duplicate analyses of ammonia concentration $C \mu\text{g}/\text{dL}$ by the waveguide method and by the Seligson technique were next carried out on 35 pooled whole blood samples. The comparison is shown in Figure 4, and corresponds to the linear relationship

$$C_w = 0.984 C_s + 0.963$$

with correlation coefficient equal to 0.92. Here, the subscripts w and s refer to the waveguide and Seligson methods, respectively.

RELATED APPLICATIONS

In investigation of related clinical applications for the optical waveguide technique, we determined that basically the same system and methodology used for blood ammonia could be employed for other measurements as well. These involve specific enzymatic reactions liberating ammonia as an end product. The tests include determinations for blood urea nitrogen (BUN), serum CPK activity, creatinine, and L-amino acids.

Blood urea nitrogen was selected for the first study because this constituent is found in fairly high concentrations, and

it is a common clinical test. The analytical scheme that is commonly used for BUN is its reaction with urease to give ammonia. Subsequent reactions may be selected for analyzing the ammonia produced by the enzymatic reaction. In our approach, BUN is reacted with urease in the usual manner, this reaction being carried out in the blood ammonia apparatus at an incubation temperature of 37 °C. A 100- μ L sample proved convenient for normal levels in blood. After a suitable incubation period has transpired, an alkalinizing agent is added to the reactants and the sensitized waveguide is placed in the reaction chamber. The method from this point on is the same as for blood ammonia.

A procedure for determining CPK activity and creatinine was also examined briefly. It was similar to that for BUN insofar as a reaction between creatinine and creatinine deaminase is incubated at 37 °C, gaseous ammonia is liberated by the addition of an alkalinizing agent, and reaction occurs with the rod. It appeared that optimization of reaction parameters could make this a viable analytical method for clinical tests.

Like BUN, L-amino acids constitute another reaction of considerable clinical interest. In this case, the amino acids react with L-amino acid oxidase to form ammonia which again can be measured by the optical waveguide approach and related to amino acid concentration. This scheme was tested with different concentrations of L-leucine (100, 200, and 300 μ g/dL). Again, no serious attempts were made to fully optimize reaction conditions but rather to demonstrate the reaction as a feasible adjunct to our ammonia approach. Measured absorbances were found to follow the different amino acid concentrations.

It should be noted, in connection with prospects for these additional tests, that in both the creatinine series and in the amino acid determination, parallel runs for blood ammonia must be made on samples of interest and subtracted from the values obtained with the enzymatic reactions. There is no problem with BUN since it is present at a much higher concentration than blood ammonia. This is not the case with creatinine and amino acids.

With regard to sensitivity of the optical waveguide method, some experiments done on scale-down of the blood ammonia technique also are of interest. We found that use of the same coated waveguides described earlier also gave a practical level of response in small reaction vessels containing 100 μ L of blood or standard sample. A suitable reaction time was 30 min. This

microscale test would find value in blood ammonia analyses on infant heel-stick samples.

ACKNOWLEDGMENT

The authors acknowledge the contributions of several individuals and key personnel at institutions supporting this work. Edgar E. Hardy, Director of the Monsanto Research Corporation, Dayton Laboratory is one of the inventors of the optical waveguide technique described and was instrumental in supporting the investigation of clinical applications. David S. Auld and Kenneth Falchuk of the Biophysics Research Laboratory, Harvard Medical School, originally suggested the blood ammonia test and the possibility of related ammonia-readout applications.

LITERATURE CITED

- (1) E. E. Hardy, D. J. David, N. S. Kapany, and F. C. Unterleitner, *Nature (London)*, **257**, 666-667 (1975).
- (2) D. J. David, M. C. Wilson, and D. S. Ruffin, *Anal. Lett.*, **9**(4), 389-404 (1976).
- (3) C. H. Glips, *Folia Med. Neerl.*, **13**, 14-26 (1970).
- (4) I. Davidson, and J. B. Henry, Ed., "Clinical Diagnosis by Laboratory Methods", 15th ed., Saunders, Philadelphia, Pa. 817-818 (1974).
- (5) D. S. Sanih, T. T. Fulton, and H. McCullough, *J. Clin. Pathol.*, **23**, 715-719 (1970).
- (6) G. J. Gabuzda, *Gastroenterology*, **53**, 806-808 (1967).
- (7) D. G. Dienst, *J. Lab. Clin. Med.*, **58**, 149-155 (1961).
- (8) G. R. Kingsley, H. S. Tager, and R. P. MacDonald, Ed., "Standard Methods in Clinical Chemistry", Academic Press, New York, Vol. 6, 1970, pp 115-125.
- (9) J. C. Fenton, *Clin. Chim. Acta*, **7**, 163-175 (1962).
- (10) G. E. Miller and J. D. Rice, Jr., *Am. J. Clin. Pathol.*, **39**, 97-103 (1963).
- (11) F. L. Forman, *Clin. Chem. (Winston-Salem, N.C.)*, **10**, 497-508 (1964).
- (12) V. G. Oberholzer, K. B. Schwarz, C. H. Smith, D. N. Dietzler, and T. L. Hanna, *Clin. Chem. (Winston-Salem, N.C.)*, **22**, 1976-1981 (1976).
- (13) H. F. Proelss and B. W. Wright, *Clin. Chem. (Winston-Salem, N.C.)*, **19**, 1162-1170 (1973).
- (14) N. J. Park and J. C. B. Fenton, *J. Clin. Pathol.*, **26**, 802-804 (1973).
- (15) H. A. M. Jacobs and F. M. F. G. Othlis, *Clin. Chim. Acta*, **43**, 81-86 (1973).
- (16) R. J. Spooner, P. A. Toseland, and D. M. Goldberg, *Clin. Chim. Acta*, **65**, 47-55 (1975).
- (17) D. Seligson and K. Hirahara, *J. Lab. Clin. Med.*, **49**, 962-974 (1957).
- (18) H. Conn and S. Meites, Ed., "Standard Methods of Clinical Chemistry", Academic Press, New York, Vol. 5, 1965, pp 43-54.
- (19) W. H. Stein and S. Moore, *Quant. Biol.*, **14**, 179-190 (1949).

RECEIVED for review September 13, 1978. Accepted January 5, 1979. This work was presented in part at the 29th National Meeting of the American Association of Clinical Chemists, Chicago, Ill., July 1977 (Paper No. 295). The generous support of the St. Elizabeth Medical Center provided one of us (P.L.S.) during the clinical testing portion of this work also is gratefully acknowledged.

Effect of Sample Thickness on the Magnitude of Optoacoustic Signals

M. J. Adams,* G. F. Kirkbright, and K. R. Menon

Chemistry Department, Imperial College of Science and Technology, London SW7 2AZ, United Kingdom

A study has been undertaken of the effects of sample thickness of thin polymer films on the magnitude of optoacoustic signals observed from these materials on irradiation with modulated ultraviolet radiation. In the ultraviolet region, the samples may be considered optically opaque. The results obtained are in good agreement with published theoretical predictions.

In recent years, there has been revived interest in the study of the optoacoustic effect and, in particular, its applications

for the examination of solid and liquid samples. In the optoacoustic effect, modulated radiant energy absorbed by the sample leads to an increase in the internal energy of the system, and subsequent deexcitation provides an increase in the temperature which may be monitored as the periodic pressure change in the gas surrounding the sample using a microphone transducer. Several workers have described spectrometers equipped with wavelength scanning facilities which enable absorption spectra to be recorded (1-3); a number of similar commercial systems have also become available recently. The technique may be considered a ra-

diometric method and employed as a spectrophotometric means of analysis (4).

Theoretical interpretations of the optoacoustic effect and its applications to the study of condensed phase sample types have been discussed by a number of workers (5-8); all agree concerning the fundamental parameters which govern the magnitude of the observed signals. Unfortunately, however, to date there have been few published results to support the theoretical interpretations; in particular, there is a dearth of results relating to the quantitative interpretation of the effects observed. Only absorbed radiation may contribute to the production of an optoacoustic signal, and the important sample characteristics determining the magnitude and nature of the signal are the optical absorption coefficient of the material studied at the wavelength of the incident radiation, the efficiency of internal radiationless deexcitation, and the thermal, heat-transfer coefficients (in particular the thermal diffusivity) for the material.

In this communication, we wish to demonstrate that the quantitative predictions for the dependence of the magnitude of the optoacoustic effect on the sample parameters can be shown to be valid for optically opaque samples of polyester films of differing thickness.

EXPERIMENTAL

Apparatus. The amplitude of the optoacoustic signals obtained from the polymer samples examined was monitored with the aid of a double-beam optoacoustic spectrometer operated in the single-beam, uncorrected mode. The constructional details and performance characteristics of this instrument have been described elsewhere (1). Continuum radiation from a 300-W xenon arc source was focused, through a variable speed rotating sector, at the entrance slit of an F/4 grating monochromator. The dispersed radiation from the exit slit entered the optoacoustic cell via a concave folding-mirror. The working spectral range of the spectrometer was ca. 250 to 2500 nm. The aluminum optoacoustic cell was fitted with a 20-mm diameter silica entrance window and a similar silica plate was employed as the sample tray. The total internal cell volume was ca. 1 cm³ and a sensitive capacitor microphone (Bruel and Kjaer Type 4166) was employed as the pressure transducer. The signal at the microphone was monitored with the aid of a lock-in amplifier, and the sample signal amplitude was displayed as a function of the wavelength of the incident radiation on a conventional potentiometric chart recorder.

Procedure. A schematic diagram demonstrating the mounting of the polymer film samples is shown in Figure 1. Disks of polymer film, 18 mm in diameter, were cut from the samples and fixed with the aid of double-sided adhesive tape to the underside of the thin-walled, highly polished stainless-steel ring which was mounted together with the sample onto a similar thin-walled ring contained within the sampling tray. This arrangement was sealed by means of locking nuts inside the optoacoustic cell and the unnormalized spectrum of each polymer sample was recorded in the wavelength interval 250 to 350 nm. The magnitude of the signal at the peak absorption wavelength of 300 nm was measured from the chart recorder display. The polyester film samples examined were all of identical composition and of thickness, 6, 12, 25, 50, 125, and 250 × 10⁻⁴ cm. Each sample was examined at modulation frequencies of 10, 30, 120, and 280 Hz.

Transmission spectra of the samples in the ultraviolet region were obtained with the aid of a conventional UV/visible spectrophotometer.

RESULTS AND DISCUSSION

Rosenzweig and Gersho (7), have developed a theoretical interpretation of the optoacoustic effect observed for solid samples in terms of the optical absorption coefficient of the sample and its heat transfer characteristics. For sinusoidal modulated radiation incident at the sample, the pressure variation in the gaseous atmosphere within the optoacoustic

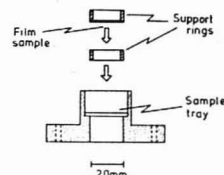


Figure 1. Sample holder and method employed to retain the polymer film.

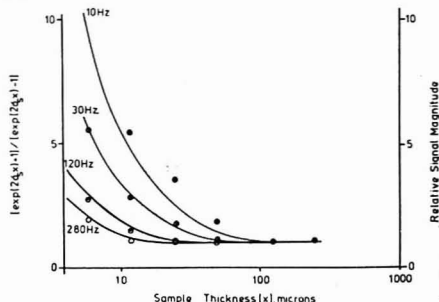


Figure 2. The function $[\exp(2\sigma_a x) + 1] / [\exp(2\sigma_a x) - 1]$ vs. x (solid lines) and the experimentally determined results for the relative optoacoustic signal magnitude for different values of sample thickness, x , as a function of modulation frequency: (a) ●, 10 Hz; (b) ○, 30 Hz; (c) ⊙, 120 Hz; (d) ○, 280 Hz. (The theoretical curves assume a value of 10^{-3} cm² s⁻¹ for the thermal diffusivity of the polymer samples)

Table I. Thermal Characteristics for Nitrogen and Polyester Samples^a

	air (N ₂)	polyester
α (cm ² s ⁻¹)	200×10^{-3}	1.0×10^{-3}
k (cal. s ⁻¹ cm ⁻¹ K ⁻¹)	6.4×10^{-5}	3.4×10^{-4}
A_1/ω (s ² cm ⁻¹)	1.58	22.4
$g = \frac{K_g A_g}{K_s A_s} = \frac{K_b A_b}{K_s A_s} = 1.33 \times 10^{-2}$		

^a Thermal data taken from ref. 9.

cell, P , is shown to be:

$$P = \frac{AB\beta}{k_a g (\beta^2 - \sigma_a^2)} \quad (1)$$

where β is the optical absorption coefficient (cm⁻¹) of the material under study and k_a is its thermal conductivity.

$$\sigma_a = (1 + j)a_a \quad (2)$$

a_a and a_g are thermal damping functions of an alternating temperature wave passing through the sample and gas respectively and are given by:

$$a_i = \left(\frac{\omega}{2\alpha_i} \right)^{1/2} \quad (3)$$

with ω the frequency of the wave (i.e., the modulation frequency) and α_i the thermal diffusivity of the material.

In Equation 1, A is a constant factor which is dependent upon the experimental arrangement and is proportional to the incident radiant energy at the sample surface and the ambient pressure within the cell.

$$B = \frac{(r-1)(b+1)\exp(\sigma_a x) - (r+1)(b-1)\exp(-\sigma_a x) + 2(b-r)\exp(-\beta x)}{(g+1)(b+1)\exp(\sigma_a x) - (g-1)(b-1)\exp(-\sigma_a x)} \quad (4)$$

B is a complex function for the system and may be expressed as in Equation 4 where x is the thickness of the sample and the other functions are given by,

$$r = \frac{(1-j)\beta}{2a_s} \quad (5)$$

$$b = \frac{k_b a_b}{k_s a_s} \quad (6)$$

$$g = \frac{k_g a_g}{k_s a_s} \quad (7)$$

The subscript "b" denotes the backing material of the sample and the product $k_b a_b$ may be considered as a thermal flux coefficient for the material.

To simplify Equation 1, it is necessary to apply assumptions which reduce Equation 4. The assumptions employed in this study of the magnitude of the optoacoustic signals derived from polymer films may be considered.

Conventional transmission spectroscopy studies were undertaken for the thin film samples and these showed that even the thinnest material, of 6×10^{-4} cm thickness, exhibited an optical density greater than 3.0 at 300 nm. Thus at this wavelength the samples may be considered opaque and β is thus very large, i.e., $\exp(-\beta x) \approx 0$ and $r \gg 1$.

The experimental conditions employed, and shown in Figure 1, ensure that the backing material is air and, hence, identical with the atmosphere above the sample top surface, i.e., $b = g$. Typical thermal characteristics of polymers and air (nitrogen) are presented in Table I and allow us to make the simplification that b and $g \ll 1$ (9).

With these assumptions we may simplify Equation 4 to provide,

$$B = r \frac{\exp(\sigma_s x) + \exp(-\sigma_s x)}{\exp(\sigma_s x) - \exp(-\sigma_s x)} \quad (8)$$

which may be rearranged,

$$B = r \frac{\exp(2\sigma_s x) + 1}{\exp(2\sigma_s x) - 1} \quad (9)$$

Substituting Equation 9 into Equation 1 and applying the assumptions yields,

$$P = \frac{A(1-j)}{2a_s k_s} \frac{\exp(2\sigma_s x) + 1}{\exp(2\sigma_s x) - 1} \quad (10)$$

With the aid of Equation 10, we may examine the effect of variation in sample thickness, x , on the magnitude of the optoacoustic signal. Examination of Equations 9 and 10 indicates that for low values of x (i.e., for thermally thin samples) the signal magnitude should decrease with increasing thickness and reaches a limiting value when B , as expressed in Equation 9, approximates to r ; at high values of x (thermally thick samples), it should become independent of sample thickness.

This manner in which the signal, as given by $[\exp(2\sigma_s x) + 1] / [\exp(2\sigma_s x) - 1]$, should vary with the thickness, x , of the sample is shown in Figure 2 for a variety of modulation frequencies. Also shown in Figure 2 are the experimentally determined data. For comparison purposes, the relative signal magnitude data is presented, i.e., the 1/10 dependence predicted at large values of x in Equation 10 has been avoided by normalization for modulation frequencies. The two cases, thermally thin and thermally thick regions, are clear from these results and good agreement is observed between the theoretical curves predicted from Equations 9 and 10 and the experimental results determined from the examination of the

optically opaque, thin polymer films.

It is interesting to consider the mechanisms of the heat-flow within the sample and cell in explaining the nature of the data shown in Figure 2. For any selected and fixed frequency of modulation we may assign to the sample under study a "thermal diffusion length" μ_s , i.e., a distance within the sample, from its upper surface, from which an alternating thermal signal may reach the upper surface without appreciable attenuation. Rosenzweig and Gersho (7) have assigned a value of $1/a_s$ ($= \mu_s$) to this active depth. For an optically opaque sample, any increase in sample thickness has a negligible effect on the amount of radiant energy absorbed and, providing the sample thickness is less than μ_s , an increase in thickness merely serves to increase the mass of the sample which may respond to the alternating thermal wave produced in the sample. Indeed, to a first approximation, we may expect the thermal wave amplitude, hence the optoacoustic signal magnitude, to be inversely proportional to the sample thickness for a constant sample area, for values of thickness, x , less than μ_s . When the sample thickness is greater than μ_s , however, the sample mass, or volume, responding to the periodic thermal wave is constant as negligible alternating thermal energy is transferred to a depth greater than μ_s by definition of μ_s . Also, as μ_s is a function of modulation frequency, decreasing with increasing frequency, the point of inflection of the two curves (inversely proportional to thickness and independent of sample thickness) moves to lower values of thickness with increasing modulation frequency.

A further observation may be made concerning Equation 10. At high values of $\exp(2\sigma_s x)$, the optoacoustic signal magnitude is independent of sample thickness, as discussed above, and Equation 10 reduces to

$$P = \frac{A(1-j) \mu_s}{2a_s k_s} \quad (11)$$

which is identical with the expression derived by Rosenzweig and Gersho (7) for the case of the optically opaque, thermally thick sample.

CONCLUSION

Unlike conventional spectrophotometric measurements by transmission, an optoacoustic measurement depends not only on the optical properties of the sample but also on its thermal characteristics. For the samples described in this work, little quantitative information concerning the samples could be gained from their ultraviolet absorption spectra because of their high opacity in this spectral region, even with relatively thin samples. The optoacoustic results, however, show very interesting trends with sample thickness and advantage may be taken of the high opacity in the ultraviolet. Furthermore, as the optoacoustic effect is concerned with a periodic thermal wave, control of the thermal diffusion length may be achieved by suitable control of the frequency of modulation of the incident radiation.

The experimental data presented above agree well with the theoretical treatment derived from Rosenzweig and Gersho (7), and we believe that it serves to illustrate the general applicability of their treatment of the optoacoustic effect. Our experimental results also show that for any thickness of sample above the thermal diffusion length, the signal magnitude is $\propto 1/W$. It may be observed from our results that the greatest errors arise at low modulation frequencies (10 Hz) and for thin samples (6×10^{-4} cm thickness). Although decreasing the frequency of modulation provides for an increase in signal magnitude (see Equation 11), at frequencies below ca. 20 Hz the experimental system employed for the studies described above suffers increasingly from "1/f" noise. Also, with thin

samples (less than ca. 10^{-3} cm) the sample arrangement discussed may give rise to erroneous results by vibration of the sample due to the enclosed air volume below the sample.

With the increasing interest being shown in optoacoustic spectrometry for the examination of condensed phase samples not easily studied by conventional techniques, more quantitative data are certain to be produced to test the current theoretical treatments and expand the currently limited knowledge of the interrelation between the optical characteristics and thermal transfer properties of a wide variety of materials.

ACKNOWLEDGMENT

We are grateful to I.C.I. Ltd. for the provision of a studentship to one of us (K.R.M.) and for provision of the samples

of polyester film employed in the studies described above.

LITERATURE CITED

- (1) M. J. Adams, B. C. Beadle, and G. F. Kirkbright, *Analyst (London)*, **102**, 569 (1977).
- (2) W. R. Harshbarger and M. B. Robin, *Acc. Chem. Res.*, **6**, 329 (1973).
- (3) A. Rosencwaig, *Anal. Chem.*, **47**, 592A (1975).
- (4) M. J. Adams, J. G. Highfield, and G. F. Kirkbright, *Anal. Chem.*, **49**, 1850 (1977).
- (5) M. J. Adams and G. F. Kirkbright, *Analyst (London)*, **102**, 678 (1977).
- (6) J. G. Parker, *Appl. Opt.*, **12**, 2974 (1973).
- (7) A. Rosencwaig and A. Gersho, *J. Appl. Phys.*, **47**, 64 (1976).
- (8) A. Hordvik and L. Skolnik, *Appl. Opt.*, **16**, 2919 (1977).
- (9) L. R. Touloukian, R. W. Powell, C. Y. Ho, and M. C. Nicolaou, "Thermal Diffusivity", IFI/Plenum, New York, 1973.

RECEIVED for review June 29, 1978. Accepted December 26, 1978.

Determination of Trace Elements in Light Element Matrices by X-ray Fluorescence Spectrometry with Incoherent Scattered Radiation as an Internal Standard

Robert D. Giauque,* Roberta B. Garrett, and Lilly Y. Goda

Energy and Environment Division, Lawrence Berkeley Laboratory, University of California, Berkeley, California 94720

A method for the direct determination of trace elements in light element matrices is described. It takes advantage of the fact that the incoherent mass scattering coefficient for 17.4 keV Mo K α radiation is relatively constant for the elements Li ($Z = 3$) \rightarrow Ca ($Z = 20$). Consequently, incoherent scattered Mo K α excitation radiation, corrected for matrix absorption, can serve as an internal standard which compensates for variations in sample mass, X-ray tube output, and sample geometry. Samples of ~ 0.5 g are prepared in the form of thin specimens (~ 0.08 cm thick) in a cell between two 0.0006-cm thick polypropylene windows. Standardization for most elements is achieved using standard aqueous solutions diluted to ~ 100 ppm. Data obtained from simultaneous transmission measurements for several X-ray energies are used to calculate matrix absorption corrections. For 15-min analysis periods, results are typically accurate to within $\pm 10\%$ when X-ray counting statistics are not the limiting factor. Sensitivities of 2 ppm or better are realized for 16 of the 22 elements determined (Ti \rightarrow Zr, Hg, Pb, Th, and U).

The determination of trace elements in light element matrices by X-ray fluorescence spectrometry requires the use of appropriate techniques to compensate for matrix absorption effects. Matrix enhancement effects usually are minor or negligible.

The literature contains a number of methods or approaches to deal with matrix absorption effects. In this paper we will limit our discussion to reported methods which have used scattered X-rays as an internal standard. These methods require minimum sample preparation and do not necessitate prior knowledge of specimen major element concentrations. Andermann and Kemp (1) initially showed that scattered X-rays could serve as internal standards to make matrix absorption corrections. Cullen (2) determined Ni, Cu, and

Ag in acid solutions using coherently scattered W L X-rays as an internal standard. Dwiggins (3) has measured both coherent and incoherent scattered W L X-rays to predict spectral background and matrix corrections for the determination of several elements in organic samples. A prerequisite is that the elements have X-rays of energy near those of the scattered X-rays. Reynolds (4) and, more recently, Feather and Willis (5) have used incoherent scattered X-rays to compensate for matrix absorption in analysis of trace elements in thick geochemical specimens. This approach is not applicable to multielement trace analysis of light element matrices because of the amount of material required to attain infinite thickness for all radiations of interest. Furthermore, it is preferable to use thin specimens, because higher peak to background ratios and, thus, improved sensitivities, are achieved. Nielson (6) has developed a numerical method for computing matrix effects in which the ratio of coherent to incoherent scattered X-rays is used to estimate the light element content in pressed disks of mass 63 mg/cm 2 .

In this paper, we describe a method for which the incoherent scattered radiation, corrected for matrix absorption, serves as an internal standard. The method takes advantage of the fact that the incoherent mass scattering coefficient for 17.4 keV Mo K α radiation is relatively constant for most light element matrices. Homogeneous specimens of thin uniform mass thickness are required for analyses.

THEORY

Figure 1 is a plot of the incoherent mass scattering coefficient (7) of the elements H ($Z = 1$) through Ca ($Z = 20$) for 17.4 keV radiation. Except for hydrogen, the coefficients are relatively constant. The incoherent mass scattering coefficient of a sample, $(\sigma_1/\rho)_{\text{Total}}$ cm 2 g $^{-1}$, is expressed

$$(\sigma_1/\rho)_{\text{Total}} = \sum_{i=1}^n (\sigma_1/\rho)_i w_i \quad (1)$$

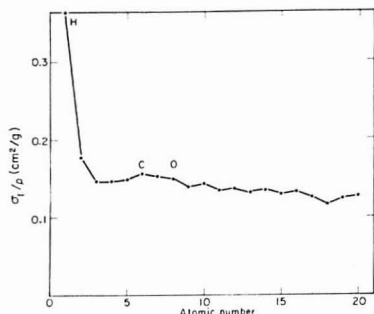


Figure 1. Incoherent mass scattering coefficients of the elements H through Ca for 17.4 keV radiation

Table I. Incoherent Mass Scattering and Total Mass Attenuation Coefficients (cm²/g)

coefficient radiation energy	σ_I/ρ Mo K α 17.4 keV	μ/ρ Fe K α 6.40 keV
matrix		
CH	0.172	7.9
CH with 2% S	0.171	11.3
CH with 2% Ca	0.171	14.1
CH ₃	0.186	7.4
C	0.156	8.6
H ₂ O	0.173	19.8
seawater	0.172	23.9
H ₂ O with 2% Ca	0.172	25.8

where $(\sigma_I/\rho)_i$ is the incoherent mass scattering coefficient of element i , and w_i is the weight fraction of element i . The weight fraction of hydrogen in most light element matrices varies between 0 and 14%. The major fraction of the light atomic number matrices are made up of other elements. Thus, the incoherent mass scattering coefficient is relatively constant for most light element matrices. Table I lists the incoherent mass scattering coefficients for some light element matrices. The coefficients typically do not vary more than a few percent from that of pure water, with a maximum deviation of 10%. Thus, the intensity of the incoherent scattered radiation, when properly corrected for matrix absorption, can be directly related to the sample mass. However, there are wide variations in the degree to which these matrices attenuate or absorb fluorescent X-rays, as is evident in Table I. For example, the total mass attenuation coefficient, μ/ρ , at 6.40 keV, Fe K α X-ray energy, varies by a factor of 3.

Giaque et al. (8) have previously shown that matrix absorption effects can be determined experimentally for thin uniform samples. Relative X-ray intensities are measured from a target located at a position adjacent to the back of the sample, with and without the sample, as illustrated in Figure 2. The combined fraction of the exciting and fluorescent radiations transmitted in the total sample thickness, m (g cm⁻²), is expressed

$$e^{-(\mu_e/\rho + \mu_f/\rho)m} = \frac{I_T - I_S}{I_T} \quad (2)$$

where I_S , I_T , and $I_{T'}$ are the intensities of the X-ray plus background from the sample alone, the target alone, and the sample plus the target, respectively. The values μ_e/ρ and μ_f/ρ are the total mass attenuation coefficients of the sample for the excitation and the fluorescent radiations, respectively.

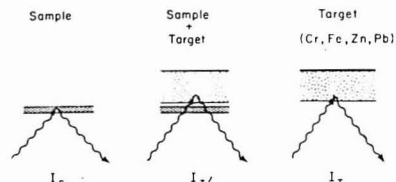


Figure 2. Schematic of experimental procedure used to determine matrix absorption effects

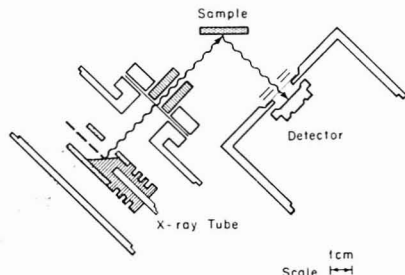


Figure 3. Schematic of X-ray fluorescence analysis system

Integration of the X-ray absorption over the thickness of the sample yields the absorption correction which is expressed

$$Ab_{corr.} = \frac{(\mu_e/\rho + \mu_f/\rho)m}{1 - e^{-(\mu_e/\rho + \mu_f/\rho)m}} \quad (3)$$

If values of $(\mu_e/\rho + \mu_f/\rho)m$ are experimentally determined for several X-ray energies and plotted vs. the fluorescence X-ray energy on a log-log scale, an approximate value for $(\mu_e/\rho)m$ can be obtained by extrapolation of the curve to the excitation radiation energy. By difference, values for $(\mu_f/\rho)m$ can be calculated, a curve for $(\mu_f/\rho)m$ values drawn, and a new value for $(\mu_e/\rho)m$ established. This procedure can be iterated several times. Using data from the latter curve, absorption corrections for all radiations of interest can be calculated from Equation 3.

EXPERIMENTAL

Equipment and Characteristics. The X-ray system, shown in Figure 3, was designed by Jaklevic and co-workers. It consists of a guard-ring detector with pulsed light feedback electronics and 512-channel pulse-height analyzer. The resolution of the system, fwhm, is 200 eV at 6.4 keV (Fe K α X-ray energy) at 8000 counts/s using an 18- μ s pulse peaking time.

A low power Mo-anode X-ray tube followed by a 0.010-cm Mo filter was used to provide the Mo K excitation radiation. The X-ray tube was operated at 45 kV. The regulated X-ray tube current was adjusted between 50 and 300 μ A for each sample to obtain a count rate of approximately 8000 counts/s. This eliminated or minimized potential spectral zero level or gain shifts, which would have produced errors in our peak unfolding routine.

Correction for system dead time, resulting either from pile-up rejection or analyzer dead time, was made using a gated clock that measured total system live time. Spectral data were recorded on magnetic tape. Computations were made using a Control Data 7600 computer. Our program required approximately 50K of core space.

Preparation of Specimens. The sample cell is illustrated in Figure 4. The cell is composed of two sections—each consisting of two rings which snap together to hold a 0.0006-cm thick polypropylene window. A spacer ring, 0.08-cm thick, is placed in the bottom section of the cell. Liquid to be analyzed (~0.5 mL) is pipetted into this section, after which the top section is

TARGET FOR ABSORPTION MEASUREMENTS

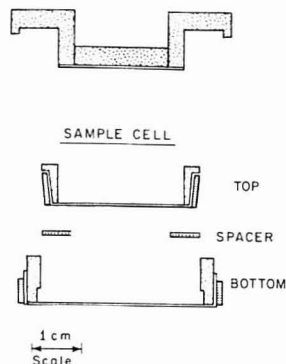


Figure 4. Sample cell and target for X-ray absorption measurements

inserted against the spacer ring. Any excess liquid is dispersed to the perimeter of the spacer ring. Viscous oils require slight heating prior to pipetting to reduce the viscosity, which usually permits specimens of uniform mass thickness to be prepared.

In the preparation of self-binding material, 250 to 350 mg of finely pulverized sample is placed in a die and a 2.5-cm o.d. disk is pressed at 15000 psi. This sample is then placed in the cell without the spacer ring for analysis.

For a non-self-binding material such as coal, 200 to 250 mg of pulverized powder is distributed in the bottom of the cell within the spacer ring. The top section of the cell is inserted and a disk is pressed at 2000 psi.

CALIBRATION METHOD

Standardization. Standards for the elements are prepared by dissolving pure metals or standard weighing forms as reported elsewhere (9). Portions of these solutions are diluted to produce element standards in the 100 to 500 ppm range. The diluted standards are pipetted into the sample cell and used to calibrate the X-ray system. Attenuation measurements are made on each of the standards to determine matrix absorption corrections. For each standard a sensitivity factor, K_i , is determined and expressed

$$K_i = \frac{I_i}{I_{\text{Incoh.}}} \times \frac{(Ab_{\text{corr.}})_i}{(Ab_{\text{corr.}})_{\text{Incoh.}}} \times \frac{1}{\text{ppm}_i} \quad (4)$$

where I_i and $I_{\text{Incoh.}}$ are the X-ray intensities from the standard element and the incoherent scattered Mo K α radiation, respectively; $(Ab_{\text{corr.}})_i$ and $(Ab_{\text{corr.}})_{\text{Incoh.}}$ are the absorption corrections for these same radiations; and ppm_i is the concentration of the standard.

Corrections for Absorption Effects. The degree to which the specimen attenuates the incident and fluorescent X-rays in the total specimen thickness is measured experimentally. Relative X-ray intensity is measured at five X-ray energies, with and without the specimen, from a target located at a position adjacent to the back of the specimen, as shown in Figure 2. The target, shown in Figure 4, is contained in a holder which seats over and within the sample cell. The composition of the target and the X-ray energies for which attenuation measurements are determined are listed in Table II.

Using data from the attenuation measurements and Equation 2, values of $(\mu_e/\rho + \mu_f/\rho)m$ are calculated for the five X-ray energies listed in Table II. These values are plotted vs. fluorescence X-ray energy on a log-log diagram. The value of $(\mu_e/\rho + \mu_f/\rho)m$ is estimated by extrapolation of the curve to 17.4

Table II. Target for Absorption Measurements

element or compound	weight, mg	X-ray lines	energy, keV
Cr	600	Cr K α	5.41
Fe ₂ O ₃	1000	Fe K α	6.40
Zn	200	Zn K α	8.63
Pb ₂ O ₃	150	Pb L α	10.54
-	-	Pb L β	12.61
cellulose	200	-	-

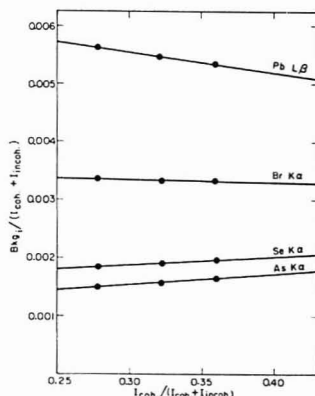


Figure 5. Spectral background curves for As, Se, Br, and Pb

keV, the energy of the excitation radiation. In turn, values for $(\mu_e/\rho)m$ are calculated, a curve for these values is drawn, and a new value for $(\mu_e/\rho)m$ is ascertained by extrapolation of this curve to 17.4 keV. This last step is iterated several times. Finally, three separate curves for $(\mu_f/\rho)m$ values are plotted between 4.50 and 7.11 keV; 7.12 and 10.54 keV; and 10.55 and 17.4 keV, using $(\mu_f/\rho)m$ values determined for Cr K α and Fe K α ; Zn K α and Pb L α ; and Pb L α and Pb L β X-rays, respectively. From these curves, values of $(\mu_f/\rho)m$ and, in turn, values of $(\mu_e/\rho + \mu_f/\rho)m$ are determined for all X-ray energies in our program. These values are used in Equation 3 to calculate the absorption corrections. The above steps are shown in the Appendix.

Corrections for Overlapping X-Rays. Our analysis program uses a fixed number of channels as a measure of X-ray intensity for each element determined. Peak overlap factors are initially established from X-ray spectra generated from thin deposits of individual element solutions nebulized onto Nuclepore polycarbonate filters.

Characteristic X-ray line ratios (e.g., K β /K α) obtained in analysis deviate from the ratios ascertained using thin deposits, since X-ray absorption increases with decreasing X-ray energy. The deviations in these ratios are determined experimentally using data from the attenuation measurements for the five X-ray lines listed in Table II. The following elements and corresponding X-ray lines are selected for analysis: Ti \rightarrow Fe, Ni \rightarrow Zr (K α); Co (K β); Hg, Th, U (L α); and Pb (L β).

Spectral Background. Spectral background under each of the X-ray lines is principally related to incoherent and coherent scattered excitation radiation intensities. Curves which relate the intensity of the spectral background to the intensities of both incoherent and coherent scattered Mo K α radiation are established from spectra acquired on three 300-mg disks (60 mg/cm²) of varying X-ray mass scattering cross sections. These disks, prepared from cellulose and sulfur

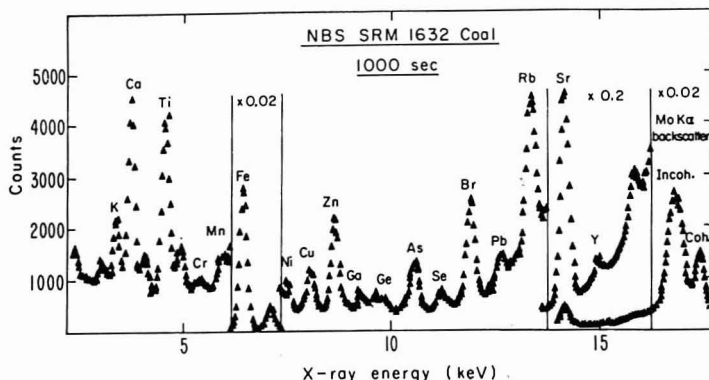


Figure 6. X-ray spectrum obtained on NBS SRM 1632 Coal

powders, are composed of 100% cellulose; 90% cellulose, 10% sulfur; and 80% cellulose, 20% sulfur. Figure 5 illustrates four X-ray line spectral background curves. All spectral background curves are expressed by the equation for a straight line

$$Bkg_i = \left[C_i + S_i \left(\frac{I_{Coh.}}{I_{Coh.} + I_{Incoh.}} \right) \right] (I_{Coh.} + I_{Incoh.}) \quad (5)$$

where S_i is the slope of the spectral background curve for element i and C_i is the intercept at $I_{Coh.} = 0$.

RESULTS

To demonstrate the capability of the method, four National Bureau of Standards trace element standard reference materials and a shale oil sample were analyzed. A flowchart illustrating the steps undertaken to calculate element concentrations is listed in the Appendix.

Ten samples (~200 to 250 mg) of SRM 1632 Coal were pulverized using an agate mortar and pestle. The powders were distributed within the sample cell spacer ring, and disks were pressed with both sample cell windows in place. Analysis periods, live time, were 1000 s for the disks alone and 100 s for the attenuation measurements. Figure 6 is a spectrum obtained on the coal.

Curves of $(\mu_a/\rho + \mu_i/\rho)m$ and $(\mu_i/\rho)m$ values determined for one specimen are shown in Figure 7. There is a minor drop in these curves at 7.11 keV, the Fe K absorption edge energy, since Fe is a minor constituent (0.8%) and not a trace element. Table III lists the results determined for 22 elements. The Ti → Mn values were corrected for overlapping Ba, La, and Ce L X-rays, using concentration values published by Ondov et al. (10). Most of the referenced values (10) were determined by instrumental neutron activation analysis at four laboratories. All results have been corrected for moisture content. We have reported results for four elements (Ga, Ge, Y, and Zr) that are not included in the NBS or referenced values. NBS values listed in parentheses are not certified.

The XRF values are generally in good agreement with the NBS and referenced values. The coal was found to be inhomogeneous with respect to Zn and Pb in that the deviation in the results was substantially larger than the precision of the XRF method. The coal has also been reported to be inhomogeneous for Sb (10). The XRF results for V are quite likely low. Six spectral lines overlap at 4.95 keV: Ti K β , V K α , Fe K β escape peak, Ba L β , La L β , and Ce L α . Using NAA results (10) for Ba, La, and Ce, the calculated intensity of the three L X-ray lines is 2.5 times that of V K α . If the samples

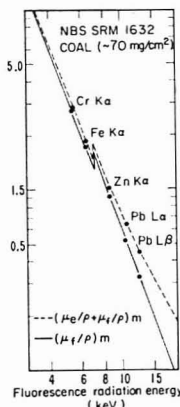


Figure 7. Curves of $(\mu_a/\rho + \mu_i/\rho)m$ and $(\mu_i/\rho)m$ values determined for a NBS SRM 1632 Coal specimen

Table III. Elemental Concentrations in NBS SRM 1632 Coal ($\mu\text{g/g} \pm 2\sigma$)

element	XRF	NBS	NAA (10)
Ti	951 ± 53	(800)	1040 ± 110
V	24 ± 8	35 ± 3	36 ± 3
Cr	22 ± 8	20.2 ± 0.5	19.7 ± 0.9
Mn	39 ± 3	40 ± 3	43 ± 4
Fe	7790 ± 360	8700 ± 300	8400 ± 400
Co	8.5 ± 4.2	(6)	5.7 ± 0.4
Ni	14.5 ± 1.2	15 ± 1	--
Cu	17.7 ± 1.5	18 ± 2	--
Zn	35.7 ± 9.9	37 ± 4	30 ± 10
Ga	6.1 ± 0.3	--	--
Ge	2.9 ± 0.2	--	--
As	4.7 ± 1.0	5.9 ± 0.6	6.5 ± 1.4
Se	3.1 ± 0.2	2.9 ± 0.3	3.4 ± 0.2
Br	17.5 ± 0.3	--	19.3 ± 1.9
Rb	20.1 ± 0.6	--	21 ± 2
Sr	151 ± 4	--	161 ± 16
Y	7.9 ± 0.6	--	--
Zr	33 ± 4	--	--
Hg	<1.1	0.12 ± 0.02	--
Pb	13.6 ± 6.5	30 ± 9	--
Th	2.7 ± 0.7	(3.0)	3.2 ± 0.2
U	<2.3	1.4 ± 0.1	1.41 ± 0.07

Table IV. Elemental Concentrations in NBS SRM 1571 Orchard Leaves ($\mu\text{g/g} \pm 2\sigma$)

element	XRF	NBS
Ti	18.0 \pm 8.5	--
V	<8	--
Cr	<5	2.6 \pm 0.3
Mn	86.5 \pm 4.9	91 \pm 4
Fe	274 \pm 19	300 \pm 20
Co	<6	(0.2)
Ni	1.2 \pm 0.5	1.3 \pm 0.2
Cu	11.5 \pm 1.0	12 \pm 1
Zn	25.3 \pm 2.1	25 \pm 3
Ga	<0.5	(0.08)
Ge	<0.4	--
As	10.1 \pm 0.8	10 \pm 2
Se	<0.3	0.08 \pm 0.01
Br	9.0 \pm 0.5	(10)
Rb	11.5 \pm 0.6	12 \pm 1
Sr	36.3 \pm 1.3	(37)
Y	<1	--
Zr	<3	--
Hg	<1	0.155 \pm 0.015
Pb	40.7 \pm 3.0	45 \pm 3
Th	<1	--
U	<2	0.029 \pm 0.005

Table V. Elemental Concentrations in NBS SRM 1577 Bovine Liver ($\mu\text{g/g} \pm 2\sigma$)

element	XRF	NBS
Ti	<11	--
V	<6	--
Cr	<4	--
Mn	9.4 \pm 1.1	10.3 \pm 1.0
Fe	267 \pm 5	270 \pm 20
Co	<6	(0.18)
Ni	<0.8	--
Cu	192 \pm 4	193 \pm 10
Zn	134 \pm 2	130 \pm 10
Ga	<0.5	--
Ge	<0.4	--
As	<0.3	(0.055)
Se	1.1 \pm 0.2	1.1 \pm 0.1
Br	8.8 \pm 0.4	--
Rb	18.4 \pm 0.4	18.3 \pm 1.0
Sr	<1	(0.14)
Y	<1	--
Zr	<3	--
Hg	<0.8	0.016 \pm 0.002
Pb	<1	0.34 \pm 0.08
Th	<1	--
U	<2	(0.0008)

are not ground sufficiently fine to eliminate particle size effects (11), an overcorrection for the L X-ray lines would be calculated and, in turn, a low result determined for V. However, our Pb result suggests that the certified value is in error for the batch of coal we purchased from NBS. Our Pb result has been substantiated by another analytical technique, Zeeman atomic absorption spectrometry (12).

Ten samples (~250 to 350 mg) of both SRM 1571 Orchard Leaves and SRM 1577 Bovine Liver were pressed into 2.5-cm o.d. disks and analyzed. Table IV and V list the results. In both cases, the XRF values are in excellent agreement with the certified values.

Twelve samples (~0.5 mL) of SRM 1634 Fuel Oil were analyzed using 400-s counting periods for the oil specimens, and 40 s for the attenuation measurements. The XRF results, listed in Table VI, are low for V and Ni. The oil was found to contain 11.5% hydrogen and 85.7% carbon by combustion analysis. Thus, the incoherent mass scattering coefficient of this oil is most likely about 4% higher than that of water or a pure hydrocarbon with a 1:1 hydrogen to carbon atomic weight ratio as shown in Table I. Even if an adjustment was

Table VI. Elemental Concentrations in NBS SRM 1634 Fuel Oil ($\mu\text{g/g} \pm 2\sigma$)

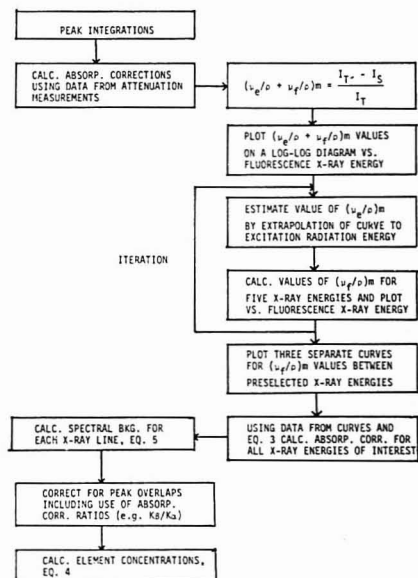
element	XRF	NBS
V	283 \pm 12	320 \pm 15
Cr	<6	(0.09)
Mn	<3	(0.12)
Fe	14.0 \pm 1.5	13.5 \pm 1.0
Ni	32.0 \pm 1.6	36 \pm 4
Cu	<0.8	--
Zn	<0.6	0.23 \pm 0.05
As	<0.4	(0.095)
Pb	<1.5	0.041 \pm 0.005

Table VII. Comparison of XRF and NAA Elemental Results for Shale Oil, S-09 ($\mu\text{g/g} \pm 2\sigma$)

element	XRF	NAA
Fe	40.3 \pm 2.0	38 \pm 3
Ni	4.5 \pm 0.6	4.2 \pm 0.2
Cu	4.9 \pm 0.6	4.6 \pm 1.8
Zn	3.3 \pm 0.3	2.4 \pm 0.4
As	18.2 \pm 1.0	18.2 \pm 1.0
Se	0.8 \pm 0.3	0.7 \pm 0.1

Chart I

FLOW CHART FOR ANALYSIS PROGRAM



made for this difference, the XRF result for V would still be low. The low V result can be attributed to the preparation of specimens of non-uniform mass thickness due to the relatively high viscosity of the oil. With non-uniform specimens, absorption corrections determined are smaller than expected. This discrepancy becomes larger at lower X-ray energies.

Table VII lists the results for a shale oil sample. Five determinations were made by XRF and two by NAA (neutron activation analysis). The NAA results were obtained by Jon Fruchter, Battelle Pacific Northwest Laboratories. Again, very good agreement has been achieved by these two instrumental analytical techniques.

APPENDIX

Chart I, a flow chart illustrating the steps undertaken to determine element concentrations is shown on page 515. For each sample, two spectra are acquired, one for the sample alone, and one with a target located at the back of the sample. Additionally, once each day, a spectrum is acquired on the target only. Using data from the above spectra, matrix absorption corrections are established for all X-ray energies of interest. These corrections are applied to the unfolding of peak overlaps, as well as to compensate for matrix absorption for the individual element determinations. The incoherent scattered radiation intensity, corrected for matrix absorption, serves as the internal standard.

ACKNOWLEDGMENT

The authors thank Joe Jaklevic and Leif Christensen for their comments on the preparation of this paper. We are grateful to Fred Goulding and members of the Department of Instrument Techniques for developing the X-ray system. We are indebted to David Gok for writing the computer program and to Vazken Tashinian for the hydrogen and carbon combustion determinations. We also greatly appreciate the encouragement and financial support for method development by Bob Stephens of the California Department of

Public Health, Vector and Waste Management Section.

LITERATURE CITED

- (1) G. Andermann and J. W. Kemp, *Anal. Chem.*, **30**, 1306 (1958).
- (2) T. J. Cullen, *Anal. Chem.*, **34**, 812 (1962).
- (3) C. W. Dwiggs, Jr., *Anal. Chem.*, **36**, 1577 (1964).
- (4) R. C. Reynolds, Jr., *Am. Mineral.*, **48**, 1133 (1963).
- (5) C. E. Feather and J. P. Willis, *X-Ray Spectrom.*, **4**, 41 (1976).
- (6) K. K. Nielson, *Anal. Chem.*, **49**, 641 (1977).
- (7) W. H. McMaster, N. K. Del Grande, J. H. Mallett, and J. H. Hubbell, "Compilation of X-Ray Cross Sections", University of California, Lawrence Livermore Lab. Report UCRL-50174, Section II, Revision 1 (1969).
- (8) R. D. Glaueque, F. S. Goulding, J. M. Jaklevic, and R. H. Pehl, *Anal. Chem.*, **45**, 671 (1973).
- (9) R. D. Glaueque, R. B. Garrett, and L. Y. Goda, *Anal. Chem.*, **49**, 1012 (1977).
- (10) J. M. Ondov, W. H. Zoller, Ihan Olmez, N. K. Aras, G. E. Gordon, L. A. Rancitelli, K. H. Abel, R. H. Filby, K. R. Shah, and R. C. Ragaini, *Anal. Chem.*, **47**, 1102 (1975).
- (11) R. Jenkins, "An Introduction to X-ray Spectrometry", Heyden & Son Ltd., London, 1974.
- (12) T. Hadeishi and R. McLaughlin, *Anal. Chem.*, **48**, 1009 (1976).

RECEIVED for review October 23, 1978. Accepted December 13, 1978. This work was done with support from both the U.S. Department of Energy and the California Department of Public Health. Any conclusions or opinions expressed are solely those of the author(s) and not necessarily those of the Lawrence Berkeley Laboratory, the U.S. Department of Energy, or the California Department of Public Health.

Comparison of Different Plasma Excitation and Calibration Methods in the Analysis of Geological Materials by Optical Emission Spectrometry

Jan-Ola Burman and Kurt Boström*

Department of Economic Geology, University of Luleå, S-951 87 Luleå, Sweden

A comparative study has been made of different dissolution and calibration methods for analyses by optical emission spectrometry (OES) utilizing inductively coupled plasma (ICP) and capacitively coupled microwave plasma (MWP) as excitation sources. The test substances were geological standard rocks, in which SiO_2 , Al_2O_3 , TiO_2 , Fe_2O_3 , MnO , MgO , CaO , Na_2O , Ba , and some traces were determined. The results show that analyses by MWP-OES are severely disturbed by matrix effects; only in the presence of large quantities of ionization buffers e.g., $[\text{Sr}(\text{NO}_3)_2]$ can MWP-OES yield rock analyses of very good quality. No buffers are needed for analyses by ICP-OES, for which the matrix effects are remarkably low. ICP-OES may suffer from annoying nebulizer disturbances when concentrated solutions are used but, with properly diluted solutions, all major and many trace elements can routinely be analyzed in 50-mg rock samples. MWP-OES on the other hand is poorly suited for trace element determinations.

Analysis by optical emission spectrometry (OES) has been used for a long time, in spite of the difficulties with arc and spark excitation. The development of plasma sources such as microwave plasma (MWP) and inductively coupled plasma (ICP) has made it even more advantageous to use OES in many applications (1-4). Furthermore, Govindaraju et al. (5)

have found that MWP excitation can be used with success for routine rock analysis. The method is based on fusing the sample with Li_2BO_3 and H_3BO_3 and an addition of a large amount of ionization buffer, $\text{Sr}(\text{NO}_3)_2$. At our laboratory we have successfully used this method, but with a simplified fusing step to get a faster preparation procedure (6). The ICP technique has also been used extensively for the analysis of geological samples: Scott et al. (7), Burman et al. (8, 9).

Larson et al. (10) showed that MWP sources are strongly influenced by high concentrations of easily ionized elements like Na, whereas their study of the Na effect on Mn, Cr, Zn, and Ca demonstrated that ICP-OES can tolerate such matrix fluctuations much better. Comparisons between MWP and ICP have also been made by Boumans et al. (11), who found ICP to be far more advantageous than MWP as an excitation source.

A problem with ICP-OES is that the nebulizer function is disturbed by concentrated solutions, an effect that is much less prominent with MWP-OES. It could therefore be of interest to study whether the MWP-OES method could be used for trace element analyses, since a concentrated solution by definition also must be richer in traces than a diluted one.

In a preliminary study, matrix effects for Al and Ba in MWP-OES were investigated (9). The results were discouraging but pointed to the importance of examining the matrix effects on other main components in rocks, namely SiO_2 , Fe_2O_3 , MgO , CaO , MnO , Na_2O , and TiO_2 . These nine elements have been examined by MWP and ICP excitation,

Table I. Spectrometer Performance for ARL 33000 CA

spectrometer: sequence reading; Paschen-Runge mounting; Rowland circle diameter, 1 m
grating: 1440 lines/mm
spectral range: 2560-6100 Å
dispersion: 7 Å/mm
entrance slit: 50 µm
exit slit: 75 µm for all elements but Fe 50 µm and Na 100 µm

Table II. Spectrometer Performance for ARL 35000 Quantoscan Monochromator

spectrometer: single channel instrument; Czerny-Turner mounting. Two mirrors with 1-m focal length; two interchangeable gratings
grating (1): 2160 lines/mm
spectral range (1): 1700-4600 Å
dispersion (1): 4 Å/mm
grating (2): 1200 Å/mm
spectral range (2): 1900-8000 Å
dispersion: 8 Å/mm
entrance slit: 20 µm
exit slit: 60 µm

Table III. Plasma Parameters for Capacitively Coupled Microwave Plasma

source: ARL capacitively coupled microwave plasma, manufactured by European ARL, and magnetron made by Philips
power: approx. 600 W
frequency: 2450 MHz
anode current: 200 mA
gas flow rate: 3 L/min N₂
sample uptake rate: 1.2 mL/min
electrode material: Ag
Nebulizer system: ARL-design. All plastic pneumatic nebulizer. Plastic spray chamber length 70 mm and diameter 32 mm
observation height: 10 mm above electrode

the measurements being made in four matrix types. Some trace element applications will also be discussed.

EXPERIMENTAL

Instrument Routines. The spectrometers are described in Tables I and II. The operational conditions for the plasma sources are described in Tables III and IV. In an early arrangement, the MWP unit was mounted on the nonscanning sequential reading ARL 33000 CA and the ICP unit on the scanning monochromator ARL 35000 Quantoscan, but subsequently both spectrometers were placed on the optical axis on each side of the ICP. All the MWP readings as well as the ICP readings for Si, Na, and Ba were performed with the ARL 33000 CA. The remaining ICP measurements for Fe, Mg, Ca, Al, Ti, and Ba were made with ARL 35000 Quantoscan, grating 1, (Table II). All the trace element measurements were made with ARL 33000 CA. The spectral lines used are given in Table V.

Each measurement involved a single 10-s integration period after a pre-flush of 60 s. Evaluation of measurements, curve fitting and plotting, and calculation of regression coefficient, standard error of estimate, and standard error of the coefficients in the calibration equation were made on a Hewlett-Packard 9825A desk computer, (24 kbytes) with a printer/plotter HP 9871A.

Major Elements. A series of test solutions were made as follows:

- (1) Metal salt solution, diluted with 2% (v/v) HNO₃.
- (2) Metal salt solution, prepared as under 1 but with 350 mg LiBO₂ added, diluted to 100 mL.
- (3) Standard rock, 50 mg (12, 13) is dissolved in HF/HClO₄ and finally diluted to 100 mL with 2% (v/v) HNO₃ (14).
- (4) Standard rock, 50 mg, is fused with 350 mg LiBO₂ and finally diluted to 100 mL with 2% (v/v) HNO₃ (6, 7).

The acids used were of analytical reagent grade and the metaborate was reagent grade, Merck 12228.

The synthetic solutions were made from Merck Titrisol ampules; for silica also, British Drug House (BDH) solutions were

Table IV. Plasma Parameters for Inductively Coupled Plasma

source: ARL inductively coupled plasma; RF generator model Henry Radio Inc., 3 kW
forward power: 1200 W
reflected power: <10 W
Ar cooling gas flow: 10 L/min
Ar plasma gas flow: 0.8 L/min
Ar central gas flow: 1.0 L/min
sample uptake rate: 0.8 mL/min
nebulizer system: J. E. Meinhard concentric glass nebulizer, type T-200-A4
spray chamber of glass barrel type
observation height: Zn, 14 mm; Ba, Mg, Si, Sr, and Zr, 18 mm; Cr and Ni, 22 mm; Al, Ca, Co, Cu, Fe, Na, Mn, Ti, and V, 26 mm

Table V. Spectral Lines Used for MWP and ICP

element	wavelength, Å ^a	element	wavelength, Å ^a
Si	2516.1 × 2	I Co	3474.0
Al	3961.5	I Cr	4254.3
Fe	3719.9	I Cu	3247.5
Mg	2795.5	II Ni	3414.7
Ca	4226.7	I Sr	4077.7
Na	5889.9	II V	4379.2
Mn	4030.7	I Zn	2138.6 × 2
Ti	3635.4	I Zr	3438.2
Ba	4554.0	II	

^a I = Atom emission line. II = Ion emission line.

used. The synthetic metal solutions were diluted to the same general concentration ranges as those in the rock solutions of series 3 and 4.

Trace Elements. A trace element study was performed by reading Co, Cr, Cu, Ni, Sr, V, Zn, and Zr in HF/HClO₄ dissolved standard rocks; 1 g/100 mL was used for ICP and 2 g/100 mL for MWP measurements.

RESULTS AND DISCUSSION

In our early plasma OES analyses, we used Govindaraju's (5) MWP method, which involves the use of Sr(NO₃)₂ as ionization buffer. However, we quickly discovered difficulties with this buffer. For some elements, e.g., Mn, there was a contamination from the buffer, which obviously is a nuisance in trace element analysis. The intensive Sr emission lines furthermore produce line broadenings which cause annoying background shift, particularly in trace element analysis. Investigations were also made eliminating the Sr buffer and with only LiBO₂ as flux. Govindaraju (5) reported that some elements like Fe, Mn, and Ti were unaffected by Sr, but that Si and Al needed buffering. In standard rock samples with 38-76% SiO₂, the standard error for SiO₂ increases by a factor of 3 when the Sr buffer is excluded. These results confirmed reported advantages with Sr buffering in MWP analysis.

We also observed early that many detection limits with MWP excitation were too poor to give satisfactory trace element data for rocks and sediments in contrast to the ICP unit; this source has detection limits that in most cases studied are lower, see Table VII.

Matrix effects in MWP and ICP sources were investigated, using the four types of test solutions without Sr buffer described above.

The aim of the investigation is to establish an accurate and simple routine method for plasma OES. The selected concentration ranges for the main elements are typical for those obtained in routine determinations in rock, sediment, slag, and coal ash samples.

We wanted to have the following questions answered:

- (i) What are the differences between calibration with synthetic solutions and standard reference samples?

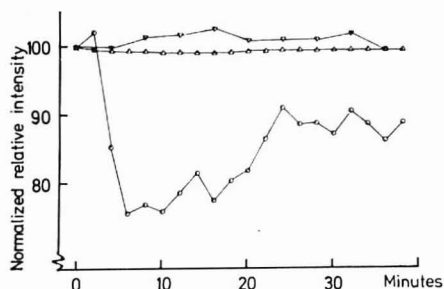


Figure 1. Instrumental drift for SiO_2 . Fused standard rock with 52.8% SiO_2 . The readings are normalized to the first intensity value = 100%. \blacktriangle = ICP, \circ = MWP Δ = lamp used for measuring deviations in readout electronics

(ii) Is it important to match calibration solutions and unknown samples with regard to amount of flux?

(iii) In what way do the excitation characteristics between MWP and ICP differ? Are there different answers to (i) and (ii) due to the excitation source?

Instrumental Drift. The MWP unit has persistently shown a considerable random drift, which was particularly annoying for SiO_2 . The effect of the drift can be minimized by reading only a few samples between each recalibration. During this study, we also noticed drift in the ICP unit, caused by high flux content. Thus, the high melaborate concentration led to nebulizer clogging after 15–20 min. All ICP measurements that involved LiBO_2 were therefore done as single element determinations since this procedure minimized the clogging by keeping each measuring cycle as short as possible. A change in the sample to flux ratio from 1:7 (this study) to 1:1 eliminates clogging; these results are reported elsewhere (8).

The drift is illustrated in Figure 1. All readings are made over a period of 40 min. Measurement with a lamp placed in the spectrometer housing to simulate the light emission from a source, gave a relative standard deviation of 0.2%, representing the deviations in the readout electronics. Standard rock DR-N, 52.8% SiO_2 , was used to compare the drift between MWP and ICP sources for samples dissolved in accordance to presently used routine methods. MWP (sample to flux 1:7) and ICP (sample to flux 1:1) gave 8.5% and 1.0%, respectively, in relative standard deviation. No in-depth study of the reasons for the serious MWP drift was performed before the use of the MWP source was stopped, but some possible explanations can be offered. Thus, although the MWP nebulizer can tolerate a much higher salt load than the ICP nebulizer, it is plausible that high Sr and flux concentrations cause drift. When high salt concentrations are nebulized in the MWP, a salt layer is built up under the silver electrode, a deposit that probably changes the gas flow through the holes in the electrode. We also observed that this salt coating occasionally broke loose and fell down from the electrode; it appears likely that such events explain the intensity revitalizations that can be observed in Figure 1.

Matrix Effects. The results for all the nine major elements are summarized in Table VI. The variation of slope of the calibration curves is used as a criterion for degree of matrix effects. For each element, the slope for series 1, 2, 3, and 4 is respectively divided by the slope for series 1, thereby giving a sensitivity ratio for different matrices. The results of the matrix effect study are also presented graphically for two major, Al and Fe, and two minor elements, Mn and Ba, in Figures 2–5. The four different calibration series are plotted

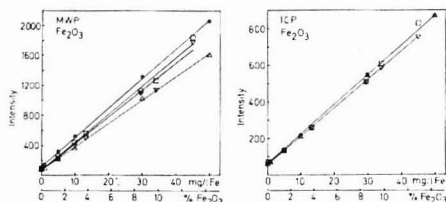


Figure 2. Fe excitation in four matrices by MWP and ICP. All the concentration axes are double-marked. One axis indicate the concentration in mg/L in the solution and the other represents concentration in % in the solid rock. Δ = series 1, \circ = series 2, \square = series 3, ∇ = series 4, as defined in Experimental

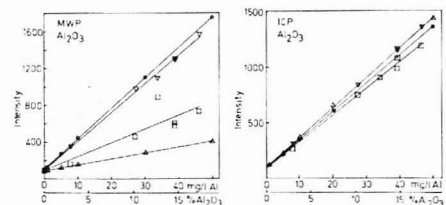


Figure 3. Al excitation in four matrices by MWP and ICP. See Figure 2 for conditions

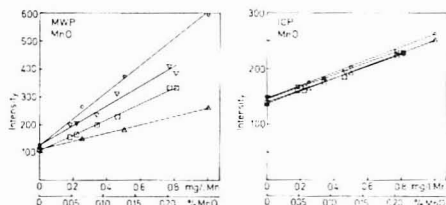


Figure 4. Mn excitation in four matrices by MWP and ICP. See Figure 2 for conditions

together to facilitate direct comparison between MWP and ICP for the same element.

It is immediately clear the MWP readings scatter much more than the ICP data, and that a given MWP intensity corresponds to a highly varying concentration due to influence from matrix. ICP excitation is superior because of the relative freedom from matrix effects.

Comments for Each Element. Fe. The matrix effects on Fe are small for both MWP and ICP excitation. The MWP results are the best obtained for any of the elements examined in this study. Figure 2 shows that the matrix effects for ICP are almost non-existent.

Al. The synthetic solutions containing Li and the fused rocks give almost the same sensitivity in the MWP case, but the Li-free samples differ a great deal in sensitivity. This indicates that the geological matrix increases the sensitivity for Al. This is also the case for Mn, Mg, Na, and Ba. The spread of the points around the calibration curve for series 3 is reproducible. One point which by MWP-OES falls off the calibration line (see Figure 3) is placed exactly on the calibration line when the same solution is read with the ICP unit. The reason for this anomalous behavior in MWP-OES is not understood.

Mn. The background shift observed in Figure 4 was caused by Mn contamination from the flux. If the curves are corrected for this shift, there is no matrix effect on Mn in the

Table VI. Sensitivity Variations in Four Different Matrices; Comparing MWP and ICP Excitations

element	MWP			
	S1/S1 ^a	S2/S1	S3/S1	S4/S1
Fe	1	1.2	1.2	1.2
Al	1	5.2	2.4	4.9
Mn	1	3.2	1.9	2.4
Ba	1	32	2.3	17
Ca	1	4.6	1.0	2.4
Si	1	0.1	-	0.5
Ti	1	3.4	1.1	2.9
Na	1	2.1	1.7	3.5
Mg	1	1.7	3.0	1.5

element	ICP			
	S1/S1	S2/S1	S3/S1	S4/S1
Fe	1	1.0	1.1	1.0
Al	1	0.9	0.9	1.0
Mn	1	1.0	0.9	0.9
Ba	1	1.0	0.9	0.9
Ca	1	1.3	1.0	1.1
Si	1	0.8	-	1.0
Ti	1	1.0	1.0	1.0
Na	1	1.1	1.4	2.4
Mg	1	0.9	1.1	1.0

^a S_n = slope for calibration curve of series n . The ratio between the slopes for series n and series 1 gives information about relative sensitivity changes depending on matrix. Series 1, which is in the denominator, contains only metal salt and acid, as defined in the text.

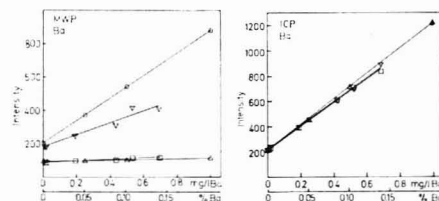


Figure 5. Ba excitation in four matrices by MWP and ICP. See Figure 2 for conditions

ICP case, whereas MWP-OES is strongly affected by matrix. These MWP results contradict those by Govindaraju (5) although we have used the same emission line. He reported that there was no matrix effect on Mn.

Ba. The differences between MWP and ICP are very striking for Ba, see Figure 5. The ICP curves converge to one single line, whereas the effects of the matrix changes are enormous by MWP-OES. There is also a background shift caused by matrix changes in the MWP. This is not a contamination shift, since it is absent in the ICP.

Ca. The maximum concentration of Ca was 50 mg/L. The self-absorption is more apparent in MWP than in ICP, as well as the other matrix effects. MWP sensitivity for Ca is the same in synthetic calibration solutions without Li as in acid dissolved rocks. This is observed only for Ca, Ti, and Fe.

Si. The two standard solutions for Si (Merck and British Drug House) have been manufactured by different fusion methods, resulting in high and differing Na concentrations in the final standard solution. The test solutions in series 1 were made from these two standard solutions. Because of their varying Na content, the slope differed by a factor of two when these test solutions were studied by MWP-OES, the higher intensities being observed in the Na-rich system. ICP-OES

Table VII. Standard Error for MWP and ICP Readings of Trace Elements in Standard Rocks

element	MWP, Sy-x, %	ICP, Sy-x, %	concn range in solid rock, ppm
Co	76	25	0-110
Cr	7	9	0-2250
Cu	31	28	0-70
Ni	5	7	0-2000
Sr	32	4	0-1350
V	120	12	0-240
Zn	33	11	0-160
Zr	78	50	0-240

tolerated these matrix fluctuations much better. No silica measurements were made in series 3, because Si was evaporated by the HF/HClO₄ treatment.

Boumans et al. (11) found that the addition of Li increased the sensitivity of many elements in MWP-OES. This is in good agreement with our results except for Si, where Li additions yield considerable sensitivity drops, see Table VI. Si is the only element for which we have noticed such a detrimental Li effect. It should be noted, however, that Sr buffers have an opposite effect on the Si sensitivity in MWP-OES; this is the main reason why MWP-OES has yielded very good Si analyses (5, 6).

Ti has also been reported (5) to be free from matrix effects in MWP-OES. Our results are different, see Table VI. ICP was not affected by matrix changes. Ti contamination from the flux was observed.

Na. This is the only element which was distinctly influenced by matrix changes in ICP-OES, but even then the results were better than those by MWP-OES.

Mg. Mg offers an exception in the MWP characteristics. This is the only case where a Li-free standard rock matrix gave greater sensitivity than the corresponding Li matrix. The changes in ICP sensitivity are negligible.

Trace Elements. The measured MWP and ICP trace elements intensities were plotted against the recommended concentrations for the standard rocks (12, 13). The spread around the calibration curve in terms of standard error, Sy-x, were almost the same for Cu, Cr, and Ni, independent of excitation source. The other trace elements, Co, Sr, V, Zn, and Zr, showed a drastic increase in Sy-x for MWP compared to ICP, see Table VII.

All errors due to uncertainty in recommended concentration values, incomplete dissolution, matrix effects, and instrumental drift are included in the standard error. The mineral zircon is not completely dissolved by a HF/HClO₄ procedure. Dissolution difficulties was the reason for high Sy-x values for both MWP and ICP. The chromite (Cr) case is analogous. This trace element study shows that the geological matrix itself causes severe effects on the trace element determinations when MWP excitation is used.

CONCLUSIONS

MWP. Analyses by MWP-OES require a careful match of samples and calibration solutions to get satisfactory results. In addition to equal amounts of flux, a large amount of ionization buffer is also needed, e.g., Sr(NO₃)₂. It is essential that calibrations be done with standard rocks since the matrix effect of the rock itself may influence the MWP excitation. Trace element analysis can be difficult because many trace elements are still poorly determined in standard rocks. The only way is to calibrate with synthetic standard solutions which in turn are difficult to make properly matched to real samples. It is furthermore impossible to analyze samples which are acid dissolved using calibration solutions from fusions and vice versa.

Nevertheless, we have analyzed a few hundred samples (sediments and rocks) in parallel by MWP-OES and ICP-OES. The results are in good agreement, except for Ba. It is indeed possible to make good routine analysis of geological samples with MWP if all the special demands on the sample preparation are fulfilled, including the addition of buffers (5, 6). However, these tricky preparation procedures make MWP-OES a highly awkward analytical method. The fact that the MWP nebulizer can stand higher salt concentration than the ICP nebulizer nevertheless makes it potentially a very interesting source, since nebulizer malfunction is a common source of disturbance in routine analysis.

In many cases it is possible to detect matrix changes from the form and size of the plasma. As the plasma changes, it is obvious that a fixed optical axis through the plasma will observe regions with different energies and thus also different excitation conditions.

ICP-OES. The freedom from matrix effects makes it very easy to prepare both samples and calibration solutions for ICP-OES. Even if different dissolution methods are mixed, it is still possible to make accurate analysis, but the contaminations from reagents can cause trouble if the same amounts of reagents are not used in all samples. The plasma unit itself can generally tolerate very large matrix changes. This led us to recommend that the samples and, if possible, the standard rocks should be uniformly prepared to minimize the effect of contamination due to reagents. There are no difficulties in making synthetic calibration solutions for trace element analysis since the absence of the main elements of a geological matrix in the calibration solutions causes no problems. This makes it easy to prepare calibration solutions for the analysis of trace elements that lack certified values.

The nebulizer and sample transportation can cause several disturbances, but these are not true matrix effects in the plasma. To avoid clogging of the nebulizer, we now use a new

preparation method, in which the sample to flux ratio is 1:1. The most critical part in an ICP system is the nebulizer unit, which needs further development. This is of importance for making a good routine analysis system better. The very low detection limits as well as the extended dynamic concentration range makes ICP-OES an ever more superior analytical method than MWP-OES.

ACKNOWLEDGMENT

The authors thank L.-G. Omberg, C. Pontér, and B. Boström for help with the MWP and ICP measurements. K. Govindaraju has kindly supported us with geological reference materials via the Working Group for Analytical Standards of Minerals, Ores, and Rocks.

LITERATURE CITED

- (1) V. A. Fassel and R. N. Kniseley, *Anal. Chem.*, **46**, 1110A-1120A, 1155A-1164A (1974).
- (2) P. W. J. M. Boumans, *Fresenius Z. Anal. Chem.*, **279**, 1 (1976).
- (3) C. C. Butler, R. N. Kniseley, and V. A. Fassel, *Anal. Chem.*, **47**, 825 (1975).
- (4) R. K. Skogerboe and G. N. Coleman, *Anal. Chem.*, **48**, 611A (1976).
- (5) K. Govindaraju, G. Meville, and C. Chouard, *Anal. Chem.*, **48**, 1325 (1976).
- (6) J.-O. Burman, B. Boström, and K. Boström, *Geol. Foeren. Stockholm Foerh.*, **99**, 102 (1977).
- (7) R. H. Scott and M. L. Kokott, *Anal. Chim. Acta*, **75**, 257 (1975).
- (8) J.-O. Burman, C. Pontér, and K. Boström, *Anal. Chem.*, **50**, 679 (1978).
- (9) J.-O. Burman and K. Boström, *Kem. Tidskr.*, **80**, 18 (1978) (In Swedish).
- (10) G. F. Larson and V. A. Fassel, *Anal. Chem.*, **48**, 1161 (1976).
- (11) P. W. J. M. Boumans, F. J. de Boer, F. J. Dahmen, H. Hölzel, and A. Meier, *Spectrochim. Acta Part B*, **30**, 449 (1975).
- (12) H. de la Roche and K. Govindaraju, "Rapport (1972) sur quatre standards géochimiques (DR-N, UB-N, BX-N and DT-N)", *Bull. Soc. Fr. Ceram.*, **100**, 49-75 (1973).
- (13) M. Roubault, H. de la Roche and K. Govindaraju, "Etat actuel (1970) des études coopératives géochimiques", *Sci. Terre*, **15**, 351-393 (1970).
- (14) J.-O. Burman, *ICP Inf. Newsl.*, **2**, 33 (1977).

RECEIVED for review October 24, 1978. Accepted December 26, 1978. This study was supported by a grant from the Swedish Board of Technical Development (STU).

Determination of Microgram Quantities of Asbestos by X-Ray Diffraction: Chrysotile in Thin Dust Layers of Matrix Material

B. A. Lange* and J. C. Haartz

U.S. Department of Health, Education, and Welfare, Public Health Service, Center for Disease Control, National Institute for Occupational Safety and Health, 4676 Columbia Parkway, Cincinnati, Ohio 45226

A method has been developed for the determination of microgram quantities of chrysotile (serpentine asbestos) which is precise, accurate, and rapid. The method utilizes X-ray diffraction techniques and has the capability of measuring microgram amounts of either pure chrysotile or small quantities of chrysotile (typically 1-10% by weight) in the presence of large amounts of matrix material. Detection limits as low as $2 \mu\text{g}/\text{cm}^2$ (on a filter) are cited. In developing this method, phase analysis procedures, methods of sample preparation, and a technique for X-ray absorption corrections were evaluated.

The detrimental health effects of airborne asbestos particles, notably asbestosis, lung cancer, and mesothelioma (1-3), have

necessitated the development of analytical techniques that can be used to monitor personal exposures to asbestos fibers. To date, the primary method of asbestos analysis has been fiber counting using optical or electron microscopy, but associated with this method is considerable variability in the measurement of asbestos concentration both within and among laboratories (4-9). Representative of this variability is data on analyses of ambient air samples (4) which show that differences between laboratories may be as high as two orders of magnitude. Along the same line, appreciable errors also occur in counting fibers collected in occupational environments (4, 6, 7). This variability is a natural consequence of factors inherent in the counting procedure, i.e., microscope quality, mounting procedure, and the necessity for interpretation by the analyst. While the present U.S. standard is still in terms of fibers per unit volume, the severe analytical problems posed

Table I. Measurement Parameters

component	ana-lytical ^a peak (s), ° 2 θ	scan range, ° 2 θ	step incr- ment, ° 2 θ	time per step incr., s
chrysotile	12.08	10.58-13.58	0.02	10
silica	24.38	22.88-25.88	0.02	10
silver	38.03	37.03-39.03	0.02	0.5
α -quartz	26.66	26.41-26.91	0.01	0.6
talc	9.32	7.82-10.82	0.02	2

^a Cu K α radiation (1.54178 Å).

by the counting method have provided impetus for developing an accurate, precise, rapid, and automated method capable of analyzing microgram quantities of airborne respirable dust. Precedence for measuring asbestos in terms of mass rather than number of fibers has been set in the adoption by West Germany of a mass standard (0.15 mg/m³) for airborne chrysotile (10). The British New Asbestos Regulations, adopted in May 1970, limited chrysotile exposure to 0.1 mg/m³ or 2 fibers/cm³ (10).

X-ray diffraction (XRD) was deemed the method most feasible for analyzing minute quantities of chrysotile and, while a number of other investigations have been made concerning the quantitative measurement of chrysotile by XRD, the quantities examined were generally in the milligram rather than microgram range. Working in a range of 1-10 mg, Crable et al. (11-13) clearly demonstrated the viability of XRD for the quantitative measurement of asbestos. Goodhead (14) used film techniques for determining percent chrysotile in a silicon matrix, and Rickards (15) cited 10 μ g as the detection limit for chrysotile by XRD and postulated that 50-100 μ g could be measured in the presence of an interference.

In the process of developing an effective method a number of factors had to be examined and evaluated. Of pivotal importance were the following: (1) the effects of the ultrasonic treatment used in sample preparation on X-ray response and particle size, (2) the cogency of the various phase analysis methods, (3) corrections for X-ray absorption by the analyte and any co-existent matrix, (4) techniques for preparing thin layers of dust on filters, (5) an evaluation of analytical bias resulting from ashing of the collection filter followed by redeposition of the analyte and (6) the detection limit and analytical parameters associated with the method. Each of these areas was thoroughly examined or developed so that, based upon the results obtained from this study, a well-documented statement can now be made about the feasibility of XRD for chrysotile analysis. Of equal importance is the fact that the fundamentals developed during the course of this work can now be extended to other serpentine and amphibole minerals, both pure and in interfering matrices.

EXPERIMENTAL

Apparatus. A Philips APD-3500 automated powder diffractometer was used with a Philips XRG-3000 X-ray generator and a scintillation counter. Small integrated peak areas were reliably measured through the use of a step scanning mode. Silver membrane filters were used as a support for the samples and, in conjunction with a pulse height selector and a focusing graphite monochromator, were used to reduce background. All measurements were obtained using a Philips long fine focus copper X-ray tube run at a power level of 1400 W. The instrumental configuration employed in this study included a 1° receiving slit and a 2 θ compensating divergence slit. The positions (2 θ) of the analytical peaks for the various analytes examined along with the associated scan ranges, step increments and count times per step increment are summarized in Table I.

Reagents. Chrysotile, obtained from Union Carbide was designated as Calidria asbestos, high purity open. Talc was obtained from the Sierra Talc and Chemical Company, a division

of Cyprus Mines Corporation. Silver membrane filters (Selas Flotronics), Millipore AA filters, and Gelman DM-450 filters were used at various stages in this study. Dispersions were produced using reagent grade isopropyl alcohol (Fisher).

Grinding, Sieving, and Particle Sizing. Chrysotile (0.8 g) was placed in a freezer mill (SPEX, Inc.), cooled to liquid nitrogen temperature and ground for 7 min at a grinding rate of ca. 5 impacts per second. Because dry grinding may lead to some decomposition of the chrysotile, the grinding rate and grinding time were kept to a minimum. The ground material was wet sieved through a 10 \pm 2 μ m sieve following the general method of Kupel (16). The talc was dry sieved as received through a 10- μ m sieve using an Allen-Bradley Sonic Sifter. All particle size determinations were performed with an RCA-EM3H transmission electron microscope.

Preparation of Suspensions. A weighed amount of the sieved chrysotile or talc was placed in 50 mL of isopropyl alcohol and the mixture subjected to an ultrasonic cell disruptor (Ultrasonics, Inc., Model W140) at an output power level of 5 W until a stable suspension was obtained. The resulting suspension was diluted to 1 L with isopropyl alcohol in a standard volumetric flask to give the desired final concentration. To prepare suspensions containing both talc and chrysotile, separate dispersions of the two minerals were first generated in the manner given above, then combined. The final concentrations of chrysotile ranged from 5-10 μ g/mL while the talc ranged from 100-1000 μ g/mL.

Deposition of Thin Dust Layers on Silver Filters. Two pore sizes of silver membrane filters were used in this study, 0.45 and 0.80 μ m. The former was used to maximize sensitivity (see Table II) and the latter for those large depositions that would clog the 0.45- μ m membranes. Two techniques were used in preparing thin dust layers on the silver filters. In the first, pipetted aliquots of the suspensions were filtered through silver membrane filters following a carefully developed procedure as follows: prior to removal of an aliquot, the suspension was first stirred for 1 min with a magnetic stirrer, then vigorously hand shaken, stirred a second time for 1 min and finally hand shaken again. The aliquot was withdrawn immediately after the second agitation during which time the dispersion was *not* stirred. A positioning collar placed on the pipet ensured that each aliquot was taken from the center of the dispersion. Three milliliters of isopropyl alcohol were then placed in the reservoir of a 2.5-cm Gelman vacuum funnel prior to the addition of the aliquot. After delivery, the pipet was rinsed into the reservoir and the mixture rapidly filtered. The sides of the reservoir were *not* rinsed after filtration. Two types of pipets were used in this method, a class A transfer pipet and a class A transfer pipet with the capillary tip removed (recalibrated).

In the second method of dust layer preparation, the required amount of material was weighed out, dispersed in isopropyl alcohol and subsequently filtered through a silver membrane filter. This method was designed to avoid the use of a pipet.

In both methods, the suspensions were filtered using the Gelman vacuum filter funnel giving an effective area of deposition of 3.46 cm²; a rectangular area 1.41 cm \times 1.59 cm (2.24 cm²) is actually irradiated by the X-ray beam.

Filter Ashing. The Millipore AA or Gelman DM-450 filters (with deposited talc and chrysotile) were ashed in an International Plasma Corporation low temperature asher for 4 h at a radio frequency (RF) power level of 100 W with an oxygen flow of 70 cm³/min.

THEORY

Corrections for X-ray Absorption. If absolute amounts of analyte are to be quantitatively measured, then corrections for X-ray absorption by the analyte and by any surrounding matrix must be made; i.e., the measured intensity I_m must be multiplied by a correction factor Γ to give the corrected intensity I_c

$$I_c = \Gamma I_m \quad (1)$$

For samples of less than "infinite thickness" (17), Williams (18) devised a method whereby the absorption coefficient of a powder could be determined at the same time as analytical intensities were being measured. This was accomplished by

mounting the powder on the surface of a metal and measuring the attenuation of the X-ray beam from the metal after it had passed through the powder. Williams went on to successfully use this method for determining quartz in various ceramics (18). Along similar lines Leroux (19, 20) derived an equation for evaluating the above correction factor based on the amount of attenuation observed for the intensity of a diffraction peak from an underlying silver filter. This correction factor is expressed as follows:

$$\Gamma = \frac{-R \ln T_n}{1 - T_n^R} \quad (2)$$

where $R = \sin \theta_{Ag} / \sin \theta_X$ (X represents analyte) and $T_n = I_{Ag}/I_{Ag}^0$ where I_{Ag} and I_{Ag}^0 represent the intensities of the attenuated and unattenuated silver peaks, respectively.

Combining Equations 1 and 2

$$I_c = I_m \frac{-R \ln T_n}{1 - T_n^R} \quad (3)$$

By plotting intensity as a function of weight for standards prepared from pure analyte (negligible absorption effects when less than 200 $\mu\text{g}/\text{filter}$), a calibration curve is generated from which slope (m_o) and intercept (b_o) may be calculated. Substituting these parameters into Equation 3 gives a general expression for the corrected, absolute weight of analyte (X_c).

$$X_c = \frac{1}{m_o} (I_c - b_o) \quad (4)$$

Calculation of Detection Limits as a Function of the Amount and Nature of a Matrix. Using some of the equations established above, an expression has been derived by this laboratory for use in calculating detection limits for an analyte at any specified concentration in various matrices. The theoretical ratio of the intensities of a silver reflection from a filter with and without the thin layer of sample is given (21) by the equation

$$T_n = I_{Ag}/I_{Ag}^0 = \exp \frac{-2\mu_s^* t \rho}{\sin \theta_{Ag}} \quad (5)$$

where t = sample thickness (cm), ρ = bulk density of the sample (g/cm^3), and

$$\mu_s^* = \sum f_i \mu_i^* \quad (6)$$

(f_i and μ_i^* are the weight fraction and mass absorption coefficient of the i th component).

Since $t = X/Af\rho$ where X = weight of pure analyte (g), A = area of deposition (cm^2), and f = weight fraction of pure analyte, then

$$T_n = \exp \frac{-2X\mu_s^*}{Af \sin \theta_{Ag}} \quad (7)$$

Defining the lower limit of detection (LLD) as the amount of material required to produce a measured intensity equal to three times the standard deviation of the background intensity (22, 23), then at the LLD

$$3s = I_m = I_c/\Gamma = \frac{m_o X + b_o}{\Gamma} \quad (8)$$

Substituting Equations 2 and 7 into 8 yields the expression

$$3s = (Xm_o + b_o) \frac{1 - [\exp(-2X\mu_s^*/Af \sin \theta_{Ag})]^R}{-R(-2X\mu_s^*/Af \sin \theta_{Ag})} \quad (9)$$

By determining a 3s level from background measurements and by specifying both the weight fraction of analyte in the matrix

Table II. Relation of Sonification Time to Sensitivity and Lower Limit of Detection (LLD)

sonification time	sensitivity, counts/ μg	LLD, $\mu\text{g}/\text{cm}^2$
2.5 h	61 (1) ^c	4
10 min ^a	95 (2)	3
10 min ^b	108 (2)	2

^a 0.8- μm pore size filters. ^b 0.45- μm pore size filters. ^c Figures in parentheses represent one standard deviation for least squares line.

(f), and the mass absorption coefficient of the sample (μ_s^*), Equation 9 can be solved for X by numerical means (24) to give the lower limit of detection for the analyte in the given matrix.

RESULTS AND DISCUSSION

With reference to the areas of proposed investigation outlined in the introduction, definitive statements can now be made concerning the effects, importance and applicability of these areas on this method for chrysotile. (1) While prolonged sonification does change X-ray response and probably particle size, those short periods of sonic treatment used in preparing dispersions have negligible effects. (2) The best method for phase analysis involves measuring integrated peak areas and normalizing by means of an external standard. (3) Corrections for X-ray absorption can readily and effectively be made when the analyte is present in a matrix such as talc at levels as low as 1% by weight. (4) Thin dust layers can be reproducibly generated by filtering suspensions containing particulate matter at concentrations as high as 1000 $\mu\text{g}/\text{mL}$. (5) Ashing of the collection filter and subsequent redeposition of the analyte introduces no analytical bias into the method. (6) The detection limit for chrysotile by this method is at a level of 2 $\mu\text{g}/\text{cm}^2$ on silver membrane filters, and the overall precision of the method (RSD) is 6.9%. A detailed discussion of these salient points is presented below.

Effects of Ultrasonic Treatment on Particle Size. To obtain stable dispersions of chrysotile and talc, ground and sieved samples of these minerals were placed in isopropyl alcohol and subjected to the action of an ultrasonic cell disruptor. Concern about the possible reduction in the length and/or diameter of the relatively brittle chrysotile fibers as a result of the sonification prompted a study on the actual effects of the sonic treatment. This concern is particularly germane should it become necessary to use ultrasonic techniques to redispense the chrysotile after the original collection filter has been asked so that the asbestos may be redeposited on silver membrane filters. In this study, comparable amounts of chrysotile were "sonified" for widely varying periods of time and subsequently both sized by electron microscopy and used in generating calibration curves. The results of this investigation indicate that prolonged ultrasonic treatment (>10 min) may be reducing particle size although insufficient sizing data have been gathered to state unequivocally that the apparent decrease in size is statistically significant. The supposition of decreased particle size is borne out by the X-ray responses of the sonified material. Calibration curves generated using the sonically treated samples show increased detection limits and decreased sensitivity (counts/ μg) with increased sonification time (Table II). These observations are probably a consequence of the fact that with increased sonification time a larger fraction of the sample is becoming small enough to either pass through the filter or lodge in the interior of the silver filter where it is shielded from X-rays. A more detailed study is presently being conducted to add statistical credence to the observation that sonification decreases particle size. At any rate, the marked response of the

Table III. Analytical Results as a Function of Phase Normalization Method

sample set	normalization procedure	RSD ^a		RSD of slope		linear correlation coefficient	
		A ^b	B ^c	A	B	A	B
I	external	8.7	7.9	2.5	2.6	0.9988	0.9986
	substrate	8.4	8.0	3.1	3.3	0.9982	0.9972
	none ^d	8.8	7.9	2.4	2.7	0.9988	0.9986
II	external	6.9	9.0	2.1	3.1	0.9991	0.9980
	substrate	6.6	9.3	2.7	3.7	0.9986	0.9972
	none ^d	6.9	9.0	1.3	1.8	0.9997	0.9993

^a $RSD = [\sum n_i(RSD_i)^2 / \sum n_i]^{1/2}$; all relative standard deviations were tested and shown to be homogeneous before being pooled (Bartlett's test at 1% significance level). ^b 7.33-Å peak of chrysotile (primary). ^c 3.65-Å peak of chrysotile (secondary). ^d Raw intensity (counts).

X-ray sensitivity to sonification time indicates that the treatment time must be kept to a minimum.

Evaluation of Phase Analysis (Normalization)

Methods. Two methods of normalizing the raw, net intensities of the diffraction peaks from pure chrysotile (no matrix) were evaluated to determine their effect on the analytical results. In the first method, corrections were made for instrumental instabilities by referencing the raw intensities to an α -quartz peak from a reference stone (external normalization). In the second method, the raw intensities were first externally normalized then referenced to a silver peak (also externally normalized) from an underlying filter to correct for any variations in the chrysotile intensity due to the orientation, height, and variability in flatness of the silver filter in the sample holder (substrate normalization). To obtain the necessary data, two sets of raw intensities were collected using two different pore size silver filters and chrysotile suspensions that had been ultrasonically treated for 10 min. The 7.33- and 3.65-Å peaks of chrysotile, the 2.36-Å peak from the underlying silver filter, and the 3.34-Å peak from the quartz reference stone were measured. The first set of data was taken using chrysotile deposited on 0.45- μ m pore size silver filters (I) and the second with chrysotile deposited on 0.80- μ m pore size silver filters (II). The overall analytical precision (RSD, pooled relative standard deviation), the linear correlation coefficients, and the relative standard deviations (RSD) of the slopes of the calibration curves were determined using each of the two methods and also the raw data. A Bartlett's test at a 1% level of significance shows that within each set of data (I or II) the RSDs and RSDs of the slopes are equal, demonstrating that both phase analysis methods give comparable results (Table III), and indicating that the physical condition of the filter is reproducible and is not a critical factor when integrated intensities are being measured. Convenience dictates the use of the external method unless a filter is heavily loaded (greater than ca. 2 mg) at which point the substrate method should be employed as it provides the means for X-ray absorption correction (see later section). Examination of Table III also reveals that in all instances the raw data give results comparable to both types of normalized data (Bartlett's test, 1% level). However, it is felt that this is simply a consequence of the excellent instrumental stability observed over the relatively short time period during which this study was conducted. Long-term stability has been found to be significantly less, and corrections should be made continuously for instrumental instability.

X-Ray Absorption Corrections. To evaluate the viability of the X-ray absorption correction method (theory section), thin dust layers containing 10%, 7%, 5%, 3%, and 1% (w/w) chrysotile in a talc matrix were deposited on silver filters and the intensities of the chrysotile and silver peaks measured.

The average silver peak intensity was determined using clean filters, and the chrysotile intensities were corrected for

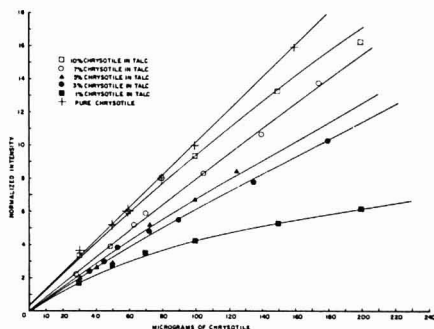


Figure 1. Intensities of the diffracted beam from chrysotile samples before X-ray absorption corrections (7.33 Å peak)

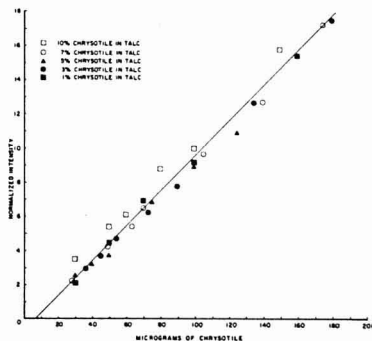


Figure 2. Intensities of the diffracted beam from chrysotile samples after X-ray absorption corrections (7.33 Å peak)

X-ray absorption using Equation 3. The slope (m_0) and intercept (b_0) values found for a calibration curve of pure chrysotile (negligible absorption effects) were then used to calculate the corrected weights according to Equation 4. A comparison of the uncorrected weights to the actual weights reveals that errors in accuracy can be significant if absorption corrections are not made. For example, at a level of 1% chrysotile in talc, a 100- μ g sample of chrysotile would give an apparent weight of 49 μ g before absorption correction and 102 μ g after correction.

The effectiveness of the correction method is shown graphically in Figures 1 and 2 where the intensities of the primary chrysotile peak are plotted before and after absorption corrections. The curves in Figure 1 correspond well with those

Table IV. Calibration Curve Slopes Derived from Plots of Corrected^a Intensity vs. Weight of Chrysotile (μg)

chrysotile in talc, %	slope, counts/ μg	linear correlation coefficient
100 ^{b,c}	108	0.9991
100 ^b	95	0.9988
10	98	0.9984
7	111	0.9978
5	92	0.9961
3	101	0.9993
1	102	0.9938

^a Corrected for X-ray absorption. ^b No X-ray absorption corrections. ^c 0.45- μm pore-size silver filters used, all other results are for 0.80- μm pore size silver filters.

^d Externally normalized.

predicted by theory (20), and the linearity of points in Figure 2 demonstrates the ability of the correction technique to compensate for absorption effects. The slopes of the corrected intensity vs. weight curves for the various percentages of chrysotile in talc are given in Table IV and by their comparable values further demonstrate the excellent correspondence between intensities that differed initially by as much as a factor of three due to X-ray absorption.

As an additional check on the principle of this correction technique, a portion of the data accumulated in this study was used in determining the mass absorption coefficient (μ^*) for talc (Equation 7). The experimentally determined value of 33.62 cm^2/g compares favorably with the calculated value of 31.2 (25) and adds further credibility to the results obtained.

Evaluation of Techniques Used for Depositing Thin Dust Layers. The thin dust layers used in this study were generated by filtering pipetted aliquots of suspensions containing particulate matter, specifically talc and chrysotile. However, there has been concern at this laboratory that errors which could significantly affect the precision and accuracy of the results may be incurred by pipetting from particulate dispersions. The primary concerns have been that the capillary tip of the pipet might foster poor precision by promoting variable amounts of particulate aggregation, and filter out a fraction of the particles, thereby introducing a bias into the analytical accuracy. To test for effects on the accuracy and precision, three different techniques were used in placing 10 mg of pure talc on three sets of 10 silver filters each. (Talc was used as it represented the mineral component that was used in highest concentration during the entire course of this investigation.) In the first technique, 10.00 \pm 0.01 mg samples of talc were weighed out, suspended in isopropyl alcohol, and the entire suspension was filtered through the silver filters. In the second and third techniques, a transfer pipet and a transfer pipet with the capillary tip removed (recalibrated) were used to draw 10-mL aliquots from a suspension containing 1000 $\mu\text{g}/\text{mL}$ of talc. The average talc diffraction peak intensities and associated standard deviations were used to assess and compare the precision and accuracy of the three techniques. The values of the mean and standard deviation found for the diffracted intensities from the weighed samples were then assumed to be the true and best values respectively.

A statistical *F*-test (two tailed) show that, at a 5% level of significance, the standard deviations associated with the samples prepared using either the regular transfer pipet or the tipless transfer pipet were not different from the standard deviation found for the weighed samples ($P = 0.638$ and 0.653, respectively). A statistical *t*-test (two tailed) showed that at a 5% level of significance the average intensity of the diffracted beam from the weighed talc samples is not different from the average beam intensities of the samples that were generated with either the regular pipet or the tipless pipet ($P = 0.151$ and 0.055, respectively). Thus this demonstrates

Table V. Detection Limits for Chrysotile in Different Matrices

matrix	chrysotile, %	detection limit, ^a $\mu\text{g}/\text{cm}^2$
...	100	2
...	100	3 (secondary peak)
talc	10	3
talc	7	3
talc	5	3
talc	3	3
talc	1	3
ZnO ₂	1	3.5
CaCO ₃	1	3.5
ZrO ₂	1	4.0
TiO ₂	1	3.5
Fe ₂ O ₃	1	4.5

^a Determined using the primary peak (7.33 Å) unless otherwise noted.

that transfer pipets can be used in taking aliquots from suspensions containing particulate matter in concentrations as high as 1000 $\mu\text{g}/\text{mL}$.

Detection Limits. The detection limit for chrysotile was defined as the amount of material required to give a diffracted X-ray intensity equal to three times the standard deviation of the background (22, 23). Using this definition in the form of Equation 9 the lower limits of detection for pure chrysotile and for the various percentages of chrysotile in talc were established (Table V). By measuring the background radiation levels of the other matrices given in Table V at angular positions comparable to those used for chrysotile background measurements, Equation 9 was also used to predict the minimum mass of chrysotile that could be detected in these matrices assuming 1% chrysotile by weight.

One of the conclusions reached during the course of this investigation is that the analysis of bulk samples for relative percent analyte should be made on samples that are less than "infinitely thick" (17). The procedure involves the deposition of a known weight of sample on a silver filter, the determination of the actual weight of analyte using the absorption correction method, and finally the calculation of percent analyte. The advantages of analyzing bulk samples in this manner are: (1) both relative and absolute amounts of analyte can be determined simultaneously, (2) it becomes unnecessary to prepare calibration curves based on varying percentages of analyte in a matrix; a single calibration curve for the pure analyte suffices, and (3) the method does not require a prior knowledge of the identity or nature of the matrix (assuming it is not an interference), it is merely required that the amount of sample placed on the filter be less than that which will absorb all of the diffracted X-rays from the underlying silver filter. By comparison, the nature of the matrix is critical in analyzing "infinitely thick" bulk samples unless an internal standard is used.

Recovery Studies. The applications of the method described in this paper are directed primarily toward the analysis of samples collected by small personal air samplers, attached to workers, which draw air through a filter at ca. 1.7 L/m. Worker movement, air currents, partial blockage of the face of the filter cassette, particle size discriminators attached to the cassette, and cassette positioning may lead to inhomogeneous deposits of analyte on the filter. The principles of the method described above require (1) homogeneous depositions of uniform thickness and (2) silver filters as support material. Therefore, to assure optimum results, the collection filters must be ashed and the chrysotile redeposited on silver membrane filters. Since concern about deposition homogeneity precludes direct sampling with silver filters, a study was carried out to evaluate the possibility of bias being in-

Table VI. Count to Mass Conversion Factors for Chrysotile

fibers/ μg^a	source	mass of 8-h sample, ^b μg	ref.
0.67×10^4	textile products	244	(27)
1.39×10^4	friction products	117	(27)
2.25×10^4	pipe products	73	(27)
5.2×10^4	commercial buildings	31	(5)
2.0×10^4	"general standard"	82	(28)
2.0×10^4	hygiene standard	82	(10)

^a Fibers $> 5 \mu\text{m}$ in length. ^b 1.7 L/m sampling rate.

produced into the analytical results as a consequence of the ashing and redeposition.

Equal amounts of chrysotile were deposited on 12 Millipore AA filters and 12 silver membrane filters (six filters at each of two levels; 100 and 150 μg). The AA filters were then ashed in a low temperature asher and the residues redeposited on silver membrane filters. The average intensities of the diffracted beams from the 12 redeposited samples were compared with those of the 12 direct deposition samples and a two tailed t -test showed that at a 5% level of significance ($P = 0.466$, 0.426, respectively) there was no difference in the means at either of the two levels of loading. Similarly, both sets of filters for each of the two levels gave comparable standard deviations (two tailed F -test, 5% level of significance $P = 0.058$, 0.182, respectively) indicating that ashing and redeposition does not introduce analytical bias or affect the precision of the method.

Count to Mass Conversion. On July 1, 1976, the Occupational Safety and Health Administration (OSHA) promulgated a standard for occupational exposure to asbestos containing an 8-hour time-weighted average (TWA) concentration exposure limit of 2 fibers/ cm^3 longer than 5 μm (26). To determine if this level is commensurate with the detection limit of the above method, it is necessary to obtain a count-to-mass conversion factor for chrysotile fibers. The results of several studies in which conversion factors were reported are summarized in Table VI. Quite clearly, the results are at variance and reflect not only the variety in the sources or uses of the fibers but also the differences in techniques used by the original investigators. However, based on these correction factors, the minimum amount of material that would be collected in a personal sample exceeds by at least a factor of three the detection limit determined for chrysotile at a level of 1% in talc and exceeds by at least a factor of five the detection limit for pure chrysotile.

CONCLUSIONS

This study clearly demonstrates the substantial potential of XRD as a routine technique for the quantitative determination of microgram quantities of serpentine asbestos. The utility of this method for both personal samples collected on filters and bulk samples is evident in its (1) specificity for chrysotile, (2) low detection limits, (3) excellent precision, particularly in comparison to the interlaboratory precisions of 30–100% (or greater) found using fiber counting methods for non-occupational (4, 5, 8), occupational (6, 7), and laboratory generated samples (9), (4) capability of making precise and accurate quantitative measurements on small quantities of chrysotile in the presence of large amounts of matrix

material, a situation where the counting method is at best difficult, (5) potential for automation, and (6) ready adaptability of the method to other asbestiform materials (e.g., tremolite) in different matrices.

No method is without its drawbacks, the primary one of which in this case is the problem of interferences. Minerals such as antigorite, lizardite, members of the kaolinite group (kandites), and possibly chlorite are potentially serious interferences with chrysotile. Sample pretreatment and X-ray line profile analysis are two approaches presently being explored in an attempt to reduce the adverse effects of interferences.

ACKNOWLEDGMENT

The authors gratefully acknowledge the guidance and assistance received during the program from J. V. Crable and from M. E. Cassinelli for her technical assistance. Special thanks also go to M. T. Abell and D. D. Dollberg for their technical and scientific consultations.

LITERATURE CITED

- (1) M. R. Becklake, *Am. Rev. Respir. Dis.*, **114**, 187 (1976).
- (2) L. Bruckman, R. A. Rubino, and B. Christine, *Air Pollut. Control Assoc. J.*, **27**, 121 (1977).
- (3) H. J. Wolltowitz and H. Valentin, *Staub-Reinhalt. Luft*, **36**, 112 (1976).
- (4) M. J. Duggan and E. W. Culley, *Ann. Occup. Hyg.*, **21**, 85 (1978).
- (5) W. J. Nicholson, A. N. Rohi, and I. Weisman, "Asbestos Contamination of the Air in Public Buildings", Research Triangle Park, N.C., *Environ. Prot. Agency (U.S.)*, Publ. 450/3-761004, Oct. 1975.
- (6) S. T. Beckett, R. K. Hey, R. Hirst, R. D. Hunt, J. L. Harris, and A. L. Rickards, *Ann. Occup. Hyg.*, **19**, 69 (1976).
- (7) G. W. Gibbs, P. Baron, S. T. Beckett, R. Dillen, R. S. J. DuToit, M. Koponen, and K. Robock, *Ann. Occup. Hyg.*, **20**, 321 (1977).
- (8) A. V. Samudra, F. C. Cook, C. F. Harwood, and J. D. Stockham, "Evaluating and Optimizing Electron Microscope Methods for Characterizing Airborne Asbestos", *Environ. Prot. Agency (U.S.)*, Contract No. 68-02-2251, July 1977.
- (9) NIOSH Report, "Precision and Accuracy Study", Proficiency Analytical Testing Program (PAT), Division of Physical Sciences and Engineering, Measurements Services Branch, November 28, 1975.
- (10) A. Schutz and H. J. Wolltowitz, *Staub-Reinhalt. Luft*, **33** (12), 445 (1973) (English).
- (11) J. V. Crable and M. J. Knott, *Am. Ind. Hyg. Assoc. J.*, **27**, 449 (1966).
- (12) J. V. Crable and M. J. Knott, *Am. Ind. Hyg. Assoc. J.*, **27**, 383 (1966).
- (13) J. V. Crable, *Am. Ind. Hyg. Assoc. J.*, **27**, 293 (1966).
- (14) K. Goodhead and R. W. Martindale, *Analyst (London)*, **94**, 985 (1969).
- (15) A. L. Rickards, *Anal. Chem.*, **44**, 1872 (1972).
- (16) R. E. Kupel, R. E. Kinser, and P. A. Maurer, *Am. Ind. Hyg. Assoc. J.*, **29**, 364 (1968).
- (17) H. P. Klug, L. E. Alexander, "X-Ray Diffraction Procedures", 2nd ed., John Wiley and Sons, New York, 1974, p. 360.
- (18) P. P. Williams, *Anal. Chem.*, **31**, 1842 (1959).
- (19) J. Leroux, *Staub-Reinhalt. Luft*, **29**, 26 (1969) (English).
- (20) J. Leroux, A. B. C. Davey, and A. Pallard, *Am. Ind. Hyg. Assoc. J.*, **34**, 409 (1973).
- (21) H. P. Klug and L. E. Alexander, "X-Ray Diffraction Procedures", 2nd ed., John Wiley and Sons, New York, 1974, p. 547.
- (22) L. S. Birks, "X-Ray Spectrochemical Analysis", Interscience, New York, 1959, p. 54.
- (23) R. Jenkins and J. L. deVries, "Worked Examples in X-Ray Analysis", Springer-Verlag, New York, 1970, p. 51.
- (24) C. F. Gerald, "Applied Numerical Analysis", Addison-Wesley Publishing Co., Reading, Mass., 1970, p. 2.
- (25) "International Tables for X-Ray Crystallography", Vol. 3, 3rd ed., Kynock Press, Birmingham, England, 1969, p. 159.
- (26) U.S. Department of Labor, Occupational Safety and Health Administration (1975): Occupational Safety and Health Standards. *Fed. Reg.*, **29 CFR** 1910.1001, 1975.
- (27) J. R. Lynch, H. E. Ayer, and D. L. Johnson, *Am. Ind. Hyg. Assoc. J.*, **31**, 598 (1970).
- (28) L. Bruckman and R. Rubino, *Air Pollut. Control Assoc. J.*, **25**, 1207 (1975).

RECEIVED for review October 19, 1978. Accepted January 2, 1979. Mention of products or trade names does not constitute endorsement by the Public Health Service.

Optimized Wide-Interval Rate Measurements of Substrate

J. E. Davis* and Brian Renoe¹

Division of Laboratory Medicine, Departments of Pathology and Medicine, Washington University and Barnes Hospital, St. Louis, Missouri 63110

Variation in the value of the rate constant of a first-order or pseudo-first-order reaction, is a major contributor to error in the estimation of substrate from the rate of reaction. Rate measurements over any arbitrary but fixed time interval can be optimized to provide impressive reduction in errors from that source. Wide-interval measurements include a large amount of the available change in absorbance and reduce the need for high precision photometers.

Estimation of chemical substances by rate methods is becoming more common as a result of instrumentation which makes rate methods convenient to use. The simplest and most common methods are based on first-order or pseudo-first-order reactions. The particular advantage of first-order reactions is the fact that at any fixed time the velocity (rate of reaction) is proportional to the initial amount of substrate (I). A great many methods measure the rate as close to zero time as possible in an attempt to measure the initial rate. For first-order reactions, it is also true that the average velocity between any two time points is proportional to the initial amount of substrate (I).

It has been shown by Atwood and DiCesare (2) that the rate constant could be adjusted to give a maximum velocity over a relatively short interval which occurred at a fixed time after initiation of the reaction. That an optimum rate constant exists, can be seen from the following argument. Suppose the rate constant were small, then the rate of reaction would be small. Increasing the rate constant would increase the rate of reaction. However, in contrast to the initial rate measurement, there comes a point at which the amount of substrate remaining at the time of measurement is so small that the rate of reaction would be small. Thus there is a compromise between an increased rate due to an increased rate constant and decreased rate due to substrate utilization. In addition to providing the maximum velocity, those same conditions provided resistance to the effects of variations in the rate constant (enzyme activity). Those authors were able to show that $\pm 20\%$ variations in the rate constant resulted in a mere 2% error in the measured rate and, hence, in the estimated substrate concentration. The same variation would cause a 20% error in results measured by initial rate methods.

Our purpose is to extend the optimization theory to the use of time intervals that are large in comparison to the time after initiation. Large time intervals will result in larger changes in absorbance which would permit the use of instruments that are neither so sensitive nor elegant as that used by Atwood and DiCesare. Techniques for quickly and simply optimizing an assay are presented and illustrated by application to the estimation of uric acid by the use of uricase.

THEORY

A first-order reaction is characterized by an exponential function of time;

$$S = S_0 \exp(-kt) \quad (1)$$

where S_0 is the initial amount of substrate, S is the amount at time t , and k is the rate constant. For an enzymatic reaction with substrate levels well below K_m , $k = V_{\max}/K_m$ (2). The average rate of reaction (velocity) between times t_1 and t_2 is;

$$V_{av} = S_0 \frac{\exp(-kt_1) - \exp(-kt_2)}{t_2 - t_1} \quad (2)$$

In order to find the optimal value of k which minimizes the variation in V_{av} for variations in k , the derivative of Equation 2 is taken with respect to k ;

$$\frac{dV_{av}}{dk} = \frac{S_0}{t_2 - t_1} (-t_1 \exp(-kt_1) + t_2 \exp(-kt_2)) \quad (3)$$

By setting this derivative equal to zero, the condition for optimization results;

$$kt_1 \exp(-kt_1) - kt_2 \exp(-kt_2) = 0 \quad (4)$$

For other than the trivial solution, $t_1 = t_2$, the solutions to this equation must be found by numerical methods. The physical situation justifies this condition as a minimum and obviates need to examine the second derivative. Furthermore, the natural variables are kt_1 and kt_2 and their use allows a general solution that does not depend on the particular time scale, i.e., minutes, seconds, hours, etc. For example, if $kt_2 = 0.5$, then Newton's method can be used to find that a value of $kt_2 = 1.7565$ will satisfy the equation within 0.01%. In a like fashion, numerous other values of kt_1 between 0 and 1 were chosen and the value of kt_2 was found. The relation between kt_1 and kt_2 is symmetrical so that values of kt_1 greater than 1 yield values of kt_2 less than 1. For that reason, kt_1 was limited to values less than 1. These data points are shown as a smooth function in Figure 1, where it is seen that the optimum value for kt_2 increases rapidly as kt_1 approaches zero. As an example in the use of Figure 1, suppose the rate constant, k , is 0.01 s^{-1} and t_1 is chosen as 50 s. The value of kt_1 is 0.5 and the optimum kt_2 is 1.76; hence the second measurement is to be made at 176 s.

Also shown in Figure 1 is the time interval of the measurement, $k\Delta t$, which of course can be calculated by subtracting kt_1 from kt_2 . Its purpose here is to illustrate that the rate measurement can be made over an interval which rapidly approaches the total time of reaction.

In some situations, the rate constant must be modified (by adjustment of the amount of enzyme) to make the optimum times coincide with predetermined measurement times. The ratio, kt_1/kt_2 shown in Figure 1, allows determination of the optimum rate constant. For example, if $t_1 = 30$ s and $t_2 = 45$ s, then the ratio is equivalent to t_1/t_2 or 0.67 since the rate constant can be factored out of the ratio. From Figure 1 it is found that $kt_1 = 0.82$ and $k = 0.027 \text{ s}^{-1}$.

In Figure 2, curve A shows the amount of material reacting within the measurement interval. Thus, in the example above where $kt_1 = 0.82$, about 15% of the original amount of material reacted to produce a difference in measurements at t_1 and t_2 . Curve B shows the amount of material reacted by the time of the final measurement, about 70% in the example above.

¹Present address: Department of Pathology, University of Virginia, Charlottesville, Va. 22901.

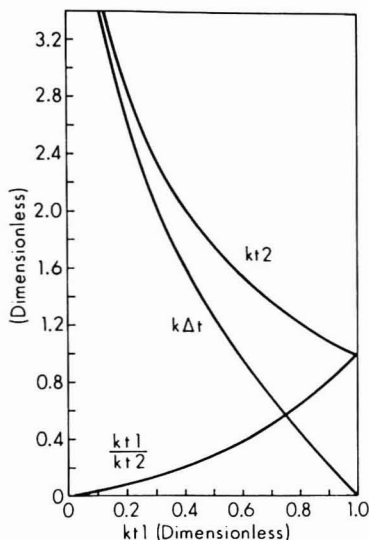


Figure 1. Optimum time relationship between measurement at the first time point, kt_1 , and the final time point, kt_2 . The time interval between those two points is shown as $k\Delta t$. Note that the rate constant has dimensions of inverse time so that kt is dimensionless

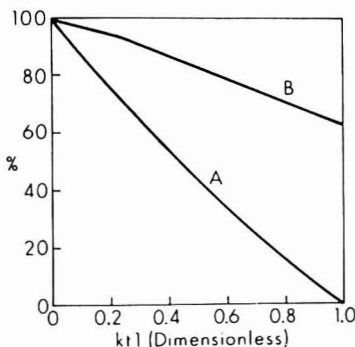


Figure 2. (A) Amount of material reacted during the optimum time interval which corresponds to an initial measurement at kt_1 . (B) Total amount of material reacted by the end of the optimum time interval which corresponds to an initial measurement at kt_1 .

Notice that at least 63% of the material will be reacted and that 100% of the material reacts in the interval when $kt_1 = 0$ and consequently kt_2 is infinite, i.e., the reaction has gone to completion.

Finally, in Figure 3 is shown the error in velocity that results from a plus, P, or minus, M, 25% variation in the rate constant when the optimum time interval is chosen. It is seen that the error decreases as kt_1 decreases and correspondingly, kt_2 increases. Ultimately, the error due to variations in rate constant goes to zero, as kt_1 goes to zero, in which case the reaction has gone to completion since the corresponding kt_2 is infinite. It is noteworthy that the error decreases rather slowly, even as the total amount of substrate converted surpasses 90% at $kt_1 = 0.3$.

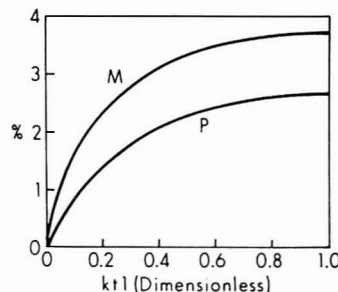


Figure 3. Variation of plus 25% (P) and minus 25% (M) in the rate constant and the resulting amount of error (decrease) in rate measurement over the optimum time interval which corresponds to an initial measurement at kt_1 .

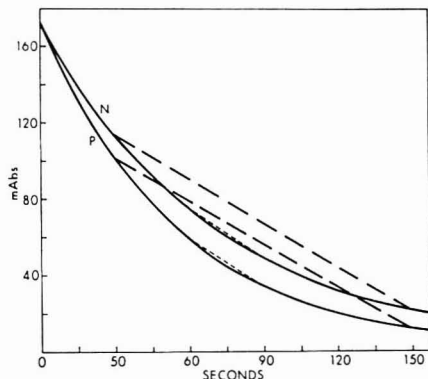


Figure 4. Absorbance vs. time for two levels of urease; N = nominal, P = +23%

EXPERIMENTAL

A CentrifChem 400 (Union Carbide, Rye, N.Y. 10580) was used to collect spectrophotometric data at 292 nm at 37 °C. Reagents for uric acid analysis were from DuPont (Automatic Clinical Analysis Division, Wilmington, Del. 19898) and were chosen because of the large K_m of the uricase obtained from *Bacillus fastidiosus* (3). Solutions of uric acid were prepared according to the method of Henry (4).

In an initial experiment wherein the reagents were reconstituted with 6.25 mL H_2O , the rate constant was measured to be $0.033 s^{-1}$ from a log velocity vs. time plot. For the purposes of illustration, it was desired to use a k value of $0.013 s^{-1}$, therefore a new set of reagents was diluted to 15.9 mL. No attempt was made to maintain the buffer capacity, ionic strength, or pH. In view of the results, this procedure was deemed adequate. Two time intervals were selected for the purposes of illustration. The first was $kt_1 = 0.4$ ($t_1 = 30$ s) and $kt_2 = 2.02$ ($t_2 = 150$ s). This condition permits a measurement of over 50% of the total absorbance available from the uric acid. A second interval was $kt_1 = 0.8$ ($t_1 = 60$ s) and $kt_2 = 1.23$ ($t_2 = 90$ s). This condition was the smallest convenient time interval surrounding one reaction time constant ($1/k$). The value of the rate constant ($0.013 s^{-1}$) was chosen so that these convenient time points would approximately satisfy the optimization conditions.

RESULTS

In Figure 4 is plotted the absorbance readings from the experiment with $k = 0.013 s^{-1}$. Inspection shows the initial rate (slope of the curves at $t = 0$) to be greater for the curve

where the rate constant was purposely increased 23% (increased amount of uricase). On the other hand, the average rates of reaction, as indicated by the slope of the long dashed lines between the absorbance at 30 and 150 s, are nearly the same. Thus, any substrate concentrations derived from the slope of those lines would be nearly the same.

In a similar way, the short dashed lines of Figure 4 have nearly the same slope and would give nearly the same results. Whether the narrow or wide measurement interval is chosen depends on the precision of the absorbance measurements and the time available for the measurement (or allowable cost for increased amounts of enzyme required for a short time scale). It can be seen from Figure 4 that narrow time intervals will exhibit a steeper average slope than wide intervals.

DISCUSSION

Measurements of analytes by rate methods are becoming increasingly important compared to end-point measurements. This is because rate methods inherently correct for blanks (interfering absorbance unrelated to the analyte). Generally, they take less time, since it is not necessary for the reaction to go to completion. Furthermore, the availability of instrumentation which permits convenient rate measurements has made the use of rate methods more popular. However, variation in the rate constant is one of the major sources of error. The rate constant in enzyme catalyzed methods is particularly sensitive to variations in temperature (often 7–8%/degree) and in amount of inhibitors and activators from the sample. Furthermore, if calibration is to be performed occasionally, then loss of enzymatic activity on storage becomes a factor. Finally, the rate constant can vary because of dilutional errors as well as variations in the amount of the second substrate in pseudo-first-order reactions. These are compelling reasons for optimizing the rate measurement to reduce the effects of such variations.

The optimization presented by Atwood and DiCesare (2) provides many advantages, not the least of which is avoidance of measurements near t_0 . In addition to those advantages, the wide-interval optimization presented here permits the measurement of larger changes in absorbance, thereby reducing the need for a high precision photometer. Furthermore, to a lesser extent the optimized wide-interval measurement is even less affected by variation in the rate constant.

When it is not practical to adjust the rate constant, then t_1 must be chosen to be less than the reciprocal of the rate

constant. With that selection, t_2 is automatically set and will be greater than the reciprocal of the rate constant. Conversely, t_2 may be selected and t_1 determined by the optimization condition. If no conditions predispose a particular selection of t_1 or t_2 , then they may be selected to achieve a particular absorbance change. On the other hand, both t_1 and t_2 may be fixed by instrumental considerations in which case the rate constant must be adjusted. All of these situations can be handled by referral to the appropriate figures.

In order to apply the methods of this paper, it has been necessary to know or to measure the rate constant. In some circumstances, it is inconvenient to measure the rate constant. The wide-interval optimization is still valid in those circumstances, in which case the average rate of reaction can be measured for a number of rate constants (or simply, amount of enzyme) and the value which maximizes the average rate of reactions selected as the optimum condition. This approach is valid since the derivative of the average rate of reaction is zero at the optimum conditions, indicating a maximal value in this case. However, measurement of the rate constant is preferred because the optimal conditions can be achieved with fewer measurements and with greater precision. Because the peak in a graph of rate vs. rate constant is broad, it is difficult to select the best value for the peak.

It is anticipated that the theory of optimization for wide-interval rate measurements can be extended to include coupled reactions as well as measurements at multiple time points in order to improve the precision. Nevertheless, the theory developed thus far is applicable to any first- or pseudo-first-order reaction, even though enzyme catalyzed reactions were treated explicitly. The optimized wide-interval rate measurement of substrate is easy to use and offers substantial advantages.

LITERATURE CITED

- (1) T. O. Tiffany, J. M. Jansen, C. A. Burtis, J. B. Overton, and C. D. Scott, *Clin. Chem.* (Winston-Salem, N.C.), **18**, 829–840 (1972).
- (2) J. G. Atwood and J. L. DiCesare, *Clin. Chem.* (Winston-Salem, N.C.), **21**, 1263–1269 (1975).
- (3) G. Lum and S. R. Gambino, *Clin. Chem.* (Winston-Salem, N.C.), **19**, 1184–1186 (1973).
- (4) J. DiGiorgio, "Clinical Chemistry Principles and Techniques", 2nd ed., R. J. Henry, D. C. Cannon and J. W. Winkelman, Ed., Harper and Row Publications, Inc., Hagerstown, Md., 1974.

RECEIVED for review September 18, 1978. Accepted December 21, 1978.

Optimization of the Coupled Enzymatic Measurement of Substrate

J. E. Davis* and Jeff Pevnick¹

Division of Laboratory Medicine, Department of Pathology and Medicine, Washington University and Barnes Hospital, St. Louis, Missouri 63110

In the kinetic analysis of substrate, factors which affect the enzymatic activity will affect the estimate of the amount of substrate. Likewise variations in the activity of coupling enzymes will affect the estimate. By proper selection of the time at which to measure the rate, variations in enzymatic activities will cause only minor variations in the rate, contrary to the case where measurements of the initial rate are made. Optimization theory is developed for variations in the activity of the primary or the coupling or both enzymes. Four methods are presented for estimating the kinetic parameters used in the optimization.

Measurement of the initial rate of reaction in an enzyme catalyzed assay for substrate is not necessarily the best rate measurement. Atwood and DiCesare (1) present a technique for optimization which measures the rate at a time when approximately 63% of the substrate has been consumed. That rate measurement exhibits an impressive resistance to variations in activity of the enzyme with a resultant improvement in methodological precision, and obviation of the need for making early absorbance measurements. While their theory is developed for simple first-order reactions, some of the methods involved one or more coupled reactions, with lag phases that were significant fractions of the time from triggering to measurement. Although they did not make a rigorous analysis of the effects of lag phase resulting from coupling reactions, they did offer an explanation which approximated the effect as a fixed time delay.

Bergmeyer (2) has investigated the kinetics of coupled reactions. The case which is of interest for the present discussion is that of consecutive irreversible first-order reactions. When the end-product is measured and the rate constants are comparable, i.e., neither step is rate limiting, a lag phase is evident in the reaction curve. Following the lag phase is the straightest portion of the reaction curve which corresponds to the maximum velocity of the reaction. This maximum velocity, which occurs at the inflection point of the velocity curve, could be substantially different from the initial rate of reaction of the first step. Nevertheless, the maximum velocity is proportional to the initial concentration of the reactant and the time at the inflection point is independent of the initial concentration. Furthermore, the product of the time at the inflection point and either rate constant is equal to a respective term which depends only on the ratio of the rate constants. In other words, the relative shape of the curve depends on the ratio of the rate constants, not their individual value.

Tiffany et al. (3) also studied the case of two irreversible first- or pseudo-first-order reactions occurring in series. They demonstrate the linear relationship between the concentration and the average rate measured between any two fixed times.

While making no claims about the desirable amount of coupling enzyme or the lag phase, they do state that the concentration of substrate must be less than $0.1 K_m$ for both enzymes.

In order to provide a firm theoretical foundation for the optimization of coupled enzymatic measurements of substrate, a kinetic analysis needs to be made for the case of two irreversible first-order reactions occurring in a series. The resulting equation will be equivalent to that derived by Bergmeyer (2), although it will be factored differently for purposes of emphasis. Subsequently, the technique of Atwood needs to be expanded to the case of coupled reactions. Thus our purpose is severalfold: (1) to derive a theory of optimization which includes the effects due to coupling enzymes, (2) to present methods for estimation of the primary and coupling rate constants, and (3) to demonstrate the improved resistance of the optimized assay with respect to variation in enzymatic activity.

EXPERIMENTAL

Reagents. Urease type III, glutamate dehydrogenase type II, 2-oxoglutarate, and NADH were from Sigma (St. Louis, Mo. 63118). All other chemicals were reagent grade. Deionized water was used throughout.

Instrumentation. A Gensac (ENI, Fairfield, N.J. 07006) was used to gather spectrophotometric data.

Procedure. The conditions of the assay were: 60 $\mu\text{mol/L}$ urea; 40 mmol/L Tris; 4.0 mmol/L EDTA; 2.0 mmol/L 2-oxoglutarate; 1400 IU/L urease, nominal; 20000 IU/L glutamate dehydrogenase, nominal; 200 $\mu\text{mol/L}$ NADH. The reagent was adjusted with HCl to a pH of 7.8 at 30 °C before the addition of enzymes or NADH.

THEORY

Assume the reactions are irreversible first order so that;



where $k_1 = V_{\text{max}}/K_m$ for the primary enzyme and $k_2 = V_{\text{max}}/K_m$ for the coupling enzyme. Differential equations representing the above can be solved to give the rate of change or velocity (V) of the final product, C ;

$$V = A_0 k_1 \exp(-k_1 t) \left[\frac{k_2}{k_2 - k_1} \right] \{1 - \exp(-(k_2 - k_1)t)\} \quad (2)$$

The term A_0 is the amount of substrate at time zero and the term $A_0 k_1 \exp(-k_1 t)$ is equal to the rate of change in substrate, A . The additional terms represent effects due to the coupling enzyme and intermediate product, B . Thus the rate of appearance of product is different from the rate of disappearance of substrate by a steady-state term in brackets and a transient term in braces.

The customary technique of measuring the initial rate is not feasible in this case because the initial rate is zero, i.e., there is a lag phase while the intermediate product builds up. An alternate technique chooses a region of the absorbance vs. time plot that approximates a straight line. The slope (da/dt) in this region is equivalent to measuring the peak velocity where the rate of change of velocity and, hence, curvature of

¹ Present address: Missouri Institute of Psychiatry, 5400 Arsenal Street, St. Louis, Mo. 63139.

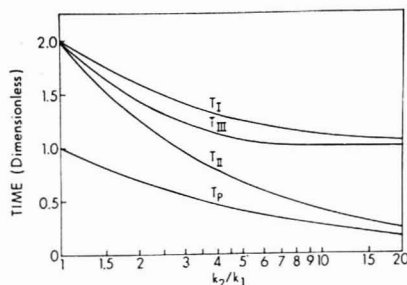


Figure 1. Optimal time (dimensionless) of rate measurement. T_I , T_{II} , and T_{III} provide maximum suppression of errors due to variations in k_1 , k_2 , and k_1 and k_2 respectively. T_P provides the peak velocity. These dimensionless times are to be divided by the rate constant, k_1 , to obtain the actual time.

the absorbance vs. time plot is smallest. However, Equation 2 reveals that the velocity is proportional to the substrate for any time greater than zero. The question can now be asked; is there an optimum time at which to measure the velocity where the greatest precision will be obtained. Of course the answer will depend on the source of the variations. Of concern here are variations in the activity of the enzymes.

In the following, the derivative of the velocity shall be set equal to zero and the resulting equation shall be solved for the time. Because there are two variables, k_1 and k_2 , the derivative can be taken with respect to one or the other or an infinite number of combinations of the two. Several conditions are particularly useful, that representing variations in k_1 , that representing variations in k_2 , and that representing equal percentage changes in k_1 and k_2 . The first situation occurs, for example, when a variable amount of inhibitor for the primary enzyme is present in the sample or when the primary enzyme is unstable and loses activity from one assay to the next. Optimization with respect to variations in k_1 shall be called Type I conditions. Similarly, when the coupling enzyme is subject to inhibition or is unstable, then optimization with respect to variations in k_2 is appropriate. This is a Type II condition. Finally, a Type III condition shall denote equal percentage changes in k_1 and k_2 . This situation would arise with dilutional errors, assuming that the ratio of enzyme activities remains constant. Also, changes in temperature would affect the enzyme activities in approximately equal proportion. Thus the optimum time will depend on which kinds of variation are most important in a particular assay. Later on, we shall be able to comment on desirable ratios of the primary and coupling enzyme.

Type I—Variations in k_1 . The derivative, set to zero, of the velocity with respect to k_1 is:

$$0 = 1 - k_1 t_1 - \frac{k_1}{k_2 - k_1} - k_1 t_1 \exp^{-(k_2 - k_1)t_1} [1 - \exp^{-(k_2 - k_1)t_1}] \quad (3)$$

where t_1 is the optimum time at which to measure the rate of reaction. In the event k_2 is very large, i.e., an excess of coupling enzyme, the last two terms of Equation 3 can be neglected and the resultant equation is equivalent to that obtained by Atwood (1). When k_2 is not particularly large, then Equation 3 must be solved in its entirety. An analytical solution for t_1 could not be found, so resort to a numerical solution was made utilizing Newton's method. In order to obtain a solution for the optimum time which was not dependent on the particular values of k_1 and k_2 , the equation was scaled using a parametric time, $T_1 = k_1 t_1$. The results are

plotted in Figure 1 where it is seen, for example, that the optimum T_1 for a ratio of k_2 to k_1 of 4 is 1.3. Thus, if $k_1 = 0.01 \text{ s}^{-1}$, then $t_1 = 1.3/0.01$ or 130 s. It is apparent from Figure 1 that the optimum time with respect to k_1 for k_2/k_1 greater than 10 is only slightly different from Atwood's limiting case with a result of 1.0.

It is appropriate to inquire whether the optimization depends on the nature of the change in the rate constant, since K_m will be affected by competitive inhibitors and V_m will be affected by noncompetitive inhibitors as well as by dilutional and temperature variations. The optimization with respect to k_1 is valid for small changes in K_m or V_m or both. Proof of this assertion is seen from the partial derivatives of k_1 :

$$dk_1 = \frac{\partial k_1}{\partial V_{\max}} dV_{\max} + \frac{\partial k_1}{\partial K_m} dK_m \quad (4)$$

and noting that

$$\frac{\partial k_1}{\partial V_{\max}} = \frac{1}{K_m} \quad (5)$$

and

$$\frac{\partial k_1}{\partial K_m} = \frac{-V_{\max}}{(K_m)^2} \quad (6)$$

Hence the derivatives are different only by a constant and would be equal to zero for the same value of time. This finding also applies to k_2 .

Type II—Variations in k_2 . The derivative, set to zero, of the velocity with respect to k_2 is:

$$0 = \frac{-k_1}{k_2 - k_1} (1 - \exp^{-(k_2 - k_1)t_1}) + k_2 t_1 \exp^{-(k_2 - k_1)t_1} \quad (7)$$

Newton's method was again used to obtain the numerical solution for t_{II} . The parametric time, $T_{II} = k_1 t_{II}$ is plotted in Figure 1.

Type III—Variations in k_1 and k_2 (Dilutional). The derivative of the velocity in the most general form is:

$$dV = \frac{\partial V}{\partial k_1} dk_1 + \frac{\partial V}{\partial k_2} dk_2 \quad (8)$$

for the particular case of dilutional errors, $dk_2 = k_2/k_1 dk_1$. Making this substitution into Equation 8 and setting $dV = 0$, gave an equation which was again solved by Newton's method to find the optimum time. The parametric time in this case was $T_{III} = k_1 t_{III}$. The result is plotted in Figure 1 where it is seen that T_{III} is generally shorter than T_I and for $k_2/k_1 > 5$, T_{III} is approximately equal to Atwood's limiting case with a result of 1.0.

Error Surface. It is instructive to consider an error surface around some optimum time. For these purposes, the optimum time was chosen as T_I for $k_2/k_1 = 4$. As will be seen, this choice will amply illustrate the distinction between T_I and T_{III} and further represents a not unlikely set of operating conditions, i.e., the observed velocity vs. time curve is characteristic of that for coupled reactions.

The error surface is plotted in Figure 2 for selected levels of error. In the center of Figure 2 is the nominal operating point. It can be seen that a $\pm 20\%$ change in k_1 is required before the velocity measured at time t_1 has changed (decreased) by 2%. On the other hand only an 8% change in k_2 is required before the velocity is changed by 2%. Note that a decrease in k_2 results in an increased velocity. Because optimization was made with respect to variations in k_1 it is not surprising that the nominal operating conditions provide the greatest resistance to changes in k_1 , nevertheless the magnitude of insensitivity to such changes is impressive. Figure 2 also shows that a $7\frac{1}{2}\%$ increase in k_1 and k_2 (un-

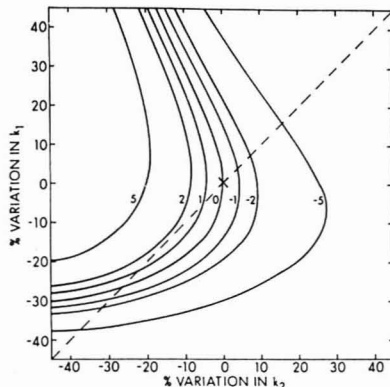


Figure 2. Error surface at T_1 for $k_2/k_1 = 4$. See text for description

derdilution or temperature change) results in 2% decrease in the velocity while a 32% decrement in k_1 and k_2 is required before a 2% change in velocity is incurred. This latter observation suggests that k_1 and k_2 could be reduced approximately 15% so that equivalent dilutional errors on the up side and the down side could be tolerated. Additionally, Figure 2 shows that such an operating point would be approximately parabolic with respect to dilutional errors, hence there would be a very small error in the velocity for small dilutional errors. However it is not really necessary to change the values of k_1 and k_2 , but merely to measure the velocity at a different time, t_{11} . This fact can be appreciated by realizing that equal changes in k_1 and k_2 are equivalent changes in the time scale. Thus decreasing in k_1 and k_2 cause the velocity curve to evolve more slowly. Equivalent results would be found by decreasing the time where the velocity was measured on the velocity curve resulting from the original values of k_1 and k_2 . This is consistent with the fact that t_{11} is less than t_1 .

Measurement of k_1 and k_2 . In order to relate the theoretical curves of Figure 1 to a physical system, the rate constants k_1 and k_2 or their equivalents must be determined by any of several approaches.

Method A. Direct purposeful variation of the activity of the primary and/or coupling enzyme activity by 10 to 25% yields a straightforward estimate of the optimum time. In particular, the intersection of the time curves for +25 and -25% variation in k_1 is virtually at t_1 . Similarly, the intersection of the curves for variation in k_1 and k_2 together is virtually t_{11} . A distinction is to be made between these crossover times and the respective optimum times since the latter is based on infinitesimal variations in the rate constants. There would be no difference if the variation in the rate were a parabolic function of variation in the rate constants. The function is only approximately parabolic. However, in practice the difference is negligible.

In many cases it is not necessary to actually determine the values for k_1 or k_2 . However, if it is desirable to change conditions, for reasons of operator convenience or instrumental constraints, then some estimate is required. An estimation of k_2/k_1 can be made from the measurement of time of crossover and the time of occurrence of the peak velocity, t_p . Because the center of the peak is difficult to locate, it is useful to use a least squares fit to the data points around the peak. For velocity data which were measured over equal intervals of time, the following simplified least squares formula is helpful,

$$\Delta X = -\frac{y_{-1} - y_{+1}}{2y_{-1} - 4y_0 + 2y_{+1}} \quad (9)$$

where y_0 is the peak velocity, y_{-1} is the velocity in the previous interval, y_{+1} is the velocity in the following interval, and ΔX is the distance to the estimated peak from the data point having the maximum velocity. The distance is in terms of the time interval, i.e., if the velocity was measured every 30 s, and ΔX were -0.3, the estimated peak occurred 9 s before the data point with maximum velocity. Returning to the estimation of k_2/k_1 , the ratio of t_p to t_1 (for a crossover determined by variation of k_1) is equal to the ratio of T_p to T_1 . The latter ratio can be determined from Figure 1 and linear interpolation used if necessary to find the appropriate k_2/k_1 .

Once k_2/k_1 is known, then the other optimal times can be determined, or individual adjustments to the activity of k_1 or k_2 can be made for improved resistance to change or to reduce the cost of the assay by using more of the inexpensive enzyme and less of the other.

Method B. From Figure 1, the value of k_2/k_1 can be determined if the value of T_p is known. Since $T_p = k_1 t_p$, measurement of k_1 , in addition to t_p , as described in Method A above, is necessary. The value of k_1 can be measured from the terminal slope of a log velocity vs. time plot. This method is convenient because both measurements can be made on a single set of velocity data.

Method C. The rate constants are determined from a nonlinear least-squares fit of Equation 10 to the data.

$$X = Y + A_0 \left\{ 1 - \exp(-k_1 t) \left[\frac{k_2}{k_2 - k_1} \right] \left(1 - \frac{k_1}{k_2} \exp(-(k_2 - k_1)t) \right) \right\} \quad (10)$$

where X represents a measured variable such as absorbance, Y is a background level, and the other terms are the same as in Equation 2. The parameters to be determined are; Y , A_0 , k_1 , k_2 , and possibly t_0 in cases where there exists a significant dead time between mixing and initiation of the reaction timer. The Box Algorithm (4) is useful in dealing with three nonlinear terms, k_1 , k_2 , and t_0 . The method requires at least 10 good data points which include some measurements around the time where the velocity is a maximum.

Method D. This method involves direct measurement of k_2 by measuring the slope of a log velocity vs. time plot resulting from a reaction mixture initially containing the intermediate substance B in Equation 1. In the example considered here, ammonium ion is the intermediate. From the terminal slope of a log velocity vs. time for a plot resulting from a reaction mixture initially containing the substrate, A, the rate constant, k_1 , can be determined also.

RESULTS

In Figure 3 are plotted the velocity data (rate of change of absorbance) for a systematic variation in k_1 (Type I variation). The curve labeled 1 corresponds to the desired enzyme activity, curve 2 corresponds to an increase of 25%, and curve 3 corresponds to a 25% decrease. The peak velocity (corresponding to the straightest portion of the absorbance curve which is not shown here) occurs approximately at the second velocity data point. At that time the velocities were 13% greater and 17% less than the unperturbed velocity depending as k_1 was greater or less than the nominal. Such variation in results would be generally unacceptable. On the other hand, the crossover point labeled A represents the time at which the various perturbations have very nearly the same velocity as the nominal, i.e., minimal error. The time of crossover, A, is virtually the same as t_1 and illustrates the finding from the error surface that increase or decrease in k_1 both result in a decrease in velocity at that time. The measured decrease was

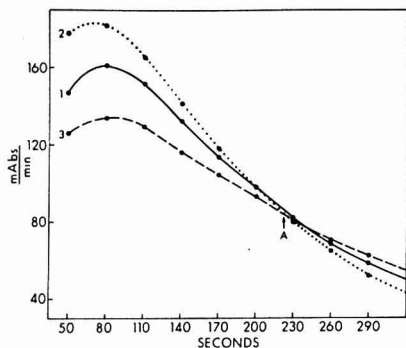


Figure 3. Velocity curves resulting from systematic variation in k_1 . Conditions: 1 = nominal, 2 = +25% k_1 , 3 = -25% k_1 .

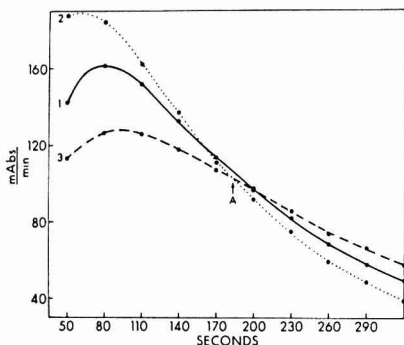


Figure 4. Velocity curves resulting from systematic variation in k_1 and k_2 together (dilutional or temperature type variations). Conditions: 1 = nominal, 2 = +25% k_1 and k_2 , 3 = -25% k_1 and k_2 .

2.5% which compares well with the predicted 2% and is a substantially smaller error than that at the peak velocity.

In Figure 4 are plotted the velocity data for a systematic variation in k_1 and k_2 together (Type III variation). The results are entirely analogous to those for perturbations in k_1 above. At crossover A, corresponding to t_{III} , the 25% perturbations resulted in a decrease in velocity of 4%.

Data for systematic variation of k_2 (Type II variation) are plotted in Figure 5. A semilogarithmic scale was chosen to illustrate estimation of k_1 from the terminal slope. At crossover A, corresponding to t_{II} , 25% perturbations in k_2 resulted in error too small to be measurable from the figure.

As expected, Figure 5 demonstrates that the three curves exhibit the same terminal slope. Also this illustrates the point that the velocity is different from that of a simple exponential decay (first-order reaction) by a steady-state term. The transient term has negligible effect on the terminal portion of the curve. For a value of k_2/k_1 of 4, a 25% increase in k_2 results in a 6.25% decrease in the value of the steady-state term. The observed decrease was about 6%.

Table I summarizes the kinetic constants estimated by the several methods. The agreement with the experimental finding is generally good. For instance, from Figure 5 the type II crossover occurred at 124 s. The estimates of t_{II} ranged from 127 to 145 s. In the latter case, it will be seen that Method C generally overestimated the various times. One would have expected Method C, the nonlinear least squares, to provide

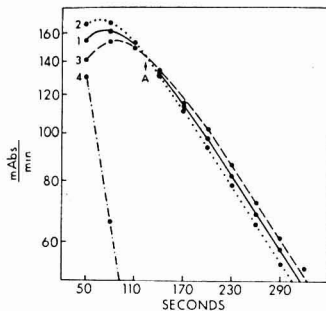


Figure 5. Semilog plot of velocity resulting from systematic variation in k_2 . Conditions: 1 = nominal, 2 = +25% in k_2 , 3 = -25% in k_2 . Curve 4 is due to the intermediate, ammonia, so that k_2 can be estimated directly from the slope.

Table I. Estimation of Kinetic Constants

measured	method of estimation ^a				
	A _I	A _{III}	B	C	D
k_1 (s ⁻¹)			0.0061	0.0060	0.0061
k_2 (s ⁻¹)				0.0205	0.0226
A (s)	223	183			
t_p (s)	78	78	78		
derived					
k_2/k_1	4.1	3.9	3.8	3.4	3.7
t_I (s)	-	210	216	227	218
t_{II} (s)	133	127	131	145	134
t_{III} (s)	194	-	187	197	189
t_p (s)	-	-	-	85	79

^a The method of estimation denotes the particular experimental manipulations. In Method A_I, one measures the time at which the rate of reaction is a maximum and also the time at which the reaction curves intersect for variations in k_1 (see point A of Figure 3). Method A_{III} is like A_I except that both k_1 and k_2 are varied keeping their ratio constant (see point A of Figure 4). In Method B, one measures the time at which the rate of reaction is a maximum and also estimates k_1 from the terminal slope of a semilog plot of the reaction data (see Figure 5). In Method C, one fits the absorbance data by a nonlinear least-squares routine. In Method D, one estimates k_1 as in Method B and also estimates k_2 by observing the reaction of the intermediate substance (see curve 4 of Figure 5). See text for full description of methods.

better agreement since the maximum deviation between the measured and fitted absorbance was only 1.6 milliabsorbance. It may be that the method was adversely affected by early measurements before the reaction mixture was fully temperature equilibrated.

DISCUSSION

In the design of an assay for a substance by kinetic methods, a great many factors have a bearing on the selection of conditions. The optimization, presented here, presumes that variations in the rate constants (enzymatic activities) are a dominant source of error. Depending on the rate constant which is most subject to variation, conditions can be selected that substantially minimize the effects of such variation. In the selection of those conditions, the optimization theory provided the time at which the rate measurement should be made. If that time were, for example, 10 min and it was desired to complete the analysis in 2 min, then both rate constants (amount of enzyme) would simply be increased by a factor of 5. It may be observed from Figure 4 or 5 that, for

a fixed analysis time, the amount of enzyme required for the optimized method is greater than that for the maximal velocity criteria (approximating an initial rate measurement) yet less than that for the end-point criteria (99% complete at 5 time constants).

In the one-step kinetic analysis described by Atwood, the rate of reaction at the optimum time was only 37% of the initial rate. Even so, that rate was the greatest rate which could be achieved at a nonzero measurement time. More or less enzyme would have given a smaller rate. By way of contrast, the coupled kinetic analysis exhibits a peak rate at some time after initiation of the reaction and the rate of reaction at the optimum time can range from 37% to 100% of that peak rate. For instance, when k_2/k_1 is greater than 5 to 10, the optimum time of type I or III, will give approximately 37% of the peak velocity, whereas a Type II condition will approach 100%. When the rate constants are approximately equal, then the velocity at the optimum time will be approximately 75% of the peak velocity in all types of optimization.

It is observed from Figure 1 that the various optimum times converge when the rate constants are equal. Under those conditions, there are minimum errors resulting from variation of k_1 or k_2 or any combination of them. This is in contrast to other conditions where, for example, selection of a Type III optimum time sacrifices the suppression of errors due to variation in k_1 alone. However, that sacrifice will be small for k_2/k_1 greater than 10 or less than 2. While the selection of equal rate constants is a generally desirable condition, other conditions might be dictated by cost consideration. Thus, less of the expensive enzyme and more of the other enzyme would be used. This strategy generally leads to amounts of enzyme proportioned for equal cost and the ratio, k_2/k_1 , is thus fixed. The actual amounts of enzyme are set by the choice of analysis time.

It has been customary to make k_2 greater than k_1 , and the theory so far has only considered k_2 equal to or greater than k_1 . However, the symmetry of the differential equations is such that the same curve would be generated for $k_2/k_1 = 4$ as for $k_2/k_1 = 1/4$. For this case ($k_2/k_1 = 0.25$), the optimum time would be obtained from Figure 1 by choosing a value of 4 for the ratio of rate constants and using the corresponding value of T_I if error from k_2 is to be minimized, T_{II} if error from k_1 is to be minimized, and T_{III} for simultaneous variations. The actual time will be calculated as from the relations; $T_I = k_2 t_I$, $T_{II} = k_2 t_{II}$, and $T_{III} = k_2 t_{III}$.

Of the various methods for determining the optimal time, Method A offers particular advantage because it is not necessary that the upside and downside variations be equal. For example, if it were expected that an increase in k_1 could

be expected because of endogenous enzyme in some samples, then the time of crossover between the nominal and exceptional sample could be chosen.

It is customary to calibrate enzymatic measurements of substrate. Even though the actual time of measurement may be far from optimum, the results will be without error if the conditions do not vary. The consequence of non-optimum conditions is only to make the analysis more sensitive to variation in conditions. It is fortunate that the optimum time need not be known with great precision since the results of Table I exhibit a considerable range of estimates for the various optimal times.

The measurement of urea under the conditions presented here was taken as an example that would be a serviceable assay. Nevertheless the conditions could be modified for the sake of cost and convenience without sacrifice in quality. The anticipated changes would reduce the amount of glutamate dehydrogenase by a factor of two and increase the amount of urease by a factor of two. This would make the rate constants approximately equal. Another set of experiments could be performed to verify that the expected conditions had been achieved. Then, possibly, the amount of both enzymes might be increased to move the optimum time to about 2 min, which time is long (to reduce the required amount of enzymes) but not affecting throughput of the centrifugal analyzer (whose sample loader limits the throughput to at least a 3-min cycle).

Extensions of the theory presented here could consider additional coupling steps. Also, wide time intervals for the measurement of the rate deserves consideration. It is not necessary that the reaction be enzyme catalyzed, but only that it be first- or pseudo-first-order in each step. Furthermore, the coupling step is mathematically equivalent to an RC filter used in analog rate measurements; hence the optimum time for the measurement of a first-order reaction by an analog ratemeter can be determined. Nevertheless, the point made here is that coupled kinetic assays for substrate can be made less subject to errors in a straightforward manner.

ACKNOWLEDGMENT

We thank a reviewer for bringing the work of H. U. Bergmeyer to our attention.

LITERATURE CITED

- (1) J. G. Atwood and J. L. DiCesare, *Clin. Chem. (Winston-Salem, N.C.)*, **21**, 1263-1269 (1975).
- (2) H. U. Bergmeyer, *Biochem. Z.*, **324**, 408-432 (1953).
- (3) T. O. Tiffany, J. M. Jansen, C. A. Burtis, J. B. Overton, and C. D. Scott, *Clin. Chem. (Winston-Salem, N.C.)*, **18**, 829-840 (1972).
- (4) G. E. P. Box, *Ann. N.Y. Acad. Sci.*, **86**, 792-816 (1960).

RECEIVED for review September 18, 1978. Accepted December 22, 1978.

Determination of Individual Ubiquinone Homologues by Mass Spectrometry and High Performance Liquid Chromatography

Sukehiro Imabayashi,* Tetsuya Nakamura, Yoshio Sawa, Jirō Hasegawa, Kenya Sakaguchi, Takeshi Fujita, Yutaka Mori, and Kiyoshi Kawabe

Eisai Research Laboratories, Eisai Co., Ltd., Koishikawa 4, Bunkyo-ku, Tokyo 112, Japan

Ubiquinone homologues in various animal tissues (liver, kidney, heart, and spleen) were determined by direct inlet selected ion monitoring. Samples were prepared by solvent extraction, after treating with lipase to eliminate substances that might interfere with the analysis. The detection limit by direct inlet selected ion monitoring for ubiquinone-10 was 0.1 ng. The same samples were also subjected to high performance liquid chromatography and results of this latter analysis were in good agreement with results by direct inlet selected ion monitoring.

The biological significance of ubiquinone as a redox carrier in the respiratory chain has been well established (1). Further, from a physiological standpoint, it was reported that localized deficiencies of ubiquinone occurred in the gingiva of patients with periodontal diseases (2), in human heart disease (3), and in leukocytes of patients with essential hypertension (4). The test was performed by measuring the variation of specific activity of succinate-dehydrogenase ubiquinone reductase in tissues (5). However, the quantitative analysis of ubiquinone has not been described in these cases. This may be due partly to the fact that a practical and reliable procedure for analysis of ubiquinone homologues in biological samples had not been developed.

However, a number of studies have been carried out on the quantitative analysis of ubiquinone homologues (i.e., ubiquinone-*n*, with *n* representing the number of isoprenoid side chains, hereafter, simply as *Q-n*) widely occurring in animals and plants. A survey of the occurrence of ubiquinone in various vertebrates has been reported (6). Ramasarma (7) described a comprehensive review of the analytical data in animal tissues, plants, and microorganisms. As a conventional method for the determination of total *Q-n*, spectrophotometric analysis (8), which is based on the difference in absorbancy of the oxidized and reduced ubiquinone at 275 nm or a modified Craven test (8), has been used. Since each of these methods utilizes the quinone nuclei as the analytical principle, they do not give satisfactory results for determination of individual homologues of ubiquinone. Casey et al. (9) developed a method using reverse-phase paper chromatography. It consists of direct estimation of individual spots developed on the paper by densitometry. The *Q-n* concentration (in human blood) is also being analyzed (10) by electron capture gas chromatography.

To develop a sensitive and simple method, the present authors attempted to determine individual ubiquinone homologues in various tissues of animals and human blood by direct inlet selected ion monitoring (DI-SIM) (11, 12), which recently drew attention as a means of microanalysis, for the determination of individual ubiquinone homologues in animal tissues and human plasma. Additionally, determination was made by high performance liquid chromatography (HPLC) (13, 14) to compare the results of both methods. For the pretreatment of samples, in place of a conventional strong alkali saponification method, a milder enzymic hydrolysis using lipase was employed.

EXPERIMENTAL

Standards. All-trans standard samples (*Q*₁₀, *Q*₉, and *Q*₈) were prepared by condensing a boric acid ester of 2,3-dimethoxy-5-methyl-1,4-benzohydroquinone with decaprenol (or isodecaprenol), solanesol, octaprenol, respectively, and oxidizing the resultant borate with Ag₂O (15). DI-SIM internal standard 2,3-dimethoxy-5-methyl-6-³,⁷,¹¹,¹⁵,¹⁹,²³,²⁷,³¹,³⁵,³⁹-decamethyl-tetracontanyl benzoquinone (hereafter referred to as IS-1) was prepared by catalytic reduction of *Q*₁₀ with a Pd-C catalyst, followed by oxidation with PbO₂ (10). HPLC internal standard 2,3,5-trimethyl-6-decaprenyl-1,4-benzoquinone (16) (hereafter referred to as IS-2) was prepared by condensing a boric acid ester of 2,3,5-trimethyl-1,4-benzohydroquinone with decaprenol (or isodecaprenol), and oxidizing the resultant borate with Ag₂O.

Humans and Animals. *Humans.* Ten healthy males (28 to 43 years of age, weighing 58 to 79 kg) were used.

Mice. Five- to six-week-old female ICR/JCL mice were purchased from CLEA Japan Inc., Tokyo. They were maintained on a NMF (Oriental Yeast Co., Tokyo) pellet diet for two weeks and mice weighing about 22 g were used in the present study.

Guinea Pigs. Healthy three-month-old males and females were maintained for two weeks on an ORC-4 diet (Oriental Yeast Co., Tokyo). The weights were about 250 g when used.

Beagles. Twenty-four- to thirty-eight-month-old males and females were maintained on a CD-1 diet (CLEA Japan Inc., Tokyo). The weights were about 10 kg.

Rats. Fifteen-week-old male and female Sprague-Dawley rats were maintained for three weeks on a CE-2 diet (CLEA Japan Inc., Tokyo).

Pretreatment of the Samples. One to two mL of plasma was placed in a Pyrex glass test tube and 2.0 μg of IS-1 was added. To the mixture 2 mL of 1% pancreatin (Sigma Chemical Company) solution and 0.2 mL of 4% sodium taurocholate (BDH Chemicals Ltd.) solution were added. Subsequently, the solution was incubated at 37 °C for 2 h. Then 5 mL of ether was added and the mixture was sufficiently shaken and centrifuged. The ether phase was collected in a Pyrex glass test tube. This extraction procedure was repeated three times. The sample was evaporated to dryness under reduced pressure. The resultant residue was dissolved in 0.2–0.5 mL of ethyl acetate.

Sample pretreatment in a quantitative analysis of *Q-n* in tissues was as follows. The rats were decapitated, the liver removed, and a portion of the liver (about 0.5 to 2 g of wet liver) was homogenized in a Potter Elvehjem homogenizer. The homogenate thus obtained was treated in the same manner as pretreatment of the plasma sample mentioned above. Extraction with ether was repeated three times to ensure complete extraction of IS and *Q-n*.

The homogenized tissues were kept in a freezer and an aliquot of the homogenate was used for determination. The determination errors in one day and between days were examined. Such errors in the DI-SIM were within ±5%. Following the present experimental procedure, it was observed that the relative recovery ratio of *Q-n* and IS-1 from the plasma and organs were almost 100%.

Direct Inlet Selected Ion Monitoring. The instruments used were a JFOL JMS-D100 and JMS-D300, both with a magnetic sector. For JMS-D300 equipment, the computer system (JMA-200Q, JEOL, Tokyo) was attached to ascertain the contaminant of interfering substances. This computer system is specially designed to detect minute amounts of interfering substances in biological samples. Measuring conditions were as follows, ionizing current, 300 μA; ionizing voltage, 25 eV; chamber

Table I. Relative Intensities of Parent Ion Peaks of Ubiquinone Homologues and Internal Standards

Q_n	m/e	ionizing voltage	
		70 eV	30 eV
Q_9	728	60	64
Q_{10}	796	31	33
Q_{10}	864	22	24
IS-1	882	100 ^a	100 ^a
IS-2	832	26	28

^a Arbitrarily assigned.

Table II. Comparison of Human Plasma Level Determined by DI-SIM or Craven Test

subject	DI-SIM $\mu\text{g/mL}$	Craven test, $\mu\text{g/mL}$
1	1.35 ± 0.11^a	1.41 ± 0.36
2	1.26 ± 0.09	1.15 ± 0.23
3	1.04 ± 0.11	1.03 ± 0.17

^a Mean \pm SEM for three determinations for a sample.

temperature, 200 °C; probe temperature programmed from 150 to 270 °C; measuring SIM: Q_9 , m/e 796 [M + 2]⁺; Q_{10} , m/e 864 [M + 2]⁺; IS-1, m/e 882 [M]⁺; IS-2, m/e 832 [M + 2]⁺. The appearance of parent ion peaks of ubiquinone homologues and internal standards under two ionizing voltage conditions is shown in Table I.

The extract was dissolved in 1 to 5 μL of ethyl acetate, the presumed content of Q_{10} being 0.1–100 ng. At this point, the solution was placed in a glass capillary, which was heated with a drier to evaporate the solvent. A standard sample for a calibration curve was prepared by adding cholesterol in the amount of 1 to 5%. The cholesterol was added only in the standard samples to stabilize evaporation of ubiquinone homologues and to obtain a typical SIM pattern. In such a case, high reproducibility was easily obtained and a linear calibration curve was obtained.

High Performance Liquid Chromatography. Chromatography was performed on a Shimadzu LC-1 pumping system, Shimadzu SPD-1 (scanning UV detector) and UVD-1 (254-nm UV detector). The column was a Shimadzu-Du Pont "permaphase ODS" (1 m \times 2.1 mm, particle size: 30 μm). A solution of degassed spectroquality methanol (HPLC grade, Wako Chemicals, Osaka) and distilled water was used as the gradient-elution mobile phase programmed for a linear 1% per minute increase in methanol concentration from a starting mixture of 80/20 (v/v) methanol/water taken to 100% methanol. The measuring temperature was 45 °C. A 1000-psi head was developed at a flow rate of 1 mL/min. Column effluent was monitored at 254 nm (UVD-1)

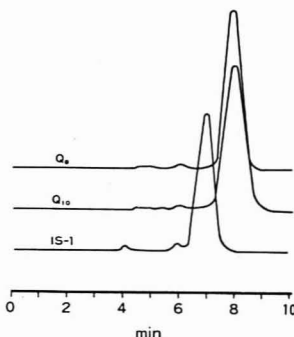


Figure 1. Direct inlet selected ion monitoring (DI-SIM) of standard Q_9 , Q_{10} , and the internal standard (IS-1). Measuring conditions: ionizing current, 300 μA ; ionizing voltage, 25 eV; chamber temperature, 200 °C; sample temperature, from 150 to 270 °C. Measuring mass fragment: Q_9 , m/e 796 [M + 2]⁺; Q_{10} , m/e 864 [M + 2]⁺; IS-1, m/e 882 [M]⁺.

and 275 nm (SPD-1). The purpose of using two differential UV detectors was to investigate interfering substances in more detail.

RESULT AND DISCUSSION

The SIM spectrum of a standard sample is shown in Figure 1 and the chromatogram of a standard sample of HPLC analysis is shown in Figure 2.

The analysis of Q_{10} in human plasma was carried out by DI-SIM and Craven test (17). The results obtained by the two methods are shown in Table II.

The range for the 10 individuals by DI-SIM was from 0.28 to 1.63 $\mu\text{g/mL}$ and the average was 0.85 $\mu\text{g/mL}$.

Analysis of DI-SIM and HPLC on individual animal tissues is shown in Table III. Results of analytical values by DI-SIM, Craven test, and HPLC were almost in agreement (Tables II and III).

For pretreatment of samples, a conventional method of alkali saponification could not entirely eliminate substances that interfered with the analysis (such as triglyceride-like compounds) by the DI-SIM. Treatment with lipase removed this difficulty. The effectiveness of the lipase pretreatment was clearly shown on the SIM pattern of extracts of tissue samples. Using DI-SIM and HPLC analysis, measurements were made for the various animal tissues. In all cases, using

Table III. Occurrence of Ubiquinone-9 and -10 in Animal Tissues^a

animal	tissue	DI-SIM		HPLC	
		Q_9	Q_{10}	Q_9	Q_{10}
mouse	liver	87.5 ± 18.4 (6) ^b	6.7 ± 2.4 (4)	83.5 ± 8.3 (4)	5.6 ± 2.3 (4)
	kidney	321.5 ± 26.1 (6)	29.1 ± 6.5 (4)	298.0 ± 35.1 (4)	26.7 ± 4.1 (4)
	heart	151.0 ± 18.6 (6)	19.1 ± 2.9 (5)		
	spleen	24.5 ± 4.6 (6)	N.D. ^c		
rat	thymus	77.5 ± 27.0 (5)	28.7 ± 11.0 (5)		
	liver	148.5 ± 18.7 (3)		169.2 ± 85.1 (15)	
	kidney	103.2 ± 22.9 (3)		128.2 ± 47.2 (15)	
guinea pig	liver		77.5 ± 7.5 (18)	4.5 ± 2.0 (18)	79.7 ± 7.9 (18)
	kidney		230.7 ± 10.5 (18)	trace	224.5 ± 10.0 (18)
	heart		220.5 ± 8.6 (18)	trace	227.8 ± 8.4 (18)
rabbit	liver				77.8 ± 10.6 (4)
	kidney				147.7 ± 12.8 (4)
beagle dog	liver		145.7 ± 14.8 (5)	trace	138.3 ± 13.9 (5)
	kidney		185.4 ± 13.6 (5)	trace	177.7 ± 14.0 (5)
mongrel dog	liver			13.8 ± 3.2 (4)	142.4 ± 29.7 (4)
	kidney			trace	213.5 ± 33.9 (4)

^a $\mu\text{g/g}$ wet tissue (mean \pm SEM). ^b Figures in the parentheses represent number of animals. ^c N.D.: not detectable.

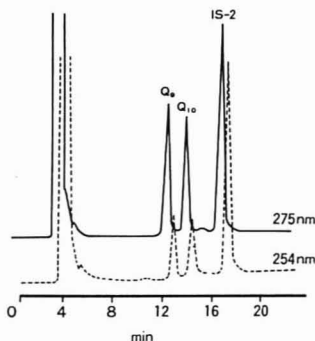


Figure 2. HPLC of standard Q-n. Measuring conditions: column, Permaphase ODS 1 m X 2.1 mm i.d.; mobile phase, MeOH (HPLC grade)-water (pH 5.0-7.0); gradient, 80/20-100/0 (MeOH/H₂O); flow rate, 1 mL/min (70 kg/cm²); temperature, 45 °C; measuring wavelengths, 254 nm (UVD-1) and 275 nm (SPD-1)

either one or the other of the two methods, consistently reproducible results were obtained (Table III).

In order to be sure of the results of the HPLC analysis, two types of detectors (SPD-1 and UVD-1) were attached to the HPLC apparatus and the measurements were made at two different wavelengths (275 and 254 nm). The analytical results obtained were always the same for the two wavelengths. This fact means that the analytical data obtained are not disturbed by contaminants.

In the DI-SIM analysis, a check was also made by mass chromatography (JEOL model JMS D-300 with computer system). By use of a mass chromatography analysis, it was possible to confirm the adequacy of the established quantitative analytical procedure with DI-SIM. A comparative study of the DI-SIM method and Craven test method was made using normal human plasma as the sample (Table II). The results obtained showed good compatibility of the ubiquinone concentration.

Theoretically, in the DI-SIM analysis, the number of simultaneous determinations of individual ubiquinone homologues is permitted in accordance with the channel number of the multi-ion detector in the apparatus.

In studying the physiological role of ubiquinone in tissues or blood, it is necessary to determine the concentration of individual homologues in the mixture in a quantitative manner. Although this can be accomplished by several methods (8, 9, 17), these procedures require large amounts of samples. However, our method is a practical recommendation for quantitative analysis of individual ubiquinone higher than Q₈ homologues, which are widely distributed in small amounts in the animal and vegetable kingdom.

ACKNOWLEDGMENT

The technical assistance of Miwako Kuroki and Kazuko Kinoshita are gratefully acknowledged. The authors are deeply indebted to Junzō Tsutsumi, R. K. Garg, Tomio Takamatsu, and Kimio Hamamura, Eisai Research Laboratories, for their cooperation. Thanks are also due to Atsushi Yamagishi, Executive Director of the Board and Director of Research Division, for encouragement and support of this study.

LITERATURE CITED

- (1) J. W. DePierre and L. Ernster, *Ann. Rev. Biochem.*, **46**, 201-262 (1977).
- (2) R. Nakamura, G. P. Littarru, K. Folkers, and E. G. Wilkinson, *Proc. Natl. Acad. Sci. U.S.A.*, **71**, 1456-1460 (1974).
- (3) G. P. Littarru, L. Ho and K. Folkers, *Int. J. Vitam. Nutr. Res.*, **42**, 413-434 (1972).
- (4) T. Yamagami, Y. Iwamoto, and K. Folkers, *Int. J. Vitam. Nutr. Res.*, **44**, 404-414 (1974).
- (5) R. Nakamura, G. P. Littarru, and K. Folkers, *Int. J. Vitam. Nutr. Res.*, **43**, 526-536 (1973).
- (6) A. T. Diplock and G. A. D. Haslewood, *Biochem. J.*, **104**, 1004-1010 (1967).
- (7) T. Ramasarma, *Adv. Lipid Res.*, **6**, 107-180 (1968).
- (8) F. L. Crane and Rita Barr, "Methods in Enzymology", D. B. McCormick and L. D. Wright, Ed., Academic Press, New York, 1971, Vol. 18, Part C, pp 137-181.
- (9) A. C. Casey, P. Myers, and A. Lee, *J. Chromatogr.*, **72**, 365-371 (1972).
- (10) H. Morimoto, I. Imada, T. Amano, M. Toyoda, and Y. Ashida, *Biochem. Med.*, **7**, 169-177 (1973).
- (11) C. G. Hammar and R. Hessling, *Anal. Chem.*, **43**, 298-306 (1971).
- (12) W. Snedden and R. B. Parker, *Anal. Chem.*, **43**, 1651-1656 (1971).
- (13) P. L. Donnan and F. W. Hemming, *Biochem. Soc. Trans.*, **3**, 775-776 (1975).
- (14) I. A. Tavares, N. J. Johnson, and F. W. Hemming, *Biochem. Soc. Trans.*, **5**, 1771-1773 (1977).
- (15) S. Kijima, I. Yamatsu, K. Hamamura, N. Minami, Y. Yamagishi and Y. Inai, U.S. Patent 3,998,858 (1976); *Chem. Abstr.*, **86**, 171664z (1977).
- (16) J. Green and D. McHale, "Biochemistry of Quinones", R. A. Morton, Ed., Academic Press, London and New York, 1965, pp 261-285.
- (17) E. Redalieu, I. M. Nilsson, T. M. Farley, K. Folkers, and F. R. Konisky, *Anal. Biochem.*, **23**, 132-140 (1968).

RECEIVED for review April 12, 1978. Accepted December 15, 1978.

Stoichiometry of the Reaction of Electrons with Bromotrichloromethane in an Electron Capture Detector

E. P. Grimsrud* and S. H. Kim

Department of Chemistry, Montana State University, Bozeman, Montana 59717

A detailed study of the reactions of CCl_3Br with electrons and positive ions under conditions existing in an electron capture detector (ECD) is reported. Measurements of ions by atmospheric pressure ionization mass spectrometry (APIMS) indicate that each CCl_3Br molecule which undergoes electron capture removes only one electron and the resulting neutral products do not undergo further electron attachment to a significant extent. Also, under the condition where electrons are in abundance in the ECD, it is shown that no significant loss of CCl_3Br due to reaction with positive ions occurs. These results lend fundamental support to assumptions of chemical reactivity inherent in the use of the ECD as a gas-phase coulometer.

The electron capture detector (ECD) responds sufficiently sensitively to certain halogen-containing compounds as to cause nearly 100% ionization of these within this detector in their analyses by gas chromatography. This observation has prompted several investigations of the use of the ECD as a gas-phase coulometer (1-3) in which the number of electrons lost as measured simply from ECD peak areas was reported to be nearly equal to the number of sample molecules passed through the cell for compounds such as SF_6 , CCl_4 , CFCl_3 , and CF_2Br_2 . The successful application of this form of gas-phase coulometry to these and perhaps to other strongly ECD-active compounds would provide an extremely useful method for trace analysis because of the considerable difficulty incurred in preparing reliable calibration standards at environmental concentration levels.

If the ECD is to be made to function successfully as a gas phase coulometer, several individual criteria of the overall method might be envisioned. These would include at least the following: (1) Electrons must be in excess of sample molecules. (2) The electron capture reaction must be nearly complete (nearly 100% destruction of sample molecules). (3) The stoichiometry of the reaction of thermal electrons with the sample molecules must be 1:1 (or some other known ratio). (4) No side reactions of the sample molecule may occur. (5) The current monitored from the ECD must reflect the absolute magnitude of electrons present in the entire ECD cell, and an ECD response must reflect absolutely the loss of these electrons to EC reactions. In previous studies of gas-phase coulometry (1-3), experiments were designed to test the apparent overall validity of the method by comparing an observed response with a known amount of sample passed through the cell. Also, with the instrumentation available in the previous studies, requirements 1 and 2 could be individually examined. By the use of tandem ECDs it was convincingly demonstrated that strongly ECD-active compounds are nearly completely consumed by the electron capture reactions within the first detector.

While these initial tests of gas phase coulometry are encouraging, it nevertheless remains desirable to examine individually the remaining criteria of this technique. From experiments we have recently reported (4), it might be ex-

pected that requirement 5 is not precisely satisfied with at least some ECD cell designs. We have shown that the cell current obtained from a pulsed ECD of the concentric pin design may be significantly reduced because of the migration of positive ions to the sampling anode pin during the period between voltage pulses. For our cell conditions, this positive ion component of the net current was shown to be about 28%. Another potential complication of requirement 5 may be positive ion-electron recombination which has recently been suggested as an important electron loss mechanism within the ECD (5). It appears, therefore, that requirement 5 of gas-phase coulometry warrants further individual study. In this article we wish to report experiments designed to test the chemical reactivity requirements 3 and 4, individually. This is done by measuring the negative ions produced by the electron capture reactions of CCl_3Br and the positive ions formed by competitive ion-molecule reactions. The mass spectrometer used is a specialized atmospheric pressure ionization mass spectrometer (APIMS) where its ion source is an actual ECD.

EXPERIMENTAL

The ECD/APIMS instrument used for this study was home-built and has been described in detail previously (4, 6). This instrument is essentially an atmospheric pressure ionization mass spectrometer (7) where the ion source has an internal volume (1 cm^3) typical of ^{63}Ni ECDs and includes a coaxial pin which serves as the ECD anode. With this instrument, the ECD response to an electron capturing compound can be monitored along with mass spectral measurement of the ions simultaneously formed in the source, as shown in Figures 1 and 2. We have shown previously, however, that the application of voltage pulses to the anode pin can adversely affect the intensity of negative ion signals simultaneously monitored (4). The cause of this interdependence is not that negative ions are destroyed or chemically altered by the field, but is thought to be due to the creation of a positive ion, space-charge field after the removal of electrons by individual voltage pulses, and the subsequent containment of negative ions within this positive-ion cloud (4). With no fields applied to the ion source, charge neutrality exists throughout the ion source (5) and the negative ions formed by electron capture reactions can be observed even in the small sample condition. For this reason, the measurement of negative ions within the ECD was always made during separate, repeated GC analyses with the ECD function of the ion source turned off. All ECD current measurements reported here were obtained by applying to the anode +48-volt pulses of $1.5\text{-}\mu\text{s}$ width and frequency 550 Hz. The ECD current shown in Figures 1 and 2 is the total unprocessed current. The standing current observed with this configuration was about 1.0 nA .

Mass spectral measurements in all cases were made with the resolution sufficiently relaxed so that the ion current due to the entire group of halogen isotope clusters in a given measurement was monitored. In the determination of the relative Cl^- and Br^- ion concentrations reported in Tables I and II, the measured ion intensity ratios such as shown in Figure 1 were corrected for mass bias of the overall mass spectrometer system. This correction factor was determined by measuring the intensities of Cl^- and Br^- produced by the addition of continuously larger samples of C_2Cl_4 and $\text{CH}_2\text{ClCH}_2\text{Br}$ until a saturated condition of the ion source was observed. It was found that at saturation with

$\text{CH}_2\text{ClCH}_2\text{Br}$, the Br^- signal is 2.0 times greater than the Cl^- signal at saturation with C_2Cl_4 . In each case, these were the only ions of significant intensity observed. Assuming that at saturation, all of the finite number of electrons within the source are converted to these negative ions, the overall mass spectrometer system was deduced to be 2.0 times more sensitive to Br^- than Cl^- . The measured intensity ratio of Br^- to Cl^- divided by 2.0, was, therefore, taken as a measure of the ratio of Br^- to Cl^- concentration within the ion source. The precise cause of the mass bias is unknown. It has been shown (5) that positive ion-negative ion recombination will be a major loss mechanism for negative ions within an API source. Thus, a difference in the recombination rates of Cl^- and Br^- would contribute to the overall measured bias. In the above experiments, however, we have also monitored the total positive-ion signal and observed no significant differences between the Cl^- saturated and Br^- saturated cases. If recombination rates differed, this should have been reflected in the positive-ion signal, and we tentatively conclude that this is not the cause of the ion measurement bias. With our instrument (6), only a very small fraction of the total number of ions present in the expanding gas stream emitted from the source enters the quadrupole mass analyzer. It seems likely that it is in this gas expansion region (where a few relatively inefficient ion focusing lenses are located), that the ion measurement bias occurs. Whatever the cause of this bias, the above procedure should provide the correction necessary so that a measure of Cl^- and Br^- production rates within the source are obtained. Furthermore, any small errors introduced by this procedure do not alter the conclusions to be drawn here.

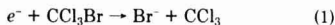
The gas chromatograph used in an Aerograph Autoprep A-700. The GC column was made from $1/8$ in. \times 10 ft stainless steel tubing packed with 10% SF-96 on Chromosorb W. The oven temperatures used were from 25 to 50 °C. The carrier gas was ultrahigh purity nitrogen (Matheson) which was further purified by passing it through a trap containing CaSO_4 and 5A molecular sieve. A heated, $1/8$ -in. stainless tube connected the GC to the ECD/APIMS.

Samples were prepared by the successive dilution of the compounds of interest (purchased from commercial suppliers) into hexane. These were injected into the sampling port of the GC with a 1- μL syringe. Repeated injections were reproducible to within $\pm 5\%$.

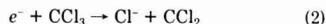
RESULTS AND DISCUSSION

In investigating the validity of requirement 3 of gas-phase coulometry, CCl_3Br provides an ideal molecule for study with our ECD/APIMS because the relative amounts of Br^- and Cl^- produced in its reaction with electrons will reflect details of the overall mechanism. Since CCl_4 has been shown to possess a very high ionization efficiency within the coulometric ECD, CCl_3Br might also be expected to be of the type susceptible to complete reaction (8). Furthermore, since the mechanism of electron capture by CCl_4 and CCl_3Br might be expected to be dissociative electron capture yielding a halide ion (9) and it is known that brominated molecules undergo electron capture more readily than chlorinated molecules (8), the neutral fragment produced most abundantly in each case is probably CCl_3 . Thus, the tests of requirement 3 for the case of CCl_3Br probably apply also to CCl_4 .

A likely first step in the electron capture by CCl_3Br is reaction 1, producing Br^- .



If this reaction is followed by further electron capture reactions of any of the neutral products, such as reaction 2



which will be accompanied by the production of Cl^- ions, a nonequivalent relationship between electrons consumed and molecules of CCl_3Br consumed would be expected. The relative importance of reaction 2 can be tested by measuring the abundances of Br^- and Cl^- in the ion source. In Figure 1 are shown ECD/APIMS chromatograms of several CCl_3Br samples where the amount of sample is varied from 2×10^{-8}

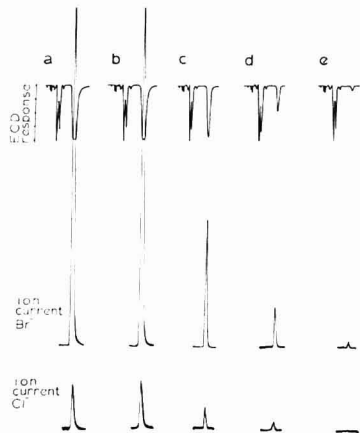


Figure 1. ECD/APIMS analyses of CCl_3Br where the ECD response and the Br^- and Cl^- ion signals are monitored for sample sizes (a) 2×10^{-8} g, (b) 2×10^{-9} g, (c) 2×10^{-10} g, (d) 2×10^{-11} g, and (e) 2×10^{-12} g. Ion source temperature is 250 °C, carrier gas flow rate 50 mL min^{-1} .

Table I. Ratio of Br^- to Cl^- Formed in Electron Capture by CCl_3Br

temperature, °C	flow rate, mL/min	sample size, g	$\text{Br}^-/\text{Cl}^-^a$
150	50	2×10^{-12}	~3.2
		2×10^{-11}	3.8
		2×10^{-10}	3.8
		2×10^{-9}	3.5
		2×10^{-8}	3.5
250	50	2×10^{-11}	3.8
		2×10^{-10}	3.6
		2×10^{-9}	3.7
		2×10^{-8}	4.1
		2×10^{-10}	3.9
250	50	2×10^{-10}	3.5
	75		4.0
	18		4.2

^a Ion concentration ratios are obtained from measured mass spectral ion signal ratios and are corrected for mass spectral bias effects as described in the Experimental section.

to 2×10^{-12} g. The two samples of highest concentration cause saturation of the ECD and the three lower concentrations cause progressively smaller responses until, in chromatogram e, the condition for coulometry that electrons be in excess of sample is clearly met. For all sample sizes, Br^- and Cl^- negative ions, and no others, were observed. The similarity of total ion intensities observed in chromatograms a and b of Figure 1 reflect the saturated condition where all available electrons have reacted to form Cl^- and Br^- ions. The decrease in total ion intensity from chromatogram c to e appears to be in harmony with the corresponding ECD responses. The indicated presence of Cl^- in Figure 1 may on first consideration suggest that reaction 2 does occur to some significant extent following reaction 1. On closer inspection, however, it is noted that the ratio of Br^- to Cl^- signals appears to be constant, about 8 to 1, in all cases. After correction for mass spectral bias, the ratio of Br^- to Cl^- concentration is about 4 to 1. Furthermore, as shown in Table I at the same temperature, 250 °C, with different carrier gas flow rates, the ratio of Br^-

to Cl^- produced is also close to 4 to 1 in all cases. The measured amounts of Br^- and Cl^- are also insensitive to variations in temperature to 150 and 300 °C. If it is assumed for the moment that Cl^- is generated from reaction 2, these results suggest the unlikely occurrence that only one and always one out of four CCl_3 radicals produced by reaction 1 undergoes electron attachment for all concentrations of CCl_3Br , for all flow rates, and at all temperatures. The relative amounts of Br^- and Cl^- which might be expected from the model comprised of reactions 1 and 2 can be calculated from the following coupled rate equations:

$$\frac{d\eta_{\text{Br}}}{dt} = k_1\eta_e\eta_{\text{CCl}_3\text{Br}} - R\eta_+\eta_{\text{Br}} \quad (3a)$$

$$\frac{d\eta_{\text{Cl}}}{dt} = k_2\eta_e\eta_{\text{CCl}_3} - R\eta_+\eta_{\text{Cl}} \quad (3b)$$

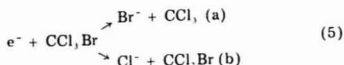
$$\frac{d\eta_{\text{CCl}_3}}{dt} = k_1\eta_e\eta_{\text{CCl}_3\text{Br}} - k_2\eta_e\eta_{\text{CCl}_3} - \frac{F}{V}\eta_{\text{CCl}_3} \quad (3c)$$

where the terms η_i are the number of densities of the indicated species i , η_+ is the total positive ion density, k_1 and k_2 are the rates of reactions 1 and 2, R is the rate constant for positive ion-negative ion recombination, F is the carrier gas flow rate, and V is the detector volume. The rate Equations 3a and 3b ignore the contribution to loss of Cl^- and Br^- due to diffusion to walls and ventilation through the detector, since these have been shown to be insignificant relative to ion recombination within an API source (5). Loss of CCl_3 by ventilation is included as the last term in Equation 3c. If the steady-state approximation is applied to reactions 3a-c, Equation 4 is obtained.

$$\frac{\eta_{\text{Br}}}{\eta_{\text{Cl}}} = 1 + \frac{F}{V k_2 \eta_e} \quad (4)$$

Since the observed ratio of $\eta_{\text{Br}}/\eta_{\text{Cl}}$ equals about 4, the second term in Equation 4 must be considered important if this model is valid. This term, however, varies with flow rate and also with η_e which, in the experiments here, has been varied by changing the sample size. Since the measured ratio of Br^- to Cl^- has been shown to be insensitive to changes in both the sample size and carrier gas flow rate, it appears that reaction 2 is not producing the Cl^- ion observed. Furthermore, any reaction scheme in which CCl_3 changes to another neutral molecule which then undergoes electron capture to produce Cl^- will also be inconsistent with the observed Br^- to Cl^- ratios.

An alternative description of the electron capture reaction of CCl_3Br might be envisioned in which reaction 1 is modified slightly to allow the formation of Cl^- competitively with Br^- , as shown in reaction 5.



Reaction 5a should be faster than reaction 5b, since reaction 5a is more exothermic than 5b by about 14 kcal (calculated from the electron affinities of Br^- and Cl^- , 78 and 83 kcal (10), respectively, and the bond dissociation energies of the C-Br and C-Cl bonds in CCl_3Br , about 54 and 73 kcal (11), respectively). However, if the rupture of a carbon-halogen bond occurs immediately upon electron attachment to the molecule (9) and prior to its stabilization by collisions, the route by which the excited molecular anion falls apart will be only somewhat sensitive to this energy difference which is small relative to the excess energy of CCl_3Br^- species, probably about 47 kcal (10). If reaction 5, alone, produces the Br^- and Cl^- ions observed, this would explain the insensitivity of the

Table II. Ratio of Br^- to Cl^- Formed in Electron Capture^a by $\text{CH}_2\text{ClCH}_2\text{Br}$ and $p\text{-ClC}_6\text{H}_4\text{Br}$

	sample size, g	Br^-/Cl^- ^b
$\text{CH}_2\text{ClCH}_2\text{Br}$	1.7×10^{-10}	8
	1.7×10^{-9}	9
	1.7×10^{-8}	17
	1.7×10^{-7}	26
$p\text{-ClC}_6\text{H}_4\text{Br}$	1.7×10^{-9}	>200
	1.7×10^{-8}	>200
	1.7×10^{-7}	>200
		>200

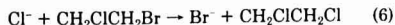
^a Ion source temperature is 250 °C. Carrier gas flow rate is 50 mL/min. ^b Ion concentration ratios are obtained from measured mass spectral ion signals and are corrected for mass spectral bias effects as described in the Experimental section.

measured Br^- to Cl^- ratios to variations in CCl_3Br concentration and to changes in the carrier gas flow rate and ion source temperature, since the relative rates in reaction 5 should be largely independent of these variables. For the same reasons as put forth in the above consideration of reactions 1 and 2, following reaction 5 no further electron capture by the neutral products, CCl_3 and CCl_2Br , apparently occurs. Since reaction 5, alone, provides the only reasonable model of electron capture events for this molecule that we can envision which is consistent with the mass spectral measurements, we conclude that it is probably valid. As this relates to our consideration here of gas-phase coulometry, it appears that requirement 3 is being met for CCl_3Br , and that the stoichiometry of its reaction with thermal electrons is 1:1. It may seem surprising that neutral products such as CCl_3 do not appear to undergo further electron attachment. Their electron affinity is nearly as large as the original substrate molecule (10). Evidently, these do not attach electrons rapidly or perhaps they are scavenged by carrier gas impurities such as H_2O , O_2 , hydrocarbons, or column bleed to form other relatively inactive compounds, such as CHCl_3 (3). Some of these impurities will always be in very great excess over electrons in any practical analysis system. For example, "oxygen-free" nitrogen may easily contain 1 ppm O_2 or about 10^{13} molecules cm^{-3} (or mL^{-1}) at one atmosphere pressure. The electron concentration in the ECD is probably about 10^8 cm^{-3} (or mL^{-1}) (5), five orders of magnitude less than that of oxygen.

Two other molecules containing both a bromine and chlorine atom, 1-bromo-2-chloroethane and p -bromochlorobenzene, were examined in the same manner as CCl_3Br to see if these might add additional insight into the CCl_3Br case. These molecules differ from CCl_3Br in that the ECD response to each is not as great, and only a small fraction of these molecules is expected to undergo electron capture. The results are reported in Table II.

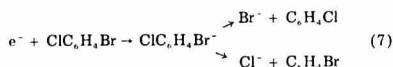
For $\text{CH}_2\text{ClCH}_2\text{Br}$, a sample size of 1.7×10^{-10} g was required before the Cl^- ion was measurable with acceptable precision. At this sample size, the ratio of Br^- to Cl^- produced is observed to be 8 to 1. If one accounts for the statistical factor that this molecule has only one chlorine atom while CCl_3Br has three, it would appear that $\text{CH}_2\text{ClCH}_2\text{Br}$ falls apart upon electron attachment in a manner roughly similar to that of CCl_3Br , without a great deal of sensitivity to the lowest energy pathway, which in this case favors Br^- production by about 7.5 kcal (bond dissociation energies of the C-Br and C-Cl bonds in this molecule are probably about 69 and 82 kcal (11), respectively). The observation that the ratio of Br^- to Cl^- increases to about 26 to 1 for the largest sample size of $\text{CH}_2\text{ClCH}_2\text{Br}$ may upon first consideration be taken to reflect a mechanism similar to reactions 1 and 2 previously discounted for CCl_3Br , where reaction 1 becomes progressively more favored over reaction 2 with the addition of excess $\text{CH}_2\text{ClCH}_2\text{Br}$. An alternative explanation, however, is that only an

electron capture reaction similar to reaction 3 again is important, but that ion molecule reaction 6



also occurs and increases the observed Br^- to Cl^- ratio under the condition of very great excess of sample. Nucleophilic displacement reactions of Cl^- with aliphatic bromides have previously been shown to occur with an appreciable rate in the gas phase (12), and the observed increase in the Br^- to Cl^- ratio with increased sample size might have been expected. A reaction analogous to reaction 6 could also be envisioned for the case of CCl_3Br when the sample is in great excess. No increase in the Br^- to Cl^- ion intensity ratio with large excess of sample was observed in this case, however, suggesting that this nucleophilic displacement reaction is not fast for CCl_3Br .

The case of *p*-bromochlorobenzene in Table II differs greatly from those previously considered in that no Cl^- was detected along with an intense Br^- signal. At the three sample sizes indicated in Table II, a minimum ratio of Br^- to Cl^- was estimated to be about 200 to 1. A search for other electron capture products of this compound, such as the M , $\text{M} - \text{Cl} + \text{O}$, and $\text{M} - \text{Br} + \text{O}$ negative ions (13), revealed none of these. The much higher ratio of Br^- to Cl^- observed for *p*-bromochlorobenzene probably reflects a greater lifetime of its molecular anion formed by the initial electron capture reaction prior to its irreversible dissociation (8), as suggested in reaction 7.



If the initial $\text{ClC}_6\text{H}_4\text{Br}^-$ species survives long enough to be collisionally stabilized, its ultimate decay to Br^- or Cl^- will be more sensitive to the energy differences of these pathways, which in this case favors Br^- production by 18 kcal (bond dissociation energies of the C-Br and C-Cl bonds are probably about 72 and 95 kcal (9, 11, 14), respectively). In an earlier ECD study, Wentworth, Becker, and Tung (9) first proposed this mechanism for the aromatic halides. It is reasonable to expect that the lifetime of excited aromatic molecular anions is longer than that of the aliphatic molecular anions, and, furthermore, molecular negative ions of some polychlorinated aromatic molecules have actually been observed by APIMS (13) whereas those of aliphatic chlorocarbons have not.

In considering requirement 4 of gas-phase coulometry, one might suspect that positive ion-molecule reactions may constitute the most likely cause of a side reaction with the sample molecule. Siegle and Fite have shown (15), for example, that positive ions of CF_2Cl_2 are readily produced in the ^{63}Ni ionization source of an APIMS. Also, we have frequently observed in studies of ECD-active compounds, such as *p*-chloronitrobenzene (4), that positive ions of the sample molecule can be formed more readily than the negative ions. In Figure 2 are shown chromatograms of CCl_3Br where the two largest positive ions detected for this molecule, CCl_3^+ and CCl_2Br^+ , are shown along with the Br^- ion for comparison. In all cases, the positive ion signals are weaker than the Br^- ion signal. In chromatogram c of Figure 2, the positive ion signals are only barely perceptible over the noise levels for this lower sample size where electrons are clearly in abundance within the ion source. This favorable result might have been expected from the consideration that the fastest ion-molecule reactions exhibit rate constants near $1 \times 10^9 \text{ cm}^3 \text{ s}^{-1}$ (16) while rates for electron capture may be as high as $4 \times 10^7 \text{ cm}^3 \text{ s}^{-1}$ (17), or 400 times greater. The fact that positive ions are observed in chromatogram b, however, where the ECD response is just short of complete saturation suggests that the positive ion-molecule reactions of CCl_3Br are almost com-

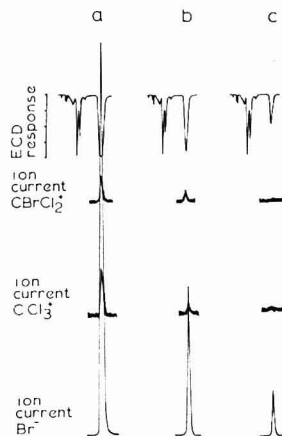


Figure 2. ECD/APIMS analyses of CCl_3Br where the EC response and the ion signals due to CBrCl_2^+ , CCl_3^+ , and Br^- are monitored for sample sizes (a) 2×10^{-9} g, (b) 2×10^{-10} g, and (c) 2×10^{-11} g. Ion source temperature is 250°C and carrier gas flow rate 50 mL min^{-1} .

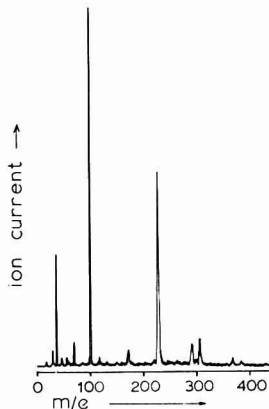


Figure 3. Mass spectrum of positive ions in ECD/APIMS ion source during no-sample condition. Carrier gas is nitrogen, temperature is 250°C .

petitive with electron capture in this case, and may therefore, constitute a point worthy of further concern. In Figure 3 the spectrum of the positive reactant ions which cause these ion-molecule reactions is shown to be dominated by three ions. The ion at m/e 37 is undoubtedly $\text{H}^+(\text{H}_2\text{O})_2$ (15). The ion at m/e 225 is present only when the GC is attached and is most likely a column bleed ion. Our column was thoroughly conditioned and is used at a temperature far below its rated maximum. Nevertheless, with it a peak m/e 225 in the positive ion spectrum always appears as do numerous other smaller positive ion signals at high masses. The ion at m/e 101 is one we have always observed with nitrogen or argon-methane carrier gas with or without a GC column attached. This ion has not appeared so dominantly in other API studies (15), and may reflect a contaminant inherent in our ion source or carrier gas flow system. An ion at m/e 102 about 6% as intense suggests the presence of several carbon atoms

in the m/e 101 ion. As the column temperature is increased, the ion at m/e 225 increases in intensity at the expense of the ions at m/e 37 and 101.

Since at least some of these ions are sufficiently reactive toward CCl_3Br as to cause a nearly competitive side reaction, it may be advisable in some applications of gas phase coulometry to intentionally dope the carrier gas with a substance which will lead to a less reactive set of reactant positive ions. Many possibilities come to mind as a result of research in chemical ionization mass spectrometry (18) where the choice of carrier gases and dopants is now a well understood variable in creating a desired positive ion flux. The intentional addition of water vapor or ammonia, for example, to the carrier gas, thereby forming the less reactive higher clusters of water or ammonia, might accomplish this. Of course, care must be taken to ensure that the dopants, themselves, do not undergo electron capture reactions and, thereby, damage the ECD base line. We found in a previous study (19) that at least 10 ppm (v/v) water vapor can be added to the carrier gas of an ECD without causing a significant effect on its base line as long as the carrier gas is relatively free of oxygen. Also, the use of lower detector temperatures will promote the formation of larger ion clusters (20).

In summary, the experiments reported here suggest that requirements 3 and 4 of gas phase coulometry are met for the case of CCl_3Br under our experimental conditions. Because CCl_4 and $CFCl_3$ are chemically similar, it seems reasonable that requirements 3 and 4 will also be met for these compounds, to which atmospheric analyses by gas phase coulometry have already been applied (3). The possibility that the success of requirement 3 and possibly requirement 4 may

depend somewhat on the unintentional presence of carrier gas impurities is being investigated further.

LITERATURE CITED

- (1) J. E. Lovelock, R. J. Maggs, and E. R. Adlard, *Anal. Chem.*, **43**, 1962 (1971).
- (2) J. E. Lovelock, *J. Chromatogr.*, **99**, 3 (1974).
- (3) D. Lillian and H. B. Singh, *Anal. Chem.*, **48**, 1060 (1974).
- (4) E. P. Grimsrud, S. H. Kim, and P. L. Gobby, *Anal. Chem.*, **51**, 223 (1979).
- (5) M. W. Siegel and M. C. McKeown, *J. Chromatogr.*, **122**, 397 (1976).
- (6) E. Grimsrud, *Anal. Chem.*, **50**, 382 (1978).
- (7) D. I. Carroll, I. Dzidic, R. N. Stillwell, M. G. Horning, and E. C. Horning, *Anal. Chem.*, **46**, 706 (1974).
- (8) E. R. Adlard, *CRC Crit. Rev. Anal. Chem.*, **5**(1), 1 (1975).
- (9) W. E. Wentworth, R. S. Becker, and R. Tung, *J. Phys. Chem.*, **71**, 1652 (1967).
- (10) H. M. Rosenstock, K. Draxl, B. W. Steiner, and J. T. Herron, *J. Phys. Chem. Ref. Data*, Vol. 6, Suppl. 1, 1977.
- (11) A. J. Gordon and R. A. Ford, "The Chemists Companion", John Wiley and Sons, New York, 1972.
- (12) J. I. Brauman, W. H. Olmstead, and C. A. Lieder, *J. Am. Chem. Soc.*, **96**, 4030 (1974).
- (13) I. Dzidic, D. I. Carroll, R. N. Stillwell, and E. C. Horning, *Anal. Chem.*, **47**, 1308 (1975).
- (14) "Handbook of Chemistry and Physics", 56th ed., The Chemical Rubber Co., Cleveland, Ohio, 1976.
- (15) M. W. Siegel and W. L. Fite, *J. Phys. Chem.*, **80**, 2871 (1976).
- (16) S. G. Lias and P. Ausloos, "Ion-Molecule Reactions", American Chemical Society, Washington, D.C., 1975, Chapter 4.
- (17) L. G. Christophorou, *Chem. Rev.*, **76**, 409 (1976).
- (18) B. Munson, *Anal. Chem.*, **43**(13) 28A, (1971).
- (19) E. P. Grimsrud and R. G. Stebbins, *J. Chromatogr.*, **155**, 19 (1978).
- (20) E. P. Grimsrud and P. Kearn, *J. Am. Chem. Soc.*, **95**, 7939 (1973).

RECEIVED for review November 13, 1978. Accepted January 15, 1979. Acknowledgement is made to the Donors of the Petroleum Research Fund, administered by the American Chemical Society; to Research Corporation; and to the National Science Foundation for support of this research.

Statistical Designs for the Optimization of the Nitrogen-Phosphorus Gas Chromatographic Detector Response

I. B. Rubin*

Bio/Organic Analysis Section, Analytical Chemistry Division, Oak Ridge National Laboratory, Oak Ridge, Tennessee 37830

C. K. Bayne

Mathematics and Statistics Research Section, Computer Sciences Division, Oak Ridge National Laboratory, Oak Ridge, Tennessee 37830

Statistically designed and evaluated factorial experiments were used to approach optimum operating conditions for the rubidium bead type of nitrogen-phosphorus gas chromatographic detector to detect small quantities of nitrogen compounds in a hydrocarbon matrix, and to study the effects of the operating variables. Simplex designs were used to define the optimum set of conditions. The test variables were hydrogen pressure, air pressure, and bead heating current. Only two 2^3 factorial designs and ten simplex vertices were needed to accomplish these purposes. Detector responses for 12 nitrogen and 12 hydrocarbon compounds were compared with both the nitrogen-phosphorus and flame ionization detectors. The average value of the ratio of nitrogen to hydrocarbon response with the nitrogen-sensitive detector was about 1000:1. Chromatography of several fractions from a chemical extractive fractionation of a coal liquefaction product oil demonstrated the discrimination capability of the nitrogen-phosphorus detector at optimum conditions.

The introduction by Kolb and Bischoff (1) of the thermionic nitrogen-phosphorus detector (NPD) which uses a rubidium silicate bead as the alkali source has greatly increased the capability for detecting nitrogen compounds in mixtures which may be composed predominately of hydrocarbons. The effectiveness of the NPD in discriminating between nitrogen- and nonnitrogen-containing compounds is a function of several operating variables: bead heating current, jet potential, carrier gas, air and hydrogen flow, as well as positioning of the bead. General conditions for the use of the NPD for given situations have been described (2-5), but as has been suggested (4), each user should check the performance of each bead before applying it to his own problem.

The usage of the NPD for the detection of nitrogenous compounds in a matrix of hydrocarbons gives rise to a complicated optimization problem. It requires maximizing the nitrogen response and minimizing the hydrocarbon response. Changing the operating variables will generally cause

both responses to move in the same direction, although, fortunately, not to the same degree. It is possible to reduce the hydrocarbon response to zero, but with an accompanying loss of nitrogen sensitivity that may not be tolerable if the nitrogen compounds are in very low concentrations. Consequently, for applications of the NPD to problems such as are addressed here, it is very likely that the operating conditions will have to be some compromise between sensitivity and discrimination. Single factor experiments (1, 2, 4) for optimizing operating conditions require taking an adequate number of data points and drawing a bewildering array of curves. Because this method does not take interactions among variables into consideration, results are sometimes ambiguous. A two-level factorial experiment for three variables measures responses at the eight different combinations of high and low levels of each variable (6, 7). A statistical analysis of the factorial experiments allows numerical evaluation of all single factor and multifactor effects (7, 8). Factorial designs are particularly useful for exploratory work to investigate these effects, and to approach the region of optimum response. As one nears this area, it may be necessary to go to a more complicated experimental design which requires more data points, and a more complex statistical analysis (9). Simplex designs require initially only one more experimental point than the number of variables and provide an uncomplicated procedure for reaching optimization in easy steps and with simple arithmetic (10, 11). A combination of factorial designs to evaluate the important variables and simplex designs to reach the optimum response yields a sophisticated, yet simple and quick, solution to optimization problems.

In the work described below, the combined use of factorial and simplex experimental designs for the optimization of the NPD operating variables is discussed, and the applicability of the NPD to the detection of nitrogen compounds in fractions of a coal liquefaction product oil is illustrated.

EXPERIMENTAL

Materials. The hydrocarbon and nitrogen standard compounds were obtained at the highest available purity from commercial suppliers. Benzene solutions of these compounds in the range of 2 to 10 mg/mL were prepared. The few compounds that were not readily soluble in benzene were dissolved in redistilled tetrahydrofuran. Working solutions were 1 mg/mL dilutions of the standard solutions. In order to demonstrate discrimination between compound type, a synthetic sample was prepared which contained 1 mg/mL of each of 12 hydrocarbons and 0.1 mg/mL of each of 12 nitrogen compounds.

Factorial Design. The design for a factorial experiment and the high and low values assigned to the three test variables for two different experiments are shown in Table IA. Each row of the table corresponds to a single trial and the entries in the row designate the value levels of each variable in that trial. Carrier gas flow was not included with the test variables because of the tendency for the flow to decrease with increasing temperature of the columns used in these tests; jet potential was treated as a constant because its effect on sensitivity and discrimination is described in the manufacturer's literature; bead position which could not be quantified, was set according to the manufacturer's instructions and was not changed.

Procedure. The work was carried out with a Perkin-Elmer Model 3920 gas chromatograph with a Perkin-Elmer Nitrogen-Phosphorus Detector in the B channel and a flame ionization detector (FID) in the A channel. Two glass columns, $1/8$ inch by about 12 feet, packed with 3% Dexsil 400 on 80/100 mesh Chromosorb W, were used. The helium carrier flow was regulated so that retention times of the hydrocarbons on each column were as closely matched as possible. Response of each detector was tested separately.

For the optimization studies, a benzene solution of 1 mg/mL each of octadecane and carbazole was used. Aliquots of 2 μ L were chromatographed. Initial oven temperature was 200 °C, with a 2 °C/min rate of increase until the carbazole was completely eluted

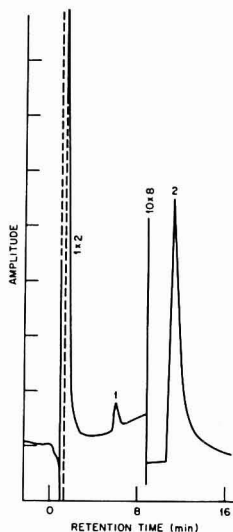


Figure 1. Typical chromatogram from an optimization study. Peak 1, octadecane. Peak 2, carbazole

at ~235 °C. Detector response, as peak area per microgram of sample injected, was measured for each compound. Standard factorial (6) and simplex (10) design schemes were followed. Operating variables were bead heating current as indicated by the dial setting, hydrogen pressure, and air pressure. Helium carrier pressure was set at 60 psig; the jet potential was set on position 3 for the factorial trials and on position 2 for the simplex trials.

For the routine chromatography of the solutions of standard compounds and of samples, temperature was programmed from 100 to 320 °C at 2 °C/min.

RESULTS AND DISCUSSION

Two factorial designs were used to define the region in which the optimum discrimination factor (ratio of carbazole to octadecane responses) was favored and to define the important experimental variables. A typical chromatogram of the responses is shown in Figure 1. The results from the first factorial design indicated that the discrimination factor was improved by using the lower air pressure level, the lower hydrogen pressure level, and the higher bead heating current level. Estimates of the variables calculated from Yates algorithm (7, 8) and data analysis using half-normal plots (12) indicated the region for the second factorial experiment. Based on the analysis of the eight points from the first factorial design, a more extensive second factorial design was conducted with a smaller range of levels for the variables redefined in the region given in Table IA. Each of the eight combinations of the three variables in the second factorial design was performed in random order with selected trials repeated to get an estimate of the variance of the experimental error. In addition, measurements were taken on a second day to test the repeatability of the response, for a total of 27 data points for each of the two responses. The responses from the factorial designs are tabulated in Tables IB and IC.

A rigorous statistical analysis of the data from the second factorial design was made by fitting models of the form: response = independent variables + error, using the method of least squares (13). Different models were formed by selecting independent variables from the following possible

Table IA. Factorial Design for Optimizing Discrimination between Nitrogen and Nonnitrogen Compounds

trial	variable		
	1 H ₂ , psig	2 air, psig	3 bead heating current, dial setting
1	-	-	-
2	+	-	-
3	-	+	-
4	+	+	-
5	-	-	+
6	+	-	+
7	-	+	+
8	+	+	+
design #1	(+) 20	42	675
	(-) 6	20	575
design #2	(+) 10	24	700
	(-) 6	18	650

Table IB. Factorial Design 1 Data

trial	peak area, cm ² /μg			
	carbazole		octadecane	
	day		day	
	1	2	1	2
1	566	16.4	0.06	0.0
2	0.0	0.1	0.0	0.0
3	922	864	19.9	9.8
4	887	1122	128	114
	1230	1112	112	111
5	1884	1925	7.9	7.3
6	69	65	26.9	21.1
7	2220	2437	21.9	21.4
8	2720	2826	123	132

Table IC. Factorial Design 2 Data

trial	peak area, cm ² /μg			
	carbazole		octadecane	
	day		day	
	1	2	1	2
1	991	47 ^a	1.1	0.0 ^a
2	495	6 ^a	0.5	0.0 ^a
	401		0.0	
3	1348	1219	10.8	8.2
	1302	1188	10.8	7.6
4	2166	2350	23.5	19.2
	1935	2258	21.9	19.9
5	1948	1843	6.0	5.5
6	2442	1820	4.2	2.1
	2286	1935	5.1	1.7
	1855		1.8	
7	2241	2431	20.4	17.5
	2158	2154	16.2	17.1
8	3087	3569	35.6	29.5
	3025		35.6	

^a Suspected values not used in the statistical analysis.

terms: (1) intercept, μ ; (2) day effect, D; (3) hydrogen pressure, H₂; (4) air pressure, AIR; (5) bead heating current, BEAD; (6) interaction of H₂ × AIR; (7) interaction of H₂ × BEAD; (8) interaction of AIR × BEAD; and (9) interaction of H₂ × AIR × BEAD. To find the significant variables, first a base model using all nine terms is fitted to the data and then compared to a smaller fitted model with terms deleted. If the error terms in the models are assumed to be independent and identically distributed as a normal distribution with zero mean

Table II. Sample Correlation Coefficients (*r*) between Carbazole, Octadecane, and Test Parameters

	carbazole	octadecane
carbazole		0.75
octadecane	0.75	
H ₂ pressure	0.27	0.15
air pressure	0.37	0.77
bead current	0.62	0.14

and constant variance, an *F*-test (13) can be used to test any significant differences between the base model and any smaller model. The best model is the model which has the fewest independent variables and is not significantly different than the base model.

From this analysis, the independent variables that have a significant effect at the 5% level are for carbazole: μ , H₂, BEAD, H₂ × AIR, and AIR × BEAD; and for octadecane: μ , D, H₂, AIR, BEAD, H₂ × AIR, and AIR × BEAD. Equations for each compound with the coefficients for the significant factors (for octadecane, the day effect is included in the intercept) are:

$$\begin{aligned} \text{Carbazole: Response} &= -14870. - 807.0 \text{ H}_2 + \\ &\quad + 43.78 (\text{H}_2 \times \text{AIR}) - 0.307 (\text{AIR} \times \text{BEAD}) \\ \text{Octadecane: Response} &= 284.5 - 12.37 \text{ H}_2 - \\ &\quad + 17.93 \text{ AIR} - 0.3503 \text{ BEAD} \\ &\quad + 0.6573 (\text{H}_2 \times \text{AIR}) + \\ &\quad + 0.02317 (\text{AIR} \times \text{BEAD}) \end{aligned}$$

These two models can also be tested for their appropriateness by partitioning each estimated error variance from the least squares analysis into the estimated variance due to lack of fit and the estimated variance of pure error due to the replicate measurements. The ratios of the lack of fit estimated variance to the pure error estimated variance for the two models are then compared with the percentile points of the *F*-distribution. This test shows that neither model had a significant lack of fit at the 5% significance level. The final estimates of the standard deviation of the observed values from their true value are the least squares estimates of $S_1 = 222$ for carbazole and $S_2 = 2.1$ for octadecane.

Contours of equal response for the carbazole and octadecane equations can be plotted, and representative drawings are shown in Figure 2. These plots depict the bead heating current vs. air pressure plane as it would intercept the hydrogen axis in a three-dimensional representation of the operating variables. In this example, hydrogen is constant at 6 psig, and the curves show the effects of changing air pressure and bead heating current. The upper portion of this figure shows a family of curves for three response levels for carbazole. Each curve represents a constant value of the response for different air pressure and bead heating current settings. For example, along a 1500 cm²/μg response curve, air pressure can be changed from 24 psig to 18 psig with a concomitant change of bead heating current setting from 666 to 680 and the same response maintained. The lower portion of Figure 2 shows a corresponding family of contours for octadecane.

The sample correlation coefficient (*r*) calculated for the carbazole and octadecane responses has a positive value of $r = 0.75$, which indicates that the two responses increase and decrease together. Sample correlation coefficients between chromatographic responses of the two standard compounds and the three operating variables show a positive correlation between octadecane response and air pressure, and between carbazole response and bead heating current. There was essentially no correlation between either response and any of

Table III. Three Factor Simplex Design

vertex no.	vertices retained	variables ^a			response		
		bead current, dial setting	air, psig	H ₂ , psig	ratio, carb/C18	area(cm ²)/μg	
1		650	20	8	197	165.8	0.84
2		670	20	8	216	201.6	0.94
3		660	22	8	283	161.3	0.57
4		660	21	10	92	204.4	2.23
5	1, 2, 3	660	20	6	504	118.4	0.24
6	2, 3, 6	677	22	7	330	145.2	0.44
7	3, 5, 6	661	23	6	394	116.4	0.27
8	5, 6, 7	672	21	5	398	111.5	0.28
9	5, 7, 8	652	21	4	990	64.4	0.065
10	5, 8, 9	662	18	4	660	59.4	0.090
5 repeat					472	99.2	0.21
9 repeat					1254	50.2	0.040

^a Steps: current setting, 20 units; air and H₂, 2 psig.

the other test variables. These correlation coefficients are shown in Table II.

The results of the factorial experiments provided the area in which the optimum pressures and bead current settings should be found, i.e., hydrogen pressure, 8–10 psig; air pressure, 18–20 psig; bead heating current setting, 650–660. To define optimum operating conditions more precisely, a simplex experiment was carried out to maximize the ratio of the carbazole response to the octadecane response. The first vertex was located at 8 psig hydrogen, 20 psig air, and a bead current of 650. The other vertices were located in the manner described by Long (8). The jet potential control knob was set in the 2 position, because there was a 5-fold increase in the discrimination factor when compared to the 3 position, although there was a loss in sensitivity for both of the test compounds. The simplex experimental data are shown in Table III. Fractional pressures required by the calculations were rounded off because of the difficulty in interpolation on the instrument gages. After the tenth vertex had been tested, it was obvious that further work would lead to an area of decreasing sensitivity and reproducibility. The hydrogen pressure boundary had arbitrarily been set at 6 psig because it was feared flow control might not be easily maintained at lower pressures, and this boundary had already been crossed at vertex 8. Consequently, vertex 5, which appeared to be a secondary maximum, was chosen as the point of optimum working conditions.

There is contradictory evidence regarding the stability of the detector bead (2, 4, 16). In the course of these studies, there was a sensible decrease in the detector response, and there were occasional short term aberrations that corrected themselves. Consequently, it is necessary to run periodic calibration checks, and if re-optimization is necessary, a short simplex series can be carried out.

The capability of the NPD to discriminate between nitrogen and hydrocarbon compounds was demonstrated by chromatographing a synthetic sample using both the NPD and FID. The composition of the mixture and the responses to each detector are shown in Table IV. Both the NPD and FID are mass flow rate detectors (14), for which sensitivity has been defined (15) as:

$$S' = (AC_1C_2)/w$$

where S' = detector sensitivity, mV-s/mg; A = peak area, cm²; C_1 = recorder sensitivity, mV/cm of chart; C_2 = reciprocal of chart speed, s/cm; and w = weight of component, mg. Therefore, response for each detector can be compared directly. Because the same recorder and same chart speed were used in both cases, C_1 and C_2 were not factored into the calculations and response was calculated as A/w with w being

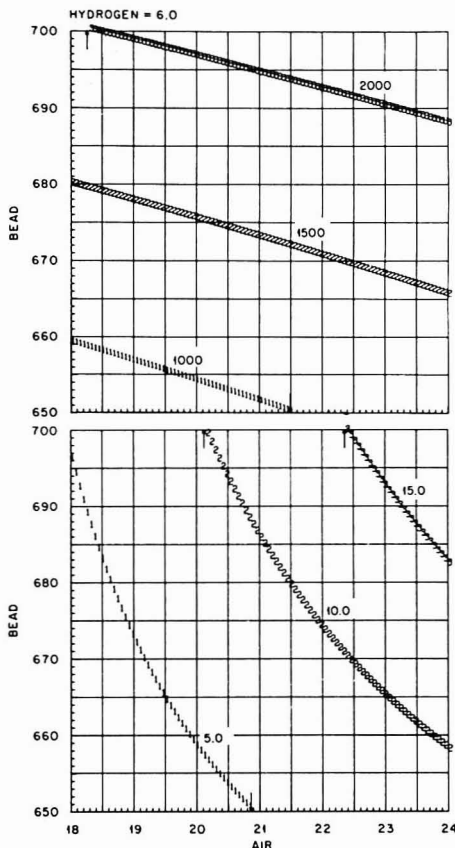


Figure 2. Contours of equal detector response for changing air pressure and bead heating current settings at constant hydrogen pressure. Upper: carbazole. Lower: octadecane

μg rather than mg. These standard compounds were selected to provide a spread over the temperature range required for sample work, and hopefully to provide some overlapping of

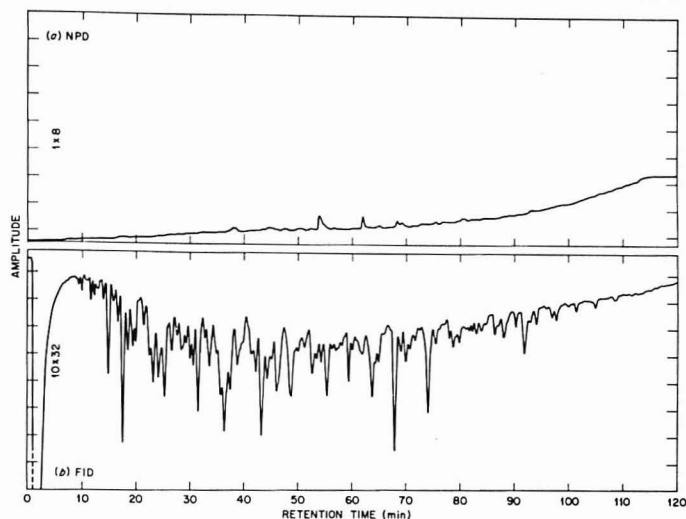


Figure 3. Chromatograms of the hexane eluate from the neutral portion of a coal-derived product oil. NPD conditions: air, 20 psig; hydrogen, 6 psig; bead heating current setting, 660; jet potential control setting, 2

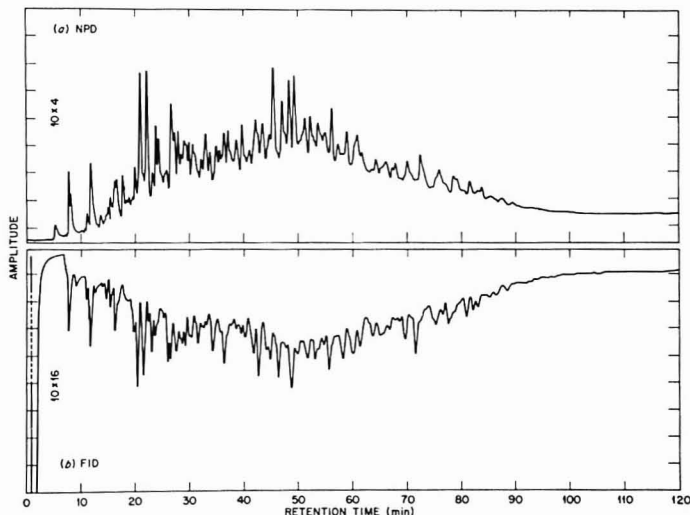


Figure 4. Chromatograms of the ether-soluble base fraction of a coal-derived product oil. NPD conditions same as Figure 3

the hydrocarbon with the nitrogen compounds. With the FID, the hexadecane does obscure the dimethylindole, while with the NPD, the reverse occurs; with the latter detector, the tetradecane is observed as a shoulder on the indole peak. Detector response was calculated from chromatography of each group of compounds at the 1 mg/mL level. The average decrease in hydrocarbon sensitivity from the FID to the NPD response was 0.5 that for the FID. When the average value of response is taken, the discrimination factor is about 1000 throughout most of the chromatogram, an order of magnitude lower than the manufacturer's literature leads one to expect.

The sensitivity for the nitrogen compounds falls off substantially starting at about 250 °C under these chromatographic conditions; this loss is probably caused by decreasing carrier gas flow. Baker has reported that response is not necessarily correlated with the number of nitrogen atoms in the molecule (16). As seen in Table IV, both 2,3-dimethylquinoxaline and phenazine had double the response of their neighbors but *o*-tolidine did not. Two other di-nitrogen compounds, harmine and benzo[c]cinnoline, with retention times near 60 min, had responses similar to acridine and carbazole. Response also varies with type of nitrogen-con-

Table IV. Composition of Synthetic Sample

retention time, min	compound	detector response, ^a area (cm ²)/μg	
		FID	NPD
A. Hydrocarbons			
9.0	<i>n</i> -dodecane	567	0.24
11.2	naphthalene	608	0.19
19.6	<i>n</i> -tetradecane	611	0.19
22.0	biphenyl	628	0.16
31.6	<i>n</i> -hexadecane	577	0.16
35.8	fluorene	559	0.13
49.1	anthracene	544	0.17
54.5	<i>n</i> -eicosane	541	<i>b</i>
68.2	pyrene	507	0.17
74.0	<i>n</i> -tetracosane	454	0.17
90.6	<i>n</i> -octacosane	420	0.18
102.5	1,3,5-triphenylbenzene	477	0.24
B. Nitrogen Compounds			
18.0	indole	398	230
22.6	7-methylindole	477	234
24.2	2,3-dimethylquinoxaline	422	463
31.5	2,3-dimethylindole	<i>c</i>	<i>c</i>
36.5	diphenylamine	487	235
45.5	phenazine	431	420
50.1	acridine	448	214
51.6	carbazole	493	237
77.8	<i>o</i> -tolidine	333	170
83.9	benz[<i>a</i>]acridine	479	161
90.0	7,9-dimethylbenz[<i>c</i>]acridine	419	117
114.0	1,2,7,8-dibenz[<i>a,i</i>]acridine	474	94

^a Based on chromatography of groups A and B separately at 1 mg/mL level. ^b Apparently contaminated with carbazole. ^c Concentration unknown.

taining compound (16), so that if one is investigating a specific compound, or class of compounds, it would be better to optimize with that compound, or a member of that class.

The lower detector response than expected may be related to the large sample size chromatographed, although studies with at least one compound (2) have shown linear detector response up to 1 μg. Chromatography of the synthetic sample with 0.1 mg/mL levels of the nitrogen compounds listed in Table IV indicates that average peak area for seven of the compounds was 170 cm²/μg as compared to 190 cm²/μg for the same compounds at the 1 mg/mL level. As stated above, in order to gain in the discrimination ratio, there must be a sacrifice in the sensitivity. By merely switching the jet potential knob from the 3 to the 2 position, one causes a drop in the nitrogen sensitivity to one-third its former value, but there is an accompanying 15-fold decrease in the hydrocarbon response.

The chromatograms in Figures 3 and 4 represent two fractions of a coal liquefaction product oil fractionated by a chemical separations procedure (17). Figure 3 shows the chromatograms of the hexane elutable material from a Florisil column. Florisil has been shown to retain nitrogenous

compounds (18) and essentially no nitrogen (<0.1%) was detected by elemental analysis of this fraction. It is evident from the chromatogram that only a few nitrogen compounds in very small quantities may be present as compared to the multiplicity of hydrocarbons revealed by the FID. Figure 4 shows chromatograms from the ether-soluble base fraction. While there are a few peaks in each chromatogram which do not appear on the other, the two chromatograms are similar qualitatively and quantitatively. This fraction comprises most of the dilute-acid extractable material from the oil, and it has been established that this portion of fossil fuels is composed predominantly of alkyl substituted pyridines and quinolines (19). This fraction was found to contain 7.1% nitrogen.

We have demonstrated that statistically organized designs can be used for the optimization of the operating conditions for the nitrogen-phosphorus detector when it is used to discriminate between hydrocarbon and nitrogenous compounds. A combination of factorial and simplex experiments proved to be effective in this study. This type of procedure can be applied not only to this detector, but to other types as well, and to other kinds of optimization studies where there are several variables. It provides a rapid and efficient method of attaining optimum operating conditions, and allows an analysis of the effects of all the variables and the interactions among them.

ACKNOWLEDGMENT

The authors thank H. G. Davis and Mrs. Nancy Cook for carrying out the elemental analysis of the sample material.

LITERATURE CITED

- (1) B. Kolb and J. Bischoff, *J. Chromatogr. Sci.*, **12**, 625 (1974).
- (2) M. J. Hartigan, J. E. Purcell, M. Novotny, M. L. McConnell, and M. L. Lee, *J. Chromatogr.*, **99**, 339 (1974).
- (3) B. Kolb, M. Auer, and P. Pospisil, *J. Chromatogr.*, **134**, 65 (1977).
- (4) J. A. Lubkowitz, J. L. Glajch, B. P. Semonian, and L. B. Rogers, *J. Chromatogr.*, **133**, 37 (1977).
- (5) R. Pigliucci, W. Averill, J. E. Purcell, and L. S. Ettre, *Chromatographia*, **8**, 165 (1975).
- (6) G. E. P. Box and J. S. Hunter, *Technometrics*, **3**, 311 (1961).
- (7) W. Volk, "Applied Statistics for Engineers", 2nd ed., McGraw-Hill, New York, 1969, pp 235-259.
- (8) F. Yates, *Imp. Bur. Soil. Sci., Tech. Commun.*, No. 35 (1937).
- (9) W. G. Cochran and G. M. Cox, "Experimental Designs", 2nd ed., John Wiley and Sons, New York, 1957, pp 335-375.
- (10) D. E. Long, *Anal. Chim. Acta.*, **46**, 192 (1969).
- (11) S. L. Morgan and S. N. Deming, *Anal. Chem.*, **46**, 1170 (1974).
- (12) G. Daniel, *Technometrics*, **1**, 311 (1959).
- (13) S. R. Searle, "Linear Models", John Wiley and Sons, New York, 1971, pp 75-134.
- (14) C. H. Hartman, *Anal. Chem.*, **43**, 113A (1971).
- (15) H. M. McNair and E. J. Bonelli, "Basic Gas Chromatography", Varian Aerograph, Palo Alto, Calif., 5th ed., 1969, p 87.
- (16) J. K. Baker, *Anal. Chem.*, **49**, 906 (1977).
- (17) I. B. Rubin, M. R. Guerin, A. A. Hardgree, and J. L. Epler, *Environ. Res.*, **12**, 358 (1976).
- (18) G. V. Dineen, J. R. Smith, R. A. VanMeter, C. S. Allbright, and W. R. Anthoney, *Anal. Chem.*, **27**, 185 (1955).
- (19) H. L. Lichte and E. R. Littmann, "The Petroleum Acids and Bases", Chemical Publishing Company, New York, 1955, pp 283-355.

RECEIVED for review August 25, 1978. Accepted January 15, 1979. Research sponsored by the Division of Biomedical and Environmental Research, U.S. Department of Energy under contract W-7405-eng-26 with the Union Carbide Corporation.

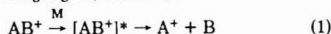
Electron Impact Excitation of Ions from Organics: An Alternative to Collision Induced Dissociation

R. B. Cody and B. S. Freiser*

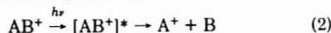
Department of Chemistry, Purdue University, West Lafayette, Indiana 47907

A technique has been developed for electron impact excitation of ions from organics (EIEIO). The technique uses trapped ion cyclotron resonance (ICR) spectroscopy and together with the ICR photochemical techniques and unusual capabilities for studying ion-molecule reactions, will aid in the evolution of ICR as an analytical instrument. It is demonstrated on a variety of substituted benzene radical cations. Ions are generated and subsequently excited in a continuous electron beam while being trapped in the source region. The spectra obtained by EIEIO are shown to be analogous to those obtained by collision induced dissociation and yield characteristic structural information.

Obtaining the fragmentation pattern generated from ionization of a neutral sample is typically the primary objective in conventional mass spectrometry. A great deal of additional information, however, is available by further probing the structures of individual ions in the mass spectrum. Such information is of obvious importance in fundamental studies of unimolecular ion and ion-molecule reactions and in separation and identification of complex mixtures (1, 2). To achieve these ends, a variety of innovative methods have been developed including collision induced dissociation (CID) (1-6) and photodissociation (PDS) (7-13). These techniques are similar in that both probe the ion structure by monitoring unimolecular dissociation following excitation, with the major difference being the mode of excitation. In CID, also referred to as collisional activation (CA), the unimolecular dissociation of an ion is monitored following excitation of the ion by collision with a target gas (Process 1).

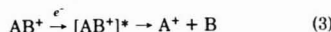


In PDS, unimolecular dissociation is monitored following light absorption by the ion (process 2).



Interestingly, photodissociation pathways need not mimic those observed by CID (6).

In this paper we report an extension of a new method utilizing ICR (14, 15) in which unimolecular dissociation is monitored following excitation by electron impact (process 3) in analogy to CID and PDS.



Until recently quantitative as well as qualitative studies of electron impact dissociative excitation of ions were limited to diatomics such as H_2^+ , D_2^+ , O_2^+ and N_2^+ (16-18). We wish to report that ICR-EIEIO techniques appear to hold not only considerable promise for routine investigation of these fundamental processes for polyatomic ions, but also provide ICR with important CID-like capabilities.

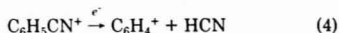
EXPERIMENTAL

The ion cyclotron resonance spectrometer used in the present study is a modified V-5900 series manufactured by Varian Associates (19, 20). The ICR cell is one which has been used extensively for studies of ion photoexcitation processes as described

in detail (7-11) and required no modification. Parent ions from the substituted benzenes (in the pressure range from $1-10 \times 10^{-7}$ Torr) were formed and subsequently excited in a continuous electron beam while being trapped in the source region. Ion formation was accomplished by switching the electron energy to a value lying a few electron volts above the ionization potential for 15 ms. For the remainder of the trapping period, the electron energy remained below the ionization potential at a value which could be varied readily. All of the electron energies given have been corrected for the space charge potential of the electron beam which has the effect of reducing the electron energy. This correction can be substantial at high emission currents and low electron energies (14). These effects also prevented data from being obtained below about 2 eV because of instability in the current. Each of the chemicals used was a commercial sample of high purity with the exception of the labeled phenetole, and was used as supplied except for freeze-pump-thaw cycles to remove noncondensable gases. Mass spectrometry revealed no detectable impurities.

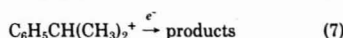
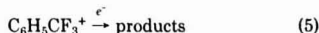
RESULTS

The phenomenon of EIEIO is particularly evident in appearance potential measurements at high emission currents as illustrated by Figure 1, which shows the intensity of $C_6H_4^+$ generated from cyanobenzene as a function of electron energy at a trapping time of 100 ms. At low emission currents, the fragment ion $C_6H_4^+$, arising from loss of HCN from the parent ion, appears at about 3.5 eV above the ionization potential of the parent neutral. This appearance potential measurement is consistent with the estimated thermodynamic threshold (14). At higher emission currents, however, $C_6H_4^+$ begins to appear with the parent cation at the ionization potential which, significantly, is not affected by emission current, eliminating the possibility of an artifact arising from electron energy distribution broadening. The striking behavior of $C_6H_4^+$ is attributed to EIEIO reaction 4.



As expected this reaction becomes even more apparent both as the emission current is increased (Figure 1), and as the trapping time is increased as illustrated in Figure 2 which shows the temporal variation of $C_6H_4^+$ and $C_6H_5CN^+$ obtained at an electron excitation energy of 7.5 eV and at an emission current of 5 μA .

It is evident from the above results that mass spectra at a particular electron energy will also be affected by emission current and trapping conditions. Figures 3 and 4 compare the conventional ICR single resonance drift spectra of trifluorotoluene, *n*-propylbenzene, and isopropylbenzene to their corresponding EIEIO spectra obtained at trapping times of 100 ms. Again the appearance of fragment ions in the EIEIO spectra are apparent, arising from reactions 5-7 (see Table I),



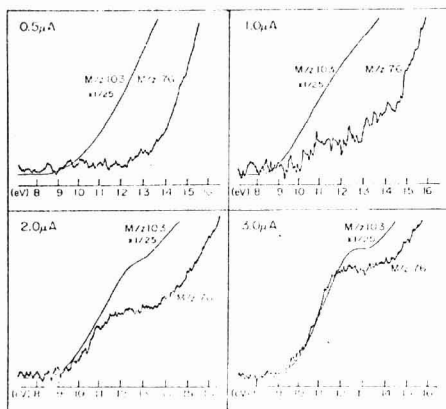


Figure 1. Appearance potential measurements on cyanobenzene at different electron emission currents. As emission current is increased, the fragment ion $C_6H_5^+$ (m/z 76) begins to appear with the parent ion (m/z 103) at the ionization potential. This behavior is attributed to EIEIO reaction 4 in text

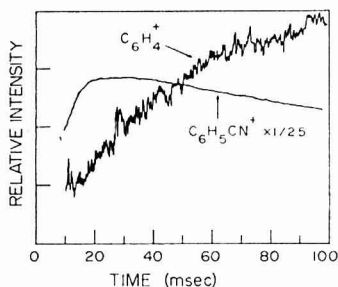


Figure 2. Temporal variation of ions involved in the process $C_6H_5CN^+ \rightarrow C_6H_4^+ + HCN$ obtained at an electron excitation energy of 7.5 eV and at an emission current of 5 μA

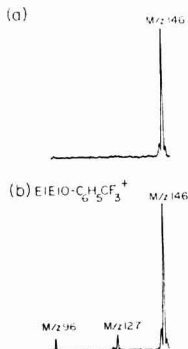


Figure 3. (a) Single resonance spectrum of trifluorotoluene at 100-ms trapping time, 14-eV and 3.5-eV electron energy ion formation and base voltages, respectively, and 3- μA emission. (b) Same conditions as (a) at 7.2-eV base voltage

whereas at the same electron energies, only the parent cations are observed in the conventional single resonance spectra.

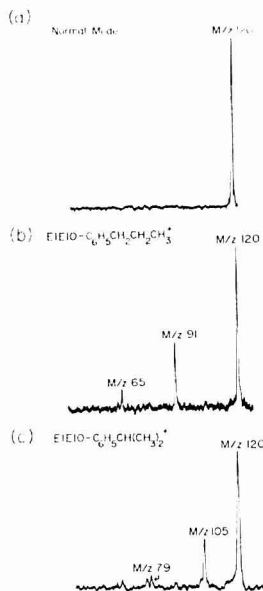


Figure 4. (a) Single resonance spectrum of *n*-propylbenzene at low emission currents. (b) Single resonance spectrum of *n*-propylbenzene under EIEIO conditions. (c) Single resonance spectrum of isopropylbenzene under EIEIO conditions

It is of interest to compare the EIEIO spectra obtained by ICR to the corresponding CID spectra. A direct comparison is made on phenetole radical cation in Figure 5. The labeled compounds used are involved in another study in our laboratory and were chosen for this experiment because of availability rather than for any mechanistic purpose. The major fragments arising from EIEIO of $C_6H_5OC_2D_5^+$ (m/z 127) at 72 ms trapping time shown in Figure 5b include loss of C_2D_4 and loss of C_3D_4O to form $C_6H_5OD^+$ (m/z 95) and $C_6H_5D^+$ (m/z 67), respectively. As shown in Figure 5c, the corresponding ions also appear as the major components in the CID spectrum of $C_6H_5OCD_2CH_3^+$ (m/z 124). Several other ions also appear in the CID spectrum, however, which are not observed in the EIEIO spectrum including, for example, loss of the ethoxy moiety to form $C_6H_5^+$ (m/z 77).

In Figure 6a the EIEIO spectrum of $C_6H_5OC_2D_5^+$ is repeated at an increased trapping time of 432 ms. The two major fragment ions, $C_6H_5OD^+$ and $C_6H_5D^+$ are again evident as well as the lower mass species m/z 39 and 40, but the ion corresponding to ethoxy loss is still not observable. Also evident in an examination of Figure 6a is that the $C_6H_5D^+$ intensity has increased relative to that of $C_6H_5OD^+$. While Figure 6b is a repetition of the CID spectrum from Figure 5c of $C_6H_5OCD_2CH_3^+$ for comparison, a straightforward explanation for the increased $C_6H_5D^+$ intensity can be derived from a comparison of the EIEIO spectrum in Figure 6a to the CID spectrum of $C_6H_5OH^+$ shown in Figure 6c. The CID spectrum of $C_6H_5OH^+$ shows loss of CO and C_3H_5O to produce $C_3H_6^+$ and $C_3H_3^+$, respectively, as the predominant fragmentation pathways (21). The corresponding products for the labeled phenol ion, $C_6H_5OD^+$, would be $C_6H_5D^+$ and both $C_3H_3^+$ and $C_3H_2D^+$ all of which are observed in Figure 6a. Thus, it is apparent that $C_6H_5OD^+$ having excess internal energy is being produced and subsequently fragmenting, and

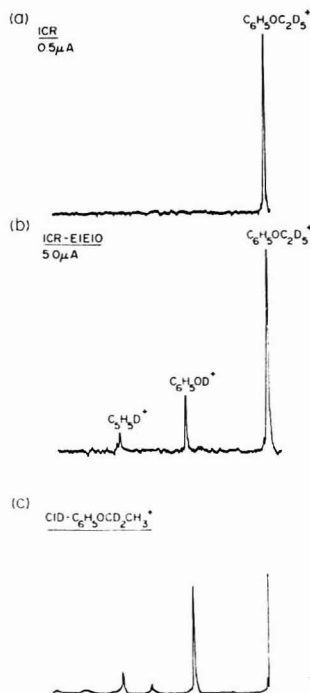


Figure 5. (a) Single resonance spectrum of labeled phenetole at low emission current. (b) Single resonance spectrum of labeled phenetole under EIEIO conditions. (c) CID spectrum of labeled phenetole

Table I. Comparison of Photodissociation, Electron Impact Excitation, and Collision Induced or Metastable Dissociation of Benzene Radical Cations

ion	PDS	EIEIO	CID/ metastable
[toluene] ⁺	-H	-H, C ₂ H ₅	-H
[<i>n</i> -propylbenzene] ⁺	-C ₂ H ₅	-C ₂ H ₅ , C ₂ H ₃	-C ₂ H ₅ , C ₂ H ₃
[isopropylbenzene] ⁺	-CH ₃	-CH ₃ , C ₂ H ₅ , C ₂ H ₃	-CH ₃ , C ₂ H ₅
[<i>p</i> -diethylbenzene] ⁺	-H	-H, C ₂ H ₅	-C ₂ H ₅
[trifluorotoluene] ⁺	-H, CF ₂ , F	-H, F, CF ₂	-H, F, CF ₂
[<i>p</i> -fluorotrifluorotoluene] ⁺	-H, F, CF ₂	-H, F, CF ₂	-H, F, CF ₂
[<i>p</i> -chlorotrifluorotoluene] ⁺	-Cl	-Cl	-Cl
[benzonitrile] ⁺	-HCN	-HCN	-HCN
[benzaldehyde] ⁺	X ^a	-CHO, H, C ₂ H ₅ O	X
[phenetole] ⁺	-C ₂ H ₅	-C ₂ H ₅ , C ₂ H ₃ O, C ₂ H ₅ O	-C ₂ H ₅ , C ₂ H ₃ O, C ₂ H ₅ O

^a X = data not available.

it is surmised that the phenol ion produced by EIEIO from phenetole ion is itself undergoing EIEIO fragmentation.

EIEIO spectra were obtained from a variety of substituted benzenes and the data are summarized in Table I. Also included in Table I are the corresponding results obtained by photodissociation and collision induced dissociation (or metastable) experiments where available for comparison.

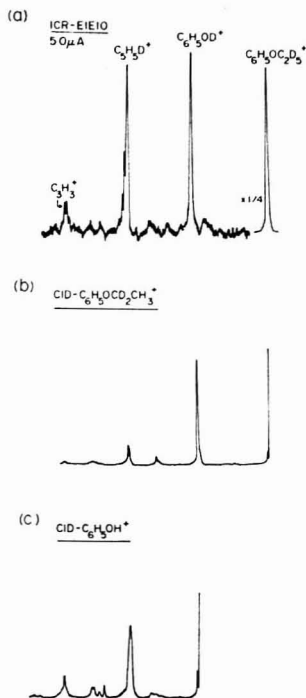
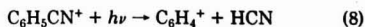
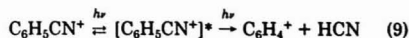


Figure 6. (a) ICR-EIEIO spectrum of labeled phenol. (b) CID spectrum of labeled phenol. (c) CID spectrum of phenol. See text for explanation

The energy of the exciting electrons, as expected, has a profound effect on both the product ion yields, i.e., the EIEIO cross section, and on the product distribution in cases where more than one ion can be observed. Figures 7 and 8 demonstrate these features. Figure 7, reported in an earlier study (14), compares the relative dissociation cross section for process 4 as a function of excitation energy to both the photoelectron spectrum of cyanobenzene reported by Rabalais and Colton (22) and to the photodissociation spectrum of C₆H₅CN⁺ reported by Orlowski et al. (10). The energy axis of the photoelectron spectrum is adjusted such that the first vertical ionization potential of cyanobenzene is zero on the photodissociation and electron impact dissociation scales. The photodissociation spectrum (Figure 7b) consists of a band at high energy obtained by monitoring process 8



and a band at low energy attributed to the two photon process (9).



Comparison of the photodissociation spectra to the photoelectron spectrum indicates that the high energy band arises from a $\pi \rightarrow \pi^*$ transition and the lower energy absorption proceeds through a $\pi \rightarrow \pi$ transition (10).

The cross section for electron impact dissociation of C₆H₅CN⁺ (Figure 7a) is observed to rise from a threshold of

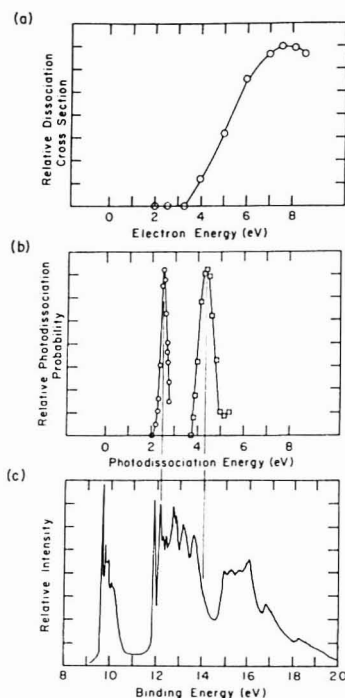


Figure 7. (a) Relative dissociation cross section for process 4 as a function of electron excitation energy. (b) Photodissociation spectra obtained for the one-photon process 8 (\square) and two-photon process 9 (\circ). (c) Photoelectron spectrum of cyanobenzene. The energy axis of the photoelectron spectrum is adjusted such that the first vertical ionization potential of cyanobenzene is zero on the photodissociation and electron dissociation energy scale.

3.0 ± 0.5 eV, near the thermodynamic threshold of 3.2 eV, to a maximum cross section estimated from the data in Figure 2 to be 6 \AA^2 at 7.5 ± 0.5 eV (14). A comparison of Figures 7a and 7b suggests that electron excitation proceeds by the same $\pi \rightarrow \pi^*$ transition as observed for the photodissociation process 8. Comparison to Figure 7c, however, indicates the presence of other states which, in the absence of the usual photon absorption selection rules, could be involved.

Loss of H, F, and CF_2 to produce $\text{C}_7\text{H}_4\text{F}_3^+$, $\text{C}_7\text{H}_2\text{F}_2^+$, and $\text{C}_6\text{H}_2\text{F}^+$, respectively, are prominent fragmentations observed in the EIEIO, PDS (23), and CID spectra of α,α,α -trifluorotoluene. Figure 8 plots the relative intensity of these fragment ions arising from EIEIO on $\text{C}_6\text{H}_5\text{CF}_3^+$ as a function of the excitation energy at 100-ms trapping time. Also shown are normalized photodissociation results (dashed lines) using laser light over a limited energy range (23). The product distribution is clearly observed to be dependent on the excitation energy, with loss of H the predominant product at low energies. Interestingly, loss of H is also the predominant species observed near threshold in photodissociation.

DISCUSSION

In a comparison of EIEIO to CID, one factor which is apparent is that the product intensity relative to the parent molecular ion intensity is substantially larger in EIEIO (up to 50% product to parent observed in Figures 5–8) than in

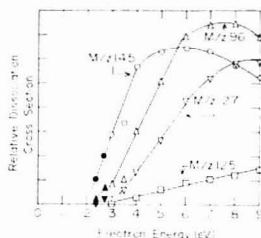


Figure 8. Relative dissociation cross sections for ion products arising from EIEIO on trifluorotoluene radical cation as a function of excitation energy. Also shown for comparison are normalized photodissociation results (dashed lines) using laser light.

CID where generally the main parent ion beam intensity is 100 to 1000 times that of the product ion intensities (1–6). This difference dramatically contrasts the capability of the ICR to monitor all of the ions in the cell, whereas scattering in CID plays a major role in reducing product ion intensities at the detector.

Choosing the electron excitation energy in the ICR experiment adds a certain flexibility in the extent of dissociation desired. This flexibility is somewhat further enhanced by choice of the trapping times used. Unlike CID which generally monitors a single event, however, in EIEIO as the trapping time is increased, daughter ions may be further excited and decomposed in the electron beam as was pointed out earlier or may undergo subsequent ion-molecule reactions modifying fragment peak intensities. For this reason caution must be exercised in interpreting ICR-EIEIO data. Relatively short trapping times (≤ 100 ms) and low pressures ($\sim 10^{-7}$ Torr) as were used in the majority of this study can be employed to minimize these complications.

Table I, for the most part, indicates that fragmentation following electron impact or collision with a neutral are quite similar, which perhaps is to be expected. The differences which do occur can be postulated as arising either from the amount of energy deposited by the two methods or the form in which it is delivered (i.e., rotational, vibrational, and electronic) (6). Further comparisons between EIEIO and CID as well as with PDS should yield insight into this question.

Finally, we feel that EIEIO gives ICR important capabilities equivalent to CID which, together with the ICR photochemical techniques and unusual capabilities for studying ion-molecule reactions, will aid in the development of ICR as an analytical instrument. Further studies are in progress.

ACKNOWLEDGMENT

The authors thank Graham Cooks and Richard Kondrat, Chemistry Department, Purdue University, for providing the CID spectra and Tom Morton, Chemistry Department, Brown University, for supplying the phenetole sample.

LITERATURE CITED

- (1) C. Koppel and F. W. McLafferty, *J. Am. Chem. Soc.*, **98**, 8293 (1976).
- (2) R. W. Kondrat and R. G. Cooks, *Anal. Chem.*, **50**, 81A (1978).
- (3) K. R. Jennings, *Int. J. Mass Spectrom. Ion Phys.*, **1**, 227 (1968).
- (4) J. Durup, "Mechanisms of Collision Induced Dissociation of Fast Ions", in "Recent Developments in Mass Spectrometry", K. Ogata and T. Hayakawa, Ed., University Park Press, Baltimore, Md., 1970.
- (5) J. H. Beynon and R. G. Cooks, *Int. J. Mass Spectrom. Ion Phys.*, **19**, 107 (1976).
- (6) V. Franchetti, B. S. Freiser, and R. G. Cooks, *Org. Mass Spectrom.*, **13**, 106 (1978).
- (7) R. C. Burnier and B. S. Freiser, *Inorg. Chem.*, in press.
- (8) D. A. McCreary and B. S. Freiser, *J. Am. Chem. Soc.*, **100**, 2902 (1978).
- (9) B. S. Freiser and J. L. Beauchamp, *J. Am. Chem. Soc.*, **99**, 3214 (1977).
- (10) T. E. Orlowski, B. S. Freiser, and J. L. Beauchamp, *Chem. Phys.*, **16**, 439 (1976).
- (11) B. S. Freiser and J. L. Beauchamp, *J. Am. Chem. Soc.*, **96**, 6260 (1974).
- (12) R. C. Dunbar, *Anal. Chem.*, **48**, 723 (1976).

- (13) E. Fu, P. P. Dymerski, and R. C. Dunbar, *J. Am. Chem. Soc.*, **98**, 337 (1976).
 (14) B. S. Freiser and J. L. Beauchamp, *Chem. Phys. Lett.*, **42**, 380 (1976).
 (15) B. S. Freiser, *Int. J. Mass Spectrom.*, **26**, 39 (1978).
 (16) G. H. Dunn, B. van Zyl, and R. N. Zare, *Phys. Rev. Lett.*, **15**, 610 (1965).
 (17) G. H. Dunn and B. van Zyl, *Phys. Rev.*, **154**, 40 (1967).
 (18) B. van Zyl and G. H. Dunn, *Phys. Rev.*, **153**, 43 (1967).
 (19) J. L. Beauchamp, *Ann. Rev. Phys. Chem.*, **22**, 527 (1971).
 (20) T. A. Lehman and M. M. Bursey, "Ion Cyclotron Resonance Spectrometry", Wiley-Interscience, New York, 1976.
 (21) F. Borchers, K. Levsen, C. B. Theissling, and N. M. M. Nibbering, *Org. Mass. Spectrom.*, **12**, 746 (1977).
 (22) J. W. Rabalais and R. J. Colton, *J. Electron. Spectrosc.*, **1**, 83 (1972).

(23) R. B. Cody and B. S. Freiser, unpublished results.

RECEIVED for review August 22, 1978. Accepted December 26, 1978. This work was supported in part by Research Corporation through a Cottrell Research Grant. The authors also wish to acknowledge the donors of the Petroleum Research Fund, administered by the American Chemical Society, and DuPont for support administered through Purdue University.

Determination of Organosulfur Compounds Extracted from Marine Sediments

Timothy S. Bates¹ and Roy Carpenter

Department of Oceanography, University of Washington, Seattle, Washington 98195

A method to characterize organosulfur compounds in the lipophilic extract of marine sediments is described. The main interference in the analysis is elemental sulfur (S_8). Techniques for its elimination are discussed. Saponification of the initial extract is shown to create organosulfur compounds. Activated copper removes S_8 from an extract and appears neither to create nor to alter organosulfur compounds. However, mercaptans and most disulfides are removed by the copper column. The extraction efficiency of several other classes of sulfur compounds is 80–90%. Extracts are analyzed with a glass capillary gas chromatograph equipped with a flame photometric detector. Detection limit is 1 ng S, precision $\pm 10\%$.

Reliable methods are needed to quantitate organosulfur compounds in the lipids extracted from marine sediments. These lipophilic organosulfur compounds (OSC) are a small but significant component of crude oils and other fossil organic materials (1). Through oil spills, runoff, and atmospheric processes, many anthropogenic organosulfur compounds are transported into the marine environment where they can be deposited along with natural organosulfur compounds in sediments (2). Natural sources include oil seeps, biosynthesis, atmospheric input from forest and grass fires, and diagenetic reactions within the sediment.

Despite the environmental and geochemical importance of these compounds, little information is available concerning the nature and amounts of organosulfur compounds in marine sediments (3). Investigations of the persistence and toxic effects of these compounds require reliable extraction and analysis techniques.

The analysis of organosulfur compounds has been greatly facilitated by the flame photometric detector (4). Volatile compounds can be separated by a glass capillary chromatographic (GC) column and the effluent split to a flame ionization detector (FID) and a flame photometric detector (FPD). The FPD response is proportional to $[S]^2$ (5, 6). The

selectivity and enhanced sensitivity of the FPD for S permits quantitation of organosulfur compounds at relatively low concentrations in complex organic mixtures. The FID trace allows the organosulfur compounds to be referenced to the more abundant aliphatic and/or polynuclear aromatic hydrocarbons (2). A FID-FPD chromatogram of Prudhoe Bay crude oil is shown in Figure 1. The upper trace (FID) is dominated by a series of aliphatic hydrocarbons found in the oil. The lower trace (FPD) shows the organosulfur compounds. The U.S. Coast Guard (7) and the Environmental Protection Agency (8) have used similar FPD traces to compare oils qualitatively.

Reliable FPD quantification of organosulfur compounds requires careful optimization of the GC parameters. Although the relative response of the FPD to various sulfur compounds remains somewhat controversial (9), analysis of organosulfur compounds by FPD is now relatively straightforward. Quantitative extraction of these compounds from marine sediments, though, has never been previously investigated. Extraction techniques are the main thrust of this study.

EXPERIMENTAL

A variety of extraction procedures were tested in this study. The methods described here were the most efficient and reliable for extracting OSC from marine sediments.

Extraction. Sediment samples were freeze-dried (Virtis, Unitrap II), weighed (80 g), and Soxhlet extracted in pre-extracted paper thimbles (43 × 123 mm Whatman single thickness) with CH_2Cl_2 for 24 h. Quantitation of the total extract was obtained by weighing an aliquot on an electrobalance (Cahn 4100). The extraction precision was 0.01 mg/g sediment dry weight (1.2% rel. std. dev., for 4 replicate analyses). After weighing, the extract was concentrated to ≈ 10 mL by rotary evaporation (ambient temperature and 50 cm of Hg vacuum) and eluted through a column of activated Cu powder to eliminate S_8 (10). The column was prepared by passing 2 N HCl, H_2O , CH_3COCH_3 , and CH_2Cl_2 through a 10-mm i.d. column containing 5 cm of Cu powder (Cu "U" metal, No. 53, made by Metal Powders, Carteret, N.J.). The column eluate was then reconcentrated to 10 mL, reweighed, and evaporated to dryness under N_2 for GC analysis. The recovery of 100 ng of individual sulfur standards added to pre-extracted sediment varied from 80–90% for sulfides, sulfones, and aromatic sulfur compounds. Mercaptans and disulfides were not recovered since these classes of compounds were retained on the Cu column.

Gas Chromatographic Analysis. A Perkin-Elmer model 3920B GC was used for all analyses. The entire system was glass

¹Present address: Pacific Marine Environmental Laboratory, Environmental Research Laboratories, National Oceanic and Atmospheric Administration, 7600 Sand Point Way N.E., Bldg. 32 Seattle, Wash. 98115.

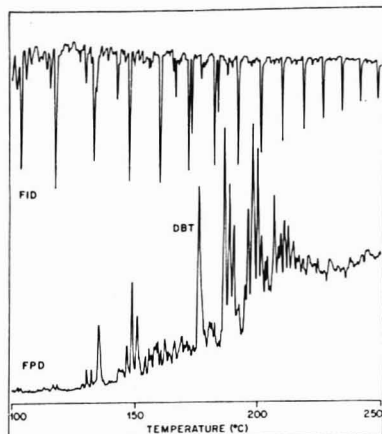


Figure 1. Gas chromatogram of unfractionated Prudhoe Bay crude oil. The sulfur-sensitive flame photometric detector (FPD) response and the flame ionization detector (FID) response were recorded simultaneously. The peak labeled DBT is dibenzothiophene. Instrumental conditions: Perkin-Elmer 3920B gas chromatograph with FID/FPD; 30 m \times 0.5 mm SCOT glass capillary column; linear temperature program 100–250 °C at 8°/min

or glass-lined to prevent chemical reactions from contact with hot metal. Support-coated, open-tubular (SCOT) SE-30 glass capillary columns (30 m \times 0.5 mm i.d., deactivated with triethanolamine) were used in preference to wall-coated columns because of the former's increased loading capacity. The column effluent was split 2:1 to the FPD and FID, respectively. The FPD detection limit was 1 ng S (S/N = 2, $\pm 10\%$ rel. std. dev. for 10 injections of dibenzothiophene over 5 days).

FPD Optimization and Calibration. Tests with SF_6 and a standard mixture of organosulfur compounds showed optimal FPD response with a H_2 flow of 55 mL/min and an air flow of 120 mL/min, in agreement with Mizany (11) but not Burnett et al. (9). H_2 flow of 75 mL/min gave an O_2/H_2 ratio of 0.32 in the flame (found optimal by Burnett et al., (9)), but the response was 10% lower at the same noise level. The flow to the FPD was 33 mL/min or 2/3 or the combined flow from the column (8 mL/min) and the make-up gas (42 mL/min).

The GC signal output (theoretically the square root of the photomultiplier response) was fed through a Spectrum model 1021A filter to reduce instrument noise, and then to a Columbia Scientific Instruments Supregrator 3 integrator. The response of the detector output vs. the injected amount was linear from 1–1500 ng for *n*-butyl sulfone, dibenzothiophene, thianthrene, benzyl disulfide, phenyl sulfide, and 2-mercaptanaphthalene (concentration = 0.88 (integrator response) + 10; $r = 0.99451$). This response was related to the number of S atoms in a molecule and not to chemical structure, in agreement with Maruyama and Kakimoto (12). Such a calibration curve was recommended by Burnett et al. (9) to avoid systematic errors associated with a nonlinear detector response.

RESULTS AND DISCUSSION

Extraction Procedures. Several extraction procedures were compared for efficiency and ease of extraction. The tests were performed upon sediment obtained with a van Veen grab sampler in Puget Sound, west of Seattle (47° 41.0' N, 122° 28.0' W). This fine-grained sediment is typical of the major basins in Puget Sound and has an organic carbon content of $\approx 2\%$. Soxhlet extraction was used since it is believed to be most efficient for lipids (13, 14). Extraction results of freeze-dried sediment were compared to those obtained with wet sediment. No significant differences were found in the

total lipids or OSC extracted. The gas chromatogram of freeze-dried sediment extract showed only the OSC that were also present in the wet sediment. The freeze drier did not form OSC artifacts, contrary to observations with alkenes (15). GC analysis of the vacuum pump oil showed no OSC.

Using freeze-dried sediment, three solvent systems were compared by gravimetric measurements of total extractable lipids and GC quantitation of OSC. Twenty-four hour extractions with benzene:methanol (50:50), dichloromethane:methanol (50:50), and dichloromethane alone gave comparable results for OSC. Dichloromethane extracted only about 1/3 as much total lipids as by the other two solvent systems. Continuing the dichloromethane extraction for a second day afforded only an additional 4% of extractable lipids, while OSC showed no significant increase.

Trace levels of OSC in marine sediments require a larger amount of sample than normally extracted in hydrocarbon analyses. Approximately twice as much sample can be extracted in the same apparatus by using a freeze-dried sediment. The use of freeze-dried sediment also permits dichloromethane to be used as the single extraction solvent which is not possible if water is present in the sample. Dichloromethane is as efficient as more polar solvents for extracting OSC and has the additional advantage of simplifying subsequent sample workup because of the absence of pigments and more polar compounds that would be extracted with more polar solvents.

S_8 Elimination. The main obstacle in the analysis of OSC in marine sediments is elemental sulfur (S_8) which is also extracted with organic solvents. Existing in nature as an eight-membered ring (16), sufficient S_8 is usually present in both oxidizing and reducing marine sediments to saturate the FPD and thereby interfere with OSC analyses. Organic extracts of primary-treated sewage effluent, storm-water runoff, crude oils, and refined petroleum products usually do not contain sufficient S_8 to cause this problem (2). However, since S_8 is present in most sediment extracts, a method is needed to eliminate it without altering OSC compositions.

Traditionally S_8 has been removed by eluting the lipid extract through a column of activated Cu powder (10). Tests with a mixture of organosulfur standards showed that this also removed mercaptans and many disulfides. Individual sulfur standards were recovered as follows: 2-mercaptanaphthalene, 0%; benzyl disulfide, 20%; thianthrene, 80%; dibenzothiophene, 86%; *n*-butylsulfone, 87%; and phenyl sulfide, 90%.

Other techniques were tested to eliminate S_8 without removing OSC. Elemental sulfur can be removed by saponification of the extract. This procedure is often used in hydrocarbon analyses to remove esters from total lipid extracts. Saponification cleaves the sulfur-8 ring, releasing water-soluble ions which can be separated from the lipophilic organic molecules. Another S_8 removal technique is its conversion to thiosulfate with tetrabutylammonium sulfite (17). The resulting thiosulfate dissolves in alcohol and can be separated from the nonpolar organic material. Elemental sulfur can also be eliminated from the lipid extract by converting S_8 to thiocyanate by adding sodium cyanide (18).

None of these methods for removing S_8 was satisfactory in this application. Thiocyanate, formed from sodium cyanide, was difficult to separate from the organic extract. It partly reacted with mercaptan and disulfide standards to give nonquantitative results for these compounds. Tetrabutylammonium sulfite removed S_8 efficiently, but the sulfite ion apparently created two additional organic sulfur compounds from the mixture of standards. Saponification removed both S_8 and mercaptans. When this procedure was applied to a surface sediment extract, the gas chromatogram showed that

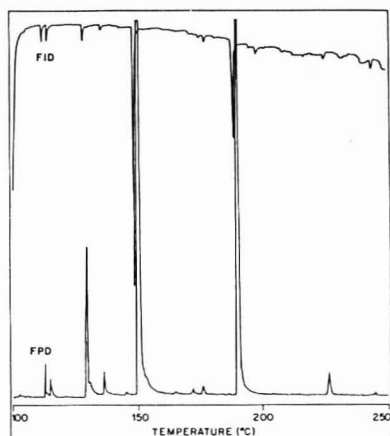


Figure 2. Gas chromatogram of a saponified sediment sample extract. Instrumental conditions are as cited in Figure 1

all the major compounds contained sulfur (Figure 2). These compounds were not removed from the extract when it was eluted through an activated Cu column. To test whether these compounds were artifacts or indigenous to the sediments, an identical sediment sample was extracted, but an activated Cu column rather than saponification was used to eliminate S_8 . The gas chromatogram was entirely different from that obtained from the saponified sample (Figure 3, bottom). The saponified sample was fractionated using silica-alumina gel chromatography (14). The compounds seen in Figure 2 were eluted from the column in the methanol fraction. The sulfur compounds in the 20% benzene in pentane and 100% benzene fractions were the same compounds that were observed in the sediment sample that was eluted through the Cu column. These results indicate that saponification created polar organosulfur compounds.

Another approach to eliminating S_8 without removing the more reactive OSC was to stabilize the mercaptans and disulfides prior to S_8 removal. Compounds such as α -bromo-2,3,4,5,6-pentafluorotoluene (19), benzoyl chloride (20), and *N*-ethylmaleimide (21) can be used to form mercaptan derivatives. Initially such derivatizing agents seemed desirable since the recoveries of the sulfur compounds were high, but base was required to form the derivatives quantitatively. Evidently, S_8 was cleaved by base and reacted with the derivatizing agents to form organosulfur by-products. This supposition was confirmed by the reaction of various mercaptan derivatizing agents with elemental sulfur which resulted in the formation of a variety of organosulfur compounds. These derivatizing agents, therefore, cannot be applied to the extraction and analysis of OSC in marine sediments.

Artifacts Produced by Photosensitized Reactions. Photochemical reactions may cause problems in extracting and analyzing OSC (22). At least one sulfur compound in the sediment extract appeared to undergo a photochemical reaction. Two samples of surface sediment were extracted by the normal procedure. One extract was left on a window sill in a transparent glass container for 5 days while the other was kept in the laboratory. Compound E in the extract left on the window sill appeared to break down to form A, B, C, and D (Figure 3). Compound D was also observed in sediment samples that remained in the sunlight after collection aboard ship. There was no evidence that the conditions of this experiment affected di-

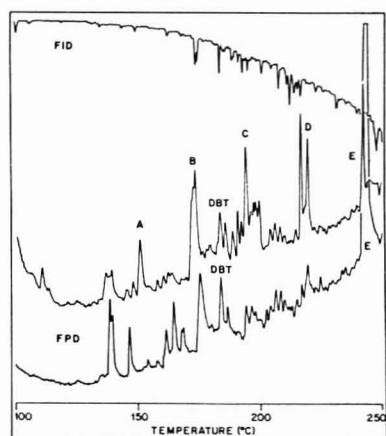


Figure 3. Gas chromatogram of a surface sediment sample extract eluted through a copper column to eliminate elemental sulfur. The bottom FPD trace was from a sample extract kept in the laboratory. The top FPD trace was from an identical sediment extract that was left on a window sill for 5 days. The FID traces for the two samples were identical. One is shown at the top of the figure. The peaks labeled DBT are dibenzothiophene. The lettered peaks are discussed in the text. Instrumental conditions are as cited in Figure 1

benzothiophene or its alkylated homologues.

Burwood and Speers (23) have suggested that photo-oxidation of petroleum creates thiocyclane oxides. This did not appear to occur in this experiment since the observed reaction products were all nonpolar. In summary, care should be taken to minimize exposure of samples and extracts to sunlight. Normal laboratory fluorescent lighting does not appear to cause artifacts during sample processing, but amber-colored glassware may minimize difficulties.

Applications to a Crude Oil. A sample of Prudhoe Bay crude oil was mixed with pre-extracted sediment, Soxhlet extracted with dichloromethane, and eluted through a column of Cu powder. GC analyses of the oil before and after the procedure showed no change in the relative abundances of the sulfur compounds (Figure 1). Evidently the dichloromethane extractable fraction of the crude oil (1) contained all the S compounds present in the oil that can be analyzed by GC, (2) contained no mercaptans or disulfides, and (3) contained no OSC formed during the procedure.

ACKNOWLEDGMENT

The authors appreciate the helpful suggestions of J. I. Hedges and R. C. Clark, Jr., and the constructive review of this manuscript by W. D. MacLeod.

LITERATURE CITED

- (1) J. A. Gransch and J. Posthuma, "On the Origin of Sulphur in Crudes", in "Advances in Organic Geochemistry", B. Tissot and F. Biener, Ed., Pergamon Press, New York, 1973.
- (2) T. S. Bates and R. Carpenter, *Geochim. Cosmochim. Acta*, in press.
- (3) J. S. Warner, "Determination of Sulfur-containing Petroleum Components in Marine Samples", in "Proceedings of the Joint Conference on the Prevention and Control of Oil Spills", American Petroleum Institute, Washington D.C., 1975, pp 97-101.
- (4) S. S. Brody and J. E. Chaney, *J. Gas Chromatogr.*, **4**, 42 (1966).
- (5) D. G. Greer and T. J. Bydalek, *Environ. Sci. Technol.*, **7**, 153 (1973).
- (6) T. Sugiyama, Y. Suzuki, and T. Takeuchi, *J. Chromatogr.*, **77**, 309 (1973).
- (7) A. P. Bert, *Anal. Chem.*, **48**, 454A (1976).
- (8) M. E. Garza, Jr., and J. Muth, *Environ. Sci. Technol.*, **8**, 249 (1974).
- (9) C. H. Burnett, D. F. Adams, and S. O. Farwell, *J. Chromatogr. Sci.*, **16**, 68 (1978).
- (10) M. Blumer, *Anal. Chem.*, **29**, 1039 (1957).
- (11) A. I. Mizary, *J. Chromatogr. Sci.*, **8**, 151 (1970).
- (12) M. Maruyama and M. Kakimoto, *J. Chromatogr. Sci.*, **16**, 1 (1978).

- (13) G. G. Rohrbach and W. E. Reed, "Evaluation of Extraction Techniques for Hydrocarbons in Marine Sediments", Publication No. 1537, Institute of Geophysics and Planetary Physics, University of California at Los Angeles, Los Angeles, Calif., 1976.
- (14) J. W. Farrington and B. W. Tripp, "A Comparison of Analysis Methods for Hydrocarbons in Surface Sediments", in "Marine Chemistry in the Coastal Environment", T. M. Church, Ed., ACS Symp. Ser., No. 18, 1975, Chapter 15.
- (15) D. Van de Meent, W. L. Maters, J. W. De Leeuw, and P. A. Schenck, *Org. Geochem.*, **1**, 7 (1977).
- (16) H. Schumann, "Reactions of Elemental Sulfur with Inorganic, Organic, and Metal-Organic Compounds" in "Sulfur in Organic and Inorganic Chemistry", A. Senning, Ed., Marcel Dekker, New York, 1972, Chapter 21.
- (17) S. Jensen, L. Renberg, and L. Reutergerd, *Anal. Chem.*, **49**, 316 (1977).
- (18) J. K. Bartlett and D. A. Skoog, *Anal. Chem.*, **26**, 1008 (1954).
- (19) F. K. Kawahara, *Environ. Sci. Technol.*, **5**, 235 (1971).
- (20) L. Gasco and R. Barrera, *Anal. Chim. Acta*, **81**, 253 (1972).
- (21) M. T. J. Murphy, B. Nagy, G. Rouser, and G. Kritchevsky, *J. Am. Oil Chem. Soc.*, **42**, 475 (1965).
- (22) W. E. Haines, G. L. Cook, and J. S. Ball, *J. Am. Chem. Soc.*, **78**, 5213 (1956).
- (23) R. Burwood and G. C. Speers, *Estuarine Coastal Mar. Sci.*, **2**, 117 (1974).

RECEIVED for review October 10, 1978. Accepted December 26, 1978. This study was supported by U.S. Department of Energy Contract AT(45-1)-2225-T40. This is Contribution No. 1059 from the Department of Oceanography, University of Washington, Seattle, Wash.

Voltammetric Ion Selective Electrode for the Determination of Nitrate

James A. Cox* and George R. Litwinski

Department of Chemistry and Biochemistry, Southern Illinois University at Carbondale, Carbondale, Illinois 62901

A sensor which uses an anion-exchange membrane to enclose a small volume electrolysis cell has been demonstrated to be suitable for nitrate determinations. The three-electrode cell includes a constrained mercury column indicator electrode; filter paper, which is impregnated with a 0.1 M KCl-0.01 M $ZrOCl_2$ electrolyte, serves as the constraining barrier and as the spacer for the thin-layer electrolysis chamber. The anion-exchange membrane sheath permits transfer of nitrate from the sample into the electrolysis chamber by Donnan dialysis and excludes several species which would otherwise interfere. Controlled potential electrolysis at -1.25 V vs. Ag/AgCl provides the sensing current, the value of which is proportional to the sample concentration of nitrate. As a steady-state current is not developed with the present design, a defined current sampling time is used. Linear response over 3 orders-of-magnitude nitrate concentration is obtained. The detection limit using the current at 8 min is 6.7×10^{-6} M NO_3^- .

Membrane-clad voltammetric sensors have been designed for the determination of certain molecular species, especially dissolved gases. The Clark oxygen electrode is probably the best known (1, 2). This system functions by using a neutral membrane to separate the sample from a small volume electrochemical cell. Oxygen diffuses into the cell where it is continuously reduced by controlled potential electrolysis at a platinum electrode; a steady-state current is developed in proportion to the oxygen concentration in the sample. Comparable sensors for ionic species have not been previously reported.

The present design is based upon our earlier work in which nitrate was determined by linear potential scan voltammetry at a hanging mercury drop electrode in the presence of a $La(III)$ catalyst (3). Donnan dialysis was used to transfer a controlled fraction of the nitrate from the sample into the 0.01 M $LaCl_3$ -0.1 M KCl electrolyte prior to the voltammetric scan in order to increase the overall sensitivity (through preconcentration) and eliminate interference by cations and sur-

factants. In the present work $ZrOCl_2$ has been used as the catalyst since, unlike in the $La(III)$ system, the mercury surface does not become passivated and dissolved oxygen does not interfere with the development of the nitrate reduction current (4).

EXPERIMENTAL

The instrumentation consisted of a three-electrode polarograph which was constructed with Teledyne Philbrick Model 1027 operational amplifiers and a Hewlett-Packard Model 1510B strip chart recorder. The chemicals were ACS Reagent Grade and were used without further purification. Because of the known effect of aging (5-7), the electrolytes were prepared from a 0.1 M $ZrOCl_2$ stock solution which had been stored for at least 3 weeks.

The ion-exchange membranes and the poly(vinyl acetate) and poly(vinyl alcohol) neutral membranes were obtained from RAI Research Corporation, Hauppauge, Long Island, N.Y. The ion-exchange membranes were pretreated by the general procedure of Blaedel and Kissel (8) except that they were stored in 0.1 M KCl-0.01 M $ZrOCl_2$ prior to use.

The membrane-clad voltammetric sensors (Figure 1) utilized Ag/AgCl reference, platinum counter, and constrained mercury column indicator electrodes. The system was constructed by cementing a 5-mm o.d. (2-mm i.d.) glass tube into a 12-mm o.d. tube with Torr Seal low vapor pressure resin, Varian Associates, Vacuum Division, Palo Alto, Calif. The tubes were placed concentrically. The reference and counter electrode wires were also cemented into the assembly. The resin face and outer tube of the sensor were machined at a 45° angle; the mercury tube was left planar.

A pair of disks of Whatman No. 40 (medium) filter paper were placed over the mercury tube and resin face. Prior to assembly they were impregnated with the KCl- $ZrOCl_2$ electrolyte. The paper served as the constraint for the mercury and as a spacer. An ion-exchange membrane was firmly drawn over the entire end of the assembly. The membrane was fixed in place by Teflon tape and a small plastic hose clamp. Mercury was poured into the inner tube and electrical contact was made by inserting a platinum wire. The length of the complete assembly was about 12 cm.

The assembly was stored in supporting electrolyte between experiments. As co-ion penetration occurs extensively with a high ionic strength solution on each side of the membrane, this step regenerates the inner solution and removes the electrolysis products. At least 5 min is allowed for this step.

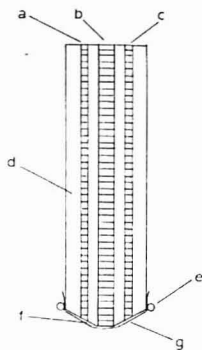


Figure 1. Design of the voltammetric sensor. (a) Pt counter electrode; (b) constrained Hg indicator; (c) Ag/AgCl reference; (d) epoxy; (e) retainer ring; (f) paper spacer and supporting electrolyte reservoir; (g) anion-exchange membrane

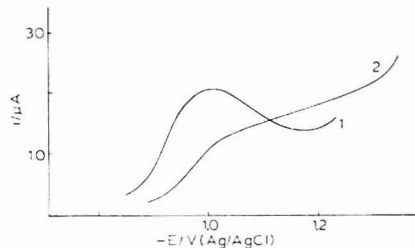


Figure 2. Linear scan voltammetric reduction of nitrate. (1) Hanging mercury drop; (2) paper-constrained mercury column indicator electrode. Solution: 10^{-3} M NO_3^- , 0.1 M KCl, 0.01 M ZrOCl_2 ; scan rate, 50 mV s^{-1}

RESULTS AND DISCUSSION

Preliminary experiments were performed to determine whether the described sensor would respond to nitrate. In these experiments, the electrode was dipped into a 10^{-4} M NaNO_3 solution for 15 min, and a linear potential scan voltammogram was subsequently obtained at a 10 mV s^{-1} scan rate. A nitrate reduction current plateau was observed in the range -1.0 to -1.3 V; at more negative potentials discharge of the supporting electrolyte occurs (Figure 2). Comparable experiments performed with a typical polarographic cell and a hanging mercury drop electrode produce a peak at -0.9 V with the Zr(IV) catalyst in agreement with the results of our recent mechanistic study (9). The high resistance of the constrained Hg electrode and immobilized electrolyte are responsible for the potential shift and lack of a distinct peak.

As the intended application uses controlled potential electrolysis, the absence of a peak current is not important, but since the paper-constrained Hg indicator electrode does not permit complete resolution of the nitrate reduction current from the supporting electrolyte discharge, other constraining materials were tested. A mercury column with a terminal coarse glass frit (10) gave similar linear scan voltammetry results; however, it was difficult to obtain good solution contact when the ion-exchange membrane was attached. Neutral membranes (poly(vinyl alcohol), poly(vinyl acetate), and cellophane) were also employed to enclose the Hg column (11); because of slow diffusion of nitrate through these materials, a nitrate reduction current was not observed. Subsequently only filter paper was used as the Hg constraint and spacer.

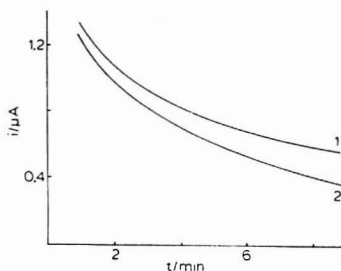


Figure 3. Current-time behavior of the nitrate voltammetric ion selective electrode. (1) NaNO_3 10^{-4} M; (2) blank (distilled H_2O). Sample volumes, 100 μL . Supporting electrolyte, 0.1 M KCl-0.01 M ZrOCl_2 . Electrolysis potential, -1.25 V vs. Ag/AgCl. Samples were deaerated for 5 min prior to measurement and were stirred.

Based upon the data in Figure 2, experiments were performed in which the nitrate sensor was dipped into deaerated samples of various concentrations; the controlled potential electrolysis current at -1.25 V was monitored. Typical results are shown in Figure 3. The above electrolysis potential was selected because it yielded the greatest signal-to-background ratio. Unlike the case of polarographic oxygen electrodes, steady-state currents were not obtained with the present sensor design. Decreasing the ratio of electrode-to-membrane areas, which decreases the time to reach steady state for the oxygen electrode (2), was not effective. Hence, working curves were prepared using the electrolysis current measured at a prescribed time after contact to the stirred sample.

Under such conditions, linear working curves were obtained. For example, with an 8-min current sampling time linear least-squares analysis of a 7-point curve over the range 1.0×10^{-5} to 1.2×10^{-4} M NO_3^- yielded the following: slope, $1.91 \pm 0.05 \times 10^5 \text{ nA/M}$; intercept, 0.34 nA; and correlation coefficient, 0.998. The slope was unchanged up to 5×10^{-3} M NO_3^- . Five replicate blank trials (distilled water instead of a nitrate sample) yielded a current of $0.42 \pm 0.01 \mu\text{A}$ with the 8-min current sampling time.

The detection limit (using the criterion of the concentration which yields a current of twice the blank uncertainty) was 6.7×10^{-6} M NO_3^- . With a 2-min sampling time, the working range was 8×10^{-5} to 1×10^{-2} M NO_3^- . A comparable least squares study at the 10^{-4} M level gave a slope of $1.37 \pm 0.04 \times 10^5 \mu\text{A/M}$, correlation coefficient of 0.9985, and intercept of $8 \times 10^{-3} \mu\text{A}$.

The major limitations of the present electrode design are the lack of a steady-state current and the physical instability of the constrained mercury indicator electrode. Both problems are associated with the Zr(IV) catalyst. The constant decrease in the blank current, which is shown in Figure 3, is probably the result of some hydrogen discharge which occurs at -1.25 V. Evidence for this discharge is the increasing current beyond -1.1 V in Figure 2 with the paper-constrained mercury indicator. The consumption of proton during the subsequent controlled potential electrolysis at -1.25 V would cause the current contribution from proton reduction to decrease with time. If the electrolysis cell could be constructed with a low internal resistance, a nitrate reduction potential could be defined at which the background electrolysis is negligible (see Figure 2). Such an electrolysis cell would presumably yield a linear scan voltammetric response identical to that of the hanging mercury drop electrode i - E curve in Figure 2. In this case an electrolysis potential of -1.0 V would result in nitrate reduction without concurrent proton reduction. Steady state would then likely be achieved. Such a cell could be made with a solid indicator electrode. Several solid electrode types were

investigated by linear scan voltammetry with the Zr(IV) catalyst, including wax-impregnated graphite, mercury-coated graphite and platinum, solid silver amalgam (12), and glassy carbon. In each case, the electrolyte discharge obscured the nitrate reduction current. An improved catalyst would permit resolving the nitrate current from the background at a solid electrode. The commonly used La(III) and UO_2Cl_2 catalysts (13, 14) failed because of passivation of the electrode and a low signal-to-background ratio, respectively. Presently catalysis by a mixed Cd, Cu deposit on graphite, which was reported by Bodini and Sawyer (15), is being tested in the membrane-clad sensor.

Species which can interfere with the measurement, and the extent to which they will interfere, can be predicted from previous work. The anion-exchange membrane will exclude neutral species, except for those of low molecular weight, and cations (3). Anions which are electroactive at -1.25 V will interfere. Fortunately these are not abundant in most samples, but nitrite, which often is present with nitrate, is in this category. Measurements in nitrite-containing samples must be performed after a separation or by an alternative approach such as with an enzymatic method (16). Anions which can affect the Zr(IV)-catalysis of the nitrate reduction will interfere. For example, sulfate in high concentrations (ca. 10^{-3} M) will shift the nitrate reduction beyond the discharge of

the supporting electrolyte (9). If the sample is not deaerated, the reduction of dissolved O_2 will add to the background current.

LITERATURE CITED

- (1) L. C. Clark, Jr., *Trans. Am. Soc. Artif. Intern. Organs*, **2**, 41 (1956).
- (2) I. Fatt, "The Polarographic Oxygen Sensor", CRC Press, Cleveland, Ohio, 1978.
- (3) G. L. Lundquist, G. Wasinger, and J. A. Cox, *Anal. Chem.*, **47**, 319 (1975).
- (4) J. A. Cox and F. Brumgard, Southern Illinois University—Carbondale, Carbondale, Ill., unpublished results, 1976.
- (5) H. W. Wharton, *J. Electroanal. Chem.*, **9**, 134 (1965).
- (6) V. M. Klyuchnikov, L. M. Zaitsev, S. S. Korovin, and I. A. Apraksin, *Zh. Neorg. Khim. (Engl. Transl.)*, **17**, 1593 (1975).
- (7) R. L. Young, J. E. Spill, H. M. Su, and R. H. Philip, *Environ. Sci. Technol.*, **9**, 1075 (1975).
- (8) W. J. Blaedel and T. R. Kissel, *Anal. Chem.*, **44**, 2109 (1972).
- (9) J. A. Cox and A. Brajter, *Electrochim. Acta*, in press.
- (10) J. H. Clausen, G. B. Moss, and J. Jordan, *Anal. Chem.*, **38**, 1398 (1966).
- (11) E. Pungor, G. Nagy, and Zs. Fehér, *J. Electroanal. Chem.*, **75**, 241 (1977).
- (12) Z. Stojek and Z. Kublik, *J. Electroanal. Chem.*, **60**, 349 (1975).
- (13) J. W. Collat and J. J. Lingane, *J. Am. Chem. Soc.*, **76**, 4214 (1954).
- (14) I. M. Kolthoff, W. E. Harris, and G. Matsuyama, *J. Am. Chem. Soc.*, **66**, 1782 (1944).
- (15) M. E. Bodini and D. T. Sawyer, *Anal. Chem.*, **49**, 485 (1977).
- (16) C. H. Kiang, S. S. Kuan, and G. G. Guilbault, *Anal. Chem.*, **50**, 1319 (1978).

RECEIVED for review November 13, 1978. Accepted January 15, 1979. This work was supported by the Water Resources Center, University of Illinois, Project A-087-ILL, in the OWRT Allotment Program.

Spectroelectrochemical Determination of Heterogeneous Electron Transfer Rate Constants

Douglas E. Albertson and Henry N. Blount*

Brown Chemical Laboratory, The University of Delaware, Newark, Delaware 19711

Fred M. Hawkrigde*

Department of Chemistry, Virginia Commonwealth University, Richmond, Virginia 23284

The theory underlying the single potential step spectroelectrochemical determination of heterogeneous electron transfer rate constants is presented. The resulting expressions are experimentally verified using the quasi-reversible oxidation of ferrocyanide at tin oxide optically transparent electrodes at pH 7.00. For this model system, good agreement is obtained between values of k_{12} and α determined spectroelectrochemically ($k_{12} = 4.6 (\pm 0.2) \times 10^{-4}$ cm/s, $\alpha = 0.328 (\pm 0.006)$) and those determined by the previously reported technique of chronocoulometry ($k_{12} = 4.0 (\pm 0.2) \times 10^{-4}$ cm/s, $\alpha = 0.323 (\pm 0.008)$). The present methodology was devised to quantitatively characterize and thereby compare the rates of heterogeneous electron transfer at chemically modified electrodes.

The recent development of chemically modified electrodes (CMEs) has stimulated considerable interest, and a variety of both novel methods of preparation and applications have been reported. Electrochemical syntheses and analyses which were intractable before the advent of CMEs have been reported, and it is expected that activity in this area will increase

as present methodologies are improved and new approaches are developed.

Methodologies which have been applied to affect CME surfaces include adsorption (1-14), amidization (15-22), silanization (22-33), formation of ether linkages (34-36), vapor deposition of phthalocyanine (37), and binding of quinones (38). Other methods for preparing modified electrode surfaces include use of plasma treatment (39) and electrochemically driven surface reactions (40-42). Species selective electrodes have also been developed for potentiometric and amperometric analyses incorporating immobilized enzymes and bacteria. Recent reports have described advances in this area of research and this family of modified electrodes will not be discussed here (43-45).

Spectroscopic and electrochemical techniques have been used to characterize the morphology of CME surfaces, the electrochemical behavior of the surface, and heterogeneous electron transfer reactions occurring at CMEs. The latter problem has been addressed using cyclic voltammetry, differential pulse polarography, and chronocoulometry. However, these techniques fail to provide species-selective heterogeneous electron transfer rate parameters in an extremely important application of CMEs, namely, electrocatalysis. The absence

of any quantitative data on the heterogeneous rate constant (k_{ah}) for a redox process driven at CMEs attests to the need for a technique which provides this information. Knowledge of the magnitude of k_{ah} for such electrochemical reactions would permit quantitative comparisons of the methods of electrode pretreatment, chemical modification procedures, and other experimental variables. The optimization of the electrocatalytic character of CMEs requires access to this information.

Spectroelectrochemical methods have been shown to provide species-specific probes with which the demeanor of a specific electrochemical process of interest may be characterized (46, 47). Theories for characterizing a variety of chemically coupled electrochemical mechanisms and the attendant kinetic parameters have been advanced using spectroelectrochemical methods (47). There has been no treatment for spectroelectrochemically determining heterogeneous electron transfer rate parameters for quasi-reversible and irreversible systems.

While chronocoulometric theory has been developed and reported for the measurement of k_{ah} (48), this technique lacks species specificity if more than one electron transfer process is occurring. It has been suggested that spectroelectrochemistry may be useful in the determination of k_{ah} (49), but this application of the technique has not been demonstrated. The theory and experimental verification of the application of spectroelectrochemistry to the determination of k_{ah} is reported here. The formulation of the theoretical expressions is analogous to the previously reported chronocoulometric treatment (48) and the results of the two techniques agree for the chosen model system, ferricyanide/ferrocyanide in pH 7.00 phosphate buffer at a tin oxide optically transparent electrode (OTE).

It is expected that the spectroelectrochemical technique will provide a useful tool with which to measure k_{ah} of heterogeneous electron transfer reactions at CME surfaces. Work in these laboratories is in progress to measure k_{ah} for heterogeneous electron transfer reactions of biological molecules at CMEs of the type that has been previously described (41, 42).

THEORY

For the charge transfer process given by Equation 1,



diffusion of the two forms of the redox couple to and from a planar electrode surface may be expressed as

$$\frac{\partial C_A(x,t)}{\partial t} = D_A \frac{\partial^2 C_A(x,t)}{\partial x^2} \quad (2)$$

and

$$\frac{\partial C_B(x,t)}{\partial t} = D_B \frac{\partial^2 C_B(x,t)}{\partial x^2} \quad (3)$$

Application of a potential step of sufficient magnitude to cause the forward reaction in Equation 1 to proceed at a rate governed by k_{th} (k_{bh} being negligible) renders the following initial and boundary conditions valid:

$$C_A(x,0) = C_A^\circ; C_B(x,0) = 0 \quad (4)$$

$$D_A \frac{\partial C_A(x,t)}{\partial x} \Big|_{x=0} = k_{th} C_A(0,t) \quad (5)$$

$$D_B \frac{\partial C_B(x,t)}{\partial x} \Big|_{x=0} = -D_A \frac{\partial C_A(x,t)}{\partial x} \Big|_{x=0} \quad (6)$$

$$C_A(x \rightarrow \infty, t) = C_A^\circ; C_B(x \rightarrow \infty, t) = 0 \quad (7)$$

where C_A° is the bulk concentration of A.

By the method of Laplace transforms, solution of Equations 2 and 3 with the initial and boundary conditions given by Equations 4–7 affords the concentration of electrode reaction product in the transform plane, namely

$$\bar{C}_B(x,s) = \frac{C_A^\circ k_{th}}{sD_B^{1/2}} \left[\frac{1}{s^{1/2} + k_{th}/D_A^{1/2}} \right] \exp\left(-\frac{s^{1/2}x}{D_B^{1/2}}\right) \quad (8)$$

In the transform plane, the optical absorbance of this electrode reaction product, observed in the transmission mode, is given by (47)

$$\bar{A}_B(\lambda,s) = \epsilon_B(\lambda) \int_0^\infty \bar{C}_B(x,s) dx \quad (9)$$

Substitution for $\bar{C}_B(x,s)$ from Equation 8 affords

$$\bar{A}_B(\lambda,s) = \frac{\epsilon_B(\lambda) k_{th} C_A^\circ}{sD_B^{1/2}} \times \left[\frac{1}{s^{1/2} + k_{th}/D_A^{1/2}} \right] \int_0^\infty \exp\left(-\frac{s^{1/2}x}{D_B^{1/2}}\right) dx \quad (10)$$

which integrates to give

$$\bar{A}_B(\lambda,s) = \epsilon_B(\lambda) k_{th} C_A^\circ \left(\frac{1}{s^{3/2}} \right) \left(\frac{1}{s^{1/2} + k_{th}/D_A^{1/2}} \right) \quad (11)$$

and, in turn inverts (50) as

$$A_B(\lambda,t) = \frac{\epsilon_B(\lambda) C_A^\circ D_A}{k_{th}} \left[\frac{2k_{th} t^{1/2}}{\pi^{1/2} D_A^{1/2}} + \exp\left(\frac{k_{th}^2 t}{D_A}\right) \operatorname{erfc}\left(\frac{k_{th} t^{1/2}}{D_A^{1/2}}\right) - 1 \right] \quad (12)$$

If the magnitude of the potential step applied to the electrode is sufficiently large to cause the forward reaction in Equation 1 to proceed at a diffusion controlled rate, then the time-dependent optical absorbance of the electrode reaction product, A_B^D , is given by (51)

$$A_B^D(\lambda,t) = \frac{2}{\pi^{1/2}} \epsilon_B(\lambda) D_A^{1/2} C_A^\circ t^{1/2} \quad (13)$$

The ratio of the kinetically controlled absorbance (Equation 12) to the diffusion controlled absorbance (Equation 13) provides the normalized absorbance, A_N , namely

$$A_N(\lambda,t) = 1 + \frac{\pi^{1/2}}{2\zeta} [\exp(\zeta^2) \operatorname{erfc}(\zeta) - 1] \quad (14)$$

where

$$\zeta = \frac{k_{th} t^{1/2}}{D_A^{1/2}} \quad (15)$$

The dependence of the normalized absorbance of the electrode reaction product on the dimensionless parameter ζ is shown in Figure 1. This working curve is of the same functional form as that obtained for the chronocoulometric response of this same system (Equations 1–7) (48). The optical measurement, however, affords a means of discerning the heterogeneous electron transfer rate constant for a single redox reaction of interest even if charge is being consumed by other diffusing and nondiffusing processes.

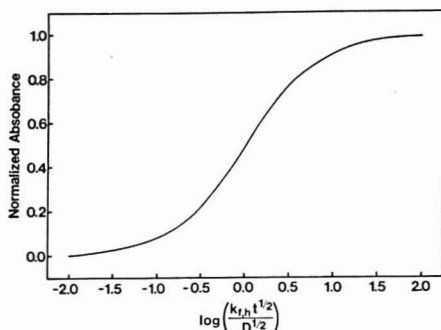


Figure 1. Working curve for spectroelectrochemical determination of heterogeneous electron transfer rate constants

EXPERIMENTAL

Materials. Deionized (Barnstead D0803), glass distilled water was used for all solution preparations. Potassium ferrocyanide (Mallinckrodt, Analytical Reagent) was used as received for the preparation of sample solutions in pH 7.00 phosphate buffer (Titrisol, Merck) containing 0.100 M sodium chloride (Fisher). Solutions were prepared by direct weighing immediately prior to use and were deoxygenated with prepurified nitrogen (Linde) which was passed over hot copper turnings and then pre-saturated with distilled water.

Apparatus. Electrochemical instrumentation, described elsewhere (52), was modified to incorporate a current follower configuration to ensure invariance of electrode potential during the potential step perturbation. Analog integration of the resulting current transients permitted chronocoulometric observation of the reaction system. Tin oxide OTEs (Corning, 10 Ω/\square) served as working electrodes in cells of a previously reported design (47). All spectroelectrochemical measurements were made at the λ_{max} of $\text{Fe}(\text{CN})_6^{3-}$, 420 nm. The electrochemical and optical systems were interfaced with a dedicated computer system for the acquisition, reduction, and presentation of data (53). The saturated calomel reference electrode employed in the experimental measurements was calibrated using a platinum electrode immersed in saturated solutions of quinhydrone (Eastman) at pHs of 7.00, 7.50, and 8.00 (54). All potentials reported here are relative to the normal hydrogen electrode. All measurements were made at 25.0 (± 0.2) $^{\circ}\text{C}$.

RESULTS AND DISCUSSION

In acidic aqueous solution, the ferricyanide/ferrocyanide couple exhibits reversible electrochemical behavior at tin oxide. This behavior, shown in Figure 2A, is consistent with that previously reported (51). With decreasing acidity, however, electron transfer between this couple and the tin oxide electrode becomes quasi-reversible (47, 55) and this behavior at pH 7.00 is shown in Figure 2B. Quasi-reversible behavior of this couple has also been observed at other electrodes, notably platinum (56–60), carbon (59–62), and gold (59, 63).

Application of potential steps of 800 mV or more to the tin oxide OTEs resulted in the diffusion controlled oxidation of ferrocyanide at pH 7.00. The integrity of diffusion control of this system under these conditions was demonstrated by both chronocoulometry and spectroelectrochemistry. In the former case, diffusion control was ascertained through linearity of the charge dependence on the square root of time over the duration of the potential step and through agreement between the electrode area determined under these experimental conditions and that evaluated at pH 2.5 where the system is known to behave reversibly (51). In the latter case, diffusion control was validated by linearity of absorbance dependence on the square root of time over the duration of the potential

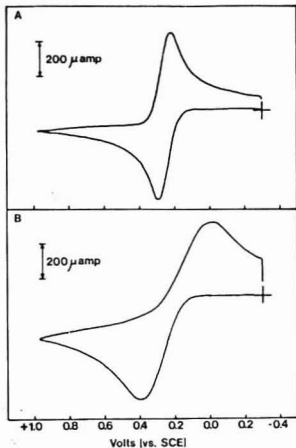


Figure 2. Cyclic voltammetric behavior of 5.0 mM ferrocyanide at tin oxide electrode. Electrode area = 0.40 cm^2 ; sweep rate = 125 mV/s. Curve A: 0.50 M glycine/HCl, pH 2.50. Curve B: 0.10 M phosphate, 0.10 M NaCl, pH 7.00

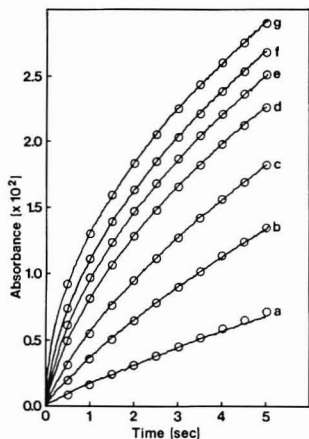


Figure 3. Absorbance-time behavior for potential step electro-oxidation of 5.34 mM ferrocyanide at tin oxide OTE at pH 7.00. Solid lines are experimental transients; open circles are theoretical responses calculated from Equation 12. Curve a: $\eta = 20$ mV, theoretical response calculated for $k_{1h} = 4.02 \times 10^{-4}$ cm/s; Curve b: $\eta = 70$ mV, theoretical response calculated for $k_{1h} = 1.05 \times 10^{-3}$ cm/s; Curve c: $\eta = 120$ mV, theoretical response calculated for $k_{1h} = 2.00 \times 10^{-3}$ cm/s; Curve d: $\eta = 170$ mV, theoretical response calculated for $k_{1h} = 4.57 \times 10^{-3}$ cm/s; Curve e: $\eta = 220$ mV, theoretical response calculated for $k_{1h} = 7.13 \times 10^{-3}$ cm/s; Curve f: $\eta = 270$ mV, theoretical response calculated for $k_{1h} = 1.41 \times 10^{-2}$ cm/s; Curve g: $\eta = 820$ mV, theoretical response calculated from Equation 13

step and through agreement between experimentally determined and previously reported (51) values of $t_{\text{Fe}(\text{CN})_6^{3-}} D^{1/2}$.

Time dependent absorbance and charge transients were determined at various potential steps of magnitudes less than those required to force diffusion-controlled electro-oxidation of ferrocyanide. Representative dynamic spectroelectro-

Table I. Heterogeneous Electron Transfer Rate Constants for the Oxidation of Ferrocyanide at Tin Oxide Evaluated by the Spectroelectrochemical Technique^a

time, s ^c	$k_{t,h}^b$ (cm/s) × 10 ³					
	$\eta^d = 20$ mV	$\eta = 70$ mV	$\eta = 120$ mV	$\eta = 170$ mV	$\eta = 220$ mV	$\eta = 270$ mV
0.50	---	1.08 (±0.02)	2.26 (±0.06)	4.06 (±0.08)	7.39 (±0.07)	13.6 (±0.4)
1.00	0.605 ^e (±0.012) ^f	1.09 (±0.02)	2.29 (±0.02)	4.00 (±0.04)	7.35 (±0.08)	13.9 (±0.3)
1.50	0.601 (±0.009)	1.08 (±0.01)	2.28 (±0.02)	4.05 (±0.05)	7.27 (±0.05)	14.2 (±0.2)
2.00	0.581 (±0.005)	1.06 (±0.01)	2.31 (±0.02)	3.96 (±0.04)	7.31 (±0.06)	13.7 (±0.2)
2.50	0.571 (±0.006)	1.05 (±0.01)	2.28 (±0.01)	3.99 (±0.05)	7.30 (±0.10)	14.1 (±0.1)
3.00	0.564 (±0.005)	1.05 (±0.01)	2.26 (±0.02)	3.99 (±0.02)	7.28 (±0.05)	14.0 (±0.2)
3.50	0.560 (±0.007)	1.04 (±0.01)	2.27 (±0.02)	3.96 (±0.03)	7.24 (±0.05)	14.5 (±0.2)
4.00	0.558 (±0.008)	1.03 (±0.01)	2.23 (±0.01)	4.01 (±0.02)	7.38 (±0.10)	14.2 (±0.4)
4.50	0.554 (±0.004)	1.03 (±0.01)	2.25 (±0.03)	4.02 (±0.02)	7.43 (±0.14)	14.2 (±0.2)
5.00	0.546 (±0.003)	1.04 (±0.02)	2.23 (±0.02)	4.02 (±0.03)	7.30 (±0.05)	14.3 (±0.2)

^a $[K_3Fe(CN)_6] = 5.34$ mM or 5.02 mM. ^b According to Equation 1. ^c Following onset of potential step. ^d Overpotential where $\eta = E_{step} + E_{ref} - E^{\circ}$; E° for $Fe(CN)_6^{3-}/Fe(CN)_6^{4-} = 424$ mV vs. NHE (55). ^e Mean value of 5 measurements. ^f Parentheses contain one standard deviation.

Table II. Heterogeneous Electron Transfer Kinetic Parameters for the Oxidation of Ferrocyanide

technique	electrode	solution conditions	$k^{\circ} t_{th}$, cm/s	α	ref.
spectroelectrochemistry	tin oxide	5 mM $K_3Fe(CN)_6$ in 0.10 M phosphate, 0.10 M NaCl, pH 7.00	$4.6 (\pm 0.2) \times 10^{-4}$	$0.328 (\pm 0.006)$	this work
chronocoulometry	tin oxide	5 mM $K_3Fe(CN)_6$ in 0.10 M phosphate, 0.10 M NaCl, pH 7.00	$4.0 (\pm 0.2) \times 10^{-4}$	$0.323 (\pm 0.008)$	this work
rotated disk electrode voltammetry	boron carbide	0.10 mM $K_3Fe(CN)_6$ in 0.10 M phosphate, pH 7.5	$3.3 (\pm 0.2) \times 10^{-4}$	$0.65 (\pm 0.02)$	59
turbulent tubular electrode voltammetry	platinum	0.10 mM $K_3Fe(CN)_6$ in 0.10 M phosphate, pH 7.5	$1.4 (\pm 0.3) \times 10^{-3}$	$0.43 (\pm 0.05)$	59
turbulent tubular electrode voltammetry	gold	0.10 mM $K_3Fe(CN)_6$ in 0.10 M phosphate, pH 7.5	$1.2 (\pm 0.3) \times 10^{-3}$	$0.37 (\pm 0.03)$	59
pulsed rotation voltammetry	glassy carbon	10 μ M $K_3Fe(CN)_6$ in 0.10 M phosphate, pH 7.5	5.4×10^{-3}	0.69	62

chemical behavior is shown in Figure 3 together with theoretical behavior calculated from Equation 12. Using the normalized absorbance (Equation 14) derived from the sub-diffusion (kinetically controlled) transient behavior and the experimentally determined diffusion-controlled response resulting from the ≥ 800 -mV potential steps, the heterogeneous electron transfer rate constants ($k_{t,h}$, Equation 1) summarized in Table I were determined. Of particular significance is the invariance of these experimentally determined rate constants over the duration of the potential steps which speaks to the validity of the theoretical expressions presented above. The slight trending in $k_{t,h}$ to lower values with time at small magnitudes of overpotential indicates that at small η , the back reaction in Equation 1 becomes significant on the time scale of the experiment.

Using the technique of chronocoulometry (48), the heterogeneous electron transfer rate constants ($k_{t,h}$, Equation 1) for the ferrocyanide system were determined over the same range of η employed for spectroelectrochemical measurements. Figure 4 shows the dependence of the logarithms of the rate constants on overpotential observed by both techniques. Linear regression analyses of these data afford the formal heterogeneous electron transfer rate constants ($k^{\circ} t_{th}$) and transfer coefficients (α) tabulated in Table II.

Of the numerous studies of the heterogeneous electron transfer kinetics of the ferri-/ferrocyanide system which have been reported, the majority have either examined the reduction of ferri-/ferrocyanide or followed the method of Randles (64) wherein both oxidation of the reduced form of the couple and reduction of the oxidized form of the couple are utilized in the determination of kinetic parameters. Representative

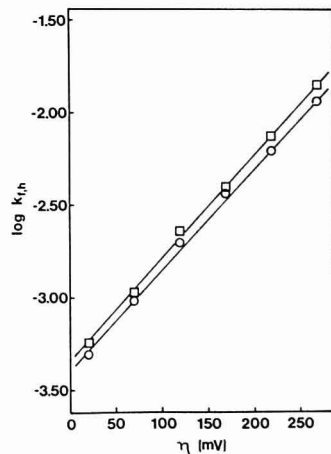


Figure 4. Dependence of $k_{t,h}$ determined by spectroelectrochemical (\square) and chronocoulometric (\circ) techniques on overpotential. Coefficients of correlation: spectroelectrochemistry, $R = 0.9993$; chronocoulometry, $R = 0.9989$.

results from studies involving the oxidation of ferrocyanide have been included in Table II for comparison with this present work.

The power of spectroelectrochemical techniques in the study of electron transfer processes has been amply demonstrated (46, 65). The major advantages of spectroelectrochemistry compared to chronocoulometry in the measurement of heterogeneous electron transfer kinetic parameters are the molecular specificity of the optical measurement and the freedom from errors associated with charge transfer processes, faradaic and nonfaradaic, other than the redox reaction of interest. In applying CMEs to the study of the electron transfer reactions of biological molecules, this latter advantage is of paramount importance. Biological sample preparations usually contain unknown impurities which may adversely affect chronocoulometric results as a consequence of the isolation and purification procedures which are extant for a given system. Further, knowledge of the electron transfer kinetics between biological molecules which participate in physiological redox reactions offers insight into the mode and mechanism of these processes. The spectroelectrochemical technique described here used in concert with CMEs which exhibit quasi-reversible electron transfer kinetics with biological molecules (41, 42) offers access to such kinetic parameters without the need for electrochemical mediators or exogenous chemical titrants. Work in these laboratories is being conducted to take advantage of this approach both in the study of electron transfer reactions of biological molecules from plant, bacterial, and mammalian sources and in the study of heterogeneous catalytic processes.

ACKNOWLEDGMENT

Helpful discussions with Harvey B. Herman and the experimental assistance of Eldonna R. Summers are gratefully acknowledged.

LITERATURE CITED

- (1) R. F. Lane and A. T. Hubbard, *J. Phys. Chem.*, **77**, 1401 (1973).
- (2) R. F. Lane and A. T. Hubbard, *J. Phys. Chem.*, **77**, 1411 (1973).
- (3) R. F. Lane and A. T. Hubbard, *J. Phys. Chem.*, **79**, 808 (1975).
- (4) R. F. Lane and A. T. Hubbard, *Anal. Chem.*, **48**, 1287 (1976).
- (5) R. F. Lane, A. T. Hubbard, K. Fukunaga, and R. J. Blanchard, *Brain Res.*, **114**, 346 (1976).
- (6) A. P. Brown, C. Koval, and F. C. Anson, *J. Electroanal. Chem.*, **72**, 379 (1976).
- (7) A. P. Brown and F. C. Anson, *Anal. Chem.*, **49**, 1589 (1977).
- (8) A. P. Brown and F. C. Anson, *J. Electroanal. Chem.*, **83**, 203 (1977).
- (9) S. Mazur, T. Matusinovic, and K. Cammann, *J. Am. Chem. Soc.*, **99**, 3888 (1977).
- (10) L. L. Miller and M. R. Van De Mark, *J. Am. Chem. Soc.*, **100**, 639 (1978).
- (11) M. R. Van De Mark and L. L. Miller, *J. Am. Chem. Soc.*, **100**, 3223 (1978).
- (12) M. T. Stankovich and A. J. Bard, *J. Electroanal. Chem.*, **75**, 467 (1977).
- (13) K. S. V. Santhanam, N. Jespersen, and A. J. Bard, *J. Am. Chem. Soc.*, **99**, 274 (1977).
- (14) A. Merz and A. J. Bard, *J. Am. Chem. Soc.*, **100**, 3222 (1978).
- (15) B. F. Watkins, J. R. Behling, E. Kariv, and L. L. Miller, *J. Am. Chem. Soc.*, **97**, 3549 (1975).
- (16) B. E. Firth, L. L. Miller, M. Mitani, T. Rogers, J. Lennox, and R. W. Murray, *J. Am. Chem. Soc.*, **98**, 8271 (1976).
- (17) C. A. Koval and F. C. Anson, *Anal. Chem.*, **50**, 223 (1978).
- (18) M. Fujihira, T. Matsue, and T. Osa, *Chem. Lett.*, 875 (1976).
- (19) J. C. Lennox and R. W. Murray, *J. Electroanal. Chem.*, **78**, 395 (1976).
- (20) J. C. Lennox and R. W. Murray, *J. Am. Chem. Soc.*, **100**, 3710 (1978).
- (21) N. Oyama and F. C. Anson, *J. Electroanal. Chem.*, **88**, 289 (1978).
- (22) J. R. Lenhard, R. Rocklin, H. Abruna, K. Willman, K. Kuo, R. Nowak, and R. W. Murray, *J. Am. Chem. Soc.*, **100**, 5213 (1978).
- (23) P. R. Moses, L. Wier, and R. W. Murray, *Anal. Chem.*, **47**, 1882 (1975).
- (24) N. R. Armstrong, A. W. C. Lin, M. Fujihira, and T. Kuwana, *Anal. Chem.*, **48**, 741 (1976).
- (25) C. M. Elliott and R. W. Murray, *Anal. Chem.*, **48**, 1247 (1976).
- (26) P. R. Moses and R. W. Murray, *J. Am. Chem. Soc.*, **98**, 7435 (1976).
- (27) D. F. Untereker, J. C. Lennox, L. M. Wier, P. R. Moses, and R. W. Murray, *J. Electroanal. Chem.*, **81**, 309 (1977).
- (28) P. R. Moses and R. W. Murray, *J. Electroanal. Chem.*, **77**, 393 (1977).
- (29) J. R. Lenhard and R. W. Murray, *J. Electroanal. Chem.*, **78**, 195 (1977).
- (30) D. G. Davis and R. W. Murray, *Anal. Chem.*, **49**, 194 (1977).
- (31) A. F. Diaz, *J. Am. Chem. Soc.*, **99**, 5838 (1977).
- (32) R. J. Burt, G. J. Leigh, and C. J. Pickett, *J. Chem. Soc., Chem. Commun.*, 940 (1976).
- (33) G. Leigh and C. J. Pickett, *J. Chem. Soc., Dalton Trans.*, 1797 (1977).
- (34) A. W. C. Lin, P. Yeh, A. M. Yacynych, and T. Kuwana, *J. Electroanal. Chem.*, **84**, 411 (1977).
- (35) A. M. Yacynych and T. Kuwana, *Anal. Chem.*, **50**, 640 (1978).
- (36) J. F. Evans, T. Kuwana, M. T. Henne, and G. P. Royer, *J. Electroanal. Chem.*, **80**, 409 (1977).
- (37) H. Tachikawa and L. R. Faulkner, *J. Am. Chem. Soc.*, **100**, 4379 (1978).
- (38) D. C. Tse and T. Kuwana, *Anal. Chem.*, **50**, 1315 (1978).
- (39) J. F. Evans and T. Kuwana, *Anal. Chem.*, **49**, 1632 (1977).
- (40) J. F. Evans and H. N. Blount, *J. Phys. Chem.*, **80**, 1011 (1976).
- (41) H. L. Landrum, R. T. Salmon, and F. M. Hawkridge, *J. Am. Chem. Soc.*, **99**, 3154 (1977).
- (42) J. F. Stargardt, F. M. Hawkridge, and H. L. Landrum, *Anal. Chem.*, **50**, 930 (1978).
- (43) H. Freiser, Ed., "Ion Selective Electrodes in Analytical Chemistry", Plenum Publishing Corp., New York, 1978.
- (44) L. D. Bowers and P. W. Carr, *Anal. Chem.*, **48**, 545A (1976).
- (45) M. Meyerhoff and G. A. Rechnitz, *Science*, **195**, 494 (1977).
- (46) T. Kuwana and W. R. Heineman, *Acc. Chem. Res.*, **9**, 241 (1976).
- (47) T. Kuwana and N. Winograd, "Spectroelectrochemistry at Optically Transparent Electrodes", in "Electroanalytical Chemistry", Vol. 7, A. J. Bard, Ed., Marcel Dekker, New York, and references therein.
- (48) J. H. Christie, G. Lauer, and R. A. Osteryoung, *J. Electroanal. Chem.*, **7**, 60 (1964).
- (49) G. C. Grant, Joint Southeast-Southwest Regional American Chemical Society Meeting, New Orleans, La., 1970; Abstracts of Papers ANAL-6.
- (50) A. Erdelyi, Ed., "Tables of Integral Transforms", Vol. I, McGraw-Hill, New York, 1954.
- (51) N. Winograd, H. N. Blount, and T. Kuwana, *J. Phys. Chem.*, **73**, 3456 (1969).
- (52) J. F. Evans and H. N. Blount, *J. Am. Chem. Soc.*, **100**, 4191 (1978).
- (53) P. F. Seelig and H. N. Blount, *Anal. Chem.*, **48**, 252 (1976).
- (54) R. Hill, in "Modern Methods of Plant Analysis", Vol. 1, K. Peach and M. V. Tracey, Ed., Springer-Verlag, New York, 1956, p. 393.
- (55) F. M. Hawkridge and T. Kuwana, *Anal. Chem.*, **45**, 1021 (1973).
- (56) J. Jordan and R. A. Javicz, *Electrochim. Acta*, **6**, 23 (1962).
- (57) S. Roffia and M. Lavacchielli, *Gazz. Chim. Ital.*, **106**, 283 (1976).
- (58) H. P. Agarwal and S. Oureshi, *J. Electroanal. Chem.*, **75**, 697 (1977).
- (59) W. J. Blaedel and G. W. Schieffer, *J. Electroanal. Chem.*, **80**, 259 (1977).
- (60) W. J. Blaedel and G. A. Mabbott, *Anal. Chem.*, **50**, 933 (1978).
- (61) Z. Galus and R. N. Adams, *J. Phys. Chem.*, **67**, 866 (1963).
- (62) W. J. Blaedel and R. C. Engstrom, *Anal. Chem.*, **50**, 476 (1978).
- (63) P. Gindra, H. Gerscher, and L. M. Peter, *J. Electroanal. Chem.*, **57**, 435 (1974).
- (64) J. E. B. Randles, *Can. J. Chem.*, **37**, 238 (1959).
- (65) T. Kuwana, *Ber. Bunsenges. Phys. Chem.*, **77**, 858 (1973).

RECEIVED for review October 25, 1978. Accepted December 26, 1978. This work was supported in part by grants from the National Institutes of Health (No. R01 HL22821) and the National Science Foundation (No. PCM 77-00867).

Thin-Layer Spectroelectrochemistry for Monitoring Kinetics of Electrogenerated Species

Elmo A. Blubaugh, Alexander M. Yacynych,¹ and William R. Heineman*

Department of Chemistry, University of Cincinnati, Cincinnati, Ohio 45221

The applicability of thin-layer optically transparent electrodes for monitoring homogeneous chemical reactions of electrogenerated species has been demonstrated. The reactive species is coulometrically generated in the thin solution layer at a minigrid electrode, and the chemical reaction is optically monitored by light passing through the transparent electrode. Single- and double-potential step techniques are demonstrated using the benzidine rearrangement as a model system. Spectra in the 200–320 nm range were obtained with a rapid scanning spectrometer during electrogeneration and reaction. Absorbance vs. time data were then displayed for analysis of the kinetics. Rate constants obtained for the acid-catalyzed benzidine rearrangement were $2.8 \times 10^{-3} \text{ s}^{-1}$ in 0.05 F HCl and $3.0 \times 10^{-2} \text{ s}^{-1}$ in 0.10 F HCl.

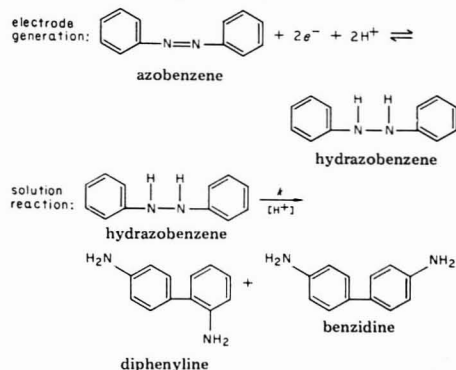
Thin-layer electrochemical cells restrict the diffusional path of the electroactive species by trapping a "thin slab" of solution between two barriers (1, 2). Exhaustive electrolysis of electroactive species in the thin solution layer can be achieved in about 10–60 s with diffusion as the only mode of mass transport. Optically transparent thin-layer electrodes (OTTLE) enable spectroscopic observation of electrogenerated species via a light beam passing through the thin layer of solution and the electrode (3, 4). Therefore, the OTTLE is potentially useful for the optical monitoring of homogeneous chemical reactions that an electrogenerated species may undergo.

The OTTLE technique offers advantages which warrant its consideration as a method for kinetic studies. (a) Since the reactive species is trapped in the thin solution layer, very slow homogeneous chemical reactions should be observable. Such slow reactions are not always amenable to study by conventional electrochemical techniques in which diffusion of the reactive species away from the electrode is unrestricted. Perturbation of concentration gradients by convection limits many semi-infinite diffusion techniques to a time domain of less than ca. 60 s. (b) Since electrogeneration of reactive species in the thin solution layer is quantitative, spectral observation of intermediates and products of the chemical reaction is not interfered with by starting material, unless a regenerative mechanism is involved. (c) The reactive species is homogeneously distributed across the thin solution layer after its quantitative generation from starting material. Such a homogeneous solution of reactive intermediate allows subsequent kinetic processes to be treated by conventional methods of data analysis for kinetics. This is less complicated than non-thin-layer electrochemical and spectroelectrochemical techniques for which appropriate diffusion equations must be solved or simulated to extract information about kinetics (5–7).

The measurement of reaction rate constants with an OTTLE was suggested during the early development of

thin-layer spectroelectrochemistry (2, 3) and electrogenerated intermediates were optically observed (8, 9). However, the quantitative measurement of rate constants has only recently been reported. Owens and Dryhurst measured the rate constant for the hydrolysis of a diimine electrogenerated by oxidation of 5,6-diaminouracil (10). McCreery reported the rate constant for the hydrolysis of electrogenerated *p*-quinone imine by a method in which the amount of reactive species was varied by potential control of the [O]/[R] ratio in the thin layer (11). This "non-quantitative generation" approach was effectively used to slow the reaction into a time frame observable with the thin-layer cell. Mark et al. have used the OTTLE to spectrally observe the homogeneous reoxidation of electrogenerated cob(II)alamin (12–14).

In this study, the utility of the OTTLE for the spectroscopic measurement of rate constants for homogeneous chemical reactions of electrogenerated species is evaluated for single- and double-potential step techniques. The benzidine rearrangement was selected as a model system. The reaction sequence involves the acid-catalyzed rearrangement of hydrazobenzene which is generated by reduction of azobenzene:



Considerable data on the benzidine rearrangement are available for comparison purposes since this reaction has been used as a model EC mechanism for evaluating numerous electrochemical techniques including polarography (15), double potential step chronoamperometry (16), double potential step chronocoulometry (17), twin-electrode thin-layer electrochemistry (18), chronopotentiometry with step current reversal and reverse ramp current (19), thin-layer chronopotentiometry (19), thin-layer potential-step chronocoulometry (19), cyclic voltammetry (20), and potential step generation with linear sweep reversal (21).

EXPERIMENTAL

Optically transparent thin-layer cells were constructed by sandwiching gold minigrid (500 lpi) between two quartz plates separated by two 2-mil Teflon tape spacers (4). Cell thicknesses were ca. 0.23 mm. The mercury-coated gold minigrid electrode was prepared by a previously reported procedure (22). The

¹ Present address: Department of Chemistry, Rutgers University, New Brunswick, N.J. 08903.

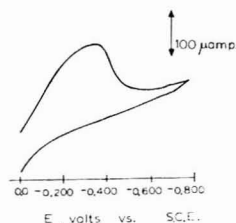


Figure 1. Cyclic voltammogram of azobenzene on Hg-Au minigridded OTTLE. 1 mM azobenzene, 0.050 F HCl, 0.200 F KCl, 44% ethanol. Scan rate, 10 mV s⁻¹.

OTTLE was masked with black vinyl tape so that the optical beam passed through a 2 × 2 mm area in the center of the minigridded. Reference and auxiliary electrodes were placed in a small solution cup into which the OTTLE was dipped. OTTLE cells were subjected to 10 min of radio-frequency plasma discharge prior to use for removal of any organic film.

A potentiostat of conventional operational amplifier design was used to provide potential control. All potentials were measured vs. an SCE using a Fluke 8008A digital voltmeter.

All chemicals were of reagent grade quality. Azobenzene (Eastman Kodak Co.) was recrystallized from ethanol until its absorption spectrum remained constant (23). A 44% ethanol-56% water solvent mixture was prepared by combination of equal volumes of 95% ethanol and deionized, doubly distilled water. Solutions were 0.050 F or 0.100 F HCl with a concentration of 1 mM azobenzene and a sufficient amount of KCl to give an ionic strength of 0.25. Solutions were deoxygenated by nitrogen bubbling before use and were kept under nitrogen and in the dark to avoid photooxidation of the azobenzene.

Single-potential step experiments were performed on mercury-coated gold minigridded OTTLEs. The electrode assembly was positioned in the deoxygenated sample compartment of a Harrick Rapid Scan Spectrometer, RSS-B. External triggering and data acquisition were accomplished through a data linkup with a Raytheon 704 computer. Spectra in the range of 220 to 320 nm were obtained at a rate of 10 spectra per second. The absorbance-time curves at fixed wavelengths of 293 and 300 nm were then plotted via data reduction procedures previously reported (24). New solution was drawn into the OTTLE from the reservoir cup before each measurement.

Double-potential step experiments were performed on a gold minigridded OTTLE. The electrode assembly was placed in the deoxygenated sample compartment of a Cary 14 spectrophotometer. Deoxygenated solution was added to the solution cup, and new solution was drawn into the cell before each measurement at different reaction times, t_R . External triggering of the potentiostat was provided by a PAR 175 Universal Programmer. Absorbance-time curves were obtained at 325 nm for different reaction times, t_R .

RESULTS AND DISCUSSION

Cyclic Voltammetry. Cyclic voltammograms of azobenzene were used to determine appropriate potentials for the potential step experiments. A typical voltammogram obtained on a mercury-coated gold minigridded (Hg-Au) OTTLE is shown in Figure 1. The wave for reduction of azobenzene to hydrazobenzene is clearly defined although somewhat distorted because of resistance in the OTTLE. The oxidation wave for hydrazobenzene to azobenzene is obscured by oxidation of the mercury film to form mercurous chloride. The Hg-Au OTTLE was used for the single-potential step experiments to facilitate comparison with previous measurements made on mercury electrodes (19) and to extend the negative potential range. The latter aspect enabled the potential to be stepped well beyond the peak potential so that resistance effects on the rate of electrolysis were minimized.

A voltammogram obtained on a gold OTTLE is shown in Figure 2. In this case, both reduction and oxidation waves

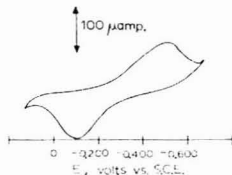


Figure 2. Cyclic voltammogram of azobenzene on Au minigridded OTTLE. 1 mM azobenzene, 0.050 F HCl, 0.200 F KCl, 44% ethanol. Scan rate, 10 mV s⁻¹.

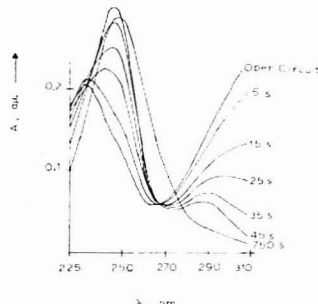


Figure 3. Spectra recorded on Hg-Au OTTLE during single-potential step spectroelectrochemistry. Potential step 0.000 V to -0.600 V vs. SCE. 1 mM azobenzene, 0.05 F HCl, 0.20 F KCl, 44% ethanol. Each spectrum represents 100 signal averaged spectra.

are reasonably well defined, although merging of the reduction wave with the onset of hydrogen evolution restricts the accessible negative potential range. The gold OTTLE was used for the double-potential step experiments so that the potential could be stepped beyond the oxidation wave for the conversion of hydrazobenzene back to azobenzene.

Cyclic voltammograms performed on a solution of hydrazobenzene after a 30-min reaction time to generate benzidine and diphenylene gave no waves between +0.2 and -0.8 V, substantiating electroinactivity of the reaction products in this potential range as previously reported (19).

Spectra. Spectra were recorded during a single-potential step experiment to enable selection of wavelengths for optically monitoring the benzidine rearrangement. Figure 3 shows spectra that were recorded during a single-potential step experiment in a Hg-Au OTTLE. The potential was stepped from 0.0 to -0.600 V vs. SCE and spectra were recorded at the rate of 10 spectra per second with the Rapid Scanning Spectrometer. Signal averaging was used to improve the signal-to-noise ratio. Each spectrum represents an average of the 100 spectra recorded during ± 5 s of the indicated time.

The spectra show azobenzene (spectrum at open circuit), which was then reduced to hydrazobenzene (5-45 s) with subsequent rearrangement to products (750 s). Severe overlap of the azobenzene peak at 233 nm, the hydrazobenzene peak at 245 nm, and the benzidine peak at 255 nm is apparent. This is quite different from previously reported spectra that exhibit less overlap of the hydrazobenzene and product spectra (23). The peaks shown in Figure 3 are shifted to shorter wavelengths than those previously reported because of protonation in the acidic media.

Single-Potential Step Thin-Layer Chronoabsorptometry. The single potential step approach to the measurement of kinetics in the OTTLE involves quantitative electrochemical reduction of azobenzene to hydrazobenzene in the

Table I. Rate Constants for Benzidine Rearrangement Determined by Thin-Layer Spectroelectrochemistry^a

technique	supporting electrolyte	λ , nm	$10^3 k$, s ⁻¹	10^3 std. dev., s ⁻¹
single-potential step	0.05 F HCl, 0.2 F KCl, 44% EtOH	293	2.7	0.36 (N = 3)
		300	2.8	0.3 (N = 3)
	0.10 F HCl, 0.15 F KCl, 44% EtOH	293	30	3.2 (N = 3)
		300	30	3.9 (N = 3)
double-potential step	0.05 F HCl, 0.2 F KCl, 44% EtOH	325	8.7 ^b	0.24 (N = 2)
		325	16 ^b	1.2 (N = 2)
	0.10 F HCl, 0.15 F KCl, 44% EtOH	325	11 ^c	1.5 (N = 2)
		325		

^a Temperature, 24.5–25.5 °C. ^b Potential step: 0.00 to -0.600 to +0.300 V vs. SCE. ^c Potential step: +0.300 to -0.600 to +0.300 V vs. SCE.

Table II. Previously Reported Rate Constants for Benzidine Rearrangement

technique	supporting electrolyte	$10^3 k$, s ⁻¹	ref
twin-electrode thin-layer	0.100 F HClO ₄ , 0.15 F NaClO ₄ , 35.5% EtOH	22.3	(18)
	0.063 F HClO ₄ , 0.15 F NaClO ₄ , 35.5% EtOH	9.0	
	0.075 F HClO ₄ , 0.15 F NaClO ₄ , 44.0% EtOH	4.23	
	0.040 F HClO ₄ , 0.15 F NaClO ₄ , 44.0% EtOH	2.16	
thin-layer current-reversal	0.0997 F HClO ₄ , 0.15 F NaClO ₄ , 38.5% EtOH	31.0	(19)
chronopotentiometry	0.0629 F HClO ₄ , 0.187 F NaClO ₄ , 38.5% EtOH	13.9	
thin-layer double-potential	0.0997 F HClO ₄ , 0.15 F NaClO ₄ , 38.5% EtOH	20.0	(19)
step	0.0629 F HClO ₄ , 0.187 F NaClO ₄ , 38.5% EtOH	8.6	
reaction quenching with	0.050 F HCl, 0.0200 F NH ₄ Cl, 44% EtOH	1.32	(25)
spectrophotometry			

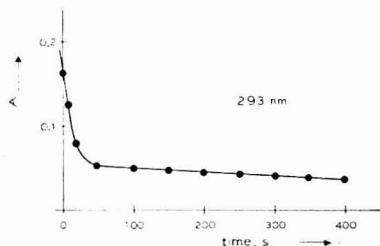


Figure 4. Absorbance-time curve at 293 nm during potential step from 0.000 to -0.600 V vs. SCE. 1 mM azobenzene, 0.050 F HCl, 0.200 F KCl, 44% ethanol

thin solution layer by a potential step from 0.00 to -0.60 V vs. SCE. The electrolysis and subsequent rearrangement of hydrazobenzene are monitored spectrally. Severe overlap at the lower wavelengths necessitated optical monitoring of the reaction at >250 nm. The wavelengths selected for the single-potential step measurements were 293 and 300 nm where the absorbance change due to the benzidine rearrangement was greatest (difference between 45- and 750-s curves) and the spectrometer signal-to-noise ratio was best. A typical absorbance-time curve at 293 nm is shown in Figure 4. The rapid decrease in absorbance during the first 30 s corresponds to the reduction of azobenzene to hydrazobenzene; the slow subsequent decrease is due to rearrangement of hydrazobenzene.

The rearrangement of hydrazobenzene is an acid-catalyzed pseudo-first-order reaction (15–21). Consequently, plots of absorbance-time data according to Equation 1 should be linear with a slope of $-k$ and an intercept of $\ln(A_0 - A_\infty)$.

$$\ln(A_t - A_\infty) = -kt + \ln(A_0 - A_\infty) \quad (1)$$

where k = pseudo-first-order rate constant, s⁻¹; A_0 = initial absorbance = $b\epsilon_{\text{HAB}}[\text{HAB}]_0$; A_∞ = final absorbance = $b(\epsilon_{\text{DP}}[\text{DP}]_\infty + \epsilon_{\text{BZ}}[\text{BZ}]_\infty)$; A_t = absorbance at time t = $b(\epsilon_{\text{HAB}}[\text{HAB}]_t + \epsilon_{\text{DP}}[\text{DP}]_t + \epsilon_{\text{BZ}}[\text{BZ}]_t)$; in which HAB = hydrazobenzene, DP = diphenylene, BZ = benzidine; b = pathlength of thin-layer cell, ϵ = molar absorptivity. A typical plot is shown in Figure 5. In all cases, the plots were linear

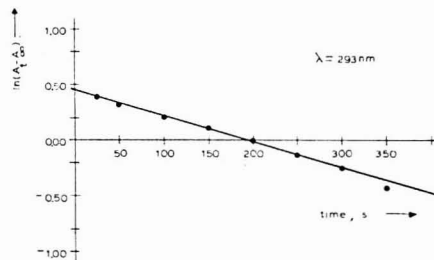


Figure 5. Kinetic plot of single-potential step absorbance-time data at 293 nm. 1 mM azobenzene, 0.050 F HCl, 0.200 F KCl solution, 44% ethanol

with the correlation coefficient being greater than 0.99. Second-order plots were nonlinear, substantiating the existence of a first-order reaction.

A summary of rate constants obtained with 0.05 F HCl and 0.10 F HCl at two monitored wavelengths is shown in Table I. The pseudo-first-order rate constant is larger for the greater acid concentration as would be expected for the acid-catalyzed rearrangement. The rate constants are in good agreement with those obtained by electrochemical techniques under similar solution conditions shown in Table II. The rate constant of $2.7 \times 10^{-3} \text{ s}^{-1}$ reported here for 0.050 F hydrochloric acid is intermediate between the twin-electrode thin-layer values of $2.16 \times 10^{-3} \text{ s}^{-1}$ and $4.23 \times 10^{-3} \text{ s}^{-1}$ for perchloric acid concentrations of 0.040 and 0.075 F, respectively (18). It also compares favorably with the $1.32 \times 10^{-3} \text{ s}^{-1}$ value obtained by a nonelectrochemical technique in 0.050 F HCl, 0.200 F NH₄Cl, 44% ethanol (25). The rate constant of $3.0 \times 10^{-2} \text{ s}^{-1}$ obtained for 0.10 F HCl is comparable to the value of $2.23 \times 10^{-2} \pm 0.06 \times 10^{-2} \text{ s}^{-1}$ reported for 0.10 F HClO₄, 35.5% ethanol obtained by the twin-electrode method (18) and $3.10 \times 10^{-2} \text{ s}^{-1}$ by thin-layer chronopotentiometry and $2.0 \times 10^{-2} \text{ s}^{-1}$ by thin-layer potential step in 0.0997 F HClO₄, 0.15 M NaClO₄, 38.5% ethanol (19).

These results were obtained under non-ideal spectroscopic conditions since the total absorbance change resulting from the benzidine rearrangement was less than 0.05 au. This

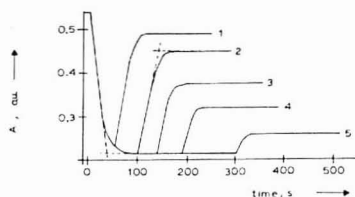


Figure 6. Double-potential step absorbance-time curves at 325 nm. Potential step from +0.000 to -0.600 to +0.300 V vs. SCE. 1 mM azobenzene, 0.100 F HCl, 0.150 F KCl, 44% ethanol. (1) $t_R = 50$ s, (2) $t_R = 100$ s, (3) $t_R = 150$ s, (4) $t_R = 200$ s, and (5) $t_R = 300$ s

indicates that good results can be obtained with rather small optical changes. The precision of repetitive measurements was within 10% for all of the runs.

The upper limit of rate constants obtainable by this method is determined by the time required for quantitative generation of reactive species in the thin solution layer. The electrolysis time for the present study was found to be about 30 s. Kinetic plots were severely curved in the region 0–30 s, so $A-t$ data at times greater than 30 s were used in the analysis. The electrolysis time can be shortened by cell designs which minimize iR drop or decrease the diffusional path length. The magnitude of lower rate constants obtainable is ultimately limited by the problem of edge effects (18) and convection. The effect of edge-diffusion into the thin-layer cell is minimized by focusing the optical beam in the center of the minigrad region (4). The minigrads above and below the beam then serve as a buffer zone between the volume being optically monitored and the edges of the minigrad. OTTEs in which the minigrad covers the entire cell can be used to eliminate the edge effect for extremely slow reactions (13).

Double-Potential Step Thin-Layer Chronoabsorptometry. The double-potential step thin-layer spectroelectrochemical approach involves first the complete reduction of azobenzene to hydrazobenzene by a potential step from 0.300 to -0.600 V vs. SCE. The potential is maintained at -0.600 V for a time interval, t_R , during which the rearrangement reaction proceeds. At the end of t_R , the remaining hydrazobenzene is electrolyzed back to azobenzene by returning the potential to 0.300 V. The double-potential step experiments were performed at a wavelength of 325 nm where the absorbance change is attributable only to azobenzene, eliminating spectral interference from hydrazobenzene and reaction products. Typical optical responses for varying lengths of reaction time t_R are shown in Figure 6. This double-potential step technique is the optical analogue of the thin-layer potential step approach with charge monitoring previously described by Oglesby, Johnson, and Reilly (19).

A pseudo-first-order rate constant can be calculated from the data in Figure 6 by Equation 2.

$$\ln \frac{\Delta A_f}{\Delta A_b} = kt_R \quad (2)$$

ΔA_f , the change in absorbance accompanying the first potential step, is a measure of the amount of hydrazobenzene generated (i.e., azobenzene electrolyzed). ΔA_b , the absorbance change accompanying the second potential step, is a measure of the amount of hydrazobenzene remaining after reaction time t_R . The reaction time, t_R , was taken as the time interval between the two intersections of the extrapolated dotted lines for the forward and reverse potential steps as shown for curve 2.

A typical plot of $\ln(\Delta A_f/\Delta A_b)$ vs. t_R is shown in Figure 7. The plot is linear as expected with the slope equal to the pseudo-first-order rate constant k . Rate constants obtained

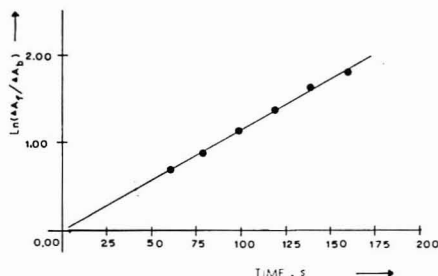


Figure 7. Kinetic plot for double-potential step absorbance-time data. Potential step from +0.300 to -0.600 to +0.300 V vs. SCE. 1 mM azobenzene, 0.100 F HCl, 0.15 F KCl

by the double-potential step method for 0.05 F and 0.10 F acid solutions are shown in Table I.

Comparison of Single- and Double-Potential Step Methods. Agreement between rate constants obtained by the single-potential step and double-potential step techniques is fair. The difference between rate constants obtained by the two techniques is attributed to uncertainty in the reaction time t_R for the double-potential step method. In this technique, the reaction is initiated by the first potential step and then quenched by the second potential step. Since exhaustive electrolysis of the thin solution layer requires about 30 s, the times of reaction initiation and quenching are estimated by the graphical procedure in Figure 6. The resulting uncertainty in t_R is significant on the time scale of the benzidine rearrangement. For slower reactions where longer values of t_R can be used, this problem diminishes. In the case of the benzidine rearrangement, further slowing of the reaction by lowering the acid concentration results in loss of the pseudo-first-order condition.

In comparing the double- and single-potential step methods, the double-potential step technique is subject to the above-mentioned uncertainty in t_R , whereas the single-potential step approach is insensitive to uncertainty in reaction initiation time for a pseudo-first-order case. The double-potential step technique requires a series of experiments at varying t_R values to obtain a kinetic plot. Kinetics information can be obtained from a single experiment by single-potential step.

An advantage of the double-potential step approach in the azobenzene system is the much larger optical change obtained as compared to the single-potential step. In principle, no optical signal due to the reaction itself is necessary for application of the double-potential step technique if the species from which the reactive species is electrogenerated has measurable spectral properties. This feature could be useful for some systems.

Adsorption Effects. Adsorption of azobenzene and hydrazobenzene has been observed on mercury electrodes (15, 17, 18). Such adsorption effects have been taken into consideration in the measurement of rate constants by electrochemical techniques, since the adsorbed material contributes directly to the current- or charge-response signal. However, the thin-layer spectroelectrochemical approach using a minigrad optically transparent electrode would be sensitive to adsorption effects only in an indirect fashion. Transparency of minigrads is due to holes which are 100% transmittant. Material which is adsorbed on the gold bars of the minigrad is not optically observable due to the nontransparency of the bars themselves. Only the small amount adsorbed on the inner edges of the holes might be observable by light grazing this surface. Thus, any adsorbed hydrazobenzene that might be

rearranging at a different rate than the solution species is not directly observed optically in the single-potential step experiment. Adsorption would affect the data only if the rearrangement products desorb into solution and spectrally contribute. This is unimportant in the azobenzene case, since the products do not interfere spectrally at the wavelength selected for monitoring.

In the double-potential step experiment, adsorption effects would also be observable only indirectly if hydrazobenzene and azobenzene adsorb differently at the two potentials involved. The extent of adsorption of these species on gold electrodes has not been reported. However, calculations indicate that greater than monolayer coverages would be necessary to affect the optical response by a measurable amount.

CONCLUSIONS

Thin-layer spectroelectrochemistry is a viable technique for measuring rate constants of reactions involving electrogenerated species when optical monitoring of the reaction is possible. The time domain of the technique as implemented in this paper restricts its applicability to slower reactions. As such, it complements the much faster spectroelectrochemical techniques involving semi-infinite diffusion conditions where the time domain is ca. 10 μ s to 60 s (7). The thin-layer method is relatively easy to implement: no solving or simulation of diffusion equations is necessary and no background corrections are required as in most electrochemical techniques where current or charge is the monitored response.

ACKNOWLEDGMENT

The authors acknowledge J. F. Goetz for suggesting the benzidine rearrangement as a model chemical system and T. H. Ridgway for helpful discussions.

LITERATURE CITED

- (1) A. T. Hubbard and F. C. Anson in "Electroanalytical Chemistry", A. J. Bard, Ed., Vol. 4, Marcel Dekker, New York, 1970, p. 129.
- (2) C. N. Reilley, *Rev. Pure Appl. Chem.*, **18**, 137 (1968).
- (3) R. W. Murray, W. R. Heineman, and G. W. O'Dom, *Anal. Chem.*, **39**, 1666 (1967).
- (4) W. R. Heineman, B. J. Norris, and J. F. Goetz, *Anal. Chem.*, **47**, 79 (1975).
- (5) H. R. Thirk and J. A. Harrison, "A Guide to the Study of Electrode Kinetics", Academic Press, New York, 1972.
- (6) S. W. Feldberg in "Electroanalytical Chemistry", A. J. Bard, Ed., Vol. 3, Marcel Dekker, New York, 1969, p. 199.
- (7) N. Winograd and T. Kuwana in "Electroanalytical Chemistry", A. J. Bard, Ed., Vol. 7, Marcel Dekker, New York, 1974.
- (8) W. R. Heineman, J. N. Burnett, and R. W. Murray, *Anal. Chem.*, **40**, 1970 (1968).
- (9) P. T. Kissinger and C. N. Reilley, *Anal. Chem.*, **42**, 12 (1970).
- (10) J. L. Owens and G. Dryhurst, *J. Electroanal. Chem.*, **80**, 171 (1977).
- (11) R. W. McCreey, *Anal. Chem.*, **49**, 206 (1977).
- (12) T. M. Kenyhercz, A. M. Yacynych, and H. B. Mark, Jr., *Anal. Lett.*, **9**, 203 (1976).
- (13) T. M. Kenyhercz and H. B. Mark, Jr., *J. Electrochem. Soc.*, **123**, 1656 (1976).
- (14) E. Itabashi, T. M. Kenyhercz, and H. B. Mark, Jr., private communication.
- (15) B. Nygaard, *Ark. Kemi.*, **20**, 163 (1963).
- (16) W. M. Schwarz and I. Shain, *J. Phys. Chem.*, **69**, 30 (1965).
- (17) R. P. Van Duyne, T. H. Ridgway, and C. N. Reilley, *J. Electroanal. Chem.*, **34**, 283 (1972).
- (18) B. McDuffie, L. B. Anderson, and C. N. Reilley, *Anal. Chem.*, **38**, 883 (1966).
- (19) D. M. Oglesby, J. D. Johnson, and C. N. Reilley, *Anal. Chem.*, **38**, 385 (1966).
- (20) R. H. Wopschall and I. Shain, *Anal. Chem.*, **39**, 1535 (1967).
- (21) W. M. Schwarz and I. Shain, *J. Phys. Chem.*, **70**, 845 (1966).
- (22) M. L. Meyer, T. P. DeAngelis, and W. R. Heineman, *Anal. Chem.*, **49**, 602 (1977).
- (23) R. B. Carlin, R. G. Neib, and R. C. Odioso, *J. Am. Chem. Soc.*, **73**, 1002 (1951).
- (24) Mark S. Denton, Ph.D. Thesis, University of Cincinnati, Cincinnati, Ohio, 1977.
- (25) D. A. Blackadder and C. Hinshelwood, *J. Chem. Soc.*, 2898 (1957).

RECEIVED for review October 23, 1978. Accepted January 2, 1979. Partial support of this research was provided by the National Science Foundation.

Metallized-Plastic Optically Transparent Electrodes

R. Cieslinski and N. R. Armstrong*

Department of Chemistry, University of Arizona, Tucson, Arizona 85721

Polyester sheets covered with thin films of metal or metal oxide can be used as optically transparent electrodes (MPOTE). These new electrodes have low sheet resistivities and high transparency to visible wavelength light—better than most optically transparent electrodes. The flexibility of these metallized polyester films may facilitate their use in unusual environments or cell geometries. Preliminary electrochemical, optical, and surface analytical data are presented for gold and indium/tin oxide MPOTES. The gold MPOTE, when covered with a thin antireflection coating of titanium oxide, exhibited unusual voltammetric behavior indicative of a porous, semi-passive electrode surface.

Films of metal or metal oxides of 1000–10000 Å thickness have been used as electrodes for several years (1–7). These materials were first developed because of their optical transparency to visible wavelength light, and the field of spectroelectrochemistry was developed as a result of their widespread use. Metal or metal oxide films can be formed

by evaporation, sputtering, or chemical vapor deposition of the conductive material onto substrates such as glass or quartz, or other metals, if optical transparency is not desired. Thin film electrodes also enjoy the advantage of reproducible surface properties (4, 7). Several electrodes can be made simultaneously which will have identical surface chemical composition and morphology. The use of thin film electrodes has been restricted to cases where rigid substrates could be employed and were difficult to fabricate into irregular or very small electrode configurations. The expense and difficulty of preparation of thin film electrodes with good optical and surface properties has been a problem (2–4, 8).

Recently, polymer sheets, covered with thin films of metal or metal oxide (metallized-plastic optically transparent electrodes, MPOTE), have become commercially available (9). Proprietary sputtering processes have resulted in the production of some polyester-polymer sheets covered with less than 1000 Å of noble metals such as gold or metal oxides like indium/tin oxide. The sheet resistivities of these materials are exceptional for their thickness (down to 10 Ω /sq. for the gold films; down to 15–200 Ω /sq. for the indium/tin oxide

films), and their transparency to visible wavelength light appears to be as good or better than previously reported for most optically transparent electrodes (OTEs) (7-8). The substrate material is very flexible with no apparent degradation of electrode properties under mechanical deformation. This fact may lead to a variety of experiments with OTEs in unusual geometries which could not have been previously attempted. The cost of these new materials is also quite low in comparison with previous thin film electrodes (\$1.50/ft² vs. \$60-100/ft²).

We report here the first of a series of experiments designed to exploit the unique properties of these new thin film electrodes. Preliminary electrochemical, optical, and surface analysis data are presented to demonstrate the utility of these materials and to foster their further application. A metal oxide coating applied to certain of the gold MPOTEs to improve their optical transparency led to unusual electrochemical behavior. Our preliminary characterizations of this new metal/metal oxide electrode material are also detailed herein.

EXPERIMENTAL

The basic cell design used for electrochemical experiments has been described previously (1). This design allows sandwich-like positioning of the metallized plastic film electrode to a Teflon body with a cell volume of approximately 10 mL. Geometric area of the electrode was 0.5 cm². A potentiostat of conventional design was used for all studies. Differential capacitance measurements were made by modulating the electrode potential with a 400 Hz, 10-20 mV sine wave and measuring the quadrature component of the potentiostat response with a Princeton Applied Research, 126, lock-in amplifier (1, 7).

Metallized plastic optically transparent electrodes (MPOTE) were obtained from Sierracin/Sylmar (Sylmar, Calif.) under trade names Intrex-G (gold) and Intrex-K (indium-tin oxide, ITO) films. The electrodes were thoroughly cleaned in an ultrasonic cleaner using successive washings of detergent, ethanol, and distilled water.

All aqueous solutions were prepared from water which had been distilled three times from alkaline KMnO₄. All buffers were prepared from potassium hydrogen phthalate, potassium dihydrogen phosphate, or sodium bicarbonate and either nitric acid or sodium hydroxide. High purity, nonaqueous solvents were obtained from Burdick and Jackson laboratories (Muskegon, Mich.) and were passed through activated alumina just prior to use. In all nonaqueous studies, tetraethyl ammonium perchlorate (TEAP) was used as the supporting electrolyte which had previously been recrystallized from ethanol and dried under vacuum. Reagent grade ferrocene (Eastman Kodak), bis(hydroxymethyl)ferrocene (Strem), and potassium ferricyanide (Mallinckrodt) were recrystallized twice from suitable solvents: methyl viologen (1,1'-dimethyl-4,4'-bipyridium) (Aldrich) was used as obtained.

XPS spectra were obtained on a GCA-McPherson ESCA 36 spectrometer using a magnesium anode operating at 300 W of power. Vacuum was maintained at ca. 10⁻⁸ Torr. Preliminary XPS spectra were also obtained by A. W. C. Lin (Ohio State University) on a Physical Electronics 548 ESCA/Auger Spectrometer. SEM analysis was carried out using an ETEC-Autocam instrument. Small amounts of carbon were vapor-deposited on the electrodes prior to analysis to prevent image-charging effects.

RESULTS AND DISCUSSION

Gold MPOTEs. Two types of gold MPOTE were investigated. One available form had a thin (ca. 300 Å) gold coating over the polyester substrate (sheet resistance ca. 6 Ω/sq.). The second and more readily available form had an additional titanium oxide coating over the gold film of ca. 1200 Å thickness (10). The visible spectra of the gold and titanium oxide-coated gold MPOTEs compared favorably with previous electrodes (2). The gold MPOTE had an absorbance minimum of $A = 0.30$ at $\lambda_{\text{min}} = 550$ nm. The addition of the titanium oxide coating improves the optical transparency ($A_{550} = 0.20$), but at the expense of certain electrochemical parameters discussed below. Preliminary XPS data indicated

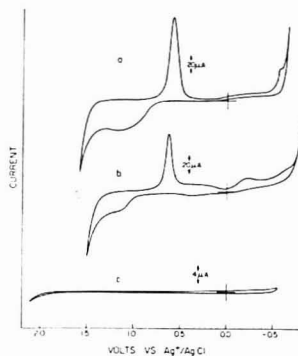


Figure 1. Cyclic voltammograms of pH 5 aqueous buffer at (a) titanium oxide-coated gold MPOTE, (b) uncoated gold MPOTE, and (c) indium/tin oxide MPOTE. Scan rate, 20.4 mV/s. Geometric area of the electrode was 0.5 cm².

that the titanium oxide coating was sufficiently thick and uniform and that no gold signal was detectable (Au 4f lines); that is, the coating thickness must be at least 30 Å thick (7). The binding energies of the O(1s) line and the Ti(2p_{3/2}) line indicated the surface to be composed chiefly of TiO₂ [O(1s) - Ti(2p_{3/2}) = 71.5 eV (11)]. The pure gold MPOTE showed only the gold XPS transitions and small amounts of oxygen and carbon which may be present as contaminants or as functionalities of the polyester substrate (12).

Scanning electron microscopy of the coated and uncoated gold MPOTE showed a uniform film structure—better than previously reported for most thin film electrodes (1). The average surface defect size was less than 0.1-μm diameter.

Figure 1 shows the voltammetric response of the gold MPOTE and the gold/titanium oxide MPOTE. Both electrodes show the response predicted for gold in aqueous media; gold oxide formation and reduction occurred near the expected potentials. The hydrogen overvoltage of these gold films was extended somewhat over bulk gold, but excursions of the MPOTE potential into the hydrogen evolution region also caused deterioration of the film. The films were otherwise stable during successive cycles of the potentials of the MPOTE over the rest of the usable voltage window. Similar results were obtained in pH 1, 3, 7, 11.7, and 13 solutions, although some film decomposition was noted in the more basic media.

We find it interesting that the presence of the titanium oxide coating appears to have little effect on the gold surface oxidation or reduction. The computed charge transferred during gold oxide reduction was nearly the same on both types of film. This observation would suggest a more porous titanium oxide film structure than observed by surface analysis. Differential capacitance studies of the uncoated and titanium oxide-coated gold MPOTE confirmed this porous surface structure (1, 4, 7). Capacitance values at +0.8 to -0.4 V vs. Ag/AgCl were ca. 3-6 μF/cm² for the uncoated gold MPOTE and were two to ten times larger for the titanium oxide-coated gold electrode depending upon solution pH. The most porous electrode structure was observed in acidic solutions, pH = 1, where some decomposition of the titanium oxide film was noted (see below). The position of the capacitance minimum was generally shifted to more cathodic potentials on the coated vs. uncoated gold electrodes.

The faradaic electrochemical response of the uncoated vs. the titanium oxide coated gold MPOTE electrodes was quite different in both aqueous and nonaqueous media. Cyclic voltammetry of 10⁻³ M ferricyanide solutions was carried out

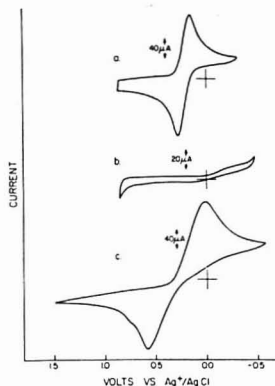


Figure 2. Cyclic voltammogram of 1×10^{-3} M ferricyanide in pH 5 aqueous buffer at (a) uncoated gold MPOTE, (b) titanium oxide coated gold MPOTE, and (c) indium/tin oxide MPOTE. (Better CV response was observed for BHMF oxidation and MV^{2+} reduction on this electrode.) Scan rate, 50.6 mV/s

for both types of gold film. In pH 1 and pH 5 buffers, the uncoated gold MPOTE showed normal electrochemical activity (Figure 2). Scanning only from 0.850 to -0.450 V vs. Ag/AgCl, the gold/titanium oxide MPOTE showed no detectable faradaic activity for ferricyanide reduction (Figure 2b). In strong acid, pH = 1 solution, typical faradaic activity for ferricyanide was restored for the coated electrode if the MPOTE potential was scanned first into the gold oxide region ($E \geq 1.4$ V). Films examined after such potential scans (with or without ferricyanide present) were different in appearance, had a lower surface resistivity than the titanium oxide-coated film and showed little titanium and significant amounts of gold when examined by XPS. The electrochemical formation of the gold oxide in strong acid media apparently solubilizes the titanium oxide overcoating allowing for uninhibited faradaic activity. In pH 5 buffers, no dissolution of the titanium oxide coating was observed even after repeated oxidation/reduction cycles of the gold. No faradaic activity of ferricyanide developed as was observed in the more acidic media.

The cyclic voltammetric oxidation of bis(hydroxymethyl)ferrocene (BHMF) and reduction of benzoquinone (BQ) were likewise completely inhibited on the titanium oxide coated gold electrode, unless the coating was electrochemically removed.

The cyclic voltammetric reduction of methyl viologen dication ($MV^{2+} + e^- \rightleftharpoons MV^{+ \cdot}$) was attempted in pH 5 and pH 7 buffers on the coated gold electrode and the electrochemical and spectroelectrochemical response compared with the normal gold MPOTE. The cathodic peak potential for the MV^{2+} reduction occurs within 200 mV of the onset of hydrogen evolution on the normal gold electrode, but can nevertheless yield reasonable cyclic voltammetric behavior for a reversible, one-electron reduction. On the oxide coated MPOTE, a small cyclic voltammetric wave for the MV^{2+} reduction was noted, superimposed upon the hydrogen evolution wave. The total peak current was ca. 10% of the value noted for the normal gold MPOTE but visual and spectrophotometric observation of the blue $MV^{+ \cdot}$ radical cation could be made after electrolysis.

The results of the aqueous voltammetric experiments show reasonable behavior for the uncoated gold electrodes, but unique response for the coated gold electrodes. The titanium oxide coating apparently allows solvent permeation to facilitate

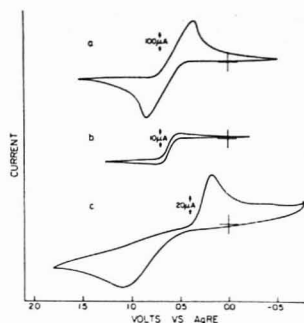


Figure 3. Cyclic voltammogram of 8×10^{-3} M ferrocene in 0.1 M TEAP, propylene carbonate solutions on (a) uncoated gold, (b) titanium oxide-coated gold, and (c) indium/tin oxide MPOTE. Scan rate, 20.4 mV/s

the gold oxide formation and reduction, but severely inhibits faradaic activity of several electroactive species—possibly by excluding them from the gold interfacial region and/or inhibiting electron transfer for all but the most negative redox couples (e.g., $MV^{2+}/MV^{+ \cdot}$) which have equilibrium potentials approaching the flat-band potential of TiO_2 .

The voltammetric behavior of the gold and gold/titanium oxide MPOTEs was also examined in several nonaqueous solvents—acetonitrile, dimethyl sulfoxide, dimethylformamide, and propylene carbonate. The stability of the films was quite good in all of these solvents. Both the conductive and nonconductive sides of the films could be exposed to the solvents without apparent degradation or appreciable swelling. The usable potential window for all solvents was 100–200 mV greater for the MPOTEs than gold films on glass. The cyclic voltammetric behavior for ferrocene was examined on both films in the above solvents—the results were similar in all cases. On the uncoated gold MPOTE, normal cyclic voltammetric behavior was observed (Figure 3a).

On the gold/titanium oxide MPOTE, quite unexpected behavior was noted (Figure 3b). As the potential was scanned anodically, an increase in current was observed at the ferrocene oxidation potential; however, the current voltage curve reached a plateau rather than a peak. The height of this current plateau was a factor of 10–20 less than the peak current for a gold electrode of the same geometric area. The magnitude of this current plateau was independent of scan rate from 1 to 500 mV/s and seemed to be independent of convection rates when the solution was stirred. If the potential was held at a point beyond the normal oxidation peak potential, little decrease in current was noted as a function of time. Upon scanning cathodically, no net negative current were observed corresponding to reduction of the ferrocenium cation. Similar results were obtained for the reduction of MV^{2+} in DMF. A current plateau was observed (ca. 10% of the normal current density) near the normal reduction potential of MV^{2+} with no reverse oxidation current seen in the cyclic voltammetric scan.

In nonaqueous solvents, the titanium oxide coating apparently inhibits both mass transfer and charge transfer in an interesting fashion. The oxidation wave for ferrocene appears as might be expected if diffusion through a semi-permeable layer were controlling the current flow rather than diffusion through solution. The lack of reversible behavior remains unexplained and is the subject of future experiments (13).

Indium/Tin Oxide Films. The indium/tin oxide (ITO) MPOTEs were specified to be less than 50 nm in thickness. This is a factor of ten less than normal ITO OTEs which leads

to a considerable improvement in the optical properties of these films. Absorbance values of less than 0.2 were observed from 400 to 800 nm with no indication of the interference fringes which plague thicker ITO or tin oxide film electrodes. This observation, coupled with the good electrochemical properties of these films, should lead to new spectroelectrochemical applications of these electrodes.

Preliminary XPS data showed the predicted elemental analysis for indium, tin, oxygen, and carbon. The indium to tin relative atomic ratio was computed from the XPS intensities (I , 11) and was found to be ca. $N_{In}/N_{Sn} = 15.0$. Previous surface analyses of ITO thin film electrodes have generally shown higher tin surface concentration, $N_{In}/N_{Sn} = 3.10$ (1).

Scanning electron microscopy of the ITO MPOTE showed a similar surface structure to that of the gold MPOTE. The average surface defect size was less than 0.1- μ m diameter; significantly better than previously reported electron microscopic data for such metal oxide electrodes (1).

Voltammetric scans of these ITO MPOTES in pH 3, 5, 7, and 10 buffers showed behavior similar to previously published experiments (Figure 1c) (1, 2). In the pH 10 buffer, the electrode coating proved unstable after one voltammetric scan. The coating appeared stable to successive scans in the other solutions. Solutions of ferricyanide and bis(hydroxymethyl)ferrocene (BHMF) and methyl viologen (MV^{2+}), 10^{-3} M, were electrochemically active on the ITO MPOTE with reasonable voltammetric response for certain electroactive species. Cyclic voltammetric peak potential separations $\Delta E_p = 600$ mV, $\Delta E_p = 120$ mV, and $\Delta E_p = 260$ mV were observed for ferricyanide (Figure 2c) and BHMF oxidations, and (MV^{2+}) reduction, respectively, at scan rates of 50.6 mV/s. The nonaqueous electrochemical behavior for these films was acceptable only for certain electroactive species. The oxidation of 10^{-3} M solutions of ferrocene in propylene carbonate gave peak potential separations of $\Delta E_p = 920$ mV whereas BHMF had a value of $\Delta E_p = 120$ mV, at a potential scan rate of 20.4 mV/s (Figure 3c).

Differential capacitance data obtained for the ITO films gave linear $1/C^2$ vs. potential relationships. A calculation of the apparent carrier density, n_a , was carried out from the Mott-Schottky (MS) relationship and was found to be $n_a = 1.7 \times 10^{20}$ cm $^{-3}$ in comparison with a value calculated from the XPS data, $n_a = 5.2 \times 10^{20}$ cm $^{-3}$. The flat-band potential determined from the $1/C^2 = 0$ intercept of the MS plots shifted ca. 60 mV/pH as expected.

Spectroelectrochemical experiments with the ITO electrodes were conducted using the one-electron reduction of methyl viologen ($MV^{2+} + e^- \rightleftharpoons MV^{\bullet+}$). The cation radical formation was easily monitored at 604 nm (λ_{max}) in chronoaabsorptometric experiments—however linear absorbance vs. $t^{1/2}$ behavior was observed only at short electrolysis times ($t < 10$ s). The absorbance/time behavior at the wavelength maximum

reached a plateau at long electrolysis times ($t > 60$ s), indicative of adsorption or depletion of the electroactive species. We have observed this phenomenon in the voltammetric response of other viologens which may lead to electrochromic display applications of the MPOTE (13).

It is clear that the indium/tin oxide films behave nearly as well as similar films of greater thickness. This property may lead to new experiments where a thicker semiconductor film would be optically or electronically undesirable (2).

CONCLUSIONS

The metallized plastic optically transparent electrode represents an interesting new development in thin film electrode technology. The low cost and excellent optical properties of the MPOTE alone are unique. The ease of manipulation of small and/or distorted electrode geometries with the metallized polyester films may facilitate their use in unusual environments. Thin-layer electrochemical cells, with the electrode bonded to the inner wall of a narrow glass tube, are easily manufactured (13). The electrodes can be inserted in any cavity to 0.003 inch with a width constrained only by the skill of the experimenter in cutting the plastic sheet. We are also exploring the possibility that chemical functionalities from the polyester substrate could be used for covalent attachment sites for purposes of electrode chemical modification (13). The titanium oxide coating on the gold MPOTE may also lend itself to such an application. Multilayered electrochemical solar cells are also a possible application of these new metallized plastic films (14).

ACKNOWLEDGMENT

The authors would like to acknowledge the gift of the metallized plastic films from John Fenn, Sierracin/Sylmar.

LITERATURE CITED

- (1) N. R. Armstrong, A. W. C. Lin, M. Fujihira, and T. Kuwana, *Anal. Chem.*, **48**, 741 (1976).
- (2) N. Winograd and T. Kuwana, in "Advances in Electroanalytical Chemistry", A. J. Bard, Ed., Marcel Dekker, New York, 1974, Vol. 7.
- (3) H. A. Latinen, C. A. Vincent, and T. M. Bednarski, *J. Electrochem. Soc.*, **115**, 1024 (1968).
- (4) R. K. Quinn, N. R. Armstrong, and N. E. Vanderborgh, *J. Vac. Sci. Technol.*, **12**, 160 (1975).
- (5) C. Y. Li and G. S. Wilson, *Anal. Chem.*, **45**, 2370 (1973).
- (6) F. Mollers and R. Memming, *Ber. Bunsenges Phys. Chem.*, **77**, 879 (1973).
- (7) N. R. Armstrong and R. K. Quinn, *Surf. Sci.*, **67**, 451 (1977).
- (8) C. A. Vincent, *J. Electrochem. Soc.*, **119**, 515 (1972).
- (9) W. P. Townsend, in "Handbook of Adhesives", 2nd ed., I. Skeist, Ed., Van Nostrand-Reinhold Co., New York, 1976, pp. 836-854.
- (10) John Fenn, Sierracin/Sylmar Corporation, private communication.
- (11) C. Sayers and N. R. Armstrong, *Surf. Sci.*, **77**, 301 (1978).
- (12) D. T. Clark, in "Characterization of Metal and Polymer Surfaces", L. H. Lee, Ed., Academic Press, New York, 1977, Vol. 2.
- (13) R. Cieslinski and N. R. Armstrong, unpublished results.
- (14) R. Shepard and N. R. Armstrong, unpublished results.

RECEIVED for review October 6, 1978. Accepted December 27, 1978. Research supported by a grant from the National Science Foundation, CHE 77-14683.

Determination of Nitrogen and Oxygen Functional Groups in Coal-Derived Asphaltenes

Irving Schwager and Teh Fu Yen*

Chemical Engineering Department, University of Southern California, University Park, Los Angeles, California 90007

Coal-derived asphaltenes and their derivatives, isolated from five demonstration coal liquefaction processes (PAMCO SRC, Catalytic Inc. SRC, HRI H-Coal, Synthoil, and FMC-COED) were analyzed for hydroxyl content by silylation followed by proton NMR analysis. Nonbasic pyrrolic nitrogen content was determined for these asphaltenes by elemental analysis after they were separated by solvent elution chromatography, and treated further by methylation with methyl iodide to remove residual basic asphaltenes. Nonhydroxylic ether oxygen, and basic pyridine-like nitrogen content were calculated by difference from total oxygen and nitrogen obtained from elemental analysis. Infrared absorptivity values were determined from the OH and NH absorption bands of these asphaltenes, and found to give linear correlations with the weight percentages of OH, and pyrrolic nitrogen:

$$\text{Absorptivity}_{\text{OH}} = 0.066 \pm 0.002 \text{ wt\% OH} \quad (1)$$

$$(\text{L/g-cm})$$

$$\text{Absorptivity}_{\text{NH}} = 0.052 \pm 0.006 \text{ wt\% pyrrolic nitrogen} \quad (2)$$

$$(\text{L/g-cm})$$

Coal-derived asphaltenes, defined operationally as soluble in benzene and insoluble in pentane, consist of highly functionalized, highly aromatic, high molecular weight components of the coal liquefaction products. All direct coal liquefaction processes produce a coal liquid which contains varying amounts of asphaltenes. Whether coal liquids are ultimately to be used directly as a utility fuel, or upgraded for use as a home heating oil, motor fuel, or chemicals feedstock, it is important to know as much as possible about the composition and character of the nitrogen- and oxygen-containing asphaltene compounds present in the liquids as they may be important in terms of air pollution, health hazards, refining conditions and catalysts, and precursors of useful chemicals.

The purpose of this work is to report such data for coal-derived asphaltenes obtained from a wide range of coal liquefaction processes (1): PAMCO SRC, Catalytic Inc. SRC, HRI H-Coal, Synthoil, and FMC-COED, and to determine infrared absorptivity values for OH and NH groups in such species which will simplify such calculations in future work. Our method of determining the concentration of phenolic groups in coal-derived asphaltenes is silylation followed by proton NMR analysis (2). Our method of determining nonbasic pyrrolic groups is chromatography of the coal-derived asphaltenes on silica gel (3). The benzene eluted fraction affords little or no pyridine-like basic asphaltenes. In order to completely remove any such basic asphaltenes, a second procedure, methylation with methyl iodide, is carried out. The isolated nonbasic asphaltenes from this step are then analyzed, and the percentage nitrogen is assumed to be pyrrolic nitrogen. This method is generally applicable except in the rare cases where amide-type nitrogen may be present.

EXPERIMENTAL

Coal-derived asphaltenes were separated by solvent fractionation (1) from coal liquids produced in five major demonstration liquefaction processes: Synthoil, HRI H-Coal, FMC-COED, Catalytic Inc. SRC, and PAMCO SRC. The asphaltenes were further separated by exhaustive solvent elution chromatography on silica gel with benzene, diethyl ether, and tetrahydrofuran (3). Baker analyzed reagent grade silica gel (60-200 mesh) was used as obtained after initial work showed no significant improvements in results could be obtained by thermally activating the silica gel. Preliminary experiments were carried out with analytical columns, at high adsorbent-to-sample ratios, to select combinations which afforded the desired separation and recovery of the asphaltenes. Preparative scale operations were then carried out with a large 50 × 500 mm column. The column was slurry packed with 400 mL of silica gel in benzene, and topped with layers of 60-80 mesh nonpolar Fluoropak 80 (The Fluorocarbon Co., Anaheim, Calif.) and sand. Accurately weighed samples (4-5 g) of asphaltenes, dissolved in a minimum volume of benzene, were carefully charged to the top of the column, and the columns exhaustively eluted with benzene (≈4L), diethylether (≈2L), and THF (≈1L). Solvents were removed by rotary evaporations, and powders were obtained directly, or by freeze-drying the samples from benzene. The nonbasic benzene-eluted fractions and, in one case, a nonbasic fraction, obtained by HCl precipitation of basic asphaltenes were further treated to remove any residual basic compounds by methylation. Methylations were carried out in benzene with a large excess (35/1) of methyl iodide. The reaction solutions were refluxed for one week, and any benzene insoluble product was removed by filtration. The benzene soluble products were recovered by freeze drying the concentrated benzene solutions.

Trimethyl silyl ethers of asphaltenes were synthesized by refluxing the asphaltene with excess 1,1,1,3,3,3-hexamethyldisilazane (HMDS), and catalytic amounts of trimethylchlorosilane and pyridine in either benzene or tetrahydrofuran (4). After removal of liquids by rotary evaporation, the silyl derivatives were freeze-dried to powders from benzene, and dried under vacuum to constant weight. The number of trimethylsilyl groups introduced was determined by proton NMR analysis (2) after the silyl derivative was checked by infrared in dilute solution to ensure complete removal of hydroxyl groups. Under the conditions used to silylate the asphaltenes, nitrogen-containing functional groups in coal have been reported not to react to form derivatives (5). We found no evidence for NH silylation by examining the NH absorption band of the asphaltenes before and after silylation by infrared spectroscopy.

Elemental analyses were carried out with standard procedures by the ELEK Microanalytical Labs., Torrance, Calif., and Huffman Laboratories, Wheatridge, Colo. Molecular weights were determined in our laboratory with a Mechrolab Model 301A Vapor Pressure Osmometer. In normal runs, 6-8 concentrations in the range of 4-39 g/L were employed in the solvents benzene or tetrahydrofuran for extrapolation to infinite dilution (6).

Infrared spectra were obtained from dilute solution of deuteriochloroform or carbon disulfide on a Beckman Acculab 6 IR or as KBr disks. The solution spectra were obtained in either sodium chloride cells, or in 1-cm matched near-infrared silica cells. The CDCl_3 spectra contain, in addition to asphaltene OH and NH bands, two water bands at 3690 and 3600 cm^{-1} from adventitious water contamination of the CDCl_3 and/or the asphaltene. Because the 3600 cm^{-1} H_2O band appears at the same

Table I. Assignment of IR Bands for Asphaltene Spectra in CDCl_3 in the OH and NH Region

wave number, cm^{-1}	assignment
3690	water
3600	water
3600	free phenolic OH
3540	associated phenolic OH or OH independent of phenolic OH
3470	pyrrolic NH
3400	other NH, possibly amines and/or amides
3400-3200 (broad)	H-bonded acidic components

Table II. Infrared Absorptivity Values for Asphaltene OH and NH Stretches

asphaltene	absorptivity, a	
	OH_{STR} (3600 cm^{-1}) (L/g-cm)	NH_{STR} (3470 cm^{-1}) (L/g-cm)
Synthoil	0.15 ^a	0.045 ^b
Synthoil benzene eluted	0.10	0.062
Synthoil ET_2O eluted	0.26	0.023
Synthoil THF eluted	0.06	0.026
HRI H-coal	0.18	0.044
FMC-COED	0.39	0.024
PAMCO SRC	0.19	0.058
Catalytic Inc. SRC	0.22	0.037

^a Typical least squares equation, $A_{\text{OH}} = 0.145 \cdot 0.003 \text{ g-cm/L} + 0.037 \pm 0.012$; correlation coefficient, 0.999.

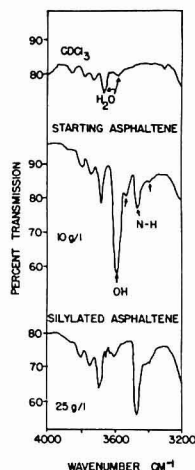
^b Typical least squares equation, $A_{\text{NH}} = 0.0454 \pm 0.0005 \text{ g-cm/L} + 0.0047 \pm 0.0005$; correlation coefficient, 0.999.

position as the asphaltene monomeric OH band, it was subtracted from the asphaltene OH band. Since the absorbance ratio of the 3600 cm^{-1} band to the 3690 cm^{-1} band is 0.32, this factor was used to correct for H_2O absorbance when quantitative measurements were carried out.

Proton NMR Spectra were obtained on a Varian T-60 Spectrometer. The solvent used was 99.8% DCCl_3 with or without 1% TMS.

RESULTS AND DISCUSSION

Assignments for the various peaks in the OH and NH region, shown in Figure 1 and Table I, are well established from earlier work on petroleum fractions (7, 8) and coal-derived asphaltenes (9) with the exception of a small 3540 cm^{-1} band. The band at 3540 cm^{-1} was assigned to a π -hydrogen bonded phenolic OH for phenolic species in petroleum distillates (7). For Synthoil asphaltene, it was reported that temperature studies indicate that the 3590 cm^{-1} and 3560 cm^{-1} bands do not change relative to one another. This was taken to mean that the second band was not from an intramolecularly π -bonded phenolic hydroxyl group (9). Workers at

**Figure 1.** Partial IR spectra of Synthoil asphaltene and silylated Synthoil asphaltene in the OH and NH region (CDCl_3 , 1-mm path)

PERC (10) report that this band was not completely removed from the infrared spectrum of the TMS derivative of a Synthoil acid/neutral asphaltene fraction although the free phenolic OH stretching band at 3600 cm^{-1} was completely removed on silylation. They suggest, therefore, that this band belongs to an independent species, and may be due to carboxylic acid structures. We, on the other hand, have observed essentially complete loss of this band on silylation of many asphaltenes (Figure 1), which suggests that this band could be from a species capable of being silylated. Others have assigned this band to an intramolecular-associated phenolic OH (and/or a weaker carboxylic acid OH) (11).

Infrared spectra were run in dilute CDCl_3 solution down to 0.3 g/L where self-association between asphaltenes is not significant (6). Plots of absorbance vs. concentrations were generally linear below concentrations of 10 g/L and could be extrapolated to a value of near zero at infinite dilution. However, some of the asphaltenes (FMC-COED, Catalytic Inc. SRC) afforded deviations from linearity at concentrations approaching 5 g/L . Such deviations support the general premise that asphaltene association via hydrogen bonding (6, 12-14) and concomitant loss of monomeric OH absorption are related. The extrapolated slopes of the linear portion of such plots were used to obtain absorptivity values (Table II). These values for a_{OH} afforded a good linear correlation with weight percent OH, determined by the silylation method (a_{OH}

Table III. Synthoil Asphaltene and Silica Gel Chromatography Fractions, Nitrogen and Oxygen Analyses

sample	oxygen, %			nitrogen, %			wt. % fraction
	total ^a	hydroxyl ^b	ether ^c	total ^d	pyrrolic ^e	basic ^f	
benzene eluted	2.39	1.61	0.78	1.07	1.24	(0)	45
ET_2O eluted	5.40	4.11	1.29	2.30	0.45	1.85	37
THF eluted	5.97	1.19	4.78	2.86	0.52	2.34	18
original asphaltene	3.89	2.67	1.22	1.74	0.93	0.81	100
calculated total asphaltene	4.15	2.45	1.69	1.84	0.82	1.02	100

^a By difference from ultimate analysis, error $\pm 1.5\%$, estimated sum of all errors. ^b From NMR analysis of trimethylsilylated asphaltene TMS area, error $\pm 3\%$, as determined by replicate measurement. ^c Total oxygen - hydroxyl = ether. ^d From ultimate analysis. ^e From IR absorptivity NH stretch, error $\pm 12\%$, as determined from least-squares standard deviation of slope of correlation line. ^f Total nitrogen - pyrrolic = basic.

Table IV. Asphaltene Oxygen and Nitrogen Analyses

asphaltene	oxygen, %			nitrogen, %		
	total ^a	hydroxy ^b	ether ^c	total ^d	pyrrolic ^e	basic ^f
Synthoil	3.89	2.67	1.22	1.74	0.93	0.81
HRI H-coal	4.96	2.92	2.04	1.61	0.88	0.73
FMC-COED	7.11	5.88	1.23	1.70	0.47	(1.23) ^g
PAMCO SRC	4.67	2.96	1.71	1.57	1.16	0.41
Catalytic Inc. SRC	4.58	3.65	0.93	1.25	0.73	0.52

^a By difference from ultimate analysis, error $\pm 1.5\%$, estimated sum of all errors. ^b From NMR analysis of trimethylsilylated asphaltene TMS area, error $\pm 3\%$, as determined by replicate measurement. ^c Total oxygen - hydroxyl = ether. ^d From ultimate analysis. ^e From IR absorptivity NH stretch, error $\pm 12\%$, as determined from least-squares standard deviation of slope of correlation line. ^f Total nitrogen - pyrrolic = basic. ^g This sample showed IR absorption at 3400 cm^{-1} which may belong to amide type NH, therefore, total nitrogen - pyrrolic = basic + amide nitrogen.

$= 0.066 \pm 0.0021\text{ wt \% OH} - 0.012 \pm 0.007$, correlation coefficient $= 0.997$), and a fair correlation between a_{NH} and weight percent pyrrolic nitrogen obtained from elemental analysis of chromatographically separated or HCl-treated asphaltenes which were also subjected to methylation to remove remaining basic nitrogen ($a_{\text{NH}} = 0.052 \pm 0.006\text{ wt \% NH} - 0.001 \pm 0.006$, correlation coefficient $= 0.96$). These methods for determining phenolic oxygen and pyrrolic nitrogen are believed to be superior to methods which require the use of low molecular weight model compounds. Snyder (7, 15) has shown that molar absorptivity values show a decrease with increasing molecular weight for carbazoles and sulfoxides from petroleum. He attributes the decrease to increased crowding of the infrared active groups by adjacent alkyl groups within the same molecule as the extent of alkyl substitution is increased.

These results may be used to calculate ether oxygen and basic nitrogen by difference from total oxygen and nitrogen. This method was applicable to all cases except for the FMC-COED asphaltene where IR absorption bands were observed at 3400 cm^{-1} and 1650 cm^{-1} which may be assigned to the NH and C=O stretches of the amide nitrogen (8). In such cases, a correlation would have to be developed for calculating separate amide and basic nitrogen concentrations. The results for Synthoil asphaltene and its silica gel chromatography fractions are presented in Table III. When the values for the separated asphaltene are arithmetically combined, the calculated total asphaltene values obtained are in good agreement with the values obtained experimentally for the original unseparated asphaltene. The results indicate that the benzene-eluted fraction contains high proportions of OH and NH ($\text{OH}/\text{O}_{\text{total}} = 0.67$, $\text{NH}/\text{N}_{\text{total}} \approx 1$). The diethyl ether-eluted fraction contains a large proportion of OH and a small fraction of NH ($\text{OH}/\text{O}_{\text{total}} = 0.76$, $\text{NH}/\text{N}_{\text{total}} = 0.20$). The THF-eluted fraction contains only small proportions of OH and NH (≈ 0.20 each). The starting unseparated asphaltene contains a majority of both OH and NH (0.69 and 0.53, respectively). The presence of phenolic and pyrrolic species in the basic fractions tends to support the idea that asphaltenes are made up of amphoteric molecules containing both acid/neutral and basic groups as well as acid/neutral, and basic molecules.

The oxygen and nitrogen analyses for asphaltenes from five demonstration processes are presented in Table IV. The

results show that the $\text{OH}/\text{O}_{\text{total}}$ values range from 0.59 to 0.83, and the pyrrolic $\text{NH}/\text{N}_{\text{total}}$ values generally range from 0.53 to 0.74. The FMC-COED pyrrolic $\text{NH}/\text{H}_{\text{total}}$ value could not be determined accurately because of the presence of possible amide type NH functional groups absorption at 3400 cm^{-1} .

CONCLUSION

We believe our infrared spectroscopic procedure for determining nitrogen and oxygen functional groups in coal-derived liquid products is simpler and more rapid than alternate procedures based on nonaqueous titrations (16).

ACKNOWLEDGMENT

The authors thank the FMC Corporation, Hydrocarbon Research, Inc., Catalytic Inc., PAMCO, and the Pittsburgh Energy Research Center of DOE for generously supplying samples of their coal liquid products, and J. G. Miller who performed some of the experimental work in this study.

LITERATURE CITED

- (1) I. Schwager and T. F. Yen, *Fuel*, **57**, 100 (1978).
- (2) F. K. Schweighardt, H. L. Retcofsky, S. Friedman, and M. Hough, *Anal. Chem.*, **50**, 368 (1978).
- (3) I. Schwager and T. F. Yen, *Fuel*, **58**, 219 (1979).
- (4) S. Friedman, M. L. Kaufman, W. A. Steiner, and I. Wender, *Fuel*, **40**, 33 (1961).
- (5) S. H. Langer, S. Connell, and I. Wender, *J. Org. Chem.*, **23**, 50 (1958).
- (6) I. Schwager, W. C. Lee, and T. F. Yen, *Anal. Chem.*, **49**, 2363 (1977).
- (7) L. R. Snyder, *Anal. Chem.*, **41**, 314 (1969).
- (8) J. F. McKay, T. E. Cogswell, J. H. Weber, and D. R. Lantham, *Fuel*, **54**, 50 (1975).
- (9) F. R. Brown, S. Friedman, L. E. Makovsky, and F. K. Schweighardt, *J. Appl. Spectrosc.*, **31**, 241 (1977).
- (10) A. G. Sharkey, J. L. Retcofsky, and F. R. Brown, *PERC/RI-77/14*, Nov. 1977.
- (11) T. Accel, R. B. Williams, R. J. Pencirov, and J. N. Karchmer, "Chemical Properties of Synthetic Products and Feeds", Final Report, prepared for U.S. ERD under Contract No. E(46-1)-8007, Sept. 1976, Exxon Research and Engineering Co., Baytown, Tex.
- (12) H. N. Sternberg, R. Raymond, and F. K. Schweighardt, *Science*, **188**, 49 (1975).
- (13) S. R. Taylor, L. G. Galya, B. J. Brown, and N. C. Li, *Spectrosc. Lett.*, **9**, 733 (1976).
- (14) F. K. Schweighardt, R. A. Friedel, and H. L. Retcofsky, *Appl. Spectrosc.*, **30**, 291 (1976).
- (15) L. R. Snyder, *Anal. Chem.*, **41**, 1084 (1969).
- (16) R. J. Baltisberger, R. A. Kaba, K. J. Klabunde, K. Saito, W. Sukalski, V. I. Stenberg, and N. F. Woolsey, *Fuel*, **57**, 529 (1978).

RECEIVED for review November 17, 1978. Accepted January 18, 1979. This research was supported by the United States Department of Energy under Contract No. EX-76-C-01-2031.

Determination of Nitrogen in Atmospheric Aerosols by Proton Activation Analysis

Mark Clemenson, Tihomir Novakov, and Samuel S. Markowitz*

Department of Chemistry and Lawrence Berkeley Laboratory, University of California, Berkeley, California 94720

Nuclear reactions induced by low-energy protons are used to determine total nitrogen in atmospheric aerosols. Radioactive ^{11}C , a 20.4-min positron emitter, is detected unambiguously via its 0.511-MeV annihilation radiation following the $^{14}\text{N}(\text{p},\alpha)^{11}\text{C}$ reaction. The detection system consists of a Ge(Li) γ -ray spectrometer that is calibrated for its absolute detection efficiency with ^{22}Na standards. The method is nondestructive of the sample, permitting the same sample to be studied by other experiments such as electron spectroscopy for chemical analysis. A comparison of nitrogen found by our proton activation method with that found by an independent but destructive combustion method gave an average percent difference of 14% for 17 samples analyzed over a concentration range that spans two orders of magnitude. Using realistic proton intensities and γ -ray detection coefficients, we estimate a nitrogen detection limit of approximately $0.1 \mu\text{g}/\text{cm}^2$, corresponding to 200 ppm in an aerosol sample of thickness $500 \mu\text{g}/\text{cm}^2$.

The recent discoveries of the important role of atmospheric aerosols in the chemistry of the polluted urban environment have led to intensified research efforts to determine the origin and nature of these particles (1-5). This research has already shown that the majority of the mass of these particles is made up of low-Z elements such as carbon, oxygen, nitrogen, and sulfur (6, 7). The development of new methods that are capable of the rapid and nondestructive determination of these elements in atmospheric aerosols on a routine basis is an important short-term goal. The work of Macias and co-workers in this area is an important contribution (8). Their method of light-element determination involves the "in-beam" measurement of γ rays from the inelastic scattering of protons. The method, however, does require lengthy use of accelerator time. This paper will describe a new method, both rapid and nondestructive, for the determination of nitrogen in aerosol particles. This simple activation method is quite sensitive and requires only a short amount of beam time (1 min in most cases) for each sample analysis. This method is also applicable to the other low-Z elements mentioned and is presently in the development stage for those elements.

The X-ray fluorescence method, an important tool in the determination of heavy-element concentrations, is of little use for low-Z elements because of large X-ray absorptive effects and low fluorescence yields. Neutron activation analysis is also limited by low reaction cross sections and the unsuitability of the induced radioactivity for counting. There has been, however, some interesting work done on the determination of sulfur in environmental materials using neutron-capture prompt γ -ray spectrometry in an elaborate setup at the Los Alamos reactor by Jurney, Curtis, and Gladney (9). Combustion analysis, of course, is a useful tool for the analysis of most of the important low-Z elements; however, it is not a very sensitive technique. It is also destructive of the sample and thus does not allow other analyses to be performed on the same sample. These difficulties have led us to develop a new method of determination of one of the low-Z elements, nitrogen, utilizing protons of sufficient energy to induce the

$^{14}\text{N}(\text{p},\alpha)^{11}\text{C}$ reaction. The radioactive decay of the 20.4-min ^{11}C is followed via its 0.511-MeV annihilation radiation. The method offers a simple approach to the problem of nitrogen analysis in atmospheric aerosols and is applicable to the routine analysis of these particles for nitrogen.

The activation analysis method offers several advantages, most of which are ideally suited to aerosol analysis: (a) high sensitivity, (b) nondestructive analysis, and (c) need for only a small amount of sample. A useful description of the charged-particle analysis method, including the pertinent equations, has been offered by Markowitz and Mahony (10); the recent article by Lyon and Ross (11) reviews current advances in the field.

EXPERIMENTAL

Targets. The targets used to determine the $^{14}\text{N}(\text{p},\alpha)^{11}\text{C}$ excitation function were prepared by vacuum-evaporation of melamine, $\text{C}_3\text{N}_6\text{H}_6$, onto 0.001-inch aluminum foils. The thickness of the melamine ranged from 0.5 to 3.5 mg/cm^2 . The targets were 2.2-cm diameter and the proton beam was collimated into a 1.3-cm diameter central spot.

Irradiation. Irradiations were performed at the Lawrence Berkeley Laboratory 88-inch cyclotron. The initial energy of the proton beam was 16.0 MeV. Aluminum foils were placed in front of the sample foils to degrade the beam from the initial energy to the desired energy for each irradiation. The range-energy tables of Williamson, Boujot, and Picard were used to calculate the required aluminum thickness (12). The length of bombardment was 1 min and the average beam intensity was $1 \mu\text{A}$. The targets were irradiated at different energies by the stacked-foil technique. The total charge received from the Faraday cup was measured by an integrating electrometer.

Counting. The irradiated samples were analyzed by detecting the 0.511-MeV positron annihilation radiation of ^{11}C using a high-resolution Ge(Li) detector coupled to a computer-controlled 4096-channel analyzer with a magnetic tape unit. The use of this system allowed the collection of γ -ray information up to 2.0 MeV with a resolution of 2.0 keV (full width at half maximum) at the 1.3325-MeV γ ray of ^{60}Co . The information obtained using this system permitted a more complete identification of the other radionuclides produced during the irradiation and also protected against γ -ray interferences which might not be detected with a low-resolution system such as NaI spectrometry (6-7% resolution). After the high-resolution system has demonstrated that there are no γ -ray interferences, a counting system consisting of a NaI detector and a single-channel analyzer could be used.

The Ge(Li) detector used for this work was manufactured by Ortec, Inc., and has an active volume of 60 cm^3 . The decay of the 0.511-MeV γ -ray photopeak of an activated melamine target is shown in Figure 1. The decay is a single component with a 20.4-min half-life corresponding to the decay of ^{11}C in the target. In the geometry ($\sim 3 \text{ cm}$ from the Ge(Li) crystal face) used to count the samples, the 0.511-MeV overall detection coefficient (ODC) was determined to be 1.86%. $\text{ODC} = (c/m)$ in the photopeak/(d/m) from the source. It was determined with a ^{22}Na calibrated standard, obtained from the International Atomic Energy Authority, Vienna. The decay curves were analyzed using the CLSQ computer code (13).

RESULTS

Excitation Function. The absolute cross sections at several energies were calculated for the $^{14}\text{N}(\text{p},\alpha)^{11}\text{C}$ reaction using the melamine targets. The result is the excitation

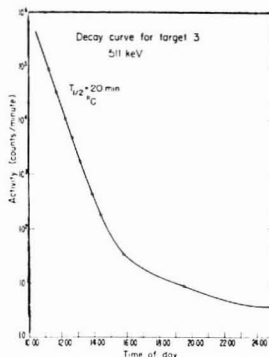


Figure 1. Decay curve of the 20-min ^{11}C annihilation radiation for a melamine target

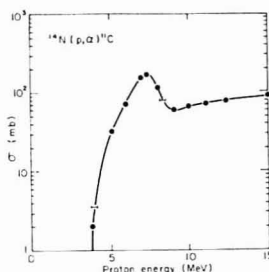


Figure 2. Excitation function for the $^{14}\text{N}(p, \alpha)^{11}\text{C}$ reaction

function shown in Figure 2. This excitation function agrees with the $^{14}\text{N}(p, \alpha)^{11}\text{C}$ excitation function measured by Ephre and Seide (14). The errors in precision are determined to be about 1% (standard deviation) for counting statistics and decay-curve calculation of the end-of-bombardment counting rate, A_0 . The other uncertainties in the excitation function include (a) determination of the integrated charge, (b) uniformity of the thickness of the targets, (c) determination of the overall detection coefficient, and (d) possible gas losses during irradiation. Any nuclear recoils of ^{11}C are caught in the aluminum. The combined uncertainties lead to an estimated accuracy in the absolute excitation function of about 5%.

Interferences. Two types of interferences must be considered in an activation analysis using γ -ray spectroscopy. The first type of interference is from the production of activities of similar half-life and γ -ray energy to the activity of interest. This type of interference can usually be minimized by use of high-resolution Ge(Li) detectors, but it does present a potential problem in the experiment being described. Because the γ ray being counted is the 0.511-MeV positron annihilation radiation, there will be contributions to this photopeak from all other β^+ -emitting nuclides that may be created in the bombardment. This type of interference, however, has not been a serious problem because the desired product, ^{11}C , is by far the dominant β^+ -emitting nuclide produced and is easily resolved in the decay-curve analysis.

The second type of interference which must be considered is the production of the radionuclide of interest from an element other than the one under analysis. If the ^{11}C radionuclide is produced from any element other than nitrogen, the amount of ^{11}C produced is not proportional to the amount

Table I. Nuclear Reaction Thresholds for the Reaction of Interest and the Principal Interfering Reactions

Reaction	threshold, MeV
$^{14}\text{N}(p, \alpha)^{11}\text{C}$	3.1
$^{11}\text{B}(p, n)^{11}\text{C}$	3.0
$^{13}\text{C}(p, pn)^{11}\text{C}$	20.3 ^a
$^{16}\text{O}(p, \alpha d)^{11}\text{C}$	25.1
$^{19}\text{F}(p, \alpha n)^{11}\text{C}$	18.1

^a The (p, d) threshold is 17.9 MeV.

of nitrogen in the sample and an error in the analysis will result. It is important that all the possible interfering reactions be identified and their significance be determined. The possible interfering nuclear reactions of importance are listed in Table I. The reaction of interest for the nitrogen analysis is listed first. Of the four possible interfering reactions listed, the last three are totally eliminated by selection of an irradiation energy below their reaction threshold. If the aerosol irradiation is carried out below a proton energy of 15 MeV, these reactions energetically cannot occur. Most notably, there is no interference from carbon, which constitutes a large fraction of the bulk aerosol. The only interfering reaction which cannot be eliminated by a proper choice of the proton energy is the $^{11}\text{B}(p, n)^{11}\text{C}$ nuclear reaction. This reaction has a threshold very similar to that of the reaction of interest. Large concentrations of boron will interfere with the nitrogen analysis. It has been shown, however (15), that boron concentrations are at least two orders of magnitude lower than nitrogen concentrations in typical urban aerosols; therefore, boron is not a significant interference.

Aerosol Sample Analyses. The silver-membrane filter was found to be the best type of filter for the collection of the ambient aerosol; it is only slightly activated during the proton irradiation. This permits the most sensitive detection of the γ radiation from the activation of the aerosol itself. The silver filter was only slightly activated because the irradiations were carried out below the Coulomb barrier of 8.4 MeV for protons on silver. Carbon- and oxygen-containing filters were found to be unsuitable because of the production of large amounts of ^{13}N and ^{18}F from the $^{16}\text{O}(p, \alpha)^{13}\text{N}$, $^{13}\text{C}(p, n)^{13}\text{N}$, and $^{18}\text{O}(p, n)^{18}\text{F}$ reactions. The production of 10.0-min ^{13}N and 109.8-min ^{18}F in quartz and Nuclepore filters interferes with the detection of the 20.4-min ^{11}C from the activation of the nitrogen in the relatively small mass of aerosol deposited on the filters.

The aerosol loading on the silver filters was approximately $500 \mu\text{g}/\text{cm}^2$ for a typical filter sample. Two filter samples were irradiated in a single stack at proton energies of 7.5 and 6.0 MeV. Aluminum foils were used to degrade the beam energy to the desired level. Following the "relative" method of activation analysis, we irradiated a melamine target, which was used as the nitrogen standard, in the same stack with the aerosol samples. The nitrogen standard was irradiated at a proton energy of 9.2 MeV. The stack was typically irradiated for 1 min at a beam intensity of $1 \mu\text{A}$. The decay of the 0.511-MeV annihilation peak was then followed for 3 or 4 h. A typical γ -ray spectrum for an aerosol sample is shown in Figure 3. Besides the 0.511-MeV annihilation peak, several other γ rays are present. All of these other γ rays are a result of the activation of the silver membrane filter. A typical decay curve for the integrated 0.511-MeV photopeak is shown in Figure 4. There are four components present in the decay curve: (a) a 10.0-min component due to ^{13}N produced from the $^{16}\text{O}(p, \alpha)^{13}\text{N}$ and $^{13}\text{C}(p, n)^{13}\text{N}$ nuclear reactions, (b) a 20.4-min component from the $^{14}\text{N}(p, \alpha)^{11}\text{C}$ reaction, (c) a 109.8-min component due to ^{18}F produced by the $^{18}\text{O}(p, n)^{18}\text{F}$ reaction, and (d) a 6.5-h component due to activation of the silver filter itself to produce ^{107}Cd by the $^{107}\text{Ag}(p, n)^{107}\text{Cd}$

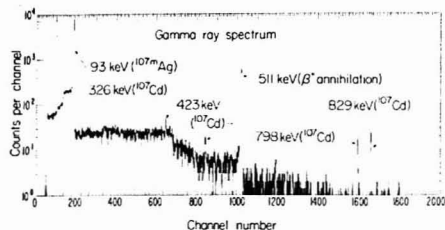


Figure 3. γ -ray spectrum of an atmospheric aerosol sample mounted on a silver filter. The 511-keV annihilation radiation and the γ rays from the silver filter are identified. A Ge(Li) detector was used.

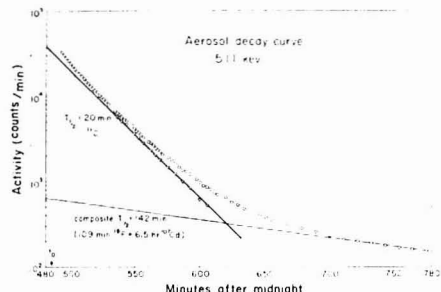


Figure 4. Decay of the 511-keV annihilation radiation intensity with time following proton irradiation of an atmospheric aerosol sample. Length of bombardment = 1 min at a beam intensity of $1 \mu\text{A}$.

nuclear reaction. By far the dominant component in this decay curve is the 20.4-min component, ^{11}C , which results from activation of the nitrogen in the aerosol. The amount of nitrogen present was calculated by comparing the A_0 value for the ^{11}C component in the aerosol to the A_0 value for the ^{11}C component in the nitrogen standard. Several blank filters were also analyzed for nitrogen and found to contain approximately $0.5 \mu\text{g}/\text{cm}^2$; this is normally a very small known correction to the total nitrogen found.

Samples containing varying amounts of nitrogen were nondestructively analyzed using the proton activation method. The same samples were then analyzed for nitrogen using a destructive combustion method. The results of these analyses are summarized in Table II. The samples can be divided into two groups. One group of samples was prepared in the laboratory by depositing either ammonium sulfate, $(\text{NH}_4)_2\text{SO}_4$, or ammonium oxalate, $(\text{NH}_4)_2\text{C}_2\text{O}_4$, on a silver-membrane filter. These samples correspond to the first nine listed in Table II. The second group of eight samples consists of ambient aerosols collected in the San Francisco Bay Area under widely varying atmospheric conditions.

DISCUSSION

Errors. The comparison of the nitrogen found by proton activation analysis and that found by the independent combustion method shows an average percent difference of 14% for the 17 samples analyzed. This difference is essentially the same whether one compares only the laboratory-prepared samples or the ambient samples. It should also be noted that the agreement between the two methods holds over a range which spans two orders of magnitude in nitrogen concentration.

Estimated Detection Limit. In order to estimate the sensitivity of the method, a set of irradiation conditions approximating those normally used will be considered. One

Table II. Comparison of Methods for Nitrogen Determination in Atmospheric Aerosols^a

sample	N found, $\mu\text{g}/\text{cm}^2$	
	proton activation	combustion
AS-1	129	144
AS-2	110	130
AS-3	326	368
AS-4	68	52
AO-1	162	147
AO-2	210	207
AO-3	261	279
AO-4	134	143
AO-5	136	133
AA-1	4.0	3.5
AA-2	8.0	6.5
AA-3	15	13
AA-4	76	99
AA-5	16	18
AA-6	59	59
AA-7	36	37
AA-8	46	54

^a AS are the laboratory-prepared ammonium sulfate samples; AO, the laboratory-prepared ammonium oxalate samples; and AA, the ambient aerosol samples.

must also consider the lowest amount of activity which can be detected accurately with the given detection system. Using this approach, we can calculate an estimated detection limit for nitrogen. The irradiation conditions are a proton beam intensity of $1 \mu\text{A}$ and an irradiation time of 4 min; the proton energy is 7.5 MeV, which is at the peak of the $^{14}\text{N}(p,\alpha)^{11}\text{C}$ excitation function ($\sigma = 165 \text{ mb}$). The overall detection coefficient for the 0.511-MeV γ ray is approximately 2%. The minimum amount of activity that could be counted is approximately 500 c/m of ^{11}C at the end of the bombardment. This minimum A_0 value takes into account the contribution of the other β^+ -emitting nuclides that are always present. These conditions correspond to a nitrogen detection limit of approximately $0.1 \mu\text{g}/\text{cm}^2$, corresponding to 200 ppm in an aerosol sample of thickness $500 \mu\text{g}/\text{cm}^2$. This detection limit could be lowered by an increase in proton beam intensity or a longer irradiation time. Considering the complexity of the aerosol, however, we believe that this represents a reasonable lower limit to the nitrogen sensitivity in a nondestructive analysis.

ACKNOWLEDGMENT

We thank the staff of the Lawrence Berkeley Laboratory 88-inch cyclotron for their hard work and technical assistance. We are grateful to C. Spicer, Battelle Memorial Institute, Columbus, Ohio, and the staff of the analytical laboratory at the University of California Chemistry Department for the combustion analyses of the samples.

LITERATURE CITED

- (1) T. Novakov, S.-G. Chang, and A. G. Harker, *Science*, **186**, 259 (1974).
- (2) S.-G. Chang and T. Novakov, *Atmos. Environ.*, **9**, 495 (1975).
- (3) G. M. Hidy et al., Science Center, Rockwell International, Report SC524-25FR, 1974.
- (4) H. Rosen and T. Novakov, *Nature (London)*, **266**, 708 (1977).
- (5) K. W. Boyer and H. A. Laitinen, *Environ. Sci. Technol.*, **9**, 457 (1975).
- (6) R. E. Lee, Jr., and J. Hein, *Anal. Chem.*, **46**, 931 (1974).
- (7) R. G. Floccini, T. A. Cahill, D. J. Shadon, S. J. Lange, R. A. Eldred, P. J. Feehey, G. W. Wolfe, D. C. Simmeroth, and J. K. Suder, *Environ. Sci. Technol.*, **10**, 76 (1976).
- (8) E. S. Macias, C. D. Radcliffe, C. W. Lewis, and C. R. Sawicki, *Anal. Chem.*, **50**, 1120 (1978).
- (9) E. T. Jurney, D. B. Curtis, and E. S. Gladney, *Anal. Chem.*, **49**, 1741 (1977).
- (10) S. S. Markowitz and J. D. Mahony, *Anal. Chem.*, **34**, 329 (1962).
- (11) W. S. Lyon and H. P. Ross, *Anal. Chem.*, **50**, 80R (1978).
- (12) C. F. Williamson, J. P. Boulot, and J. Picard, Centre d'Etudes Nucleaires de Saclay, France, Report CEA-R 3042, 1966.
- (13) J. B. Cumming, in "Applications of Computers to Nuclear and Radiochemistry," G. D. O'Kelly, Ed., National Academy of Science-National

Research Council, *Nucl. Sci. Ser.*, **NAS-NS 3107**, 25 (1963).
 (14) M. Ephre and C. Seide, *Phys. Rev. C*, **3**, 2167 (1971).
 (15) J. A. Cooper, Battelle Northwest Laboratories, Report BNWL-SA-4690.

RECEIVED for review November 20, 1978. Accepted January

23, 1979. This work is supported by the National Science Foundation and the Division of Biomedical and Environmental Research of the Department of Energy. It was presented (by S.S.M.) at the 176th Meeting of the American Chemical Society, Miami Beach, Fla., September 10-15, 1978.

Continuum Source Atomic Fluorescence Detector for Liquid Chromatography

Darryl D. Siemer,*¹ Prabhakaran Koteel, Daniel T. Haworth,* William J. Taraszewski, and Stephen R. Lawson

Department of Chemistry, Marquette University, Milwaukee, Wisconsin 53233

A preliminary study of interfacing of a high pressure liquid chromatography instrument with a continuous source atomic fluorescence detector is reported. The chemical system investigated is the acetylation reaction of ferrocene by acetic anhydride. The retention data from the conventional UV molecular absorption detector are in excellent agreement with those obtained using the atomic fluorescence detector monitoring the iron fluorescence signal. The metal-containing compounds are more easily quantitated with the fluorescence detector, both because it does not respond to purely organic interferants co-eluting with the compounds of interest and because the integrated response is insensitive to the chemical form of the compound.

High pressure liquid chromatography (HPLC) detectors have been reviewed by several authors (1-7). Detectors based on refractive index, UV or visible light absorption, heat of absorption, electrical conductivity, flame ionization and molecular fluorescence are commercially available. Koen et al. (8) have described a polarographic detector. Other detectors described in the literature include light scattering (9), IR absorption (10), vapor pressure (11), and scintillation (12).

Metal specific detection methods such as atomic absorption simplify the complex chromatograms obtained when other compounds are run with mixtures of organometallic compounds. Gonzales and Rose (13) and Longbottom (14) used atomic absorption for the detection of mercury after separation from alkylated mercuric compounds by gas chromatography. Manahan and Jones (15) used atomic absorption as a detector for HPLC, and Fernandez (16) reviewed atomic absorption chromatography detectors for use in metal speciation applications. VanLoon (17) was the first to report a line source atomic fluorescence detector for HPLC.

Continuum source atomic fluorescence spectroscopy (CSAFS) shows promise for use as a metal specific HPLC detector. Flame atomization CSAFS possesses sub-part per million sensitivity for many elements and is readily amenable for multielement analysis by using either a rapid scanning monochromator or a dedicated polychromator/multiple photomultiplier system. Interfacing of a HPLC instrument with a CSAFS detector system can be accomplished very

simply by connecting the outlet of the chromatograph to the nebulizer pick-up tube of the burner. Eimac xenon lamp excited CSAFS does not require the operator to obtain different source lamps for each element as is the case with the atomic absorption or line source AFS detectors previously described. This fact makes the CSAFS detector inherently more flexible than line source based instruments. This paper describes the use of a first generation CSAFS detector with an HPLC instrument to follow the progress of a typical organometallic reaction.

This particular reaction (the acetylation of ferrocene giving both acetylferrocene and diacetylferrocene) has been studied by several workers (18-21) using other analytical techniques to follow the relative concentrations of reactants and products throughout the reaction. In Haworth and Liu's study (21) the reaction was monitored by HPLC using a conventional fixed wavelength (254 nm) UV absorption detector, and both the chromatographic system and the sample preparation steps used in that work were largely duplicated in this project.

EXPERIMENTAL

Equipment. A Tracor 995 isochronic pump with a Tracor 960 UV absorption detector (254 nm) equipped with an injection port was used for the separation of ferrocene (Fc), acetylferrocene (Fc₁) and diacetylferrocene (Fc₂).

The outlet of the UV detector from the HPLC instrument was connected to the aspirator of a homemade acetylene-air capillary tube burner which was mounted on a Perkin-Elmer nebulizer scavenged from a PE model 290 atomic absorption unit. The burner was constructed of 20-gage stainless steel disposable syringe needles embedded in high temperature ceramic furnace cement (Sauerisen) in a 1.2-cm i.d. thin wall (0.7 mm), aluminum tube. This tube was centered in a 2.5-cm diameter copper tube, and the gap between the concentric tubes was filled with 18-gage needles embedded in more cement. A flow of argon could be directed through the outer row of tubes to sheath the flame from the atmosphere. A Varian 300 W Eimac xenon continuum lamp powered by a Varian PS 300-1 power supply served as the spectral excitation source. A 2.5-cm diameter, 8-cm focal length quartz lens focused an image of the illuminated portion of the flame onto the entrance slit of the monochromator. Conventional 90° optical geometry was used. A light baffle made from a 2-inch copper "cross T" plumbing fitting was used to keep stray-light to a practical minimum (Figure 1). Holes (2-cm diameter) were drilled at right angles to the plane of the fitting at the juncture of the "T"s to permit viewing of the signal. No attempt was made to obtain multiple passes of the excitation source beam through the flame through the use of a reflector on the side of the flame opposite of the lamp because of the potential of overheating the lamp. The monochromator used was an *f* 3.5, 100-mm efl Oriel

¹ Present address, Allied Chemical Corporation, CPP-602, 550 2nd Street, Idaho Falls, Idaho 83401.

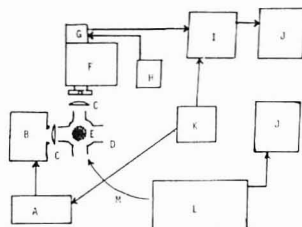


Figure 1. Block diagram of instrument. (A) Xenon lamp power supply; (B) Xe lamp housing; (C) quartz lens; (D) copper light shield; (E) top of burner; (F) monochromator; (G) photomultiplier; (H) PMT power supply; (I) lock-in amplifier; (J) recorder; (K) 50-Hz square wave signal generator; (L) HPLC instrument; (M) exit tube from UV detector

Model 7249 equipped with a 2400 lines/mm grating. A variable width entrance slit and a fixed width exit slit giving a bandpass of approximately 1 nm was used for most of the work. The light detector was an IP 28 photomultiplier tube powered with a Fluke regulated high voltage supply.

In an attempt to correct for the very considerable molecular fluorescence error signals encountered from PO bands in the vicinity of the iron resonance lines, some experiments were performed using a wavelength modulation system instead of the more conventional source lamp modulation AFS system. This was implemented by vibrating (25 Hz) a 9-cm focal length, 2.5-cm diameter, quartz lens in front of the monochromator exit slit within the monochromator with a miniature (6 V, 50 Ω) relay and using the lock-in amplifier in "2f" mode. The lens was glued to a 2-cm long strip of thin phosphor bronze which was itself spot welded to the armature of the relay. In these experiments, the xenon lamp was run at a dc current of 22 A. The PM tube was run at -1000 V with equal voltage decrements between the cathode, down the dynode string to ground. The photocurrent was converted to a voltage and amplified with a homemade 3-stage, tuned amplifier, and that signal was demodulated with a Model 9501 E ORTEC Brookdeal lock-in amplifier. For the conventional AFS experiments, the xenon lamp was pulsed at about 50 Hz and synchronized with the lock-in amplifier with a 5-V square wave signal generated by one half of a TTL dual flip-flop integrated circuit chip (74107) which was itself fed by a 100-Hz signal from an astable multivibrator integrated circuit chip (Signetics 555), used with appropriate R and C values. The lamp current was pulsed between 30 and 10 A. The UV and CSAFS detectors were each provided with separate strip chart recorders in order to read responses simultaneously. A more complete description of the optical, electronic, and mechanical components used in both the conventional pulsed source and the wave length modulated systems may be found in Lawson's thesis (22).

Reagents. Pure ferrocene, acetylferrocene, diacetylferrocene, and dibenzoylferrocene were dissolved in either chloroform or methanol. Potassium hexacyanoferrate(III) was dissolved in 80% methanol-water. The organometallic chemicals were obtained from the Aldrich Chemical Company.

Analytical Procedure. The acetylation of ferrocene was done with acetic anhydride in phosphoric acid at 70 °C. Details of the workup of the reaction mixture and of the extraction of the ferrocene and its derivatives with chloroform are given elsewhere (19-21). Five samples were obtained from the reaction flask at various time intervals after initiation of the reaction. Two- to eight-microliter aliquots of these samples were injected. The liquid chromatograph was operated under the following conditions: Chromasorb S (50 cm \times 2 mm) column packed with pellicular 10 μ m silica gel; flow rate was varied from 0.5 to 2.0 mL/min; 40:1 diethyl ether:methanol solvent mixture; 300 psi; 22 °C; UV absorption detector with wavelength fixed at 254 nm. The polypropylene pick-up tube of the AFS burner was connected to the small bore stainless steel tube exiting from the UV detector with vinyl electrical heat shrink tubing. The solvent flow rates and total tubing volumes between the UV detector and the AFS burner were such that there was a delay of about 5 s, depending on solvent flow rate, between the appearance of analytical peaks

Table I. Resolution Data

detection method	Fc/Fc ₁	Fc ₁ /Fc ₂	Fc/Fc ₂
UV ^a	0.4	1.18	1.77
CSAF ^b	1.0	1.41	2.36

^a Flow rate (1.5 mL/min at 300 psi (2 mPa)), UV detector at 254 nm. ^b Fe line at 248.3 nm. Pulsed source, lock-in at 100-mV sensitivity, C₂H₂:air burner; standard solution 12, 25, and 25 mg of Fe, Fc₁, and Fc₂, respectively.

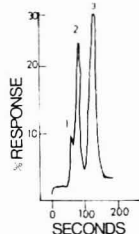


Figure 2. UV detector chromatogram of a standard solution. Flow rate of 1.50 mL/min at 300 psi, UV detector. (1) Fc, (2) Fc₁, (3) Fc₂. Standard solutions of 12 mg of Fc, 25 mg each of Fc₁ and Fc₂ in 25-mL CHCl₃; 5 μ L injected. Attenuation 16. Retention times 60, 70, and 105 s for Fc, Fc₁, and Fc₂, respectively

on the two detectors. Aliquots of the crude reaction mixture as well as samples cleaned up by an extraction procedure (21) were chromatographed.

The flame was "run" slightly "rich" (about 150 mL/min acetylene, 3 L/min air, 1.50 mL/min solvent (diethyl ether)) for most of this work. This stoichiometry gives a slight green "feather" over the inner flame cones.

RESULTS AND DISCUSSION

At low flow rates (0.5 mL/min), the separation of ferrocene, 1-acetylferrocene and 1,1'-diacetylferrocene are accomplished with good resolution using the UV detector. At higher flow rates (greater than 1.0 mL/min) the ferrocene peak is apparently not cleanly resolved and appears only as a shoulder on the acetylferrocene peak.

At a flow rate of 0.5 mL/min, although ferrocene is resolved from acetylferrocene, (as indicated by the UV absorption detector), the peaks seen with the AFS detector are broad with a poor signal-to-noise ratio. Increasing the solvent flow rate increases the flux of iron to the burner and gives improved sensitivity but poorer resolution. Table I gives a comparison of resolution between UV and CSAFS chromatograms at solvent flow rates of 1.50 mL/min, and the corresponding UV and CSAFS chromatograms are shown in Figures 2 and 3, respectively. The tabulated figures are defined as $2(V_2 - V_1)/(W_1 + W_2)$ where V_i = retention volume of the compounds compared and W_i = width of the base of each peak in volume units. The apparently better resolution of the AFS detector is due only to the fact that the much greater ultraviolet molar extinction coefficient of acetylferrocene as compared to ferrocene exaggerates the difference in the size of the big peak upon which the smaller one is situated in the UV detector chromatograms.

Most of the noise in the CSAF spectrum is due to the variation in molecular fluorescence background and "flicker" noise originating in the flame. A concentric argon sheath (about 12 L/min of gas passed through the outer ring of tubes surrounding the inner burner tubes) did reduce this "noise" somewhat but proved to be too expensive to implement in view of the rather limited improvement it afforded. The iron line

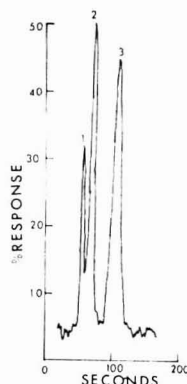


Figure 3. CSAF detector chromatogram of standard solution. Same HPLC conditions as in Figure 2. Lock-in at 100 mV, Fe line at 248.3 nm, pulsed Xe arc source, C_2H_2 /air burner; retention times 65, 75, and 110 s for Fc , Fc_1 , and Fc_2 , respectively.

Table II. Detector Data

UV detector data for extracted Fe samples ^a				
sample no.	weight percentage			Fc_1/Fc_2 ratio
	Fc	Fc_1	Fc_2	
1	27.9	70.5	—	—
2	16.0	77.7	6.3	12.3
3	—	91.7	8.3	11.4
4	—	88.9	11.1	8.0
5	—	83.8	16.2	5.2
CSAF detector data for extracted Fe samples ^b				
1	28.7	69.3	—	—
2	11.2	81.0	7.0	11.6
3	—	91.4	8.6	10.6
4	—	87.5	12.5	7.0
5	—	85.1	14.9	5.7

^{a, b} See footnotes in Table I.

normally used (248.3 nm) is situated on the shoulder of a molecular (PO) fluorescence background band originating from the phosphine present in the acetylene.

The quantitative data for the ferrocene acetylation reaction as seen with the CSAFS detector are contained in Table II. The agreement between UV detector data and CSAF data obtained simultaneously generally seems to be good. However, quantitation of the acetylferrocene peak with the UV detector is difficult because acetic anhydride co-eluted with it. Acetic anhydride has a similar retention time (70 s at a solvent flow rate of 1.50 mL/min) to that of acetylferrocene and has a non-zero molar extinction coefficient.

The peak areas obtained with the UV detector must be related to eluent concentrations with empirically determined calibration factors which correct for the different molar extinction coefficients of each compound at the specific wavelength used. Haworth and Liu (21) described how these response factors for the various compounds investigated in this study were obtained. From the corrected UV detector peak areas, weight percentages were calculated, and the ratio of acetylferrocene to diacetylferrocene in the reaction mixture at a given time is gathered in Table II.

With the CSAFS detector, the peak areas obtained correspond to the iron content only. The integrated peak area is a measure of the number of moles of each iron-containing

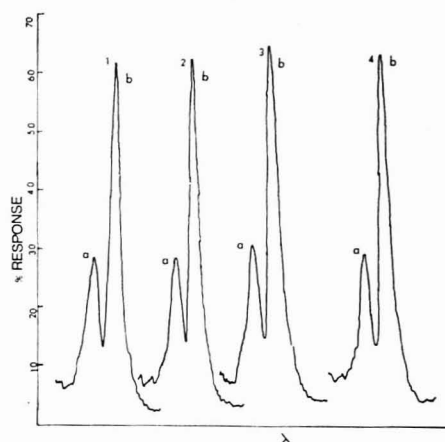


Figure 4. CSAF detector responses for various iron complexes. Wavelength scan without interfacing with HPLC. (1) Dibenzoylferrocene. (2) Fc . (3) $K_3Fe(CN)_6$. (4) Fc_1 . Four ppm standard solutions of (1–4) in methanol, run independently. Fe lines shown: (a) 252.2 nm, (b) 248.3 nm. Lock-in at 100 mV.

compound eluted with an uncertainty only of how many iron atoms are associated with each molecule of the compound—a small whole number. Proportionality of peak heights to the concentration of each compound was established in this project by running standard solutions of each compound both separately and in mixtures. A typical AFS detector response for a standard solution is shown in Figure 3. The molecular fluorescence interference of phosphorus can be considerably reduced by passing the acetylene through a filter before burning it. This was accomplished by passing the acetylene through a series of absorption tubes which contained mixtures of mercury(II) chloride, iron(III) chloride, manganese oxide, and diatomaceous earth using a recipe found in Mavrodineanu and Boiteaux's classic text (23). The phosphine in the acetylene is converted to phosphoric acid which is in turn absorbed by the diatomaceous earth. The wavelength modulation system briefly discussed in the Experimental portion of this paper did not give as good detection limits for iron as did the source modulated CSAFS system (when used with purified acetylene) and was dropped from further consideration for the application. Because ether (a "fuel") was used as one of the mobile phase solvents, the proportion of total fuel to oxidant in the flame would have varied if solvent programming had been used. This perturbs the flame chemistry and changes the response of the detector somewhat to a given flux of iron. This loss of an important experimental variable may prove to be a serious weakness of flame atomization atomic spectrometric HPLC detectors in general.

In order to verify the expected insensitivity of the detector to changes in the chemical environment of the iron, solutions of ferrocene, acetylferrocene, dibenzoylferrocene, and potassium hexacyanoferrate(III) in methanol were aspirated into the burner and the CSAF response was measured. Each solution contained 4 ppm of iron. The monochromator was scanned over a wavelength interval containing two iron lines. The response as shown in Figure 4, corresponds to the iron content only. These iron lines are 248.3- and 252.2-nm resonance lines.

The extraction procedure used in some cases to separate the ferrocenes from the bulk of the reactant mixture (21) is fairly tedious and not easily made quantitative. Excessively

Table III. CSAF Data for Crude Mixture

sample no. ^a	weight percentage			Fc ₁ /Fc ₂ ratio
	Fc	Fc ₁	Fc ₂	
1	21.3	78.7	—	—
2	9.8	83.0	7.2	11.5
3	—	84.1	15.9	5.3
4	—	75.5	24.5	3.1
5	—	71.4	28.6	2.5
6	—	61.2	38.8	1.6
7	—	57.8	42.3	1.4
8	—	57.2	42.8	1.3

^a Samples 1 to 7 taken at 15-min intervals. Sample 8 taken after 24 h. Conditions same as given in Table I for CSAF.

large amounts of sodium bicarbonate have to be used to neutralize the reaction mixture. The final resulting aqueous solution is almost saturated with sodium salts. Any organic compound (for example, acetic anhydride) extracted by the ether which is less volatile than ether can lead to a complicated chromatogram with the UV absorption detector. If the retention times of these compounds are similar to those of the products being monitored, the question arises whether a particular peak is due to a derivative of ferrocene or due to an interferent. Identification and quantitation can become difficult in many cases without the use of a metal specific detector.

To investigate the specificity of the CSAFS detector, the acetylation reaction was run with excess acetic anhydride in phosphoric acid, and samples were drawn at 15-min intervals and injected into the instrument without any prior separation or chemical treatment. The results of this experiment are shown in Table III. Great difficulty was encountered in the removal of the excess reactants (phosphoric acid and to a lesser extent acetic anhydride), and routine injection of the raw reaction mixtures into an HPLC system not incorporating a clean-up pre-column is not recommended for routine work. Both the UV detector responses and those of the AFS detector seen for this experiment are shown in Figure 5. Acetic anhydride enhances the acetylferrocene peak seen with the conventional UV detector giving rise to a false apparent composition. As the reaction progresses, more and more acetic acid is produced giving rise to another peak (peak D in the UV detector response plots) appearing as a shoulder on the acetylferrocene peak. Other smaller peaks are seen at lower flow rates with the UV detector. The corresponding CSAFS response shows only peaks from the ferrocenes and, as expected, the acetic anhydride, the acetic acid, and other purely organic compounds in the reaction mixture did not give any response. The progress of the reaction can be more conveniently followed and quantitated with that detector. In our work, we did not observe the presence of any iron-containing products other than acetylferrocene and diacetylferrocene. The reactant, ferrocene, disappears in the reaction mixture after 30 min at 70 °C. First there is a gradual increase of acetylferrocene compared to ferrocene. As the acetylation reaction proceeds the diacetylferrocene/acetylferrocene ratio increases until an equilibrium is reached. After 24 h, no appreciable change in the ratio was observed (Sample 8 in Table III).

Advantages of using the continuum source AFS detector may include any or all of the following depending upon the application: considerable reduction of the analysis time by reducing the amount of sample "clean-up" required (a pre-column is recommended, especially, for "raw" samples); positive identification of the compounds of interest in the presence of purely organic interferents; good sensitivity; and easily implemented applicability to the determination of other

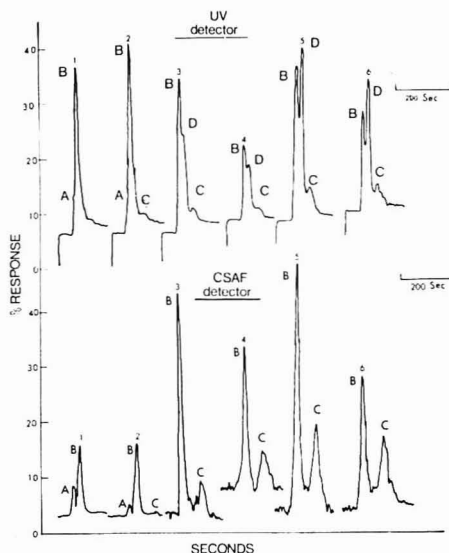


Figure 5. UV-CSAF detector responses for crude mixture. 1-6: Sample numbers. (A) Fc. (B) Fc₁. (C) Fc₂. (D) Acetic acid. HPLC conditions as in Figure 2. 2-8 μ L injected. Interfaced CSAF: Fe line (248.3 nm), pulsed Xe arc source, lock-in at 1 mV for sample 1 and 2 and 100 mV for 3-6

metal atom-containing compounds by simply changing the monochromator wavelength setting. In comparison to line source (for example, pulsed EDL or laser) excited AFS, the continuum source based detector suffers in that it is not as specific (that is to say, with line source itself, not the monochromator, largely determines the resolution and consequently the specificity), and in that molecular fluorescence and scattering error signals are much larger relative to the useful atomic fluorescence signal. However, bright line sources suitable for AFS are often quite expensive and/or difficult to obtain and to operate reliably, and, generally, as is the case with conventional AAS, a separate source is required for every element studied.

CONCLUSIONS

The use of HPLC separation with CSAFS detection offers a powerful tool for solving problems in inorganic and organometallic chemistry. Possible applications include the monitoring of inorganic chemical reactions involving both transition and nontransition metal; the monitoring of typical organic reactions with organometallic catalysts or reagents to get a better insight of the reaction mechanisms; speciation of environmental metal-bearing pollutants; and metal speciation of complex products of coal (for example, artificial crude oil). Another interesting application of the detector is that it is possible to obtain molecular weights of metal-containing molecules. The only requirement is that a known mass of the compound be injected and that the detector's integrated peak response as a function of the amount of that same metal be known. Of course, the "molecular weight" so obtained is really a measure of the mass of compound per mole of metal in the compound and is subject to an uncertainty of how many metal atoms are in each molecule. Some of the more flexible of the molecular fluorescence detection systems commercially available have optical and electronic capabilities superior to those of the equipment used in this work and could

be readily modified (by substituting a nebulizer-burner assembly for the cuvette) to permit element specific detection.

ACKNOWLEDGMENT

The authors express their thanks to John Naleway of Marquette University, for his continued support of our research efforts.

LITERATURE CITED

- (1) L. R. Snyder, "Chromatography", 2nd ed., E. Heftmann, Ed., Reinhold Publishing Corp., New York, 1967, pp 93-95.
- (2) J. F. K. Huber, *J. Chromatog. Sci.*, **7**, 172 (1969).
- (3) R. D. Conlon, *Anal. Chem.*, **41**, 107A (1969).
- (4) M. N. Munk, *J. Chromatog. Sci.*, **8**, 491 (1970).
- (5) H. Veening, *J. Chem. Educ.*, **47**, A549, A675, A749 (1970).
- (6) S. H. Byrne, Jr., "Modern Practices of Liquid Chromatography", J. J. Kirkland, Ed., Wiley-Interscience, New York, 1971, Chapter 3.
- (7) M. N. Munk, in "Basic Liquid Chromatography", N. Haden et al., Ed., Varian Aerograph, Palo Alto, Calif., 1971, Chapter 6.
- (8) J. G. Koen, J. F. K. Huber, H. Poppe, and G. den Boef, *J. Chromatog. Sci.*, **8**, 192 (1970).
- (9) D. L. Ford and W. Kennard, *J. Oil Colour Chem. Assoc.*, **49**, 299 (1966).

- (10) H. N. Tenney and F. E. Sturgis, *Anal. Chem.*, **28**, 946 (1954).
- (11) J. C. Sternberg and W. Kennard, *J. Chromatog.*, **2**, 53 (1959).
- (12) E. T. McGuinness and M. C. Culen, *J. Chem. Educ.*, **47**, A9 (1970).
- (13) J. G. Gonzales and R. T. Ross, *Anal. Lett.*, **5**, 683 (1972).
- (14) J. E. Longbottom, *Anal. Chem.*, **44**, 111 (1972).
- (15) S. E. Manahan and D. R. Jones, *Anal. Lett.*, **6**, 745 (1973).
- (16) F. Fernandez, *At. Absorp. Newsl.*, **16**(2), 33 (1977).
- (17) J. C. VanLoon, J. Lichew, and B. Radzick, *J. Chromatog.*, **136**, 301 (1977).
- (18) P. T. Graham, R. V. Lindsey, G. W. Parshall, M. L. Peterson, and G. M. Whitman, *J. Am. Chem. Soc.*, **79**, 3416 (1957).
- (19) R. E. Bozak, *J. Chem. Educ.*, **43**, 73 (1966).
- (20) J. E. Herz, *J. Chem. Educ.*, **43**, 599 (1966).
- (21) D. T. Haworth and T. Liu, *J. Chem. Educ.*, **53**, 730 (1976).
- (22) S. R. Lawson, M.S. Thesis, Marquette University, Milwaukee, Wis., 1978.
- (23) R. Mavrodineanu, "Flame Spectroscopy", R. Mavrodineanu and H. Boileau, Ed., 1965, Part 1, p. 62.

RECEIVED for review April 5, 1978. Accepted January 25, 1979. Acknowledgment is made to the donors of the Petroleum Research Fund, administered by the American Chemical Society, and to the Committee of Research, Marquette University, for support of this research.

AIDS FOR ANALYTICAL CHEMISTS

Microprocessor-Controlled Digital Integrator for Nuclear Magnetic Resonance Measurements

F. Morley, I. K. O'Neill,¹ M. A. Pringuer,² and P. B. Stockwell*

Laboratory of the Government Chemist, Cornwall House, Stamford St., London SE 9NQ, United Kingdom

Continuous wave nuclear magnetic resonance (NMR) spectroscopic observation of ^1H nuclei (1) is an inherently quantitative phenomenon that has been used for the analysis of pharmaceuticals (2), polymers (3), and many other materials. Commercial NMR spectrometers, however, are designed primarily for qualitative measurements. Many improvements in sensitivity and resolution have been incorporated into instruments in recent years but there have been no significant advances in integration techniques. Experience of quantitative ^1H NMR analyses (4, 5) at the Laboratory of the Government Chemist indicated that significant effort could be saved through automation of the spectrometer integration functions. Commercially available gas chromatographic integrators were unsuitable because data output from the scanning of sequential NMR peaks was too rapid. Subsequently, a digital integrator was constructed (6, 7), primarily to handle NMR data. This paper describes an evaluation of an automatic system for quantitative measurements, using a microprocessor to effect the various control and data processing steps. A similar system has been constructed (8) for the determination of fluorine by interfacing a commercial computer to a NMR spectrometer. This is restricted because it will accept only Gaussian peaks free of ringing.

EXPERIMENTAL

A JEOL C60-HL spectrometer was coupled to the microprocessor controlled integration system shown in Figure 1. A National Semiconductor IMP 16-C microprocessor controls all

aspects of the integration procedure and performs all the necessary data processing functions. The system which will be described in detail elsewhere (9) is a plug-in retrofit module which does not degrade spectrometer performance.

Integration. For integration purposes, the NMR spectrum is divided into discrete zones; a maximum of six zones can be used. Each zone is positioned so that the beginning and end of each zone can be positioned anywhere within the spectrum but must not overlap another zone. The sixth zone is used to specify a reference peak for quantitative measurements and can be positioned anywhere within the spectrum and not necessarily sequentially with the other zones. As a spectrum is scanned, the position of the zones is detected by a wiper mounted on the pen carriage and a linear transducer mounted along the top edge of the recorder chart. The NMR signal is amplified, fed to a voltage-to-frequency converter, and the output pulses are gated within the integration zone to a five-decade counter. This displays a digital value representing the area of the peak or multiplet of peaks within a zone and is reset to zero between each zone.

Spectrometer Control. The spectrometer parameters are optimized manually. A spectrum of the sample is recorded and the various zone positions and the number of zones to be accumulated are entered using the thumb wheel switches, on the integrator front panel. Automatic control is initiated through a teletype command. The various data input is also entered at this time; namely, the values of the proton equivalent weight of the analyte under test and the weight of the standard used for reference. The microprocessor sets in motion the pen carriage of the recorder (which is linked to the spectrometer field sweep) and at the end of each traverse returns it for a further scan, until the total number of scans reaches a preset level. In addition, the microprocessor causes a dot to be marked on the chart at the start and end of each integration zone.

Data Processing. As each zone is integrated, the integral value is passed to the computer memory store where a running average is maintained of each zone integration value. Then the proton equivalent weights (p.e.w.) for each zone and the averaged in-

¹ Presently on secondment to RTZ Services Ltd, York House, Bond Street, Bristol BS1 3PE, United Kingdom.

² Present address, Life Science Research, Stock, Essex CH4 9PE, United Kingdom.

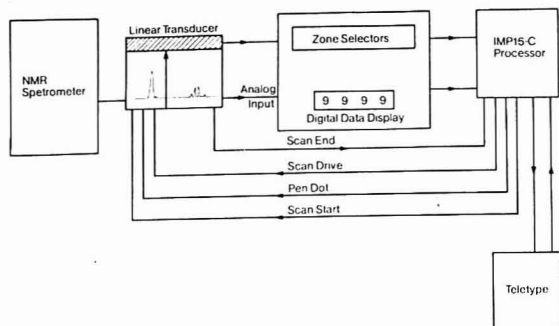


Figure 1. Layout of spectrometer control system

Table I. Comparison of Digital and Capacitance Integration of Ethylbenzene

	calculated number of protons (from average integral of 10 scans) ^a		
	C ₆ H ₅	CH ₂	CH ₃
capacitance integration	5 (97.1 mm) <i>s</i> = 2.02%	1.84	2.82
digital integration	5 (2988 counts) <i>s</i> = 0.57%	1.92	2.97
theoretical value	5	2	3

^a Scan rate = 22 Hz s⁻¹. *s* = standard deviation.

egrated areas for sample and standard peaks are used in calculations according to the equation:

$$\% \text{ wt sample} = \frac{\text{wt standard}}{\text{wt sample}} \times \frac{\text{p.e.w.sample} \times I(\text{sample}) \times 100}{\text{p.e.w. standard} \times I(\text{standard})}$$

(The p.e.w. of a substance is the molecular weight of the molecule or polymer unit divided by the number of protons responsible for the absorption of interest; this figure is entered on thumb-wheel switches mounted on the control panel). Results are printed on the teletype and may be expressed either as the quantity of the material present in the sample or as a relative purity.

Samples. Samples of 10% w/v ethylbenzene in deuteriochloroform were examined using the aromatic peak as a reference. Also, with a known composition samples of polydimethylsiloxane (PMS) in a pharmaceutical preparation (5) were examined. This preparation, a suspension, contains according to its manufacturers 0.5% PMS, 4% w/w aluminum hydroxide and 4% w/w magnesium hydroxide in a spearmint flavored medium. Weighed amounts of the preparation and hexamethylbenzene (99.90% pure obtained from the High Purity Organic Standard range of the National Physical Laboratory, Teddington) were dissolved with shaking in deuteriochloroform in 5-mm o.d. NMR tubes. The spectra were integrated at a sweep rate of 22 Hz s⁻¹ using a total of 10 scans for signal averaging.

RESULTS AND DISCUSSIONS

The integration characteristics of the digital integrator and the original spectrometer capacitance integrator are compared in Tables I and II. Ethylbenzene (Figure 2), which has a proton ratio of 5:2:3 for aromatic, methylene and methyl protons is used for this experiment because it is widely employed as a standard to evaluate NMR spectrometer and integrator performance. These results show that the digital integrator gives somewhat better integral ratios and relative standard deviations than the capacitance integrator. The capacitance integrator has disadvantages in that it is in-

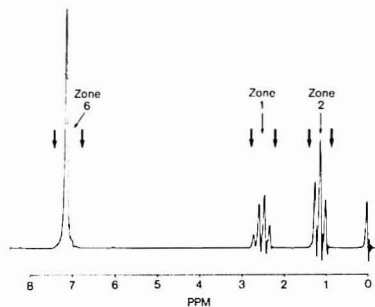


Figure 2. Spectrum of ethylbenzene showing zones for digital integration

Table II. Assay of a Commercial Formulation Containing Polymethylsiloxane

	% w/w PMS	
	capacitance integration	digital integration
	0.457	0.446
	0.460	0.523
	0.542	0.477
	0.529	0.449
	0.498	0.540
mean value	0.50	0.49
std. dev.	0.039	0.043

herently less stable than the digital integrator because of leakage, minor environmental changes, and variable drift, all of which must be corrected manually before each set of integrations.

The digital integrator is designed to accumulate positive signals above a preset threshold value; thus positive peaks associated with the ringing characteristics of many NMR peaks will also be integrated. The net effect of this is that the digital integrator will give a higher relative integral value for peaks with ringing than a capacitance integrator which averages the positive and negative peaks of the ringing. This is readily overcome either by a slight degradation of the resolution to minimize ringing or by setting the end of an integration zone to a precise position, thus avoiding the inclusion of the ringing within the zone. The latter procedure was used in this evaluation. The spectrometer scan rate did not significantly affect the accuracy of the integral value with the exception of the normal spectroscopic constraint of

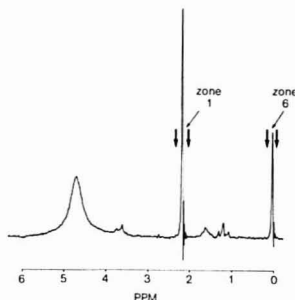


Figure 3. Spectrum of commercial preparation of polymethylsiloxane

saturation which occurs at the slowest scan rates.

The microprocessor-controlled integrator performance was further demonstrated by the determination of the PMS content of a commercial pharmaceutical preparation (Figure 3). The results shown in Table II compare favorably with those previously obtained using the capacitance integration technique. The automated control system has the advantage that, once the initial spectrum is obtained and the control parameters are set, the operator initiates the microprocessor to control the marking of integration zones, measuring and averaging integrals, performs the calculations, and prints out the results. The operator is then released for other work.

A dot is marked automatically on the chart paper at the start and end of each integration zone and acts as a safety check if the spectrometer field-frequency lock stabilization fails to prevent excessive drift during unattended operation; a movement of a peak through a zone boundary will be in-

dicated by a vertical displacement of successive dots. The operator is assured of the validity of the results obtained during unattended operation, especially when the spectrometer is used under external field-frequency lock which is most often the case with low cost NMR spectrometers which are most susceptible to field drift.

The advantages of speed, accuracy, and automation recommend this system, especially in the application of routine repetitive quality control. The system could be used as an accessory to almost any continuous-wave NMR spectrometer with a few minor modifications. Many of these spectrometers are functioning routinely, although they have been superseded qualitatively by more advanced NMR instrumentation. Addition of a microprocessor-controlled integration accessory to these spectrometers would enable them to perform a routine quality control task. This would be less expensive than the additional capital expenditure on more modern instrumentation and would extend the full working life of the existing instrumentation.

LITERATURE CITED

- (1) J. W. Emsley, J. Feeney and L. H. Sutcliffe, "High Resolution Nuclear Magnetic Resonance Spectroscopy", Vol. 1, Pergamon Press, London, 1965, p. 236.
- (2) D. Rackham, *Talanta*, **23**, 264 (1976).
- (3) F. Kessler, "Quantitative Analysis by NMR Spectroscopy", Academic Press, London, 1973.
- (4) I. K. O'Neill and M. A. Pringuer, *Chem. Ind. (London)*, 494 (1975).
- (5) I. K. O'Neill, M. A. Pringuer, and H. J. Prosser, *J. Pharm. Pharmacol.*, **27**, 222 (1975).
- (6) W. Bunting, M.Sc. Thesis, Polytechnic of Central London, 1974.
- (7) W. Bunting, Brit. Patent No. 1 483 552, Aug. 1977.
- (8) R. J. Warren, A. D. Bender, D. B. Staiger, and J. E. Zarembo, *Anal. Chem.*, **50**, 426, (1978).
- (9) F. Morley, I. K. O'Neill, M. A. Pringuer, and P. B. Stockwell, *J. Automatic Chemistry*, in press.

RECEIVED for review July 12, 1978. Accepted November 3, 1978.

Graphite Plate Sample Holders for X-Ray Photoelectron Spectroscopy

David M. Aylmer, Hossein Razzavi, and James C. Carver¹

Department of Chemistry, Texas A&M University, College Station, Texas 77843

During the past decade, numerous methods for examining nonvolatile powders have been tried for use in X-ray photoelectron spectroscopy (XPS or ESCA). The most widely used techniques include simply sprinkling the powder on double sided sticky tape, imbedding the sample in indium foil (1), and pressing the sample into a pellet. We have developed another method which seems to offer certain advantages over those methods available because (1) only 1 mg or less of the sample is required, and (2) the sample holder and all transfer devices lead to virtually no contamination, except for the holder material. This technique makes use of graphite planchets cut or machined to precisely fit one's spectrometer. We have a Hewlett-Packard 5950A ESCA, and our sample holders were prepared by cutting a graphite rod into 1.0 × 1.2 cm rectangles, 1 mm thick. The graphite used was electrolytic grade, obtained from Wale Apparatus Co., Heltown, Pa. Since these holders cost only about ten cents apiece, they are normally discarded after use, although reuse is certainly possible.

The graphite planchets are first soaked in 50% nitric acid

for about 20 min. After thorough rinsing in deionized water, the graphite is heated to red hot in a Bunsen burner flame. Upon cooling, the holder is ready to be loaded. The cleaning process removes all metals (nitric acid), and all organics, and most of the oxygen (heating). The powder sample is loaded onto the graphite plate by means of two freshly prepared glass spatulas. These devices are made by sealing the ends of two pieces of 3-mm glass tubing in a flame immediately before use. If care is taken that the freshly prepared glass surfaces and the graphite surface do not come into contact with possible contaminants, including dust from the air, transfer of a sample can be accomplished with almost no detectable contamination. The two freshly prepared glass rods are used to abrade the sample onto the graphite plate. Extremely small (submilligram) samples, when compared to the other techniques, can be easily examined. Also, samples can be easily loaded onto these cleaned graphite planchets in an inert atmosphere, such as in a glove box directly attached to the spectrometer.

It is often very difficult to obtain reliable intensity and peak positions for oxygen from powdered samples by ESCA. By using this technique, very little oxygen contamination is observed on the blank holder, and the intensity data for oxygen-containing compounds agree well with what is expected

¹ Present address: EXXON Research and Development Laboratories, P.O. Box 2226, Baton Rouge, La. 70821.

Table I. Comparative Intensities and Binding Energies for Powdered Ni Compounds on Different Sample Holders^a

compound	graphite		holder		in foil	
	intensity	BE	intensity	BE	intensity	BE
NiO						
Ni2p _{3/2}	45	855.0	100	855.0	63	855.6
O 1s	10	530.2	23	529.9	12	530.0
O/Ni	1.10		1.15		0.95	
NiS						
Ni2p _{3/2}	60	857.7	35	857.9	12	857.1
S 2p	9	162.3	3	162.1	2	161.7
	6	163.4				
	17	169.2	12	169.5	6	168.1
S/Ni	0.93		0.72		1.09	
NiSO ₄ ·x(H ₂ O)						
Ni2p _{3/2}	28	858.2	20	858.8	19	857.1
O 1s	40	532.1	31	532.7	28	531.5
S 2p	14	169.5	15	169.4	12	168.9
O/Ni	7.14		11.11		7.14	
S/Ni	0.87		0.77		0.91	
Ni(NO ₃) ₂ ·xH ₂ O						
Ni2p _{3/2}	8.5	856.4	20	856.8	38	856.7
O 1s	10	532.3	20	531.9	43	532.4
N 1s	11	406.2	37	406.6	40	406.6
O/Ni	5.87		4.99		5.69	
N/Ni	1.10		1.36		0.85	

^a Intensities are given in thousands of counts and binding energies in electron volts. Experimental ratios are corrected for counting times and photoionization cross sections (2). The relative error in the absolute intensities is about $\pm 10\%$.

from the stoichiometry. Further, the carbon 1s peak from the graphite itself can be used as a convenient calibrant for binding energies. Obviously, if one is interested in the carbon signal from a sample containing unoxidized carbon, he will have great difficulty in distinguishing the sample signal from that of the graphite. However, it would be possible to look at carbon bound to electronegative species.

For comparative purposes, several samples have been examined by XPS by loading each sample (1) on graphite, (2) on double sided sticky tape, and (3) imbedded in indium foil. Most of the samples examined were not easily pressed into pellets. The results of the comparison are shown in Table I. Each value is an average of two or more determinations. Comparative intensities for powdered Ni compounds on different sample holders are given in thousands of counts, and binding energies in electron volts. The theoretical intensity ratios are found from the formula, while the experimental ratios have been corrected for photoionization cross sections by using Scofield's values (2) and for counting times. The absolute intensity of the spectra obtained from samples on graphite, double sided sticky tape, and indium foil are generally about the same, with variations due to differences in the amount of sample adhering to the surface. It should be noted that in the cases of graphite and indium, complete coverage of the surface of the holder often was not attained. The intensity obtained from pellets is usually best. However, pellets require far more material, are often fragile, and, in a glove box, are difficult to load into the spectrometer. In addition, making a pellet enables the sample to be contaminated from the press and/or the die. The graphite holders are easy to load and they require no supports or covers, as do tape, indium foil, and pellets. Graphite is a conductor and, with the aid of an electron flood gun, presents no problem arising from the charging of the surface.

The NiS shows a peak of approximately 168.4 eV, indicating the presence of SO₄²⁻, caused by surface contamination of the sample by oxygen. The S/Ni ratio obtained for NiS, therefore, may not be representative of the bulk sample. The sulfate and nitrate were of the form NiSO₄·6H₂O and Ni(NO₃)₂·6H₂O. These samples showed a change of color upon being removed from the spectrometer, and the ratio of O/Ni was less than

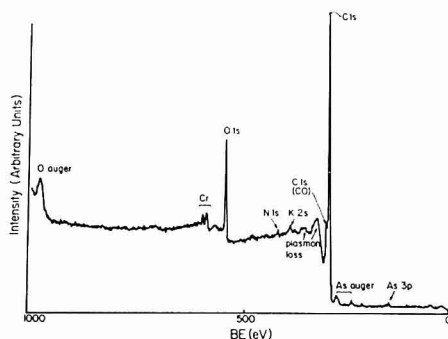


Figure 1. Wide scan of a graphite plate which contains 250 μ L of a nitric acid solution which is 500 ppm in Cr, 375 ppm in K, and 500 ppm in As.

expected, probably because of the loss of water due to the effects of the X-ray and the vacuum. If the intensities are used to predict stoichiometry, it appears that no waters of hydration remain on the nitrate compound but that the sulfate still retains about 2 waters of hydration. The binding energies were referenced to the carbon 1s peak from the sample using a value of 285.0 eV (3). The intensity ratios found for NiO seem to center about 1, which is predicted from stoichiometry. The experimental ratios, however, may be in error since the photoionization cross sections are taken from calculations. The small variations in ratios observed between holders is not unexpected because of uncertainty in absolute intensities.

One recent advancement in XPS has been its use in trace analysis. Analysis of microliter quantities of ppm solutions has been accomplished by observing the residue of such solutions on specially treated Al (4) and calcite plates (5). The graphite plates were also examined for use in trace analysis of solutions using XPS. Graphite might be a better choice for such an analysis because it has fewer interfering peaks. Since graphite can absorb a liquid, rapid evaporation of the

solvent was necessary. After the graphite planchet is cleaned, it is placed on a glass plate on a hot plate, and heated to between 60–80 °C. The solution is then added, 50 μ L at a time, with the water quickly evaporating. Figure 1 shows the spectra of 250 μ L of a solution containing 500 ppm Cr and 375 ppm K (from $K_2Cr_2O_7$), and 500 ppm As in nitric acid, loaded onto the graphite as described above. This preliminary evaluation of the holder in quantitative studies is promising.

In summary, these graphite planchets seem to have many advantages as routine sample holders in XPS. They are simple to use, inexpensive, and, when treated carefully, virtually free of contaminants. They have proved useful in examining oxygen-containing compounds and seem to have potential in trace analysis by ESCA.

LITERATURE CITED

- (1) G. E. Theriault, Thomas L. Batty, and M. J. B. Thomas, *Anal. Chem.*, **47**, 1492 (1975).
- (2) J. H. Scofield, *J. Electron Spectrosc.*, **8**, 129 (1976).
- (3) G. Johansson, J. Hedmann, A. Berndtsson, M. Klasson, and R. Nilsson, *J. Electron Spectrosc.*, **2**, 295 (1973).
- (4) D. Briggs, V. S. Givson, and J. K. Beccossall, *J. Electron Spectrosc.*, **11**, 343 (1977).
- (5) G. M. Bancroft, J. R. Brown, and W. S. Fyfe, *Anal. Chem.*, **49**, 1044 (1977).

RECEIVED for review September 8, 1978. Accepted October 31, 1978. Acknowledgement is made to the Robert A. Welch Foundation and to the donors of the Petroleum Research Fund, administered by the American Chemical Society for the support of the research.

Blank Limitations in Laser Excited Solution Luminescence

T. G. Matthews and F. E. Lytle*

Department of Chemistry, Purdue University, West Lafayette, Indiana 47907

In fluorimetry, the instrumental sensitivity is directly proportional to the intensity of the exciting radiation. This parameter, in turn, depends upon the source intensity, the throughput of the excitation optics, and, for a continuum source, the bandwidth of the monochromator. As a result, lasers have been demonstrated to be a very advantageous excitation source for trace luminescence analysis (1–4). An increase in sensitivity does not, however, produce a corresponding improvement in the lower limit of detection because most practical samples are blank limited. Parker has outlined several contributing factors including elastic scattering of the exciting radiation, inelastic Raman scattering from the solvent, and fluorescence from the cuvette, the solvent, and any sample impurities (5). The reduction of the total blank emission is therefore crucial to capitalizing on the laser as a source in studies involving either trace, high quantum yield or bulk, low quantum yield emitters in solution. This paper demonstrates that an improvement in the lower limit of detection can be achieved by a detailed consideration of the blank luminescence from both the cell and the solvent. A survey of high purity and spectral grade commercial solvents, including a complete range of polarity and several glass-forming mixtures, shows possible orders of magnitude variation in the blank. Simple purification procedures are found to be very effective in lowering reagent grade solvent emission, but none are competitive with high purity commercial solvents.

EXPERIMENTAL

The fluorimeter used for these experiments was constructed around a Phase-R Model N21K nitrogen laser providing 3- μ J, 4.5-ns pulses at a repetition rate of 28 Hz. Sample luminescence was focused through a Corning 0-52 filter (laser scatter attenuation X1000) into a Jarrell-Ash Model 82-405, $\frac{1}{4}$ -m monochromator providing a 4-nm bandpass. Emission detection was achieved by an RCA 1P28B photomultiplier. A detailed description of this instrument will be published at a later date.

Although the fluorimeter provided subnanosecond time resolution, all spectra were recorded at a time coincident with the peak of the laser pulse to more closely resemble the results expected with steady-state excitation. Data shown in the figures are corrected for the spectral response of the monochromator-photomultiplier combination.

Unless otherwise stated, all solvents were tested as received from the manufacturer. Quinine bisulfate was purchased from

Eastman Kodak and recrystallized twice from ethanol.

RESULTS AND DISCUSSION

Cell Design. Scatter and fluorescence from the cuvette can be conveniently reduced well below solvent emission levels by designing a cell consisting of a 1-cm i.d. quartz tube epoxied to a 1.2-cm² plate cut from a Corning 7-54 filter. Exciting vertically through the bottom of the cell, the filter passes the laser beam with minimal scatter and fluorescence, and irradiates the solution without impinging upon the walls. An increased path length can also be achieved in this configuration for greater signal strength.

Solvent Considerations. Solvent scatter and fluorescence present a far more complicated problem than cell design. In most cases, the total emission spectrum consists of temporally and spectrally sharp elastic and inelastic scattering bands (C-H, O-H), and some degree of a spectrally broad, impurity fluorescence tail ($\tau_f < 2$ ns). This is consistent with considerations of typical cross-sections for Rayleigh, vibrational Raman, and fluorescence processes. Despite the dramatically lower cross-sections for the scattering processes, the high number density of the solvent molecules causes both the Rayleigh and Raman signals to be comparable or greater in integrated intensity than the fluorescence emission from impurities in ultra-clean solvents.

Although not the principal topic of this paper, it should be noted that an instrument employing pulsed laser excitation is of obvious value in isolating long-lived sample emission from solvent impurity fluorescence and Raman scattering (2). Naturally, for fluorophores with lifetimes of similar magnitude to those of solvent impurities or the laser pulse width, time resolution is of little value. For this latter case, the blank emission can be reduced only by solvent purification or a judicious choice of manufacturer.

A survey of solvent emission (Figures 1–3) was taken including many very common solvents, a wide range of solvent polarity, and several manufacturers. Impurity fluorescence intensity varied by more than two orders of magnitude between spectral grade and high purity solvents. Only Burdick and Jackson (B&J) high purity, distilled-in-glass solvents were found to have uniformly low backgrounds. Individual solvent comparisons between spectral grade and B&J high purity are

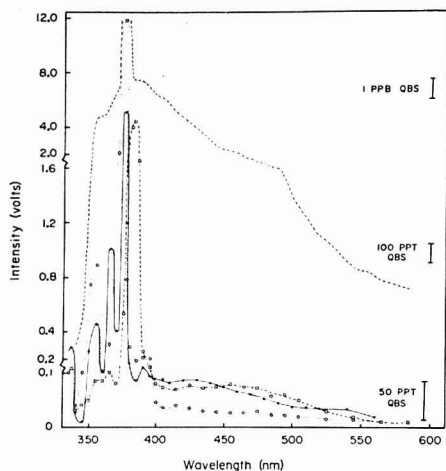


Figure 1. Solvent luminescence, (---) Spectral grade benzene, $E_T = 34.5$ kcal/mol. (●—●—●) B&J acetone, 46.0 kcal/mol. (□—□—□) Distilled water, 63.1 kcal/mol. (○—○—○) Cyclohexane, 31.2 kcal/mol

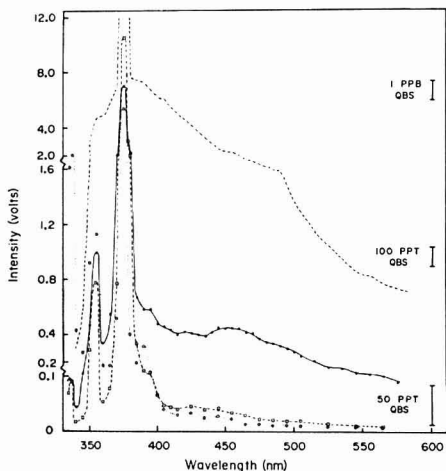


Figure 2. Solvent luminescence, (---) Spectral grade benzene. (●—●—●) USP grade ethanol, $E_T = 51.9$ kcal/mol. (□—□—□) B&J methanol, 55.5 kcal/mol. (○—○—○) B&J benzene

shown for benzene (Figure 2) and carbon tetrachloride (Figure 3). Significant improvement was noted with B&J carbon tetrachloride and orders of magnitude of difference was noted with B&J benzene. In all cases, the luminescence intensity (450 nm, 0.1 M H_2SO_4) of a particular concentration of quinine bisulfate (QBS) is shown for comparison. It should be noted that residual fluorescence for the better solvents corresponds roughly to compounds having a concentration-quantum yield product of 10^{-12} , e.g., 10^{-9} M and $\phi_f = 0.001$.

Figures 1, 2, and 3 illustrate the extensive range of polarity available in high quality solvents. Applying the E_T (25 °C) values developed by Reichardt and Dimroth (6) to classify solvent polarity, the largest gap between cyclohexane and

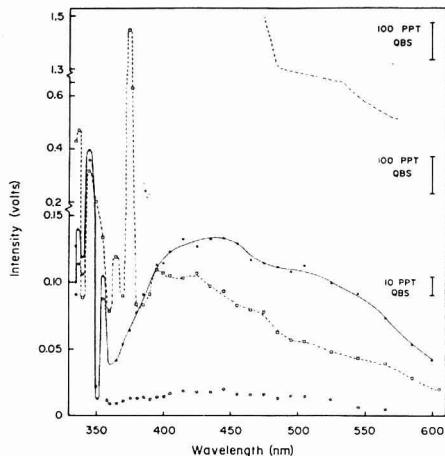


Figure 3. Solvent luminescence, (---) Spectral grade benzene. (●—●—●) Spectral grade carbon tetrachloride, $E_T = 32.5$ kcal/mol. (□—□—□) B&J chloroform, 39.1 kcal/mol. (○—○—○) B&J carbon tetrachloride

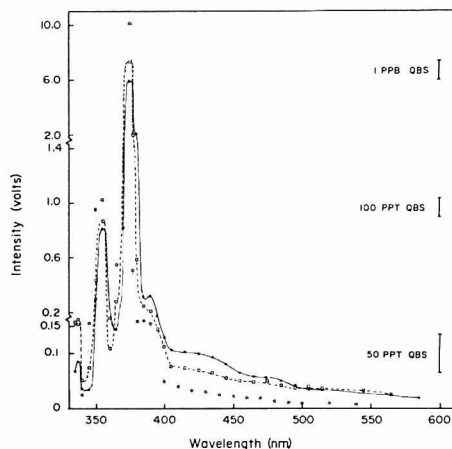


Figure 4. Glass-forming solvents. (●—●—●) 10% USP grade ethanol, 90% B&J methanol. (□—□—□) 29% B&J propanol or butanol, 71% B&J ethyl ether. (○—○—○) 50% B&J pentane, 50% B&J cyclopentane

water was 7.6 kcal/mol (see Figure captions). Incorporating other B&J high purity solvents and a few binary water mixtures for gaps at the polar end of the scale, separations of less than 2 kcal/mol could easily be achieved.

Three weakly luminescent glass-forming solvent mixtures of low (1:1 pentane/cyclohexane), intermediate (2:5 propanol/ether), and high (1:9 ethanol/methanol) polarity are presented in Figure 4. The 1:9 alcohol mixture represents the least fluorescent combination of several mixtures of these two solvents which forms a stable glass (7).

Solvent Purification. To ascertain the practicality of simple solvent purification procedures, a fractional distillation was attempted. Methyl cyclohexane was chosen for purification because it is used in several glass-forming solvent

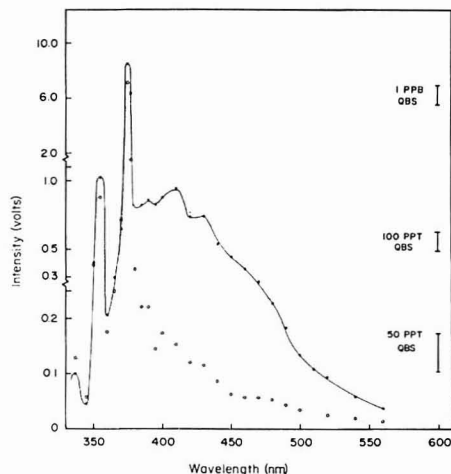


Figure 5. Methylcyclohexane purification. (●—●—●) Unpurified. (○—○—○) Purified

mixtures but can only be purchased in less than spectral grade quality. The luminescence of the best of 4 equal fractions collected from a packed Vigreux column (~10 theoretical plates) is presented in Figure 5. Although significant improvement was made, much more elaborate purification procedures would be necessary before results competitive with

high purity commercial solvents could be achieved.

CONCLUSION

Solvent scatter and luminescence have been shown to be major factors controlling the limits of detection in the conventional fluorescence technique. Solvent luminescence can frequently be reduced by orders of magnitude with careful selection or purification. Temporal resolution would also be valuable for isolating any sample emission long lived in comparison to the fluorescent impurities of the solvent. Spectral resolution is of little value, however, unless the emission is greatly red-shifted from the excitation energy. In contrast, the interference caused by scattered emission can frequently be attenuated with either spectral or time resolution, because of its sharp spectral and fast temporal characteristics.

ACKNOWLEDGMENT

We thank J. M. Harris for the initial work on the low cost cell design and the laser system.

LITERATURE CITED

- (1) R. E. Brown, K. D. Legg, M. W. Wolf, and L. A. Singer, *Anal. Chem.*, **46**(12), 1690 (1974).
- (2) F. E. Lytle and M. S. Kelsey, *Anal. Chem.*, **46**(7), 855 (1974).
- (3) R. N. Zare and M. R. Berman, *Anal. Chem.*, **47**(7), 1200 (1975).
- (4) J. H. Richardson and S. M. George, *Anal. Chem.*, **50**(4), 618 (1978).
- (5) C. A. Parker, *Photoluminescence of Solutions*, Elsevier, New York, 1968.
- (6) C. Reichardt, and K. Dimroth, *Fortschr. Chem. Forsch.*, **11**, 1-89 (1968).
- (7) F. J. Smith, J. K. Smith, and S. P. McGlynn, *Rev. Sci. Instrum.*, **33**(12), 1367 (1962).

RECEIVED for review November 16, 1978. Accepted January 18, 1979. This research was supported in part through funds provided by the National Science Foundation under Grants MPS75-05907 and CHE77-24312.

Algorithm for the Determination of Decay Rate Constants by Reversal Current Chronopotentiometry

Donald A. Tryk and Su-Moon Park*

Department of Chemistry, The University of New Mexico, Albuquerque, New Mexico 87131

Current-reversal chronopotentiometry (CRCP) is a technique which can complement cyclic voltammetry by providing quantitative kinetic data for slow following reactions investigated qualitatively by cyclic voltammetry. CRCP has perhaps been under-utilized because of the difficulties of its data treatment. We wish to report a convenient algorithm for the computation of pseudo-first-order decay rate constants of electrogenerated species using the method of current-reversal chronopotentiometry.

For the case where the forward electrolysis current, i_f , equals the reversal current, i_r , the diffusion equation yields the analytical solution (1).

$$2 \operatorname{erf} \sqrt{k\tau} = \operatorname{erf} \sqrt{k(t + \tau)} \quad (1)$$

where t is the forward electrolysis time, τ is the time elapsed between the current polarity switching time and the transition time for the electrogenerated species, and k is the pseudo-first-order decay rate constant. For the case in which $i_r \neq i_f$, the solution is (2)

$$(u + 1) \operatorname{erf} \sqrt{k\tau} = \operatorname{erf} \sqrt{k(t + \tau)} \quad (2)$$

where $u = i_r/i_f$.

The usual method for the computation of k has been to read values of the dimensionless quantity kt from a graph or table of kt vs. the experimental dimensionless quantity, τ/t (1). Herman has outlined a method for computer-generating such a table (3). In order to increase the precision of k , the experiment may be run at various values of t to obtain a series of values of kt . These may be plotted against t , the slope of the line being k (1). In terms of computer programming, however, a method requiring the use of a stored table and interpolation therefrom suffers from defects in storage economy, speed, and precision.

Another approach is to recast Equation 1 in an explicit form, giving the quantity t/τ as a function of $k\tau$:

$$t/\tau = \frac{1}{k\tau} [\operatorname{erf}^{-1}(2 \operatorname{erf} \sqrt{k\tau})]^2 - 1 \quad (3)$$

where erf^{-1} is the inverse of the error function. The inverse error function is readily implemented as a subroutine using the Newton method (4), since the derivative of the error function is available (5), and the error function itself is commonly available as a subroutine. The geometric form of Equation 3 is shown in Figure 1. At large values of t/τ , $k\tau$

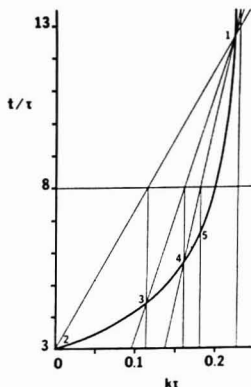


Figure 1. Theoretical curve for CRCP based on Equation 3. The thinner lines demonstrate the operation of the False Position algorithm. The asymptote lies at $kt = 0.2275$.

becomes insensitive to changes in t/τ , but this characteristic is inherent in Equation 1.

The problem then becomes one of finding roots of Equation 3 so that values of kt can be computed for input values of t/τ . Rather than attempting to derive a derivative of t/τ with respect to kt , which would be necessary in order to employ the Newton method, the False Position method (4) may be used. This method does not require a derivative to be known and is nearly as efficient as the Newton method. Also, the False Position method required less than half the average number of iterations required by a simple stepping search when used on a sample data set. Equation 3 was fitted to several different differentiable functional forms in order that the Newton method could be used directly, but a good fit could not be obtained.

In its simplest form, the False Position method may be set up using the origin (point 2) and a point on the curve in Figure 1 arbitrarily close to the asymptote, $kt = 0.22$ (point 1), as the starting points. In geometric terms, a line is drawn between the two points, and the intersection of this line with the horizontal line corresponding to an experimental t/τ value is found. The kt coordinate of this point is used to compute a value of t/τ using Equation 3. This coordinate pair corresponds to a point on the curve (point 3) from which a second line is drawn to point 1. Again the intersection with the horizontal t/τ line is found, and the kt value used to compute the t/τ coordinate of a new point on the curve (point 4). The process is continued until the desired accuracy is obtained. The iteration formula is then:

$$(kt)_{i+1} = (kt)_i \frac{(t/\tau)_1 - (t/\tau)_d}{(t/\tau)_1 - (t/\tau)_i} + (kt)_1 \frac{(t/\tau)_d - (t/\tau)_i}{(t/\tau)_1 - (t/\tau)_i}$$

Digestion Tube Diffusion and Collection of Ammonia for Nitrogen-15 and Total Nitrogen Determination

William A. O'Deen* and L. K. Porter

USDA, Science & Education Administration, Agricultural Research, P. O. Box E, Fort Collins, Colorado 80522

Total N in seeds, plants, soils, manures, sludges, organic residues, and organic compounds has traditionally been determined by Kjeldahl analysis. The Kjeldahl digestion

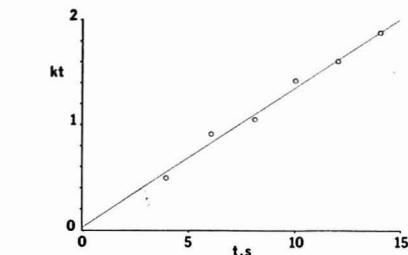


Figure 2. Experimental data with computer-generated kt values. Each point is averaged from three experiments (See text for experimental details).

where $(t/\tau)_d$ is the desired experimental value.

In order to achieve the efficiency indicated above for this algorithm, the curve was divided into two parts, and t/τ values below 5.6970 were treated using (0.1600, 5.6970) as the point of false position. Values of t/τ above this were treated using (0.2200, 12.6524). This treatment can easily be extended to encompass situations in which $i_r \neq i_l$ by using Equation 2.

Having now a value for kt for an experimental value of t/τ , one computes kt and plots values of kt vs. t as in Ref. 1. Figure 2 shows a plot using computer-generated values for an experiment similar to one run by Testa and Reinmuth (1) on the oxidation of *p*-aminophenol (PAP). Twice-recrystallized PAP was 1.13 mM in 0.0965 M H_2SO_4 , run at a current of $\pm 1 \mu A$ using a Pt disk electrode of area 0.021 cm^2 . The k value was $0.132 \pm 0.008 s^{-1}$ at the 90% confidence level. This compares well with the value of Testa and Reinmuth (1), which was $0.103 \pm 0.003 s^{-1}$ for 0.102 M H_2SO_4 and with that of Herman and Bard (6) determined by cyclic chronopotentiometry, which was $0.115 s^{-1}$ for 0.10 M H_2SO_4 . All of these values are at 30.0 °C.

A print-out of a FORTRAN IV program using the False Position method with least-squares and plotting subroutines is available from the authors.

LITERATURE CITED

1. A. C. Testa and W. H. Reinmuth, *Anal. Chem.*, **32**, 1512 (1960); C. Furlani and G. Morpurgo, *J. Electroanal. Chem.*, **1**, 351 (1959-60).
2. O. Fischer and O. Dracka, *J. Electroanal. Chem.*, **75**, 301 (1977); O. Dracka, *Collect. Czech. Chem. Comm.*, **25**, 338 (1960).
3. H. B. Herman in "Electrochemistry: Calculations, Simulation and Instrumentation", J. S. Mattson, H. B. Mark, and H. S. MacDonald, Jr., Ed., Marcel Dekker, New York, 1972, p. 63.
4. F. S. Acton, "Numerical Methods That Work", Harper and Row, New York, 1972, p. 52.
5. M. Abramowitz and I. A. Stegun, Ed., "Handbook of Mathematical Functions", NBS Applied Mathematics Series, No. 55, U.S. Government Printing Office, 1965, p. 311.
6. H. B. Herman and A. J. Bard, *Anal. Chem.*, **36**, 510 (1964).

RECEIVED for review July 17, 1978. Accepted December 19, 1978.

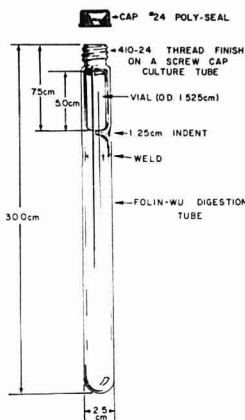


Figure 1. Construction details of a tube for tube-diffused collection of NH_3 .

formed in the digestion has normally been determined by colorimetric methods or by titration of the NH_3 trapped in various acidic solutions following alkaline distillation (2). Classically, isotope analyses for N have consisted of recovering the NH_4^+ by distillation and concentrating the NH_4^+ for subsequent oxidation to N_2 by alkaline hypobromite for mass spectrometry or emission spectrometry analysis (3).

This paper reports a simple procedure for the diffusion of NH_3 and its quantitative recovery as NH_4Cl from semimicro Kjeldahl digests. The recovered NH_4Cl can be used for N isotope and total N analyses. The procedure is similar in concept to the Yoneyama and Kumazawa (4) reabsorption system for obtaining NH_4Cl for Dumas combustion and subsequent isotope analysis, and is an extension of digestion-microdiffusion methods for total N determination detailed by Conway (5).

The primary advantage of this semimicro diffusion technique over the distillation technique now commonly employed is that the diffusion and subsequent evaporation of the excess HCl to recover the NH_4Cl salt are essentially unattended operations. Our present distillation procedure allows only 20 total N determinations and simultaneous isotopic N sample preparations in one day. This requires the full time attention of a laboratory analyst. Following tube-diffusion and acquisition of NH_4Cl , hundreds of gravimetric total N determinations, which are immediately ready for N isotope analysis, can be performed in the same one-day period.

MATERIALS AND METHODS

Special screw-cap digestion-diffusion tubes, 2.5 by 30 cm (Figure 1), were constructed by cutting off the bottoms of screw-cap culture tubes (Corning #9826) and glass blowing them to Folin-Wu digestion tubes (Corning #7940). Caps with conical polyethylene liners (Poly-Seal Caps, A. H. Thomas Co.) provided excellent seals. Glass indents 7.5 cm from the top of the tubes were formed to support the NH_3 absorption vials. The disposable glass shell vials (1.5 dram, or 5.0 by 1.525 cm) were the same vials used in the isotopic N inlet system conversion apparatus of Porter and O'Deen (6).

Isotopic Fractionation. Isotopic N fractionation resulting from the diffusion of NH_3 was studied with alkaline salt solutions containing 1.3 atom % ^{15}N ($\text{NH}_4)_2\text{SO}_4$ and Na_2SO_4 . Solutions made from $(^{15}\text{N})_2\text{SO}_4$ (1 mg N/mL) and Na_2SO_4 (220 mg/mL) were made alkaline with 1 mL of 13 N NaOH. (The Na_2SO_4 solution closely approximates the inorganic matrix of a neutralized Kjeldahl digest.) Immediately after making the solutions basic,

vials containing 3 mL of 1 N HCl were inserted into the tubes using reverse action forceps. The tubes were then capped and placed in a 40-hole Tecator or Technicon block digester.

At selected time intervals, tubes were removed and cooled for 5 min prior to vial removal. The extent of NH_3 diffusion was determined by steam distillation of the NH_3 remaining in the Na_2SO_4 matrix solutions followed by titration with HCl. The NH_4Cl in the vials was taken to dryness on a 95 °C steam table in an aluminum block holder (6). One-mg N levels were used for fractionation studies. One mg N as NH_4Cl , when oxidized by alkaline hypobromite, produces optimum N_2 pressure in the inlet system of the AEI-MS-20 isotope-ratio mass spectrometer and inlet system which we used (6). Fractionation can occur if NH_3 recovery is less than quantitative (7).

Recovery of $\text{NH}_4^+\text{-N}$. Two simple and direct methods were used to determine whether the N as NH_4Cl had been recovered quantitatively. Gravimetric determination was used by weighing number etched vials prior to diffusion and following evaporation of the excess HCl on the 95 °C steam table. The vials were left on the steam table for 0.5 h after vial and salt appeared dry and no odor of HCl could be detected. Vials left on the steam table for 6 h showed no weight losses. After evaporation of the HCl, the outside of the vials was cleaned with water-wet tissues and then with methanol. They were then stored in a desiccator. At normal isotopic abundance, 11.46 mg NH_4Cl are equivalent to 3 mg N.

A second method employing a solid-state Cl^- electrode was used to confirm quantitative recovery of the N as NH_4Cl . Since N is directly related to Cl^- in NH_4Cl , the potential of the Cl^- electrode may be used to determine N concentration in solutions of NH_4Cl . An Orion solid-state chloride electrode (Model 94-117A) and an Orion pH meter (model 701) in combination with an Orion double-junction reference electrode (model 90-02-00) were used to measure N concentration. The vials containing the NH_4Cl were placed on their sides in 600-mL beakers and 50 mL of water were pipetted into each beaker. The NH_4Cl in each vial was dissolved and transferred to a 100-mL beaker for nitrogen measurement. Three-minute readings were employed, followed by successive reimmersion of the electrodes and readings at 2 minutes. A standard curve of EMF vs. mg N/50 mL plotted on semilogarithmic paper was linear between 0.4 mg N/50 mL and 8 mg N/50 mL with nearly Nernstian behavior.

Total N Analyses. To demonstrate that both plant and soil samples could be carried through the tube-diffusion procedure with quantitative recovery of the N as NH_4Cl , 0.3 g of ball-milled corn ear tissue and 1 g of ball-milled Rago silt loam surface soil from Akron, Colo., were digested and then diffused. Total N digestions modified to include NO_3^- -N were performed according to semimicro-Kjeldahl procedures described by Bremner (2). Block temperature was 375 °C and digestion continued for 4 h. The digests were cooled and 24 mL of water were added to plant samples and 16 mL to soil samples to prevent solidification. The samples were made alkaline by addition of refrigerated 13 N NaOH in two increments with a 5-min cooling in cold water prior to the addition of each increment.

Total solution volume was 42 mL for plant samples and 38 mL for soil samples. Contents were thoroughly mixed by capping and inverting, and the caps were rinsed and the rims of the tubes wiped before insertion of the vials. The tubes were capped and diffused. (A 130 °C temperature and a 2-day period of diffusion were selected for soil sample diffusion because of bumping at 140 °C and physical characteristics of the soil diffusion solution.) 140 °C is a maximum safe diffusion temperature.

RESULTS AND DISCUSSION

The recovery of NH_3 from the diffusion process was highly dependent upon temperature and diffusion interval (Table I). At 80 °C, nitrogen isotope fractionation was significant. *t*-tests of the ^{15}N values for the various fractions vs. standard are all significantly different in ^{15}N content at the 1% probability level. When NH_3 recovery exceeds 95% (168 h), the ^{15}N value approaches that of the standard and differs from the standard by less than 5 parts per thousand. At 140 °C, mean separation tests employing the error mean square and appropriate LSD values show significant differences at the

Table I. The Amount of NH_4Cl Diffusion and Isotopic Fractionation as a Function of Temperature and Diffusion Interval with a Fixed Volume of 70 mL and an N Level of 1 mg (80°C , $n = 8$; and 140°C , $n = 10$)

temperature	diffusion period, h						standard
	8	24	48	72	96	168	
80°C							
% diffusion	--	34.1	60.2	73.1	--	95.5	--
fractionation	--	1.2883	1.2884	1.2930	--	1.3100	1.3144
(atom % ^{15}N)							
variance $\times 10^{-3}$	--	10.3	16.3	50.7	--	0.714	0.127
140°C							
% diffusion	63.6	94.7	98.3	98.6	99.0	--	--
fractionation	1.3078	1.3072	1.3073	1.3093	1.3072	--	1.3135
(atom % ^{15}N)							
variance $\times 10^{-3}$	0.903	1.13	1.16	0.523	0.633	--	0.128

Table II. The Extent of Diffusion and Isotopic N Fractionation as a Function of Salt Solution Volume and Diffusion Period with a Constant N Level of 1 mg/tube and a Diffusion Temperature of 140°C (8 h, $n = 4$; and 24 h, $n = 5$)^a

	volume, mL					
	50	30 8 h	10	50	30 24 h	10
amount of diffusion %	69.2	90.9	99.8	98.7	99.4	100
fractionation	1.3030	1.3059	1.3147	1.3113	1.3109	1.3153
(atom % ^{15}N)						
deviation from standard	9.95	7.75	1.06	3.65	3.95	0.61
(parts/1000 low)						

^a Atom % ^{15}N of standard was 1.3161Table III. Gravimetric Determinations of NH_4Cl Recovered

	standards			samples	
	3 mg N ^a	3 mg N ^b	1 mg N ^b	plant ^c	soil ^d
mean NH_4Cl weight	11.50	11.50	3.86	13.14 ^e	3.04 ^e
for 5 determinations (mg)					
deviation from expected (%)	+0.35	+0.35	+1.05	+0.38	+3.05
coefficient of variation (%)	1.37	1.23	5.37	1.15	2.94

^a Evaporated without diffusion. ^b Diffused 1 day at 140°C from 50 mL. ^c Diffused 1 day at 140°C from 42 mL.^d Diffused 2 days at 130°C from 38 mL. ^e Expected values were calculated from 5 corresponding steam distillation determinations. Gravimetric blank determinations had no measurable weight.

1% probability level for the standard ^{15}N values vs. fractions from other time intervals. However, atom % ^{15}N values for the various time intervals differ from the standard by less than 5 parts per thousand.

Table II shows that a reduction in sample volume greatly increased the recovery for the 8-h collection period and also influenced the atom % ^{15}N values. With a 10-mL sample volume and a 1-day collection period, lowering of the ^{15}N values is no longer significant. Table I shows that quantitative recovery of small N-level samples would take longer than quantitative recovery of high N-level samples. Diffusion of a 1-mg N sample from a 70-mL volume at 140°C for 1 day results in 94.7% recovery. Proceeding from 94.7% recovery (53 μg N remaining in solution) to 99% recovery (10 μg N remaining in solution) requires 3 days. Only 81% of the 53 μg N in solution would be recovered in 3 days. It also follows that in a fixed interval of diffusion, a higher percentage of a high N-level sample would be recovered than a low N-level sample. Use of this semimicro tube-diffusion apparatus for microgram quantities of N would require additional diffusion time to achieve quantitative recoveries.

Isotopic fractionation of nitrogen in tube-diffusion can therefore be minimized by decreasing sample volume, increasing N level, and increasing the diffusion time. This parallels the percentage recovery of nitrogen under the same experimental conditions. The fractionation is inconsequential

in most ^{15}N -enriched laboratory, greenhouse, and field experiments, but would produce errors in very exact ^{15}N determinations involving normal abundance studies.

Martin and Ross (8) reported extensive losses of NH_4Cl upon evaporation and recovery of the salt. Under our experimental conditions, no loss occurred. A water bath temperature of 95°C and the upper vial structure acting as a condenser for NH_4Cl vapor eliminated any volatile loss of NH_4Cl . Table III shows that both 3 mg-N standard evaporated without diffusion and 3 mg-N standard evaporated following diffusion resulted in quantitative recovery of the NH_4Cl . Slightly over 3 mg N diffused from digested plant samples also yielded quantitative recovery of the N as NH_4Cl . Although quantitative recovery of N as NH_4Cl occurred for 1 mg N when diffused from standard solutions or from digested soil samples, diffusion of 1 mg N resulted in a higher gravimetric coefficient of variation (CV) due to a larger relative weighing error. However, for gravimetric determination of 3 mg N and above, the CV of 1.4 and below is better than the CV of 2.45 reported for the block digestion-steam distillation procedure or the CV of 3.64 reported for the block digestion- NH_3 electrode procedure (9).

Solid-state chloride electrode determinations performed on 3 vials saved from corn tissue gravimetric determinations of N yielded values 0.63% higher, 0.96% lower, and 1.05% lower (mean = 0.46% lower) than values of N calculated from the

corresponding gravimetric values, providing additional evidence that the N as NH_4Cl was quantitatively recovered. The NH_4Cl may therefore be used not only for isotopic N analysis but for total N determinations. More sensitive N-detection methods, such as indophenol blue (10) and halide pulse polarography (11), might also be used with the resulting NH_4Cl , especially if this semimicro system were used for microgram quantities of N.

LITERATURE CITED

- (1) G. E. Schuman, M. A. Stanley, and D. Knudsen, *Soil Sci. Soc. Am. Proc.*, **37**, 480 (1973).
- (2) J. M. Bremner in "Methods of Soil Analysis", C. A. Black, Ed., American Society of Agronomy, Madison, Wis., 1965, pp 1149-1178.
- (3) J. M. Bremner in "Methods of Soil Analysis", C. A. Black, Ed., American Society of Agronomy, Madison, Wis., 1965, pp 1256-1286.
- (4) T. Yoneyama and K. Kumazawa, *Plant Cell Physiol.*, **15**, 655 (1974).
- (5) E. Conway, "Microdiffusion Analysis and Volumetric Error", Crosby Lockwood, London, 1957, pp 139-153.
- (6) L. K. Porter and W. A. O'Deen, *Anal. Chem.*, **49**, 514 (1977).
- (7) R. D. Hauck and J. M. Bremner, *Adv. Agron.*, **28**, 219 (1976).

- (8) A. E. Martin and P. J. Ross, *Trans. Int. Congr. Soil Sci.*, **9th**, **3**, 521 (1968).
- (9) R. N. Gallaher, C. O. Weldon, and F. C. Boswell, *Soil Sci. Soc. Am. J.*, **40**, 887 (1976).
- (10) J. K. Fawcett and J. E. Scott, *J. Clin. Pathol.*, **13**, 156 (1960).
- (11) W. A. O'Deen and R. A. Osteryoung, *Anal. Chem.*, **43**, 1879 (1971).

RECEIVED for review August 23, 1978. Accepted December 26, 1978. The work reported here was presented in part at the Third International Conference on Stable Isotopes, Oak Brook, Ill., 1978, and at the 20th Annual Rocky Mountain Conference on Analytical Chemistry, Denver, Colorado, 1978. Contribution of USDA, Science and Education Administration, Agricultural Research, Fort Collins, Colorado, in cooperation with Colorado State University Experiment Station, Fort Collins, Colorado. Trade names used in text are included for the reader's convenience, and such inclusion does not constitute any preferential endorsement of products named over similar products available on the market.

General Method for Overcoming Photoacoustic Saturation in Highly Colored Organic and Inorganic Solids

William H. Fuchsman*

Chemistry Department, Oberlin College, Oberlin, Ohio 44074

Ann J. Silversmith

Gilford Instrument Laboratories, Inc., 132 Artino Street, Oberlin, Ohio 44074

Recent interest in the application of photoacoustic spectroscopy (1, 2) to samples which absorb visible light has led not only to the commercial production of photoacoustic spectrometers but also to careful examination (2) of the advantages and limitations of the technique. A general problem in the application of photoacoustic spectroscopy to highly colored solids is saturation, which results in featureless spectra.

Saturation occurs when light is so effectively absorbed that the spectrum ceases to be dependent on the sample absorptivity. In photoacoustic spectroscopy, a layer of material with thickness approximately equal to the thermal diffusion length μ of the material can contribute to the signal; $\mu \propto f^{-1/2}$, where f is the frequency of modulation. The relative sizes of μ and the optical penetration depth $1/\beta$ determine whether saturation occurs. If the material is so highly absorbing that all of the light is absorbed in the first thermal diffusion length ($1/\beta \ll \mu$) over a range of wavelengths, then the photoacoustic spectrum is independent of sample absorptivity, and saturation occurs. Saturation can be avoided either by increasing the modulation frequency or by making the sample thickness so small that it is on the order of $1/\beta$ (cf. Figure 1, Reference 3).

EXPERIMENTAL

Tetraphenylporphyrin and its dication were synthesized by literature methods (4, 5). Photoacoustic spectra were obtained on a Gilford R-1500 spectrometer. Samples were attached to an aluminum sample holder by two-sided adhesive Cellophane tape. Diffuse reflectance spectra were obtained on a Beckman Acta IV spectrophotometer with reflectance sphere attachment. Samples were lightly spread on adhesive Cellophane tape; a BaSO_4 powder sample was behind the tape. The reference was BaSO_4 powder.

Solution absorbance spectra were obtained on a Cary 17 spectrophotometer. Scanning electron microscopy was performed on an AMR 1000-A instrument. Thin-layer grade alumina was purchased from Woelm; infrared grade KBr was purchased from Harshaw Chemical Company.

RESULTS

In our initial attempts to obtain photoacoustic spectra of solid porphyrins, even with high (2 kHz) chopper frequencies and thoroughly ground samples, we obtained typical saturated spectra (Figure 1A). In order to break up the sample particles still further, we ground tetraphenylporphyrin with thin-layer grade alumina. By so doing, we were able to obtain well defined photoacoustic spectra of tetraphenylporphyrin in the 400-700 nm visible region (Figure 1). The visible region photoacoustic spectrum of tetraphenylporphyrin ground with alumina exhibited λ_{max} values of 422, 519, 553, 594, and 652 nm. The photoacoustic spectrum of tetraphenylporphyrin ground with alumina was similar to the diffuse reflectance spectrum of pure tetraphenylporphyrin (Figure 1A) and the solution absorption spectrum of tetraphenylporphyrin dissolved in chlorobenzene (Figure 1B). Diffuse reflectance spectra of pure tetraphenylporphyrin and tetraphenylporphyrin ground with alumina showed no evidence of change resulting from grinding with alumina. We also obtained well defined photoacoustic spectra of tetraphenylporphyrin ground with infrared grade KBr.

Grinding samples with a white inorganic solid appears to be a general procedure for obtaining photoacoustic spectra of intensely colored solids. Saturation prevented successful visible region photoacoustic spectroscopy on pure solid potassium chromate, pure solid potassium dichromate, and pure solid copper phthalocyanine (2). Figure 2 shows visible region photoacoustic spectra of potassium chromate and potassium

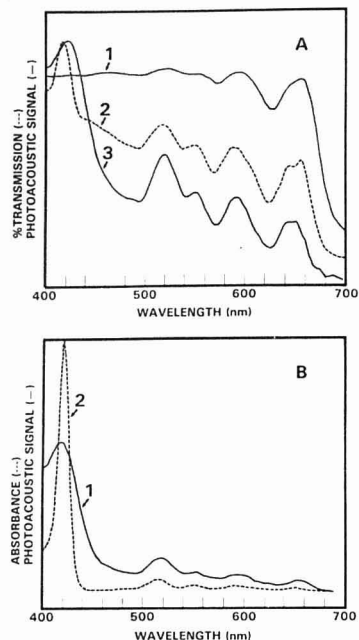


Figure 1. (A). (1) Photoacoustic spectrum of pure solid tetraphenylporphyrin, $f = 2$ kHz; (2) diffuse reflectance spectrum of pure solid tetraphenylporphyrin in percent transmittance; (3) photoacoustic spectrum of solid tetraphenylporphyrin ground with alumina (1 mg/g alumina), $f = 100$ Hz. (B). (1) Photoacoustic spectrum of solid tetraphenylporphyrin ground with alumina (1 mg/g alumina), $f = 100$ Hz; (2) absorbance spectrum of tetraphenylporphyrin dissolved in chlorobenzene

dichromate, each ground with alumina. After grinding samples with alumina, we also obtained visible region photoacoustic spectra of potassium permanganate, copper phthalocyanine, hemin, and chlorophyllin.

Grinding time appeared to be important for some samples. Tetraphenylporphyrin dication (with trifluoroacetate counterions) was converted to tetraphenylporphyrin by prolonged grinding but not by brief grinding with KBr.

Samples ground with KBr were successfully examined both as powders and as pieces of KBr pellets which had been used for infrared and Raman spectroscopy.

The degree of saturation, particularly in the 400–450 nm region of most intense absorption by tetraphenylporphyrin, depended upon the relative amounts of tetraphenylporphyrin and white inorganic solid which were ground together. Lower tetraphenylporphyrin:alumina and lower tetraphenylporphyrin:KBr mass ratios gave samples which exhibited less extensive saturation. The solid dilution effect is consistent with the proposal that organic solids ground with inorganic diluents are coated onto the surfaces of the inorganic particles rather than divided into smaller discrete particles (6). When examined by scanning electron microscopy, alumina ground with tetraphenylporphyrin appeared to have bits of tetra-

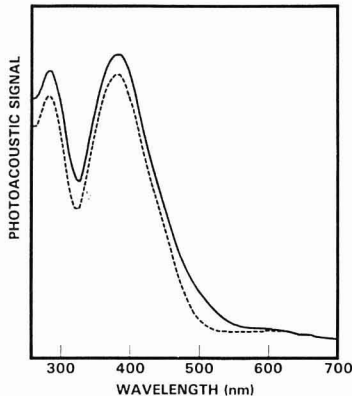


Figure 2. Photoacoustic spectra of solid $K_2Cr_2O_7$ ground with alumina (—) and solid K_2CrO_4 ground with alumina (---), $f = 100$ Hz

phenylporphyrin coating the alumina particles.

White alumina and KBr by themselves showed no absorption of visible light during photoacoustic spectroscopy.

Successful application of photoacoustic spectroscopy to pure, solid hemeproteins has been possible (7, 8) despite their large molar absorptivities and despite similarities in structure and optical properties of hemeproteins and tetraphenylporphyrin. Lack of saturation effects in solid hemeproteins might be associated with lower chromophore density (in moles/volume) in hemeproteins than in protein-free porphyrin compounds. Such chromophore concentration effects have been observed in photoacoustic spectra of methylene blue in aqueous solution (3) and tetraphenylporphyrin in chlorobenzene solution (9).

ACKNOWLEDGMENT

We thank D. J. Salasek, Ferro Corporation Technical Center, for aid in obtaining diffuse reflectance spectra and J. W. Smith, Ferro Corporation Technical Center, for obtaining scanning electron micrographs. We thank R. E. Blank, Gilford Instrument Laboratories, Inc., for advice and support and J. M. Long, Gilford Instrument Laboratories, Inc., for aid in computer-adjusting spectra from different instruments to consistent size.

LITERATURE CITED

- (1) A. Rosencwaig, *Anal. Chem.*, **47**, 592A–599A (1975).
- (2) F. W. Karasek, *Res. Dev.*, **28** (Sept.), 38–46 (1977).
- (3) J. F. McClelland and R. N. Kniseley, *Appl. Phys. Lett.*, **28**, 467–469 (1976).
- (4) A. D. Adler, F. R. Longo, J. D. Finarelli, J. Goldmacher, J. Assour, and L. Korsakoff, *J. Org. Chem.*, **32**, 476 (1967).
- (5) W. H. Fuchsman, J. M. Goldberg, D. D. Levy, and Q. R. Smith, *Bioinorg. Chem.*, **9**, 461–467 (1978).
- (6) G. Kortüm, "Reflectance Spectroscopy", Springer Verlag, Berlin, 1969, p 176.
- (7) A. Rosencwaig, *Science*, **181**, 657–658 (1973).
- (8) M. J. Adams, B. C. Beadle, A. A. King, and G. F. Kirkbright, *Analyst (London)*, **101**, 553–561 (1976).
- (9) W. H. Fuchsman and A. J. Silversmith, unpublished data, 1978.

RECEIVED for review October 10, 1978. Accepted January 23, 1979. This work was supported in part by grants to W.H.F. from the Research Corporation and by the donors of the Petroleum Research Fund, administered by the American Chemical Society.

Automatic Device to Monitor and Terminate a Distillation

Robert R. Lowry

Department of Agricultural Chemistry, Oregon State University, Corvallis, Oregon 97331

To obtain the level of purity presently required for many chromatographic techniques, it is often necessary to redistill solvents. This is true even with reagent grade material, as well as lesser grades and solvents that have been stored for a period of time.

Distillation is time-consuming and can be hazardous. If left unattended, broken hoses result in floods while overheated mantles result in damaged mantles and/or broken flasks, any of which may cause fires. These hazards are minimized using the device described below. Any failure of either the power or the water flow right up to the exit into the drain will result in the shutting off of both the water and the power. Further, an adjustable sensor permits the distillation to be turned off, both power and water, with a previously chosen level of solvent remaining in the still flask. This level can be chosen at any time before or during the distillation.

DESIGN

All electrical connections and circuits are outside the still itself with only a float made of glass or glass and metal in the solvent chamber. Standard flasks and mantles are used; the only requirement is that the flask have two necks, one of which should be a $\frac{3}{4}$ 45/50. If necessary, all the circuitry can be solid state. The drawings shown, however, have an electromechanical relay and two manual switches. A low voltage system is used to minimize arcing and other electrical hazards.

Figure 1 shows the equipment added to a regular still, in this case a 5-L flask and mantle. A glass guideway is made using a through-type $\frac{3}{4}$ 24/40 joint with a 12-mm upper diameter. This in turn sits upon a stock $\frac{3}{4}$ 24/40 to 45/50 adapter. Inside, a float consisting of two glass spheres on the ends of a wire, is free to rise and fall with the solvent level. The upper sphere is made of an opaque glass. If necessary, the wire could be replaced with a fine glass rod or tube.

Also shown is the sensor head containing a light source, PL; a light activated silicon controlled rectifier, PC; a switch, S1;

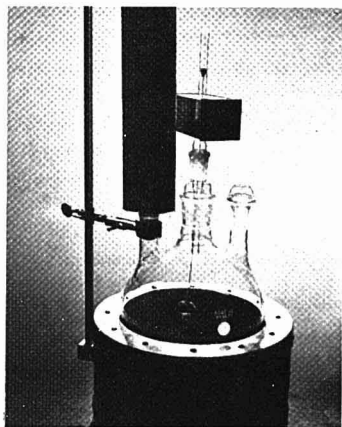


Figure 1. View of flask, solvent, float, float guideway, and sensor head

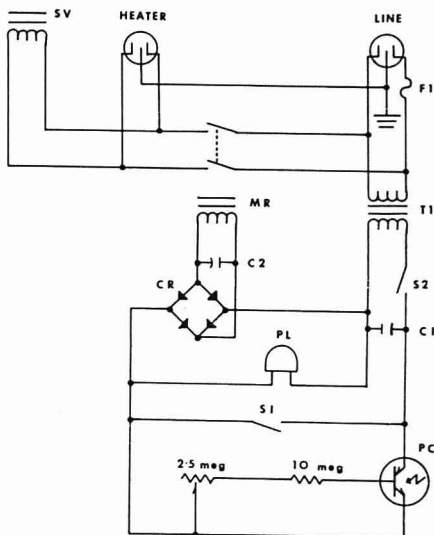


Figure 2. Schematic of device

Table I. Parts List for the Device

C1	0.1 μ f, 50 V dc	capacitor
C2	100 μ f, 50 V dc	capacitor
PL	18-24 V	pilot light
PC	General Electric L911F	photo SCR
MR	Potter & Brumfield KRP1DG	relay
F1	for mantle plus T1	fuse
T1	14 V, 0.25 A secondary	transformer
SV	Sporlan, 115 V, NC	solenoid valve
CR	SEN2A1	bridge rectifier
S1	push button, NO	switch
S2	Cherry #E22, NO	microswitch

and the resistors, R1 and R2, shown in Figure 2 and listed in Table I. The sensor head height is adjusted by a rubber grommet stop that is on the glass tube. When the opaque sphere interrupts the light beam from PL to PC, the circuit path to the relay coil is broken.

This can only be reset by manually closing switches S1 and S2 simultaneously. Switch S1 is a momentary push button and S2 is a flow switch consisting of a microswitch with a small plate of aluminum attached. This is located immediately above the drain and is so positioned that the exit stream of the condenser cooling water holds it in the closed position.

The relay controls the 110-V power to the heater and solenoid valve that controls the water supply. The latter is "hard" plumbed into the line and contains a constrictor for the water flow. With this arrangement, any loss of a hose connection or breakage of the condenser immediately stops the water flow and turns off the power.

In normal operation, once the distillation is proceeding and the solvent cut desired is being collected, it is necessary only

to have the sensor head located at the correct height for unattended operation.

The device described has been in use for eight years without a failure of any sort. It has permitted the distillation of hundreds of liters of a variety of organic solvents safely and economically in a system that is essentially of all glass

construction with a minimum of technical attention.

RECEIVED for review December 18, 1978. Accepted January 15, 1979. This work was supported by the Oregon Agricultural Experiment Station, Technical Paper No. 4917.

CORRECTION

Anodic Stripping Peak Currents: Electrolysis Potential Relationships for Reversible Systems

In this article (Zirino, A.; Kounaves, S. P. *Anal. Chem.* 1977, 49, 56), an inconsistency for the derivation of an equation for the half-wave ($E_{1/2}$) potential of a "polarogram" generated from peak currents or peak areas (charges) obtained by anodic stripping voltammetry has been found. The corrected equation should be

$$E_{1/2} = E^\circ + \frac{RT}{nF} \ln \left(\frac{2\gamma_0 \delta_0 r_0}{3D_0 \gamma_R} \right) - \frac{RT}{nF} \ln(t)$$

This expression differs from the previously derived equation by the "2" in

$$\ln \left(\frac{2\gamma_0 \delta_0 r_0}{3D_0 \gamma_R} \right)$$

The difference occurs from our failure to integrate the equation for the surface concentration of the reduced component under conditions of constant flux (Shain, I.; Lewinson, J. *Anal. Chem.* 1961, 33, 187.). We equated $\bar{C}_R(O)$ with $C_R(O)$ which in practice sets the mean value of $C_R(O)$ over the interval to the final value of $C_R(O)$ at the end of the electrolysis. That this is incorrect can also be seen intuitively from the following. Since diffusion within the drop can be neglected, $C_R(O)$ can be shown to increase linearly with t even at very low overvoltages. Thus $\bar{C}_R(O)$ lies between zero and $C_R(O)$ at t , and $\bar{C}_R(O) = C_R(O)/2$.

The resolution of our data is not sufficient to clearly distinguish the factor of 2 experimentally. Differences in junction potentials and E° between our experimental conditions and those which produced reference values (Harned, H. S.; Owen, B. B. "The Physical Chemistry of Electrolyte Solutions"; Reinhold: New York, 1958.), as well as the lack of comparative values for γ_0 and γ_R make this impossible at present (Ben Yaakov, S.; private communication.).

In accordance with the above, the corresponding equation for the half-wave potential of a stripping polarogram generated on a thin Hg film of thickness " l " should be

$$E_{1/2} = E^\circ + \frac{RT}{nF} \ln \left(\frac{2\gamma_0 \delta_0 l}{D_0 \gamma_R} \right) - \frac{RT}{nF} \ln(t)$$

The expanded equation for the potential-current relationship should be similarly corrected.

Author Index

Adams, M. J.	508	Gibson, H. W.	483		
Albertson, D. E.	556	Goda, L. Y.	511		
Armstrong, N. R.	565	Grimsrud, E. P.	537		
Aylmer, D. M.	581				
		Haartz, J. C.	520		
Bailey, F. C.	483	Hasegawa, J.	534	Markowitz, S. S.	572
Bates, T. S.	551	Hawkrigge, F. M.	556	Martin, B. R.	488
Bayne, C. K.	541	Haworth, D. T.	575	Matthews, T. G.	583
Blount, H. N.	556	Heineman, W. R.	561	Menon, K. R.	508
Blubaugh, E. A.	561	Hirschfeld, T.	495	Mori, Y.	534
Boström, K.	516			Morley, F.	579
Brakke, N. B.	499	Imabayashi, S.	534		
Burman, J.-O.	516	Imasaka, T.	502	Nakamura, T.	534
		Ishibashi, N.	502	Novakov, T.	572
Carpenter, R.	551	Jánossy, A. G. S.	491	O'Deen, W. A.	586
Carver, J. C.	581			Ogawa, T.	502
Cieslinski, R.	565			O'Neill, I. K.	579
Clemenson, M.	572	Kawabe, K.	534	Orofino, T. A.	505
Cody, R. B.	547	Kim, S. H.	537		
Cox, J. A.	554	Kirkbright, G. F.	508	Park, S.-M.	585
		Koteel, P.	575	Pevnick, J.	529
Davis, J. E.	526, 529	Kovács, K.	491	Pochan, J. M.	483
				Porter, L. K.	586
Freiser, B. S.	547	Lange, B. A.	520	Pringuer, M. A.	579
Fuchsman, W. H.	589	Lawson, S. R.	575		
Fujita, T.	534	Lifwinski, G. R.	554	Quinney, P. R.	499
		Lowry, R. R.	591		
Gale, L. H.	466	Lytte, F. E.	583	Raymond, R. H.	466
Garrett, R. B.	511				
Giauque, R. D.	511	McGuire, G. E.	488		
				Razzavi, H.	581
				Renoe, B.	526
				Rubin, I. B.	541
				Sakaguchi, K.	534
				Sawa, Y.	534
				Schwager, I.	569
				Siemer, D. D.	575
				Silversmith, A. J.	589
				Smock, P. L.	505
				Spencer, W. S.	505
				Stockwell, P. B.	579
				Taraszewski, W. J.	575
				Tóth, I.	491
				Tryk, D. A.	585
				Vance, J. A.	499
				Wagner, C. D.	466
				Wooten, G. W.	505
				Yacynych, A. M.	561
				Yen, T. F.	569

Gas Chromatographic Determination of Benzene and Toluene in Crude Oils

P. L. Grizzle and H. J. Coleman

Determination of Arsenic and Sulfur Species in Environmental Samples by Ion Chromatography

L. D. Hansen, B. E. Richter, D. K. Rollins, J. D. Lamb, and D. J. Eatough

Estimation of Particle Size Distributions from Turbidimetric Measurements

K. C. Yang and R. Hogg

Generalized Standard Addition Method

B. E. H. Saxberg and B. R. Kowalski

Calibration Curves with Nonuniform Variance

L. M. Schwartz

Mechanism of Low Pressure Chemical Ionization Mass Spectrometry

R. L. Hunter and R. T. McIver, Jr.

Electrochemical Removal of Phenolic Films from a Platinum Anode

R. C. Koile and D. C. Johnson

Design of a Phosphoroscope and the Examination of Room Temperature Phosphorescence of Nitrogen Heterocycles

C. D. Ford and R. J. Hurtubise

Future Articles

Optical System for Gathering Simultaneous Time and Spatial Data from Transient Events

S. G. Salmon and J. A. Holcombe

Direct Reaction Mixture Analysis by Probe Insertion Chemical Ionization Mass Spectrometry

R. J. Weinkam and H.-S. Lin

Plasma Emission Determination of Trace Heavy Metals in Salt Water Matrices

D. D. Nygaard

Determination of Cobalt by Lucigenin Chemiluminescence

L. M. Montano and J. D. Ingle, Jr.

Investigation of the Lucigenin Chemiluminescence Reaction

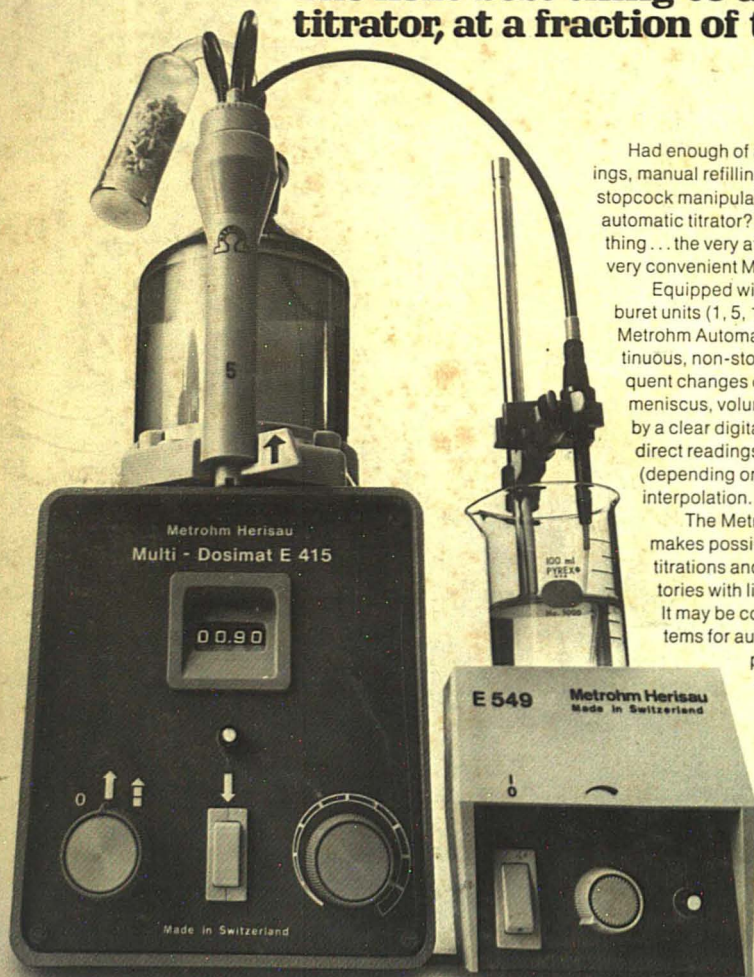
L. A. Montano and J. D. Ingle, Jr.

Comparison of the Negative Reactant Ions Formed in the Plasma Chromatography by Nitrogen, Air, and Sulfur Hexafluoride as the Drift Gas with Air as the Carrier Gas

T. W. Carr

LOOK... NO MENISCUS READING PROBLEMS!

**The Metrohm Automatic Buret.
The next best thing to an automatic titrator, at a fraction of the cost.**



Had enough of inaccurate meniscus readings, manual refilling of burets and tedious stopcock manipulation? Can't afford a fully-automatic titrator? Then consider the next best thing... the very affordable, very accurate and very convenient Metrohm Automatic Buret.

Equipped with interchangeable 'snap-in' buret units (1, 5, 10, 20 and 50ml), the Metrohm Automatic Buret will perform continuous, non-stop titrations even with frequent changes of titrant. Instead of a meniscus, volume indication is provided by a clear digital display which gives direct readings to 0.01ml or 0.001ml (depending on buret size) without interpolation.

The Metrohm Automatic Buret makes possible faster, more accurate titrations and is the answer for laboratories with limited equipment budgets. It may be coupled to ancillary systems for automatic determinations of potentiometric or colorimetric end points.

For informative literature, write: Metrohm Division, Brinkmann Instruments, Inc., Cantigue Road, Westbury, N.Y. 11590. In Canada: Brinkmann Instruments (Canada), Ltd.



Metrohm Automatic Buret

CIRCLE 21 ON READER SERVICE CARD

7.3.10.222